Pertanika Journal of

TROPICAL AGRICULTURAL SCIENCE

JTAS

VOL. 46 (4) NOV. 2023

PERTANIKA JOURNALS

A scientific journal published by Universiti Putra Malaysia Press

Pertanika Journal of Tropical Agricultural Science
Pertanika Journal of Tropical Agricultural Science

PERTANIKA JOURNAL OF TROPICAL AGRICULTURAL SCIENCE

About the Journal

Overview

Pertanika Journal of Tropical Agricultural Science is an official journal of Universiti Putra Malaysia. It is an open-access online scientific journal. It publishes the scientific outputs. It neither accepts nor commissions third party content.

Recognised internationally as the leading peer-reviewed interdisciplinary journal devoted to the publication of original papers, it serves as a forum for practical approaches to improving quality in issues pertaining to tropical agriculture and its related fields.

Pertanika Journal of Tropical Agricultural Science is a **quarterly** (*February*, *May*, *August*, and *November*) periodical that considers for publication original articles as per its scope. The journal publishes in **English** and it is open for submission by authors from all over the world.

The journal is available world-wide.

Aims and scope

Pertanika Journal of Tropical Agricultural Science aims to provide a forum for high quality research related to tropical agricultural research. Areas relevant to the scope of the journal include agricultural biotechnology, biochemistry, biology, ecology, fisheries, forestry, food sciences, genetics, microbiology, pathology and management, physiology, plant and animal sciences, production of plants and animals of economic importance, and veterinary medicine.

History

Pertanika was founded in 1978. Currently, as an interdisciplinary journal of agriculture, the revamped journal, *Pertanika* Journal of Tropical Agricultural Science now focuses on tropical agricultural research and its related fields.

Vision

To publish journals of international repute.

Mission

Our goal is to bring the highest quality research to the widest possible audience.

Quality

We aim for excellence, sustained by a responsible and professional approach to journal publishing. Submissions are guaranteed to receive a decision within 90 days. The elapsed time from submission to publication for the articles averages 180 days. We are working towards decreasing the processing time with the help of our editors and the reviewers.

Abstracting and indexing of Pertanika

Pertanika Journal of Tropical Agricultural Science is now over 45 years old; this accumulated knowledge has resulted in *Pertanika* Journal of Tropical Agricultural Science being abstracted and indexed in SCOPUS (Elsevier), Clarivate Web of Science (ESCI), EBSCO, DOAJ, Agricola, ASEAN CITATION INDEX, ISC, Microsoft Academic, Google Scholar, National Agricultural Science (NAL), and MyCite.

Citing journal articles

The abbreviation for *Pertanika* Journal of Tropical Agricultural Science is *Pertanika J. Trop. Agric. Sci*.

Publication policy

Pertanika policy prohibits an author from submitting the same manuscript for concurrent consideration by two or more publications. It prohibits as well publication of any manuscript that has already been published

either in whole or substantial part elsewhere. It also does not permit publication of manuscript that has been published in full in proceedings.

Code of Ethics

The *Pertanika* journals and Universiti Putra Malaysia take seriously the responsibility of all its journal publications to reflect the highest publication ethics. Thus, all journals and journal editors are expected to abide by the journal's codes of ethics. Refer to *Pertanika*'s **Code of Ethics** for full details, available on the official website of *Pertanika*.

Originality

The author must ensure that when a manuscript is submitted to *Pertanika*, the manuscript must be an original work. The author should check the manuscript for any possible plagiarism using any program such as Turn-It-In or any other software before submitting the manuscripts to the *Pertanika* Editorial Office, Journal Division.

All submitted manuscripts must be in the journal's acceptable **similarity index range**:
≤ 20% – *PASS*; **> 20%** – *REJECT*.

International Standard Serial Number (ISSN)

An ISSN is an 8-digit code used to identify periodicals such as journals of all kinds and on all media–print and electronic. All *Pertanika* journals have an e-ISSN.

Pertanika Journal of Tropical Agricultural Science: e-ISSN 2231-8542 (Online).

Lag time

A decision on acceptance or rejection of a manuscript is expected within 90 days (average). The elapsed time from submission to publication for the articles averages 180 days.

Authorship

Authors are not permitted to add or remove any names from the authorship provided at the time of initial submission without the consent of the journal's Chief Executive Editor.

Manuscript preparation

For manuscript preparation, authors may refer to *Pertanika*'s **INSTRUCTION TO AUTHORS**, available on the official website of *Pertanika*.

Editorial process

Authors who complete any submission are notified with an acknowledgement containing a manuscript ID on receipt of a manuscript, and upon the editorial decision regarding publication.

Pertanika follows a double-**blind peer review** process. Manuscripts deemed suitable for publication are sent to reviewers. Authors are encouraged to suggest names of at least 3 potential reviewers at the time of submission of their manuscripts to *Pertanika,* but the editors will make the final selection and are not, however, bound by these suggestions.

Notification of the editorial decision is usually provided within 90 days from the receipt of manuscript. Publication of solicited manuscripts is not guaranteed. In most cases, manuscripts are accepted conditionally, pending an author's revision of the material.

The journal's peer review

In the peer review process, 2 or 3 referees independently evaluate the scientific quality of the submitted manuscripts. At least 2 referee reports are required to help make a decision.

Peer reviewers are experts chosen by journal editors to provide written assessment of the **strengths** and **weaknesses** of written research, with the aim of improving the reporting of research and identifying the most appropriate and highest quality material for the journal.

Pertanika Journal of Tropical Agricultural Science
Pertanika Journal of Tropical Agricultural Science

Pertanika Journal of Tropical Agricultural Science
Pertanika Journal of Tropical Agricultural Science

Operating and review process

What happens to a manuscript once it is submitted to *Pertanika*? Typically, there are 7 steps to the editorial review process:

1. The journal's Chief Executive Editor and the Editor-in-Chief examine the paper to determine whether it is relevance to journal needs in terms of novelty, impact, design, procedure, language as well as presentation and allow it to proceed to the reviewing process. If not appropriate, the manuscript is rejected outright and the author is informed.

2. The Chief Executive Editor sends the article-identifying information having been removed, to 2 or 3 reviewers. They are specialists in the subject matter of the article. The Chief Executive Editor requests that they complete the review within 3 weeks.

   Comments to authors are about the appropriateness and adequacy of the theoretical or conceptual framework, literature review, method, results and discussion, and conclusions. Reviewers often include suggestions for strengthening of the manuscript. Comments to the editor are in the nature of the significance of the work and its potential contribution to the research field.

3. The Editor-in-Chief examines the review reports and decides whether to accept or reject the manuscript, invite the authors to revise and resubmit the manuscript, or seek additional review reports. In rare instances, the manuscript is accepted with almost no revision. Almost without exception, reviewers' comments (to the authors) are forwarded to the authors. If a revision is indicated, the editor provides guidelines to the authors for attending to the reviewers' suggestions and perhaps additional advice about revising the manuscript.

4. The authors decide whether and how to address the reviewers' comments and criticisms and the editor's concerns. The authors return a revised version of the paper to the Chief Executive Editor along with specific information describing how they have answered' the concerns of the reviewers and the editor, usually in a tabular form. The authors may also submit a rebuttal if there is a need especially when the authors disagree with certain comments provided by reviewers.

5. The Chief Executive Editor sends the revised manuscript out for re-review. Typically, at least 1 of the original reviewers will be asked to examine the article.

6. When the reviewers have completed their work, the Editor-in-Chief examines their comments and decides whether the manuscript is ready to be published, needs another round of revisions, or should be rejected. If the decision is to accept, the Chief Executive Editor is notified.

7. The Chief Executive Editor reserves the final right to accept or reject any material for publication, if the processing of a particular manuscript is deemed not to be in compliance with the S.O.P. of *Pertanika.* An acceptance notification is sent to all the authors.

   The editorial office ensures that the manuscript adheres to the correct style (in-text citations, the reference list, and tables are typical areas of concern, clarity, and grammar). The authors are asked to respond to any minor queries by the editorial office. Following these corrections, page proofs are mailed to the corresponding authors for their final approval. At this point, **only essential changes are accepted**. Finally, the manuscript appears in the pages of the journal and is posted on-line.

Pertanika Journal of

TROPICAL AGRICULTURAL SCIENCE

Vol. 46 (4) Nov. 2023

PERTANIKA JOURNALS

A scientific journal published by Universiti Putra Malaysia Press

PJTAS

***Pertanika* Journal of Tropical Agricultural Science**

AN INTERNATIONAL PEER-REVIEWED JOURNAL

EDITORIAL OFFICE

JOURNAL DIVISION

Putra Science Park

1st Floor, IDEA Tower II

UPM-MTDC Technology Centre

Universiti Putra Malaysia

43400 Serdang, Selangor Malaysia.

Gen Enquiry

Tel. No: +603 9769 1622 | 1616

E-mail:

executive_editor.pertanika@upm.edu.my

URL: www.journals-jd.upm.edu.my

PUBLISHER

UPM PRESS

Universiti Putra Malaysia

43400 UPM, Serdang, Selangor, Malaysia.

Tel: +603 9769 8851

E-mail: penerbit@putra.upm.edu.my

URL: http://penerbit.upm.edu.my

ABSTRACTING AND INDEXING OF PERTANIKA JOURNALS

The journal is indexed in SCOPUS (Elsevier), Clarivate-Emerging Sources Citation Index (ESCI), BIOSIS, National Agricultural Science (NAL), Google Scholar, MyCite, ISC. In addition, Pertanika JSSH is recipient of "CREAM" Award conferred by Ministry of Higher Education (MoHE), Malaysia.

Pertanika Journal of Tropical Agricultural Science
Vol. 46 (4) Nov. 2023

Contents

Foreword

Welcome to the fourth issue of 2023 for the Pertanika Journal of Tropical Agricultural Science (PTAS)!

PJTAS is an open-access journal for studies in Tropical Agricultural Science published by Universiti Putra Malaysia Press. It is independently owned and managed by the university for the benefit of the world-wide science community.

This issue contains 21 articles; one review article; two short communications; and the rest are regular articles. The authors of these articles come from different countries namely Bangladesh, Brazil, Brunei Darussalam, Indonesia, Kazakhstan, Malaysia, Nigeria, Philippines and Thailand.

Dayang Safinah Nayan and Suhaila Fouzi from Malaysia Agriculture Research and Development Institute evaluated the effects of individual zinc (Zn) and iron (Fe) foliar applications on growth, dry matter, and nutrient uptake by lettuce (*Lactuca sativa*). The application of Zn and Fe in the form of sulfate salt showed a lower toxicity effect in terms of growth and dry matter of plants than Fe and Zn in the form of ethylenediaminetetraacetic acid (EDTA). It was found that there was a significant difference observed compared to the control, especially when 3 kg/ha Zn was applied, regardless of whether it was in the form of sulfate or EDTA. Furthermore, there was an increase in Fe uptake observed with increased Zn application. In contrast, the Fe application showed no difference in Fe intake compared to the control. It was found that there is a decrease in Zn uptake observed with increasing application of Fe rate. It is believed that sufficient Fe content is already available in the soil, and plants only take up what is needed for growth. The detailed information of this article is available on page 1111.

A regular article entitled "Effects of Paracetamol on the Development of Zebrafish (*Danio rerio*)" investigated the impact of paracetamol on the development of zebrafish embryos. The results showed that paracetamol negatively affects the hatching and survival rates of zebrafish. In addition, spinal abnormalities, pericardial edema, hypopigmentation, reduced heart rate, and spontaneous movement were also appeared in zebrafish larvae. The developmental abnormalities in zebrafish were more significant with higher concentrations and longer exposure times. The further details of this study are found on page 1173.

A selected article entitled "Antioxidant Capacity, Alpha Amylase Inhibition, and Calorie Value of Dark Chocolate Substituted with Honey Powder" evaluated the effect of substituting sugar with 70% honey powder on the antioxidant, alpha-amylase inhibition, and calorie value of dark chocolate. The results proved that the antioxidant activity and alpha-amylase inhibition were increased, indicating that the phenolic content of the honey powder was preserved. Among the samples, dark chocolate containing honey/maltodextrin (H/M) exhibited the highest antioxidant

and alpha-amylase inhibition, demonstrating the effective preservation of phenolic content by maltodextrin. Therefore, chocolate containing H/M could be formulated as a functional food that may help decrease the risk of diabetes. Full information of this study is presented on page 1205.

In the last 12 months, of all the manuscripts peer-reviewed, 40% were accepted. This seems to be the trend in PJTAS.

We anticipate that you will find the evidence presented in this issue to be intriguing, thought-provoking and useful in reaching new milestones in your own research. Please recommend the journal to your colleagues and students to make this endeavour meaningful.

All the papers published in this edition underwent Pertanika's stringent peer-review process involving a minimum of two reviewers comprising internal as well as external referees. This was to ensure that the quality of the papers justified the high ranking of the journal, which is renowned as a heavily-cited journal not only by authors and researchers in Malaysia but by those in other countries around the world as well.

We would also like to express our gratitude to all the contributors, namely the authors, reviewers, Editor-in-Chief and Editorial Board Members of PJTAS, who have made this issue possible.

PJTAS is currently accepting manuscripts for upcoming issues based on original qualitative or quantitative research that opens new areas of inquiry and investigation.

Chief Executive Editor
Mohd Sapuan Salit
executive_editor.pertanika@upm.edu.my

Pertanika J. Trop. Agric. Sci. 46 (4): 1083 - 1096 (2023)

PERTANIKA JOURNALS

TROPICAL AGRICULTURAL SCIENCE

Journal homepage: http://www.pertanika.upm.edu.my/

Optimisation of Bioflocculation Using *Anabaena* sp. and *Navicula* sp. for Harvesting of Glagah Microalgae Consortium

Erik Lawijaya, Dwi Umi Siswanti and Eko Agus Suyono*

Faculty of Biology, Universitas Gadjah Mada, Jl. Teknika Selatan, Sleman, 55281 Yogyakarta, Indonesia

ABSTRACT

One of the problems in microalgae is harvesting. Currently, many chemical methods are used that impact the environment. Not all of them can be used as a filter, so bioflocculation is used because there is no need to change the medium. This method is an environmentally friendly and efficient alternative to chemical flocculants that usually cause contamination of biomass and health. Previous studies have shown that different ratios of auto-flocculated microalgae in cocultures affect the flocculation rate. This research was carried out by the Glagah Consortium bioflocculation using *Anabaena* sp. and *Navicula* sp., which had never been done before. The study aims to study the effect of the mixing ratio on the flocculation rate, carbohydrates, and lipid content of the Glagah Consortium. The consortium uses *Anabaena* sp. and *Navicula* sp. as bioflocculants. Glagah and *Anabaena* sp. consortium was cultured in Bold Basal Medium, while *Navicula* sp. was cultured in F/2 medium. Cell density was measured every 24 hr for 8 days with a hemocytometer. The cultures were harvested in the stationary phase, then mixed between non-flocculated microalgae (Glagah Consortium) and flocculated microalgae (*Anabaena* sp., *Navicula* sp.) in a ratio of 1:1, 1:0.5, and 1:0.25 for 24 hr. Bioflocculation was measured by spectrophotometer at 750 nm 0 and 24 hr after mixing. Carbohydrate levels were measured using the phenol sulfuric acid method, while lipid measurements were performed using the Bligh and Dyer method. The addition of *Anabaena* sp. and *Navicula* sp. as bioflocculant in Glagah Consortium culture results in an increase in flocculation rate with an effective ratio of 1:0.25 for *Anabaena* sp. (81%) and 1:1 for *Navicula* sp. (95%). Mixing of *Anabaena* sp. and Glagah Consortium results in carbon source competition, reducing carbohydrate content at higher mixing ratios (0.172, 0.364, and

ARTICLE INFO

Article history:
Received: 03 February 2023
Accepted: 04 April 2023
Published: 22 September 2023

DOI: https://doi.org/10.47836/pjtas.46.4.01

E-mail addresses:
eriklawijaya@mail.ugm.ac.id (Erik Lawijaya)
dwiumi@ugm.ac.id (Dwi Umi Siswanti)
eko_suyono@ugm.ac.id (Eko Agus Suyono)
* Corresponding author

ISSN: 1511-3701
e-ISSN: 2231-8542

0.500 mg/ml on 1, 1:0.5, and 1:0.25) while increasing lipid content as a result of lipid production in stationary phase (highest on ratio 1:1 = 0.011 mg/ml). *Navicula* sp. and Glagah Consortium mixture caused no significant changes to carbohydrate content but showed an increased amount of lipid at all ratios as a result of osmotic stress on Glagah Consortium from saline F/2 medium (highest on ratio 1:1 = 0.162 mg/ml).

Keywords: *Anabaena* sp., bioflocculation, co-culture, Glagah Consortium, *Navicula* sp.

INTRODUCTION

Biomass harvesting is an extensive process in microalgae biomass production, taking up 20-30% of the total production costs. Methods commonly used to harvest microalgae are centrifugation, filtration, and flocculation. Centrifugation is inefficient due to high upkeep costs, while filtration is ineffective in harvesting strains with smaller cell sizes (Matter et al., 2019; Salim et al., 2011). Flocculation is the most efficient method to harvest microalgae because it is simple, fast, and does not incur significant damage or changes to the harvested biomass (G. Singh & Patidar, 2018). The conventional flocculation method uses chemicals such as aluminium sulphate and iron chloride, which are pH-dependent and cause contamination and health risks. For example, in the flocculation process, using either alum or chitosan (Gupta et al., 2018). An alternative, more efficient method is required for microalgal biomass harvesting, and one such method is bioflocculation (Matter et al., 2019; Rahman, 2020). Bio-flocculation is the formation of flocs by adhesion and interparticle contact by microorganisms, usually done by co-culturing non-flocculating cultures with self-flocculating microorganisms or adding bio-flocculant agents into the culture (A. Singh et al., 2011; Lutfi et al., 2019; Matter et al., 2019; Y. Li et al., 2018). Bio-flocculation is an environmentally friendly and efficient method since it is biodegradable and allows the reuse of cultivation medium after dewatering (Matter et al., 2019; Salim et al., 2011). This process is attributed to the exopolymer substances (EPS) produced by auto-flocculating microalgae. In nature, EPS is used by microalgae to attach to substrates, gather nutrients, reduce diffusion, and protect cells from desiccation. EPS contribute to the formation of flocs in biofilm via the bridging effect, where EPS forms a matrix that holds non-flocculating microalgae in place (Klock et al., 2007; Salim et al., 2011).

Glagah Consortium is a local microalgae strain isolated from Glagah Beach, Yogyakarta, Indonesia, which contains 6 different species of microalgae and a symbiotic relationship with bacteria (Suyono et al., 2015, 2018). This strain has the potential to be used as a source of biofuel due to its high lipid content, reaching up to 13.58% and a lower ratio of polyunsaturated fatty acids (Sadaatkhah et al., 2020; Suyono et al., 2016). Using microalgae, bacteria, and fungi as bioflocculants resulted in higher coculture flocculation rates. However, it should be noted that bacteria and fungi may cause microbial contamination in microalgal biomass. Microalgae as

bioflocculant has a lower contamination risk, easier biomass purification, and does not require additional nutrients in the media for bioflocculant growth (Barros et al., 2015; Matter et al., 2019).

The genus *Anabaena* and *Navicula* are microalgae capable of forming aggregations in the form of cyanobacterial mats and biofilms as a defensive response to environmental change (Klock et al., 2007). EPS plays an important part in forming this aggregate by providing adhesion. Both genera can be used as bioflocculants as they can produce large amounts of EPS (Congestri & Albertano, 2011; Gómez-Ramírez et al. 2019). EPS release depends on microalgal cell growth under optimal temperature, pH, luminosity, nutrition, and salinity (Moreira et al., 2022). Previous research on Glagah Consortium bioflocculation using *Anabaena* sp. and *Navicula* sp. has yet to be done. The use of *Navicula* sp. as a microalgae culture bioflocculant still rarely does. This research is important to find a potential bioflocculant as a biofuel material, which can be seen from its lipid content. This research aims to discover the efficiency of Glagah Consortium flocculation using *Anabaena* sp. and *Navicula* sp. The research measures the effect of the mixing ratio on the flocculation rate, carbohydrates, and lipid content.

MATERIALS AND METHODS

Algal Cultures

Glagah isolates were obtained from the Laboratory of Biotechnology, Faculty of Biology, Universitas Gadjah Mada, while *Anabaena* sp. isolates were obtained from Indonesia Culture Collection (InaCC) Lembaga Ilmu Pengetahuan Indonesia (LIPI). *Navicula* sp. isolates were obtained from Pertamina Ltd. Cultivation of Glagah Consortium and *Anabaena* sp. were done in Bold's Basal Medium (BBM, PhytoTech Labs, USA) (Bold, 1949) while *Navicula* sp. cultivation was done in F/2 medium (PT Pertamina, Indonesia) with modification of silicate removal (Guillard, 1975). Cultures were grown for 8 days in 500 ml glass bottles under aeration, with an inoculum: medium ratio of 1:4. The biomass of *Anabaena variabilis* significantly increased when grown on the optimized medium (Refaay et al., 2022).

Cultivation Consortium of Glagah and *Navicula* sp. was done in a bottle culture volume of 500 ml with an inoculum: medium ratio of 1: 4 and a final volume of 500 ml at 28±2°C. The homogenization of nutrients was carried out by aeration and light shaking of *Navicula* sp. as much as 2 times a day. Ratio 1:4 was carried out between the Glagah Consortium and *Anabana* sp. and *Navicula* sp. because both have been proven to have the potential to be used as bioflocculants as they have the capability to produce large amounts of EPS.

Determination of Cell Density

Cell density in cultures was measured by cell count method using a light microscope and Haemocytometer Neubauer 1 mm (Electron Microscopy Sciences, USA) every 24 hr from the start of cultivation.

Samples were homogenized by shaking; 0.8 ml of samples were taken and mixed with 0.2 ml of 70% alcohol (Sigma-Aldrich, USA) for fixation (Sudibyo et al., 2017). The following formula calculated cell density:

$$\text{Cell density (cell/ml)} = n \times 10{,}000 \quad (1)$$

where, n = Average cell counted (Chalid et al., 2010).

Mixing of Cultures on Different Ratios

Samples of Glagah Consortium, *Anabaena* sp., and *Navicula* sp. were taken on day 3, 4, and 5 of cultivation, respectively. The sample was then put into a 15 ml tube with a mixing ratio between non-flocculating microalgae (Glagah Consortium) and flocculated microalgae (*Anabaena* sp., *Navicula* sp.) of 1:1, 1:0.5, and 1:0.25 (Salim et al., 2012). Samples were left undisturbed for 24 hr to determine bioflocculation rate, carbohydrate, and lipids content.

Determination of Bioflocculation Rate

The bioflocculation rate of the mixed cultures was measured using a UV-Vis spectrophotometer (MRC Laboratory-Instruments, United Kingdom) at 750 nm wavelength at T0 and T24 of mixing. The resulting absorbance was used to determine the sedimentation rate of the samples.

$$\text{Sd}(\%) = \frac{\text{OD}_{750}(\text{T0}) - \text{OD}_{750}(\text{Tn})}{\text{OD}_{750}(\text{T0})} \times 100\% \quad (2)$$

where, Sd (%) = Sedimentation rate; OD_{750} T0 = Optical density at 750 nm in 0 hr; Tn = Optical density at 750 nm in 24 hr (Salim et al., 2011).

Determination of Carbohydrate Content

Carbohydrate content was measured using the phenol sulphuric acid method (DuBois et al., 1956). Fifteen (15) ml of samples were centrifuged at 2,058 × *g* for 10 min, supernatant was removed, and 0.5 ml 5% phenol (Spectrum Chemicals, USA) was added into the pellet. Samples were then homogenized using a vortex and left for 10 min. One ml of concentrated sulfuric acid (Merck, USA) was added to the sample, followed by homogenization by the vortex. The sample was left for 20 min. Absorbance was measured using a UV-Vis spectrophotometer (MRC Laboratory-Instruments, United Kingdom) at 490 nm. Carbohydrate concentration was calculated from absorbance reading using the glucose standard curve as follows:

$$y = 0.0884x + 0.0095$$

Determination of Lipid Content

Lipid content was measured using Bligh and Dyer (1959) method. Fifteen (15) ml of samples were centrifuged at 2,683 × *g* for 15 min at 4°C. The supernatant was removed, and 2 ml methanol (Sigma-Aldrich, USA) and 1 ml chloroform (Sigma-Aldrich, USA) were added to the pellet. Samples were homogenized with vortex for 1 min, 1 ml equates (Sigma-Aldrich,

USA), and 1 ml chloroform was added, followed by homogenization for 1 min and centrifugation at 544 × *g* 4°C for 15 min. The sample will form 3 layers with lipids at the bottom. The layer containing lipids was moved into a Petri dish, then incubated at 33°C for 12 hr. Lipid content was calculated using the following:

$$\text{Lipid content } \left(\frac{\text{mg}}{\text{ml}}\right) = \frac{\text{Wn} - \text{W0}}{\text{W0} \times \text{V}} \quad (3)$$

where, Wn = Weight of filled Petri dish (g); W0 = Weight of empty Petri dish (g); V = Sample volume (ml) (Novaryatiin et al., 2011)

RESULTS

Cell Density

Figure 1 shows the cell density of Glagah Consortium, *Anabaena* sp., and *Navicula* sp. culture over the period of 8 days. The highest cell density of Glagah Consortium was found on day 3 (2.07 × 10^6 cell/ml), *Anabaena* sp. on day 4 (2.58 × 10^6 cell/ml), and *Navicula* sp. on day 6 (3.02 × 10^6 cell/ml). *Navicula* sp. culture showed a higher cell count from inoculation until the end of the culture period compared to Glagah Consortium and *Anabaena* sp. culture.

Bioflocculation Rate

The flocculation rate of the cultures under different mixing ratios is shown in Figure 2. The highest flocculation rate was achieved on the mixing ratio of 1:0.25 for Glagah and *Anabaena* sp. mix (Figure 2a) with a flocculation rate of 81%, mixing ratio of 1:1 is observed on Glagah and *Navicula* sp. mix with a flocculation rate of 95% (Figure 2b). The lower ratio of *Anabaena* sp. in the mix showed an increase in bioflocculation rate, while the larger mixing ratio of *Navicula* sp. showed an increase in bioflocculation rate.

Carbohydrate Content

Figure 3 shows the relation of the mixing ratio of microalgae to the carbohydrate content.

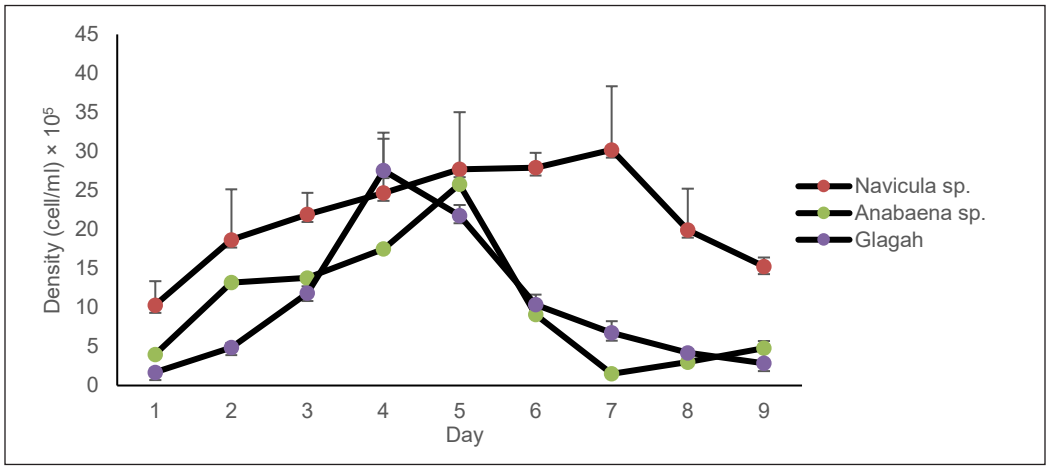

Figure 1. The cell density of Glagah Consortium, *Anabaena* sp., and *Navicula* sp. culture (Lawijaya, 2022)

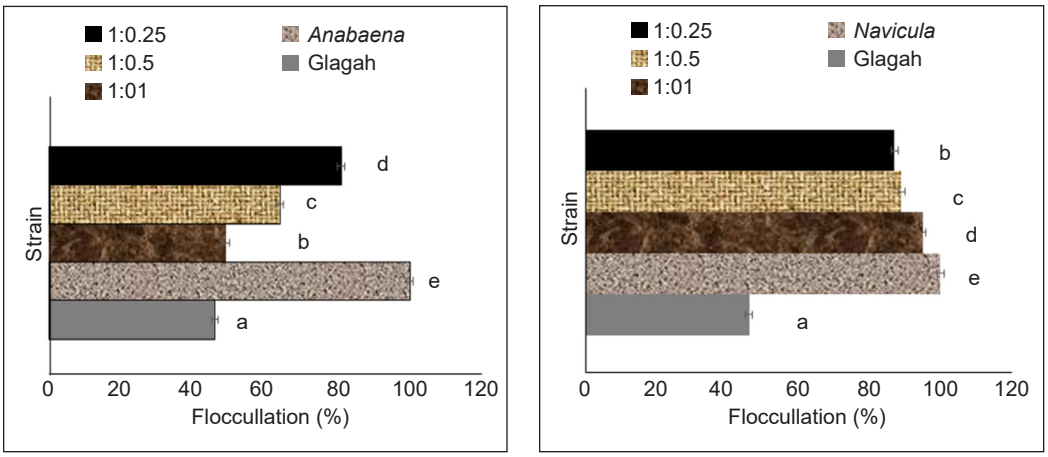

(a) (b)

Figure 2. Flocculation rates of: (a) Glagah strain and *Anabaena* sp.; (b) Glagah strain and *Navicula* sp. under different mixing ratios (Lawijaya, 2022)
Note. Different superscript letters above bars indicate significant differences (p<0.05)

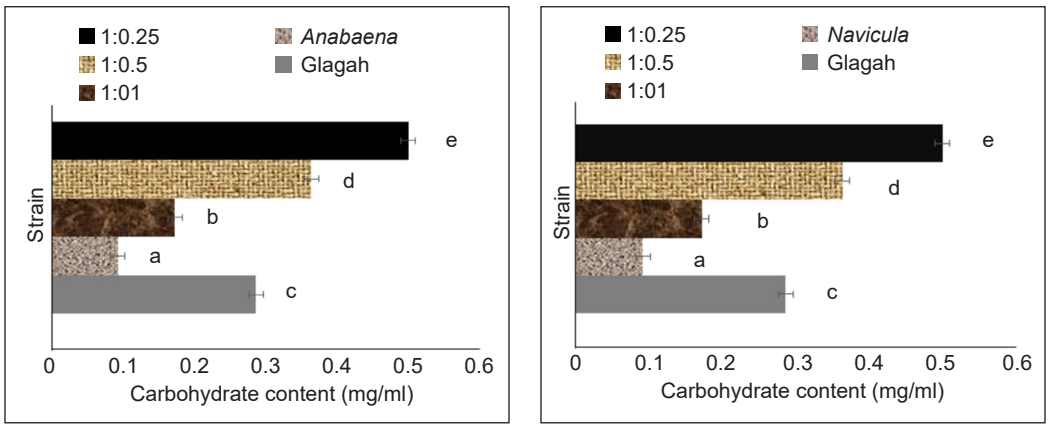

(a) (b)

Figure 3. The carbohydrate content of: (a) Glagah strain and *Anabaena* sp.; (b) Glagah strain and *Navicula* sp. under different mixing ratios (Lawijaya, 2022)
Note. Different superscript letters above bars indicate significant differences (p<0.05)

Glagah Consortium and *Anabaena* sp. mix (Figure 3a) showed higher carbohydrate content on lower mixing ratios, with the highest carbohydrate content at 1:0.25 ratio (0.500 mg/ml), *Anabaena* sp. control showed lower carbohydrate content than mixed samples at 0.092 mg/ml. A different trend was observed in Glagah Consortium and *Navicula* sp. mix (Figure 3b), which showed increased carbohydrate content at a higher mixing ratio, with the highest carbohydrate content found on a 1:1 mixing ratio (0.290 mg/ml). All mixed samples showed a lower amount of carbohydrates compared to the *Navicula* sp. control sample.

Lipid Content

The lipid content of cultures is shown in Figure 4. Glagah Consortium and *Anabaena* sp. mix (Figure 4A) showed a decrease in lipid content on a lower mixing ratio. The same pattern is observed on Glagah Consortium and *Navicula* sp. mix. The mixing ratio 1:1 showed the highest lipid content in Glagah and *Anabaena* sp. mix (0.011 mg/ml) and Glagah and *Navicula* sp. mix (0.162 mg/ml). *Navicula* sp. produced significantly higher lipid content than Glagah Consortium and *Anabaena* sp.

DISCUSSION

Cell Density

An increment of cell density in the culture indicates the usage of nutrients by microalgae for cell metabolism. In fast-growing microalgae, photosynthetic products are used for asexual reproduction and are kept as carbohydrates in microalgae with slow metabolisms (Jiménez et al., 2003). Cell density is used to indicate the growth phases of the culture. The lag phase of the Glagah Consortium occurs from day 0 to day 1 with a peak population of 4.3 × 10^5 cell/ml. This phase is characterized by a small increase in cell density due to cells adjusting to new living conditions (Fachrullah, 2011). The exponential growth phase occurs from days 1 to 3, with a peak cell density of 2.07 × 10^6 cell/ml on day 3. The stationary phase occurs from days 3 to 4, which shows no significant change in cell density, while the death phase occurs from day 4 to day 8, where a significant drop in cell density from 1.84 × 10^6 to 7.7 × 10^5 cell/ml. The mutualistic interaction between Glagah causes a large increase in cell density during the exponential growth phase.

Consortium and bacteria. Glagah Consortium supplies oxygen and organic substances via photosynthesis, while the

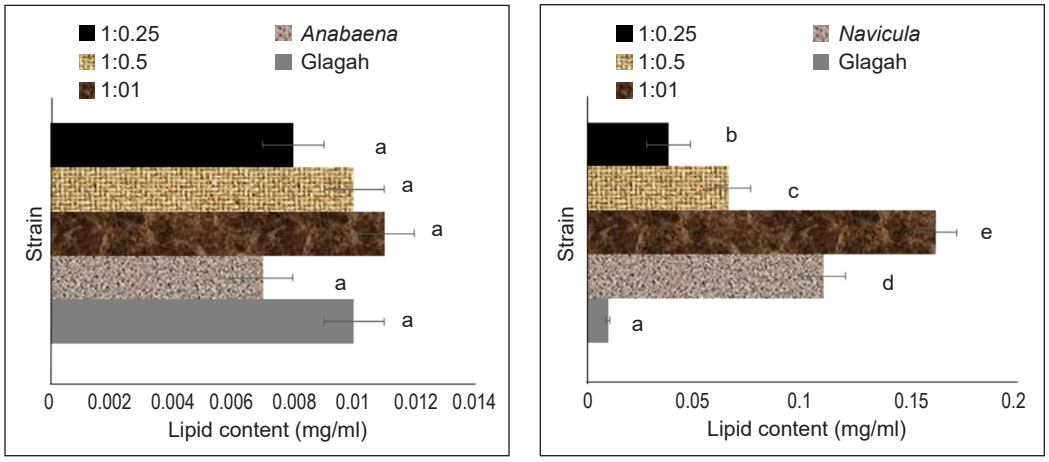

(a) (b)

Figure 4. Lipid content of: (a) Glagah strain and *Anabaena* sp.; (b) Glagah strain and *Navicula* sp. under different mixing ratios (Lawijaya, 2022)
Note. Different superscript letters above bars indicate significant differences (p<0.05)

bacteria provide vitamin B and indole-3-acetic-acid (IAA), which in turn increases the growth speed of Glagah Consortium (Fuentes et al., 2016; Rahmawati et al., 2020; Suyono et al., 2018).

Anabaena sp. culture showed a lag phase on day 0 to 1 of cultivation, followed by exponential growth until day 4, with a peak cell density of 2.58×10^6 cell/ml. The stationary phase occurs on days 4–5, and the death phase on days 5–8, indicated by the decline of cell density. *Navicula* sp. culture experienced a lag phase from day 0 to day 1, a log phase until day 5, and a stationary phase until day 6 of cultivation. The highest cell density was obtained on day 6 of cultivation at 3.02×10^6 cell/ml. The death phase occurs from day 6 to day 8. Silicate is an important component in the growth and division of diatom cells (Pandit et al., 2017). The silicate removal from the F/2 medium does not cause a slower growth rate in the culture due to the slow consumption cycle of silicate. Silicate deficiency usually affects older cultures (Sadaatkhah et al., 2020) as well as the growth inhibition of *A. platensis* was significantly ($p<0.01$) increased as a result of salt stress (Z. Li et al., 2022). The death phase of microalgae is caused by the scarcity of nutrients or accumulation of organic matter (NO_2^- and NH_4^+), which is toxic to microalgae, disturbing oxygen and nutrient intake (Nugroho, 2006; Suantika et al., 2009). Harvesting of the microalgae is done at the early stationary phase, where peak cell density is achieved. At this phase, nutrient stress occurs due to the limited nutrient in the media. It causes a drop in cell density and changes in cell metabolism (Guschina & Harwood, 2006).

Bioflocculation Rate

Harvesting of microalgae was done at the end of exponential growth, where secondary metabolite production is abundant (Cruz et al., 2020; Lutfi et al., 2019; Suyono et al., 2015). Mixing the Glagah Consortium with *Anabaena* sp. and *Navicula* sp. was done to induce the formation of flocs between microalgae, increasing the flocculation rate of the Glagah Consortium.

Anabaena sp. bioflocculation showed a higher rate of flocculation on a lower mixing ratio of flocculants. It is caused by the composition of EPS produced by *Anabaena* sp., mostly protein. It could be assumed that one of the proteins produced and excreted by the cyanobacteria is classified as an anatoxin (Gangl et al., 2015; Tiwari et al., 2015). Anatoxin could potentially inhibit the metabolism of Glagah Consortium and causes cell death in the culture mix, lowering the flocculation rate at a higher mixing ratio.

Navicula sp. is a benthic diatom with a tendency to form biofilms. As *Navicula* cells come into contact with Glagah Consortium, the cells form flocs between each other and fall onto the bottom of the media. Contact between *Navicula* sp. and Glagah Consortium could be attributed due to polysaccharides in the cell wall and colloidal exopolysaccharides excreted by *Navicula* sp., which helps in the formation of biofilm (Salim et al., 2011). This

interaction between microalgae causes the increase of flocculation rate on the addition of *Navicula* sp. to Glagah Consortium. The increase of bioflocculant rate to a higher flocculant ratio showed similar trends to Salim et al. (2012).

Carbohydrate Content

Carbohydrate is a product of photosynthesis and the main component in cell wall construction (Yen et al., 2013). It is commonly stored in the cell wall or plastids for energy storage (Domozych et al., 2012; Ho et al., 2012). Carbohydrate and lipid content are usually inversely proportional to each other. Lower amounts of carbohydrates in *Anabaena* sp. are caused by culture growth entering the stationary phase. In this phase, microalgae prioritize the hydrolysis of carbohydrates and accumulation of lipids in the cell (Sayanova et al., 2017). This results in the higher carbohydrate content on a lower mixing ratio because of lower amounts of *Anabaena* sp. competing for a carbon source.

Navicula sp. and Glagah Consortium produced a different result; a higher mixing ratio produced more carbohydrate content caused by a difference in medium salinities. *Navicula* sp. is cultivated in an F/2 medium with a salinity of 30%. When the cultures are mixed, osmotic stress will occur in Glagah Consortium cells, increasing carbon storage in cell walls, such as cellulose and hemicellulose (Suyono et al., 2015). No significant differences were observed between Glagah Consortium control and the mixed samples. Exopolysaccharides excreted by diatoms can act as substrates for heterotrophic bacteria growth, which also suggests the possibility of interaction between Glagah Consortium symbiotic bacteria and *Navicula* sp., causing a slight decrease in carbohydrate content (Amin et al., 2012).

Lipid Content

Glagah Consortium is a strain composed of multiple microalgae and bacteria species capable of fast, exponential growth. Interaction between species increases the productivity of lipids because the cells can use carbon sources optimally (Behl et al., 2011; Rahmawati et al., 2020; Suyono et al., 2015). Glagah Consortium contains 1.25% lipid, which could be increased up to 13.58% in response to saline stress (Suyono et al., 2016).

Anabaena sp. and Glagah Consortium mix produced significantly lower amounts of lipids compared to *Navicula* sp. and Glagah Consortium mix lipid content. It results from cultivation under normal conditions without stress (Rawat et al., 2013). A higher ratio of *Anabaena* sp. caused an increase in lipid production due to nutrient stress. At the stationary phase, microalgae compete in a limited nutrient condition, thus causing a change in metabolism (Guschina & Harwood, 2006). Microalgae will convert carbohydrates into lipids during this period.

Navicula sp. and Glagah Consortium mixture produced the highest lipid content at a 1:1 ratio, which is caused by exposure of Glagah Consortium to osmotic shock after mixing with *Navicula* sp., causing an

increase in lipid production as an adaptation to higher salinity. The impact of salt media increases the lipid content of the Glagah Consortium from 5.86% in brackish water to 13.58% in saltwater media (Suyono et al., 2015). Removal of silicate affects the growth and division of the cell as it is a component of the diatom frustule. Silicate deficiency and saline cause an increase in lipid production and the ratio of saturated and monounsaturated fatty acids while decreasing polyunsaturated fatty acids (Sadaatkhah et al., 2020; Seckbach & Kociolek, 2011).

The individual *Navicula* sp. or *Anabaena* sp. exposure gave a higher flocculation rate, but the contents of carbohydrate and lipid of the *Navicula* sp. or *Anabaena* sp. exposure were much lower than the mixed exposure because the lipid and carbohydrate content not only from the two microalgae but also from the Glagah Consortium.

Mixing Glagah Consortium and *Navicula* sp. cause the mixing of fuel growth medium with medium F/2, which has high salinity. In the ratio of mixing to the volume of *Navicula* sp., which is higher, the volume of medium F/2 mixed with medium BBM will be increased, thus causing a hyperosmotic condition in the culture. The Glagah Consortium and *Navicula* sp. would be hypoosmotic conditions because the medium F/2 dissolves in a non-saline BBM medium. Hyperosmotic conditions in the Glagah Consortium increased carbohydrate production, as seen in the research results. The increase is due to the influence of salinity in medium F/2 when mixing, which causes salinity stress at the Glagah Consortium. Salinity stress and water composition sea in medium F/2 results in carbon storage in cell walls as cellulose and hemicellulose (Suyono et al., 2015). One factor in increasing carbohydrate production is the Glagah Consortium, which is still in the progress log phase, so the production of carbohydrates as a cell wall material still takes precedence. Salinity stress on the Glagah Consortium also resulted in oxidative stress, increasing lipid content. On the Consortium mix Glagah with volume *Navicula* sp. lower ratios like 1:0.5 and 1:0.25, Glagah Consortium does not experience stress due to salinity, which can be seen from the lipid data that it shows lower content, and it does not significantly different from the Glagah Consortium control.

CONCLUSION

Adding *Anabaena* sp. and *Navicula* sp. as bioflocculant in the Glagah Consortium culture increases the flocculation rate with an effective ratio of 1:0.25 for *Anabaena* sp. and 1:1 for *Navicula* sp. Mixing of *Anabaena* sp. and Glagah Consortium results in carbon source competition, reducing carbohydrate content at a higher mixing ratio while increasing lipid content because of lipid production in the stationary phase. *Navicula* sp. and Glagah Consortium mixture caused no significant changes to carbohydrate content but showed an increased amount of lipid at all ratios because of osmotic stress on Glagah Consortium from saline F/2 medium. This study proves

that bioflocculation is an effective way to harvest microalgae, as evidenced by using *Anabaena* sp. and *Navicula* sp. to gather the Glagah Consortium from the coast of Yogyakarta, Indonesia.

ACKNOWLEDGEMENTS

This manuscript is a part of the first author's thesis. The authors are grateful to the Laboratory of Biotechnology, Faculty of Biology, Universitas Gadjah Mada, The National Research and Innovation Agency, and Alga Biotechnology Indonesia (ALBITEC) for their assistance in providing microalgae strains and facilities used in this research.

REFERENCES

Amin, S.A., Parker, M. S., & Armbrust, E. V. (2012). Interactions between diatoms and bacteria. *Microbiology and Molecular Biology Reviews*, *76*(3), 667-684. https://doi.org/10.1128/MMBR.00007-12

Barros, A.I., Gonçalves, A.L., Simões, M., & Pires, J. C. M. (2015). Harvesting techniques applied to microalgae: A review. *Renewable and Sustainable Energy Reviews*, *41*, 1489-1500. https://doi.org/10.1016/j.rser.2014.09.037

Behl, S., Donval, A., & Stiborb, H. (2011). The relative importance of species diversity and functional group diversity on carbon uptake in phytoplankton communities. *Limnology and Oceanography*, *56*(2), 683-694. https://doi.org/10.4319/lo.2011.56.2.0683

Bligh, E. G., & Dyer, W. J. (1959). A rapid method of total lipid extraction and purification. *Canadian Journal of Biochemistry and Physiology*, *37*(8), 911-917. https://doi.org/10.1139/o59-099

Bold, H. C. (1949). The morphology of *Chlamydomonas chlamydogama*, sp. Nov. *Bulletin of the Torrey Botanical Club*, *76*(2), 101-108. https://doi.org/10.2307/2482218

Chalid, S. Y., Amini, S., & Lestari, S. D. (2010). Kultivasi *Chlorella* sp. pada media tumbuh yang diperkaya dengan pupuk anorganik dan soil extract [Cultivation of *Chlorella* sp. on growing media enriched with inorganic fertilizers and soil extract]. *Jurnal Kimia Valensi*, *1*(6), 398-404. https://doi.org/10.15408/jkv.v1i6.242

Congestri, R., & Albertano, P. (2011). Benthic diatoms in biofilm culture. In. J. Seckbach & P. Kociolek (Eds.), *The diatom world: Cellular origin, life in extreme habitats and astrobiology* (Vol. 19, pp. 227-243). Springer. https://doi.org/10.1007/978-94-007-1327-7_10

Cruz, D., Vasconcelos, V., Pierre, G., Michaud, P., & Delattre, C. (2020). Exopolysaccharides from Cyanobacteria: Strategies for bioprocess development. *Applied Sciences*, *10*(11), 3763. https://doi.org/10.3390/app10113763

Domozych, D. S., Ciancia, M., Fangel, J. U., Mikkelsen, M. D., Ulvskov, P., & Willats, W. G. T. (2012). The cell walls of green algae: A journey through evolution and diversity. *Frontiers in Plant Science*, *3*, 82. https://doi.org/10.3389/fpls.2012.00082

DuBois, M., Gilles, K. A., Hamilton, J. K., Rebers, P. A., & Smith, F. (1956). Colorimetric method for determination of sugars and related substances. *Analytical Chemistry*, *28*(3), 350-356. https://doi.org/10.1021/ac60111a017

Fachrullah, M. R. (2011). *Laju pertumbuhan mikroalga penghasil biofuel jenis* Chlorella *sp. dan* Nanochloropsis *sp. yang dikultivasi menggunakan air limbah hasil penambangan timah di Pulau Bangka* [The growth rate of microalgae producing biofuels *Chlorella* sp. and *Nanochloropsis* sp., which is cultivated using

wastewater from tin mining on Bangka Island] [Master's thesis, IPB University]. IPB University Scientific Repository. https://repository.ipb.ac.id/handle/123456789/52202

Fuentes, J. L., Garbayo, I., Cuaresma, M., Montero, Z., González-del-Valle, M., & Vilchez, C. (2016). Impact of microalgae-bacteria interactions on the production of algal biomass and associated compounds. *Marine Drugs*, *14*(5), 100. https://doi.org/10.3390/md14050100

Gangl, D., Zelder, J. A., Rajakumar, P. D., Martinez, E. M. R., Riseley, A., Wlodarczyk, A., Purton,S., Sukaragi, Y., Howe, C. J., Jensen, P. E., & Robinson, C. (2015). Biotechnological exploitation of microalgae. *Journal of Experimental Botany*, *66*(22), 6975- 6990. https://doi.org/10.1093/jxb/erv426

Gómez-Ramírez, A. L., Enriquez-Ocaña, L. F., Miranda-Baeza, A., Esquivel, B.C., López-Elías, J. A., & Martínez-Córdova, L. R. (2019). Biofilm-forming capacity of two benthic microalgae, *Navicula incerta* and *Navicula* sp., on three substrates (Naviculales: Naviculaceae). *Revista de Biologia Tropical*, *67*(3), 599-607. https://doi.org/10.15517/rbt.v67i3.35117

Guillard, R. R. L. (1975). Culture of phytoplankton for feeding marine invertebrates. In W. L. Smith & M. H. Chanley (Eds.), *Culture of marine invertebrate animals* (pp. 29-60). Springer. https://doi.org/10.1007/978-1-4615-8714-9_3

Gupta, S. K., Kumar, N. M., Guldhe, A., Ansari, F. A., Rawat, I., Nasr, M., & Bux, F. (2018). Wastewater to biofuel: Comprehensive evaluation of various flocculants on biochemical composition and yield of microalgae. *Ecological Engineering*, *117*, 62-68. https://doi.org/10.1016/j.ecoleng.2018.04.005

Guschina, I. A., & Harwood, J. L. (2006). Lipids and lipid metabolism in eukaryotic algae. *Progress in Lipid Research*, *45*(2), 160-186. https://doi.org/10.1016/j.plipres.2006.01.001

Ho, S.-H., Huang, S.-W., Chen, C.-Y., Hasunuma, T., Kondo, A., & Chang, J.-S. (2012). Characterization and optimization of carbohydrate production from an indigenous microalga *Chlorella vulgaris* FSP-E. *Bioresource Technology*, *135*, 157-165. https://doi.org/10.1016/j.biortech.2012.10.100

Jiménez, C., Cossío, B. R., Labella, D., & Niell, F. F. (2003). The feasibility of industrial production of *Spirulina* (*Arthrospira*) in Southern Spain. *Aquaculture*, *217*(1-4), 179-190. https://doi.org/10.1016/s0044-8486(02)00118-7

Klock, J.-H., Wieland, A., Seifert, R., & Michaelis, W. (2007). Extracellular polymeric substances (EPS) from cyanobacterial mats: Characterisation and isolation method optimisation. *Marine Biology*, *152*, 1077-1085. https://doi.org/10.1007/s00227-007-0754-5

Lawijaya, E. (2022). *Pemanenan Konsorsium Glagah menggunakan* Anabaena *sp. dan* Navicula *sp. sebagai bioflokulan* [Harvesting the Glagah Consortium using *Anabaena* sp. and *Navicula* sp. as the bioflocculant] [Unpublished Undergraduate thesis]. Universitas Gadjah Mada.

Li, Y., Xu, Y., Song, R., Tian, C., Liu, L. Zheng, T., & Wang, H. (2018). Flocculation characteristics of a bioflocculant produced by the actinomycete *Streptomycetes* sp. Hsn06 on microalgae biomass. *BMC Biotechnology*, *18*, 58. https://doi.org/10.1186/s12896-018-0471-9

Li, Z., Liu, Y., Zhou, T., Cao, L., Cai, Y., Wang, Y., Cui, X., Yan, H., Ruan, R., & Zhang, Q. (2022). Effect of culture conditions on the performance or *Arthrospora platensis* and its production of exopolysaccharides. *Foods*, *11*(14), 2020. https://doi.org/10.3390/foods11142020

Lutfi, M., Nugroho, W. A., Fridayetsu, W. P., Susilo, B., Pulmar, C., & Sandra, S. (2019). Bioflocculation of two species of microalgae by exopolysaccharide of *Bacillus subtilis*. *Nature*

Environment and Pollution Technology, *18*(1), 167-173.

Matter, I. A., Bui, V. K. H., Jung, M., Seo, J. Y., Kim, Y.-E., Lee, Y.-C., & Oh, Y.-K. (2019). Flocculation harvesting techniques for microalgae: A review. *Applied Sciences*, *9*(15), 3069. https://doi.org/10.3390/app9153069

Moreira, J. B., Kutzler, S. G., Bezerra, P. Q. M., Cassuriaga, A. P. A., Zaparoli, M. M., da Silva, J. L. V., Costa, J. A. V., & de Morais, M. G. (2022). Recent advances of microalgae exopolysaccharides for application as bioflocculants. *Polysaccarides*, *3*(1), 264-276. https://doi.org/10.3390/polysaccharides3010015

Novaryatiin, S. (2011). *Isolasi dan karakterisasi potensi biodiesel mikroalga air tawar yang dikoleksi dari beberapa perairan umum sekitar Tangerang dan Bogor* [Isolation and characterization of potential freshwater microalgae biodiesel collected from several public waters around Tangerang and Bogor] [Doctoral thesis, Universitas Al Azhar Indonesia]. Repository Digital Universitas Al Azhar Indonesia. http://eprints.uai.ac.id/id/eprint/305

Nugroho, C. (2006). *Efek Pb terhadap laju pertumbuhan dan biomassa* Spirulina platensis [Effect of Pb on growth rate and biomass of *Spirulina platensis*]. [Unpublished Master's thesis]. Universitas Gadjah Mada.

Pandit, P. R., Fulekar, M. H., & Karuna, M. S. L. (2017). Effect of salinity stress on growth, lipid productivity, fatty acid composition, and biodiesel properties in *Acutodesmus obliquus* and *Chlorella vulgaris*. *Environmental Science and Pollution Research*, *24*, 13437-13451. https://doi.org/10.1007/s11356-017-8875-y

Rahman, K. M. (2020). Food and high value products from microalgae: Market opportunities and challenges. In M. D. Alam, J. L. Xu, & Z. Wang (Eds.), *Microalgae biotechnology for food, health and high value products* (pp. 3-27). Springer. https://doi.org/10.1007/978-981-15-0169-2_1

Rahmawati, B., Ilmi, M., Budiman, A., & Suyono, E. A. (2020). Screening of IAA production on the interaction of microalgae and bacteria in the Glagah Consortium. *Biosciences Biotechnology Research Asia*, *17*(1), 45-52. https://doi.org/10.13005/bbra/2808

Rawat, I., Ranjith Kumar, R., Mutanda, T., & Bux, F. (2013). Biodiesel from microalgae: A critical evaluation from laboratory to large scale production. *Applied Energy*, *103*, 444-467. https://doi.org/10.1016/j.apenergy.2012.10.004

Refaay, D. A., Abdel-Hamid, M. I., Alyamani, A. A., Mougib, M. A., Ahmed, D. M., Negm, A., Mowafy, A. M., Ibrahim, A. A., & Mahmoud, R. M. (2022). Growth optimization and secondary metabolites evaluation of *Anabaena variabilis* for acetylcholinesterase inhibition activity. *Plants*, *11*(6), 735. https://doi.org/10.3390/plants11060735

Sadaatkhah, A., Sobhanian, H., Zoufan, P., Amini, F., & Soltani, N. (2020). Interaction of nitrogen and silicate fluctuations with salt stress on growth, and lipid production in *Navicula* sp. *Iranian Journal of Fisheries Sciences*, *19*(6), 3310-3326. https://doi.org/10.22092/ijfs.2020.350889.0

Salim, S., Bosma, R., Vermuë, M. H., & Wijffels, R. H. (2011). Harvesting of microalgae by bio-flocculation. *Journal of Applied Phycology*, *23*, 849-855. https://doi.org/10.1007/s10811-010-9591-x

Salim, S., Vermuë, M. H., & Wijffels, R. H. (2012). Ratio between autoflocculating and target microalgae affects the energy-efficient harvesting by bio-flocculation. *Bioresource Technology*, *118*, 49-55. https://doi.org/10.1016/j.biortech.2012.05.007

Sayanova O., Mimouni, V., Ulmann, L., Morant-Manceau, A., Pasquet, V., Schofs, B., & Napier, J. A. (2017). Modulation of lipid biosynthesis by stress in diatoms. *Philosophical Transactions of the Royal Society B: Biological Sciences*, *372*, 20160407. https://doi.org/10.1098/rstb.2016.0407

Seckbach, J., & Kociolek, J. P. (Eds.). (2011). *The diatom world*. Springer. https://doi.org/10.1007/978-94-007-1327-7

Singh, A., Nigam, P. S., & Murphy, J. D. (2011). Mechanism and challenges in commercialisation of algal biofuels. *Bioresource Technology*, *102*(1), 26-34. https://doi.org/10.1016/j.biortech.2010.06.057

Singh, G., & Patidar, S. K. (2018). Microalgae harvesting techniques: A review. *Journal of Environmental Management*, *217*, 499-508. https://doi.org/10.1016/j.jenvman.2018.04.010

Suantika., Pingkan, G., & Yusuf. (2009). *Pengaruh kepadatan awal inokulum terhadap kualitas kulturv* Chaetoceros gracilis *(Schuut) pada sistem batch* [Effect of initial inoculum density on culture quality of *Chaetoceros gracilis* (Schuut) in batch system] [Unpublished Master's thesis]. Institut Teknologi Bandung.

Sudibyo, H., Pradana, Y. S., Samudra, T. T., Budiman, A., Indarto, I., & Suyono, E. A. (2017). Study of cultivation under different colors of light and growth kinetic study of *Chlorella zofingiensis* Dönz for biofuel production. *Energy Procedia*, *105*, 270-276. https://doi.org/10.1016/j.egypro.2017.03.313

Suyono, E. A., Fahrunnida., Nopitasari, S., & Utama, I. V. (2016). Identification of microalgae species and lipid profiling of Glagah consortium for biodiesel development from local marine resource. *ARPN Journal of Engineering and Applied Sciences*, *11*(16), 9970-9973.

Suyono, E. A., Haryadi, W., Zusron, M., Nuhamunada, M., Rahayu, S., & Nugroho, A. P. (2015). The effect of salinity on growth, dry weight and lipid content of the mixed microalgae culture isolated from Glagah as biodiesel substrate. *Journal of Life Sciences*, *9*, 229-233. https://doi.org/10.17265/1934-7391/2015.05.006

Suyono, E. A., Retnaningrum, E., & Ajijah, N. (2018). Bacterial symbionts isolated from mixed microalgae culture of Glagah strains. *International Journal of Agriculture and Biology*, *20*(1), 33-36.

Tiwari, M. O., Khangngembam, R., Shamjetshabam, M., Sharma, A. S., Oinam, G., & Brand, J. J. (2015). Characterization and optimization of bioflocculant exopolysaccharide production by cyanobacteria isolate *Glagah* BTA97 and *Anabaena* sp. BTA990 in culture conditions. *Applied Biochemistry Biotechnology*, *176*, 1950-1963. https://doi.org/10.1007/s12010-015-1691-2

Yen, H.-W., Hu, I.-C., Chen, C.-Y., Ho, S.-H., Lee, D.-J., & Chang, J.-S. (2013). Microalgae-based biorefinery - From biofuels to natural products Hong-Wei. *Bioresource Technology*, *135*, 166-174. https://doi.org/10.1016/j.biortech.2012.10.099

Pertanika J. Trop. Agric. Sci. 46 (4): 1097 - 1110 (2023)

PERTANIKA JOURNALS

TROPICAL AGRICULTURAL SCIENCE

Journal homepage: http://www.pertanika.upm.edu.my/

Short Communication

Growth Performance of Broiler Chicken Supplemented with *Bacillus velezensis* D01Ca and *Bacillus siamensis* G01Bb Isolated from Goat and Duck Microbiota

Gary Antonio Lirio[1], James Jr. Cerado[1], Jenine Tricia Esteban[1], Jeffrey Adriano Ferrer[1] and Claire Salvedia[2]*

[1]Center for Life Sciences Research, Institute for Science and Technology Research, Polytechnic University of the Philippines, 1008 Manila, Philippines
[2]Animal Science Department, College of Agriculture, Mindanao State University, 9700 Marawi, Philippines

ABSTRACT

The increasing global demand for sustainable agricultural practices and the quest for food security has intensified the need for alternative solutions to promote healthy growth in farm animals. One potential strategy is the use of probiotics derived from diverse sources, which remains relatively uncharted. In this context, this study aimed to assess the probiotic potentials of *Bacillus velezensis* D01Ca and *Bacillus siamensis* G01Bb, strains sourced from the gut of ducks and goats. Using two completely randomized experimental designs with 150-day-old broiler chickens, two distinct set-ups were implemented. In the first, broilers were subjected to either a control condition, a single dose of *B. velezensis* D01Ca at 2.4×10^7 cfu/ml, or its double dose. The second set-up followed a similar setup, but with *B. siamensis* G01Bb at 2.29×10^7 cfu/ml. Throughout the 42-day trial, all broilers consumed a commercial ration ad libitum and accessed water freely, with specific groups receiving the supplemented water based on the treatment. Results show that the feed intake of broilers remained unaffected by the probiotic supplementation, with no significant difference ($P \leq 0.05$). However, broilers in the supplemented groups exhibited a noticeable increase in body weight and body weight gain when compared to the control. The feed conversion ratio, crucially, was consistent across all test groups. Conclusively, our findings suggest that *B. velezensis* D01Ca and *B. siamensis* G01Bb hold promise as viable probiotics for

ARTICLE INFO

Article history:
Received: 03 February 2023
Accepted: 20 March 2023
Published: 22 September 2023

DOI: https://doi.org/10.47836/pjtas.46.4.02

E-mail addresses:
gaclirio@pup.edu.ph (Gary Antonio Lirio)
jamesjr.cerado@gmail.com (James Jr. Cerado)
jtb.esteban@iskolarngbayan.pup.edu.ph (Jenine Tricia Esteban)
jeffrey.ferrer.hh@gmail.com (Jeffery Adriano Ferrer)
claire.salvedia@msumain.edu.ph (Claire Salvedia)
* Corresponding author

ISSN: 1511-3701
e-ISSN: 2231-8542

broiler chickens, offering potential strides toward sustainable agricultural practices and enhanced food security.

Keywords: *Bacillus velezensis* D01Ca, *Bacillus siamensis* G01Bb, broiler chicken, growth performance, gut microbiota

INTRODUCTION

In recent years, animal production and consumption levels have rapidly increased due to the demand for animal protein. According to Hosain et al. (2021), this demand also denotes the changes in food production and feeding regimens, including increased antimicrobial use (AMU) in the livestock sector. Under intensive production systems to achieve high economic efficiency, chickens predominantly use antimicrobials to avoid stress, overcrowding, and unfavorable ambient conditions, ensuring good health. According to Elliott et al. (2017), the repeated misuse of antibiotics in food-producing animals is a key factor accelerating the emergence of drug-resistant microorganisms that has become a global public health challenge. Restrictions on the use of antimicrobials at sub-therapeutic concentrations in livestock due to the growing concerns of antimicrobial resistance (AMR) have prompted poultry researchers to look for a viable alternative.

Using growth promoters such as probiotics, prebiotics, symbiotics, organic acid, and bioactive compounds is currently being studied as an alternative to antibiotics. These are proven safe and have no negative impact on the environment, and are safe for livestock production, improved growth performance, and immunity (Callaway et al., 2008; Firth et al., 2019; Markowiak & Śliżewska, 2018). Various types of probiotics are being researched in the poultry industry to improve chicken performance. Boirivant and Strober (2007) define probiotics as viable and non-pathogenic microorganisms (bacteria and yeast) that can reach the intestines in sufficient numbers to confer benefits to the host. When probiotics are consumed in sufficient quantities, they will benefit the host by assisting digestion and nutrient absorption (Liu et al., 2009). Probiotics were initially used to prevent episodic diarrhea in poultry because they lessen intestinal salmonella and *Clostridium perfringens* (Bailey et al., 2000). However, Khan et al. (2007) found that probiotics also encouraged weight gain in broiler chickens, even in the absence of diarrheal outbreaks. Khaksefidi and Ghoorchi (2006) also reported that probiotic supplementation to broiler chickens has been shown to benefit feed intake, weight gain, and feed conversion ratio (FCR). Mountzouris et al. (2010) and Shabani et al. (2012) also reported similar observations.

Among the species of bacteria, the genus *Bacillus* is of particular interest as a probiotic. Based on the study conducted by Elshaghabee et al. (2017) and Liu et al. (2009), *Bacillus* spp. has been found to have high stability to the surrounding atmospheric conditions such as heat, gastric conditions, and moisture. Bailey et al. (2000) added that the ability of *Bacillus* to form spores ensures their stability and viability during feed manufacturing processes, storage,

and movement through the gastrointestinal tract, implying their suitability for adoption in the poultry industry (Bernardeau et al., 2017). The study by Bailey et al. (2000) reported that *Bacillus* probiotics positively influenced the feed intake, FCR, and body weight gain (BWG) of disease-challenged broiler chickens. The same results were also reported by Adhikari et al. (2019) and Roy et al. (2015). However, according to Mingmongkolchai and Panbangred (2018), the efficacy of probiotics may vary from one study to the other due to differences in *Bacillus* probiotics composition, dosage, duration of supplementation, and strain used as well as chicken's age and health status. The current study aims to evaluate *B. velezensis* D01Ca and *B. siamensis* G01Bb isolated from the gut of ducks and goats as probiotics for broiler chickens. Specifically, to evaluate if *B. velezensis* D01Ca and *B. siamensis* G01Bb will enhance the growth performance, such as the feed intake, BWG, and FCR of the broiler chickens.

MATERIALS AND METHODS

Isolation, Morphological, and Enzymatic Testing

Three mature female grazing pekin ducks (4–6 months old) and one mature upgraded native female goat (12 months old) were chosen as the source of the gut. These animals were grazed freely and exposed to environmental conditions ranging from 35–45ºC, where *Bacillus* spp. are predominant, as described by Garbeva et al. (2003). The animals were slaughtered following the slaughtering method described in the Bureau of Agriculture and Fisheries Standards (BAFS) (2015, 2017) for ducks and goats. The gut was extracted, homogenized, serially diluted to 10^{-2}, and subjected to heat shock at 85-90ºC for 10 min. The mixture was plated using trypticase soy agar (HiMedia, India) and incubated at 37ºC till the appearance of microbial colonies.

Colonies that appeared in plates were sub-cultured and modified through microscopy after a series of staining procedures. A total of 72 isolates were obtained from the guts of ducks and goats (36 bacterial isolates for each animal). Of these 72 isolates, only 30 were identified as *Bacillus* species (Table 1). Morphological identification of the isolates was based on Elliott et al. (2017). Further testing reveals that 25 of the 36 *Bacillus* species isolated from ducks were Gram-positive, with 20 endospore formers. At the same time, 31 Gram-positive and 19 endospore formers *Bacillus* species were identified from goats. The top *Bacillus* isolates were found to be all catalase positive.

Only 20 of the 31 pre-screened suspected *Bacillus* isolates passed the antibiotics and acid tolerance tests, indicating that only 20 can be tested for acid-bile tolerance (Table 2). All these strains were susceptible to ofloxacin (TM Media, India), and G01Ab was the most resistant to ofloxacin, followed by D02ha.

Twelve *Bacillus* strains from duck and goat isolates were tested for acid bile tolerance test (Figure 1).

Enzymatic activities were conducted on the top-performing *Bacillus* spp. from

duck and goat isolates. The procedure for protease was adopted from Vijayaraghavan and Vincent (2013), cellulase, lipase (Zarei et al., 2021), amylase (Abd-Elhalem et al., 2015), and chitinase (Xia et al., 2011). The summary of the enzymatic activity of the potentially viable *Bacillus* strains is presented in Figure 2. Based on the tests,

Table 1
Morphological and biochemical characterization of Bacillus *species*

Top performing isolates	Gram staining (+/-)	Endospore staining (+/-)	Catalase test (+/-)	Motility test (+/-)	Indole test (+/-)
D01Ca	+	+	+	+	-
D01Db	+	+	+	+	-
D01Gb	+	+	+	+	-
D02Aa	+	+	+	+	-
D02Hb	+	+	+	+	-
G01Bb	+	+	+	+	-
G01Hb	+	+	+	+	-
G02Aa	+	+	+	+	-
G02Ab	+	+	+	+	-
G02Ia	+	+	+	+	-

Note. + = Gram positive, endospore former, catalase positive, motile, and endole positive; - = Gram negative, non-endospore former, catalase negative, and endole negative

Table 2
Antibiotic assay of the selected Bacillus *isolates against ofloxacin (OF5)*

Antibiotic assay results			
Gut *Bacillus* isolates from duck	Average (mm)	Gut *Bacillus* isolates from goat	Average (mm)
D01Ca*	23.345±3.472	G01Ab	26.240±1.542
D01Da	26.575±0.728	G01Ba	29.425±0.516
D01Db*	22.640±0.325	G01Bb*	21.555±0.149
D01Ea*	24.070±1.697	G01Ca*	21.155±0.898
D01Eb*	23.710±0.778	G01Cb*	22.110±0.057
D01Gb*	24.755±0.431	G01Ga	24.980±0.679
D01Ha	25.505±2.128	G01Gb	26.255±1.195
D02Aa*	23.550±0.467	G01Ha	25.815±0.149
D02Ba*	22.775±0.078	G01Hb*	24.100±0.141
D02Ca*	22.815±0.205	G01Ia	25.945±0.035
D02Ea	26.085±0.092	G01Ib*	23.725±0.347
D02Ha*	21.535±0.035	G02Aa*	23.065±1.138
D02Hb*	24.025±0.035	G02Ab*	21.145±0.757
D02Ia*	24.275±0.389	G02Gb*	24.685±0.05
		G02Hb	25.880±0.085
		G02Ia*	24.445±0.361
		G02Ib	25.600±0.283

Note. * Denotes that the isolates were selected to continue further processes

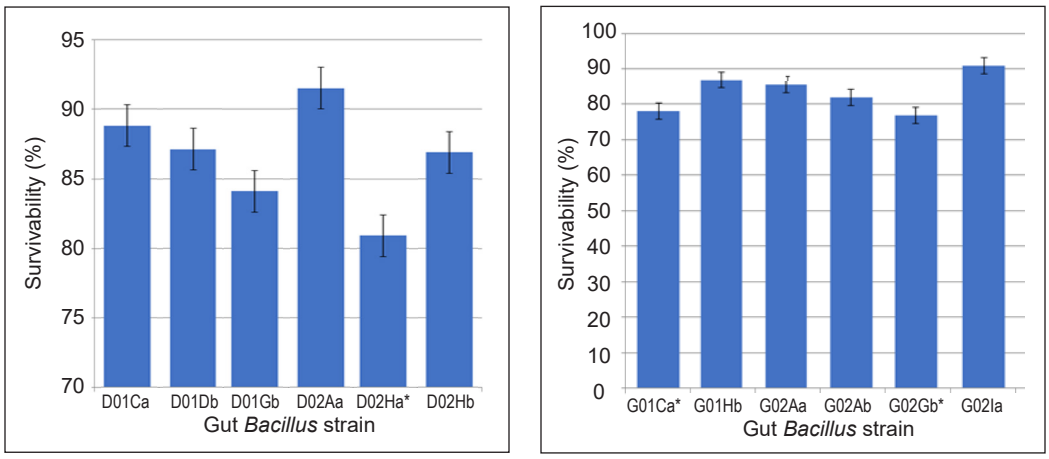

(a) (b)

Figure 1. Acid-bile tolerance test of the selected *Bacillus* strains that were isolated from duck (a) and goat (b), respectively

Note. * Denotes elimination form enzymatic assays

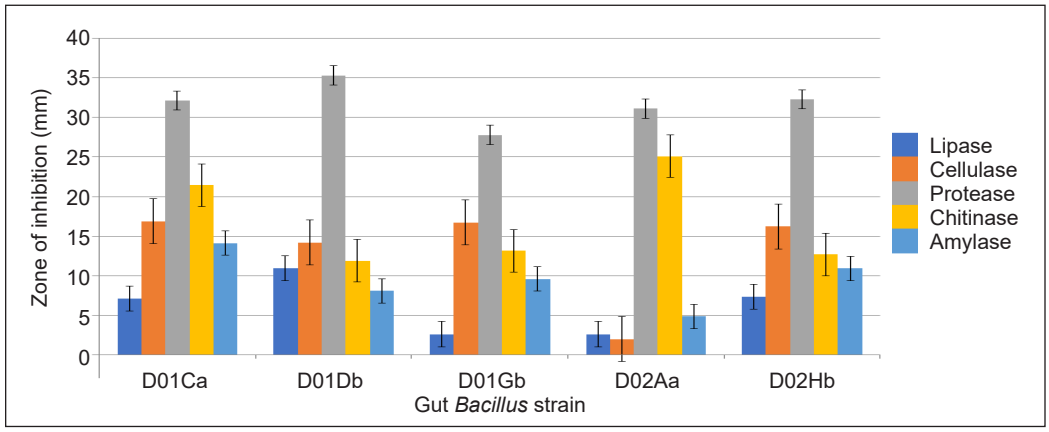

(a)

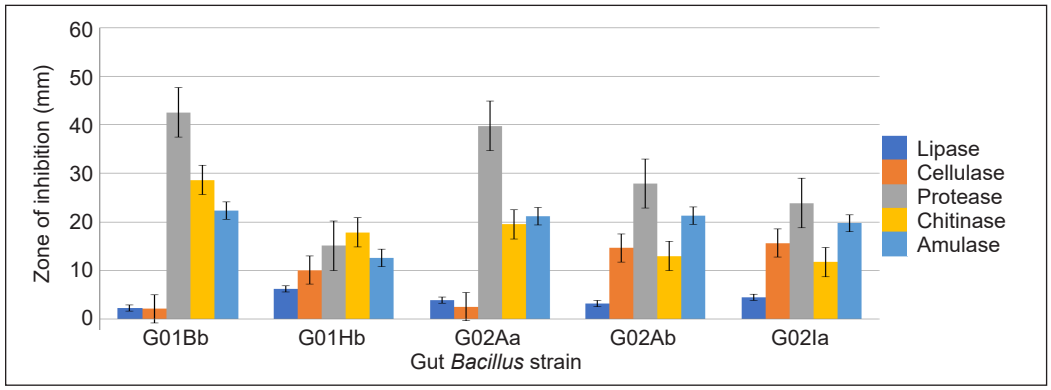

(b)

Figure 2. Enzymatic activity of the selected strain of *Bacillus* isolated from duck (a) and goat (b)

Bacillus strains D01Ca and G01Bb emerged as the top-performing isolates among both groups, with respective inhibitions of 18.332 and 17.938 mm.

Molecular Identification

Pure culture isolates were streaked on the appropriate agar and incubated at 30°C for 48 hr under aerobic conditions. The InstaGene Matrix Kit (Bio-Rad Laboratories, United Kingdom) was used for the DNA extraction according to the manufacturer's instructions. DNA purity was verified via a spectrophotometer after extraction and stored at -20°C (Olson & Morrow, 2012). Molecular identification was done in Macrogen (Korea). The sequence gathered was analyzed using Basic Local Alignment Search Tool (BLAST) software from National Center for Biotechnology Information (NCBI). Further confirmatory identification was done through the construction of a phylogenetic tree by the maximum-likelihood (ML) method and bootstrapped 10,000x for the confirmation of the identity of the isolated *Bacillus* to the nearest likely neighbor. D01Ca was confirmed and identified as *B. velezensis*; meanwhile, G01Bb diverged early from its group and was temporarily identified as *B. siamensis* G01Bb.

Animals and Experimental Design

One-hundred fifty (150) day-old Ross broiler chickens were randomly distributed into two experimental setups in a complete randomized design (CRD) with five replications per treatment containing five birds per replicate. SET A: T1—control (no probiotics), T2—single-dose *B. velezensis* D01Ca at 2.4×10^7 cfu/ml, T3—double-dose; SET B: T1—control (no probiotics), T2— single dose *B. siamensis* G01Bb at 2.29×10^7 cfu/ml; T3—double dose. The experiment was carried out for 42 days at the Center for Life Science Research Laboratory, Polytechnic University of the Philippines, Philippines, from February to April 2018.

Probiotic Preparation and Administration

Spore solution was prepared using the Arret-Kirshbaum Agar #2 (HiMedia, India) method adapted from Arret and Kirshbaum (1959). The single and double-dose concentration of the *B. velezensis* D01Ca and *B. siamensis* G01Bb was achieved using spectrophotometry (Spectronic 20D) for OD reading. Double dosage was achieved by adding a pure spore solution containing a single dosage in microtubules until the desired OD reading was doubled. After which, the pure spore solutions were added to 1 liter of sterilized water and provided to the broiler chickens daily for 42 days, according to treatments. Water is replaced daily or as needed to avoid contamination and disease outbreaks.

Experimental Diet

The broiler chickens were provided commercial feeds *ad libitum* throughout the experimental trial. Feed offered, including the leftover, were recorded. The feeds used were changed periodically based on their age group, emulating the practice of

poultry farmers. For a day-old to day-14, Chick Booster Mash™ (Philippines, GMP-1) was used; Broiler Starter Crumble™ (Philippines, GMP-2) on week 4, and Broiler Finisher Crumble™ (Philippines, GMP-3) on week 6.

Housing Preparation

An open-sided and wire mesh-sided poultry house was used. The house was cleaned and well-disinfected prior to the commencement of the experiment. A total of 15 pens were used, providing an average of 1.5 sq. ft. per bird as floor requirements. Each pen had one drinker and feeders to ensure ad libitum feeding. The temperature of the poultry house was properly monitored and maintained at 30–32ºC during brooding as recommended by Ketelaars (2005) and then decreased to 18–22ºC during the growing stage (Daghir et al., 2009).

Data Collection and Analysis

Body weight (BW) and body weight gain (BWG) was tabulated weekly to keep track of the broiler's growth performance following the protocol from Liu et al. (2009). Daily intake of feeds collated every seven days, BWG, and FCR were calculated using the following formula:

$$BWG = BW_{Wpresent} - BW_{Wprevious}$$

$$FCR = \frac{\text{Feed intake}}{\text{Weekly weight gain}}$$

The data gathered were analyzed statistically following the analysis of variance (ANOVA) run in SPSS (version 20) with homogeneity of variance tested using Levene's test. A significant difference between treatments was analyzed using the least significant difference (LSD) at $P \leq 0.05$.

RESULTS AND DISCUSSION

The weekly feed intake of the broiler chicken supplemented with *B. velezensis* D01Ca and *B. siamensis* G01Bb from two experimental setups is presented in Table 3. It was revealed that probiotic-treated groups from the two experimental setups had slightly elevated feed intake compared to the control groups, but based on ANOVA, these differences in feed intake were non-significant ($P \geq 0.05$).

Table 3
Mean weekly feed intake of broiler chickens supplemented with Bacillus velezensis *D01Ca* and B. siamensis *G01Bb (in grams)*

Week	*Bacillus velezensis* D01ca			*Bacillus siamensis* G01Bb		
	Control	Single dose	Double dose	Control	Single dose	Double dose
1	130.00±1.23	150.00±1.02	155.00±1.75	150.00±1.07	180.00±0.78	190.00±1.67
2	255.00±0.95	248.00±2.45	267.00±3.12	280.00±1.53	275.00±1.23	286.00±2.19
3	380.00±1.55	490.00±5.12	450.00±3.03	400.00±1.65	480.00±2.67	450.00±3.09
4	512.00±2.03	580.00±4.09	620.00±2.16	565.00±4.02	560.00±2.55	545.00±3.12
5	720.00±1.35	750.00±3.13	740.00±2.09	760.00±2.33	800.00±4.12	820.00±3.54
6	1,150.00 ±3.21	1285.00±2.43	1,300.00±4.08	1,120.00±7.06	1,345.00±5.32	1,260.00±5.09

Note. Means are non-significant at $P<0.05$

During the sixth week, broiler chickens supplemented with *Bacillus* species had a slightly elevated feed intake compared to the control groups in both experimental setups. However, based on ANOVA, no significant differences ($P \geq 0.05$) were noted between the treatments and the two experimental setups.

In the evaluation of the weekly body weights of the broiler chickens, a significant difference ($P \leq 0.05$) was observed between the treated groups compared to the control (Table 4). The body weight of the groups supplemented with *B. velezensis* D01Ca was heavier compared to the control during the fourth and sixth weeks of the experimental trial. The comparison between treatments revealed that a single dosage of *B. velezensis* D01Ca obtained a significant ($P \leq 0.05$) heavier body weight compared to the double doses and the control. The supplementation of *B. siamensis* G01Bb, on the other hand, also affected the body weights of the broiler chickens. Heavier body weight was also noted in broiler chickens supplemented with double doses of *B. siamensis* G01Bb compared to the single dose and the control during the fifth and the sixth weeks.

The body weight gain assessment revealed that groups supplemented with *B. velezensis* D01Ca and *B. siamensis* G01Bb obtained elevated weight gain compared to the control (Figure 3). This significant improvement in body weight gain from the treated groups ($P \leq 0.05$) was noted during the fourth week for *B. velezensis* D01Ca and during the third and fourth weeks for *B. siamensis* G01Bb. The body weight gain of broiler chickens supplemented with a single dose of *B. velezensis* D01Ca significantly obtained heavier body weight gain compared to the double dose and the control ($P \leq 0.05$) (Figure 3). The single dose and double doses of *B. siamensis* G01Bb significantly obtained heavier body weight gain during the third week of the experimental trial compared to the control ($P \leq 0.05$). However, during the fourth week of observation, a significant increase in body weight gain on the double dose of *B. siamensis* G01Bb was recorded compared to the single dose and the control ($P \leq 0.05$). Comparison between the two experimental setups revealed that the body weight gain of broiler chickens supplemented with *B.*

Table 4
Mean weekly body weights of broiler chickens supplemented with Bacillus velezensis D01Ca and *B. siamensis G01Bb (in grams)*

Week	*Bacillus velezensis* D01ca			*Bacillus siamensis* G01Bb		
	Control	Single dose	Double dose	Control	Single dose	Double dose
1	160.00±1.23	185.00±1.02	175.00±1.75	175.00±1.07	180.00±0.78	190.00±1.67
2	365.00±0.95	415.00±2.45	450.00±3.12	330.00±1.53	445.00±1.23	430.00±2.19
3	765.00±1.55	825.00±5.12	885.00±3.03	725.00±1.65	880.00±2.67	795.00±3.09
4	1,015.00±2.03^{b}	1,295.00±4.09^{a}	1,880.00±2.16^{a}	1,995.00±4.02^{a}	1,115.00±2.55^{a}	1,212.00±3.12^{a}
5	1,280.00±1.35^{b}	1,550.00±3.13^{a}	1,375.00±2.09^{b}	1,195.00±2.33^{c}	1,365.00±4.12^{b}	1,550.00±3.54^{a}
6	1,680.00±3.21^{b}	1,890.00±2.43^{a}	1,860.00±4.08^{a}	1,545.00±7.06^{b}	1,755.00±5.32^{b}	1,840.00±5.09^{a}

Note. ^{a,b,c} Mean within rows having different superscripts = Significant difference at $P \leq 0.05$

siamensis G01Bb significantly differs from the body weight gain of broiler chickens supplemented with *B. velezensis* D01Ca (Figure 3) ($P \leq 0.05$).

The FCR from the two experimental setups showed that treatments supplemented with both *B. velezensis* D01Ca and *B. siamensis* G01Bb obtained better FCR compared to the control, but these differences showed non-significant ($P \geq 0.05$) (Figure 4).

Though not significant, the single dose of *B. velezensis* D01Ca showed better FCR compared to the double dose. Furthermore, the single dose of *B. siamensis* G01Bb also showed better FCR compared to double those compared to the control.

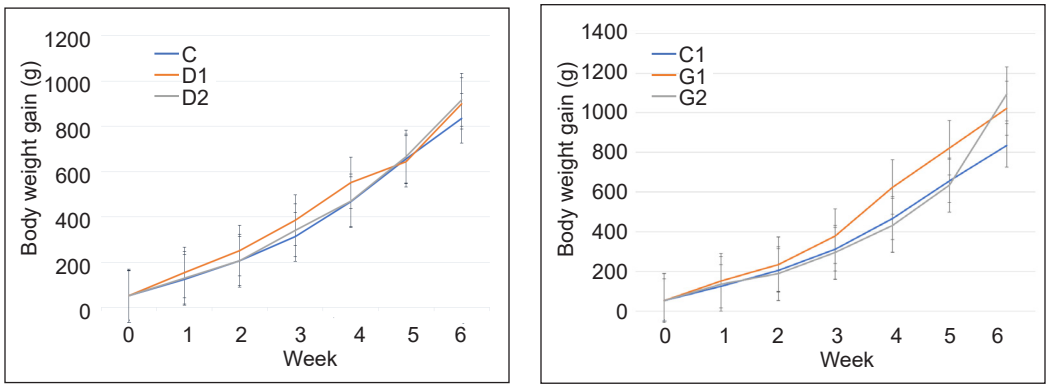

(a) (b)

Figure 3. Average weekly weight gain of broiler chickens supplemented with *Bacillus velezensis* D01Ca (a), and *B. siamensis* G01Bb (b). Body weight gain in broiler chickens supplemented with *B. siamensis* G01Bb differed significantly from those supplemented with *B. velezensis* D01Ca ($P \leq 0.05$)
Note. C = Without probiotic supplementation; D1 = Single dose supplementation with *B. velezensis* D01Ca; D2 = Double dose supplementation with *B. velezensis* D01Ca; G1 = Single dose supplementation with *B. siamensis* G01Bb; G2 = Double dose supplementation with *B. siamensis* G01Bb

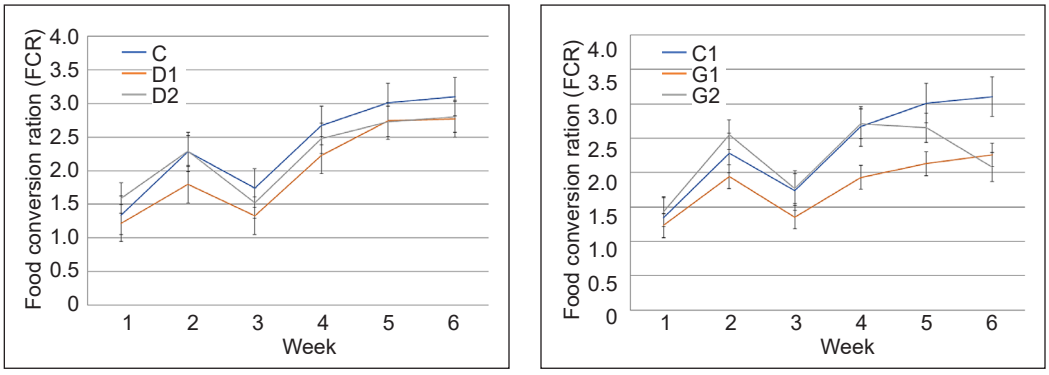

(a) (b)

Figure 4. Feed conversion ratio of broiler chickens supplemented with *Bacillus velezensis* D01Ca (a), and *B.* siamensis G01Bb (b). No significant difference at ($P<0.05$)
Note. C = Without probiotic supplementation; D1 = Single dose supplementation with *B. velezensis* D01Ca; D2 = Double dose supplementation with *B. velezensis* D01Ca; G1 = Single dose supplementation with *B. siamensis* G01Bb; G2 = Double dose supplementation with *B. siamensis* G01Bb

DISCUSSION

These findings indicated that supplementation with *B. velezensis* D01Ca and *B. siamensis* G01Bb improved broiler chicken performance, as evidenced by increased body weight and weight gain. The non-significant results observed from the broilers' feed intake in the two experimental setups is an indication that the supplementations of *B. velezensis* D01Ca and *B. siamensis* G01Bb either in a single dose or double doses maintain the feed intake of broiler chickens. This result contradicts the previous reports of Nunes et al. (2012) and Zulkifli et al. (2000), who observed increased feed intake in broiler chickens supplemented with *Bacillus* spp.

In the current study, supplementation of *B. velezensis* D01Ca and *B. siamensis* G01Bb resulted in increased body weight and weight gain compared to the control group. This result indicates that *B. velezensis* D01Ca and *B. siamensis* G01Bb survived and resisted instability inside the broiler chicken's gut, modulating better nutrient absorption and enhancing body weight and weight gain while maintaining feed intake. Guo et al. (2010) reiterated the importance of the survivability and instability of probiotics inside the intestine as it prevents pathogenic bacteria adhesion that leads to enhanced nutrient utilization and absorption. Khaksefidi and Ghoorchi (2006) similarly noted an improved weight gain with the supplementation of 50 mg/kg probiotics compared to the control. Recently, Liu et al. (2009) reported improved body weight and weight gain in broiler chickens supplemented with *Bacillus licheniformis* in drinking water. Several authors also reported the positive effect of supplementing probiotics on the body weight gain of broiler chickens (Awad et al., 2009; Timmerman et al., 2006; Zulkifli et al., 2000). Moreover, enhanced body weight and weight gain are noticeable in the single dose of *B. velezensis* D01Ca compared to the double dosage. At the same time, the double dose of *B. siamensis* G01Bb had elevated body weights and gain during the fourth and fifth weeks compared to the single dose. This variation could be attributed to the action of probiotics inside the GIT. Probiotic actions and effects inside the intestinal tract are affected by numerous factors such as strain type, probiotic doses, feed, and hygienic conditions (Patterson & Burkholder, 2003).

Though insignificant, better FCR was noticeable in treated groups compared to the control. Supplementation of *Bacillus* spp. has been reported to reduce *C. perfringens* (Jayaraman et al., 2013; Jeong & Kim, 2014; Teo & Tan, 2005), Enterobacteriaceae (Jeong & Kim, 2014), and *Campylobacter* (Guyard-Nicodème et al., 2016). The exclusion of these microorganisms inside the GIT of the broiler chicken promotes better health and absorption of essential nutrients from the feed (Ray et al., 2012). Aside from pathogenic exclusion, *Bacillus* spp. are known to produce different antioxidants (Latorre et al., 2016) and antimicrobials (Urdaci et al., 2004), such as bacteriocins and high amounts of peptides and polyketides. In the research study of Bailey et al. (2000), they observed that

Bacillus probiotics improved the FCR of broiler chickens. Kabir (2005) and Khan et al. (2007) also reported similar observations. Recently, Lin et al. (2017) and Zhang et al. (2011) well-documented the improvement of the performance of broiler chicken supplemented with *Bacillus* probiotics.

CONCLUSION

Bacillus velezensis D01Ca and *B. siamensis* G01Bb, either in single or double doses, did not affect broiler chicken feed intake. Moreover, the single and double doses of *B. velezensis* D01Ca and *B. siamensis* G01Bb improve broiler chicken body weights and weight gain during the fourth and sixth weeks of experimental trials. Therefore, both *B. velezensis* D01Ca and *B. siamensis* G01Bb can be safely used in broiler production as probiotics ensuring better performance during the finishing stage.

RECOMMENDATION

Further studies *in vivo* must be conducted to assess the efficacy of *B. velezensis* D01Ca and *B. siamensis* G01Bb as probiotic supplements for broiler chickens and other poultry animals, emphasizing dosage to the different health conditions challenges such as diarrhea, light stress, and heat stress.

ACKNOWLEDGMENTS

The researchers acknowledged the support provided by the Center for Natural Sciences and Resources Research, Research Institute for Science and Technology of the Polytechnic University of the Philippines for the shared laboratory facilities during the conduct of the study (Memo number: PUP-072018).

REFERENCES

Abd-Elhalem, B. T., El-Sawy, M., Gamal, R. F., & Abou-Taleb, K. A. (2015). Production of amylases from *Bacillus amyloliquefaciens* under submerged fermentation using some agro-industrial by-products. *Annals of Agricultural Sciences*, *60*(2), 193–202. https://doi.org/10.1016/j.aoas.2015.06.001

Adhikari, B., Hernandez-Patlan, D., Solis-Cruz, B., Kwon, Y. M., Arreguin, M. A., Latorre, J. D., Hernandez-Velasco, X., Hargis, B. M., & Tellez-Isaias, G. (2019). Evaluation of the antimicrobial and anti-inflammatory properties of *Bacillus*-DFM (Norum™) in broiler chickens infected with *Salmonella* Enteritidis. *Frontiers in Veterinary Science*, *6*, 282. https://doi.org/10.3389/fvets.2019.00282

Arret, B., & Kirshbaum, A. (1959). A rapid disc assay method for detecting penicillin in milk. *Journal of Milk Food Technol*ogy, *22*(11), 329-331. https://doi.org/10.4315/0022-2747-22.11.329

Awad, W. A., Ghareeb, K., Abdel-Raheem, S., & Böhm, J. (2009). Effects of dietary inclusion of probiotic and synbiotic on growth performance, organ weights, and intestinal histomorphology of broiler chickens. *Poultry Science*, *88*(1), 49–56. https://doi.org/10.3382/ps.2008-00244

Bailey, J. S, Stern, N. J., & Cox, N. A. (2000). Commercial field trial evaluation of mucosal starter culture to reduce *Salmonella* incidence in processed broiler carcasses. *Journal of Food Protection*, *63*(7), 867–870. https://doi.org/10.4315/0362-028x-63.7.867

Bernardeau, M., Lethtinen, M. J., Forssten, S. D., & Nurminen, P. (2017). Importance of the gastrointestinal life cycle of *Bacillus* for probiotic functionality. *Journal of Food Science*

and Technology, *54*, 2570-2584. https://doi.org/10.1007/s13197-017-2688-3

Boirivant, M., & Strober, W. (2007). The mechanism of action of probiotics. *Current Opinion in Gastroenterology*, *23*(6), 679–692. https://doi.org/10.1097/mog.0b013e3282f0cffc

Bureau of Agriculture and Fisheries Standards. (2015). *Code of slaughtering practices for goats*. BAFS. https://www.bafs.da.gov.ph/bafs_admin/admin_page/pns_file/2021-02-24-PNS%20BAFS%20164_2015%20Code%20of%20Slaughtering%20Practice%20for%20Goats.pdf

Bureau of Agriculture and Fisheries Standards. (2017). *Good animal husbandry practices for ducks*. BAFS. https://members.wto.org/crnattachments/2017/SPS/PHL/17_4779_00_e.pdf

Callaway, T. R., Edrington, T. S., Anderson, R. C., Harvey, R. B., Genovese, K. J., Kennedy, C. N., Venn, D. W., & Nisbet, D. J. (2008). Probiotics, prebiotics, and competitive exclusion for prophylaxis against bacterial disease. *Animal Health Research Reviews*, *9*(2), 217–225. https://doi.org/10.1017/s1466252308001540

Daghir, N. J., Beirut., & Lebanon. (2009). Nutritional strategies to reduce heat stress in broilers and broiler breeders. *Lohman Information*, *44*(1), 6-15.

Elliott, K. A., Kenny, C., & Madan, J. (2017). *A global treaty to reduce antimicrobial use in livestock*. Center for Global Development. http://www.cgdev.org/publication/global-treaty-reduce-antimicrobial-use-livestock

Elshaghabee, F. M. F., Rokana, N., Gulhane, R. D., Sharma, C., & Panwar, H. (2017). *Bacillus* as potential probiotics: Status, concerns, and future perspectives. *Frontiers in Microbiology*, *8*, 1490. https://doi.org/10.3389/fmicb.2017.01490

Firth, C. L., Käsbohrer, A., Egger-Danner, C., Fuchs, K., Pinior, B., Roch, F.-F., & Obritzhauser, W. (2019). Comparison of defined course doses (DCD_{vet}) for blanket and selective antimicrobial dry cow therapy on conventional and organic farms. *Animals*, *9*(10), 707. https://doi.org/10.3390/ani9100707

Garbeva, P., van Veen, J. A., & van Elsas, J. D. (2003). Predominant *Bacillus* spp. in agricultural soil under different management regimes detected via PCR-DGGE. *Microbial Ecology*, *45*, 302-316. https://doi.org/10.1007/s00248-002-2034-8

Guo, X.-H., Kim, J.-M., Nam, H.-M., Park, S.-Y., & Kim, J.-M. (2010). Screening lactic acid bacteria from swine origins for multistrain probiotics based on *in vitro* functional properties. *Anaerobe*, *16*(4), 321–326. https://doi.org/10.1016/j.anaerobe.2010.03.006

Guyard-Nicodème, M., Keita, A., Quesne, S., Amelot, M., Poezevara, T., Le Berre, B., Sánchez, J., Vesseur, P., Martín, Á., Medel, P., & Chemaly, M. (2016). Efficacy of feed additives against *Campylobacter* in live broilers during the entire rearing period. *Poultry Science*, *95*(2), 298–305. https://doi.org/10.3382/ps/pev303

Hosain, M. Z., Kabir, S. M. L., & Kamal, M. M. (2021). Antimicrobial uses for livestock production in developing countries. *Veterinary World*, *14*(1), 210–221. https://doi.org/10.14202/vetworld.2021.210-221

Jayaraman, S., Thangavel, G., Kurian, H., Mani, R., Mukkalil, R., & Chirakkal, H. (2013). *Bacillus subtilis* PB6 improves intestinal health of broiler chickens challenged with *Clostridium perfringens*-induced necrotic enteritis. *Poultry Science*, *92*(2), 370–374. https://doi.org/10.3382/ps.2012-02528

Jeong, J. S., & Kim, I. H. (2014). Effect of *Bacillus subtilis* C-3102 spores as a probiotic feed supplement on growth performance, noxious gas emission, and intestinal microflora in broilers. *Poultry Science*, *93*(12), 3097–3103. https://doi.org/10.3382/ps.2014-04086

Kabir, S., M. L., Rahman, M. M., Rahman, M. B., Hosain, M. Z., Akand, M. S. I., & Das, S. K. (2005). Viability of probiotics in balancing intestinal flora and effecting histological changes of crop and caecal tissues of broilers. *Biotechnology*, *4*(4), 325–330. https://doi.org/10.3923/biotech.2005.325.330

Ketelaars, E. H. (2005). *Lecture notes on chicken farming in warm climate zones* (1st ed.). Agromisa Foundation. https://survival.tcb13.com/Animal_Production/Poultry/Notes_On_Chicken_Farming_In_Warm_Climate_Zones_2005.pdf

Khaksefidi, A., & Ghoorchi, T. (2006). Effect of probiotic on performance and immunocompetence in broiler chicks. *The Journal of Poultry Science*, *43*(3), 296–300. https://doi.org/10.2141/jpsa.43.296

Khan, M., Raoult, D., Richet, H., Lepidi, H., & La Scola, B. (2007). Growth-promoting effects of single-dose intragastrically administered probiotics in chickens. *British Poultry Science*, *48*(6), 732–735. https://doi.org/10.1080/00071660701716222

Latorre, J. D., Hernandez-Velasco, X., Wolfenden, R. E., Vicente, J. L., Wolfenden, A. D., Menconi, A., Bielke, L. R., Hargis, B. M., & Tellez, G. (2016). Evaluation and selection of *Bacillus* species based on enzyme production, antimicrobial activity, and biofilm synthesis as direct-fed microbial candidates for poultry. *Frontiers in Veterinary Science*, *3*, 95. https://doi.org/10.3389/fvets.2016.00095

Lin, Y., Xu, S., Zeng, D., Ni, X., Zhou, M., Zeng, Y., Wang, H., Zhou, Y., Zhu, H., Pan, K., & Li, G. (2017). Disruption in the cecal microbiota of chickens challenged with *Clostridium perfringens* and other factors was alleviated by *Bacillus licheniformis* supplementation. *PLOS One*, *12*(8), e0182426. https://doi.org/10.1371/journal.pone.0182426

Liu, C.-H., Chiu, C.-S., Ho, P.-L., & Wang, S.-W. (2009). Improvement in the growth performance of white shrimp *Litopenaeus vannamei*, by a protease-producing probiotic, *Bacillus subtilis* E20, from natto. *Journal of Applied Microbiology*, *107*(3), 1031–1041. https://doi.org/10.1111/j.1365-2672.2009.04284.x

Markowiak, P., & Śliżewska, K. (2018). The role of probiotics, prebiotics, and synbiotics in animal nutrition. *Gut Pathogens*, *10*, 21. https://doi.org/10.1186/s13099-018-0250-0

Mingmongkolchai, S., & Panbangred, W. (2018). *Bacillus* probiotics: An alternative to antibiotics for livestock production. *Journal of Applied Microbiology*, *124*(6), 1334–1346. https://doi.org/10.1111/jam.13690

Mountzouris, K. C., Tsitrsikos, P., Palamidi, I., Arvaniti, A., Mohnl, M., Schatzmayr, G., & Fegeros, K. (2010). Effects of probiotic inclusion levels in broiler nutrition on growth performance, nutrient digestibility, plasma immunoglobulins, and cecal microflora composition. *Poultry Science*, *89*(1), 58–67. https://doi.org/10.3382/ps.2009-00308

Nunes, R. V., Scherer, C., Pozza, P. C., Eyng, C., Bruno, L. D. G., & Vieites, F. M. (2012). Use of probiotics to replace antibiotics for broilers. *Revista Brasileira de Zootecnia*, *41*(10), 2219–2224. https://doi.org/10.1590/s1516-35982012001000012

Olson, N. D., & Morrow, J. B. (2012). DNA extract characterization process for microbial detection methods development and validation. *BMC Research Notes*, *5*, 668. https://doi.org/10.1186/1756-0500-5-668

Patterson, J. A., & Burkholder, K. M. (2003). Application of prebiotics and probiotics in poultry production. *Poultry Science*, *82*(4), 627–631. https://doi.org/10.1093/ps/82.4.627

Ray, A. K., Ghosh, K., & Ringø, E. (2012). Enzyme-producing bacteria isolated from

fish gut: A review. *Aquaculture Nutrition*, *18*(5), 465–492. https://doi.org/10.1111/j.1365-2095.2012.00943.x

Roy, B. C, Chowdhury, S. D, & Kabir, S. L. (2015). Effects of feeding *Bacillus subtilis* to heat stressed broiler chickens with or without an antibiotic growth promoter. *Asian Journal of Medical Biological Research*, *1*(1), 80–88. https://doi.org/10.3329/ajmbr.v1i1.25502

Shabani, R., Nosrati, M., Javandel, F., & Kioumarsi, H. (2012). The effect of probiotics on carcass and internal organs of broilers. *Annals of Biological Research*, *3*(12), 5475-5477.

Teo, A. Y.-L., & Tan, H.-M. (2005). Inhibition of *Clostridium perfringens* by a novel strain of *Bacillus subtilis* isolated from the gastrointestinal tracts of healthy chickens. *Applied and Environmental Microbiology*, *71*(8), 4185–4190. https://doi.org/10.1128/aem.71.8.4185-4190.2005

Timmerman, H. M., Veldman, A., van den Elsen, E., Rombouts, F. M., & Beynen, A. C. (2006). Mortality and growth performance of broilers given drinking water supplemented with chicken-specific probiotics. *Poultry Science*, *85*(8), 1383–1388. https://doi.org/10.1093/ps/85.8.1383

Urdaci, M. C., Bressollier, P., & Pinchuk, I. (2004). *Bacillus clausii* probiotic strains: Antimicrobial and immunomodulatory activities. *Journal of Clinical Gastroenterology*, *38*, S86–S90. https://doi.org/10.1097/01.mcg.0000128925.06662.69

Vijayaraghavan, P., & Vincent, S. G. P. (2013). A simple method for the detection of protease activity on agar plates using bromocresolgreen dye. *Journal of Biochemical Technology*, *4*(3), 628-630.

Xia, J.-L., Xiong, J., Zhang, R.-Y., Liu, K.-K., Huang, B., & Nie, Z.-Y. (2011). Production of chitinase and its optimization from a novel isolate *Serratia marcescens* XJ-01. *Indian Journal of Microbiology*, *51*, 301–306. https://doi.org/10.1007/s12088-011-0139-9

Zarei, N., Golmakani, M.-T., Keramat, M., Majdinasab, M., & Karami, A. (2021). Process intensification for the autocatalytic esterification of citronellol using microwave radiation. *LWT*, *145*, 111358. https://doi.org/10.1016/j.lwt.2021.111358

Zhang, B., Yang, X., Guo, Y., & Long, F. (2011). Effects of dietary lipids and *Clostridium butyricumon* the performance and the digestive tract of broiler chickens. *Archives of Animal Nutrition*, *65*(4), 329–339. https://doi.org/10.1080/1745039x.2011.568274

Zulkifli, I., Abdullah, N., Azrin, N. M., & Ho, Y. W. (2000). Growth performance and immune response of two commercial broiler strains fed diets containing *Lactobacillus* cultures and oxytetracycline under heat stress conditions. *British Poultry Science*, *41*(5), 593–597. https://doi.org/10.1080/713654979

Pertanika J. Trop. Agri. Sci. 46 (4): 1111 - 1125 (2023)

PERTANIKA JOURNALS

TROPICAL AGRICULTURAL SCIENCE

Journal homepage: http://www.pertanika.upm.edu.my/

The Effect of Zinc and Iron Applications from Different Sources to Growth, Dry Matter, Zink and Ion Uptake by Lettuce (*Lactuca sativa*)

Dayang Safinah Nayan* and Suhaila Fouzi

Soil Science, Water and Fertilizer Research Centre, Malaysia Agriculture Research and Development Institute, 43400 Serdang, Selangor, Malaysia

ABSTRACT

Zinc (Zn) and iron (Fe) are among the micronutrients humans need. However, the main food sources in developing countries such as Malaysia have low micronutrients, making it insufficient to supply the minimum daily requirement. Foliar fertilization is one of the most effective and safe ways to enrich important micronutrients in plants. This study investigated variations in Zn and Fe sources to evaluate the effects of individual Zn and Fe foliar applications on growth, dry matter, and nutrient uptake by lettuce (*Lactuca sativa*). Based on the result, the application of Zn and Fe in the form of sulfate salt showed a lower toxicity effect in terms of growth and dry matter of plants than Fe and Zn in the form of ethylenediaminetetraacetic acid (EDTA). In terms of Zn uptake, it was found that there was a significant difference observed compared to the control, especially when 3 kg/ha Zn was applied, regardless of whether it was in the form of sulfate or EDTA. Furthermore, there was an increase in Fe uptake observed with increased Zn application. In contrast, the Fe application showed no difference in Fe intake compared to the control. It was found that there is a decrease in Zn uptake observed with increasing application of Fe rate. Sufficient Fe content is already available in the soil, and plants only take up what is needed for growth.

Keywords: Biofortification, foliar fertilizer, leaves number, plant height, toxicity

ARTICLE INFO

Article history:
Received: 20 March 2023
Accepted: 08 May 2023
Published: 22 September 2023

DOI: https://doi.org/10.47836/pjtas.46.4.03

E-mail addresses:
dayangsn@mardi.gov.my (Dayang Safinah Nayan)
suhailafauzi@mardi.gov.my (Suhaila Fouzi)
*Corresponding author

INTRODUCTION

Humans require at least 22 nutritional elements to maintain their health, and one of the ways is by consuming food sources that are rich in nutrients (Rugeles-Reyes et al., 2019). Zinc (Zn) and iron (Fe) are among the micronutrients needed by humans, with the daily requirement for adults at 4.3–6.6 and 10–29 mg/day, respectively (Ministry

ISSN: 1511-3701
e-ISSN: 2231-8542

of Health [MOH], 2017). Although it is important in human health, the main food sources in developing countries such as Malaysia have low micronutrients, making it insufficient to supply the minimum daily requirement.

Incidents of nutrient deficiency, especially Zn and Fe, are widely reported. It is estimated that 17.3% of the world population is at risk for inadequate Zn intake. The prevalence of insufficient Zn intake can range from 7.5% in high-income areas to 30% or more in areas of South and Southeast Asia, Sub-Saharan Africa, and Central America (Wessells et al., 2012). In Malaysia, iron deficiency or anemia was the main cause of years of living with disability among children and teenagers in 2013 (Kyu et al., 2016). Therefore, biofortification strategies have been developed to overcome this issue to enrich the food with essential nutrients for human nutritional needs.

In general, these beneficial elements are naturally present in the soil. Mineral elements found in the soil exist in many forms. Among them are free ions, ions adsorbed on mineral or organic surfaces, dissolved or precipitated compounds, or as part of the lattice structure contained in the soil biota. The paramount soil properties determining mineral accessibility are soil pH, redox conditions, cation exchange capacity, microbial activity, soil structure, organic matter, and water content. Although high concentrations of Fe and Zn occur in many soils, soil properties often limit the phytoavailability of these mineral elements (White et al., 2009).

Therefore, applying fertilizers to the leaves can enhance the uptake and transport of micronutrients to edible parts of the plant. Foliar fertilization is one of the most effective and safe ways to enrich important micronutrients in plants. Moreover, foliar spray with micronutrients is one of the ways to improve plant production, reduce the adverse effects on the environment, and need little infrastructure compared to other plant nutrient applications (Zahed et al., 2021).

Leaf application material can enter the inside of the leaf either through the penetration of the cuticle or through the stomatal pathway. However, the gap between beneficial and toxic concentrations is often quite close. Therefore, the right sources of raw materials aimed at the accumulation of micronutrients that contribute to human health must be obtained, and at the same time, do not negatively affect the plant's growth (Rouphael et al., 2018).

The concept of vegetable biofortification is very new in Malaysia. Currently, no health-beneficial nutrient-enriched products are available in the market, particularly for Zn and Fe. However, as time goes by, consumer awareness of health-based products is increasing. For consumers concerned about the need for these micronutrients, the easiest option available is buying synthetically processed supplement tablets. Therefore, producing vegetables enriched with these beneficial nutrients is very relevant nowadays. Apart from food safety issues, producing nutritious food that meets human dietary needs is also a challenge

in the agricultural sector. Urgent action is needed to overcome this issue, and vegetable biofortification is seen as the strategic way to enhance micronutrients in the edible portion of crops.

Many factors need to be considered to develop a vegetable biofortification program. Biofortification strategies depend on a number of factors, such as the chemical form, application rate, environmental conditions, growth stage, and plant types. Loose leaf lettuce (*Lactuca sativa*) was chosen in this study because lettuce is among the most consumed leafy vegetables in Malaysia. Based on the planted area, lettuce is among the major vegetables produced in Malaysia. There is an area of 4,728.23 ha of lettuce planted in Malaysia, producing 75,546.04 metric tons in 2021 (Department of Agriculture [DOA], 2021).

Many biofortification studies on lettuce have been conducted abroad and indirectly show its potential to be developed as a functional food. However, no study has been done on the effect of using different Zn and Fe raw materials on the biofortification of lettuce in Malaysia. Identifying raw materials for vegetable biofortification is the first thing that needs to be studied. Hence, variations in the source of Zn and Fe raw materials were investigated in this study to evaluate the effects of individual Zn and Fe foliar application on plant growth, i.e., plant height and leaves number of loose-leaf lettuce (*L. sativa*). In addition, the effect on plant dry weight and plant uptake of Zn and Fe was also investigated. The findings of this study are the identification of suitable raw materials for salad biofortification with Zn and Fe without causing a reduction in yield and crop quality.

MATERIALS AND METHODS

Glasshouse Experiment

A glasshouse experiment was conducted in Serdang, Selangor, Malaysia. The soil used for the glasshouse experiments had not been fertilized before; therefore, residual effects from previous fertilizer applications in the soil are assumed to be absent. The initial properties of the soil used for the glasshouse experiment are shown in Table 1.

Table 1
Initial chemical properties of the soil media used in the glasshouse experiment

Parameters	
pH (H_2O)	5.6 ± 0.04
Electrical conductivity (µS/cm)	219 ± 13.04
Cation exchange capacity ($cmol_{(+)}$/kg)	6.08 ± 0.26
Exchangeable bases ($cmol_{(+)}$/kg)	
K	0.44 ± 0.03
Ca	3.22 ± 0.20
Mg	0.06 ± 0.04
Na	1.02 ± 0.05

Table 1 *(Continue)*

Parameters		
Carbon (%)		1.05 ± 0.05
Nutrient concentration (%)		
	N (%)	0.11 ± 0.01
	P (%)	0.05 ± 0.002
	K (%)	0.40 ± 0.02
	Fe (%)	1.92 ± 0.24
	Zn (mg/kg)	27.06 ± 1.65 (Zarcinas et al., 2004—Mean Zn concentration: 38 mg/kg)

Note. Means (± standard error)

Experimental setups for Zn and Fe were done separately, as Zn and Fe were applied individually. For each setup, the experimental layout was in factorial (2 x 4) randomized complete block design (RCBD). Eight treatments with three replications totaled 24 planting boxes (50 cm x 20 cm). Each treatment received the same amount of 15–15–15 fertilizer (YaraMila™, Malaysia), which was applied to the soil equivalent to a rate of 500 kg/ha. In each setup, two different raw materials were tested: zinc sulfate ($ZnSO_4$) and Zn-EDTA at 0, 0.5, 1.5, and 3.0 kg/ha Zn, respectively. Meanwhile, iron sulfate ($FeSO_4$) and Fe-EDTA were applied at rates 0, 0.5, 1.0, and 2.0 kg/ha Fe, respectively.

Lettuce seeds are sown in seedling trays and transferred to planting boxes 10 days after sowing. The planting distance between plants is 10 cm, with five plants per plant box. Zinc and iron solutions were manually sprayed on the leaf surface according to treatment 20 days after planting. The amount of Zn and Fe sprayed is calculated based on the pot area for 5 plants. Due to the very small amounts of Zn and Fe, a solution with a concentration of 1,000 mg/L Zn and 1,000 mg/L Fe was prepared. For the Zn setup, the amount sprayed was 8, 24, and 48 ml/pot. Meanwhile, the amount sprayed for Fe was 8, 16, and 32 ml/pot.

The effect of Zn and Fe application on growth, i.e., plant height and the number of leaves, was recorded 30 days after planting. Plant height measurement begins from the base of the stem (at the soil surface) to the highest part of the plant by supporting the stem if needed without lifting or extending the leaves. Visible leaves number was counted, including the new leaves. Each plant's height and leaf number were measured and recorded as an average for each pot.

Dry Matter and Nutrient Analysis

At 45 days after sowing, five plant samples from each replicate of each treatment were harvested. Due to the small plant size and insufficient samples for analysis, five plants from each pot were composited to become

one sample. Plant samples were washed in the laboratory and divided into roots and upper parts. The plant samples were dried at 60°C until a constant weight was obtained. Then, the dried sample was weighed to determine its dry mass before being ground into a fine powder.

The dried plant sample was digested with nitric acid at 110°C for 2 hr or until the yellow fumes disappeared and the sample solution became clear. After cooling, hydrochloric acid was added, and digestion was continued for half an hour or so until a clear solution was obtained. The sample was then diluted to 100 ml with distilled water before determining Zn and Fe was performed using inductively coupled plasma optical emission spectrometry (ICP-OES, Thermo Fisher Scientific, USA). Nutrient uptake by plants is calculated by multiplying the nutrient concentration by the dry weight of the plant part.

Statistical Analysis

Data on plant height, number of leaves, dry matter, and nutrient uptake of lettuce were analyzed by two-factor analysis of variance (ANOVA), i.e., by making raw material and application rate as fixed factors affecting all the parameters mentioned above. Differences between treatment means were tested using Tukey's honestly significant difference (HSD) at $p \leq 0.05$ significance level. All data were analyzed using the SAS Statistical Analysis System (SAS version 9.4).

RESULTS AND DISCUSSION

Effect of Zinc Fertilization on Plant Height and Leaves Number of Lettuces

Foliar Zn application is an effective way to increase Zn concentration in food crops. Zinc sulfate is the inorganic form often used as a soil-applied Zn fertilizer, while the chelating source is Zn-EDTA (Doolette et al., 2018). However, to develop a more efficient foliar Zn fertilizer, information on the appropriate raw material and its effect on plant growth needs to be known in depth. The effect of Zn fertilization on plant height and leaves number of lettuces is shown in Table 2. Based on the table, there is an interaction between the raw material of Zn used and its rates on plant height and leaves number of lettuces. Hence, the plant height and leaves number of lettuces sorted by raw material of Zn used are presented in Figure 1.

Based on Figure 1, no significant difference was observed in plant height and the number of lettuces when the $ZnSO_4$-treated and untreated plants were compared. This result shows that $ZnSO_4$ might not affect plant height and the number of lettuce leaves. Zinc is an essential plant nutrient that has a vast effect if it is deficient in plants. However, this experiment was conducted in non-problematic conditions where the plant might have accumulated a somewhat satisfactory concentration of Zn from the soil; therefore, the external application of $ZnSO_4$ through foliar might not affect plant height and leaves number of lettuces significantly. Similar findings were also observed in the study by Munirah et al. (2015).

Table 2
The number of plant heights and leaves of biofortified lettuce with Zn

Treatment	Plant height	Leaves number
Raw material, n = 12		
$ZnSO_4$	26.25 ± 1.07 a	29.92 ± 1.86 a
Zn-EDTA	18.67 ± 2.08 b	21.58 ± 3.39 b
Zn rates (kg/ha); n = 6		
0	24.33 ± 1.03 a	30.17 ± 3.20 a
0.5	23.83 ± 1.87 a	30.67 ± 2.01 a
1.5	21.33 ± 2.20 a	23.83 ± 1.49 ab
3.0	20.33 ± 4.90 a	18.33 ± 6.53 b
Significance level		
Raw material	**	**
Zn rates	ns	**
Raw material x Zn rates	*	***
Mean	22.46	25.75
CV	21.83	21.21

Note. Means (± standard error) with different letters are significantly different ($p \leq 0.05$) using Tukey's honestly significant difference (HSD) test; * $p \leq 0.05$; ** $p \leq 0.01$; *** $p \leq 0.001$; ns = Not significant

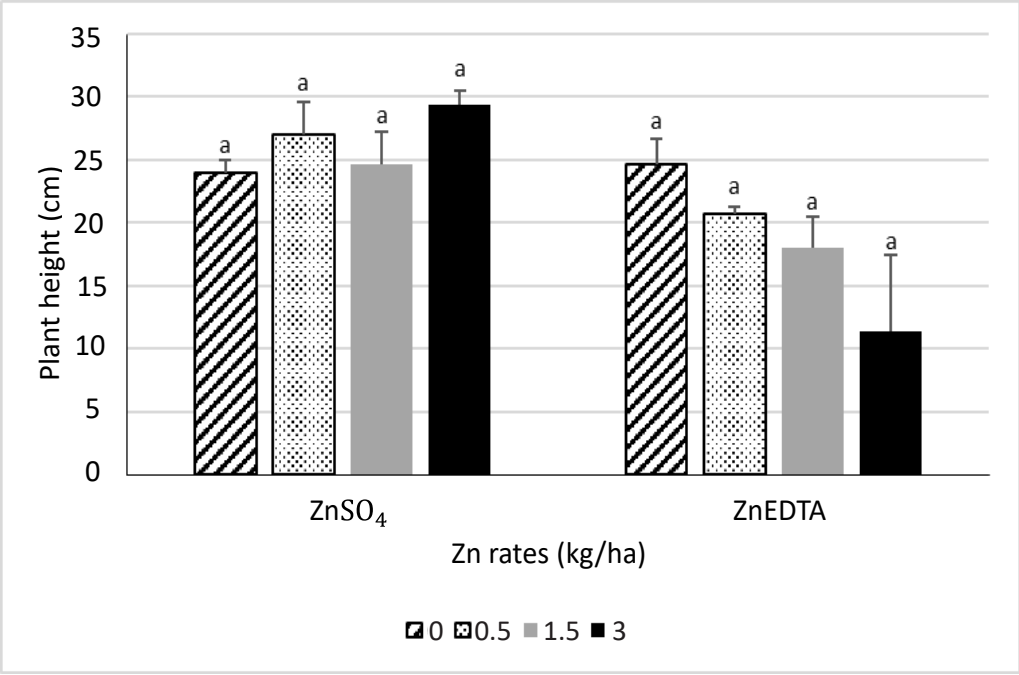

(a)

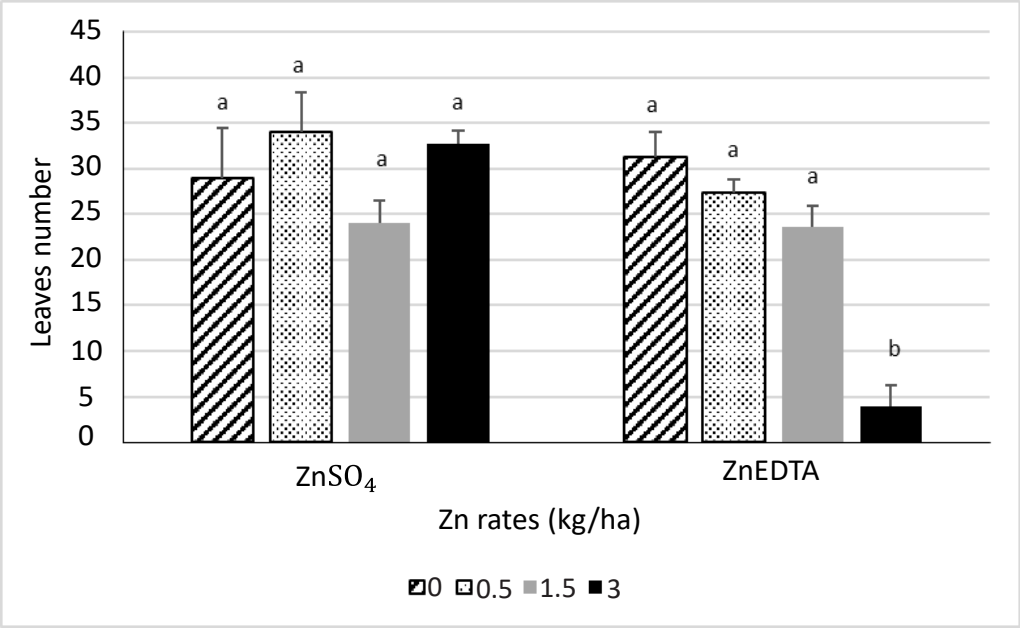

(b)

Figure 1. Plant height (a) and leaves number (b) of lettuces sorted by Zn raw material
Note. Means with different letters for each raw material are significantly different ($p \leq 0.05$) using Tukey's honestly significant difference (HSD) test

No significant difference was observed in plant height applied with various rates of Zn-EDTA; however, leaf numbers had reduced significantly when 3 kg/ha Zn-EDTA was applied as compared to other treatments. According to Vadlamudi et al. (2020), Zn will become highly toxic to plants when it reaches a concentration of 200 ppm. Symptoms shown are smaller leaf size, green disease on new leaves, stunted growth of the entire plant, and reduced root growth. In addition, a high intake of Zn also affects the intake of other nutrients such as P, Fe, and Mn, resulting in plant structure deficiencies.

Effect of Fe Fertilization on Plant Height and Leaves Number of Lettuces

Iron is the third most limiting nutrient for plant uptake and plant metabolism, and this is due to its low solubility when in the oxidized ferric form and aerobic environments. Symptoms of Fe deficiency that can be seen in plants are interveinal chlorosis on young leaves and stunted root growth (Rout et al., 2015). The effect of Fe fertilization on plant height and leaf number is shown in Table 3. There is an interaction between the raw material of Fe used and its rates on plant height and leaves number of lettuces. Hence, the plant height and leaves number of lettuces sorted by raw material

of Fe used are presented in Figure 2. No significant difference was observed in plant height and the number of lettuces applied with various rates of $FeSO_4$. This result shows that $FeSO_4$ fertilization might not affect plant height and leaves the number of lettuces.

Iron deficient symptoms do not happen to plants without Fe foliar application, which means its effect on growth cannot be seen significantly if sufficient Fe content is already available. According to El-Jendoubi et al. (2014), Fe fertilization on plants will re-green the leaves and increase biochemical and metabolic compounds in the leaves. Meanwhile, with Fe-EDTA application, plant height and leaves number reduced significantly when 2 kg/ha Fe was applied compared to the control (0 kg/ha Fe). Iron is an important nutrient for plants that functions to receive and donate electrons in the electron transport chain for photosynthesis and respiration. However, if iron accumulates at high levels, it becomes toxic and acts as a catalyst through the Fenton reaction to produce hydroxyl radicals, which can cause damage to lipids, proteins, and DNA (Connolly & Guerinot, 2002). It is found that tissue Fe concentration ranges between 500 and 5,000 mg/kg will cause yield losses between 40 to 100% (Zahra et al., 2021).

Table 3
The number of plant heights and leaves of biofortified lettuce with Fe

Treatment	Plant height	Leaves number
Raw material, n = 12		
$FeSO_4$	25.79 ± 0.78 a	26.17 ± 1.27 a
Fe-EDTA	16.42 ± 2.58 b	13.75 ± 2.41 b
Fe rates (kg/ha); n = 6		
0	25.67 ± 1.47 a	26.83 ± 1.49 a
0.5	23.00 ± 2.07 a	19.50 ± 2.99 b
1.0	20.75 ± 2.24 ab	19.67 ± 2.85 b
2.0	15.00 ± 5.07 b	13.83 ± 5.21 b
Significance level		
Raw material	***	***
Fe rates	**	***
Raw material x Fe rates	**	*
Mean	21.10	19.96
CV	18.77	17.91

Note. Means (± standard error) with different letters are significantly different ($p \leq 0.05$) using Tukey's honestly significant difference (HSD) test; * $p \leq 0.05$; ** $p \leq 0.01$; *** $p \leq 0.001$; ns = Not significant

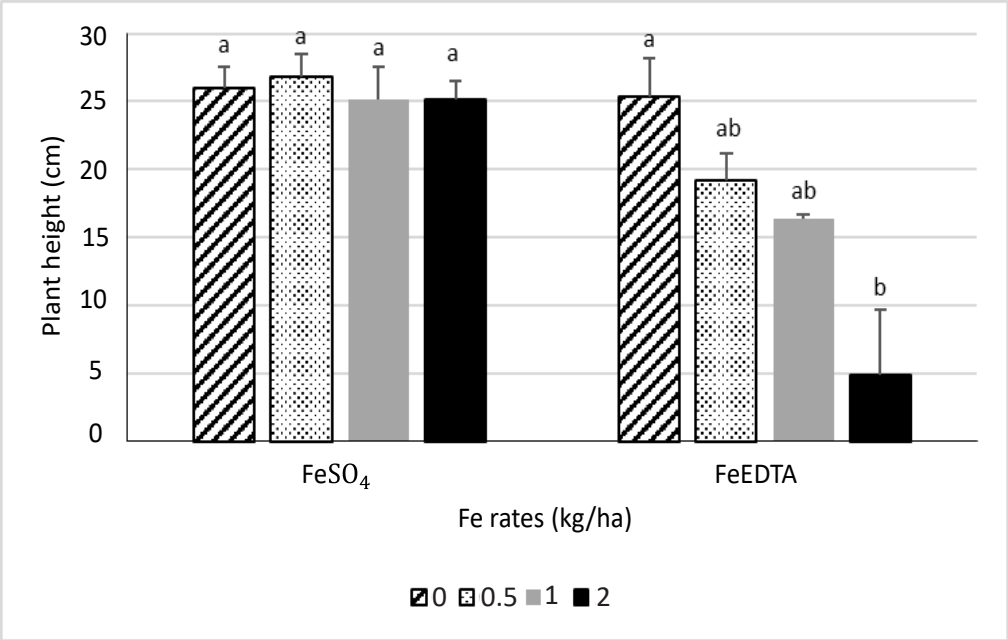

(a)

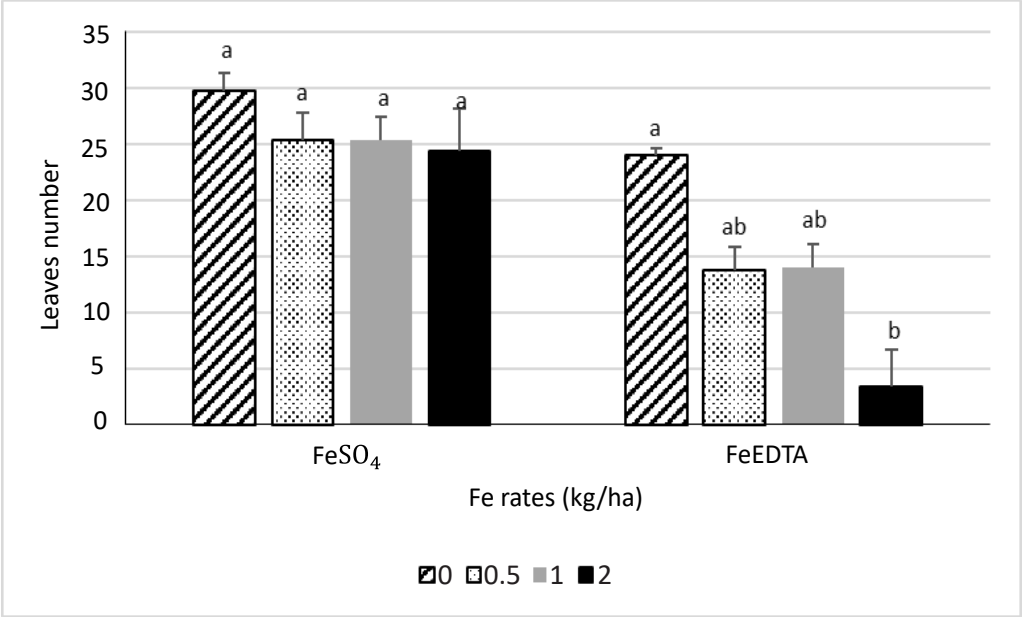

(b)

Figure 2. Plant height and leaves number of lettuces sorted by Fe raw material
Note. Means with different letters for each raw material are significantly different ($p \leq 0.05$) using Tukey's honestly significant difference (HSD) test

Dry Matter, Zn, and Fe Uptake in Leaves of Zn Biofortified Lettuces

Zinc is essential for plant metabolism, as it plays the main role in chloroplast development, protein synthesis, and metabolism of carbohydrates, lipids, and nucleic acids (Buturi et al., 2021). Results from the glasshouse study show that the raw materials at different levels of Zn rates affected the dry matter of lettuce. As shown in Table 4, there is an interaction between raw materials and Zn rates. Hence, the dry weights of lettuce sorted by raw material are presented in Figure 3.

Based on Figure 3, no significant difference was observed among the treatments when $ZnSO_4$ was applied at 0–3 kg/ha Zn. In contrast to Zn-EDTA, significant differences between treatments were observed. Particularly between control (without Zn fertilization) and Zn at 3 kg/ha. Increasing Zn-EDTA rates reduced the dry matter of lettuce. The Zn concentration in plant samples that received 3 kg/ha Zn as Zn-EDTA was between 503.2–831.5 ppm. Compared with the same rate as $ZnSO_4$, the recorded Zn concentration was only between 234.9–354.4 ppm. A high concentration of Zn has affected the growth of the plants, thus giving a lower yield. As stated in Rugeles-Reyes et al. (2019), the majority of plants showed reduced yield when foliar

Table 4
Dry matter, zinc, and iron uptake in Zn biofortified lettuce

Treatment	Dry weight (g/5 plants)	Zinc uptake (mg/5 plants)	Iron uptake (mg/5 plants)
Raw material, n = 12			
$ZnSO_4$	35.52 a	6.74 a	34.64 a
Zn-EDTA	26.39 b	5.98 a	36.00 a
Zn rates (kg/ha); n = 6			
0	33.15 a	2.22 c	24.80 a
0.5	34.38 a	4.60 bc	35.81 a
1.5	28.55 b	6.98 b	38.71 a
3.0	27.73 b	11.64 a	41.97 a
Significance level			
Raw material	***	ns	ns
Zn rates	**	***	ns
Raw material x Zn rates	***	ns	ns
Mean	30.95	6.36	35.32
CV	8.296	24.13	57.81

Note. Means (± standard error) with different letters are significantly different ($p \leq 0.05$) using Tukey's honestly significant difference (HSD) test; * $p \leq 0.05$; ** $p \leq 0.01$; *** $p \leq 0.001$; ns = Not significant

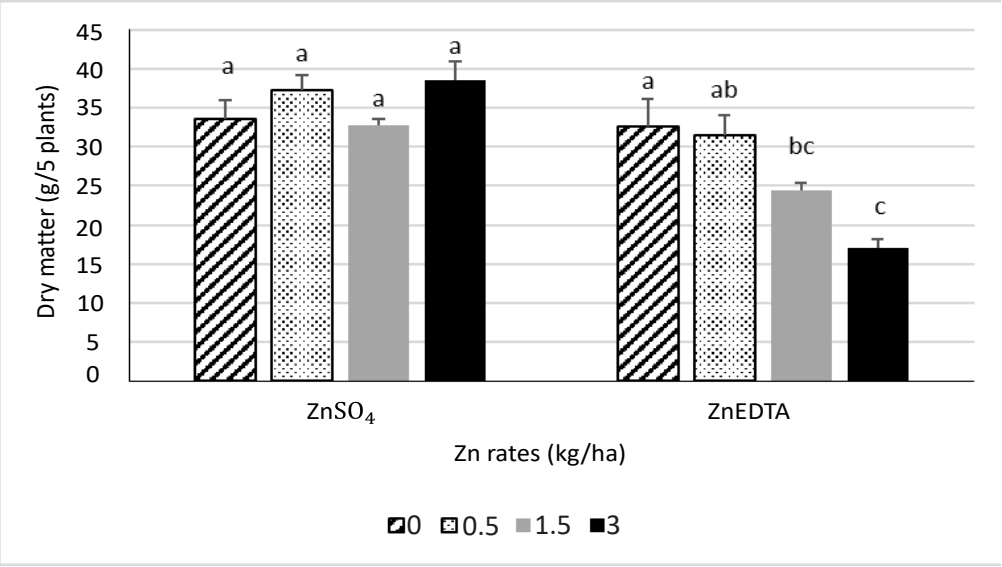

Figure 3. Dry matter of leaves of Zn biofortified lettuce sorted by Zn raw material
Note. Means with different letters for each raw material are significantly different ($p \leq 0.05$) using Tukey's honestly significant difference (HSD) test

Zn concentration was higher than 100 ppm. As well as what is stated by Buturi et al. (2021), phytotoxicity symptoms are usually apparent at leaf Zn concentrations higher than 100-700 ppm, where the symptoms shown are growth and yield reduction, leaf chlorosis and necrosis, restricted stomatal conductance, and carbon dioxide (CO_2) fixation, and also changes in chlorophyll structure and concentration. This study found that lettuce has a high Zn tolerance of more than 300 ppm, so it is more appropriate for studies of Zn biofortification.

Apart from dry weight, plants biofortified with Zn were also tested in terms of Zn and Fe uptake. Plants have different abilities to accumulate nutrients in their tissues, and the Zn hyperaccumulation characteristic is mostly seen in Brassicaceae members until many biofortification studies have been done on leafy brassicas. Meanwhile, for non-brassica, higher Zn susceptibility was also found in hydroponically grown lettuce by Barrameda-Medina et al. (2014), where Zn concentration in the leaves increased by 270% compared to the control; however, there was a decrease in biomass. Based on Table 4, there is no interaction between the raw material of Zn used and its rates on Zn and Fe uptake of lettuce. Lettuce applied with $ZnSO_4$ and Zn-EDTA shows no difference in Zn and Fe uptake. According to Buturi et al. (2021), biofortification of Zn, mainly in the form of sulfate, increases the content of Zn in vegetables; however, no differences were observed in this study.

In terms of rates, lettuce treated with 3 kg/ha Zn showed higher Zn uptake and differed significantly from the control. It is shown by the significant difference in Zn concentration between the two, which is 57.8–80.7 ppm for the control, while

234.9–831.5 ppm for those treated with 3 kg/ha Zn. In contrast to Fe uptake, no significant differences were observed at all Zn rates applied. According to Zou et al. (2019), foliar Zn application increased Fe concentrations in grain, and foliar Zn spray probably caused the formation of Zn binding compounds in grain, which most likely act as a sink for Fe transport and storage. Although Fe uptake in lettuce is seen to increase with the increasing Zn rates, no statistically significant difference was observed in this study, which shows that the application of Zn to plants does not affect the uptake of Fe in lettuce.

Dry Matter, Zn, and Fe Uptake in Leaves of Fe Biofortified Lettuces

The concentration of Fe in the soil often exceeds the plant's needs, which is between 20-40 mg/kg; however, not all amount is available for plant nutrition (Buturi et al., 2021). Iron deficiency symptoms in plants always occur in overly limed or alkaline soil, where the observed symptoms are interveinal chlorosis in younger leaves (Uchida, 2000). Results from the glasshouse study show that the dry matter of lettuce was not affected by the raw materials at different levels of Fe rates because there is no interaction between the raw material of Fe used and its rates on the dry matter of lettuce (Table 5). Lettuce with $FeSO_4$ generally shows higher dry matter than plants treated with Fe-EDTA. However, in terms of Fe rates, it was found that lower dry weights were obtained for all Fe rates compared to controls.

Table 5
Dry matter, zinc, and iron uptake in Fe-biofortified lettuce

Treatment	Dry weight (g/5 plants)	Zinc uptake (mg/5 plants)	Iron uptake (mg/5 plants)
Raw material, n = 12			
$FeSO_4$	32.63 a	2.08 a	39.30 a
Fe-EDTA	19.00 b	1.07 b	26.35 a
Fe rates (kg/ha); n = 6			
0	34.25 a	2.22 a	23.47 a
0.5	28.78 ab	1.48 ab	35.30 a
1.0	22.18 b	1.33 b	35.13 a
2.0	18.05 b	1.25 b	37.40 a
Significance level			
Raw material	***	***	ns
Fe rates	**	*	ns
Raw material x Fe	ns	ns	ns
Mean	25.82	1.57	32.83
CV	26.50	28.47	62.60

Note. Means (± standard error) with different letters are significantly different ($p \leq 0.05$) using Tukey's Honestly Significant Difference (HSD) test; * $p \leq 0.05$; ** $p \leq 0.01$; *** $p \leq 0.001$; ns = Not significant

Significant differences with control were observed when Fe was applied at 1 and 2 kg/ha Fe. Although Fe is an important nutrient for plants, excessive Fe uptake by plant cells will result in toxicity and a reduction in crop yield. Various symptoms can be associated with high Fe in plants, including stunted growth, reduced leaf size, brown or black spots or necrotic spots on leaves, blackened leaf tips and stem bases, hardening of stems, stunted roots, lack of root branching, formation precipitate on the roots (Rout et al., 2015).

In terms of Zn and Fe uptake, there was no interaction between the raw material of Fe used and the rates of Zn and Fe uptake by lettuce. Based on Table 5, Zn uptake by plants treated with $FeSO_4$ was significantly higher than plants treated with Fe-EDTA. It was expected because the higher plant weight when $FeSO_4$ was applied caused it to accumulate more nutrients, including Zn. However, it was found that the increasing rate of Fe fertilization resulted in lower Zn uptake significantly. It happened maybe due to the reduced plant size based on the dry weight data in Table 5, so the accumulation is also low. However, this is different when Zn is applied, where Fe uptake increases with increasing Zn application rate, although there is a decrease in plant size. The application of Fe to lettuce does not have a synergistic effect on Zn uptake.

For Fe intake, no significant difference was seen regardless of the Fe raw material used. Similarly, for Fe rates, no difference was seen in Fe uptake by lettuce on all Fe treatments applied. The same explanation for the effect of Fe use on plant height and the number of leaves also applies to this, where sufficient Fe content is already available in the soil; therefore, the plant only takes what it needs for growth. According to Hochmuth (2011), Fe uptake depends on the plant's ability to convert Fe^{3+} to Fe^{2+} and separate it from complex compounds or chelates. This reduction occurs on the cell surface, and the electrons in the cell are used. The same thing also happens at the root tip, where Fe absorption occurs a lot; that is, Fe chelated in the soil solution moves to the root through mass flow or diffusion. Fe is reduced and removed from chelating molecules in roots and moves through the cell membrane. However, Fe uptake can be disturbed if there are other cations in the soil solution, such as manganese (Mn) and calcium (Ca).

CONCLUSION

In the biofortification program, value over volume is preferred. However, the effect of biofortification on growth still needs to be emphasized so that the plant yield obtained is not lower than conventional cultivation methods. Applying Zn and Fe in the form of sulfate salt showed a lower toxicity effect in terms of growth and dry matter of plants than Fe and Zn in the form of EDTA. Although the beneficial effects of applying $ZnSO_4$ and $FeSO_4$ on lettuce plant height and leaf number are not seen, they do not adversely affect crop growth and yield. Perhaps the beneficial effects on plant growth and yield may be observed in plants grown in Zn and Fe-deficient conditions.

In terms of Zn uptake, it was found that there was a significant difference observed compared to the control, especially when 3 kg/ha Zn was applied, regardless of whether it was in the form of sulfate or EDTA. Furthermore, there was an increase in Fe uptake observed with increased Zn application compared to the control. In contrast to Fe, the Fe application did not show any difference in Fe intake compared to the control. It was found that there is a decrease in Zn uptake observed with increasing application of Fe rate. It is believed that sufficient Fe content is already available in the soil, and plants only take up what is needed for growth.

ACKNOWLEDGEMENTS

The authors are gratefully thank the Malaysia Agriculture Research and Development Institute (MARDI) for providing financial support under the 12th Malaysia Plan Development Project (RMK12) (P-RP515). The assistance rendered by Nurul Husna Baharuddin, Ismail Mohd, and other laboratory staff while conducting this study is greatly appreciated.

REFERENCES

Barrameda-Medina, Y., Montesinos-Pereira, D., Romero, L., Ruiz, J. M., & Blasco, B. (2014). Comparative study of the toxic effect of Zn in *Lactuca sativa* and *Brassica oleracea* plants: I. Growth, distribution, and accumulation of Zn, and metabolism of carboxylates. *Environmental and Experimental Botany*, *107*, 98-104. https://doi.org/10.1016/j.envexpbot.2014.05.012

Buturi, C. V., Mauro, R. P., Fogliano, V., Leonardi, C., & Giuffrida, F. (2021). Mineral biofortification of vegetables as a tool to improve human diet. *Foods*, *10*(2), 223. https://doi.org/10.3390/foods10020223

Connolly, E. L., & Guerinot, M. L. (2002). Iron stress in plants. *Genome Biology*, *3*(8), reviews1024.1. https://doi.org/10.1186/gb-2002-3-8-reviews1024

Department of Agriculture. (2021). *Vegetables and cash crop statistics Malaysia 2021*. DOA. http://www.doa.gov.my/index/resources/aktiviti_sumber/sumber_awam/maklumat_pertanian/perangkaan_tanaman/statistik_tanaman_sayur_tanaman_kontan_2021.pdf

Doolette, C. L., Read, T. L., Li, C., Scheckel, K. G., Donner, E., Kopittke, P. M., Schjoerring, J. K., & Lombi, E. (2018). Foliar application of zinc sulphate and zinc EDTA to wheat leaves: Differences in mobility, distribution, and speciation. *Journal of Experimental Botany*, *69*(18), 4469–4481. https://doi.org/10.1093/jxb/ery236

El-Jendoubi, H., Vázquez, S., Calatayud, A., Vavpetič, P., Vogel-Mikuš, K., Pelicon, P., Abadía, J., Abadía, A., & Morales, F. (2014). The effects of foliar fertilization with iron sulfate in chlorotic leaves are limited to the treated area. A study with peach trees (*Prunus persica* L. Batsch) grown in the field and sugarbeet (*Beta Vulgaris* L.) grown in hydroponics. *Frontiers in Plant Science*, *5*, 2. https://doi.org/10.3389/fpls.2014.00002

Hochmuth, G. (2011). Iron (Fe) nutrition of plants: SL353/SS555, 8/2011. *EDIS*, *2011*(8). https://doi.org/10.32473/edis-ss555-2011

Kyu, H. H., Pinho, C., Wagner, J. A., & Brown, J. C. (2016). Global and national burden of diseases and injuries among children and adolescents between 1990 and 2013: Findings from the global burden of disease 2013 study. *JAMA Pediatrics*, *170*(3), 267-287. https://doi.org/10.1001/jamapediatrics.2015.4276

Ministry of Health. (2017). *Recommended nutrients intake (RNI) for Malaysia: A report of the technical working group on nutritional*

guidelines. MOH. https://hq.moh.gov.my/nutrition/wp-content/uploads/2017/05/FA-Buku-RNI.pdf

Munirah, N., Lah, M. K. C., Nordin, M. N., Khandaker, M. M., Mat, N., & Jahan, M. S. (2015). The effects of zinc application on physiology and production of corn plants. *Australian Journal of Basic and Applied Sciences*, *9*(5), 161-165.

Rouphael, Y., & Kyriacou, M. C. (2018). Enhancing quality of fresh vegetables through salinity eustress and biofortification applications facilitated by soilless cultivation. *Frontiers in Plant Science*, *9*, 1254. https://doi.org/10.3389/fpls.2018.01254

Rout, G. R., & Sahoo, S. (2015). Role of iron in plant growth and metabolism. *Reviews in Agricultural Science*, *3*, 1-24. https://doi.org/10.7831/ras.3.1

Rugeles-Reyes, S. M., Filho, A. B. C., Lopez Aguilar, M. A., & Silva, P. H. S. (2019). Foliar application of zinc in the agronomic biofortification of arugula. *Food Science and Technology*, *39*(64), 1011-1017. https://doi.org/10.1590/fst.12318

Uchida, R. (2000). Essential nutrients for plant growth: Nutrient functions and deficiency symptoms. In J. A. Silva & R. Uchida (Eds.), *plant nutrient management in Hawaii's soils approaches for tropical and subtropical agriculture* (pp. 31-55). University of Hawaii Press.

Vadlamudi, K., Upadhyay, H., Singh, A., & Reddy, M. (2020). Influence of zinc application in plant growth: An overview. *European Journal of Molecular and Clinical Medicine*, *7*(7), 2321-2327.

Wessells, K. R., & Brown, K. H. (2012). Estimating the global prevalence of zinc deficiency: Results based on zinc availability in national food supplies and the prevalence of stunting. *PLOS One*, *7*(11), e50568. https://doi.org/10.1371/journal.pone.0050568

White, P. J., & Broadley, M. R. (2009). Biofortification of crops with seven mineral elements often lacking in human diets – Iron, zinc, copper, calcium, magnesium, selenium and iodine. *New Phytologist*, *182*(1), 49–84. https://doi.org/10.1111/j.1469-8137.2008.02738.x

Zahed, Z., Kumar, S. S., Mahale, A. G., Krishna, J. R., & Mufti, S. (2021). Foliar micro-nutrition of vegetable crops - A critical review. *Current Journal of Applied Science and Technology*, *40*(7), 1-12. https://doi.org/10.9734/cjast/2021/v40i731322

Zahra, N., Hafeez, M. B., Shaukat, K., Wahid, A., & Hasanuzzaman, M. (2021). Fe toxicity in plants: Impacts and remediation. *Physiologia Plantarum*, *173*(1), 201–222. https://doi.org/10.1111/ppl.13361

Zarcinas, B. A., Ishak, C. F., McLaughlin M. J., & Cozens, G. (2004). Heavy metals in soils and crop in Southeast Asia. *Environmental Geochemistry and Health*, *26*, 343-357. https://doi.org/10.1007/s10653-005-4669-0

Zou, C., Du, Y., Rashid, A., Ram, H., Savasli, E., Pieterse, P.J., Ortiz-Monasterio, I., Yazici, A., Kaur, C., Mahmood, K., Singh, S., Le Roux, M. R., Kuang, W., Onder, O., Kalayci, M., & Cakmak. I. (2019). Simultaneous biofortification of wheat with zinc, iodine, selenium, and iron through foliar treatment of a micronutrient cocktail in six countries. *Journal of Agricultural and Food Chemistry*, *67*(29), 8096-8106. https://doi.org/10.1021/acs.jafc.9b01829

Pertanika J. Trop. Agri. Sci. 46 (4): 1127 - 1150 (2023)

PERTANIKA JOURNALS

TROPICAL AGRICULTURAL SCIENCE

Journal homepage: http://www.pertanika.upm.edu.my/

Assessment of a Monthly Data Structure for Growth and Yield Projections from Early to Harvest Age in Hybrid Eucalypt Stands

Gianmarco Goycochea Casas[1]*, Carlos Pedro Boechat Soares[1], Márcio Leles Romarco de Oliveira[2], Daniel Henrique Breda Binoti[3], Leonardo Pereira Fardin[1], Mathaus Messias Coimbra Limeira[1], Zool Hilmi Ismail[4], Antonilmar Araújo Lopes da Silva[5] and Hélio Garcia Leite[1]

[1]Department of Forest Engineering, Universidade Federal de Viçosa, 36570-900 Viçosa, Minas Gerais, Brazil
[2]Department of Forestry, Universidade Federal dos Vales do Jequitinhonha e Mucuri, 39100-000 Diamantina, Minas Gerais, Brazil
[3]Dap Florestal, Rua Papa João XXIII, n 9, Lourdes, 36572-006 Viçosa, Minas Gerais, Brazil
[4]Center for Artificial Intelligence and Robotics, Universiti Teknologi Malaysia, 54100 Kuala Lumpur, Malaysia
[5]Rua Visconde de Mauá, n 755, Nobre City, 35162-391 Ipatinga, Minas Gerais, Brazil

ABSTRACT

Whole-stand Models (WSM) have always been fitted with permanent plot data organised in a sequential age-matched database, i.e., *i* and *i*+1, where *i* = 1, 2, ... *N* plot measurements. The objectives of this study were (1) to evaluate the statistical efficiency of a monthly distributed data structure by fitting the models of Clutter (1963), Buckman (1962) in the version modified by A. L. da Silva et al. (2006), and deep learning, and (2) to evaluate the possibility of gaining accuracy in yield projections made from an early age to harvest age of eucalypt stands. Three alternatives for organizing the data were analyzed. The first is with data paired in sequential measurement ages, i.e., *i* and *i*+1, where *i* = 1, 2, ... *N* plot measurements. In the second, all possible measurement intervals for each plot were considered, i.e., *i*, *i*+1; i, *i*+2; ...; *i*, *N*; *i*+1, *i*+2; ..., *N*-1, *N*. The third has data paired by month (*j*), always with an interval of one month, i.e., *j*, *j*+1; *j*+1, *j*+2; *j*+*M*-1, *M*, where *M* is the stand age of the plot measurement in months. This study shows that the accuracy and consistency of the projections depend on the organization of the monthly distributed data, except for the Clutter model. A better alternative to

ARTICLE INFO

Article history:
Received: 29 March 2023
Accepted: 02 May 2023
Published: 22 September 2023

DOI: https://doi.org/10.47836/pjtas.46.4.04

E-mail addresses:
gianmarco.casas@ufv.br (Gianmarco Goycochea Casas)
csoares.ufv@gmail.com (Carlos Pedro Boechat Soares)
marcioromarco@gmail.com (Márcio Leles Romarco de Oliveira)
danielhbbinoti@gmail.com (Daniel Henrique Breda Binoti)
leopfard@gmail.com (Leonardo Pereira Fardin)
mathaus.limeira@ufv.br (Mathaus Messias Coimbra Limeira)
zool@utm.my (Zool Hilmi Ismail)
antonilmar@gmail.com (Antonilmar Araújo Lopes da Silva)
hgleite@ufv.br (Hélio Garcia Leite)
*Corresponding author

ISSN: 1511-3701
e-ISSN: 2231-8542

increasing the statistical assumptions of the forecast from early to harvest age is based on a monthly distributed data structure using a deep learning method.

Keywords: Buckman, clutter, deep learning, forest management, volumetric projection

INTRODUCTION

The growth and yield modeling of even-aged stands is essential to forest management (Campos & Leite, 2017; Davis & Johnson, 1987). The models estimate harvest stocks for different prescriptions and thus support management plans, especially in hierarchical planning. Models are also important to figure out the average productivity at different sites used as inputs in studies related to the sustainability of production.

Growth and yield models can be used for prediction or projection. In the first case, growth and future yield are independent of current yield. In the second, the model's functional relationships use the current yield (in basal area and/or volume) as a predictor variable (i.e., an independent variable). A prediction model can be transformed and applied to differentiate future production according to current production, however, with the same growth trend (Campos & Leite, 2017). Estimating wood stocks for defined ages in a strategic planning model is known as prognosis; this term refers to any procedure that generates an expectation of future production. According to Burkhart and Tomé (2012) and Castro et al. (2013), the prediction describes the change in the size of the individual population over time.

One of the components or elements in forest management is prognosis, which is usually done using growth and yield models. Despite significant advances in studies of growth and yield modeling of forest stands with regression, problems persist. One of these problems is the low accuracy of projections made from early ages, for example, from two or three years of age to harvest age, which in Brazil is generally six or seven years for eucalypt stands to produce cellulose pulp or charcoal. This difficulty is related to the heteroscedastic nature of the relations between dominant height (*Hd*) and volume (*V*) with age (*A*), with less variance at early ages. In most cases, the dispersion of *Hd* and *V* at ages 1.5 to 2.5 years, in eucalypt stands, is relatively small. As the years go by, the variance of *Hd* and *V* increases, indicating that heteroscedasticity occurs naturally.

The main models used in Brazil are Whole-stand Models (WSM) for the use of wood, most often to produce cellulose pulp or charcoal. These aspects are discussed by Campos and Leite (2017) with reference to exponential and sigmoid models, in addition to the Buckman (1962) and Clutter (1963) models. In their discussions, they report that using simpler functional relationships requires more intense data stratification for modeling.

Buckman model (1962) had not been used on a commercial scale in Brazil despite several researchers intending to demonstrate its feasibility in its use (A. L. da Silva et al., 2006; Burkhart & Sprinz, 1984; Guera et al., 2019; Trevizol Jr., 1985). On the other

hand, the Clutter model has always been used in different regions of Brazil since the 1985s (Miguel et al. 2016; Penido et al. 2020; Salles et al., 2012; Soares et al., 2004; Trevizol Jr., 1985).

Authors have shown that for ranking productive capacity (site index) using mathematical regression models, the evaluation of estimates and statistical parameters depends on both the model and the data structure used for modeling (Cao, 1993; Cieszewski, 2002; Hirigoyen et al., 2018; Strub & Cieszewski, 2006).

Another example influenced by the organization of data is also carried out when modeling with metaheuristic techniques such as Artificial Neural Networks (ANNs) for WSM, such is the case of irregular intervals (da Silva Binoti et al., 2015), i.e., i and i+1, where i = 1, 2, ... N plot measurements, for the prediction of the performance of different initial ages and intervals of prediction are necessary for hierarchical planning. Nonetheless, works related to the Buckman (1962) and Clutter (1963) models were not found.

ANNs have been increasingly used for various purposes in forest engineering (Araújo Júnior et al., 2019; de Freitas et al., 2020; Gavilán-Acuña et al., 2021; Lopes et al., 2020; S. Silva et al., 2020). In general, the accuracy of yield estimates at the stand level has been higher when ANN is employed compared to growth and yield models (Casas, Fardin, et al., 2022; de Oliveira Neto et al., 2022). The higher accuracy is partially explained by including categorical variables in the ANN. Despite the gain in accuracy with the use of ANN, the problem of inefficient projection for about 2 years (in the case of eucalypt stands) persists.

Deep learning is part of the broader field of machine learning and artificial intelligence that uses artificial neural networks. The difference with a conventional network is that deep networks allow computational models of multiple processing layers to learn data representations with various levels of abstraction (Aggarwal, 2018; LeCun et al., 2015). Understanding the irrational effectiveness of deep learning is very complex and is still being studied through advanced mathematics and neuroscience, as it is an inspirational source in the brain's architecture (Sejnowski, 2020). Deep learning has been increasingly used in research involving complex structures in different forestry and environmental areas, where studies have been reported on the hypsometric relationship between tree diameter and height (Casas, Gonzáles, et al., 2022), individual tree detection and species classification of Amazonian palms (Ferreira et al., 2020), forest damage assessment (Hamdi et al., 2019), analysis of drone-acquired forest images (Kentsch et al., 2020), automatic identification of charcoal origin (de Oliveira Neto et al., 2021), plant identification in the natural environment (Sun et al., 2017) and wood filtering, and tree species classification from terrestrial laser scanning (Xi et al., 2020).

Most studies using machine learning for prognosis comparisons are made using regression modeling. The following question arises: Is there any gain or loss in statistical efficiency when fitting the Clutter model,

Buckman model, and deep learning when using a monthly distributed data organization from continuous inventories with permanent plots? The objectives of this study were to (1) evaluate the statistical efficiency of a monthly distributed data structure by fitting the models of Buckman (1962) and Clutter (1963) in the version modified by A. L. da Silva et al. (2006) and deep learning, and (2) evaluate the possibility of gaining accuracy in yield projections in eucalypt stands made from initial ages of approximately two years to the age of harvest with ages of six and seven years.

MATERIALS AND METHODS

Study Area Description

The data used in this study were measured from 1,243 permanent 400 m^2 rectangular plots distributed in 243 project stands of the hybrid *Eucalyptus urophylla* x *Eucalyptus grandis*, with a spacing of 3 x 3 m^2, located in the Midwest region of the Minas Gerais state, Brazil. Stand locations were at a mean altitude of 743 m, a mean annual precipitation of 1,163 mm, and a mean annual temperature of 27°C (Alvares et al., 2013). The database consisted of annual dasometric measurements from 2006 to 2015 for each permanent plot. The variables used in this study were dominant height (m), basal area (m^2/ha), and volume (m^3/ha). The statistical description of the dasometric variables for each region can be found in Table 1.

Structuring of Processing Data

Regression and deep learning methods were used. In the regression method, two WSM models were used: The Buckman

Table 1
Statistical description of dasometric variables of hybrid eucalypt stands located in the Midwest Region in the Minas Gerais state, Brazil

Subregion	Variable	Valid N	Mean	Minimum	Maximum	Variance	Standard deviation	Standard error
A	Age (months)	3,442	46.78	18.00	95.00	373.70	19.33	0.33
	Dominant Height (m)	3,442	21.59	7.63	39.24	35.23	5.94	0.10
	Basal Area (m^2/ha)	3,442	15.98	0.22	40.31	41.10	6.41	0.11
	Volume (m^3/ha)	3,442	153.84	1.22	558.11	9,243.80	96.14	1.64
B	Age (months)	2,576	39.47	20.00	82.00	209.68	14.48	0.29
	Dominant Height (m)	2,576	19.47	7.23	35.87	22.63	4.76	0.09

Table 1 *(Continue)*

Subregion	Variable	Valid N	Mean	Minimum	Maximum	Variance	Standard deviation	Standard error
C	Basal Area (m^2/ha)	2,576	14.41	1.53	34.48	26.53	5.15	0.10
	Volume (m^3/ha)	2,576	138.82	5.03	444.22	6,001.68	77.47	1.53
	Age (months)	1,976	37.10	19.00	73.00	158.39	12.59	0.28
	Dominant Height (m)	1,976	19.87	8.67	33.57	24.56	4.96	0.11
	Basal Area (m^2/ha)	1,976	14.45	3.11	28.91	26.56	5.15	0.12
	Volume (m^3/ha)	1,976	132.17	11.15	397.83	5,953.52	77.16	1.74

model (1962) and the Clutter model (1963), modified by A. L. da Silva et al. (2006). Three different data structures were fit for growth and yield modeling:

I. The two variable density models are equipped with the following data structure: paired data considering ascending intervals without overlap ([A_1-A_2], [A_2-A_3], . . . [A_n-A_{n+1}]). This structure has historically been used for fitting variable-density growth and yield models and other projection models.

II. ANN techniques are used with the following data structure: considering An as age at measurement n = 1, 2, 3, …. N in a measurement plot, the database was organized considering all possible age intervals for each plot, i.e. paired data considering all possible ascending age intervals ([A_1-A_2], [A_1-A_3], ... [A_2-A_3], [A_2-A_4], . . . [A_n-A_{n+1}], [A_n-A_{n+2}]). It was necessary so that the networks could be trained to generalize to different early ages and projection intervals and usually be used for these cases.

III. In this study, the following data structure was proposed: paired data is considered with ascending intervals without overlap by month (j), always with an interval of one month, i.e., j, j+1; j+1, j+2; j+M-1, M, where M is the stand age of the plot measurement in months. Linear interpolations were made between each plot's values to set up this structure.

Monthly structured data must be converted to Data Structure II to apply the deep learning method. In the case of any regression method, it is not necessary to perform the conversion for Data Structure II. By performing this conversion, we obtain the Data Structures II-A and II-B (Figure 1). Training the networks to generalize to different early ages and projection intervals was necessary.

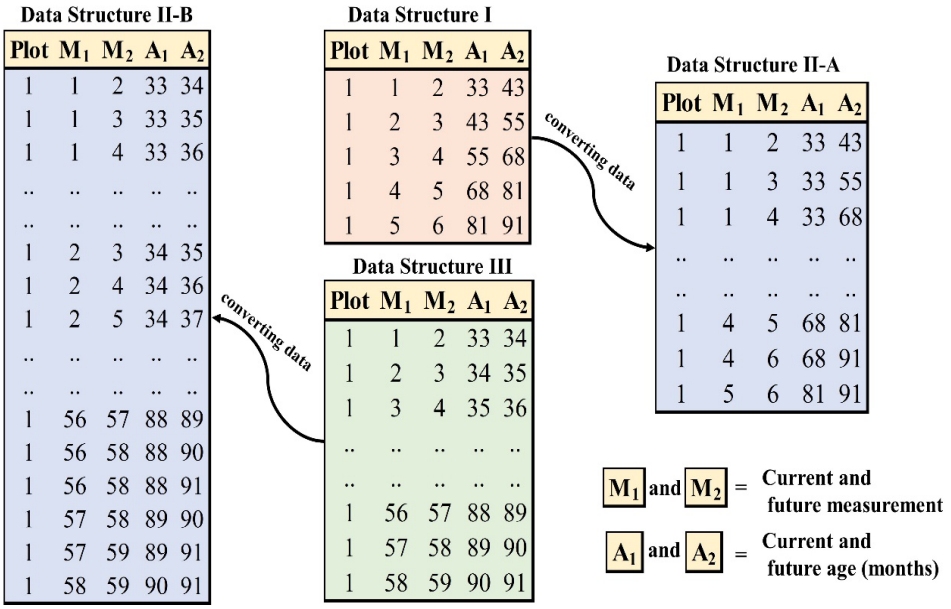

Figure 1. Example of a one-plot database structure used to fit Buckman model (1962) and Clutter model (1963) modified by A. L. da Silva et al. (2006) (Data Structures I and III) and deep learning (Data Structures II-A and II-B) models and the process of converting data from one structure to another structure according to the method to be used

Fitting the Data with the Variable Density Models

The growth and yield models for this study were the Clutter (Equations 1 and 2) and Buckman, modified by A. L. da Silva et al. (2006) (Equations 3 and 4). The Clutter model was fitted by the two-stage least squares method using applied econometrics with an R (AER) package (Kleiber & Zeileis, 2008) and the Buckman model by ordinary least squares in R. The equations are shown below:

$$\left.\begin{aligned} LnB_2 &= LnB_1\left(\frac{A_1}{A_2}\right)+\alpha_0\left(1-\frac{A_1}{A_2}\right)+\alpha_1\left(1-\frac{A_1}{A_2}\right)S+\varepsilon_1 \\ LnV_2 &= \beta_0+\beta_1\left(\frac{1}{A_2}\right)+\beta_2 S+\beta_3 LnB_2+\varepsilon_2 \end{aligned}\right\} \quad \text{(Equations 1 and 2)}$$

$$\left.\begin{aligned} LndB &= \alpha_0+\alpha_1 A_2+\alpha_2 S+\alpha_3 A_2^{-1}+\alpha_4 LnB_{1_1}+\varepsilon_1 \\ LnV_2 &= \beta_0+\beta_1 A_2^{-1}+\beta_2 S+\beta_3 LnB_2+\varepsilon_2 \end{aligned}\right\} \quad \text{(Equations 3 and 4)}$$

where V_2 = future yield (m³/ha); A_1 and A_2 = current and future age (months); S = site index in the current age (m); B_1 and B_2 = current and future basal areas (m²/ha); dB = increase in basal area between A_1 and A_2; Ln = neperian logarithm; α and β = model parameters; ε_1 and $\varepsilon_{2;}\, \varepsilon_k \sim NID(0;\, \sigma^2)$ and $B_2 = B_1 + \sum_{j=A_1}^{j=A_2} dB_j$.

The guide curve method figured out the site indexes for each measurement (Clutter et al., 1983). In our study to figure out the site index, the Gompertz (1825) model has been selected since this model is the most adequate to estimate the dominant height as a function of age for eucalypt stands (Reis et al., 2022). The index age (Ai) was 72 months. This index age is appropriate for the eucalypt species in Brazil.

Thus, considering the classical transformation of the guide curve method, in which:

$Hd = \beta_0 e^{-e^{\beta_1 - \beta_2 A}} + \varepsilon$ with observe *Hd* at the age A

$S = \beta_0 e^{-e^{\beta_1 - \beta_2 Ai}} + \varepsilon$ at the index age Ai of 72 months

Therefore, the site index equation (Equation 5) was established by taking the differences between the above equations and expressing them explicitly in terms of S:

$$S = Hd\, e^{-e^{\beta_1 - 72\beta_2}} / e^{-e^{\beta_1 - \beta_2 A}} \quad \text{(Equation 5)}$$

where Hd = dominant height (m) observed at age A, S = site index (m), and β_1 and β_2 = parameter estimates of the Gompertz model.

Fitting the Data with Deep Learning

Input and Output Variables. In the output layer, the variable was future volume (V_2). From this variable in the output layer, we set the variables of the input layer using the following function (Equation 6):

$$V_2 = f(\text{Project stand}, A_1, A_2, B_1, H_d, V_1) \quad \text{(Equation 6)}$$

where V_2 = future volume (m^3/ha) in the output layer; A_1 = current age (month); A_2 = future age (month); B_1 = current basal area (m^2/ha); *Hd* = dominant height (m); and V_1 = current volume (m^3/ha) in the input layer. The project stand had categorical variables in the input layer.

Hyperparameter Tuning with Grid Search for Deep Learning. A Cartesian grid search was performed. It has performed the procedure for implementing the deep learning method and trained models for every combination of the hyperparameter values. For each function, 162 models were trained for the deep learning method. The data were processed in R (R Core Team, 2020) using the H2O package (Fryda et al., 2020). Their architectures had one input layer, two, three, and four hidden layers, and one output layer. The numbers of neurons in the hidden layer were 50:25, 50:25:5, 100:50, 100:50:25, 100:50:25:5, and 200:100:50. The functions of activations in the hidden layer were Tanh (Equation 7), Rectified Linear (Equation 8), and Maxout (Equation 9):

$$\text{Tanh}\left[f(\alpha) = \frac{e^{\alpha} - e^{-\alpha}}{e^{\alpha} + e^{-\alpha}}\right]; f(x) \in [-1,1] \quad \text{(Equation 7)}$$

Rectified Linear

$$[f(\alpha) = \max \quad 0, \alpha)]; f(.) \in \mathbb{R}_+ \quad \text{(Equation 8)}$$

Maxout

$$\left[f(.) = \max(w_i x_i + b)\right]; f(.) \in [-\infty, 1]\ ;$$

rescale if max $f(.) \geq 1$ (Equation 9)

In the output layer, it has configured Linear activation function $[f(\alpha)=\alpha]$ for all trained models, where *f* is the function that represents the non-linear activation used in the entire neural network; *b* is the bias for the neuron activation threshold; x_i and w_i denote the input values of the unit or neuron and their weights; α denotes the weighted combination: $\alpha=\sum_{j=1}^{n} w_i x_i + b$

Gaussian distribution function was configured as an equivalent to weighted mean squared error (wMSE) (Equation 10):

$$f(.)=\omega\left(y-f\right)^2 \qquad \text{(Equation 10)}$$

where *y* is a true response, *f* is a predicted response and ω is weighted.

The loss function chosen was quadratic (Equation 11):

$$L(W,B\left|j\right.)=\frac{1}{2}\left\|t^{(j)}-o^{(j)}\right\|_2^2 \qquad \text{(Equation 11)}$$

where $t^{(j)}$ and $o^{(j)}$ are the predicted output and actual output; *j* and *W* are the collection $\{W_i\}1{:}N\text{-}1$, which W_i denotes the weight matrix connecting layers *i* and *i* + 1 for a network of *N* layers; *B* is the collection $\{b_i\}_{1:N-1}$, which b_i denotes the column vector of biases for layer *i* + 1.

The mini-batch was of size 1, the number of epochs was 1,000, and the type of regularization was the early stopping system, with 5 stop rounds, a stop tolerance of 0.001, and the MSE stop metric.

The adaptive learning rate algorithm (ADADELTA) (Equation 12) (Zeiler, 2012) was used:

$$\begin{aligned}
&1.\ \textit{Accumulate gradient}:\ E[g^2]_t=\rho * E[g^2]_{t-1}+(1-\rho)*g_t^2\\
&2.\ \textit{Compute update}:\ \Delta x_t=-RMS[\Delta x]_{t-1}/RMS[g]_t * g_t\\
&3.\ \textit{Accumulate updates}:\ E[\Delta x^2]_t=\rho * E[\Delta x^2]_{t-1}+(1-\rho)*(\Delta x_t)^2\\
&4.\ \textit{Apply update}:\ x_{t+1}=x_t+\Delta x_t
\end{aligned} \qquad \text{(Equation 12)}$$

where g_t is the gradient at time step *t*; $E\left[g^2\right]_t$ is the running average of the squared gradient at time step *t*; Δx_t is the update at time step *t*; $RMS[\Delta x]_{t-1}=\sqrt{E\left[\Delta x^2\right]_{t-1}+\in}$ is the running average of the squared updates at time step *t*; $RMS[g]_t=\sqrt{E\left[g^2\right]_t+\in}$ is the root mean square of updates at time step *t*; $RMS[g]_t=\sqrt{E\left[g^2\right]_t+\in}$ is the root mean square of gradients at time step *t*; ρ (Rho) is the decay rate; $\in$ (Epsilon) is a small constant for numerical stability.

This algorithm works with two parameters (Rho and Epsilon), which were configured with 0.9, 0.95, and 0.999 for Rho

and $1e^{-06}$, $1e^{-08}$, and $1e^{-10}$ for Epsilon while g_t denoting the parameters at the *t*-th iteration, g_t as the computed gradient, *t* is the time, and RMS is the root mean squared error.

Model Performance

The databases were split into training (70%) and validation (30%). The following statistics were used in the validation data: the linear correlation coefficient between observed and corresponding projected yields ($r_{y\hat{y}}$) (Equation 13), mean absolute deviations (MAD) (Equation 14), percent root mean square error (RMSE%) (Equation 15), Bias (Equation 16), percent Bias% (Equation 17) and percent relative error (RE%) (Equation 18). In addition, the distribution graph of RE% *vs*. fitting was interpreted. The estimators used were:

$$r_{y\hat{y}} = \frac{n^{-1}\sum_{i=1}^{n}(Y_{pi}-\bar{Y}_m)(Y_i-\bar{Y})}{\sqrt{n^{-1}\sum_{i=1}^{n}(Y_{pi}-\bar{Y}_m)^2 n^{-1}\sum_{i=1}^{n}(Y_i-\bar{Y})^2}};\ Y_m = n^{-1}\sum_{i=1}^{n}Y_{pi} \quad \text{(Equation 13)}$$

$$MAD = \left(n^{-1}\sum_{i=1}^{n}\left|\hat{Y}i - Yi\right|\right); \quad \text{(Equation 14)}$$

$$RMSE\% = 100\overline{Y}_i^{-1}\sqrt{n^{-1}\sum_{i=1}^{n}(\hat{Y}_i - \mathrm{Y}_I)^2}; \quad \text{(Equation 15)}$$

$$Bias = \sum_{i=1}^{n}\frac{\left(\hat{Y}_i - Y_i\right)}{n}; \quad \text{(Equation 16)}$$

$$Bias\% = 100\overline{Y}_i^{-1}\sum_{i=1}^{n}\frac{\left(\hat{Y}_i - Y_i\right)}{n}; \quad \text{(Equation 17)}$$

$$RE\% = 100\left(\frac{\hat{Y}_i - Y_i}{Y_i}\right) \quad \text{(Equation 18)}$$

where *n* = number of observations; $\overline{\hat{Y}}$ = projected yield; $\overline{Y}$ = observed yield; and $\overline{Y}$ = mean observed yield.

RESULTS

Assessment of Growth and Yield Projection

Assessment of Production Capacity. The parameter estimates of the Gompertz model are shown in Table 2, where all coefficients were significant ($p < 0.01$). The same table shows the precision and accuracy statistics obtained from the fit when applied to the validation data with r = 0.9112, MAD = 1.7104, RMSE% = 11.8216, bias = 0.1200, and bias% = 0.0066.

Table 2
Statistical indicators and evaluation parameters obtained using the Gompertz model in hybrid eucalypt stands

Gompertz model								
Parameter	Coefficient	Standard error	*t*-statistic	r	MAD	RMSE (%)	Bias	Bias (%)
β_1	29.3806	0.3676	79.94					
β_2	0.9578	0.0387	24.73	0.9112	1.7104	11.8216	0.12	0.0066
β_3	0.0511	0.002	25.85					

Note. r = Correlation between observed and estimated dominant height (*Hd*); MAD = Mean absolute deviation; RMSE% = Percent mean square error; Bias% = Percent bias

The limit tables of dominant heights were established from the obtained coefficients and applied to the site index equation (Equation 5), being able to construct the site index curves at an index age of 72 months to stand for the productive capacity (Figure 2) illustratively. The site index has been set from 22 to 32 m with an amplitude of 2 m.

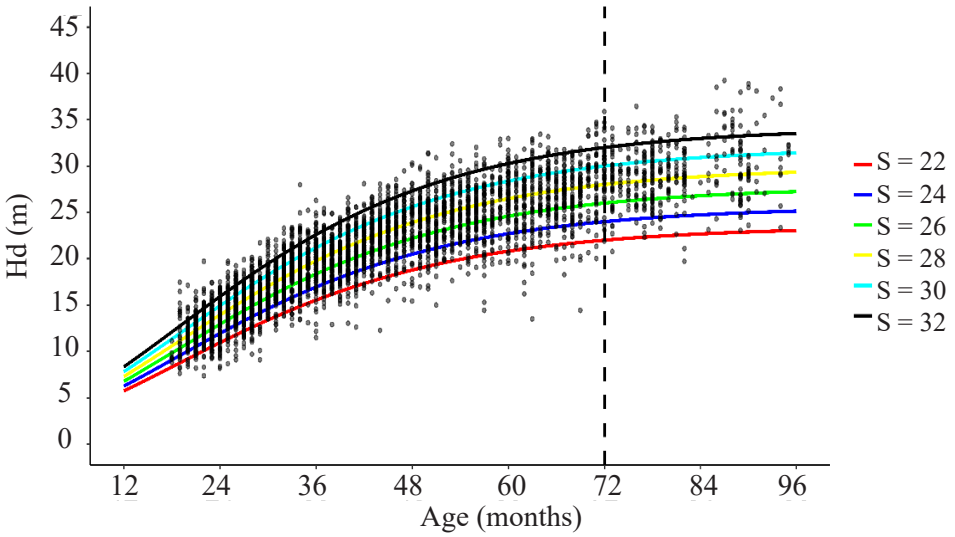

Figure 2. Site index (S) curves at the index age of 72 months in hybrid eucalypt stands

Evaluation of Variable Density Models. The parameter estimates of the Clutter and Buckman model modified by A. L. da Silva et al. (2006) for Data Structures I and III are shown in Table 3, where all coefficients were significant ($p < 0.01$). The results of the statistical parameters evaluated for both models and the data structures evaluated are also shown.

The comparison of fits between Data Structures I and III reveals that, in the case of the Clutter model (1963), Data Structure I provides superior statistical estimates, with r = 0.9262, MAD = 23.6587, RMSE% = 14.6257, bias = -4.3151, and bias% = -0.0187.

In the case of the Buckman model modified by A. L. da Silva et al. (2006), a large difference is observed in their statistical estimations of the future yield. The Structure III database was clearly better than the structure I database with r = 0.8658, MAD = 33.3512, RMSE% = 20.4896, bias = -164,653, and bias% = -0.0712.

The Clutter model fitted using Data Structure I (Figure 4A) showed a better constant variance than Data Structure III (Figure 4B). An improvement in its residual distribution was also observed when fitting the Buckman model modified by A. L. da Silva et al. (2006) using Data Structure III (Figure 4D) rather than using Data Structure I (Figure 4C).

Table 3
Parameter estimates and their respective precision and accuracy statistics of Clutter and Buckman's models fitted with Database Structures I and III in hybrid eucalypt stands

Clutter model (1963)									
Data Structure I									
	Coefficient	Std. error	*t*-statistic	Variable	r	MAD	RMSE (%)	Bias	Bias (%)
α_0	3.932558	0.038727	101.5454						
α_1	-0.008756	0.001392	-6288644	B_2	0.9236	1.3949	9.2528	-0.1118	-0.0053
b_0	0.877906	0.044012	19.94678						
b_1	-10.24837	0.481462	-21.28594						
b_2	0.018141	0.000727	24.94387	V_2	0.9262	23.6587	14.6257	-4.3151	-0.0187
b_3	1.38008	0.014437	95.59182						

Clutter model (1963)									
Data Structure III									
	Coefficient	Std. error	*t*-statistic	Variable	r	MAD	RMSE (%)	Bias	Bias (%)
α_0	3.981974	0.033332	119.4652						
α_1	-0.0128	0.001217	-1051407	B_2	0.9219	1.4789	9.9031	-0.6373	-0.0302
b_0	1.603696	0.007266	220.7228						
b_1	-22.6567	0.100077	-226.3926						
b_2	0.035006	0.000139	251.6177	V_2	0.9143	26.0424	16.1049	-9.8251	-0.0425
b_3	1.06014	0.002439	434.6499						

Buckman model modified by A. L. da Silva et al. (2006)									
Data Structure I									
	Coefficient	Std. error	*t*-statistic	Variable	r	MAD	RMSE (%)	Bias	Bias (%)
α_0	2.735686	0.200096	13.672						
α_1	0.009577	0.001975	4.85						
α_2	0.050674	0.003933	12.883	B_2	0.4655	4.0692	27.3475	-0.1448	-0.0069
α_3	-3.344789	4.096659	-0.816						
α_4	-1.194655	0.040544	-29.466						
b_0	1.008	0.04	24.82						
b_1	0.0193	0	27.19	V_2	0.5766	60.0655	38.0952	-4.495	-0.0194
b_2	-11.42	0.46	-25.04						
b_3	1.333	0.01	102						

Table 3 *(Continue)*

Buckman model modified by A. L. da Silva et al. (2006)								
Data Structure III								
Coefficient	Std. error	*t*-statistic	Variable	r	MAD	RMSE (%)	Bias	Bias (%)
-2.7700256	0.0610517	-45.37						
-0.0173024	0.0004176	-41.43						
-0.0239686	0.000876	-27.36	B_2	0.823	2.3147	14.9104	-1.1643	-0.0552
42.9365767	1.077054	39.87						
0.721791	0.0150107	48.09						
1.598209	0.007283	219.4						
0.034926	0.000139	251.3	V_2	0.8658	33.3512	20.4896	-16.4653	-0.0712
-22.581012	0.100189	-225.4						
1.062248	0.002439	435.6						

Note. r = Correlation between observed and projected future yield (V_2); MAD = Mean absolute deviation; RMSE% = Percent mean square error; Bias% = Percent bias

Evaluation of Deep Learning Models. In the beginning, 167 deep learning models were trained with different hyperparameter configurations for each II-A and II-B data structure. However, in Data Structure II-A, only 159 models found an optimal solution, and in Data Structure II-B, only 157 models found an optimal solution. The best-trained model for Structure II-A presented the following hyperparameter configuration: activation = Maxout, epsilon = $1.00e^{-10}$, hidden layer = [200,100,50], rho = 0.9, and epoch = 66.23. The best-trained model for structure II-B presented the following hyperparameter configuration: activation = Rectifier, epsilon = $1.00e^{-08}$, hidden layer = [100,50], rho = 0.999, and epoch = 4.59. Initially, 1,000 epochs were configured, but these were not necessary to complete since the early stopping configuration allows the training to stop early during the creation and scoring of the model, thus avoiding overfitting. The Status of neuron layers of the best models can be seen in Table S1. It has also evaluated the learning curves of each best model of the II-A (Figure 3A) and II-B (Figure 3B) Data Structures, both for the training data set and the validation data set in which it has used the RMSE over the number of epochs. Both results were adequately representative; however, using a monthly Data Structure (II-B Data Structure), a greater number of epochs were not needed compared to the II-A Structure.

Statistical indicators of both Data Structures were analyzed (Table 4). The results showed that using the II-B Data Structure, there was a statistical gain in its parameters with R = 0.9758, MAD = 14.0096, RMSE% = 8.5838, bias = -4.5534, and bias% = -0.0197.

Illustratively, regular distribution of the residuals is observed when trained with an II-B Data Structure (Figure 4F), i.e., the residuals were randomly distributed around the zero value and, in fact, with a statistical gain compared to the II-A Structure (Figure 4E).

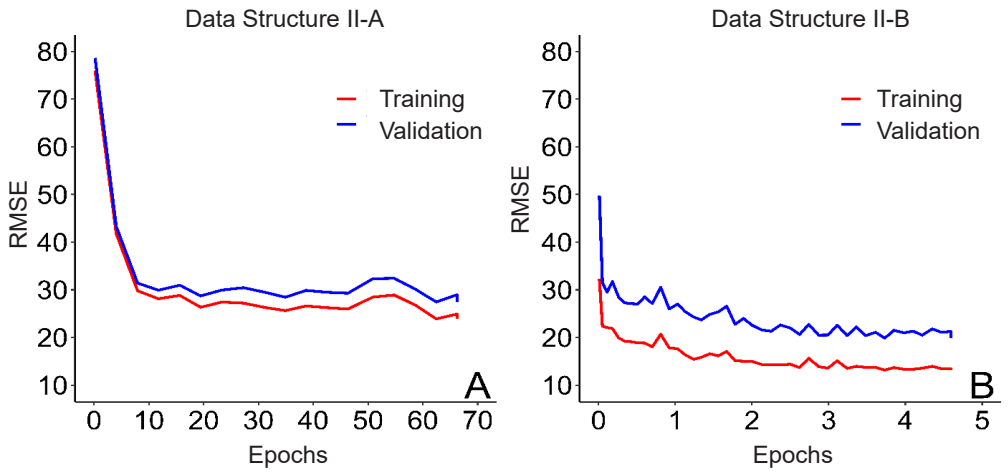

Figure 3. Model learning performance over the number of epochs trained in hybrid eucalypt stands
Note. A = Learning performance using Data Structure II-A; B = Learning performance using Data Structure II-B; RMSE = Root mean square error

Table 4
Precision and accuracy statistics of deep learning model fitted with database structures II-A and II-B in hybrid eucalypt stands

Model	Data Structure	Variable	r	MAD	RMSE (%)	Bias	Bias (%)
Deep learning	II-A	V_2	0.9506	19.4537	11.8697	-1.3161	-0.0057
	II-B	V_2	0.9758	14.0096	8.5838	-4.5534	-0.0197

Note. r = Correlation between observed and projected future yield (V_2); MAD = Mean absolute deviation; RMSE% = Percent mean square error; Bias% = Percent bias

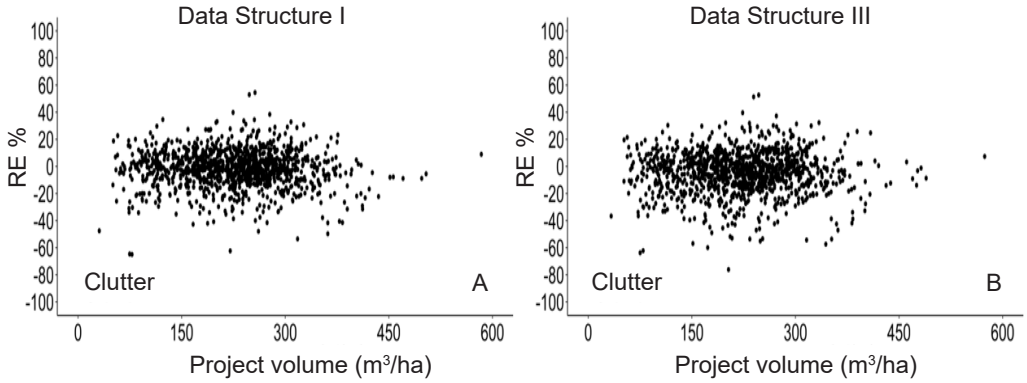

Figure 4. Dispersions of percent relative errors (RE%) as a function of estimated performance for the data structures and models in hybrid eucalypt stands

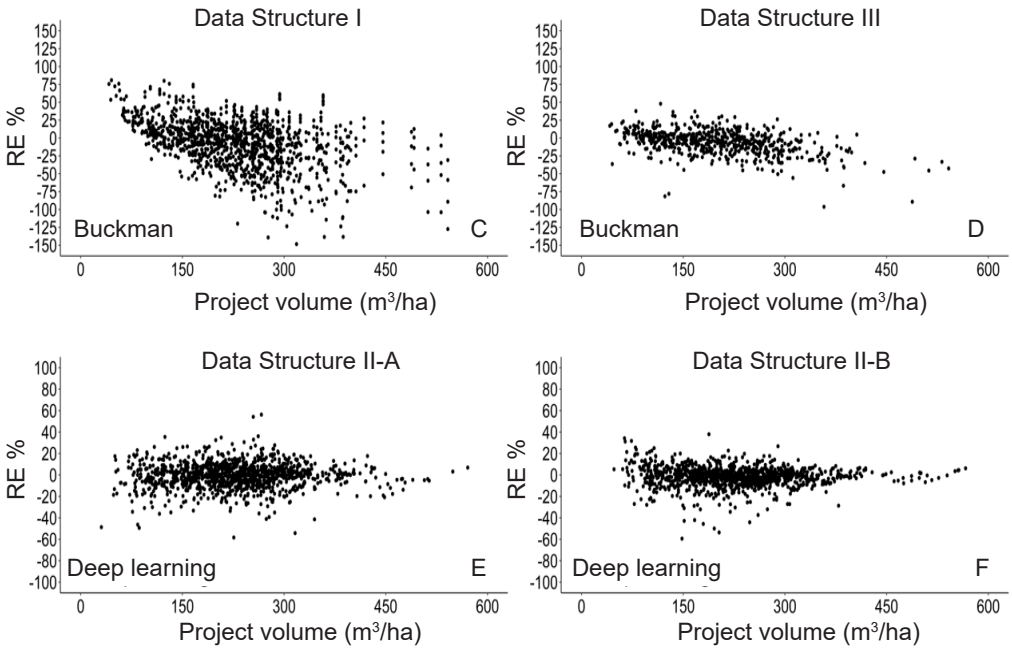

Figure 4. (Continue)
Note. A = Fitting the Clutter model using Data Structure I; B = Fitting the Clutter model using Data Structure III; C = Fitting the modified Buckman model using Data Structure I; D = Fitting the modified Buckman model using Data Structure III; E = Fitting the deep learning model using the Data Structure II-A; F = Fitting the deep learning model using the Data Structure II-B

Evaluation of Growth and Yield Projections from Early Age to Harvest Age

A statistical comparison was made with the methods and data structure evaluated to evaluate the accuracy of the volumetric projections from the early ages (two years) to the harvest age (six and seven years) (Table 5). The RMSE% plot was performed for each projection at the harvest age of 6 years (Figure 5A) and 7 years (Figure 5B) throughout the early ages to understand the behavior of the projections. The deep learning with Data Structure II-B presented greater precision in its statistics, which resulted in a lower variation of values between ages compared to the other methods and data structure. The accuracy generally increases as the early age increases except with the Buckman model with Structure III when the projection is for six years, but it has a resounding effect when the projection is for two years for both projection ages.

The methods used with a monthly data structure in this study present good estimates for volume projections from an early age, but when using artificial intelligence as a method of deep artificial neural networks, there is a tendency to decrease the RMSE%, an important indicator in volume projections, which can be considered in decision-making and influence the management plan. In the case of the Clutter model, despite not

having statistical gain with a Structure III, it presents good statistical estimates; however, it is always recommended to fit the model as is typically done, employing Structure I.

Table 5
Statistical results of volumetric projections from early to harvest age by Clutter, Buckman, and deep learning models using a study data structure in hybrid eucalypt stands

Model	Data Structure	Early age	Harvest age	r	MAD	RMSE (%)	Bias	Bias (%)
Clutter	I	2	6	0.6045	33.0581	15.4798	-13.0763	-0.0487
		3		0.7425	25.9512	12.8617	5.2079	0.0201
		4		0.8488	21.0546	10.1621	0.4931	0.0018
		5		0.9332	11.7644	5.6019	-0.5465	-0.002
		2	7	0.4788	32.3557	18.2733	-3.6332	-0.012
		3		0.7516	49.6076	18.9629	-20.3878	-0.0617
		4		0.9058	41.4839	14.9614	-30.8371	-0.0879
		5		0.9105	7.8335	5.3841	-4.6331	-0.0138
	III	2	6	0.5292	40.6503	18.8847	-25.016	-0.0931
		3		0.6717	29.6257	14.33	-0.9692	-0.0037
		4		0.8396	22.4827	10.4329	-3.1825	-0.0118
		5		0.9373	11.5962	5.6741	-5.1036	-0.019
		2	7	0.4031	37.1509	19.9158	-9.5745	-0.0318
		3		0.6969	53.9502	20.3385	-26.7242	-0.0809
		4		0.8759	47.0845	17.0584	-37.7946	-0.1077
		5		0.927	8.8185	5.827	-7.1168	-0.0211
Buckman modified by A. L. da Silva et al. (2006)	I	2	6	0.0045	93.5816	39.5078	-86.1337	-0.3205
		3		0.2467	53.8019	25.3614	-14.2639	-0.055
		4		0.2547	56.9629	25.9555	17.8658	0.0659
		5		0.2706	48.8036	24.7695	26.8213	0.1001
		2	7	-0.1793	61.3515	32.1259	-44.8372	-0.1487
		3		0.025	102.6234	37.2318	-70.2897	-0.2128
		4		0.3843	64.9168	23.739	-20.1564	-0.0574
		5		0.786	11.6204	8.5094	9.1789	0.0272
	III	2	6	0.6481	36.9178	16.8792	-23.2161	-0.0864
		3		0.6345	33.2872	16.3512	-13.6835	-0.0528
		4		0.5674	38.6764	17.7144	-17.3354	-0.0639
		5		0.5943	33.5235	15.9619	-22.4244	-0.0837
		2	7	0.5108	34.3482	18.7104	-9.8646	-0.0327
		3		0.6816	59.2349	21.8192	-37.5963	-0.1138
		4		0.7783	60.4282	20.4033	-48.3494	-0.1378
		5		0.7383	13.5624	8.3983	-5.7556	-0.0171

Table 5 *(Continue)*

Model	Data Structure	Early age	Harvest age	r	MAD	RMSE (%)	Bias	Bias (%)
Deep learning	II-A	2	6	0.7348	26.7587	12.7355	-9.2113	-0.0343
		3		0.7818	23.9604	11.964	1.7124	0.0066
		4		0.8934	17.9795	8.5486	1.4199	0.0052
		5		0.9413	10.3057	5.2914	0.7683	0.0029
		2	7	0.7403	24.1687	14.1892	-0.1785	-0.0006
		3		0.8565	32.7332	13.6318	0.9818	0.003
		4		0.939	23.7861	8.5571	-7.8113	-0.0223
		5		0.9537	5.127	3.3905	-0.1354	-0.0004
	II-B	2	6	0.8992	20.6304	10.0871	-15.4392	-0.0574
		3		0.9353	15.0248	7.3165	-7.045	-0.0272
		4		0.9634	12.2011	5.3415	-3.6078	-0.0133
		5		0.9395	12.9134	5.9563	-6.9718	-0.026
		2	7	0.9066	16.847	9.3742	-7.648	-0.0254
		3		0.9284	21.8407	10.01	-10.6502	-0.0322
		4		0.9711	14.9505	5.7711	-5.8769	-0.0167
		5		0.9777	4.0758	2.8731	-3.0824	-0.0091

Note. r = Correlation between observed and projected future yield (V_2) from early to harvest age; MAD = Mean absolute deviation; RMSE% = Percent mean square error; Bias% = Percent bias

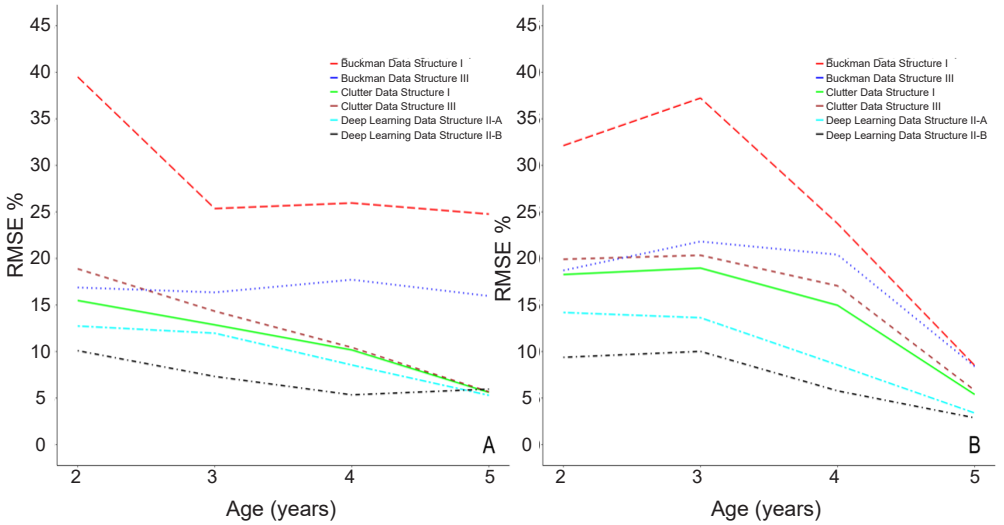

Figure 5. Percent root mean square error (RMSE%) of volumetric projections from early to harvest age by Clutter, Buckman, and deep learning models using a study data structure in hybrid eucalypt stands
Note. A = Harvest age at 6 years; B = Harvest age at 7 years

DISCUSSION

This study analyzed the effect of a monthly data structure on the accuracy and projection of the Clutter, Buckman modified by A. L. da Silva et al. (2006), and deep learning models.

In the case of WSM, the site index was acquired by utilizing the guide curve method and fitting the Gompertz model. This model is very well suited to represent the dominant height growth in eucalypt stands (Reis et al., 2022) since it follows a pattern of biological realism indicating an inflection point at its maximum growth rate, and from there, it indicates its decrease and stagnation of growth (W. S. Silva et al., 2021), a usual asymptotic characteristic in the growth of trees. Although the guide curve method has indeed been criticized for a long time (Socha & Tymińska-Czabańska, 2019), it is the method most used by the forest industries in Brazil, due to its ease of application and without prejudice to growth and yield projections. However, if the purpose is purely to classify the productive capacity, it may present errors, and it is up to the modeler in charge of the study area to be careful.

These two variable density models usually have a database structure with fixed age intervals between two consecutive measurements. Likely, the Clutter model was always fitted using a data structure in which the information was organized by pairing the ages as i as $i+1$. For example, if measurements were taken at 2, 3, 4, and 5 years then, to fit the Clutter model, the data were paired in 2–3, 3–4, and 4–5, that is, four records or lines from a permanent plot are transformed into three records.

The idea of changing the database structure with growth intervals to fit growth and production models arose from the principle of implementing non-parametric methods (Mongus et al., 2018; Vieira et al., 2018). Furthermore, statistical assumptions are likely to be violated due to the longitudinal characteristics of the data. Nevertheless, it is essential to consider that the growth intervals can be utilized for obtaining the parameters (Dorado, 2004), and the data can also be organized for the evaluations of volumetric projections.

The Clutter model is widely used in the forestry field and is the most widespread model in Brazil (Campos & Leite, 2017), with many studies conducted and preferred by researchers that over the years, it has served as a reference to express other growth and production (Soares et al., 2004), which gives it a fundamental relevance in forestry measurement works.

Authors highlighted using the modified Buckman model for volumetric estimates (A. L. da Silva et al., 2006; Guera et al., 2019), but the model is not used commercially in Brazil. This study presented results of its volumetric estimates that were highly biased when fitted with the usual data structure (Data Structure I); however, the model had an increase in accuracy when fitted with Data Structure III. The model may not have been used in Brazil due to inconsistencies in the projections because of how the database is organized. The repeated solutions method was used to obtain the basal area, which

consists of repeated solutions based on the basal area and involves solving the growth equation for a given site index, age, and population density. The growth is then added to the early density, one month is added to the age, and the equation is solved again (A. L. da Silva et al., 2006). The database structure may rely on an equation for future studies to obtain the monthly data.

The data to fit the Buckman model can, in principle, be arranged in constant one-year (or monthly) intervals for all plots. However, the organization in one-year intervals limits the application of the model in strategic planning because it is often necessary to make production projections for each management unit for a single reference month, for example, December of each year. In this case, monthly projections are needed since the early measurements of the plot are not the same.

The use of artificial neural networks has solved several problems in forest management and, in most cases, with higher accuracy than regression models. In general, many studies have demonstrated the effectiveness of the use of artificial neural networks (da Rocha et al., 2021; da Silva Binoti et al., 2013; de Alcântra et al., 2018; de Freitas et al., 2020; dos Reis Martins et al., 2016), even when comparing artificial neural networks with regression methods, ANNs show superiority in their statistical results (Casas, Fardin, et al., 2022; da Silva Binoti et al., 2014; da Silva Tavares Júnior et al., 2019; Lopes et al., 2020; M. L. M. da Silva et al., 2009; Vendruscolo et al., 2017).

A large amount of data was used in this study, which led to the use of the deep learning method. Deep learning has a hierarchical structure, which makes it particularly suitable for learning knowledge hierarchies (Nielsen, 2015). This evidence can be seen when analyzing their residual distribution graphs, in which deep learning develops with robust and constant variance, and even more so when Data Structure II-B is used (Figure 4F).

The volumetric projections were statistically analyzed for projection ages of 6 and 7 years, and it was seen that the deep learning method presents superiority in its statistical evaluation, especially when using a monthly distributed data structure (Data Structure II-B). Using the deep learning method with an II-B Data Structure, the percent mean square error (RMSE%) decreased more than the other methods and data structure (Figure 5B). However, it still does not achieve statistical performance (when the early age is 2 or 3 years) equal to that achieved when the early age is close to the projection age, i.e., from the early age of five years to a projection age of six or seven years.

Models to predict future yield improve the understanding of tree growth in forest plantations (Lhotka, 2017). Project for close ages is recommended, as yield can be overestimated when projected for lengthy intervals (Weiskittel et al., 2016). This study's findings confirm a consistent pattern observed in growth modeling studies: lower accuracy in projections when conducted from an early age (around two years), irrespective of the chosen model.

This study confirms what has been seen in growth modeling studies, i.e., lower accuracy when the projection is made from an early age (approximately two years), regardless of the model used.

It is highly likely that this could vary if a larger number of categorical variables, such as soil type, were used (Casas, Fardin, et al., 2022); however, not all forest industries have access to such information. This study has made an effort to utilize simple models and readily available variables accessible to the forestry scientific community and the forest industry.

CONCLUSION

A better alternative to increase the statistical assumptions of the forecast from early to harvest age is based on a monthly distributed data structure using the deep learning method. It is set up so that the Clutter model should be fitted in the usual way it has been fitted, i.e., with the Data Structure I. Fitting the Buckman model requires uniform intervals between measurements. In the case of eucalypt stands, it must be a monthly interval to be effectively applied in strategic planning. The Buckman model was most accurate when data were organized month-by-month and without overlap, corresponding to Data Structure III evaluated in this study. Investing more in research is necessary to obtain greater assertiveness and precision in projections from an early age with variables that are easy to get.

FUNDING

This study was financed in part by the "Fundação de Amparo à Pesquisa do Estado de Minas Gerais—FAPEMIG"—Financing Code 507, and the "Coordenação de Aperfeiçoamento de Pessoal de Nível Superior, Brasil—CAPES"—Financing Code 001, in collaboration with the "Fundação Arthur Bernardes—FUNARBE."

ACKNOWLEDGMENTS

The authors are grateful to the "Fundação de Amparo à Pesquisa do Estado de Minas Gerais—FAPEMIG"—Financing Code 507, "Coordenação de Aperfeiçoamento de Pessoal de Nível Superior, Brasil—CAPES"—Financing Code 001, "Fundação Arthur Bernardes—FUNARBE" and Federal University of Viçosa, Brazil.

REFERENCES

Aggarwal, C. C. (2018). *Neural networks and deep learning*. Springer. https://doi.org/10.1007/978-3-319-94463-0

Alvares, C. A., Stape, J. L., Sentelhas, P. C., Gonçalves, J. D. M., & Sparovek, G. (2013). Köppen's climate classification map for Brazil. *Meteorologische Zeitschrift*, *22*(6), 711-728. https://doi.org/10.1127/0941-2948/2013/0507

Araújo Júnior, C. A., de Souza, P. D., de Assis, A. L., Cabacinha, C. D., Leite, H. G., Soares, C. P. B., da Silva, A. A. L., & Castro, R. V. O. (2019). Artificial neural networks, quantile regression, and linear regression for site index prediction in the presence of outliers. *Pesquisa Agropecuária Brasileira*, *54*, e00078. https://doi.org/10.1590/S1678-3921.pab2019.v54.00078

Buckman, R. E. (1962). *Growth and yield of red pine in Minnesota*. AgEcon Search: Research in Agricultural and Applied Economics. https://doi.org/10.22004/ag.econ.170997

Burkhart, H. E., & Sprinz, P. T. (1984). Compatible cubic volume and basal area projection equations for thinned old-field loblolly pine plantations. *Forest Science*, *30*(1), 86–93. https://doi.org/10.1093/forestscience/30.1.86

Burkhart, H. E., & Tomé, M. (2012). *Modeling forest trees and stands*. Springer. https://doi.org/10.1007/978-90-481-3170-9

Campos, J. C. C., & Leite, H. G. (2017). *Mensuração florestal: Perguntas e respostas* (5. ed. atual. e ampl.) [Forest measurement: Questions and answers (5th ed.)]. Editora Universidade Federal de Viçosa.

Cao, Q. V. (1993). Estimating coefficients of base-age-invariant site index equations. *Canadian Journal of Forest Research*, *23*(11), 2343–2347. https://doi.org/10.1139/x93-288

Casas, G. G., Fardin, L. P., Silva, S., de Oliveira Neto, R. R., Binoti, D. H. B., Leite, R. V., Domiciano, C. A. R., de Sousa Lopes, L. S., da Cruz, J. P., do Reis, T. L., & Leite, H. G. (2022). Improving yield projections from early ages in eucalypt plantations with the clutter model and artificial neural networks. *Pertanika Journal of Science and Technology*, *30*(2), 1257–1272. https://doi.org/10.47836/pjst.30.2.22

Casas, G. G., Gonzáles, D. G. E., Villanueva, J. R. B., Fardin, L. P., & Leite, H. G. (2022). Configuration of the deep neural network hyperparameters for the hypsometric modeling of the *Guazuma crinita* Mart. in the Peruvian Amazon. *Forests*, *13*(5), 697. https://doi.org/10.3390/f13050697

Castro, R. V. O., Soares, C. P. B., Martins, F. B., & Leite, H. G. (2013). Growth and yield of commercial plantations of eucalyptus estimated by two categories of models. *Pesquisa Agropecuária Brasileira*, *48*(3), 287–295. https://doi.org/10.1590/S0100-204X2013000300007

Cieszewski, C. J. (2002). Comparing fixed-and variable-base-age site equations having single versus multiple asymptotes. *Forest Science*, *48*(1), 7–23. https://doi.org/10.1093/forestscience/48.1.7

Clutter, J. L. (1963). Compatible growth and yield models for loblolly pine. *Forest Science*, *9*(3), 354–371.

Clutter, J. L., Fortson, J. C., Pienaar, L. v., Brister, G. H., & Bailey, R. L. (1983). *Timber management: A quantitative approach*. John Wiley & Sons Inc.

da Rocha, J. E. C., Junior, M. R. N., da Silva Tavares Júnior, I. S., de Souza, J. R. M., de Sousa Lopes, L. S., da Silva, M. L. (2021). Configuration of artificial neural networks for height-diameter relationship of *Eucalyptus* spp. *Scientia Forestalis*, *49*(132), e3706. https://doi.org/10.18671/scifor.v49n132.08

da Silva Binoti, M. L. M., Binoti, D. H. B., & Leite, H. G. (2013). Application of artificial neural networks to estimate the height of equine eucalyptus stands. *Revista Árvore*, *37*(4), 639–645. https://doi.org/10.1590/S0100-67622013000400007

da Silva Binoti, M. L. M., Binoti, D. H. B., Leite, H. G., Garcia, S. L. R., Ferreira, M. Z., Rode, R., & da Silva, A. A. L. (2014). Neural networks for estimating of the volume of trees. *Revista Árvore*, *38*(2), 283–288. https://doi.org/10.1590/S0100-67622014000200008

da Silva Binoti, M. L. M., Leite, H. G., Binoti, D. H. B., & Gleriani, J. M. (2015). Stand-level prognosis of eucalyptus clones using artificial neural networks. *Cerne*, *21*(1), 97-105. https://doi.org/10.1590/01047760201521011153

da Silva Tavares Júnior, I., da Rocha, J. E. C., Ebling, Â. A., de Souza Chaves, A., Zanuncio, J. C., Farias, A. A., & Leite, H. G. (2019). Artificial neural networks and linear regression reduce sample intensity to predict the commercial volume of *Eucalyptus* clones. *Forests*, *10*(3), 268. https://doi.org/10.3390/f10030268

da Silva, A. L., Campos, J. C. C., Leite, H. G., de Souza, A. L., & Lopes, P. F. (2006). Growth and

yield prediction using the modified Buckman model. *Revista Árvore*, *30*(5), 787–793. https://doi.org/10.1590/S0100-67622006000500012

da Silva, M. L. M., Binoti, D. H. B., Gleriani, J. M., & Leite, H. G. (2009). Adjustment of the Schumacher and Hall model and application of artificial neural networks to estimate volume of eucalyptus trees. *Revista Árvore, 33*(6), 1133–1139. https://doi.org/10.1590/S0100-67622009000600015

Davis, L. S., & Johnson, K. N. (1987). *Forest management* (3rd ed.). McGrawHill Book Company.

de Alcântra, A. E. M., de Albuquerque Santos, A. C., da Silva, M. L. M., Binoti, D. H. B., Soares, C. P. B., Gleriani, J. M., & Leite, H. G. (2018). Use of artificial neural networks to assess yield projection and average production of eucalyptus stands. *African Journal of Agricultural Research*, *13*(42), 2285–2297. https://doi.org/10.5897/ajar2017.12942

de Freitas, E. C. S., de Paiva, H. N., Neves, J. C. L., Marcatti, G. E., & Leite, H. G. (2020). Modeling of eucalyptus productivity with artificial neural networks. *Industrial Crops and Products*, *146*, 112149. https://doi.org/10.1016/j.indcrop.2020.112149

de Oliveira Neto, R. R., Leite, H. G., Gleriani, J. M., & Strimbu, B. M. (2022). Estimation of eucalyptus productivity using efficient artificial neural network. *European Journal of Forest Research*, *141*, 129–151. https://doi.org/10.1007/s10342-021-01431-7

de Oliveira Neto, R. R., Rodrigues, L. F., Mari, J. F., Naldi, M. C., Milagres, E. G., Vital, B. R., de Cássia Oliveira Carneiro, A., Binoti, D. H. B., Lopes, P. F., & Leite, H. G. (2021). Automatic identification of charcoal origin based on deep learning. *Maderas. Ciencia y tecnología*, *23*(65), 1-12. https://doi.org/10.4067/S0718-221X2021000100465

Dorado, F. C. (2004). *Modelo dinámico de crecimiento para las masas de "*Pinus radiata *D. Don" en Galicia* [Dynamic growth model for stands of "*Pinus radiata* D. Don" in Galicia] [Doctoral dissertation, Universidade de Santiago de Compostela]. Dialnet. https://dialnet.unirioja.es/servlet/tesis?codigo=106294

dos Reis Martins, E., da Silva Binoti, M. L. M., Leite, H. G., Binoti, D. H. B., & Dutra, G. C. (2016). Configuração de redes neurais artificiais para estimação do afilamento do fuste de árvores de eucalipto [Configuration of artificial neural networks to estimate the thinning of the shaft of *Eucalyptus* trees]. *Revista Brasileirade Ciencias Agrarias*, *11*(1), 33–38. https://doi.org/10.5039/agraria.v11i1a5354

Ferreira, M. P., de Almeida, D. R. A., de Almeida Papa, D., Minervino, J. B. S., Veras, H. F. P., Formighieri, A., Santos, C. A. N., Ferreira, M. A. D., Figueiredo, E. O., & Ferreira, E. J. L. (2020). Individual tree detection and species classification of Amazonian palms using UAV images and deep learning. *Forest Ecology and Management*, *475*, 118397. https://doi.org/10.1016/j.foreco.2020.118397

Fryda, T., LeDell, E., Gill, N., Aiello, S., Fu, A., Candel, A., Click, C., Kraljevic, T., Nykodym, T., Aboyoun, P., Kurka, M., Malohlava, M., Poirier, S., Wong, W., Rehak, L., Eckstrand, E., Hill, B., Vidrio, S., Jadhawani, S., … Novotny, M. (2020). *H2O: R interface for the 'H2O' scalable machine learning platform*. https://CRAN.R-project.org/package=h2o

Gavilán-Acuña, G., Olmedo, G. F., Mena-Quijada, P., Guevara, M., Barría-Knopf, B., & Watt, M. S. (2021). Reducing the uncertainty of radiata pine site index maps using an spatial ensemble of machine learning models. *Forests*, *12*(1), 77. https://doi.org/10.3390/f12010077

Gompertz, B. (1825). On the nature of the function expressive of the law of human mortality, and on a new mode of determining the value of life contingencies. In a letter to Francis Baily, Esq. FRS &c. *Philosophical Transactions of the Royal Society of London*, *115*, 513-583. https://doi.org/10.1098/rstl.1825.0026

Guera, O. G. M., da Silva, J. A. A., Ferreira, R. L. C., Lazo, D. A. Á., & Medel, H. B. (2019). Alternatives to growth and yield prognosis for *Pinus caribaea* var. *caribaea* Barrett & Golfari. *Floresta e Ambiente*, *26*(4), e20170381. https://doi.org/10.1590/2179-8087.038117

Hamdi, Z. M., Brandmeier, M., & Straub, C. (2019). Forest damage assessment using deep learning on high resolution remote sensing data. *Remote Sensing*, *11*(17), 1976. https://doi.org/10.3390/rs11171976

Hirigoyen, A., Franco, J., & Diéguez, U. (2018). Dynamic stand model for *Eucalyptus globulus* (L.) in Uruguay. *Agrociencia Uruguay*, *22*(1), 63–80. https://doi.org/10.31285/AGRO.22.1.7

Kentsch, S., Caceres, M. L. L., Serrano, D., Roure, F., & Diez, Y. (2020). Computer vision and deep learning techniques for the analysis of drone-acquired forest images, a transfer learning study. *Remote Sensing*, *12*(8), 1287.https://doi.org/10.3390/rs12081287

Kleiber, C., & Zeileis, A. (2008). *Applied econometrics with R*. Springer. https://doi.org/10.1007/978-0-387-77318-6

LeCun, Y., Bengio, Y., & Hinton, G. (2015). Deep learning. *Nature*, *521*, 436–444. https://doi.org/10.1038/nature14539

Lhotka, J. M. (2017). Examining growth relationships in *Quercus* stands: An application of individual-tree models developed from long-term thinning experiments. *Forest Ecology and Management*, *385*, 65–77. https://doi.org/10.1016/j.foreco.2016.11.029

Lopes, L. S. S., Rode, R., Pauletto, D., Baloneque, D. D., dos Santos, F. G., Silva, A. R., Binoti, D. H. B., & Leite, H. G. (2020). Uso de regressão e redes neurais artificiais na estimativa do volume de *Khaya ivorensis* [Use of regression and artificial neural networks in the estimation of *Khaya ivorensis* volume]. *Ciência da Madeira*, *11*(2), 74-84. https://doi.org/10.12953/2177-6830/rcm.v11n2p74-84

Miguel, E. P., de Oliveira, C. S., Marthins, T. O., Matias, R. A. M., Rezende, A. V., Angelo, H., & Martins, I. S. (2016). Growth and yield models by total stand (MPT) in *Eucalyptus urophylla* (s.t. Blake) plantations. *Australian Journal of Basic and Applied Sciences*, *10*(13), 79–85.

Mongus, D., Vilhar, U., Skudnik, M., Žalik, B., & Jesenko, D. (2018). Predictive analytics of tree growth based on complex networks of tree competition. *Forest Ecology and Management*, *425*, 164–176. https://doi.org/10.1016/j.foreco.2018.05.039

Nielsen, M. A. (2015). *Neural networks and deep learning*. Determination Press.

Penido, T. M. A., Lafetá, B. O., Nogueira, G. S., Alves, P. H., Gorgens, E. B., & de Oliveira, M. L. R. (2020). Growth and production models for volumetric estimates in commercial eucalypt stands. *Scientia Forestalis*, *48*(128), e3340. https://doi.org/10.18671/scifor.v48n128.06

R Core Team. (2020). *R: A language and environment for statistical computing*. R Foundation for Statistical Computing. https://www.r-project.org

Reis, T., Silva, S., Junior, I. T., Leite, R., Taquetti, M., Atanazio, K., Fardin, L., Cruz, J., & Leite, H. (2022). Assessing alternatives for growth and yield modelling in eucalypt stands. *Southern Forests*, *84*(1), 34–43. https://doi.org/10.2989/20702620.2021.2011468

Salles, T. T., Leite, H. G., de Oliveira Neto, S. N., Soares, C. P. B., de Paiva, H. N., & dos Santos, F. L. (2012). Clutter model in modeling growth and yield of eucalyptus in crop-livestock-forest integration systems. *Pesquisa Agropecuária Brasileira*, *47*(2), 253–260. https://doi.org/10.1590/S0100-204X2012000200014

Sejnowski, T. J. (2020). The unreasonable effectiveness of deep learning in artificial intelligence. *Proceedings of the National Academy of Sciences*, *117*(48), 30033–30038. https://doi.org/10.1073/pnas.1907373117

Silva, S., de Oliveira Neto, S. N., Leite, H. G., de Alcântara, A. E. M., de Oliveira Neto, R. R., & de Souza, G. S. A. (2020). Productivity estimate using regression and artificial neural networks in small familiar areas with agrosilvopastoral

systems. *Agroforestry Systems*, *94*, 2081–2097. https://doi.org/10.1007/s10457-020-00526-1

Silva, W. S., Fernandes, F. A., Muniz, F. R., Muniz, J. A., & Fernandes, T. J. (2021). *Eucalyptus grandis* x *Eucalyptus urophylla* growth curve in different site classifications, considering residual autocorrelation. *Revista Brasileira de Biometria*, *39*(1), 122–138. https://doi.org/10.28951/rbb.v39i1.511

Soares, C. P. B., Leite, H. G., de Oliveira, M. L. R., & Carvalho, A. (2004). Specifying a model of forest growth and yield. *Revista Árvore*, *28*(6), 831–837. https://doi.org/10.1590/S0100-67622004000600007

Socha, J., & Tymińska-Czabańska, L. (2019). A method for the development of dynamic site index models using height-age data from temporal sample plots. *Forests*, *10*(7), 542. https://doi.org/10.3390/f10070542

Strub, M., & Cieszewski, C. J. (2006). Base–age invariance properties of two techniques for estimating the parameters of site index models. *Forest Science*, *52*(2), 182-186.

Sun, Y., Liu, Y., Wang, G., & Zhang, H. (2017). Deep learning for plant identification in natural environment. *Computational Intelligence and Neuroscience*, *2017*, 7361042. https://doi.org/10.1155/2017/7361042

Trevizol Jr., T. L. (1985). *Análise de um modelo compatível de crescimento e produção em plantações de* Eucalyptus grandis *(W. Hill ex Maiden)* [Analysis of a compatible model of growth and production in plantations of *Eucalyptus grandis* (W. Hill ex Maiden)] [Unpublished Master's dissertation]. Universidade Federal de Viçosa.

Vendruscolo, D. G. S., Chaves, A. G. S., Medeiros, R. A., da Silva, R. S., Souza, H. S., Drescher, R., & Leite, H. G. (2017). Height estimation of *Tectona grandis* L.f. trees using regression and artificial neural networks. *Nativa: Pesquisas Agrárias e Ambientais*, *5*(1), 52-58. https://doi.org/10.5935/2318-7670.v05n01a09

Vieira, G. C., de Mendonça, A. R., da Silva, G. F., Zanetti, S. S., da Silva, M. M., & dos Santos, A. R. (2018). Prognoses of diameter and height of trees of eucalyptus using artificial intelligence. *Science of The Total Environment*, *619–620*, 1473–1481. https://doi.org/10.1016/j.scitotenv.2017.11.138

Weiskittel, A., Kuehne, C., McTague, J. P., & Oppenheimer, M. (2016). Development and evaluation of an individual tree growth and yield model for the mixed species forest of the Adirondacks Region of New York, USA. *Forest Ecosystems*, *3*, 26. https://doi.org/10.1186/s40663-016-0086-3

Xi, Z., Hopkinson, C., Rood, S. B., & Peddle, D. R. (2020). See the forest and the trees: Effective machine and deep learning algorithms for wood filtering and tree species classification from terrestrial laser scanning. *ISPRS Journal of Photogrammetry and Remote Sensing*, *168*, 1–16. https://doi.org/10.1016/j.isprsjprs.2020.08.001

Zeiler, M. D. (2012). ADADELTA: An adaptive learning rate method. *arXiv*. https://doi.org/10.48550/arXiv.1212.5701

SUPPLEMENTARY

Table S1

Status of neuron layers of the best models trained with the deep learning method for each Data Structure II-A and II-B in hybrid eucalypt stands

Data Structure II-A								
Status of neuron layers: projection V_2, regression, Gaussian distribution, quadratic loss, 96,751 weights/biases, 183,078 training samples, mini-batch size 1								
Layer	Units	Type	mean_rate	rate_rms	mean_weight	weight_rms	mean_bias	bias_rms
2	200	Maxout	0.1394	0.3614	0.0002	0.0803	0.4891	0.0516
3	100	Maxout	0.1435	0.3666	-0.0018	0.0826	0.9977	0.0056
4	50	Maxout	0.3001	0.4548	-0.0015	0.1142	0.9996	0.0019
5	1	Linear	0	0	-0.0486	0.1955	0.0022	0
Data Structure II-B								
Status of neuron layers: projection V_2, regression, Gaussian distribution, quadratic loss, 16,701 weights/biases, 3,104,698 training samples, mini-batch size 1								
Layer	Units	Type	mean_rate	rate_rms	mean_weight	weight_rms	mean_bias	bias_rms
2	100	Rectifier	0.1125	0.1714	-0.0114	0.3045	-0.4842	0.6457
3	50	Rectifier	0.1088	0.1225	-0.1333	0.4122	0.5021	0.5974
4	1	Linear	0.0049	0.0058	0.0006	0.2037	0.3875	0

Pertanika J. Trop. Agric. Sci. 46 (4): 1151 - 1172 (2023)

PERTANIKA JOURNALS

TROPICAL AGRICULTURAL SCIENCE

Journal homepage: http://www.pertanika.upm.edu.my/

Evaluation of Sowing Methods and Herbicide Mixtures for Weed Management and Productivity in Sesame (*Sesamum indicum* L.)

Emmanuel Oyamedan Imoloame* and Lukman Funsho Abubakar

Department of Crop Production, Kwara State University, Malete, P.M.B. 1530, Ilorin, Kwara State, Nigeria

ABSTRACT

Sesame is an oil seed crop with great economic value. However, the production of this crop has been limited by weed competition, which prompted a field experiment during the 2021 cropping season in two locations: Teaching and Research Farm, Kwara State University, Malete, and National Centre for Agricultural Mechanization (NCAM), Idofian, Ilorin, Kwara, Nigeria. The aim was to determine the treatment combinations of sowing methods and herbicide mixtures for the effective management of weeds and for increasing sesame productivity in the southern Guinea savanna of Nigeria. The experiment consisted of twenty treatments comprising two sowing methods (dibbling and drilling) and ten weed control methods. Results showed that all the weed control methods reduced weed dry matter (67.15–186.20 and 42.00–92.45 g/m^2) than the weedy check (291.55 and 155.55 g/m^2) at Malete and NCAM, respectively. They also reduced the weed density (48.40–68.45 and 34.00–50.00/m^2) compared to the weedy check (103.60 and 73.15 g/m^2) at Malete and NCAM, respectively, from 6 to 12 weeks after planting (WAP). Dibbling (85.15 and 48.81 m^2) proved superior to the drilling method (172.42 and 51.58/m^2) for the management of weeds from 6–12 WAP and for promoting higher crop yield (dibbling: 78.90 and 422.70 kg/ha; drilling: 37.50 and 326.80 kg/ha) in Malete and NCAM, respectively. The treatment combinations with the highest gross margin were hoeing twice at 3 and 6 WAP × dibbling ($ -191.15 and $ 318.57), pendimethalin (P) + diuron (D) at 0.5 + 0.5 kg a.i./ha ($ -199.88 and $ 182.43), 2.0 + 1.5 × dibbling ($ -273.59 and $ 156.65) and butachlor (B) + diuron (D) at 1.5 + 1.0 kg a.i./ha × drilling ($ -269.59 and $ 177.38) at Malete and NCAM, respectively. Therefore, it is recommended that the dibbling sowing method at a spacing of 30 cm × 30 cm and thinned to 3 plants/stand integrated

ARTICLE INFO

Article history:
Received: 25 March 2023
Accepted: 18 May 2023
Published: 07 November 2023

DOI: https://doi.org/10.47836/pjtas.46.4.05

E-mail addresses:
oyaimoloame@yahoo.com (Emmanuel Oyamedan Imoloame)
funshoabubakar3@gmail.com (Lukman Funsho Abubakar)
* Corresponding author

ISSN: 1511-3701
e-ISSN: 2231-8542

with herbicide mixtures of pendimethalin at 0.5 + 0.5 kg a.i./ha is recommended as an alternative to hoe weeding for effective weed control, higher yield of sesame, and economic returns.

Keywords: Agro-chemical, dibbling method, drilling sowing method, economic returns, weed control

INTRODUCTION

Sesame (*Sesamum indicum* L.) is cultivated in almost all tropical and sub-tropical countries of Asia and Africa for its highly nutritious and edible seeds. It is an oil crop grown in 26 states of Nigeria, including areas in the northeast, north-central, middle belt, and Federal Capital Territory (Ibirogba, 2021). Sesame seeds are very nutritious and, therefore, confer health benefits. Sudan is Africa's largest producer of sesame, with an output of 11.2 million tons in 2019. Sudan alone accounts for 45.8% of the total output of the top six African countries. Nigeria is the second largest producer in Africa, as her production output constitutes 18.2% (Muktar, 2021). The crop is a very important cash crop, which Nigeria is exporting. The sesame seeds exported to Japan account for 40% of sesame consumed in Japan, which netted $ 143,650,800 for Nigeria in 2021 (Odunewu, 2022). The average grain yield of sesame per hectare in Africa is still low, between 150-250 kg/ha (Adefeko, 2017), while the global sesame grain yield is around 500 kg/ha (Myint et al., 2020). The low productivity has discouraged growers, reducing the total area under sesame cultivation. Among the factors responsible for low yield in Nigeria are poor agronomic practices by Nigerian farmers, inappropriate sowing methods, and weed control problems (Take-tsaba et al., 2011).

Most peasant smallholder sesame farmers use a broadcast method of sowing for sesame production. However, this method has been reported to be inferior to the drilling method as it lacked the ability to suppress weeds and increase sesame yield compared to the drilling method in the Sudan savanna zone of Nigeria (Imoloame et al., 2007). Furthermore, in the same agroecological zone of Nigeria, the drilling method was reported to promote sesame yield rather than dibbling and broadcasting (Katanga et al., 2017). In contrast to this, Ngala et al. (2013) reported that the dibbling method, with crop spacing of 50 cm x 25 cm, and 4–6 plants per stand (320,000–480,000 plant/ha) was the best combination for optimizing the agronomic performance of sesame. Also, Take-tsaba et al. (2011) reported that dibbling of sesame seeds at a spacing of 30 cm × 30 cm with 3 plants per stand resulted in maximum sesame yield. Aside from the method of sowing, weed competition is another factor that reduces the yield of sesame (Mane et al., 2017). When weed control is not adopted, especially during the initial periods, sesame yield may be reduced by up to 75% (Bhadauria et al., 2012). It is similar to the findings of Ijlal et al. (2011), who reported reduced sesame yield by 35–70% due to uncontrolled weeds. Using a single herbicide for a prolonged period may not provide effective weed control due to the

diverse nature of the weed community and the fact that it can result in the development of herbicide-resistant weeds or weed flora shift (Das, 2011). Therefore, to ensure more effective weed control and an eco-friendly environment, several researchers have advocated integrated weed management or herbicide mixtures (Imoloame, 2021; Lawal et al., 2019; Young et al., 2017).

Dibbling and drilling have been identified as more promising methods of sowing than broadcast methods for optimizing sesame yield in the Sudan savanna zone of Nigeria. However, there is a dearth of information comparing the effectiveness of these sowing methods for the management of weeds and for promoting sesame yield in the Southern Guinea savanna of Nigeria. Therefore, any research that seeks to find out the best combination of sowing method and herbicide mixture for effective weed management and increasing sesame yield would constitute an important production package that could be recommended to farmers for boosting sesame production and economic returns in the southern Guinea savanna of Nigeria. The objectives of this study were to determine the appropriate sowing, weed control method, and the best treatment combination that will provide effective weed management and higher productivity of sesame.

MATERIALS AND METHODS

Site

Field trials were established during the wet season of 2021 at the Teaching and Research (T&R) Farm of the Kwara State University, Malete, (8˚23'N, 4˚43'E) and National Centre for Agricultural Mechanization (NCAM), Idofian, Ilorin, Kwara (8°71'N, 4°41'E) both locations are in the southern Guinea savanna zone of Nigeria. The soil in both locations was sandy loam. However, the soil at NCAM was richer than Malete's in terms of total nitrogen, available phosphorus, and organic carbon (Table 1). Furthermore, the soil in Malete has been subjected to more years of cultivation than NCAM.

Treatment and Experimental Design

The experiment was a 2 × 10 factorial in a randomized complete block design (RCBD) with three replications. The main plot was assigned sowing methods (drilling and dibbling), while the sub-plots contained the herbicides mixtures, namely tank mixture of butachlor (B, SunRice, China) + diuron (D, Arrow, China) at 1.0 + 0.5, 1.5 + 1.0, 2.0 + 1.5, 1.0 + 0.5 kg a.i./ha + one supplementary hoe weeding (1 SHW) at 6 WAP; pendimethalin (P, Force Up, China) + diuron (D, Arrow, China) at 0.5 + 0.5, 1.0 + 1.0, 2.0 + 1.5, 0.5 + 0.5 kg a.i./ha + 1 SHW at 6 WAP, hand weeding at 3 and 6 WAP and a weedy check. The herbicides were applied pre-emergence a day after sowing.

Field Establishment and Management Practices

After the experimental fields were prepared and demarcated into subplots of 3 m × 3 m, sesame seeds (variety E8, National Cereals Research Institute, Nigeria) at 8 kg/ha were dibbled and spaced at 30 cm × 30 cm in one of the main plots, while the other plots were drilled with the same

sesame seed rate per hectare at a spacing of 60 cm × 60 cm. The emerged seedlings from the dibbled plots were thinned to 3 plants/stand at 4 WAP to maintain a plant population of 333,333 plants/ha, while the drilled seedlings were not thinned. Sowing was done at the T&R Farm on August 3 and 10, 2021, at NCAM. All the herbicide mixtures were tank-mixed and applied pre-emergence a day after sowing sesame seeds using a knapsack sprayer and a green nozzle calibrated to deliver herbicide solution at 250 L/ha. Spraying was done on August 4, 2021, at the T&R Farm and August 11, 2021, at NCAM. Two hoeing was done at 3 and 6 WAP for one of the treatments (weeded control), while the other control (weedy control) was left weedy throughout the season, and two other treatments received 1 SHW at 6 WAP. Fertilizer (NPK:15:15:15) was applied to provide nutrients at the rate of 92 kg nitrogen (N_2), 22 kg phosphorus pentoxide (P_2O_5), and 22 kg potassium oxide (K_2O) to sesame. It was applied in two split doses at planting and 6 WAP. Harvesting was done at the T&R Farm on October 14, while that of NCAM was on November 8, 2021. The inner rows were harvested, while the last rows on either side of the plots were jettisoned**.** The dried pods from the net plots were threshed manually to separate the seeds from the pods, followed by winnowing to separate the grains from the chaff.

Parameters Measured

Weed Sampling

Weed density (no./m^2) and weed biomass (g/m^2) were measured at 6 and 12 WAP. Weed density was measured by counting the number of weed species in a 1 m^2 quadrat, randomly thrown in three locations in each plot, and the weed dry matter was determined by uprooting and gathering weed species within a 1 m^2 quadrat thrown randomly in three locations within each plot, oven-dried at 80^{o}C for two days and weighed to determine total dry matter per treatment.

Growth Assessment

Plant height was taken using a measuring tape to measure the height of five tagged plants in each plot (net plot) from the soil surface to the apex at 9 and 12 WAP.

Yield Component and Grain Yield Measurement

Pods from each of the five tagged plants in each plot (net plot) were counted at 8 and 10 WAP, and the average was calculated and recorded. Seeds harvested from the net plot in each plot were weighed and converted to kilogram per hectare for analysis.

Economic Evaluation

The economic performance of different treatment combinations of weed control treatments and sowing methods was obtained by calculating the total cost of production, total revenue, and gross income. Production cost (PC) was determined by adding the cost of inputs and farm operations used. These included seeds, herbicides, fertilizers, land preparation, labor for planting, herbicide and application, weeding, fertilizer application, harvest, and processing operations.

$$PC = PC_1 + PC_2 + PC_3 + \text{----------} PCn \quad (1)$$

Gross revenue (GR) = Crop yield (Y) × Open market price (P) (2)

Gross margin/Net revenue (NR) = Gross Revenue (GR) - Production cost (PC) (3)

Eni et al. (2013)

Data Analysis

Data collected were subjected to analysis of variance (ANOVA) using the GENSTART (version 5.32) package, and means were separated using Turkey's honestly significant difference (HSD) test at a 5% level of probability.

RESULTS

Soil Physico-chemical Characteristics

The soil of the experimental sites at Malete and NCAM was loamy sand. However, the soil at NCAM was richer than the one at Malete in terms of total nitrogen, available phosphorus, and organic carbon (Table 1).

Rainfall

The total rainfall recorded in 2021 at NCAM was 1,881.10 mm, while that of Malete was 1,233.90 mm (Table 2).

Weeds

Among the weed control methods, herbicide mixtures, P + D and B + D at 2.0 +1.5 kg a.i./ha (67.15 and 109.75 g/m^2, respectively), and hoeing twice (88.90 g/m^2) resulted in the least weed dry biomass compared to the weedy check (291.55 g/m^2) in Malete, while at NCAM, hoeing twice (42.00 g/m^2), B + D at 1.5 + 1.0 kg a.i./ha (53.25 g/m^2), P + D 0.5 + 0.5 kg a.i./ha (58.70 g/m^2) and at 0.5 + 0.5 kg a.i./ha + I SHW (63.10 g/m^2) resulted in the least weed biomass compared to the other treatments and weedy check (155.55 g/m^2) at 6 WAP (Table 3). Dibbling (85.15 g/m^2) significantly ($P < 0.05$) reduced weed biomass than the drilling method (172.42 g/

Table 1
Physical and chemical properties of the soil at the experimental site

Soil parameters	T&R Farm Malete	NCAM
Sand (%)	80.0	79.0
Silt (%)	9.0	13.0
Clay (%)	11.0	8.0
Textural class	Sandy loam	Sandy loam
Organic carbon (%)	0.72	1.21
Total nitrogen (%)	0.10	0.14
Available phosphorus (mg/kg)	6.56	6.68
pH	6.80	6.9
Exchangeable Mg (cmol/kg)	1.19	1.38
Exchangeable K (cmol/kg)	0.37	0.24
Exchangeable Ca (cmol/kg)	4.25	1.98
Exchangeable Na (cmol/kg)	0.79	0.70
Exchangeable acidity (cmol/kg)	0.40	0.30
Mn (mg/kg)	140.0	110.0
Fe (mg/kg)	130.0	98.0
Cu (mg/kg)	1.23	1.04
Zn (mg/kg)	0.90	0.92

Note. T&R Farm Malete = Teaching and Research (T&R) Farm of the Kwara State University, Malete; NCAM = National Centre for Agricultural Mechanization (NCAM), Idofian, Ilorin, Kwara, Nigeria

Table 2
Monthly rainfall (mm) at the experimental sites

Month	T&R Farm Malete	NCAM
January	0.00	0.00
February	0.00	0.00
March	10.00	29.60
April	100.50	123.80
May	120.80	131.80
June	200.60	335.30
July	150.00	121.90
August	276.00	234.70
September	366.00	508.70
October	40.00	229.30
November	0.00	166.00
December	0.00	0.00
Total	1,233.90	1,881.10

Note. T&R Farm Malete = Teaching and Research (T&R) Farm of the Kwara State University, Malete; NCAM = National Centre for Agricultural Mechanization (NCAM), Idofian, Ilorin, Kwara, Nigeria; Source for NCAM = Kwara State Agricultural Development Project (Hydrology section), Ilorin, 2021; Source for Malete = Faculty of Agriculture, Kwara State University, Malete (Meteorological Station), 2021

m^2) at Malete between 6 and 12 WAP. The same trend occurred at NCAM as dibbling (48.81 g/m^2) significantly controlled weed better than the drilling (51.58 g/m^2). At both locations at 6 and 12 WAP, Malete had significantly ($P < 0.05$) higher amounts of weeds (149.06 and 128.79 g/m^2) than NCAM (77.17 and 50.20 g/m^2) (Tables 3 and 4). Also, the interaction effect of location and sowing methods was significant ($P < 0.05$) on weed biomass at 12 WAP, as dibbling provided more effective weed control than the drilling method in both locations (Table 4). Similarly, in both locations, all the weed control methods significantly reduced weed density compared to the weedy check at 6 and 12 WAP (Tables 5 and 6). However, twice hoeing (48.40/m^2) and P + D at 0.5 + 0.5 kg a.i./ha had the least weed density (54.45/m^2) in Malete, while at NCAM, P + D at 0.5 + 0.5 kg a.i./ha resulted in the least weed dry matter (34.00/m^2) at 6 WAP (Table 5). Also, B + D at 1.0 + 0.5 and 1.5 + 1.0 kg a.i./ha resulted in the least weed density (38.55 and 8.65/m^2) in Malete and NCAM at 12 WAP, respectively (Table 6). Malete had significantly ($P < 0.05$) higher weed density (62.66 and 46.27/m^2) than NCAM (45.53 and 12.60/m^2) at 6 and 12 WAP, respectively (Tables 5 and 6). At 12 WAP, the interaction effect of location and sowing method on weed density was significant ($P < 0.05$) as plots treated with the dibbling method of sowing had significantly lower weed density than the drilling methods in Malete, while drilling was better in reducing weed density at NCAM (Table 6).

Crop Growth

In Malete, all the weed control treatments produced sesame plants of comparable height but were significantly taller than those in the weedy check. A similar trend was observed at NCAM as the weedy check resulted in significantly shorter plants than all the weed control treatments ($P < 0.05$). Comparing the two locations, sesame plants in Malete were significantly shorter (88.77 cm) than those at NCAM (105.09 cm) at 9 WAP ($P \leq 0.05$) (Table 7). The interaction effects of the sowing method and weed control were significant as the hoe weeding and drilling method resulted in the tallest

Table 3
Effects of weed control and sowing methods on weed biomass (g/m²) at 6 weeks after planting (WAP)

Weed control (WC)	Location (L)	T&R Farm Malete			NCAM		
	Sowing method (SM)	DB	DL	WC Mean	DB	DL	WC mean
B + D 1.0 + 0.5 kg a.i./ha		181.30	96.90	139.10	95.00	64.90	79.95
B + D 1.0 + 0.5 kg a.i./ha + 1 SHW (6 WAP)		226.70	112.90	169.80	105.80	30.20	68.00
B + D 1.5 + 1.0 kg a.i./ha		88.00	136.00	112.00	45.30	61.20	53.25
B + D 2.0 + 1.5 kg a.i./ha		149.30	70.20	109.75	61.40	71.10	66.25
Hoe weeding (3 and 6 WAP)		48.00	129.80	88.90	48.90	35.10	42.00
P + D 0.5 + 0.5 kg a.i./ha		90.70	218.50	154.60	65.80	51.60	58.70
P + D 1.0 + 1.0 kg a.i./ha		174.20	168.90	171.55	98.70	86.20	92.45
P + D 2.0 + 1.5 kg a.i./ha		43.60	90.70	67.15	117.30	67.50	92.40
P + D 0.5 + 0.5 kg a.i./ha + 1 SHW (6 WAP)		189.30	183.10	186.20	90.60	35.60	63.10
Weedy check		331.50	251.60	291.55	163.50	147.60	155.55
SM mean		152.26	145.86	149.06	89.23	65.10	77.17
Tukey ($P < 5\%$)	Standard error						
L	13.46*						
SM	13.66						
WC	30.56*						
L × SM	19.33						
L × WC	43.21						
SM × WC	43.21						
L × SM × WC	61.11						

Note. T&R Farm Malete = Teaching and Research (T&R) Farm of the Kwara State University, Malete; NCAM = National Centre for Agricultural Mechanization (NCAM), Idofian, Ilorin, Kwara, Nigeria; Standard error = Standard error of the difference between treatment mean; * = Significant at $P < 0.05$; DB = Dibbling sowing method; DL = Drilling sowing method; B = Butachlor; D = Diuron; P = Pendimerhalin; 1 SHW = One supplementary hoe weeding

Table 4
Effects of weed control and sowing methods on weed biomass (g/m²) at 12 weeks after planting (WAP)

Weed control (WC)	Location (L)	T&R Farm Malete			NCAM		
	Sowing method (SM)	DB	DL	WC mean	DB	DL	WC mean
B + D 1.0 + 0.5 kg a.i./ha		88.90	166.70	127.80	40.10	49.40	44.75
B + D 1.0 + 0.5 kg a.i./ha + 1 SHW (6 WAP)		98.10	244.40	171.25	28.20	30.40	29.30
B + D 1.5 + 1.0 kg a.i./ha		105.60	209.30	157.45	68.90	52.80	60.85
B + D 2.0 + 1.5 kg a.i./ha		109.30	192.60	150.95	39.10	49.50	44.30
Hoe weeding (3 and 6 WAP)		41.70	161.10	101.40	29.90	23.80	26.85
P + D 0.5 + 0.5 kg a.i./ha		81.50	225.90	153.70	38.00	39.80	38.90
P + D 1.0 + 1.0 kg a.i./ha		65.30	113.00	89.15	34.50	49.20	41.85

Table 4 *(continue)*

Weed control (WC)	Location (L)	T&R Farm Malete			NCAM		
	Sowing method (SM)	DB	DL	WC mean	DB	DL	WC mean
P + D 2.0 + 1.5 kg a.i./ha		113.90	174.00	143.95	63.80	54.70	59.25
P + D 0.5 + 0.5 kg a.i./ha + 1 SHW (6 WAP)		88.00	105.70	96.85	46.70	51.70	49.20
Weedy check		59.20	131.50	95.35	98.90	114.50	106.70
SM mean		85.15	172.42	128.79	48.81	51.58	50.20
Tukey ($P < 5\%$)	Standard error						
L	12.51*						
SM	12.51*						
WC	27.97						
L × SM	17.69*						
L × WC	39.51						
SM × WC	39.55						
L × SM × WC	55.94						

Note. T&R Farm Malete = Teaching and Research (T&R) Farm of the Kwara State University, Malete; NCAM = National Centre for Agricultural Mechanization (NCAM), Idofian, Ilorin, Kwara, Nigeria; Standard error = Standard error of the difference between treatment mean; * = Significant at $P < 0.05$; DB = Dibbling sowing method; DL = Drilling sowing method; B = Butachlor; D = Diuron; P = Pendimerhalin; 1 SHW = One supplementary hoe weeding

Table 5
Effect of weed control and sowing method on weed density (no./m^2) at 6 weeks after planting (WAP)

Weed control (WC)	Location (L)	T&R Farm Malete			NCAM		
	Sowing method (SM)	DB	DL	WC mean	DB	DL	WC Mean
B + D 1.0 + 0.5 kg a.i./ha		58.70	49.80	54.25	38.20	34.20	36.20
B + D 1.0 + 0.5 kg a.i./ha + 1 SHW (6 WAP)		43.60	64.40	54.00	40.50	59.50	50.00
B + D 1.5 + 1.0 kg a.i./ha		40.90	79.10	60.00	49.80	46.20	48.00
B + D 2.0 + 1.5 kg a.i./ha		52.30	54.20	53.25	31.80	43.10	37.45
Hoe weeding (3 and 6 WAP)		55.10	41.70	48.40	32.40	43.10	37.75
P + D 0.5 + 0.5 kg a.i./ha		47.60	61.30	54.45	35.10	32.90	34.00
P + D 1.0 + 1.0 kg a.i./ha		62.20	65.80	64.00	42.20	53.40	47.80
P + D 2.0 + 1.5 kg a.i./ha		72.40	60.00	66.20	40.50	49.80	45.15
P + D 0.5 + 0.5+ 1 SHW (6 WAP)		77.80	59.10	68.45	48.00	43.60	45.80
Weedy check		84.50	122.70	103.60	76.50	69.80	73.15
SM mean		59.51	65.81	62.66	43.50	47.56	45.53
Tukey ($P < 5\%$)	Standard error						
L	3.64*						
SM	3.82						
WC	8.14*						

Table 5 *(continue)*

	Standard error
L × SM	5.15
L × WC	11.51
SM × WC	11.51
L × SM × WC	16.28

Note. T&R Farm Malete = Teaching and Research (T&R) Farm of the Kwara State University, Malete; NCAM = National Centre for Agricultural Mechanization (NCAM), Idofian, Ilorin, Kwara, Nigeria; Standard error = Standard error of the difference between treatment mean; * = Significant at $P < 0.05$; DB = Dibbling sowing method; DL = Drilling sowing method; B = Butachlor; D = Diuron; P = Pendimerhalin; 1 SHW = One supplementary hoe weeding

Table 6
Effect weed control and sowing method on weed density (no./m²) at 12 weeks after planting (WAP)

Weed control (WC)	Location (L)	T&R Farm Malete			NCAM		
	Sowing method (SM)	DB	DL	WC mean	DB	DL	WC Mean
B + D 1.0 + 0.5 kg a.i./ha		36.43	40.67	38.55	9.77	13.37	11.57
B + D 1.0 + 0.5 kg a.i./ha + 1 SHW (6 WAP)		44.00	45.77	44.89	9.77	11.10	10.44
B + D 1.5 + 1.0 kg a.i./ha		41.33	48.43	44.88	6.20	11.10	8.65
B + D 2.0 + 1.5 kg a.i./ha		41.33	47.57	44.45	12.87	5.33	9.10
Hoe weeding (3 and 6 WAP)		35.57	48.90	42.24	13.77	11.10	12.44
P + D 0.5 + 0.5 kg a.i./ha		41.77	44.90	43.34	12.00	8.87	10.44
P + D 1.0 + 1.0 kg a.i./ha		41.33	51.57	46.45	9.33	12.90	11.12
P + D 2.0 + 1.5 kg a.i./ha		44.43	49.50	46.97	12.00	12.43	12.22
P + D 0.5 + 0.5 kg a.i./ha + 1 SHW (6 WAP)		42.67	44.03	43.35	14.23	10.23	12.23
Weedy check		60.87	74.23	67.55	34.23	21.33	27.78
SM mean		42.97	49.56	46.27	13.42	11.78	12.60
Tukey ($P < 5\%$)	Standard error						
L	1.286*						
SM	1.346						
WC	2.876*						
L × SM	1.819*						
L × WC	4.068						
SM × WC	4.068						
L × SM × WC	5.753						

Note. T&R Farm Malete = Teaching and Research (T&R) Farm of the Kwara State University, Malete; NCAM = National Centre for Agricultural Mechanization (NCAM), Idofian, Ilorin, Kwara, Nigeria; Standard error = Standard error of the difference between treatment mean; * = Significant at $P < 0.05$; DB = Dibbling sowing method; DL = Drilling sowing method; B = Butachlor; D = Diuron; P = Pendimerhalin; 1 SHW = One supplementary hoe weeding

Table 7
Effect weed control and sowing method on plant height (cm) at 9 weeks after planting (WAP)

Weed control (WC)	Location (L)	T&R Farm Malete			NCAM		
	Sowing method (SM)	DB	DL	WC mean	DB	DL	WC mean
B + D 1.0 + 0.5 kg a.i./ha		91.10	96.50	93.80	115.80	110.10	112.95
B + D 1.0 + 0.5 kg a.i./ha + 1 SHW (6 WAP)		90.00	89.10	89.55	119.00	102.10	110.55
B + D 1.5 + 1.0 kg a.i./ha		90.10	90.40	90.25	112.30	105.70	109.00
B + D 2.0 + 1.5 kg a.i./ha		81.90	96.70	89.30	106.10	112.30	109.20
Hoe weeding (3 and 6 WAP)		88.90	97.60	93.25	108.00	117.80	112.90
P + D 0.5 + 0.5 kg a.i./ha		95.50	87.50	91.50	97.00	106.50	101.75
P + D 1.0 + 1.0 kg a.i./ha		94.70	83.10	88.90	102.00	101.70	101.85
P + D 2.0 + 1.5 kg a.i./ha		90.90	87.40	89.15	103.00	106.80	104.90
P + D 0.5 + 0.5 kg a.i./ha + 1 SHW (6 WAP)		89.70	85.90	87.80	94.60	111.70	103.15
Weedy check		69.10	79.20	74.15	53.50	115.70	84.60
SM mean		88.19	89.34	88.77	101.13	109.04	105.09
Tukey ($P < 5\%$)	Standard error						
L	2.64*						
SM	2.91						
WC	5.89*						
L × SM	3.73						
L × WC	8.34						
SM × WC	8.22*						
L × SM × WC	11.79						

Note. T&R Farm Malete = Teaching and Research (T&R) Farm of the Kwara State University, Malete; NCAM = National Centre for Agricultural Mechanization (NCAM), Idofian, Ilorin, Kwara, Nigeria; Standard error = Standard error of the difference between treatment mean; * = Significant at $P < 0.05$; DB = Dibbling sowing method; DL = Drilling sowing method; B = Butachlor; D = Diuron; P = Pendimerhalin; 1 SHW = One supplementary hoe weeding

plants in Malete, while the B + D 1.0 + 1.5 kg a.i./ha + 1 SHW and dibbling method produced the tallest plant at NCAM. At 12 WAP in Malete, the weedy check resulted in the tallest plants but not statistically different from the other weed control treatments except B + D 1.0 + 0.5, B + D 1.0 + 1.5 kg a.i./ha + 1 SHW, and B + D at 1.5 + 1.0 kg a.i./ha, which had significantly shorter plants. While at NCAM, B + D at 1.5 + 1.0 kg a.i./ha resulted in taller plants, comparable to other weed control methods but significantly taller than plants treated with P + D at 1.0 + 1.0 kg a.i./ha (Table 8). The interaction effect of location and weed control method on plant height was significant as the weedy check produced taller plants in Malete, while B + D at 1.5 + 1.0 kg a.i./ha produced the tallest plant at NCAM.

Table 8
Effect weed control and sowing method on plant height (cm) at 12 weeks after planting (WAP)

Weed control (WC)	Location (L)	T&R Farm Malete			NCAM		
	Sowing method (SM)	DB	DL	WC mean	DB	DL	WC mean
B + D 1.0 + 0.5 kg a.i./ha		91.30	100.40	95.85	115.70	118.70	117.20
B + D 1.0 + 0.5 kg a.i./ha + 1 SHW (6 WAP)		86.70	110.40	98.55	115.00	117.30	116.15
B + D 1.5 + 1.0 kg a.i./ha		98.10	100.80	99.45	117.40	139.80	128.60
B + D 2.0 + 1.5 kg a.i./ha		91.70	110.70	101.20	110.10	132.40	121.25
Hoe weeding (3 and 6 WAP)		102.40	105.10	103.75	106.10	119.00	112.55
P + D 0.5 + 0.5 kg a.i./ha		123.20	100.90	112.05	117.60	126.50	122.05
P + D 1.0 + 1.0 kg a.i./ha		104.20	95.60	99.90	76.20	42.20	59.20
P + D 2.0 + 1.5 kg a.i./ha		115.40	106.60	111.00	91.30	118.10	104.70
P + D 0.5 + 0.5 kg a.i./ha + 1 SHW (6 WAP)		123.80	92.80	108.30	103.70	116.50	110.10
Weedy check		117.00	110.40	113.70	103.00	117.50	110.25
SM mean		105.38	103.37	104.38	105.61	114.80	110.21
Tukey ($P < 5\%$)	Standard error						
L	3.16						
SM	3.16						
WC	7.07*						
L × SM	4.47						
L × WC	10.00*						
SM × WC	10.01						
L × SM × WC	14.15						

Note. T&R Farm Malete = Teaching and Research (T&R) Farm of the Kwara State University, Malete; NCAM = National Centre for Agricultural Mechanization (NCAM), Idofian, Ilorin, Kwara, Nigeria; Standard error = Standard error of the difference between treatment mean; * = Significant at $P < 0.05$; DB = Dibbling sowing method; DL = Drilling sowing method; B = Butachlor; D = Diuron; P = Pendimerhalin; 1 SHW = One supplementary hoe weeding

Yield Component and Grain Yield

In Malete, dibbling produced significantly ($P < 0.05$) higher number of pods (8.88) than drilling (8.19). A similar observation was recorded at NCAM, where dibbling produced more pods (16.60) than drilling (11.63) at 8 WAP (Table 9). At Malete, B + D at 1.5 + 1.0 kg a.i./ha resulted in the highest number of pods (11.87), which was not different from other weed control methods, except P + D at 1.0 + 1.0 kg a.i./ha (6.25), P + D at 2.0 + 1.5 kg a.i./ha (7.50), and the weedy check (5.90), which produced significantly lesser number of pods ($P < 0.05$). At NCAM, P + D at 1.0 + 1.0 kg a.i./ha (13.94), 2.0 + 1.5 kg a.i./ha (9.03), 0.5 + 0.5 kg a.i./ha + 1 SHW (10.44), and the weedy check (11.07) resulted in significantly lesser number of pods compared to B + D at 1.0 + 0.5 kg a.i./ha (19.04) and other weed control methods, which produced significantly ($P < 0.05$) higher number of pods. Comparing the

locations, sesame plants had a significantly lesser number of pods (8.53) in Malete than NCAM (14.12). Also, the location x sowing method interaction effect on the number of pods was significant at 8 WAP as dibbling produced a higher number of pods ($P < 0.05$) in the two locations (Table 9). In Table 10, hoe weeding gave the highest number of pods, which was comparable to only B + D at 1.0 + 0.5 kg a.i./ha + 1 SHW but was significantly higher than all the other weed control methods; however, weedy check produced significantly lowest amount of pods/plant in Malete. At NCAM, B + D at 1.5 + 1.0 kg a.i./ha produced the highest number of pods comparable to two hoe weeding, B + D at 2.0 + 1.5 and 1.0 + 0.5 kg a.i./ha, but significantly higher than other weed control methods. Weedy check and P + D at 1.0 + 1.0 kg a.i./ha significantly produced the lowest numbers of pods. In terms of location, Malete supported a significantly lower number of pods (17.34) compared to NCAM (23.89) (Table 10).

Table 9
Effect weed control and sowing method on the number of pods at 8 weeks after planting (WAP)

Weed control (WC)	Location (L)	T&R Farm Malete			NCAM		
	Sowing method (SM)	DB	DL	WC mean	DB	DL	WC mean
B + D 1.0 + 0.5 kg a.i./ha		10.97	6.13	8.55	22.8	15.27	19.04
B + D 1.0 + 0.5 kg a.i./ha + 1 SHW (6 WAP)		7.27	6.53	6.90	17.33	7.73	12.53
B + D 1.5 + 1.0 kg a.i./ha		12.67	11.07	11.87	18.33	12.53	15.43
B + D 2.0 + 1.5 kg a.i./ha		8.87	12.80	10.84	23.87	9.3	16.59
Hoe weeding (3 and 6 WAP)		9.60	12.00	10.80	17.73	18.5	18.12
P + D 0.5 + 0.5 kg a.i./ha		10.20	6.47	8.34	17.47	12.53	15.00
P + D 1.0 + 1.0 kg a.i./ha		6.97	5.53	6.25	15	12.87	13.94
P + D 2.0 + 1.5 kg a.i./ha		8.53	6.47	7.50	12.73	5.33	9.03
P + D 0.5 + 0.5 kg a.i./ha + 1 SHW (6 WAP)		9.20	7.60	8.40	11.07	9.8	10.44
Weedy check		4.47	7.33	5.90	9.67	12.47	11.07
SM mean		8.88	8.19	8.53	16.60	11.63	14.12
Tukey ($P < 5\%$)	Standard error						
L	0.926*						
SM	0.921*						
WC	2.070*						
L × SM	1.309*						
L × WC	2.928						
SM × WC	2.931						
L × SM × WC	4.141						

Note. T&R Farm Malete = Teaching and Research (T&R) Farm of the Kwara State University, Malete; NCAM = National Centre for Agricultural Mechanization (NCAM), Idofian, Ilorin, Kwara, Nigeria; Standard error = Standard error of the difference between treatment mean; * = Significant at $P < 0.05$; DB = Dibbling sowing method; DL = Drilling sowing method; B = Butachlor; D = Diuron; P = Pendimerhalin; 1 SHW = One supplementary hoe weeding

Dibbling (78.90 and 422.70 kg/ha) resulted in significantly higher grain yield than drilling (37.50 and 326.80 kg/ha) in Malete and NCAM, respectively (Table 11). Though there was no significant difference in grain yield between the weed control treatments in both locations, hoe weeding, P + D at 2.0 + 1.5, P + D at 0.5 + 0.5, B + D at 1.0 + 0.5, and B + D at 1.5 + 1.0 kg a.i./ha increased sesame yield by 97.20, 70.0, 58.1, 57.2, and 56.3%, respectively at NCAM, while at Malete, hoeing twice, P + D at 0.5 + 0.5, B + D at 2.0 + 1.5 kg a.i./ha increased sesame yield by 52.0, 28.0, and 22%, respectively. Between the two locations, the grain yield (58.20 kg/ha) of sesame in Malete was significantly ($P < 0.05$) lower than that at NCAM (374.75 kg/ha) (Table 11).

Economic Assessment

In Malete, a treatment combination of hoe weeding at 3 and 6 WAP × dibbling method

Table 10
Effect of location, weed control, and sowing method on the number of pods at 10 weeks after planting (WAP)

Weed control (WC)	Location (L)	T&R Farm Malete			NCAM		
	Sowing method (SM)	DB	DL	WC mean	DB	DL	WC mean
B + D 1.0 + 0.5 kg a.i./ha		15.27	17.67	16.47	26.73	25.20	25.97
B + D 1.0 + 0.5 kg a.i./ha + 1 SHW (6 WAP)		19.93	25.50	22.72	29.20	19.13	24.17
B + D 1.5 + 1.0 kg a.i./ha		16.13	16.60	16.37	36.73	26.67	31.70
B + D 2.0 + 1.5 kg a.i./ha		9.00	12.47	10.74	34.53	21.73	28.13
Hoe weeding (3 and 6 WAP)		29.33	26.13	27.73	32.40	23.40	27.90
Mean		17.29	17.40	17.34	24.49	23.30	23.89
P + D 1.0 + 1.0 kg a.i./ha		23.47	17.27	20.37	19.23	23.33	21.28
P + D 2.0 + 1.5 kg a.i./ha		16.63	12.53	14.58	20.87	22.67	21.77
P + D 0.5 + 0.5 kg a.i./ha + 1 SHW (6 WAP)		13.40	17.93	15.67	15.47	27.87	21.67
Weedy check		8.00	15.47	11.74	10.20	18.67	14.44
Mean		17.29	17.40	17.34	24.49	23.30	23.89
Tukey ($P < 5\%$)	Standard error						
L	1.604*						
SM	1.614						
WC	3.587*						
L × SM	2.268						
L × WC	5.072						
SM × WC	5.081						
L × SM × WC	7.173						

Note. T&R Farm Malete = Teaching and Research (T&R) Farm of the Kwara State University, Malete; NCAM = National Centre for Agricultural Mechanization (NCAM), Idofian, Ilorin, Kwara, Nigeria; Standard error = Standard error of the difference between treatment mean; * = Significant at $P < 0.05$; DB = Dibbling sowing method; DL = Drilling sowing method; B = Butachlor; D = Diuron; P = Pendimerhalin; 1 SHW = One supplementary hoe weeding

Table 11
Effect of location, weed control, and sowing methods on grain yield (kg/ha)

Weed control (WC)	Location (L)	T&R Farm Malete			NCAM		
	Sowing method (SM)	DB	DL	WC mean	DB	DL	WC mean
B + D 1.0 + 0.5 kg a.i./ha		91.00	22.00	56.50	442.00	388.00	415.00
B + D 1.0 + 0.5 kg a.i./ha + 1 SHW (6 WAP)		85.00	17.00	51.00	254.00	325.00	289.50
B + D 1.5 + 1.0 kg a.i./ha		52.00	35.00	43.50	256.00	569.00	412.50
B + D 2.0 + 1.5 kg a.i./ha		125.00	17.00	71.00	196.00	343.00	269.50
Hoe weeding (3 and 6 WAP)		135.00	43.00	89.00	744.00	297.00	520.50
P + D 0.5 + 0.5 kg a.i./ha		114.00	35.00	74.50	571.00	264.00	417.50
P + D 1.0 + 1.0 kg a.i./ha		36.00	24.00	30.00	527.00	227.00	377.00
P + D 2.0 + 1.5 kg a.i./ha		51.00	57.00	54.00	564.00	334.00	449.00
P + D 0.5 + 0.5 kg a.i./ha + 1 SHW (6 WAP)		66.00	42.00	54.00	421.00	245.00	333.00
Weedy check		34.00	83.00	58.50	252.00	276.00	264.00
SM mean		78.90	37.50	58.20	422.70	326.80	374.75
Tukey ($P < 5\%$)	Standard error						
L	32.2*						
SM	32.4*						
WC	72.1						
L x SM	45.6						
L x WC	101.9						
SM x WC	99.5						
L x SM x WC	144.2						

Note. T&R Farm Malete = Teaching and Research (T&R) Farm of the Kwara State University, Malete; NCAM = National Centre for Agricultural Mechanization (NCAM), Idofian, Ilorin, Kwara, Nigeria; Standard error = Standard error of the difference between treatment mean; * = Significant at $P < 0.05$; DB = Dibbling sowing method; DL = Drilling sowing method; B = Butachlor; D = Diuron; P = Pendimerhalin; 1 SHW = One supplementary hoe weeding

of sowing resulted in the highest yield of sesame (135.71 kg/ha), followed by B + D at 2.0 + 1.5 kg a.i./ha × dibbling and P + D at 0.5 + 0.5 kg a.i./ha × dibbling method, while B + D at 1.0 + 0.5 kg a.i./ha × drilling and P + D at 1.0 + 1.0 kg a.i./ha × drilling produced the least yield (22.13 kg/ha) and (23.83 kg/ha), respectively (Table 12). The highest cost of production emanated from P + D at 2.0 +1.5 kg a.i./ha × dibbling and P + D at 0.5 + 0.5 kg a.i./ha + 1 SHW at 6 WAP × dibbling method ($ 315.97 and $ 311.49, respectively) compared to the rest of the treatments and hoeing twice, while the treatment combinations with the least cost were weedy check × dibbling method ($ 244.56). The highest income was generated by treatment combination of twice hoeing × dibbling ($ 113.66) followed by B + D at 2.0 + 1.5 kg a.i./ha × dibbling ($ 105.05) and P + D at 0.5 + 0.5 kg a.i./ha × dibbling ($ 95.76). The least income resulted from B +

D at 2.0 + 1.5 kg a.i./ha × drilling ($ 13.93) and B + D at 1.0 + 1.5 kg a.i./ha + 1 SHW at 6 WAP × drilling ($ 13.93). The treatment combinations with the least monetary losses were weedy check × drilling ($ -177.52), followed by B + D at 2.0 + 1.5 kg a.i./ha × dibbling ($ -191.02) and P + D at 0.5 + 0.5 kg a.i./ha × dibbling ($ -199.88). The treatment combination of B + D 1.0 + 0.5 kg a.i./ha + 1 SHW × drilling attracted the highest monetary loss ($ -294.31).

In comparison, at NCAM, the treatment combination which produced the highest sesame yield was hoe weedy × dibbling (744.3 kg/ha) followed by P + D at 0.5 + 0.5 kg a.i./ha × dibbling (570.8 kg/ha) and B + D at 1.5 + 1.0 kg a.i./ha × drilling (569.1 kg/ha) and P + D at 2.0 + 1.5 kg a.i./ha × dibbling (564.3 kg/ha) while P + D at 1.0 + 1.0 kg a.i./ha × drilling resulted in the lowest yield (227.5 kg/ha). The treatment combinations with the highest cost of production were P + D 2.0 + 1.5 kg a.i./ha × dibbling and P + D 0.5 + 0.5 kg a.i./ha + 1 SHW × dibbling ($ 315.97 and $ 311.49, respectively), while the least cost was incurred by weedy check × dibbling ($ 244.56). The highest income was generated by hoe weeding × dibbling ($ 623.38) followed by P + D at 0.5 + 0.5 kg a.i./ha × dibbling ($ 478.07), B + D at 1.5 + 1.0 kg a.i./ha × drilling ($ 476.64) and P + D at 2.0 + 1.5 kg a.i./ha × dibbling ($ 472.62), while the treatment combinations with the least income were B + D at 2.0 + 1.5 kg a.i./ha × dibbling ($ 163.82). The highest gross margin resulted from hoe weeding × dibbling ($ 318.57) followed by P + D at 0.5 + 0.5 kg a.i./ha × dibbling ($ 182.43), B + D at 1.5 + 1.0 kg a.i./ha × drilling ($ 177.38) and P + D at 2.0 + 1.5 kg a.i./ha × dibbling ($ 156.65), while the treatment combination with the least gross margin was B + D at 2.0 + 1.5 kg a.i./ha × dibbling ($ -129.71) (Table 12).

DISCUSSION

Sesame has been reported to be one of the cash crops in Nigeria with huge economic potential and an important foreign exchange revenue earner. Therefore, identifying a combination of herbicide mixtures and sowing methods for effectively managing weeds and increasing crop production will help boost the country's total production of this crop. This study was carried out in two locations**:** Malete, which had a total rainfall of 1,233.90 mm, while NCAM recorded a total rainfall of 1,881.10 mm. It corroborates with Paul and Oluwatimi (2011) that the total annual rainfall in Kwara State ranges from 800 to 1,200 mm in the Northwest and 1,000 to 1,500 mm in the Southeast. The soil in the two locations was sandy loam. However, NCAM was richer than Malete in terms of total nitrogen, available phosphorus, and organic carbon. It may be due to the more prolonged continuous cultivation that the Malete site has been subjected to compared to NCAM, which was recently cultivated after many years of fallow.

The earlier establishment of the experiment and higher rainfall at Malete caused higher weed infestation at this site than NCAM in the early part of the season. However, this trend was reversed in the

Table 12
Economic analysis of the use of different treatment combinations of herbicide to produce sesame in United States dollar ($)

Treatment	Malete Yield (kg/ha)	TC ($)	Income ($)	GM ($)	NCAM Yield (kg/ha)	TC ($)	Income ($)	GM ($)
B + D 1.0 + 0.5 kg a.i./ ha (DB)	91.47	292.20	76.61	-215.59	441.8	292.20	370.03	77.83
B + D 1.0 + 0.5 kg a.i./ ha (DL)	22.13	288.66	18.53	-270.13	388.4	288.66	325.30	36.64
B + D 1.0 + 0.5 kg a.i./ha + 1 SHW (6 WAP, DB)	85.40	308.21	71.53	-236.68	253.6	308.21	212.40	-95.81
B + D 1.0 + 0.5 kg a.i./ha + 1 SHW (6 WAP, DL)	16.63	308.24	13.93	-294.31	324.8	308.24	269.49	-38.75
B + D 1.5 + 1.0 kg a.i./ ha (DB)	52.37	290.71	43.86	-246.85	255.9	290.71	214.33	-76.38
B + D 1.5 + 1.0 kg a.i./ ha (DL)	35.43	299.26	29.67	-269.59	569.1	299.26	476.64	177.38
B + D 2.0 + 1.5 kg a.i./ ha (DB)	125.43	296.07	105.05	-191.02	195.6	293.53	163.82	-129.71
B + D 2.0 + 1.5 kg a.i./ ha (DL)	16.63	297.18	13.93	-283.25	342.9	297.18	287.19	-9.99
Hoe weeding (DB)	135.71	304.81	113.66	-191.15	744.3	304.81	623.38	318.57
Hoe weeding (DL)	42.63	289.23	35.70	-253.53	296.8	289.23	248.58	-40.65
P + D 0.5 + 0.5 kg a.i./ ha (DB)	114.33	295.64	95.76	-199.88	570.8	295.64	478.07	182.43
P + D 0.5 + 0.5 kg a.i./ ha (DL)	35.30	284.51	29.57	-254.94	264.3	284.51	221.36	-63.15
P + D 0.5 + 0.5 kg a.i./ha + 1 SHW (DB)	65.70	311.49	55.03	-256.46	421.3	311.49	352.86	41.37
P + D 0.5 + 0.5 kg a.i./ha + 1 SHW (DL)	41.67	305.70	34.90	-270.80	244.8	305.70	204.36	-101.34
P + D 1.0 + 1.0 kg a.i./ ha (DB)	36.40	299.98	30.49	-269.49	527.1	299.98	441.47	141.49
P + D 1.0 + 1.0 kg a.i./ ha (DL)	23.83	290.97	19.96	-271.01	227.5	290.97	190.54	-100.43
P + D 2.0 + 1.5 kg a.i./ ha (DB)	50.60	315.97	42.38	-273.59	564.3	315.97	472.62	156.65
P + D 2.0 + 1.5 kg a.i./ ha (DL)	56.53	309.49	47.35	-262.14	333.7	309.49	279.49	-30.00
Weedy check (DB)	34.23	244.56	28.67	-215.89	252.4	244.56	211.40	-33.16
Weedy check (DL)	82.53	246.64	69.12	-177.52	276.3	246.64	231.41	-15.23

Note. TC = Total cost; GM = Gross margin = = Income – TC; NCAM = National Centre for Agricultural Mechanization; Income = Selling price x Open market price of sesame; DB = Dibbling sowing method; DL = Drilling sowing method; B = Butachlor; D = Diuron; P = Pendimerhalin; 1 SHW = One supplementary hoe weeding; WAP = Weeks after planting

middle and later part of the season, probably as a result of higher rainfall and better soil conditions existing at NCAM than at Malete, which created a conducive atmosphere for vigorous vegetative growth and early closure of canopy for weed suppression, hence, the lower weed infestation at NCAM. It is in line with Ramesh et al. (2017) that an increase in rainfall would lead to additional weed pressure. Furthermore, Daniya et al. (2019) reported the easy formation of sesame canopy and better weed control in the plots seeded with 2 kg/ha of sesame. Dibbling appeared to be more effective in controlling weed density and biomass than the drilling method of sowing in the two locations, probably because of its ability to maintain a higher plant population of sesame, thereby facilitating early canopy closure for the shading and smothering of weeds. All the herbicide mixtures and two hoeing effectively reduced weed density and biomass, suggesting the efficacy of all the herbicide mixtures in weed control. However, the herbicide mixtures that have proved to be most effective were P + D 2.0 + 1.5, P + D 0.5 + 0.5, B + D 1.5 + 1.0 B + D 1.0 + 0.5, and B + D 2.0 + 1.5 kg a.i./ha. Therefore, these herbicide mixtures can be used as alternatives to hoeing twice to reduce drudgery in sesame production.

The significantly taller plants at NCAM compared to Malete could be attributed to the utilization of more moisture, nutrients, and sunlight for better growth occasioned by higher rainfall, better soil conditions, and the lower weed infestation recorded at NCAM. All the herbicide mixtures and two hoe weeding resulted in taller sesame plants compared to the weedy check in both locations at 9 WAP. It is probably due to the effectiveness of the herbicide mixtures and hoe weeding to minimize weed infestation, resulting in more growth resources for better performance, thus corroborating with Khan (2016) that a weed-free plot gave rise to taller plants. However, at 12 WAP at Malete, the weedy check achieved sesame plant height not different from plants in the plots treated with herbicide mixture and hoe weeding. It could have resulted from weed competition for light in the weedy check. Daniya et al. (2019) attributed the taller plant height of sesame seeded at a density of 8 kg/ha to intra-specific competition for growth resources, which resulted in the elongation of internodes and taller plants.

NCAM location increased the number of sesame pods compared to the Malete location at 8 and 10 WAP. It could be attributed to the higher rainfall, better soil conditions, and weed control, which resulted in the uptake and utilization of higher amounts of nutrients, moisture, and sunlight to produce taller plants and the number of pods/plants. Daniya et al. (2019) attributed the production of more capsules/plants of sesame to taller plants, which translated into more nodes from where leaves are produced. Furthermore, Imoloame (2009) reported a significant positive correlation between the amount of pods/plants of sesame and plant height. The dibbled sesame could have suffered less intra-specific competition compared to the drilled ones and, coupled with the greater ability of the dibbled

method to minimize weed infestation, could have freed more nutrients and moisture for the plants to produce a higher number of pods in both locations at Malete at 8 WAP.

The effectiveness of herbicide mixtures B + D 1.5 + 1.0, B + D 2.0 + 1.5, P + D 0.5 + 0.5, and P + D 0.5 + 0.5 kg a.i./ha + 1 SHW and hoeing twice to control weeds in Malete, promoted the ability of the sesame crop to produce the highest number of pods. A similar trend played out at NCAM. At both locations, the weedy check produced the least number of pods due to intense weed competition with the sesame crop, which led to poor performance. At 10 WAP, at Malete hoeing twice, B + D 1.0 + 0.5 kg a.i./ha + 1 SHW and P + D 1.0 + 1.0 kg a.i./ha produced the highest number of pods than the other weed control methods and weedy check. However, at NCAM, all the herbicide mixtures and hoeing twice, except P + D 1.0 + 1.0 kg a.i./ha, produced a significantly higher number of pods than the weedy check. The faster vegetative growth and early canopy formation of sesame enhanced the herbicide mixtures and hoe weeding ability to control weeds better and produce a higher number of pods at NCAM than Malete. It corroborates the findings of Ndarubu et al. (2003) that effective weed control in sesame occurred using a combination of herbicide mixture of metolachlor + metobromuron at 0.75 + 0.75 kg a.i./ha[1] and drilling method at an interrow spacing of 30 cm.

The grain yield of sesame was abysmally lower in Malete than NCAM because of a lower amount of rainfall, late sowing, higher weed infestation, and poorer soil conditions, resulted in the uptake and utilization of lesser growth resources, which supported shorter plants, lower number of pods and grain yield.

Dibbling resulted in higher sesame grain yield than drilling, which could be attributed to a higher plant population in the dibbled plots than in the drilled plots, where sesame crops suffered higher intense intra-plant competition and plant mortality. Furthermore, the higher plant population and close spacing in the dibbled plots encouraged early closure of the canopy and the ability of sesame to control weeds more effectively. It subsequently made more growth resources available for uptake and utilization by the dibbled sesame for better performance. This result agrees with Ndor and Nasir (2019), who reported that dibbling produced a higher grain yield of sesame than the broadcast method but differed from the findings of Katanga et al. (2017), who recommended drilling as the best sowing method dibbling and broadcast methods to produce sesame. Though there was no significant difference in the grain yields among weed control treatments in the two locations, two hoeing at 3 and 6 WAP, P + D 2.0 + 1.5 and 0.5 + 0.5 kg a.i./ha, B+ D 1.0 + 1.5 and 1.5 + 1.0 kg a.i./ha increased sesame grain yield by 97, 70, 58.1, 57.2, and 56.3%, respectively at NCAM, while at Malete, two hoe weeding, P + D 0.5 + 0.5 and B + D 2.0 + 1.5 kg a.i./ha increased sesame yield by 52.0, 28.0, and 22%, respectively. These herbicide mixtures showed synergism as they proved more effective in controlling

weeds than the other treatments. They can be integrated with the dibbling method of sowing at 30 cm × 30 cm for effective weed control and higher grain yield of sesame, which is similar to Ndarubu et al. (2003) that a combination of herbicide mixture of metolachlor + metobromuron at 0.75 + 0.75 kg a.i./ha and drilling method of sowing at 30 cm inter-row spacing was effective for weed control and production of higher grain yield of sesame.

In Malete, a combination of hoeing twice × dibbling sowing method, B + D 2.0 + 1.5 kg a.i./ha × dibbling and P + D 0.5 + 0.5 kg a.i./ha × dibbling resulted in higher sesame yields, while at NCAM higher yields were produced by treatment combinations of two hoe weeding at 3 and 6 WAP × dibbing, P + D 0.5 + 0.5 kg a.i./ha × dibbling, B + D 1.5 + 1.0 × drilling method and P + D 2.0 + 1.5 kg a.i./ha. The above treatment combinations could have provided effective weed control and enabled the uptake of more growth factors for higher yield. The treatment combination of P + D and B + D at 1.0 + 1.0 kg a.i./ha × drilling resulted in the least yield as they failed to provide effective weed control. The highest cost of production in both NCAM and Malete was the treatment combinations of P + D 2.0 + 1.5 and P + D 0.5 + 0.5 kg a.i./ha + 1 SHW × dibbing method. It could be attributed to the higher cost of higher doses of herbicides and the extra cost of one supplementary hoe weeding, which increased the cost of production, which is contrary to the findings of Imoloame (2017) that hoeing twice was the most expensive weed control method than the use of herbicides. This contradiction could have been caused by Nigeria's 18.6% inflation rate, which has affected the prices of goods (herbicides) and services (Oyekanmi, n.d.). The treatment combinations of hoeing twice × dibbling, P + D 2.0 + 1.5, and 0.5 + 0.5 kg a.i./ha × dibbling gave the highest incomes at Malete, probably due to their ability to produce higher grain yields.

However, the gross margin generated from all the treatments in Malete was losses, probably due to the low sesame yields from this location due to the late planting, low rainfall, and higher weed infestation. However, at NCAM, the same treatment combinations of hoeing twice × dibbling, P + D 2.0 + 1.5 kg a.i./ha, and at 0.5 + 0.5 × dibbling and B + D 1.5 kg a.i./ha + 1.0 kg a.i./ha × drilling method resulted in the highest (gross margin/profit) compared to the other treatments. These combinations improved weed control, producing better growth and higher sesame yields. Therefore, the best treatment combinations for effective weed control, higher yields, and economic returns were hoeing twice × dibbling, P + D 0.5 + 0.5 and 2.0 + 1.5 kg a.i./ha × dibbling method, and B + D 1.5 + 0.5 × drilling method.

CONCLUSION

From the findings of this study, it can be concluded that hoeing twice at 3 and 6 WAP, P + D at 2.0 + 1.5 and 0.5 + 0.5 kg a.i./ha, B + D at 1.0 + 0.5 and at 1.5 + 1.0 kg a.i./ha increased sesame grain yield by 97, 70, 58.1, 57.2, and 56.3%, respectively, at NCAM,

while at Malete, hoeing twice, P + D 0.5 + 0.5 kg a.i./ha and B + D 2.0 + 1.5 kg a.i./ha increased sesame yield by 52, 28, and 22%, respectively. Dibbling was more effective than the drilling method for the management of weeds and for promoting crop growth and yield. The best treatment combinations for effective weed control, higher yields, and economic returns are hoe weeding at 3 and 6 WAP × dibbling, P + D 0.5 + 0.5, and 2.0 + 1.5 kg a.i./ha × dibbling and B +D 1.5 +1.0 kg a.i./ha × drilling. NCAM location produced significantly higher sesame grains than Malete. Dibbling sowing method at a spacing of 30 cm × 30 cm and thinned to 3 plants/stand integrated with pendimethalin + diuron 0.5 + 0.5 kg a.i/ha is recommended for higher yield, effective weed management, economic returns, and as an eco-friendly alternative to two hoe weeding.

ACKNOWLEDGEMENT

The authors express their gratitude to Mr. Tayo Jimoh and Mr. Mohammed Usman for collecting field data, harvesting, and processing sesame from the experimental site.

REFERENCES

Adefeko, A. (2017, May 31). Sesame farming in Africa: The little seeds with big potential. *TheCable*. https://www.thecable.ng/sesame-farming-africa-little-seeds-big-potential

Bhadauria, N., Yadav, K. S., Rajput, R. L., & Singh V. B. (2012). Integrated weed management in sesame. *Indian Journal of Weed Science*, *44*(4), 235–237.

Daniya, E., Dadari, S. A., Ndahi, W. B., Kuchinda, N. C., & Babaji, B. A. (2019). Seed rate and nitrogen fertilizer effects on weed biomass, growth and yield of two sesame (*Sesamum indicum* L.) varieties. *Nigerian Journal of Weed Science*, *12*, 35-53.

Das, T. K. (2011). *Weed science: Basics and applications*. Jain Brothers.

Eni, E. I., Phillip, B. B., Lagoke, S. T. O., & Adigun, J. A. (2013). Economic performance of maize-groundnut intercrop in response to weed control methods and cropping patterns in Nigeria. *Nigerian Journal of Weed Science*, *26*, 13-21.

Ibirogba, F. (2021, November 18). Increased sesame production, value chain will boost economic recovery. *The Guardian Newspaper*. https://www.pressreader.com/nigeria/the-guardian-nigeria/20211118/282097754960617

Ijalal, Z., Tanveer, A, Safdar, M. E, Aziz, A., Ashraf, M., Akhtar, N., Atif, F. A., Ali, A., & Maqbool, M. M. (2011). Effects of weed crop competition period on weeds and yield and yield components of sesame (*Sesamum indicum* L.). *Pakistan Journal of Weed Science Research*, *17*(1), 51-63.

Imoloame, E. O. (2017). Evaluation of herbicide mixtures and manual weed control method in maize (*Zea mays* L.) productivity in the Southern Guinea agro-ecology of Nigeria. *Cogent Food and Agriculture*, *3*(1), 1375378. https://doi.org/10.1080/23311932.2017.1375378

Imoloame, E. O. (2009). *Effects of pre- and post-emergence herbicides on weed infestation and productivity of sesame (*Sesame indicum *L.) in a Sudan savanna zone of Nigeria* [Unpublished Doctoral dissertation]. University of Maiduguri.

Imoloame, E. O., Gworgwor, N. A., & Joshua, S. D. (2007). Sesame (*Sesamum indicum* L.) weed infestation, yield and yield components as influenced by sowing method and seed rate

in Sudan Savanna agro-ecology of Nigeria. *African Journal of Agricultural Research*, *2*(10), 528-533.

Imoloame. E. O. (2021). Agronomic and economic performance of maize (*Zea mays* L.) as influenced by seed bed configuration and weed control treatments. *Open Agriculture*, *6*(1), 445-455. https://doi.org/10.1515/opag-2021-0030

Katanga, Y. N., Danmaigoro, O., & Buba, Y. (2017). Effect of sowing methods, seed rate and variety on yield and seed quality of sesame (*Sesamum indicum* L.) and its implication on returns in Sudan savanna of Nigeria. *Asian Journal of Agricultural Sciences*, *6*(4), 1-7. https://doi.org/10.9734/ARJA/2017/29589

Khan, I. A., Hassan, G., Malik, N., Khan, R., Khan, H., & Khan, S. A. (2016). Effect of herbicides on yield and yield components of hybrid maize (*Zea mays*). *Planta Daninha*, *34*(4), 729-736. https://doi.org/10.1590/s0100-83582016340400013

Lawal, M. D., Olorunmaiye, P. M., Adeyemi, O. R., & Aiyelaagbe, I. O. O. (2019). Influence of weeding regimes on cassava production intercropped with okra under three legume cover crops. *Nigerian Journal of Weed Science*, *32*, 21-34.

Mane, S. V., Kanade, V. M., Shendage, G. B., Sarawale, P. P., & Shetye, V. N. (2017). Weed management in sesame (*Sesamum indicum* L.) grown under coastal region of Maharashtra. *Journal of the Indian Society of Coastal Agricultural Research*, *35*(1), 31-33.

Muktar, F. (2021, March 30). Nigeria's sesame market, lucrative but weighed by challenges. *Premium Times*. https://www.premiumtimesng.com/news/top-news/452157-nigerias-sesame-market-lucrative-but-weighed-down-by-challenges.html?tztc=1

Myint, D., Gilani, S. A., Kawase, M., & Watanabe, K. N. (2020). Sustainable sesame (*Sesame indicum* L.) production through improved technology: An overview of production, challenges and opportunities in Myanmar. *Sustainability*, *12*(9), 3515. https://doi.org/10.3390/su12093515

Ndarubu, A. A., Adejonwo, K. O., Adigun, Y., & Chiezey, F. (2003). Effects of weed control treatments and interrow spacing on the growth and yield of sesame (*Sesamum indicum* L.). *Nigerian Journal of Weed Science*, *16*, 15-22.

Ndor, E., & Nasir, I. U. (2019). Response of sesame (*Sesamum indicum* L.) to sowing methods and fertilizer types on degraded soil of southern Guinea savanna agroecological zone, Nigeria. *East Scholars Journal of Agricultural and Life Sciences, 2*(6), 312-316.

Ngala, A. L., Dugje, I. Y., & Yakubu, H. (2013). Effects of inter-row spacing and plant density on performance of sesame (*Sesamum indicum* L.) in a Nigerian Sudan savanna. *Science International*, *25*(3), 513-519. https://doi.org/10.13140/2.1.2230.3368

Odunewu, S. (2022, August 21). Sesame seeds account for 40% of Nigeria's annual export to Japan. *Blueprint Newspapers*. https://blueprint.ng/sesame-seeds-account-for-40-of-nigerias-annual-export-to-japan/#:~:text=Sesame%20seeds%20account%20for%2040%25%20of%20Nigeria%E2%80%99s%20annual,-per%20cent%20of%20sesame%20seeds%20consumed%20in%20Japan.

Oyekanmi, S. (n.d.). Nigeria's inflation rate increases to 19.64% in July 2022. *Nairametrics*. https://nairametrics.com/2022/08/15/breaking-nigerias-inflation-rate-surges-to-a-17-year-high-of-19-64-in-july-2022/

Paul, I. I., & Oluwaseun, O. (2011). Rainfall characteristics and maize yield in Kwara state, Nigeria. *Indian Journal of Fundamental Applied Life Sciences*, *1*(3), 60-65.

Ramesh, K., Matoob, A., Aslam, F., Florentine, S. K., & Chauhan, B. S. (2017). Weeds in a changing climate: Vulnerable types, consequences and implications for future weed management. *Frontiers in Plant Science*, *8*, 95. https://doi.org/10.3389/fpls.2017.00095

Take-tsaba, A. I., Yakubu, A. I., Ibrahim, N. D., & Aliero, B. I. (2011). Effects of herbicide and manual weeding regimes on yield of sesame (*Sesamum indicum* L.) in the Sudan savannah zone of Nigeria. *Nigerian Journal of Weed Science*, *24*, 31-35.

Young, S. L., Pitla, S. K., Van Evert, F. K., Schueller, J. K., & Pierce, F. J. (2017). Moving integrated weed management from low level to a truly integrated and highly specific weed management systems using advanced technologies. *Weed Research*, *57*(1), 1-5. https://doi.org/10.1111/wre.12234

Pertanika J. Trop. Agric. Sci. 46 (4): 1173 - 1188 (2023)

PERTANIKA JOURNALS

TROPICAL AGRICULTURAL SCIENCE

Journal homepage: http://www.pertanika.upm.edu.my/

Effects of Paracetamol on the Development of Zebrafish (*Danio rerio*)

Ajeng Istyorini Asmoning Dewanti[1], Tony Prince Kunjirika[1], Raden Roro Risang Ayu Dewayani Putri[1], Ascarti Adaninggar[1], Anita Restu Puji Raharjeng[2], Bambang Retnoaji[1], Ardaning Nuriliani[1], Fajar Sofyantoro[1], Nur Indah Septriani[1] and Hendry T. S. S. G. Saragih[1]*

[1]Faculty of Biology, Universitas Gadjah Mada, 55281 Yogyakarta, Indonesia
[2]Faculty of Science and Technology, Universitas Islam Negeri Raden Fatah Palembang, 30126 Sumatera Selatan, Indonesia

ABSTRACT

The misuse of paracetamol is becoming more prevalent worldwide. Due to non-compliance with recommended dosage and regulations, paracetamol consumption can result in serious health issues such as liver necrosis, kidney damage, heart damage, and hematological changes. This study sought to investigate the impact of paracetamol on the development of zebrafish embryos, which are often used as a model for assessing the effect of drug exposure on animals. The results indicated that paracetamol negatively affects the hatching and survival rates of zebrafish. Additionally, paracetamol exposure caused spinal abnormalities, pericardial edema, hypopigmentation, reduced heart rate, and spontaneous movement in zebrafish larvae. The developmental abnormalities in zebrafish were more significant with higher concentrations and longer exposure times. These findings may provide valuable insights into the detrimental impact of paracetamol on aquatic animals.

Keywords: *Danio rerio*, embryo development, paracetamol, pigmentation, zebrafish

ARTICLE INFO

Article history:
Received: 18 March 2023
Accepted: 17 May 2023
Published: 31 October 2023

DOI: https://doi.org/10.47836/pjtas.46.4.06

E-mail addresses:
ajengistyorini@mail.ugm.ac.id (Ajeng Istyorini Asmoning Dewanti)
tonyprince512@gmail.com (Tony Prince Kunjirika)
rrrisang96@mail.ugm.ac.id (Raden Roro Risang Ayu Dewayani Putri)
ascarti.adaninggar@mail.ugm.ac.id (Ascarti Adaninggar)
anitaraharjeng_uin@radenfatah.ac.id (Anita Restu Puji Raharjeng)
bambang.retnoaji@ugm.ac.id (Bambang Retnoaji)
ardaning@ugm.ac.id (Ardaning Nuriliani)
fajar.sofyantoro@ugm.ac.id (Fajar Sofyantoro)
nurindahseptriani@ugm.ac.id (Nur Indah Septriani)
saragihendry@ugm.ac.id (Hendry T.S.S.G. Saragih)
* Corresponding author

INTRODUCTION

Paracetamol usage has been on the rise globally, likely due to the widespread availability of this medication (Alchin et al., 2022; Franzellitti et al., 2015). Its popularity is due to the perception among the public that it is a safe and effective pain reliever (Ishizuka et al., 2020; Jóźwiak-Bebenista & Nowak, 2014). This trend is further

ISSN: 1511-3701
e-ISSN: 2231-8542

exacerbated during the ongoing COVID-19 pandemic, in which people tend to self-treat by purchasing and consuming paracetamol (Leal et al., 2021).

In Indonesia, paracetamol is widely available and belongs to over-the-counter (OTC) drugs that can be obtained without a prescription from a medical professional (Kuswinarti et al., 2020). It falls under the category of non-opioid drugs, along with several non-steroidal anti-inflammatory drugs (NSAIDs), and is legally regulated by the World Health Organization (WHO) (Freo et al., 2021). The misuse of paracetamol by the public has become a global concern, with numerous studies investigating attitudes toward self-medication with paracetamol and other analgesics. For instance, Chakraborty et al. (2015) conducted a study on the prevalence of paracetamol abuse among Indian students, while Faqihi and Sayed (2021) investigated the practice of self-medication with analgesics among students at Jazan University in Saudi Arabia. In addition, Hidayati and Kustriyani (2020), as well as Kuswinarti et al. (2020), have examined the issue of paracetamol overuse within different communities in Indonesia.

Several studies have demonstrated that dependence and overdosing on paracetamol, which occurs when it is consumed improperly and not according to the recommended dosage, can lead to health problems such as liver necrosis, kidney damage, heart damage, and hematological changes (Chiew et al., 2020; Hodgman & Garrad, 2012; Mostafa et al., 2022). Incorrect doses of paracetamol in pregnant and lactating women can also endanger both the mother and fetus. Experimental and epidemiological research has found that prenatal exposure to paracetamol can disrupt fetal development and pose risks for developing neurological, reproductive, and urogenital disorders. Prenatal paracetamol exposure has been linked to an increased risk of neurological and behavioral disorders, such as attention deficit hyperactivity disorder (ADHD), autism spectrum disorders, delayed language skills, and reduced intellectual abilities (Leppert et al., 2019; Liew et al., 2016; Skovlund et al., 2016). These findings suggest that paracetamol can easily cross the placenta and blood-brain barrier (Koehn et al., 2020).

The extensive use of paracetamol is closely associated with the increased environmental waste of this medication, particularly in aquatic environments. Many studies have investigated the presence of paracetamol contamination in these environments, including studies by Patel et al. (2022). Recent research has revealed the presence of paracetamol contamination in Jakarta Bay, with concentrations of 610 ng/L and 420 ng/L (Koagouw et al., 2021). These levels are exceptionally high compared to those found in other areas, such as the study by Shigei et al. (2021), which found paracetamol with a 40–70 ng/L concentration in the Zarqa River in Jordan. Groundwater, a drinking water source in Atlanta, Georgia, in America, was also contaminated with paracetamol (Al-Kaf et al., 2017).

The contamination of paracetamol in the aquatic environment indicates its accumulation in aquatic organisms. The pharmacologically active compounds in paracetamol can be harmful to aquatic organisms and have the potential to accumulate in the food chain. According to a study by Rivera-Utrilla et al. (2013), medical contaminants with a molecular mass of <500 Da have varying complex molecular contents and may have an affinity with other pollutants in the aquatic environment, such as heavy metals and microplastics. These factors are further influenced by human anthropogenic activities, rising water temperatures, and increasing rate of water acidification (Daniel et al., 2022).

Using animal models is an alternative to studying the effects of paracetamol contamination in aquatic environments. Folarin et al. (2019) examined the effect of paracetamol and diclofenac on African freshwater fish *Clarias gariepinus* and found disturbances in liver function and anti-oxidative enzyme stress. Blue mussels (*Mytilus edulis*) exposed to paracetamol for 24 days showed disrupted reproductive processes, including modulation of several important genes such as estrogen receptor 2 and vitellogenin (Koagouw et al., 2021). Studies on zebrafish (*Danio rerio*) have also examined the effects of paracetamol (Cedron et al., 2020; Xia et al., 2017; Xu et al., 2010). These studies have shown that paracetamol affects zebrafish larvae's hatching rate and survival rate (Xia et al., 2017; Xu et al., 2010) and can cause edema and pigmentation disorders (Cedron et al., 2020). The abundance of research papers on the effects of paracetamol on zebrafish highlights the importance of using zebrafish as an animal model, especially considering their habitat in rivers, which are closely related to water pollution caused by human activities (Xia et al., 2017).

This study aimed to examine the effects of paracetamol on zebrafish development up to 72 hr post-fertilization (hpf). The development of zebrafish larvae, including measuring the intensity of eye pigmentation and spontaneous movement abnormalities, was observed. The findings from this study can be utilized as a reference for understanding the effects of paracetamol on humans and aquatic animals.

MATERIALS AND METHODS

Preparation of Brine, Egg Media, and Paracetamol Solutions

Three types of solutions were utilized in this study: brine solution, egg media, and paracetamol solution (PT. Mersifarma, Indonesia). All the solutions were prepared and dissolved using reverse osmosis (RO) water to maintain a stable pH. The brine solution was prepared by adding 35 g of salt (PT. Duta Kencana Swaguna, Indonesia) to one liter of water and stirring it with a spatula until it dissolved. For the egg medium solution, 1.5 ml of brine solution, one drop of methylene blue (Merck, India), and one liter of water were mixed and stirred until the mixture became homogeneous. The paracetamol solution was prepared using 500 mg of paracetamol tablets (PT. Mersifarma,

Indonesia). Based on previous studies, the paracetamol stock solution was then dissolved using the egg media solution to obtain a dosage of 3 and 5 mM (Cedron et al., 2020; Nogueira et al., 2019; Xia et al., 2017).

Paracetamol Exposure

The study started with the process of spawning zebrafish to obtain their eggs. A $30 \times 20 \times 15$ cm^3 aquarium was filled with water that had been aerated for 24 hr, and a spawning vessel was added. Broodstock zebrafish, approximately 3 months old and exhibiting good morphology and movement, were chosen for the experiment. Two male zebrafish were placed outside the mating chamber area, while one female was placed inside. The male and female fish were put together in spawning containers and left overnight in a dark environment. The following day, the fish were exposed to natural lighting and lamps for one hour to stimulate spawning. Once a successful spawning process was identified by the number of eggs in the aquarium, the parental fishes were returned to the original aquarium, and the fish eggs were harvested and placed in a petri dish filled with egg water media. The harvested eggs were then washed with egg water media to remove any dirt or debris and selected using a microscope for the study. A total of 20 healthy eggs with 2 replicates (40 eggs in total) were each placed in three Petri dishes containing 3- or 5-mM paracetamol solution, and egg water media was used as a control. These dishes were kept at room temperature for 72 hpf or three days. This methodology follows Arias-Alpizar et al. (2021) and Halder et al. (2010).

Observation of Developmental Abnormalities

Observation of zebrafish development was carried out at 24, 48, and 72 hpf, utilizing a Leica DM 500 microscope (Germany) with a magnification of $4 \times 10 - 10 \times 10$ (Cedron et al., 2020; Kimmel et al., 1995; Nogueira et al., 2019). The study focused on survival rate, hatching rate, and observable morphological changes. Morphological parameters such as spinal abnormalities, pericardial edema and blood clots, eye pigmentation, heart rate, and spontaneous movements were observed before and after hatching.

Statistical Analysis

Quantitative data on survival rate, hatchability, spinal abnormalities, spontaneous movements, pericardial edema, and heart rate were analyzed using Microsoft Excel 2013. Pigmentation analysis was conducted utilizing Image J. Statistical analysis was carried out using two-way analysis of variance (ANOVA), with a significance level of 0.05. The Tukey's honestly significant difference (HSD) test was then employed to determine the location of the significant differences.

RESULTS AND DISCUSSION

Effect of Paracetamol on Hatching and Survival Rate

Paracetamol is a teratogen that negatively affects the hatching rate of zebrafish.

Statistical analysis indicated that each treatment group's hatching rate differed significantly (p<0.05). Tukey's HSD analysis showed that the paracetamol concentrations of 3- and 5-mM considerably impacted the hatching rate compared to the control group. However, there was no significant difference between the hatching rates of the 3- and 5-mM concentrations, as illustrated in Figure 1.

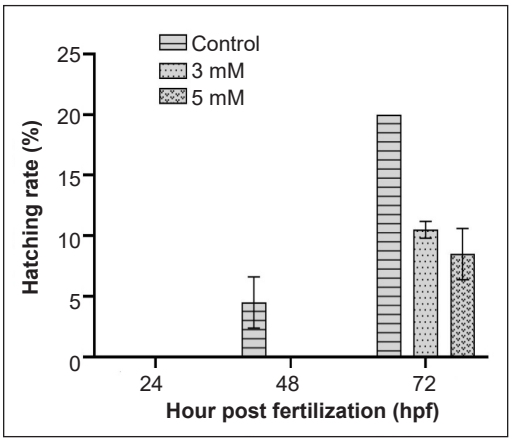

Figure 1. Effects of paracetamol exposure on the hatching rate of zebrafish

In this study, the evaluation of the hatching rate began at 48 to 72 hpf. The control group exhibited a higher hatching rate than those exposed to 3- and 5-mM paracetamol concentrations. These findings suggest that paracetamol delays the hatchability of embryos into larvae. The percentage of hatching rate at 72 hpf for embryos exposed to 3- and 5-mM concentrations was 52.5 and 42.5%, respectively, of the total embryos. Moreover, this study found that most embryos exposed to paracetamol experienced hatch failure and died. These results are consistent with Jyotsna's (2016) research on a concentration of 10 mM paracetamol and Glasco et al. (2022) study on a concentration of 3.9 mM paracetamol.

The hatching period of zebrafish usually occurs within 72 hpf, as observed in the control group. However, this study showed a lower hatching rate, particularly in embryos exposed to 5 mM paracetamol. This finding is similar to the study conducted by Xia et al. (2017), which reported that paracetamol reduced egg hatchability and affected cell survival (Cedron et al., 2020). The exposure to paracetamol was carried out until 72 hpf, and there was no transfer to a drug-free medium, which is consistent with the findings of Kantae et al. (2016), who reported that paracetamol accumulation was present in the larvae after more than 2 hr of exposure. Paracetamol induces reactive oxygen species (ROS) and disrupts apoptosis, leading to spinal abnormalities in the embryo. Consequently, the movement of the embryo's spine, crucial in the hatching process, is disrupted (Glasco et al., 2022; Xia et al., 2017).

Similar to the hatching rate, the larval survival rate decreases over time. The statistical analysis demonstrated significant differences in the survival rate among each treatment group (p<0.05). According to Tukey's HSD analysis, 3- and 5-mM paracetamol had a significant effect on the survival rate compared to the control, with 5 mM treatment demonstrating a more significant effect, as depicted in Figure 2, which shows that the survival rate of zebrafish exposed to 3- and 5-mM

paracetamol decreased sharply at 72 hpf, to 70 and 22.5% of the total embryos, respectively. These results are consistent with studies conducted by Cedron et al. (2020) and Rosas-Ramírez et al. (2022), where paracetamol reduced the hatchability and survival rate of zebrafish embryos and larvae by up to 75%.

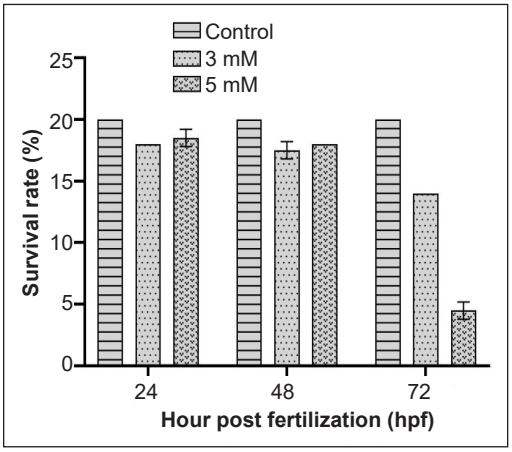

Figure 2. The impact of paracetamol exposure on the survival rate of zebrafish

Spinal Abnormalities

A scoring method was utilized to assess the severity of spinal abnormalities, with a score of 0 for normal straight spine, 1 for mild curvature (<10°), 2 for moderate curvature (10°–30°), 3 for severe curvature (>30°), and 4 for a vertebra that failed to form. At 72 hpf, exposure to paracetamol at a concentration of 3 mM resulted in moderate spinal curvature (score 2), whereas exposure to 5 mM paracetamol led to severe spinal curvature (score 3). Although spinal abnormalities were observed from 24 hpf at 3 mM, no formation of failed (score 4) spines was observed in this study. The results indicate that exposure to paracetamol affected the development of zebrafish. At 24 hpf, spinal abnormalities were observed, which may cause delays in hatching. Statistical analysis showed significant differences in each exposure treatment $p<0.05$. Tukey's HSD analysis revealed that paracetamol concentrations of 3 and 5 mM significantly affected spinal abnormalities compared to the control group (Figure 3). At 24 hpf, spinal curvature occurence (Figure 3) was found in embryos exposed to 3- and 5-mM paracetamol, accounting for 7.5% and 10% of the total embryos, respectively. The percentage of these abnormalities increased with age. At 48 hpf, larvae exposed to 5 mM paracetamol showed a spine abnormality increase of up to 67.5%. By 72 hpf, larvae exposed to paracetamol 3- and 5-mM showed spinal abnormalities, including 80 and 92.5% of the total embryos, respectively (Figure 4). These findings are consistent with the study reported by Raharjeng et al.

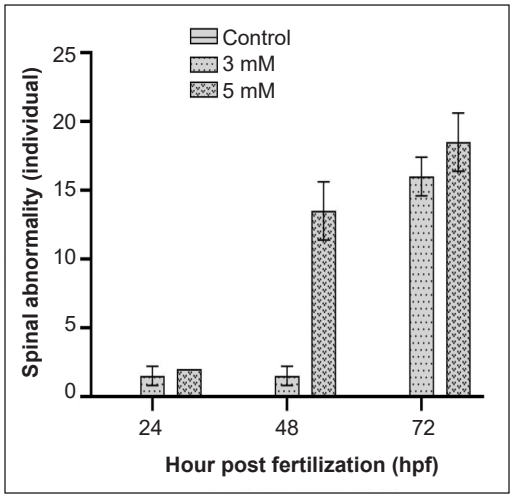

Figure 3. The influence of paracetamol exposure on the development of the spinal column in zebrafish

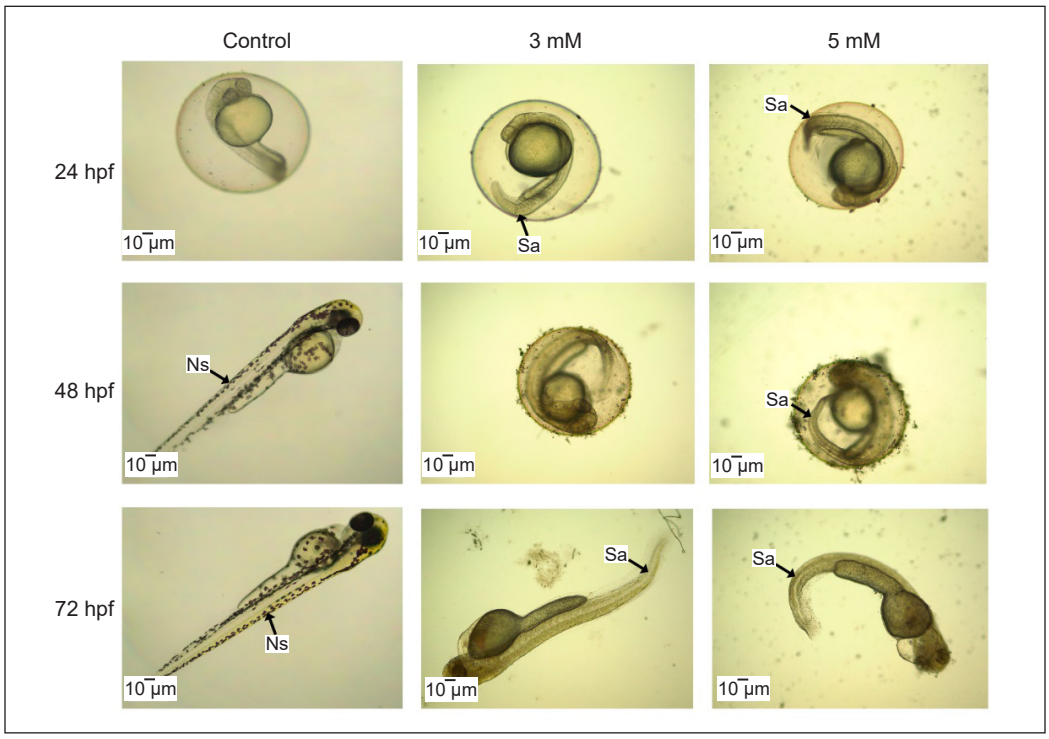

Figure 4. Spinal abnormalities in zebrafish embryos exposed to different paracetamol concentrations
Note. Ns = Nervous system; Sa = Spinal abnormalities

(2021), which suggests that developmental abnormalities in zebrafish embryos may or may not be related to bone. The results of this study show that higher concentrations and duration of paracetamol exposure led to increased spinal abnormalities, in line with previous studies by Cedron et al. (2020), Nogueira et al. (2019), and Xia et al. (2017). These spinal abnormalities suggest that paracetamol affects the development of the spinal cord, which has also been shown in the research by Cedron et al. (2020).

Zebrafish embryos have neural crest cells (NC Cells), pluripotent cells formed during the early developmental period of vertebrates, specifically at the border of the neural tube (Cedron et al., 2020). Upon closure of the neural tube, NC cells differentiate into various types of cells, such as sensory nerves, autonomic nerves, pigment cells, bone, and cartilage. Rosas-Ramírez et al. (2022) found that NC cells activate the soxE gene, which determines the development of NC tissue.

When paracetamol enters the human body, it undergoes biotransformation mediated by cytochrome P450 and converts into *N*-acetyl-*p*-benzoquinone-imine (NAPQI) (Cedron et al., 2020; Rosas-Ramírez et al., 2022). NAPQI is a metabolite compound that is produced during the process of xenobiotic metabolism of paracetamol/analgesia. NAPQI is typically eliminated by a conjugation

reaction with glutathione (GSH) in the liver, but high doses of paracetamol can lead to the accumulation of NAPQI, which can cause mutations in the soxE gene in NC cells, affecting the process of cell specification and differentiation (Bastiaan Vliegenthart et al., 2015; Glasco et al., 2022; Gum & Cho, 2013). Additionally, NAPQI induces apoptosis in differentiated cells, such as those in the spinal column, leading to neurological abnormalities characterized by the bending of the body or tail of a fish (Cedron et al., 2020; Rosas-Ramírez et al., 2022).

Pericardial Edema

A scoring system was implemented to evaluate the severity of pericardial edema. The score starts at 0 for normal/no edema and increases as follows: 1 for mild edema (enlargement < 10%), 2 for moderate edema (enlargement 10%–45%), 3 for severe edema (enlargement 46%–70%), and 4 for very severe edema (>70% enlargement). None of the groups showed pericardial edema at 24 hpf, but at 48 hpf, the 3mM group had mild pericardial edema (score 1), while the 5 mM group showed severe edema (score 3). At 72 hpf, exposure to 3 mM paracetamol resulted in moderate edema (score 2), whereas, at 5 mM exposure, severe edema (score 4) was observed. Statistical analysis showed significant differences in each treatment (p<0.05). Tukey's HSD analysis showed that concentrations of 3- and 5-mM paracetamol significantly affected pericardial edema compared to controls. However, there was no significant difference in pericardial edema between concentrations of 3- and 5-mM (Figure 5). The control group showed no pericardial edema. At 48 hpf, exposure to 3- and 5-mM paracetamol caused pericardial edema in 62.5 and 82.5% of the total embryos, respectively. 3- and 5-mM paracetamol exposure caused pericardial edema in 87.5 and 92.5% of total embryos at 72 hpf. Figure 6 shows the increased pericardial edema at 72 hpf on exposure to paracetamol 3 and 5 mM. The results are consistent with those of Cedron et al. (2020) and Kang et al. (2020).

Pericardial edema in this study (Figure 6) is believed to be caused by impaired transport and membrane permeability from exposure to paracetamol. Paracetamol is known to reduce water export, which affects blood circulation and kidney function. Specifically, it obstructs glomerular formation and electrolyte reabsorption, disrupting the osmotic balance in the fish's body (Cedron et al., 2020). Exposure to

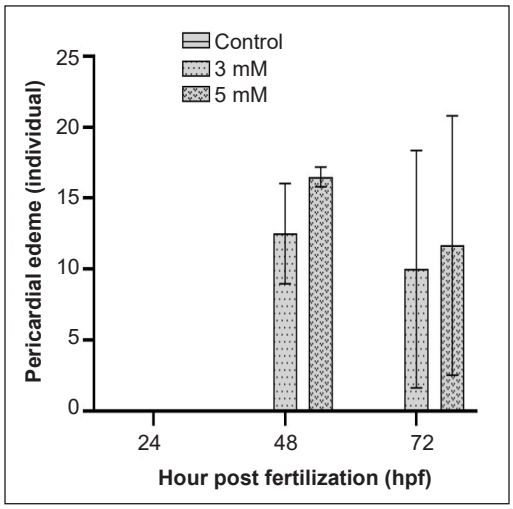

Figure 5. Pericardial edema in zebrafish induced by paracetamol exposure

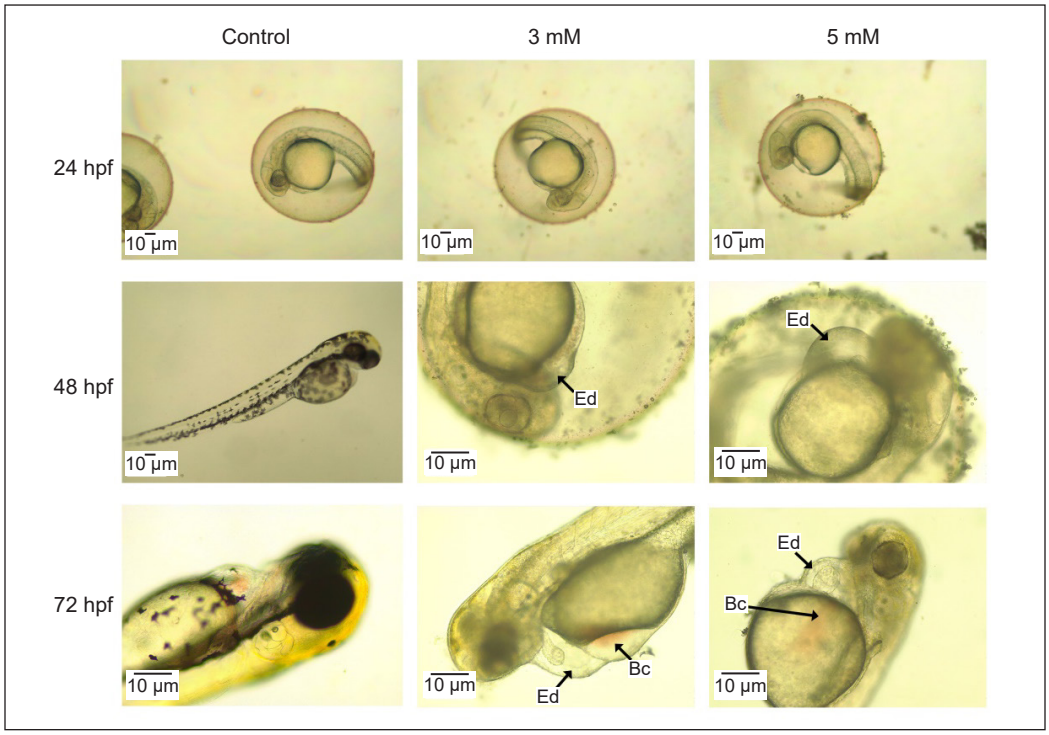

Figure 6. Representative images of pericardial edema and blood clot induced in zebrafish embryos exposed to different paracetamol concentrations
Note. Bc = Blood clot; Ed = Edema

paracetamol also induces ROS, which can disrupt gene regulation of pax2a, sim1, and wt1 homologs, preventing proper nephron and kidney development and function (Hill et al., 2003; Kang et al., 2020).

Research by Kitipaspallop et al. (2021) has shown that pericardial edema can also result from oxidative stress and inflammation, which are related to the expression of tumor necrosis factor-alpha (TNF-α) and interleukin-1b. These three genes are also associated with apoptosis and hematopoiesis. The expression of Tal1 and gata1 influences the hematopoiesis process, where Tal1 is a transcription factor that regulates Spilb and mpx hematopoietic stem cells, while gata1 regulates erythroid cells. The discovery of pericardial edema and blood clots in zebrafish, an animal model, is also found in the human body due to the consumption of analgesic drugs in inappropriate dosages. The formation of edema and blood clots can affect heart function, leading to myocardial infarctions, cardiac dysfunction, cardiac arrhythmias, and even heart failure due to an acetaminophen overdose (KhabazianZadeh et al., 2019).

Eyes Pigmentation Abnormalities

A grading system was implemented to assess the eye pigment abnormalities. The

grading score ranged from 0 to 4, where 0 corresponded to dark black eyes with pigment levels above 90%, 1 for black eyes with pigment levels ranging from 63–90%, 2 for dark gray eyes with pigment levels from 36–62%, 3 for gray eyes with pigment levels between 10–36%, and 4 for light gray eyes with pigment levels less than 10%. Exposure to 3 mM and 5 mM concentrations of paracetamol resulted in a significant decrease in the formation of eye pigment. At 72 hpf, embryos exposed to 3 mM paracetamol displayed gray eyes with a score of 3, while those exposed to 5 mM paracetamol exhibited light gray eyes with a score of 4.

In zebrafish, pigmentation is due to the presence of melanocytes, iridophores, and xanthophores, pigmentation cells derived from NC cells (Cedron et al., 2020). Melanocytes produce black pigment at the embryonic age of 24 hpf, and research shows that exposure to acetaminophen hinders the formation of black pigment along the spinal column and head to eyes (Cedron et al., 2020). In this study, the percentage of eye pigmentation was measured, and it was found that exposure to paracetamol caused hypopigmentation. The statistical analysis results indicated significant differences in each treatment (p<0.05). Additionally, Tukey's HSD analysis revealed that paracetamol concentrations of 3 and 5 mM significantly affected eye pigmentation compared to controls (Figure 7).

The black spots in the zebrafish eye and body pigmentation can be observed at 24 hpf and are more prominent at 48 and 72 hpf in the control groups. However, exposure to paracetamol resulted in hypopigmentation or incomplete pigment formation, causing the larvae to appear transparent (Figure 8). The analysis of eye pigmentation was conducted by measuring the percentage of blackness in the eyes with Image J. At 24 hpf, the control group had an eye pigmentation of 4.72%, while the 3- and 5-mM paracetamol exposure groups had 1.72 and 0.88% eye pigmentation, respectively. At 48 hpf, the control group's eye pigmentation increased sharply to 66.78%, while the paracetamol exposure groups did not show a significant increase, with 3.68 and 2.40% eye pigmentation at 3 and 5 mM, respectively. At 72 hpf, the control group's eyes were darker, with a percentage of 93.26%, whereas the paracetamol exposure groups at 3 and 5 mM were 18.43 and 9.69%, respectively.

This study's results suggest that paracetamol impacts pigmentation, as

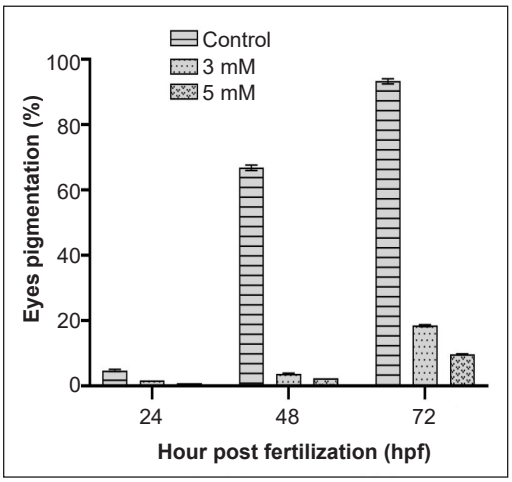

Figure 7. Eye pigmentation in zebrafish exposed to different concentrations of paracetamol

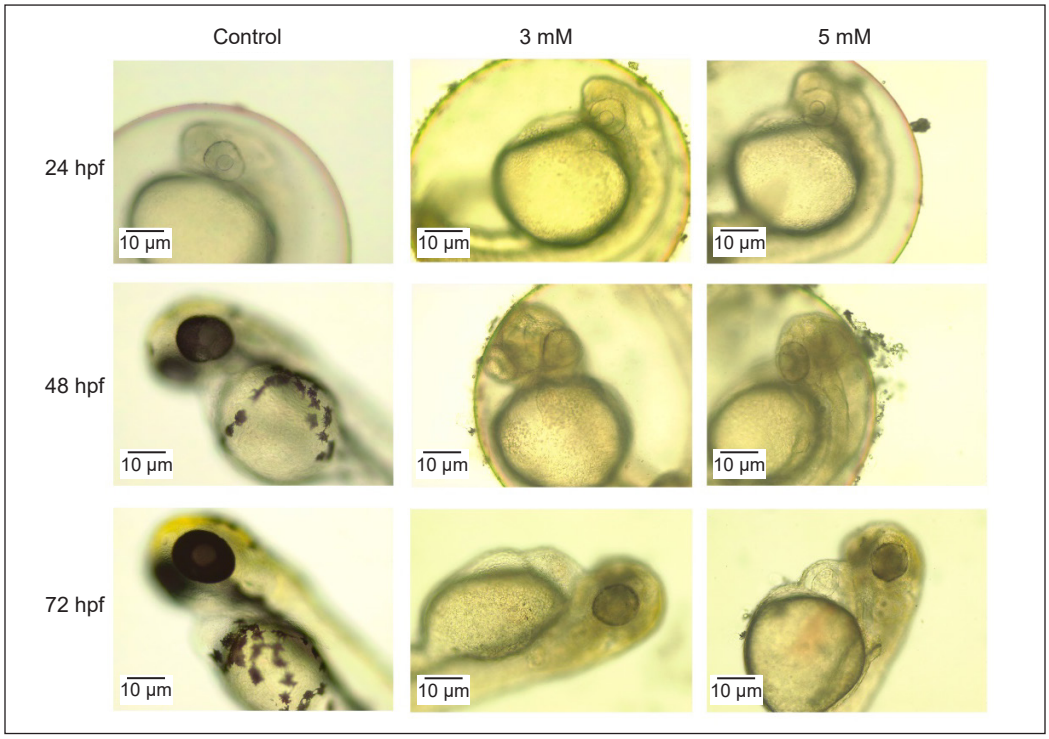

Figure 8. Abnormalities in eye pigmentation in zebrafish embryos exposed to different concentrations of paracetamol

evidenced by hypopigmentation. Cedron et al. (2020) found that exposure to acetaminophen in zebrafish significantly reduced melanocyte levels at ages 48, 72, and 96 hpf. Similarly, Wrześniok et al. (2016) reported that cell cultures showed hypopigmentation due to defects in melanin synthesis and cell survival. Nogueira et al. (2019) discovered that paracetamol caused a decrease in melanocytes and induced oxidative stress and epigenetic modification.

Heartbeat Abnormalities

Abnormalities in the hearts of zebrafish embryos can include edema and blood clots, causing disruptions to the heartbeat and blood circulation. A study by Xia et al. (2017) found that acetaminophen caused a decrease in the average heart rate per minute. Statistical analysis showed significant differences between treatments ($p<0.05$). Tukey's HSD analysis revealed that paracetamol concentrations of 3 and 5 mM significantly affected heartbeat abnormalities compared to the control group, with the concentration of 5 mM having a greater effect.

At 48 hpf, the control group had a normal heart rate of 137 beats/min, while those exposed to 3- and 5-mM paracetamol had 67.90 and 62.65 beats/min rates, respectively. The decrease in heart rate was more pronounced at 72 hpf, with exposure to 3- and 5-mM paracetamol resulting

in rates of 61.68 and 13.99 beats/min, respectively (Figure 9). The metabolism of vitamin A is affected by both the deficiency or excess of retinoic acid (RA) and N.N-diethylaminobenzaldehyde (DEAB) inhibitors, and this can have an impact on heart development by altering retinoid metabolic pathways (Jarque et al., 2020).

Abnormalities in Spontaneous Movement

This study analyzes spontaneous swimming activity as it is the first movement in the development of zebrafish, resulting from the development of muscle motoneurons, triggering hatching or emergence (Xia et al., 2017). The statistical analysis showed significant differences in each treatment (p<0.05). Furthermore, Tukey's HSD analysis revealed that 3- and 5-mM paracetamol concentrations significantly affected spontaneous movement compared to the control (Figure 10). The observation of spontaneous movements was conducted until 48 hpf because, by 72 hpf, all embryos had hatched. There is a notable difference in the observation of 48 hpf, where spontaneous movements were still observed at 3 mM paracetamol exposure, at a rate of 7.5%, and the rate is even higher at 5 mM exposure, reaching 67.5%.

Paracetamol exposure has been found to induce diverse abnormalities in zebrafish, an important model organism for studying freshwater animals. While paracetamol has been detected in high concentrations in seawater (Koagouw et al., 2021) and drinking water (Al-Kaf et al., 2017), the possibility of its presence in freshwater environments raises concerns about the potential deleterious effects on the growth and development of aquatic fauna. Findings from this study may serve as valuable evidence or a reference point for investigating the prevalence of paracetamol in freshwater systems and inform the implementation of waste management practices, particularly regarding medicinal

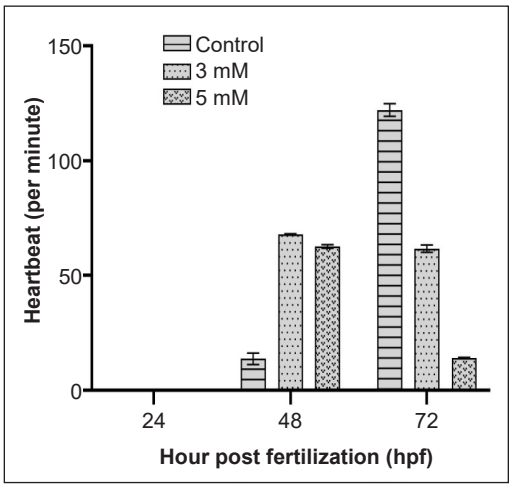

Figure 9. Abnormal heartbeat rate in zebrafish embryos upon exposure to paracetamol

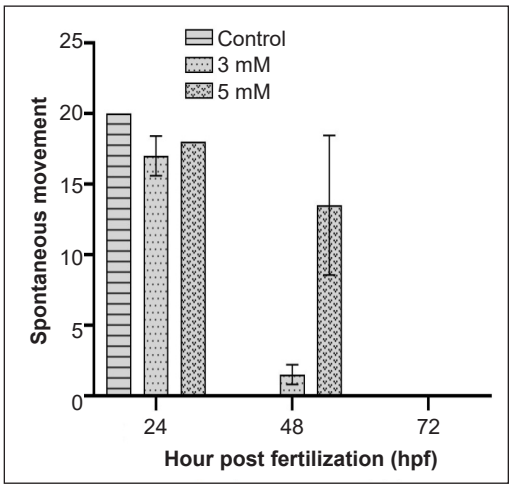

Figure 10. Abnormalities of spontaneous movement in zebrafish embryos exposed to paracetamol

waste, to mitigate the risk of environmental contamination.

Lastly, assessing the impact of paracetamol contamination on the aquatic environment also requires knowledge of the amount of paracetamol residue in various parts of the fish body. Future research should prioritize collecting residue data of paracetamol in different organs, such as gills, liver, muscle, and skin, to address this knowledge gap. Additionally, the study could focus on different fish species and their geographic locations to develop a comprehensive understanding of residue level variations. Also, further research could explore the effect of paracetamol contamination in non-fish aquatic organisms. The findings of such research could help develop better policies and guidelines for ensuring the protection of aquatic ecosystems.

CONCLUSION

Exposure to paracetamol at concentrations of 3 and 5 mM has been shown to impact the development of zebrafish embryos and larvae significantly. The negative effects on the egg hatchability, survival rate, spontaneous movement, spinal development, pericardial edema, blood clots, eye hypopigmentation, and heart rate become more pronounced with increasing concentrations and prolonged exposure time.

ACKNOWLEDGEMENTS

The authors thank the Faculty of Biology, Gadjah Mada University, Indonesia, especially the Laboratory of Animal Structure and Development, for supporting this research. They dedicated this study to their colleague Tonny Prince Kunjirika†, who passed away on December 5, 2022.

REFERENCES

Alchin, J., Dhar, A., Siddiqui, K., & Christo, P. J. (2022). Why paracetamol (acetaminophen) is a suitable first choice for treating mild to moderate acute pain in adults with liver, kidney, or cardiovascular disease, gastrointestinal; disorders, asthma, or who are older? *Current Medical Research and Opinion*, *38*(5), 811-825. https://doi.org/10.1080/03007995.2022.2049551

Al-Kaf, A. G., Naji, K. M., Abdullah, Q. Y. M., & Edrees, W. H. A. (2017). Occurrence of paracetamol in aquatic environments and transformation by microorganisms: A review. *Chronicles of Pharmaceutical Science*, *1*(6), 341-355.

Arias-Alpizar, G., Bussmann, J., & Campbell, F. (2021). Zebrafish embryos as a predictive animal model to study nanoparticle behavior *in vivo*. *Bio-protocol*, *11*(19), e4173. https://doi.org/10.21769/BioProtoc.4173

Bastiaan Vliegenthart, A. D., Antonie, D. J., & Dear, J. W. (2015). Target biomarker profile for the clinical management of paracetamol overdose. *British Journal of Clinical Pharmacology*, *80*(3), 351-362. https://doi.org/10.1111/bcp.12699

Cedron, V. P., Wiener, A. M. J., Vera, M., & Sanchez, L. (2020). Acetaminophen affects the survival, pigmentation, and development of craniofacial structures in zebrafish (*Danio rerio*) embryos. *Biochemical Pharmacology*, *174*, 113816. https://doi.org/10.1016/j.bcp.2020.113816

Chakraborty, T., Baidya, M., & Chakraborty, A. (2015). Paracetamol - A self-medicated popular drug abused by the young student community. *Biomedical and Pharmacology Journal*, *2*(1), 99-103.

Chiew, A. L., Reith, D., Pomerleau, A., Wong, A., Isoardi, K. Z., Soderstrom, J., & Buckley, N. A. (2020). Updated guidelines for the management of paracetamol poisoning in Australia and New Zealand. *Medical Journal of Australia*, *212*(4), 175-183. https://doi.org/10.5694/mja2.50428

Daniel, D., Nunes, B., Pinto, E., Ferreira, I. M. P. L. V. O., & Correia, A. T. (2022). Assessment of paracetamol toxic effects under varying seawater pH conditions on the marine polychaete *Hediste diversicolor* using biochemical endpoints. *Biology*, *11*(4), 581. https://doi.org/10.3390/biology11040581

Faqihi, A. H. M. A., & Sayed, S. F. (2021). Self-medication practice with analgesics (NSAIDs and acetaminophen), and antibiotics among nursing undergraduates in University College Farasan Campus, Jazan University, KSA. Annales Pharmaceutiques Françaises, *79*(3), 275-285. https://doi.org/10.1016/j.pharma.2020.10.012

Folarin, O. S., Otitoloju, A. A., Amaeze, N. H., & Saliu, J. K. (2019). Occurrence of acetaminophen, amoxicillin, diclofenac, and methylparaben in Lagos and Ologe lagoons, Lagos, Nigeria. *Journal of Applied Sciences and Environmental Management*, *23*(12), 2143-2149. https://doi.org/10.4314/jasem.v23i12.10

Franzellitti, S., Buratti, S., Du, B., Haddad, S. P., Chambliss, C. K., Brooks, B. W., & Fabbri, E. (2015). A multi-biomarker approach to explore interactive effects of propranolol and fluoxentine in marine mussels. *Environmental Pollution*, *205*, 60-69. https://doi.org/10.1016/j.envpol.2015.05.020

Freo, U., Ruocco, C., Valerio, A., Scagnol, I., & Nisoli, E. (2021). Paracetamol: A review of guideline recommendations. *Journal of Clinical Medicine*, *10*(15), 3420. https://doi.org/10.3390/jcm10153420

Glasco, D. M., Wang, Z., Kang, S., & Funkhouser, A. T. (2022). Acetaminophen disrupts the development of pharyngeal arch-derived cartilage and muscle in zebrafish. *Journal of Developmental Biology*, *10*(3), 30. https://doi.org/10.3390/jdb10030030

Gum, S. I., & Cho, M. K. (2013). The amelioration of N-acetyl-p-benzoquinone imine toxicity by ginsenoside Rg3: The role of Nrf2-mediated detoxification and Mrp1/Mrp3 transports. *Oxidative Medicine and Cellular Longevity*, *2013*, 957947. https://doi.org/10.1155/2013/957947

Halder, M., Léonard, M., Iguchi, T., Oris, J. T., Ryder, K., Belanger, S. E., Braunbeck, T. A., Embry, M. R., Whale, G., Norberg-King, T., & Lillicrap, A. (2010). Regulatory aspects on the use of fish embryos in environmental toxicology. *Integrated Environmental Assessment and Management*, *6*(3), 484–491. https://doi.org/10.1002/ieam.48

Hidayati, H. B., & Kustriyani, A. (2020). Paracetamol, migraine, and medication overuse headache (MOH). *Journal of Pain, Headache, and Vertigo*, *1*(2), 42-47. https://doi.org/10.21776/ub.jphv.2020.001.02.5

Hill, A., Howard, C. V., Strahle, U., & Cossins, A. (2003). Neurodevelopmental defects in zebrafish (*Danio rerio*) at environmentally relevant dioxin (TCDD) concentrations. *Toxicology Sciences*, *76*(2), 392-399. https://doi.org/10.1093/toxsci/kfg241

Hodgman, M. J., & Garrard, A. R. (2012). A review of acetaminophen poisoning. *Critical Care Clinic*, *28*(4), 499-516. https://doi.org/10.1016/j.ccc.2012.07.006

Ishizuka, K., Yoshida, T., Kawabata, T., Imai, A., Mori, H., Kimura, H., Inada, T., Okahisa, Y., Egawa, J., Usami, M., Kushima, I., Morikawa, M., Okada, T., Ikeda, M., Branko, A., Mori, D., Someya, T., Iwata, N., & Ozaki, N. (2020). Functional characterization of rare *NRXN1* variants identified in autism spectrum disorders and schizophrenia. *Journal of Neurodevelopmental*

Disorders, *12*, 25. https://doi.org/10.1186/s11689-020-09325-2

Jarque, S., Rubio-Brotons, M., Ibarra, J., Ordoñez, V., Dyballa, S., Miñana, R., & Terriente, J. (2020). Morphometric analysis of developing zebrafish embryos allows for predicting teratogenicity modes of action in higher vertebrates. *Reproductive Toxicology*, *96*, 337-348. https://doi.org/10.1016/j.reprotox.2020.08.004

Jóźwiak-Bebenista, M., & Nowak, J. Z. (2014). Paracetamol: Mechanism of action, applications, and safety concern. *Acta Poloniae Pharmaceutica*, *71*(1), 11-23.

Jyotsna, S. Y. (2016). Effect of flavonoids in acetaminophen-induced liver injury in *Danio rerio*. *International Journal of Health Sciences and Research*, *6*(2), 352-359.

Kang, A. M., Padilla-Jones, A., Fisher, E. S., Akakpo, J. Y., Jaeschke, H., Rumack, B. H., Gerkin, R. D., & Curry, S. C. (2020). The effect of 4-methyl pyrazole on oxidative metabolism of acetaminophen in human volunteers. *Journal of Medical Toxicology*, *16*, 169-176. https://doi.org/10.1007/s13181-019-00740-z

Kantae, V., Krekels, E. H., Ordas, A., González, O., van Wijk, R. C., Harms, A. C., Racz, P. I., van der Graaf, P. H., Spaink, H. P., & Hankemeier, T. (2016). Pharmacokinetic modeling of paracetamol uptake and clearance in zebrafish larvae: Expanding the allometric scale in vertebrates with five orders of magnitude. *Zebrafish*, *13*(6), 504-510. https://doi.org/10.1089/zeb.2016.1313

KhabazianZadeh, F., Kazemi, T., Nakhaee, S., Ng, P. C., & Mehrpour, O. (2019). Acetaminophen poisoning-induced heart injury: A case-based review. *DARU Journal of Pharmaceutical Sciences*, *27*, 839-851. https://doi.org/10.1007/s40199-019-00307-x

Kimmel, C. B., Ballard, W. W., Kimmel, S. R., Ullman, B., & Schilling, T. F. (1995). Stages of embryonic development of the zebrafish. *Developmental Dynamics*, *203*(3), 253-310. https://doi.org/10.1002/aja.1002030302

Kitipaspallop, W., Sillapaprayoon, S., Taepavarapruk, P., Chanchao, C., & Pimtong, W. (2021). Evaluation of developmental and transcriptional effects of α-mangosteen on zebrafish embryos. *Toxicological and Environmental Chemistry*, *103*(3), 254-268. https://doi.org/10.1080/02772248.2021.1960349

Koagouw, W., Arifin, Z., Olivier, G. W. J., & Ciocan, C. (2021). High concentrations of paracetamol in effluent-dominated waters of Jakarta Bay, Indonesia. *Marine Pollution Bulletin*, *169*, 112558. https://doi.org/10.1016/j.marpolbul.2021.112558

Koehn, L. M., Huang, Y., Habgood, M. D., Kysenius, K., Crouch, P. J., Dziegielewska, K. M., & Saunders, N. R. (2020). Effects of paracetamol (acetaminophen) on gene expression and permeability properties of the rat placenta and fetal brain. *F1000Research*, *9*, 573. https://doi.org/10.12688/f1000research.24119.2

Kuswinarti, K., Rohim, A. B. M., & Aminah, S. (2020). Attitude and behavior towards self-medication using non-steroidal anti-inflammatory drugs and paracetamol among housewives in Hegarmanah Village, Jatinangor. *Althea Medical Journal*, *7*(1), 25-30. https://doi.org/10.15850/amj.v7n1.1721

Leal, N. S., Yu, Y., Chen, Y., Fedele, G., & Martins, L. M. (2021). Paracetamol is associated with a lower risk of COVID-19 infection and decreased ACE2 protein expression: A retrospective analysis. *COVID*, *1*(1), 218-229. https://doi.org/10.3390/covid1010018

Leppert, B., Havdahl, A., Riglin, L., Jones, H. J., Zheng, J., Davey Smith, G., Tilling, K., Thapar, A., Reichborn-Kjennerud, T., & Stergiakouli, E. (2019). Association of maternal neurodevelopmental risk alleles

with early-life exposures. *JAMA Psychiatry*, *76*(8), 834-842. https://doi.org/10.1001/jamapsychiatry.2019.0774

Liew, Z., Ritz, B., Virk, J., & Olsen, J. (2016). Maternal use of acetaminophen during pregnancy and risk of autism spectrum disorders in childhood: A Danish national birth cohort study. *Autism Research*, *9*(9), 951-958. https://doi.org/10.1002/aur.1591

Mostafa, E. M. A., Tawfik, A. M., & Abd-Elrahman, K. M. (2022). Egyptian perspectives on the potential risk of paracetamol/acetaminophen-induced toxicities: Lessons learned during COVID-19 pandemic. *Toxicology Reports*, *9*, 541-548. https://doi.org/10.1016/j.toxrep.2022.03.035

Nogueira, A. F., Pinto, G., Correia, B., & Nunes, B. (2019). Embryonic development, locomotor behavior, biochemical, and epigenetic effects of the pharmaceutical drugs paracetamol and ciprofloxacin in larvae and embryos of *Danio rerio* when exposed to environmental realistic levels of both drugs. *Environmental Toxicology*, *34*(11), 1177-1190. https://doi.org/10.1002/tox.22819

Patel, R., Sushko, K., van den Anker, J., & Samiee-Zafarghandy, S. (2022). Long-term safety of prenatal and neonatal exposure to paracetamol: A systematic review. *International Journal of Environmental Research and Public Health*, *19*(4), 2128. https://doi.org/10.3390/ijerph19042128

Raharjeng, A. R. P., Kusumaningtyas, A. A., Widatama, D. A., Zarah, S., Pratama, S. F., & Dani, H. B. (2021). The effects of the plant extract on embryonic development of zebrafish (*Danio rerio*). *Tropical Genetics*, *1*(1), 6-11.

Rivera-Utrilla, J., Sánchez-Polo, M., Ferro-García, M. Á., Prados-Joya, G., & Ocampo-Pérez, R. (2013). Pharmaceuticals as emerging contaminants and their removal from water. A review. *Chemosphere*, *93*(7), 1268-1287. https://doi.org/10.1016/j.chemosphere.2013.07.059

Rosas-Ramírez, J. R., Orozco-Hernández, J. M., Elizalde-Velázquez, G. A., Raldúa, D., Islas-Flores, H., & Gómez-Oliván, L. M. (2022). Teratogenic effects induced by paracetamol, ciprofloxacin, and their mixture on *Danio rerio* embryos: Oxidative stress implications. *The Science of the Total Environment*, *806*(Part 2), 150541. https://doi.org/10.1016/j.scitotenv.2021.150541

Shigei, M., Assayed, A., Hazaymeh, A., & Dalahmeh, S. S. (2021). Pharmaceutical and antibiotic pollutant levels in wastewater and the waters of the Zarqa River, Jordan. *Applied Sciences*, *11*(18), 8638. https://doi.org/10.3390/app11188638

Skovlund, C. W., Mørch, L. S., Kessing, L. V., & Lidegaard, Ø. (2016). Association of hormonal contraception with depression. *JAMA Psychiatry*, *73*(11), 1154-1162. https://doi.org/10.1001/jamapsychiatry.2016.2387

Wrześniok, D., Oprzondek, M., Hechmann, A., Beberok, A., Otreba, M., & Buszman, E. (2016). Effect of paracetamol on melanization process in human epidermal melanocytes. *Acta Poloniae Pharmaceutica*, *73*(3), 653-658.

Xia, L., Zheng, L., & Zhou, J. L. (2017). Effects of ibuprofen, diclofenac, and paracetamol on hatch and motor behavior in developing zebrafish (*Danio rerio*). *Chemosphere*, *182*, 416-425. https://doi.org/10.1016/j.chemosphere.2017.05.054

Xu, X., Xu, X., Huang, X., Xia, W., & Xia, S. (2010). A high-throughput analysis method to detect regions of interest and quantify zebrafish embryo images. *Journal of Biomolecular Screening*, *15*(9), 1152-1159. https://doi.org/10.1177/1087057110379155

Pertanika J. Trop. Agric. Sci. 46 (4): 1189 - 1204 (2023)

PERTANIKA JOURNALS

TROPICAL AGRICULTURAL SCIENCE

Journal homepage: http://www.pertanika.upm.edu.my/

Review Article

Regulation of Potato Plant's Growth Functions

Irina Anikina[1]*, Viktor Kamkin[2], Zhastlek Uakhitov[2], Mayra Zhagiparova[1], Ulan Tileubek[1] and Galiya Kazhibayeva[1]

[1]*Department of Biotechnology, Faculty of Agricultural Sciences, Toraighyrov University, 140008 Pavlodar, Kazakhstan*

[2]*Department of Agrotechnology, Faculty of Agricultural Sciences, Toraighyrov University, 140008 Pavlodar, Kazakhstan*

ABSTRACT

Ontogenesis control is important for developing methods for modeling and yield forecasting potatoes. Knowledge of the mechanisms of phyto-regulation allows for a directed impact on plant ontogenesis. Phytohormone analogs are widely used both in culture *in vitro* and *in vivo*; under their influence, the processes of differentiation and callusogenesis take place, morphogenesis and tuberization are induced *in vitro*, a root formation is induced, seed dormancy is overcome, plant resistance to abiotic stress factors is increased, and protective properties against phytoinfections increases the content of valuable substances and yield. Currently, the list of drugs with pronounced regulatory activity has expanded significantly. Among chemical alternatives, preparations based on microorganisms are most widely used in practice as yield stimulants and resistance inducers. At the same time, there is a growing interest in herbal preparations containing a huge amount of valuable biologically active substances with a different spectrum of action. The growing role and importance of plant growth and development regulators necessitates a deep study of the action nature of these compounds using modern biochemical and molecular genetic methods. At the same time, the search for new strains and drugs that can positively influence plant health and growth under various growth conditions, especially under stress conditions, is relevant. Works

ARTICLE INFO

Article history:
Received: 27 March 2023
Accepted: 23 May 2023
Published: 31 October 2023

DOI: https://doi.org/10.47836/pjtas.46.4.07

E-mail addresses:
anikina.i@mail.ru (Irina Anikina)
vikkamkin@mail.ru (Viktor Kamkin)
zhassan-kozgan@mail.ru (Zhastlek Uakhitov)
maira010579@mail.ru (Mayra Zhagiparova)
ulan.tleubekov@gmail.com (Ulan Tileubek)
docent-1965@mail.ru (Galiya Kazhibayeva)
* Corresponding author

Current affiliation:
Galiya Kazhibayeva
Department of Food Technology and Processing Products, Technical Faculty, S. Seifullin Kazakh, Agrotechnical Research University, 010011 Astana, Kazakhstan

ISSN: 1511-3701
e-ISSN: 2231-8542

in this direction should be intensified due to the constant climatic risks. Creating a science-based system of growth regulation can provide reliable, stable results for potatoes growing in any field conditions of future agriculture.

Keywords: Biological preparations, growth regulators, mechanisms of action, phytohormones, tuberization

INTRODUCTION

Throughout the development of plant breeding, the problems of growth and development control of plant organisms have attracted researchers in many countries. Quantitative levels of endogenous phytohormones and their antagonists underlie all correlations in the plant organism (Jing & Strader, 2019). With their changes, the growth centers move from one organ system to another (Zhao et al., 2022). For example, a high concentration of auxin leads to the formation of nutrients' attraction centers. As a result, growth processes in some organs are delayed, and in others, they are activated (Kurepa & Smalle, 2022). Over two centuries, great success has been made in studying growth regulators, their influence on individual development, and the periodicity of plant growth. The molecular and genetic basis of regulation of plant development processes in ontogeny and phylogeny have been revealed.

Now, a general schematic diagram of the formation of phytohormones, the implementation of their regulatory action, including the biosynthesis of a precursor, binding to a hormone-specific protein receptor with the formation of an active hormone-receptor complex, and the effect of this complex on the plant genome and the activity of enzyme systems have been identified. At the same time, the analysis of the study of the issues showed that the main studies were aimed at studying the effect of phytohormones and their chemical analogs on the growth and yield characteristics of the plants, and this is understandable because chemical growth regulators are now a day a mandatory element of successful agricultural production (Amoanimaa-Dede et al., 2022). It has been reliably established that they not only affect growth and development but also activation of the plants' internal potential, contribute to the activation of internal reserves of the plant organism, the process of photosynthesis, and growth of leaf mass, increase the supply of nutrients from the soil (Ahmed et al., 2021; Mitrofanov & Novikov, 2020).

Modern Approaches to Plant Growth Regulation

The number of compounds with hormonal activity in plants has expanded. In addition to the long-known auxins, cytokinins, gibberellins, abscisic acid, and ethylene, many new physiologically active compounds have been added, i.e., brassinosteroids, jasmonic acid, salicylic acid, and fusicoccin. All these phytohormones and their analogs have common properties, i.e., they are formed in plants in small quantities, easily move from one part to another, and cause significant metabolic and morphogenesis effects (Vural et al., 2018). Modern

biochemical and molecular genetic methods are being used to identify the specific role of phytohormones in tuber formation. Representation of great interest is the study of directed changes in the endogenous content of hormones in potato plants using a transgenic approach. Genetic engineering methods have created chimeric gene structures that include effective regulatory and promoter regions and carry marker and coding genes.

Obtaining transgenic plants with the help of such chimeric genes made it possible to elucidate the features of regulating the activity of poetin genes and study the functions performed by these storage proteins. Thus, it was found that the inclusion of markers, for example, the luciferase gene, in the chimeric gene, constructs carrying poetin genes, makes it possible to detect by using a luminometer, the inclusion, and exclusion of the genes of these proteins in connection with the control of tuberi formation both *in vitro* and *in vivo* plants (Hannapel et al., 2017). Great interest in studying plant growth regulation and development is associated with this area's important theoretical and practical significance. Growth regulators are currently an integral element of modern crop production, which allows for solving many problems, as well as an effective and affordable tool for increasing the profitability of agricultural crop production (Marenych et al., 2019). The studies of Mani and his co-authors showed the effectiveness of pre-plant treatment of tubers with thiourea to stop the dormant period and the germination of potatoes. Under the action of thiourea, the activity of catalase was suppressed, and the concentration of hydrogen peroxide increased, which caused an interruption of dormancy of tubers. Other researchers have shown a positive effect of thiourea on the formation and height of potato stems and tuber yield (Mani et al., 2013).

Using Phytohormones

The works of Murashev and his associates showed a positive effect of potato treatments with growth regulators based on amino acids on productivity, which increased by 20–30%. At the same time, a reduction in the interphase period of development by 20% and a reduction in the growing season by 5–10 days were noted (Murashev et al., 2020). Preparations of the retardants group are most often used in agricultural crop production (Singh & Jambukiya, 2020). In potato seed production, these preparations are used to increase the reproduction rate; one of the characteristic manifestations of their action is the inhibition of growth, which increases the mechanical strength of stem tissues, which positively affects the survival rate of meristem potato seedlings (Anikina et al., 2015). Several researchers found that spraying potato plants with chlorcholine chloride inhibited stem growth by reducing the length and number of internodes, increasing the number of leaves and their size, reducing the length of stolons, and accelerating tuber maturation (Hossain et al., 2019). It has been shown that as a result of leaf treatment of potato plants with chlorcholine chloride at a dose of 2.0 g/L,

the content of indoleacetic-3-acid (IAA) and zeatin (Z) increased in the leaves, while the content of abscisic acid decreased. It was determined that this preparation has a significant regulatory role in plant photosynthesis; stomatal conductance, net photosynthesis rate, and transpiration rate increased under its influence. Consequently, the yield and quality of tubers increased (Wang & Xiao, 2008). The use of cytokinins to improve the growth of agricultural plants under conditions of increased salinity and waterlogged soil is well understood (Li et al., 2020).

Growth regulators are of great importance for the reproduction of potatoes *in vitro*. Two groups of growth regulators, i.e., auxins and cytokinins, control the processes of differentiation and callusogenesis. In addition, they affect the processes of morphogenesis and tuberization *in vitro*. Tuberization is a multifaceted, specific process caused by a combination of external and internal stimuli and is associated with changes in the synthesis and transport of substances. Phytohormones act as internal stimuli; among them, auxins, cytokinins, and gibberellins also play a special role in tuber ontogenesis. Other hormones are also involved, but to a lesser extent (Vural et al., 2018; Wróbel et al., 2017). In the case of auxins, it was found that the introduction of indole acetic acid (IAA) in potato cultivation medium increased the number and accelerated the growth of tubers (Aksenova et al., 1999), and larger tubers grown in the soil contained more IAA than smaller ones. In addition, it was found that the auxins concentration in the stolon tips increases several times immediately before tuber initiation (Kolachevskaya et al., 2019), pointing out the essential role of auxins in tuber initiation and growth. In this regard, interest arose to study the effects of directed changes in the endogenous content of auxins in potato plants by using a transgenic approach (Kolachevskaya et al., 2019).

There are many publications on the influence of kinetin on the induction of *in vitro* tuberization (Kolachevskaya et al., 2021). Confirming data on the role of cytokinins in the formation of tubers were obtained from the study of transgenic plants with the expression of the isopentenyl transferase gene (iptTi plasmids of *Agrobacterium tumefaciens*) (Guivarc'h et al., 2002). Subsequently, a great deal of research has been done in this direction (Kumlay et al., 2021; Meenakshi, 2021; Vural et al., 2018).

The important role of gibberellins in the process of tuberization has been proved. Treatments with gibberellins enhanced the length of plant stem organs, stimulated the initiation, growth, and branching of stolons in potatoes (Külen et al., 2011), and prevented the formation of tubers *in vitro*. There is evidence of gibberellic acid's effect on the expression of potato genes associated with carbohydrates and protein metabolism in leaves and the genes associated with photoperiodic regulation of tuberization. Data have been obtained on the participation of recently recognized phytohormones in tuber formation *in vitro*. In studies by Vural and his co-authors, a

jasmonic acid compound called methyl jasmonate at 1.0 ppm in Nitsch and Nitsch medium stimulated the formation of micro-tubers (Vural et al., 2018). According to Z. J. Zhang et al. (2006), while using jasmonic acid in Murashige and Skoog medium at a concentration of 0.2-2 mg/dm^3, the shoot and root formation was significantly increased when cultivating regenerated potatoes of Favorita and Helanwuhua varieties. When studying the joint effect of jasmonic acid compounds and benzyladenine cytokinin on potato tuberization (*Solanum tuberosum* L.) *in vitro*, it was observed that benzyladenine suppressed the action of jasmonates and inhibited root growth and tuberization (Sarkar et al., 2006). The *in vitro* method of potato propagation opened a new milestone in potato breeding. Using virus-free starting material has become the basis of modern potato seed production. Growth regulators are actively used at every stage of seed multiplication, starting from the meristem crop (Anikina et al., 2015; Kolachevskaya et al., 2021; Kumlay et al., 2022).

Hormones play a key role in the formation and growth of potato tubers. It was found that the same chemicals, i.e., gibberellic acid, indole butyric acid, and kinetin, which are involved in tuber formation *in vitro*, showed a positive result on tuber formation *in vivo* when they treated potato foliage during the phase of budding flowering (Prasad, 2022; Zhao et al., 2022).

Ali and employees confirmed that the gibberellic acid (GA_3) significantly impacted the morphogenesis of the *in vitro* potatoes and was effective in acclimatizing plantlets of potatoes in the field (Ali et al., 2018). The property of growth regulators to increase the adaptive functions of the plant organism is of great importance in crop reproduction. Kanmani et al. (2017) found that the growth regulator brassinolide under saline conditions increased the rate of photosynthesis and chlorophyll fluorescence in plants, as well as showed that the plant growth regulators based on gibberellic acids and kinetin can be used to improve the physiological performance of plants under stress conditions.

Recently, there has been increased interest in the preparations of natural origin, which are derived from plant or microbial raw materials, and they are not inferior in their effect to synthetic hormonal preparations. Therefore, Dahshan et al. (2018) found a positive effect of treatments with both traditional phytohormones, i.e., gibberellic acid (GA_3), indole butyric acid (IBA), and solutions of natural preparations, i.e., garlic extract, yeast extract, and green tea extract on potato yield.

Use of Microorganisms

The use of biopreparations has become a biosafety alternative to reduce the use of agrochemicals (Pirttilä et al., 2021). Among biopreparations, microorganism-based preparations are the most widespread in practice. Efforts of many scientists have laid the scientific basis for clarifying the role of microorganisms as yield stimulators and resistance inducers (Dasgupta et al., 2023; Khan et al., 2020; Meena et al., 2020). The use of mycorrhiza in crop

production is particularly interesting in this area. Mycorrhizae, or mycorrhiza, is a symbiotic association between fungus and plant roots. As a result of this interaction, plants' uptake of water and nutrients is improved, and plant growth is accelerated (Chifetete & Dames, 2020; Jansa et al., 2020; Shuab et al., 2017). Mycorrhizae continue to influence plant growth even after the fungi die, as fungal neuromas have been shown to stimulate crop biomass (Jansa et al., 2020). Lone et al. (2015) found that inoculation with mycorrhiza had a stimulating effect not only on the morphogenic parameters of potato plants but also caused an increase in chlorophyll content. Wu and his co-workers showed that mycorrhizal plants have significantly greater root length, projection area, surface area, and volume than non-mycorrhizal plants (Wu et al., 2016). The stimulating effect of mycorrhiza on potato tuber formation has long been proven. Lone concluded that tuber initiation by mycorrhiza action is hormonally mediated (Lone et al., 2015).

The ability of bacteria to mobilize nutrients from difficult-to-dissolve soil components has led to the widespread use of commercial bacterial preparations in agricultural crop production, which are erroneously called bacterial fertilizers, although their functions are not limited to this property (Htwe et al., 2018; Kudoyarova et al., 2019). Various studies revealed that plant inoculation with consortia of symbiotic bacteria has a synergistic effect on plant growth and helps in alleviating abiotic and biotic stresses by producing various defense compounds (Bulgarelli et al., 2013; Hakim et al., 2021). In addition, bacteria can release substances of hormonal nature and biofungicides, which improve plant growth and increase their resistance against various biotic and abiotic stresses (Table 1).

Table 1
The results of the influence of rhisobacteria on plant development

Influence on plants	Source
Stimulation of root system development	Hong et al. (1991); Llorente et al. (2016); Mantelin and Touraine (2004); Rahman et al. (2018); Vicente and Plasencia (2011)
Improving the water budget of plants	Chifetete and Dames (2020); Jansa et al. (2020); Kaushal and Wani (2016); Khan and Bano (2016); Marulanda et al. (2010); Shuab et al. (2017)
Stimulation of photosynthesis	Khan et al. (2020); Marulanda et al. (2010); R. Zhang et al. (2017); Shi et al. (2010)
Induction of hormone synthesis	Jha and Saraf (2015); Lone et al. (2015); Ruzzi and Aroca (2015); Spaepen et al. (2014); Tsukanova et al. (2017); Vacheron et al. (2013)
Increasing the content of organic matter	Chifetete and Dames (2020); Fan et al. (2017); Naseri et al. (2013); Shuab et al. (2017); Ul Hassan and Bano (2015)
Stimulation of protective functions against phytopathogens	Bulgarelli et al. (2013); Chen et al. (2020); Hakim et al. (2021); Mącik et al. (2020); Polyksenova (2009); Puopolo et al. (2011); Rahman et al. (2018)
Stimulation of resistance to abiotic factors	Han et al. (2014); Harb et al. (2015); Kasim et al. (2016); Khan and Bano (2016, 2019); Khan et al. (2018); Mahmood et al. (2016); Nadeem et al. (2014); Shahzad et al. (2017); Subramanian et al. (2016); Xun et al. (2015)

It should be noted that microbial preparations of different origins positively affect plants. It was found that secondary metabolites of microorganisms can stimulate growth and increase plant resistance (bacteria *Bacillus*, *Fusarium* fungi, symbiotrophic endophyte fungi, and trout fungi). In addition, the positive role preparation of yeast-based treatments that contain many valuable plant substances, *viz*. cytokinins, carbohydrates, amino acids, enzymes, and vitamins B_1, B_2, and B_3, on potato development and productivity has been proved (Dahshan et al., 2018).

The role of rhizosphere bacteria in the stimulation of plant growth and synthesis of various types of bacteriocins and exo-toxin proteins, which are biologically active peptide fragments with fungicidal action has been most studied, e.g., *Azospirillum brasilense*, *Agrobacterium* spp., *Bradyrihizobium* spp., *Enterobacter* spp., and *Rhizobium legominosarum*, can produce indole-3-acetic acid (IAA), an auxin that promotes plant growth (Oleńska et al., 2020). Other mechanisms include synergistic relationships, root growth stimulation, and biocontrol (Dahshan et al., 2018; Hakim et al., 2021; Karthika et al., 2020). Studies reported the antifungal and chitinolytic actions of *Serratia marcescens* to inhibit pathogenic fungi such as *Fusarium oxysporum* and *Rhizoctonia solani* (Karthika et al., 2020). The great interest in plant growth-promoting rhizobacteria (PGPR) has contributed to the development of numerous commercial microbial preparations, which contribute to the efficiency of crop production. The use of beneficial PGPRs such as *Azotobacter*, *Pseudomonas*, *Bacillus*, and *Azospirillum* in the form of biofertilizers can be an alternative to conventional chemical fertilizers (Htwe et al., 2018). They promote plant growth by affecting plant hormone production, iron binding by siderophore, stress management by key enzymes, such as 1-aminocyclopropane-1-carboxylate, and soil organic matter decomposition.

Bacteria can interact closely with the host plant. Thus, they can be effective biocontrol agents in sustainable agricultural production (Hakim et al., 2021). Soil bacteria exhibit antifungal properties through the production of various enzymes that are part of their lytic system and allow the uptake of hyphae as a nutrient substrate (Chen et al., 2020).

Using Plant-based Preparations

At the same time, there is increasing interest in biologically active substances of plants, which also show positive results in increasing productivity and adaptive properties and as inducers of resistance to phytopathogens. Plants are available raw materials containing a huge number of valuable biologically active substances of different spectrum of action, which have been used since ancient times, including plant breeding (Abbas & Hussain, 2020; Abd-El-Khair & Haggag, 2007; Anikina & Issayeva, 2023).

Davidyants (2011) generalized the results of numerous studies and suggested that triterpene glycosides are involved in the regulation of physiological and

biochemical processes underlying the growth, development, and stress resistance of plants. According to her research, plants containing this class of biologically active compounds can act as raw materials for plant growth stimulants. Efforts of many scientists have proven the role of plant biologically active substances (BAS: epibrassinolide, flavonoids, steroid glycosides, triterpene, and hydroxycinnamic acids) in the regulation of growth processes and increasing the yield and resistance to stress and pathogens (Gorbyleva & Borovskii, 2018). Many researchers noted the positive effect of using biopreparations based on steroid glycosides (secondary plant metabolites), including potato crops. When using the preparations pavstim, moldstim, and emistim in the tomato crop in protected ground, the yield increase was more than 30%, while the quality of fruits was improved, and the infectious potential of soil was reduced (Godlewska et al., 2021). Steroid glycosides have a particularly significant immunoregulatory result under biotic and abiotic stresses. These statements are confirmed by the results of Anikina, who conducted an experiment under the conditions of Northeast Kazakhstan and obtained data indicating a significant stimulating effect of black nightshade infusion, which contains steroid glycosides, steroid alkaloids, and steroid oligoglycosides on potato productivity. The increase in total weight of tubers of one bush after treatment with the preparation averaged 34%. The increase in the food fraction of tubers was 46% (Anikina & Issayeva, 2023).

Regulating activity of extracts isolated from Siberian fir (*Abies sibirica* Ledeb.) was established, and the number of preparations was developed on their basis, i.e., Silk, Biosil, and Novosil, which are widely used in the cultivation of crops. Such preparations have a wide range of favorable properties, having a growth-regulating and fungicidal effect on the plant. Application of these preparations increases plant resistance against various diseases, while the activity of stress resistance genes increases (Gorbyleva & Borovskii, 2018).

Thus, Zaitseva (2017) proposed to use medicinal plants of Yakutia as raw material for stimulating preparations that increase seed germination of cultivated plants and resistance against stressful environmental factors. As raw materials for stimulating drugs, she proposed to use such plants as *Melilotus officinalis* (L.) Pall., *Melilotus albus* Medikus, *Oberna behen* (L.) Ikonn., *Sanguisorba officinalis* L, *Plantago major* L., *Ribes fragrans* Pall., *Ledum palustre* L., *Artemisia lagocefala* (Bess.), *Chamaenerion angustifolium* (L.) Scop., *Trifolium pratense* L., *Tanacetum vulgare* L., *Rubus idaeus* L., *Artemisia vulgaris* L., *Equisetum arvense* L., *Artemisia integrifolia* L., and *Galium album* Mill. In these studies, it was found that treatment with plant extracts not only increased seed germination but also significantly increased the stress tolerance of treated plants. Table 2 presents the generalized results of different researchers by type of plant growth regulators.

Table 2
Results of different researchers by type of plant growth regulators

Type of the drug	Reference
Microorganism-based biopreparations	Bulgarelli et al. (2013); Chen et al. (2020); Dahshan et al. (2018); Hakim et al. (2021); Htwe et al. (2018); Jansa et al. (2020); Karthika et al. (2020); Khan and Bano (2019); Khan et al. (2020); Mitrofanov and Novikov (2020); Oleńska et al. (2020); Polyksenova (2009); Shainidze et al. (2022); Vissey (2003)
Influence of mycoriza	Chifetete and Dames (2020); Lone et al. (2015); Shuab et al. (2017); Xu and Tong (2018)
Analogs of phytohormones	Ahmed et al. (2021); Aksenova et al. (1999); Ali et al. (2018); Amoanimaa-Dede et al. (2022); Anikina et al. (2015); Dasgupta et al. (2023); Guivarc'h et al. (2002); Hossain et al. (2019); Jing and Strader (2019); Kanmani et al. (2017); Kolachevskaya et al. (2019); Külen et al. (2011); Kumlay et al. (2021); Kurepa and Smalle (2022); Meena et al. (2020); Meenakshi (2021); Pavlista (2011); Sarkar et al. (2006); Singh and Jambukiya (2020); Vural et al. (2018); Wróbel et al. (2017); Z. J. Zhang et al. (2006); Zhao et al. (2022)
Plants-based biopreparations	Abbas and Hussain (2020); Abd-El-Khair and Haggag (2007); Anikina and Issayeva (2023); Dahshan et al. (2018); Davidyants (2011); Godlewska et al. (2021); Gorbyleva and Borovskii (2018); Polyksenova (2009); Zaitseva (2017)

CONCLUSION

The increasing role and importance of plant growth and development regulators cause the need for an in-depth study of the nature of the action of these compounds. At present, certain success has been achieved in studies of growth regulators' influence on the process of vegetation and establishing their correlation links with abiotic and biotic factors of crop yield formation. Understanding and using the mechanisms of growth regulation based on the control of ontogenesis in each case will optimize the processes of modeling and forecasting potato yield, as well as obtaining certain fractions of tubers, which is important for seed production.

It is known that the biosynthesis of phytohormones and inhibitors, their inactivation, and functioning are under direct control of the cell nucleus. In turn, phytohormones influence the functioning of the nucleus and other genetic structures in the cell through cytoplasmic inducers and inhibitors. With a better understanding of the signals controlling tuber formation, a molecular approach to improve yield may soon become available.

At the same time, the search for new strains and drugs that can positively influence plant health and growth under various growth conditions, especially under stress conditions, is relevant. Works in this direction should be intensified due to the constant climatic risks. Creating a science-based system of growth regulation can provide reliable, stable results for potatoes growing in any field conditions of future agriculture.

ACKNOWLEDGEMENT

The authors thank the Toraighyrov University Kazakhstan for providing support throughout the writing.

REFERENCES

Abbas, M. M., & Hussain, W. S. (2020). Biostimulants of pepper and eggplant by using plants aqueous extract. *Plant Cell Biotechnology and Molecular Biology*, *21*(65&66), 78-82.

Abd-El-Khair, H., & Haggag, W. M. (2007). Application of some Egyptian medicinal plant extracts against potato late and early blights. *Research Journal of Agriculture and Biological Sciences*, *3*(3), 166-175.

Ahmed, I. H. M., Ali, E. F., Gad, A. A., Bardisi, A., El-Tahan, A. M., Esadek, O. A. A., El-Saadony, M. T., & Gendy, A. S. (2021). Impact of plant growth regulators spray on fruit quantity and quality of *Capsicum annuum* L. cultivars grown under plastic tunnels. *Saudi Journal of Biological Sciences*, *29*(4), 2291-2298. https://doi.org/10.1016/j.sjbs.2021.11.062

Aksenova, N. P., Konstantinova T. N., Golyanovskaya S. A., Schmülling T., Kossmann J., Willmitzer L., & Romanov G. A. (1999). *In vitro* growth and tuber formation by transgenic potato plants harboring *rolC* or *rolB* genes under control of the patatin promoter. *Russian Journal of Plant Physiology*, *46*(4), 513-519.

Ali, S., Khan, N., Nouroz, F., Erum, S., Nasim, W., & Shahid, M. A. (2018). *In vitro* effects of GA3 on morphogenesis of CIP potato explants and acclimatization of plantlets in field. *In Vitro Cellular and Developmental Biology – Plant*, *54*, 104–111. https://doi.org/10.1007/s11627-017-9874-x

Amoanimaa-Dede, H., Su, C., Yeboah, A., Zhou H, Zheng, D., & Zhu, H. (2022). Growth regulators promote soybean productivity: A review. *PeerJ*, *10*, e12556. https://doi.org/10.7717/peerj.12556

Anikina, I., & Issayeva, K. (2023). Use of the preparation based on *Solanum nigrum* as a potato yield stimulator. *Bulgarian Journal of Agricultural Science*, *29*(2), 272–276.

Anikina, I., Bekseitov, T., & Dzhaksybaeva, G. (2015). Use of the preparation chlormequat chloride to increase resistance of regenerated potato. *International Journal of Pharma and Bio Sciences*, *6*(2), B417-B422.

Bulgarelli, D., Schlaeppi, K., Spaepen, S., van Themaat, E. V. L., & Schulze-Lefert, P. (2013). Structure and function of bacterial microbiota of plants. *Annual Review of Plant Biology*, *64*, 807-838. https://doi.org/10.1146/annurev-arplant-050312-120106

Chen, M., Wang, J., Liu, B., Zhu, Y., Xiao, R., Yang, W., Ge, C., & Chen, Z. (2020). Biocontrol of tomato bacterial wilt by the new strain *Bacillus velezensis* FJAT-46737 and its lipopeptides. *BMC Microbiology*, *20*, 160. https://doi.org/10.1186/s12866-020-01851-2

Chifetete, V. W., & Dames, J. F. (2020). Mycorrhizal interventions for sustainable potato production in Africa. *Frontiers in Sustainable Food Systems*, *4*, 593053.

Dahshan, A. M. A., Zaki, H. E. M., Moustafa, Y. M. M., Abdel-Mageed, Y. T., & Hassan M. A. M. (2018). Effect of some growth regulators and natural extracts on yield and quality of potato. *Minia Journal of Agriculture Research and Development*, *38*(2), 271-295.

Dasgupta, D., Paul, A., Acharya, K., Minkina, T., Mandzhieva, S., Gorovtsov, A. V., Chakraborty, N., & Keswani, C. (2023). Bioinoculant mediated regulation of signalling cascades in various stress responses in plants. *Heliyon*, *9*(1), e12953. https://doi.org/10.1016/j.heliyon.2023.e12953

Davidyants, E. S. (2011). Vliyanie triterpenovyh glikozidov na aktivnost' α i β-amilaz i obshchee soderzhanie belka v prorostkah pshenicy [Effect of triterpene glycosides on α and ß amylase activity and total protein content in wheat seedlings]. *Prikladnaya Biohimiya i Mikrobiologiya*, *5*(47), 530-536.

Fan, X., Zhang, S., Mo, X., Li, Y., Fu, Y., & Liu, Z. (2017). Effects of plant growth-promoting rhizobacteria and N source on plant growth and N and P uptake by tomato grown on calcareous soils. *Pedosphere*, *27*(6), 1027–1036. https://doi.org/10.1016/S1002-0160(17)60379-5

Godlewska, K., Ronga, D., & Michalak, I. (2021). Plant extracts - Importance in sustainable agriculture. *Italian Journal of Agronomy*, *16*(2), 1851. https://doi.org/10.4081/ija.2021.1851

Gorbyleva, E. L., & Borovskii, G. B. (2018). Biostimulyatory rosta i ustoychivosti rasteniy terpenoidnoy prirody i drugie biologicheski aktivnye soedineniya, poluchennye iz hvoynyh porod [Growth and stability biostimulators for plants containing terpenoids and other biologically active compounds]. *Izvestiya Vuzov: Prikladnaya Khimiya i Biotekhnologiya*, *8*(4), 32–41.

Guivarc'h, A., Rembur, J., Goetz, M., Roitsch, T., Noin, M., Schmülling, T., & Chriqui, D. (2002). Local expression of the *ipt* gene in transgenic tobacco (*Nicotiana tabacum* L. cv. SR1) axillary buds establishes a role for cytokinins in tuberization and sink formation. *Journal of Experimental Botany*, *53*(369), 621-629.

Hakim, S., Naqqash, T., Nawaz, M. S., Laraib, I., Siddique, M. J., Zia, R., Mirza, M. S., & Imran, A. (2021). Rhizosphere engineering with plant growth-promoting microorganisms for agriculture and ecological sustainability. *Frontiers in Sustainable Food Systems*, *5*, 617157. https://doi.org/10.3389/fsufs.2021.617157

Han, Q.-Q., Lü, X.-P., Bai, J.-P., Qiao, Y., Paré, P. W., Wang, S.-M., Zhang, J.-L., Wu, Y.-N., Pang, X.-P., Xu, W.-B., & Wang, Z.-L. (2014). Beneficial soil bacterium Bacillus subtilis (GB03) augments salt tolerance of white clover. *Frontiers in Plant Science*, *5*, 525. https://doi.org/10.3389/fpls.2014.00525

Hannapel, D. J., Sharma, P., Lin, T., & Banerjee, A. K. (2017). The multiple signals that control tuber formation. *Plant Physiology*, *174*(2), 845-856. https://doi.org/10.1104/pp.17.00272

Harb, A., Awad, D., & Samarah, N. (2015). Gene expression and activity of antioxidant enzymes in barley (*Hordeum vulgare* L.) under controlled severe drought. *Journal of Plant Interactions*, *10*(1), 109–116. https://doi.org/10.1080/17429145.2015.1033023

Hong, Y., Glick, B. R., & Pasternak, J. J. (1991). Plant microbial interaction under gnotobiotic conditions - A scanning electron-microscope study. *Current Microbiology*, *23*, 111–114. https://doi.org/10.1007/BF02092259

Hossain, M. S., Hossain, M. M., Hossain, T., Haque, M. M., Quamruzzaman, M., & Sarkar, M. D. (2019). Varietal response to benzylaminopurine and chlorocholine chloride on *in vitro* tuberization of potato. *Agricultural Research*, *8*, 452-460. https://doi.org/10.1007/s40003-018-0392-9

Htwe, A. Z., Moh, S. M., Moe, K., & Yamakawa, T. (2018). Effects of co-inoculation of *Bradyrhizobium japonicum* SAY3-7 and *Streptomyces griseoflavus* P4 on plant growth, nodulation, nitrogen fixation, nutrient uptake, and yield of soybean in a field condition. *Soil Science and Plant Nutrition*, *64*(2), 222-229. https://doi.org/10.1080/00380768.2017.1421436

Jansa, J., Šmilauer, P., Borovička, J., Hršelová, H., Forczek, S. T., Slámová, K., Řezanka, T., Rozmoš, M., Bukovská, P., & Gryndler, M. (2020). Dead *Rhizophagus irregularis* biomass mysteriously stimulates plant growth. *Mycorrhiza*, *30*, 63-77. https://doi.org/10.1007/s00572-020-00937-z

Jha, C. K., & Saraf, M. (2015). Plant growth promoting rhizobacteria (PGPR): A review. *Journal of Agricultural Research and Development*, *5*(2), 108–119. https://doi.org/10.13140/RG.2.1.5171.2164

Jing, H., & Strader, L. C. (2019). Interplay of auxin and cytokinin in lateral root development. *International Journal of Molecular Sciences*, *20*(3), 486. https://doi.org/10.3390/ijms20030486

Kanmani, E., Ravichandran, V., Sivakumar, R., Senthil, A., Krishna Surendar, K., & Boominathan, P. (2017). Influence of plant growth regulators on physiological traits under salinity stress in constrasting rice varieties (*Oryza sativa* L.). *International Journal of Current Microbiology and Applied Sciences*, *6*(5), 1654-1661. https://doi.org/10.20546/ijcmas.2017.605.180

Karthika, S., Midhun, S. J., & Jisha, M. (2020). A potential antifungal and growth-promoting bacterium *Bacillus* sp. KTMA4 from tomato rhizosphere. *Microbial Pathogenesis*, *142*, 104049. https://doi.org/10.1016/j.micpath.2020.104049

Kasim, W. A., Gaafar, R. M., Abou-Ali, R. M., Omar, M. N., & Hewait, H. M. (2016). Effect of biofilm forming plant growth promoting rhizobacteria on salinity tolerance in barley. *Annals of Agricultural Sciences*, *61*(2), 217–227. https://doi.org/10.1016/j.aoas.2016.07.003

Kaushal, M., & Wani, S. P. (2016). Plant-growth-promoting rhizobacteria: Drought stress alleviators to ameliorate crop production in drylands. *Annals of Microbiology*, *66*, 35–42. https://doi.org/10.1007/s13213-015-1112-3

Khan, N., & Bano, A. (2016). Role of plant growth promoting rhizobacteria and Ag-nano particle in the bioremediation of heavy metals and maize growth under municipal wastewater irrigation. *International Journal of Phytoremediation*, *18*(3), 211–221. https://doi.org/10.1080/15226514.2015.1064352

Khan, N., & Bano, A. (2019). Exopolysaccharide producing rhizobacteria and their impact on growth and drought tolerance of wheat grown under rainfed conditions. *PLOS One*, *14*(9), e0222302. https://doi.org/10.1371/journal.pone.0222302

Khan, N., Bano, A., & Curá, J. A. (2020). Role of beneficial microorganisms and salicylic acid in improving rainfed agriculture and future food safety. *Microorganisms*, *8*(7), 1018. https://doi.org/10.3390/microorganisms8071018

Khan, N., Bano, A., & Zandi, P. (2018). Effects of exogenously applied plant growth regulators in combination with PGPR on the physiology and root growth of chickpea (*Cicer arietinum*) and their role in drought tolerance. *Journal of Plant Interactions*, *13*(1), 239–247. https://doi.org/10.1080/17429145.2018.1471527

Kolachevskaya, O. O., Lomin, S. N., Arkhipov, D. V., & Romanov, G. A. (2019). Auxins in potato: Molecular aspects and emerging roles in tuber formation and stress resistance. *Plant Cell Reports*, *38*, 681-698. https://doi.org/10.1007/s00299-019-02395-0

Kolachevskaya, O. O., Myakushina, Y. A., Getman, I. A., Lomin, S. N., Deyneko, I. V., Deigraf, S. V., & Romanov, G. A. (2021). Hormonal regulation and crosstalk of auxin/cytokinin signaling pathways in potatoes *in vitro* and in relation to vegetation or tuberization stages. *International Journal of Molecular Sciences*, *22*(15), 8207. https://doi.org/10.3390/ijms22158207

Kudoyarova, G., Arkhipova, T. N., Korshunova, T., Bakaeva, M., Loginov, O., & Dodd, I. C. (2019). Phytohormone mediation of interactions between plants and non-symbiotic growth promoting bacteria under edaphic stresses. *Frontiers in Plant Science*, *10*, 1368. https://doi.org/10.3389/fpls.2019.01368

Külen, O., Stushnoff, C., Davidson, R. D., & Holm, D. G. (2011). Gibberellic acid and ethephon alter

potato minituber bud dormancy and improve seed tuber yield. *American Journal of Potato Research*, *88*, 167-174. https://doi.org/10.1007/c12230-010-9178-8

Kumlay, A. M., Kaya, C., & Yıldırım, B. (2021). Different plant growth regulators on improvement of potato (*Solanum tuberosum* L.) micropropagation. *Journal of the Institute of Science and Technology*, *11*(2), 1603-1615. https://doi.org/10.21597/jist.873537

Kurepa, J., & Smalle, J. A. (2022). Auxin/cytokinin antagonistic control of the shoot/root growth ratio and its relevance for adaptation to drought and nutrient deficiency stresses. *International Journal of Molecular Sciences*, *23*(4), 1933. https://doi.org/10.3390/ijms23041933

Li, S.-M., Zheng, H.-X., Zhang, X.-S., & Sui, N. (2020). Cytokinins as central regulators during plant growth and stress response. *Plant Cell Reports*, *40*, 271–282. https://doi.org/10.1007/s00299-020-02612-1

Llorente, B. E., Alasia, M. A., & Larraburu, E. E. (2016). Biofertilization with *Azospirillum brasilense* improves *in vitro* culture of *Handroanthus ochraceus*, a forestry, ornamental and medicinal plant. *New Biotechnology*, *33*(1), 32–40. https://doi.org/10.1016/j.nbt.2015.07.006

Lone, R., Shuab, R., Sharma, V., Kumar, V., Mir, R., & Koul, K. K. (2015). Effect of arbuscular mycorrhizal fungi on growth and development of potato (*Solanum tuberosum*) plant. *Asian Journal of Crop Science*, *7*, 233-243. https://doi.org/10.3923/ajcs.2015.233.243

Mącik, M., Gryta, A., & Frąc, M. (2020). Biofertilizers in agriculture: An overview on concepts, strategies and effects on soil microorganisms. *Advances in Agronomy*, *162*, 31–87. https://doi.org/10.1016/bs.agron.2020.02.001

Mahmood, S., Daur, I., Al-Solaimani, S. G., Ahmad, S., Madkour, H., Yasir, M., Hirt, H., Ali, S., & Ali, Z. (2016). Plant growth promoting rhizobacteria and silicon synergistically enhance salinity tolerance of mung bean. *Frontiers in Plant Science*, *7*, 876. https://doi.org/10.3389/fpls.2016.00876

Mani, F., Bettaieb, T. Doudech, N., & Hannachi, C. (2013). Effect of hydrogen peroxide and thiourea on dormancy breaking of microtubers and field-grown tubers of potato. *African Crop Science Journal*, *21*(3), 221-234.

Mantelin, S., & Touraine, B. (2004). Plant growth-promoting bacteria and nitrate availability: Impacts on root development and nitrate uptake. *Experimental Botany*, *55*(394), 27–34.

Marenych, M. M., Hanhur, V. V, Len, O. I., Hangur, Y. M., Zhornyk, I. I., & Kalinichenko, A. V. (2019). The efficiency of humic growth stimulators in pre-sowing seed treatment and foliar additional fertilizing of sown areas of grain and industrial crops. *Agronomy Research*, *17*(1), 194-205. https://doi.org/10.15159/AR.19.023

Marulanda, A., Azcón, R., Chaumont, F., Ruiz-Lozano, J. M., & Aroca, R. (2010). Regulation of plasma membrane aquaporins by inoculation with a *Bacillus megaterium* strain in maize (*Zea mays* L.) plants under unstressed and salt-stressed conditions. *Planta*, *232*(2), 533–543. https://doi.org/10.1007/s00425-010-1196-8

Meena, M., Swapnil, P., Divyanshu, K., Kumar, S., Harish., Tripathi, Y. N., Zehra, A., Marwal, A., & Upadhyay, R. S. (2020). PGPR-mediated induction of systemic resistance and physiochemical alterations in plants against the pathogens: Current perspectives. *Journal of Basic Microbiology*, *60*(10), 828-861. https://doi.org/10.1002/jobm.202000370

Meenakshi, K. (2021). Effect of kinetin on growth and development of microtubers of potato (*Solanum tuberosum* L.). *International Journal of Multidisciplinary Research Configuration*, *4*(1), 48-54. https://doi.org/10.52984/ijomrc1408

Mitrofanov, S. V., & Novikov, N. N. (2020). Efficiency of using stimulating preparations in pre-treatment of spring barley seeds. *Bulgarian Journal of Agricultural Science*, *26*(5), 958-965.

Murashev, S. V., Kiru, S. D., Verzhuk, V. G., & Pavlov, A. V. (2020). Potato plant growth acceleration and yield increase after treatment with an amino acid growth stimulant. *Agronomy Research*, *18*(2), 494-506. https://doi.org/10.15159/ar.20.036

Nadeem, S. M., Ahmad, M., Zahir, Z. A., Javaid, A., & Ashraf, M. (2014). The role of mycorrhizae and plant growth promoting rhizobacteria (PGPR) in improving crop productivity under stressful environments. *Biotechnology Advances*, *32*(2), 429–448. https://doi.org/10.1016/j.biotechadv.2013.12.005

Naseri, R., Maleki, A., Naserirad, H., Shebibi, S., & Omidian, A. (2013). Effect of plant growth promoting rhizobacteria (PGPR) on reduction nitrogen fertilizer application in rapeseed (*Brassica napus* L.). *Middle East Journal of Scientific Research*, *14*(2), 213–220. https://doi.org/10.5829/idosi.mejsr.2013.14.2.1951

Oleńska, E., Małek, W., Wójcik, M., Swiecicka, I., Thijs, S., & Vangronsveld, J. (2020). Beneficial features of plant growth-promoting rhizobacteria for improving plant growth and health in challenging conditions: A methodical review. *Science of the Total Environment*, *743*, 140682. https://doi.org/10.1016/j.scitotenv.2020.140682

Pavlista, A. D. (2011). Growth regulators increased yield of Atlantic potato. *American Journal of Potato Research*, *88*, 479–484. https://doi.org/10.1007/s12230-011-9214-3

Pirttilä, A. M., Tabas, H. M. P., Baruah, N. & Koskimäki, J. J. (2021). Biofertilizers and biocontrol agents for agriculture: How to identify and develop new potent microbial strains and traits. *Microorganisms*, *9*(4), 817. https://doi.org/10.3390/microorganisms9040817

Polyksenova, V. D. (2009). Inducirovannaya ustoychivost' rasteniy k patogenam i abioticheskim faktoram stressa [Induced plant steadiness to pathogens and abiotic stress factors]. *Byulleten' BGU*, *1*, 48-60.

Prasad, R. (2022). Cytokinin and its key role to enrich the plant nutrients and growth under adverse conditions - An update. *Frontiers in Genetics*, *13*, 883924. https://doi.org/10.3389/fgene.2022.883924

Puopolo, G., Raio, A., Pierson III, L. S., & Zoina, A. (2011). Selection of a new *Pseudomonas chlororaphis* strain for the biological control of *Fusarium oxysporum* f. sp. *radicis-lycopersici*. *Phytopathologia Mediterranea*, *50*(2), 228-235.

Rahman, S. F. S. A., Singh E., Pieterse C. M. J., & Schenk P. M. (2018). Emerging microbial biocontrol strategies for plant pathogens. *Plant Science*, *267*, 102–111. https://doi.org/10.1016/j.plantsci.2017.11.012

Ruzzi, M., & Aroca, R. (2015). Plant growth-promoting rhizobacteria act as biostimulants in horticulture. *Scientia Horticulturae*, *196*, 124–134. https://doi.org/10.1016/j.scienta.2015.08.042

Sarkar, D., Pandey, S. K., & Sharma, S. (2006). Cytokinins antagonize the jasmonates action on the regulation of potato (*Solanum tuberosum*) tuber formation *in vitro*. *Plant Cell Tissue and Organ Culture*, *87*, 285-295. https://doi.org/10.1007/s11240-006-9166-3

Shahzad, R., Khan, A. L., Bilal, S., Waqas, M., Kang, S.-M., & Lee, I.-J. (2017). Inoculation of abscisic acid-producing endophytic bacteria enhances salinity stress tolerance in *Oryza sativa*. *Environmental and Experimental Botany*, *136*, 68–77. https://doi.org/10.1016/j.envexpbot.2017.01.010

Shainidze, O., Lamparadze, S., Beridze, N., Chkubadze, G., & Macharadze, G. (2022). Effect of different doses of insectofungicidal biopreparatione (Gaupsin) against *Phytophthora*

of tomato in Adjara, Georgia. *Bulgarian Journal of Agricultural Science*, *28*(3), 437-442.

Shi, Y., Lou, K., & Li, C. (2010). Growth and photosynthetic efficiency promotion of sugar beet (*Beta vulgaris* L.) by endophytic bacteria. *Photosynthesis Research*, *105*(1), 5–13. https://doi.org/10.1007/s11120-010-9547-7

Shuab, R., Lone, R., & Koul, K. K. (2017). Influence of arbuscular mycorrhizal fungi on storage metabolites, mineral nutrition, and nitrogen-assimilating enzymes in potato (*Solanum tuberosum* L.) plant. *Journal of Plant Nutrition*, *40*(10), 1386-1396. https://doi.org/10.1080/01904167.2016.1263317

Singh, C., & Jambukiya, H. (2020). Effect of foliar application of plant growth regulators on growth and yield attributing characters of green gram (*Vigna radiata* L. Wilczek). *Journal of Crop and Weed*, *16*(2), 258-264. https://doi.org/10.22271/09746315.2020.v16.i2.1347

Spaepen, S., Bossuyt, S., Engelen, K., Marchal, K., & Vanderleyden, J. (2014). Phenotypical and molecular responses of *Arabidopsis thaliana* roots as a result of inoculation with the auxin-producing bacterium *Azospirillum brasilense*. *New Phytologist*, *201*(3), 850–861. https://doi.org/10.1111/nph.12590

Subramanian, S., Souleimanov, A., & Smith, D. L. (2016). Proteomic studies on the effects of lipo-chitooligosaccharide and thuricin 17 under unstressed and salt stressed conditions in *Arabidopsis thaliana*. *Frontiers in Plant Science*, *7*, 1314. https://doi.org/10.3389/fpls.2016.01314

Tsukanova, K. A., Chebotar, V. K., Meyer, J. J. M., & Bibikova, T. N. (2017). Effect of plant growth-promoting Rhizobacteria on plant hormone homeostasis. *South African Journal of Botany*, *113*, 91–102. https://doi.org/10.1016/j.sajb.2017.07.007

Ul Hassan, T., & Bano, A. (2015). The stimulatory effects of L-tryptophan and plant growth promoting rhizobacteria (PGPR) on soil health and physiology of wheat. *Journal of Soil Science and Plant Nutrition*, *15*(1), 190–201.

Vacheron, J., Desbrosses, G., Bouffaud, M.-L., Touraine, B., Moënne-Loccoz, Y., Muller, D., Legendre, L., Wisniewski-Dyé, F., & Prigent-Combaret, C. (2013). Plant growth-promoting rhizobacteria and root system functioning. *Frontiers in Plant Science*, *4*, 356.

Vicente, M. R.-S., & Plasencia, J. (2011). Salicylic acid beyond defence: Its role in plant growth and development. *Experimental Botany*, *62*(10), 3321–3338. https://doi.org/10.1093/jxb/err031

Vissey, J. K. (2003). Plant growth promoting rhizobacteria as biofertilizers. *Plant and Soil*, *255*, 571-586. https://doi.org/10.1023/A:1026037216893

Vural, G. E., Özsan, T., Gozen, V., & Onus, A. N. (2018). *In vitro* micro tuber formation in potato (*Solanum tuberosum* L.): Is there any relation between methyl jasmonate, sugars, and explants? *International Journal of Biotech Trends and Technology*, *8*(1), 1-8. https://doi.org/10.14445/22490183/IJBTT-V8I1P601

Wang, H., & Xiao, L. (2008). Effects of chlorocholine chloride on phytohormones and photosynthetic characteristics in potato (*Solanum tuberosum* L.). *Journal of Plant Growth Regulation*, *28*, 21-27. https://doi.org/10.1007/s00344-008-9069-0

Wróbel, S., Kęsy, J., & Treder, K. (2017). Effect of growth regulators and ethanol on termination of dormancy in potato tubers. *American Journal of Potato Research*, *94*, 544-555. https://doi.org/10.1007/s12230-017-9592-2

Wu, Q.-S., Cao, M.-Q., Zou, Y.-N., Wu, C., & He, X.-H. (2016). Mycorrhizal colonization represents functional equilibrium on root morphology and carbon distribution of trifoliate orange grown in a split-root system. *Scientia Horticulturae*, *199*, 95–102. https://doi.org/10.1016/j.scienta.2015.12.039

Xu, H., Lu, Y., & Tong, S. (2018). Effects of arbuscular mycorrhizal fungi on photosynthesis and chlorophyll fluorescence of maize seedlings under salt stress. *Emirates Journal of Food and Agriculture*, *30*(3), 199-204. https://doi.org/10.9755/ejfa.2018.v30.i3.1642

Xun, F., Xie, B., Liu, S., & Guo, C. (2015). Effect of plant growth-promoting bacteria (PGPR) and arbuscular mycorrhizal fungi (AMF) inoculation on oats in saline-alkali soil contaminated by petroleum to enhance phytoremediation. *Environmental Science and Pollution Research*, *22*, 598–608. https://doi.org/10.1007/s11356-014-3396-4

Zaitseva, N. V. (2017). Biologicheski aktivnye preparaty dlya proizvodstva selskohozyaystvennyh kultur iz rastitelnogo materiala YUzhnoy YAkutii [Biologically active preparations for crop production from plant raw materials of South Yakutia]. *Uspekhi Sovremennoy Estestvennoy Nauki*, *7*, 30-35. https://doi.org/10.17513/use.36473

Zhang, R., Vivanco, J. M., & Shen, Q. (2017). The unseen rhizosphere root-soil-microbe interactions for crop production. *Current Opinion in Microbiology*, *37*, 8–14. https://doi.org/10.1016/j.mib.2017.03.008

Zhang, Z. J., Zhou, W. J., Li, H. Z., Zhang, G. Q., Kaisrajan, S., & Yu, J. Q. (2006). Effect of jasmonic acid on *in vitro* explant growth and micro-tuberization in potato. *Biologia Plantarum*, *50*, 453-456. https://doi.org/10.1007/s10535-006-0069-2

Zhao, Z., Wang, C., Yu, X., Tian, Y., Wang, W., Zhang, Y., Bai, W., Yang, N., Zhang, T., Zheng, H., Wang, Q., Lu, J., Lei, D., He, X., Chen, K., Gao, J., Liu, X., Liu, S., Jiang, L., … Wan, H. (2022). Auxin regulates source-sink carbohydrate partitioning and reproductive organ development in rice. *Proceedings of the National Academy of Sciences*, *119*(36), e2121671119. https://doi.org/10.1073/pnas.2121671119

Pertanika J. Trop. Agric. Sci. 46 (4): 1205 - 1219 (2023)

PERTANIKA JOURNALS

TROPICAL AGRICULTURAL SCIENCE

Journal homepage: http://www.pertanika.upm.edu.my/

Antioxidant Capacity, Alpha Amylase Inhibition, and Calorie Value of Dark Chocolate Substituted with Honey Powder

Aida Amirah Rusli, Nizaha Juhaida Mohamad*, Azizah Mahmood and Nor Hayati Ibrahim

Faculty of Fisheries and Food Science, Universiti Malaysia Terengganu, 21030 Kuala Nerus, Terengganu, Malaysia

ABSTRACT

The antioxidant and antidiabetic properties of honey have led to studies exploring using honey powder as a sugar substitute in chocolate innovation for its health benefits. In this study, sugar was substituted with 70% honey powder to evaluate the effect on the antioxidant, alpha-amylase inhibition, and calorie value of dark chocolate. The honey powder was produced by adding 70% of either dextrose (honey/dextrose, H/D), maltodextrin (honey/maltodextrin, H/M), or sucrose (honey/sucrose, H/S) and vacuum dried at 40°C for 6 hr. The substitution of honey powder into chocolate at a 70% level was based on the preliminary study, which showed the most acceptable particle size value. The addition of honey powder into dark chocolate showed a significant increase ($p < 0.05$) in antioxidant capacity, assessed by 2,2-diphenyl-1-picrylhydrazyl and ferric reducing antioxidant power. Chocolate containing H/M showed the highest antioxidant capacity for both assays, followed by chocolate with H/D, H/S, and the control. Alpha amylase inhibition was also significantly higher ($p < 0.05$) for H/M chocolate relative to other samples. The calorie values of dark chocolate were not affected by the honey powder substitution, which remained at 600 kcal/100 g. Therefore, chocolate containing H/M showed the best properties due to its highest antioxidant capacities and alpha-amylase inhibition effect. Hence, it can be recommended for further application in chocolate.

ARTICLE INFO

Article history:
Received: 22 April 2023
Accepted: 23 May 2023
Published: 31 October 2023

DOI: https://doi.org/10.47836/pjtas.46.4.08

E-mail addresses:
aidaamirahrusli@gmail.com (Aida Amirah Rusli)
niezaju@umt.edu.my (Nizaha Juhaida Mohamad)
azizah.m@umt.edu.my (Azizah Mahmood)
yati@umt.edu.my (Nor Hayati Ibrahim)
* Corresponding author

Keywords: Diabetes, functional food, honey powder, polyphenols, Tualang honey

INTRODUCTION

Chocolates comprise approximately 70% sugar and cocoa in fine solid particles suspended in cocoa butter, which serves as the continuous fat phase (Afoakwa et

ISSN: 1511-3701
e-ISSN: 2231-8542

al., 2007). Chocolates can be classified into various types, including dark, milk, and white chocolate, which differ in their composition of cocoa solids, cocoa butter, sugar, and milk fat content. Dark chocolate was reported to have more benefits compared to other chocolate varieties due to the high percentage of cocoa and higher phenolic antioxidant compounds (Montagna et al., 2019). Cocoa, from a cocoa tree fruit (*Theobroma cacao*), has been identified as one of the richest naturally occurring sources of antioxidants, higher than red wine, blueberries, and green tea (Shafi et al., 2018). Cocoa contains relatively high amounts of flavonoids, including catechin, epicatechin, and procyanidin (Övet, 2015). However, up to 50% of the sucrose in chocolate evokes health concerns, especially on the risk of diabetes and other cardiovascular diseases. Therefore, the impact of sucrose replacement was investigated using sugar alcohols (maltitol, isomalt, xylitol, lactitol, sorbitol, and mannitol), intense sweetener (acesulfame K, aspartame, sucralose, and steviosides), bulking agent (inulin, polydextrose, and maltodextrin) and natural sweetener (stevia, lucuma, yacon, dried carrot, acacia flowers, palm sugar, and coconut sugar) in several previous studies (Aguilar-Villa et al., 2020; Aidoo et al., 2013; A. M. E. Ali et al., 2021; Cikrikci et al., 2017; Furlán et al., 2017; Kusumadevi et al., 2021; Palazzo et al., 2011).

Honey has been shown to have a variety of beneficial impacts on human health, including antioxidant, antidiabetic, anti-cancer, antibacterial, anti-inflammatory, treatment of cardiovascular disorders, and wound-healing properties (Ahmed & Othman, 2013; Meo et al., 2017). In Malaysia, Tualang honey (*Apis dorsata*) is the most favourable as it has a darker brown colour, which correlates to its high phenolic content (Ahmed & Othman, 2013). Previous studies have reported that Tualang honey shows superior antioxidant and free radical scavenging activities compared to other local honey varieties like Gelam, Acacia, Pineapple, Borneo, and Kelulut, which is likely due to its elevated levels of phenolics and flavonoids (Khalil et al., 2011; Kishore et al., 2011; Mohamed et al., 2010; Moniruzzaman et al., 2013). Gallic, benzoic, syringic, p-coumaric, trans-cinnamic, and caffeic acids are phenolic compounds found in Tualang honey, along with catechin, naringenin, kaempferol, luteolin, and apigenin as flavonoids (Khalil et al., 2011). These compounds may act as antidiabetic agents and contribute to alpha-amylase inhibition activity in Tualang honey (H. Ali et al., 2020). Additionally, Tualang honey has an intermediate glycaemic index, according to a study on healthy individuals, suggesting a positive role in regulating blood glucose levels (Ahmed & Othman, 2013; Robert & Al-Safi, 2009). Furthermore, Tualang honey has the potential to reduce cardiovascular risk factors (Ahmed & Othman, 2013; Yaghoobi et al., 2008).

Honey powder is gaining popularity in the food industry due to its health and functional properties. It has been used as a sucrose replacer in bread (Ram, 2011;

Sathivel et al., 2013; Tong et al., 2010), cookies (Kılınç & Demir, 2017), and isotonic drinks (Tomczyk et al., 2020). Studies have shown that using honey powder in bread reduces the staling rate and increases the food's phenolic content (Kılınç & Demir, 2017; Sathivel et al., 2013). Replacing some sucrose in chocolate with honey powder can increase the polyphenol content of the chocolate due to the combination of cocoa and honey powder polyphenols. This synergistic effect can enhance the health properties of the chocolate, particularly its antioxidant and antidiabetic properties. This study compares the substitution effect of vacuum-dried honey powder on the antioxidant properties, alpha-amylase inhibition, and caloric value of chocolate using three different sugar carriers (dextrose, maltodextrin, and sucrose).

MATERIALS AND METHODS

Materials

Cocoa mass (54% fat content) and cocoa butter were purchased from Barry Callebaut (Banbury, United Kingdom), and soy lecithin from Eugene Chemical Sdn. Bhd. (Malaysia), and castor sugar (Kijang, Malaysia) from a local supermarket in Malaysia. Tualang honey was obtained from Hutan Hujan Tasik Kenyir, Kuala Terengganu, supplied by Koperasi Pemungut Madu Lebah Terengganu Berhad (Malaysia). The DE 10 maltodextrin was procured from Sim Supplies Sdn. Bhd., Malaysia and the dextrose was obtained from Eugene Chemical Sdn. Bhd., Malaysia. The solvents and reagents used in this study included hexane, acetone, acetic acid, sodium hydrogen phosphate, methanol, TPTZ (2,4,6-tripyridyl-s-triazine), ferric chloride hexahydrate, hydrochloric acid, and sodium chloride obtained from the EMSURE®, Merck (Germany), diethyl ether from Fisher Scientific (United Kingdom), dinitrosalicyclic acid (DNS) colour reagent from Santa Cruz Biotechnology Inc. (USA), trolox, 2,2-diphenyl-1-picrylhydrazyl (DPPH), amberlite XAD-2-resin with a pore size of 9 nm, and particle size of 0.2-0.8 µm, sodium acetate, and α-amylase were procured from Sigma Aldrich (USA).

Honey Powder Preparation

Honey powder containing either dextrose (H/D), maltodextrin (H/M), and sucrose (H/S) were used as a sucrose substitute. The proportions, time, and drying temperature were determined based on preliminary studies. Honey and carrier (dextrose/maltodextrin/sucrose) at 30:70 was homogenised for 15 min at 4,000 rpm with a homogeniser (Ultra-turrax® T25 Digital Disperser, IKA, China). Subsequently, 10 g of every sample was weighed and evenly spread onto a Petri dish before drying in a vacuum oven (Binder, USA) at 40°C under 25 in Hg for 6 hr. After being dried, the samples were pulverised into a powder using a mortar and pestle and stored in a desiccator until they were analysed.

Dark Chocolate Preparation

Dark chocolate samples with a total fat content of 37.7% were prepared according to the formulation (Table 1). The formulation

categorises dark chocolate as "semisweet" based on its cocoa component content, which falls between more than 38% and less than 72%, in accordance with the method outlined by Belščak-Cvitanović et al. (2012). In the formulation, sucrose was substituted with honey powder at a 70% level (w/w). The dark chocolate was prepared using a tabletop wet grinder (Lakshmi Platinum Plus, India) as the mixer. The drum and stones were pre-heated for 20 min with a hot air gun (Stanley Stel670, China) to ensure smooth grinding. This friction warmed the stones, breaking the cocoa mass faster (Masonis et al., 2017). Cocoa butter and cocoa mass were added to the wet grinder and mixed for 10 min before incorporating sugar, honey powder, and lecithin. A hot air gun was used throughout the mixing process to maintain a constant temperature of around 45°C for 30 min. Afterwards, the hot air gun was removed as the wet grinder generated sufficient heat to maintain a 42–52°C. The temperature was monitored using a food digital thermometer (Dr Yonimed®, India). The mixing period for each formulation was set to 12 hr. Extending the mixing period to 14 and 16 hr did not yield further particle size reduction for all any samples of dark chocolate, as observed using a grindometer. The molten dark chocolate was subsequently stored in an airtight container and placed in a freezer at -20°C for further analysis.

Table 1
Dark chocolate formulations

Ingredients	Percentage (g/100 g)	
	Control	Treated
Sugar	36.5	10.9
Honey powder	0	25.6
Cocoa mass	55	
Cocoa butter	8	
Lecithin	0.5	

Chocolate Defatting

The samples were defatted to remove lipids before analysing their antioxidant capacity and alpha-amylase inhibition. The chocolate sample weighing 20 g was subjected to three rounds of extraction using 100 ml of hexane each time. The resulting defatted cocoa solids were left to air-dry at room temperature for 24 hr to remove any residual organic solvent (Todorovic et al., 2015).

Sample Extraction for Antioxidant Capacity

The method for extracting antioxidants was followed by the procedure outlined by Todorovic et al. (2015). Firstly, approximately 1 g of defatted dark chocolate was weighed and placed in a screw-cap tube. Polyphenols were extracted by adding 5 ml of a solvent extraction solution, which consisted of a mixture of acetone, distilled water, and acetic acid in a ratio of 70:29.8:0.2 (v/v/v). The extraction was enhanced by vortexing the mixture for 1 min and then sonicated for 30 min in an ultrasonic bath (Power Sonic 410, Hwashin Technology, Korea). Afterwards, the mixture was centrifuged for 10 min at 2,516 × *g*. Afterwards, the supernatant was filtered through the Whatman No.1 filter paper, and the extraction step was repeated twice.

Determination of DPPH Radical Scavenging Assay

The assessment of antioxidant activity was carried out using DPPH assays, which gauged the electron donation ability of a substance towards a hydrogen atom. This ability was determined by monitoring the reduction reaction of DPPH, which caused a change in its colour from purple to yellow hue. The method used for the DPPH assays followed the protocol outlined by Brand-Williams et al. (1995) with minor adjustments. Initially, a fresh stock solution of 0.06 mM DPPH was prepared by dissolving 1.2 mg of DPPH powder in 50 ml of 70% methanol. The flask containing the DPPH stock solution was wrapped with aluminium foil and then stirred on a magnetic stirrer (HEB Heating Magnetic Stirrer, China) until the DPPH was fully dissolved in the methanol. The solution was then stored in a bottle covered with aluminium foil at room temperature.

Aliquoted samples or standard (200 µl) were mixed with 2.8 ml of the DPPH radical solution in a screw-cap test tube. After combining the samples or standards with the DPPH radical solution, the mixture was vigorously shaken and then incubated in a dark place by wrapping the test tube with aluminium foil for 1 hr at room temperature. The capacity of the compounds to scavenge free radicals was assessed by measuring the absorbance at 525 nm. The antioxidant activity of the sample was determined by constructing a calibration curve of the standard within the range of 0.2–0.7 mmol Trolox/ml. The outcomes were expressed as µM Trolox Equivalents (TE) per gram of the samples. The scavenging activity percentage was then calculated using Equation 1:

$$\% \text{ Inhibition} = \frac{A_{525\ control} - A_{525sample/standard}}{A_{525control}} \times 100\% \quad [1]$$

where,

$A_{525\ control}$ = Absorbance of control (a methanol solution)

$A_{525sample/standard}$ = Absorbance of the sample's extract or standard

Determination of Ferric Reducing Antioxidant Power Assay (FRAP)

This method was conducted based on the protocol established by Benzie and Strain (1996), with some minor alterations. The FRAP reagent was prepared freshly by mixing acetate buffer, 2,4,6-tri(2-pyridyl)-s-triazine (TPTZ), and ferric chloride hexahydrate ($FeCl_3.6H_2O$) in a ratio of 10:1:1 (v/v/v). Approximately 25 ml of 300 mM acetate buffer solution was mixed with 2.5 ml of TPTZ solution (prepared by dissolving in 40 mM hydrochloric acid) before being added to 2.5 ml of 20 mM of ferric chloride hexahydrate. Then, the solution was warmed at 37°C using a water bath for 30 min. About 100 µl of extracted sample were mixed with 3,000 µl of FRAP reagent in a screw cap test tube and shaken vigorously. The absorbance of the reaction mixture was measured using a spectrophotometer (Varian Cary 50 Probe, Malaysia) at 593 nm after 40 min in dark conditions. The calibration curve determined the antioxidant activity within

the 0.1–0.8 mmol Trolox/ml range. The findings were then reported in µM Trolox Equivalents (TE)/g of the samples.

Sample Extraction for Alpha-Amylase Inhibition

Approximately 25 g of dark chocolate samples were dissolved in 250 ml of distilled water, and the pH of the resulting solution was adjusted to pH 2.0 by adding concentrated HCl. The sample solution was then passed through an Amberlite XAD-2 resin column. An additional 250 ml of water acidified with HCl to pH 2 was added to flush the sample solution into the column. The column was then washed with 300 ml of distilled water to eliminate sugars or other polar substances in the honey. A total of 250 ml of methanol was used to elute the phenolic chemicals from the sorbent. The methanol extracts were then evaporated under a vacuum in a rotary evaporator (Buchi Rotavapor R-300EL, Switzerland) at 40°C until most of the methanol was evaporated. The residue was diluted with 5 ml of distilled water and subjected to extraction three times, each with 5 ml of diethyl ether to eliminate non-flavonoid phenolic compounds. The ether extracts were combined, and the diethyl ether was eliminated by flushing the solution with nitrogen gas (Devarajan & Venugopal, 2012).

Determination of Alpha Amylase Inhibition

The procedure utilised for the inhibition assay of alpha-amylase was adapted from Devarajan and Venugopal (2012). The test tube was filled with 500 µl of 0.02 M sodium phosphate buffer (pH 6.9) containing 0.006 M sodium chloride and 0.5 mg/ml of alpha-amylase solution. Then, different sample concentrations (4, 8, 12, 16, and 20 µg/ml) in methanol were added and vigorously shaken. The alpha-amylase solution was incubated at 25°C for 10 min. After pre-incubation, 500 µl of 1% starch solution was added to each tube. Afterwards, the reaction mixtures were incubated at 25°C for 10 min. One millilitre of dinitrosalicylic acid (DNS) colour reagent was added to halt the reaction. The test tubes were then subjected to a boiling water bath at 100°C for 5 min, then cooled to room temperature. After adding 10 ml of distilled water, the reaction mixture was further diluted, and its absorbance was subsequently measured at 540 nm. The formula utilised to determine the calculation of enzyme inhibition is expressed in Equation 2:

$$\% \text{ Inhibition} = \frac{A_{540\ control} - A_{540extract}}{A_{540control}} \times 100\% \quad [2]$$

where,

$A_{540\ control}$ = Absorbance of control (a buffer solution)

$A_{540\ extract}$ = Absorbance of the sample's extract

Determination of Calorie Value

The caloric value measurement was carried out using a bomb calorimeter (Model-IKA® C 2000, China) following the outlined preparation of the sample and procedure in

the Operating Instruction Manual (2010). Approximately 1.0 ± 0.1 g of dark chocolate sample was weighed in an empty beaker using a digital balance. The sample was pressed into a pellet shape using a pellet press maker (IKA® Werke GmbH & Co, Germany). The sample was carefully removed from the pellet press maker and re-weighed before being placed in a crucible. The crucible was placed inside the decomposition vessel and transferred into the bomb calorimeter. After combustion, the vessel was automatically removed, and the analytical value of the energy content was recorded. The analysis was conducted in triplicate.

Statistical Analysis

The statistical analysis was carried out using Statistical Product and Service Solutions (SPSS) (version 23) (IBM Corp, USA). One-way analysis of variance (ANOVA) was utilised, and significance was determined using Tukey's post-hoc test. A significant difference was defined as a probability level of $p < 0.05$. Based on measurements made in triplicate, all data are provided as means ± standard deviations (SD).

RESULTS AND DISCUSSION

Antioxidant Capacity

The DPPH and FRAP of dark chocolate containing honey powder (H/D, H/M, and H/S) are shown in Figure 1. The substitution of sucrose with honey powder in dark chocolate has increased the antioxidant capacity of chocolate samples, demonstrating that honey powder has high antioxidant properties even though the amount of honey was only 30% in the honey powder. It proves that the low drying temperature (40°C) used during honey powder production helps preserve the antioxidant properties of the honey powder. Studies have shown that exposure to temperatures below 50°C can protect phenolic compounds in honey from degradation (Halim et al., 2021; Keke & Cinkmanis, 2021; Ramli et al., 2017). Previous studies also observed the same trend, where the addition of black mulberry, raspberry, and sea buckthorn to dark chocolate has resulted in higher antioxidant content, leading to increased DPPH and FRAP values compared to control dark chocolate (Godočiková et al., 2017; Todorovic et al., 2015).

Dark chocolate containing H/M honey powder exhibited the highest antioxidant capacity, followed by H/D, H/S, and control. Maltodextrin possesses excellent

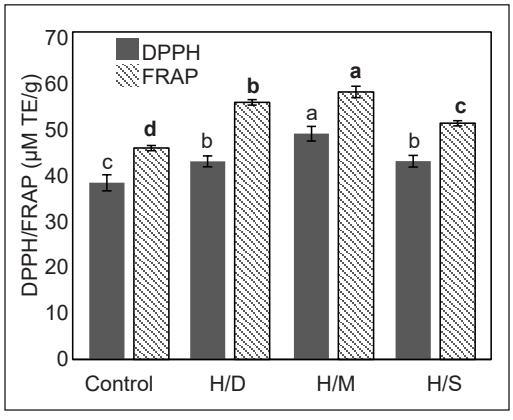

Figure 1. Antioxidant capacity in dark chocolate
Note. Control = Dark chocolate with no honey powder; H/D = Dark chocolate with honey/dextrose; H/M = Dark chocolate with honey/maltodextrin; H/S = Dark chocolate with honey/sucrose. Different letters indicate statistically significant differences ($p < 0.05$) between samples

encapsulating properties and is widely used as a drying agent due to its low viscosity, low bulk density, and high solubility in water and produce solutions that are monochromic in appearance (Buljeta et al., 2022; Hussain et al., 2018; Yang et al., 2022). Maltodextrin can effectively and stably encapsulate naturally occurring active compounds derived from plants, such as honey and cocoa (Jafari et al., 2008; Luna-Guevara et al., 2017). Studies have reported that adding maltodextrin to Mahkota Dewa fruit and pomegranate juice increased their antioxidant capacity and phenolic content compared to other encapsulating agents (Adetoro et al., 2020; Kathiman et al., 2020;). Maltodextrin has also been utilised to protect polyphenols in chokeberry, blackberry powder and acai (Ćujić-Nikolić et al., 2019; Ferrari et al., 2012; Tonon et al., 2010).

Alpha Amylase Inhibition

The inhibition percentage of dark chocolate extract against amylase enzyme is shown in Figure 2. Alpha amylase exhibited a concentration-dependent inhibitory action at 4, 8, 12, 16, and 20 extracted concentrations. The findings revealed a consistent trend for all samples, wherein the inhibition of alpha-amylase increased with an increase in concentration. The figure demonstrated that dark chocolate with honey powder had a significantly higher ($p < 0.05$) inhibition

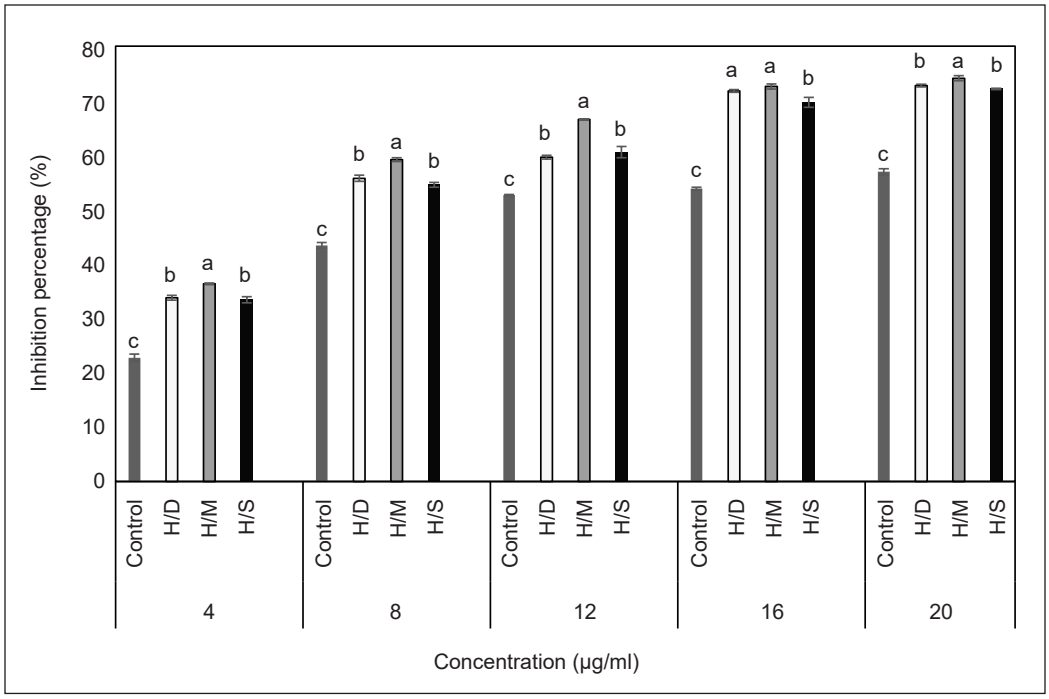

Figure 2. Alpha amylase inhibition in dark chocolate
Note. Control = Dark chocolate with no honey powder; H/D = Dark chocolate with honey/dextrose; H/M = Dark chocolate with honey/maltodextrin; H/S = Dark chocolate with honey/sucrose. Different letters indicate statistically significant differences ($p < 0.05$) between samples

percentage than the control. This finding indicates that combining cocoa polyphenols and honey may promote hypoglycemic effects due to their high antioxidant value. The high correlation between the inhibitory activity of enzymes and the antioxidant activity in the samples is attributed to polyphenols. Research has shown that honey has a specific antidiabetic role as it inhibits the enzyme alpha-amylase and treats glycemia by lowering blood glucose levels when consumed (Adefegha et al., 2018; H. Ali et al., 2020). Devarajan and Venugopal (2012) stated that flavonoid compounds in the honey extract are the source of antidiabetic behaviour. Additionally, another study suggested that luteolin, myrcetin, and quercetin in honey have potent inhibitory effects against the amylase enzyme (Tadera et al., 2006).

Flavonoids, including kaempferol, and phenolic acids, such as caffeic acid and *p*-coumaric acid, have been identified as the active ingredients in Tualang honey that contribute to the inhibition of alpha-amylase (Ahmed & Othman, 2013; Bharti et al., 2018; H. Ali et al., 2020). Chocolate is also a rich source of flavonoids, which are responsible for inhibiting alpha-amylase, as the samples demonstrate. Flavanols, such as catechin, epicatechin, and procyanidin, are flavonoids in cocoa that inhibit the alpha-amylase enzyme (Ramos et al., 2017; Yusuf et al., 2021). Furthermore, tannins, such as proanthocyanin and ellagitannin, in cocoa have also been reported to impact the inhibition of the amylase enzyme (Barrett et al., 2013). As a result, the combination of chocolate and honey extract can delay the digestion and absorption of starch by inhibiting alpha-amylase activity.

Dark chocolate containing H/M showed the highest inhibition effect compared to other dark chocolate samples. This study found a proportional relationship between alpha-amylase inhibition activity and antioxidant capacity, with dark chocolate containing H/M showing the highest DPPH and FRAP scavenging activities. Maltodextrin has been reported to efficiently preserve polyphenols and other bioactive compounds during drying, resulting in high antidiabetic activity demonstrated by encapsulated plant extract powder (Cian et al., 2019; Ćujić-Nikolić et al., 2019; Nguyen et al., 2022; Nurhayati et al., 2020; Tran et al., 2020).

Calorie Value

The caloric value of control dark chocolate and dark chocolate containing honey powder is shown in Figure 3. The figure shows no significant difference ($p > 0.05$) between all the samples. It represents that all dark chocolate has a calorie value of about 600 kcal/100 g. This value obtained was comparable to previous studies of dark chocolate, which ranged between 533 to 604 kcal/100 g (Ali et al., 2021).

The result demonstrates that the substitution of honey powder did not influence the caloric value of dark chocolate. According to the Malaysian Food Composition Database (1997), honey has a lower caloric value (313 kcal/100 g) than sucrose (398 kcal/100 g). However, as

the honey powder contained sugar carriers such as dextrose, maltodextrin, and sucrose at 70%, the value showed no significant difference ($p > 0.05$) to the control when the honey powder was incorporated into the chocolate. The caloric value of dextrose and maltodextrin was reported to be similar to sucrose (Lê et al., 2016; Tiefenbacher, 2017).

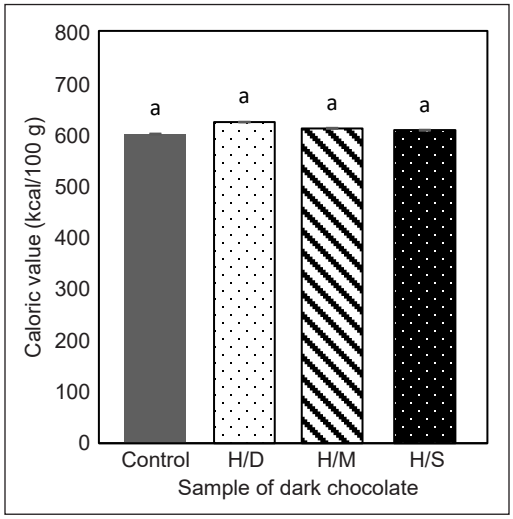

Figure 3. The caloric value of dark chocolate
Note. Control = Dark chocolate with no honey powder; H/D = Dark chocolate with honey/dextrose; H/M = Dark chocolate with honey/maltodextrin; H/S = Dark chocolate with honey/sucrose. Different letters indicate statistically significant differences ($p < 0.05$) between samples

CONCLUSION

The incorporation of honey powder into dark chocolate had been shown to increase its antioxidant activity and alpha-amylase inhibition, indicating that the phenolic content of the honey powder was preserved. Among the samples, dark chocolate containing H/M exhibited the highest antioxidant and alpha-amylase inhibition, demonstrating the effective preservation of phenolic content by maltodextrin. Therefore, chocolate containing H/M could be formulated as a functional food that may help decrease the risk of diabetes. However, to confirm the efficiency of the chocolate for human benefits, further studies on the bioavailability of polyphenol need to be carried out. An *in vivo* study on rats is suggested as the first stage for this confirmation.

ACKNOWLEDGMENTS

The research was supported by the Fundamental Research Grant Scheme (FRGS), Ministry of Higher Education, Malaysia, with project number FRGS/1/2018/WAB01/UMT/03/5. Also, thank you to the Faculty of Fisheries and Food Science, Universiti Malaysia Terengganu, for the support and facilities during this study.

REFERENCES

Adefegha, S. A., Oboh, G., & Olabiy, A. A. (2018). Nutritional, antioxidant and inhibitory properties of cocoa powder enriched wheat-plantain biscuits on key enzymes linked to type 2 diabetes. *International Food Research Journal*, *25*(2), 793–803.

Adetoro, A. O., Opara, U. L., & Fawole, O. A. (2020). Effect of carrier agents on the physicochemical and technofunctional properties and antioxidant capacity of freeze-dried pomegranate juice (*Punica granatum*) powder. *Foods*, *9*(10), 1388. https://doi.org/10.3390/foods9101388

Afoakwa, E. O., Paterson, A., & Fowler, M. (2007). Factors influencing rheological and textural qualities in chocolate - A review. *Trends in Food*

Science and Technology, *18*(6), 290–298. https://doi.org/10.1016/j.tifs.2007.02.002

Aguilar-Villa, C., Acosta-Otálvaro, E. V., Rodríguez-Sandoval, E., & Mazo-Rivas, J. C. (2020). Sucrose-free milk chocolate manufacture using bulking agents and a non-caloric sweetener. *Food Science and Technology*, *40*(1), 62–67. https://doi.org/10.1590/fst.32418

Ahmed, S., & Othman, N. H. (2013). Review of the medicinal effects of tualang honey and a comparison with manuka honey. *Malaysian Journal of Medical Sciences*, *20*(3), 6-13.

Aidoo, R. P., Depypere, F., Afoakwa, E. O., & Dewettinck, K. (2013). Industrial manufacture of sugar-free chocolates - Applicability of alternative sweeteners and carbohydrate polymers as raw materials in product development. *Trends in Food Science and Technology*, *32*(2), 84–96. https://doi.org/10.1016/j.tifs.2013.05.008

Ali, A. M. E., Shekib, L. A., Elshimy, N. M., & Sharara, M. S. (2021). Producing and quality attributes of low calories dark chocolate using different intense sweeteners and wheat fiber isolate. *American Journal of Food Science and Technology*, *9*(1), 1–7. https://doi.org/10.12691/ajfst-9-1-1

Ali, H., Abu Bakar, M. F., Majid, M., Muhammad, N., & Lim, S. Y. (2020). *In vitro* anti-diabetic activity of stingless bee honey from different botanical origins. *Food Research*, *4*(5), 1421–1426. https://doi.org/10.26656/fr.2017.4(5).411

Barrett, A., Ndou, T., Hughey, C. A., Straut, C., Howell, A., Dai, Z., & Kaletunc, G. (2013). Inhibition of α-amylase and glucoamylase by tannins extracted from cocoa, pomegranates, cranberries, and grapes. *Journal of Agricultural and Food Chemistry*, *61*(7), 1477-1486. https://doi.org/10.1021/jf304876g

Belščak-Cvitanović, A., Komes, D., Benković, M., Karlović, S., Hečimović, I., Ježek, D., & Bauman, I. (2012). Innovative formulations of chocolates enriched with plant polyphenols from *Rubus idaeus* L. leaves and characterization of their physical, bioactive and sensory properties. *Food Research International*, *48*(2), 820-830. https://doi.org/10.1016/j.foodres.2012.06.023

Benzie, I. F., & Strain, J. J. (1996). The ferric reducing ability of plasma (FRAP) as a measure of "antioxidant power": The FRAP assay. *Analytical Biochemistry*, *239*(1), 70-76. https://doi.org/10.1006/abio.1996.0292

Bharti, S. K., Krishnan, S., Kumar, A., & Kumar, A. (2018). Antidiabetic phytoconstituents and their mode of action on metabolic pathways. *Therapeutic Advances in Endocrinology and Metabolism*, *9*(3), 81–100. https://doi.org/10.1177/2042018818755019

Brand-Williams, W., Cuvelier, M. E., & Berset, C. (1995). Use of a free radical method to evaluate antioxidant activity. *LWT - Food Science and Technology*, *28*(1), 25–30. https://doi.org/10.1016/S0023-6438(95)80008-5

Buljeta, I., Pichler, A., Šimunović, J., & Kopjar, M. (2022). Polysaccharides as carriers of polyphenols: Comparison of freeze-drying and spray-drying as encapsulation techniques. *Molecules*, *27*(16), 5069. https://doi.org/10.3390/molecules27165069

Cian, R. E., Campos-Soldini, A., Chel-Guerrero, L., Drago, S. R., & Betancur-Ancona, D. (2019). Bioactive *Phaseolus lunatus* peptides release from maltodextrin/gum arabic microcapsules obtained by spray drying after simulated gastrointestinal digestion. *International Journal of Food Science and Technology*, *54*(6), 2002-2009. https://doi.org/10.1111/ijfs.14031

Cikrikci, S., Yucekutlu, M., Mert, B., & Oztop, M. H. (2017). Physical characterization of low-calorie chocolate formulations. *Journal of Food Measurement and Characterization*, *11*, 41–49. https://doi.org/10.1007/s11694-016-9369-1

Ćujić-Nikolić, N., Stanisavljević, N., Šavikin, K., Kalušević, A., Nedović, V., Samardžić, J., & Janković, T. (2019). Chokeberry polyphenols preservation using spray drying: Effect of encapsulation using maltodextrin and skimmed milk on their recovery following *in vitro* digestion. *Journal of Microencapsulation*, *36*(8), 693-703. https://doi.org/10.1080/02652048.2019.1667448

Devarajan, S., & Venugopal, S. (2012). Antioxidant and α-amylase inhibition activities of phenolic compounds in the extracts of Indian honey. *Chinese Journal of Natural Medicines*, *10*(4), 255–259. https://doi.org/10.1016/S1875-5364(12)60051-X

Ferrari, C. C., Germer, S. P. M., Alvim, I. D., Vissotto, F. Z., & de Aguirre, J. M. (2012). Influence of carrier agents on the physicochemical properties of blackberry powder produced by spray drying. *International Journal of Food Science and Technology*, *47*(6), 1237–1245. https://doi.org/10.1111/j.1365-2621.2012.02964.x

Furlán, L. T. R., Baracco, Y., Lecot, J., Zaritzky, N., & Campderrós, M. E. (2017). Effect of sweetener combination and storage temperature on physicochemical properties of sucrose free white chocolate. *Food Chemistry*, *229*, 610–620. https://doi.org/10.1016/j.foodchem.2017.03.002

Godočiková, L., Ivanišová, E., & Kačániová, M. (2017). The influence of fortification of dark chocolate with sea buckthorn and mulberry on the content of biologically active substances. *Advanced Research in Life Sciences*, *1*(1), 26-31. https://doi.org/10.1515/arls-2017-0004

Halim, N. F., Basrawi, M. F., Azman, N. A. M., Sulaiman, S. A., & Razak, S. B. A. (2021). The effect of temperature on low temperature vacuum drying with induced nucleate boiling for stingless bees honey. In *IOP Conference Series: Materials Science and Engineering* (Vol. 1078, No. 1, p. 012018). IOP Publishing. https://doi.org/10.1088/1757-899X/1078/1/012018

Hussain, S. A., Hameed, A., Nazir, Y., Naz, T., Wu, Y., Suleria, H. A. R., & Song, Y. (2018). Microencapsulation and the characterization of polyherbal formulation (PHF) rich in natural polyphenolic compounds. *Nutrients*, *10*(7), 843. https://doi.org/10.3390/nu10070843

Jafari, S. M., Assadpoor, E., He, Y., & Bhandari, B. (2008). Encapsulation efficiency of food flavours and oils during spray drying. *Drying Technology*, *26*(7), 816-835. https://doi.org/10.1080/07373930802135972

Kathiman, M. N., Mudalip, S. K. A., & Gimbun, J. (2020). Effect of encapsulation agents on antioxidant activity and moisture content of spray dried powder from Mahkota Dewa fruit extract. In *IOP Conference Series: Materials Science and Engineering* (Vol. 99, No. 1, p. 012040). IOP Publishing. https://doi.org/10.1088/1757-899X/991/1/012040

Keke, A., & Cinkmanis, I. (2021). Total phenolic content and antiradical activity of honey powders. *Research for Rural Development*, *36*, 104–110. https://doi.org/10.22616/rrd.27.2021.015

Khalil, M. I., Alam, N., Moniruzzaman, M., Sulaiman, S. A., & Gan, S. H. (2011). Phenolic acid composition and antioxidant properties of Malaysian honeys. *Journal of Food Science*, *76*(6), C921-C928. https://doi.org/10.1111/j.1750-3841.2011.02282.x

Kishore, R. K., Halim, A. S., Syazana, M. S. N., & Sirajudeen, K. N. S. (2011). Tualang honey has higher phenolic content and greater radical scavenging activity compared with other honey sources. *Nutrition Research*, *31*(4), 322–325. https://doi.org/10.1016/j.nutres.2011.03.001

Kılınç, M., & Demir, M. K. (2017). The facilities of spray dried honey powder use as a substitute for sugar in cookie production. *Journal of Food*

and Health Science, *3*(2), 67–74. https://doi.org/10.3153/JFHS17009

Kusumadevi, Z., Saputro, A. D., Dewi, A. K., Irmandharu, F., Oetama, T., Setiowati, A. D., Rahayoe, S., & Bintoro, N. (2021). Physical characteristics of compound chocolate made with various flavouring agents produced using melanger as a small scale chocolate processing device. In *IOP Conference Series: Earth and Environmental Science* (Vol. 653, No. 1, p. 012036). IOP Publishing. https://doi.org/10.1088/1755-1315/653/1/012036

Lê, K.-A., Robin, F., & Roger, O. (2016). Sugar replacers: From technological challenges to consequences on health. *Current Opinion in Clinical Nutrition and Metabolic Care*, *19*(4), 310–315. https://doi.org/10.1097/MCO.0000000000000288

Luna-Guevara, J. J., Ochoa-Velasco, C. E., Hernández-Carranza, P., & Guerrero-Beltrán, J. A. (2017). Microencapsulation of walnut, peanut and pecan oils by spray drying. *Food Structure*, *12*, 26-32. https://doi.org/10.1016/j.foostr.2017.04.001

Malaysian Food Composition Database. (1997). *Food groups: Sugars and syrups*. https://myfcd.moh.gov.my/myfcd97/index.php/site/detail_product/107002/0/10/honey/0/0/

Masonis, T., D'alesandre, G., Vega, L., & Gore, M. (2017). *Making chocolate: From bean to bar to S'more: Dandelion chocolate*. Clarkson Potter Publishers.

Meo, S. A., Ansari, M. J., Sattar, K., Chaudhary, H. U., Hajjar, W., & Alasiri, S. (2017). Honey and diabetes mellitus: Obstacles and challenges – Road to be repaired. *Saudi Journal of Biological Sciences*, *24*(5), 1030–1033. https://doi.org/10.1016/j.sjbs.2016.12.020

Mohamed, M., Sirajudeen, K. N. S., Swamy, M., Yaacob, N. S., & Sulaiman, S. A. (2010). Studies on the antioxidant properties of tualang honey of Malaysia. *African Journal of Traditional, Complementary and Alternative Medicines*, *7*(1), 59–63. https://doi.org/10.4314/ajtcam.v7i1.57256

Moniruzzaman, M., Sulaiman, S. A., Khalil, M. I., & Gan, S. H. (2013). Evaluation of physicochemical and antioxidant properties of sourwood and other Malaysian honeys: A comparison with manuka honey. *Chemistry Central Journal*, *7*, 138. https://doi.org/10.1186/1752-153X-7-138

Montagna, M. T., Diella, G., Triggiano, F., Caponio, G. R., De Giglio, O., Caggiano, G., Di Ciaula, A., & Portincasa, P. (2019). Chocolate, "food of the gods": History, science, and human health. *International Journal of Environmental Research and Public Health*, *16*(24), 4960. https://doi.org/10.3390/ijerph16244960

Nguyen, M.-T., Chuyen, H. V., Tran, M. D., & Nguyen, Q.-V. (2022). Microencapsulation of *Syzygium zeylanicum* (L.) DC. extract using spray drying: Effects of wall materials on physicochemical characteristics and biological activities of the microcapsules. *Journal of Food Processing and Preservation*, *46*(7), e16647. https://doi.org/10.1111/jfpp.16647

Nurhayati, R., Miftakhussolikhah., Oktavianingrum, D. A., & Pratiwi, R. (2020). The effect of encapsulated *Pediococcus lolii* L2 on its cell viability and α-glucosidase inhibition activity. In *IOP Conference Series: Earth and Environmental Science* (Vol. 462, No. 1, p.012024). IOP Publishing. https://doi.org/10.1088/1755-1315/462/1/012024

Operating Instruction Manual. (2010). *Oxygen bomb calorimeter*. https://www.parrinst.com/wp-content/uploads/downloads/2011/06/442M_Parr_6200-Calorimeter-Operating-Instructions-pre-Oct-2010.pdf

Övet, B. (2015). *Investigation of antioxidant capacity and phenolic contents of chocolates in the Turkish market* [Master's thesis, Middle East Technical University]. ODTÜ Library: Thesis. https://

open.metu.edu.tr/bitstream/handle/11511/24658/index.pdf

Palazzo, A. B., Carvalho, M. A. R., Efraim, P., & Bolini, H. M. A. (2011). The determination of isosweetness concentrations of sucralose, rebaudioside and neotame as sucrose substitutes in new diet chocolate formulations using the time-intensity analysis. *Journal of Sensory Studies*, *26*(4), 291–297. https://doi.org/10.1111/j.1745-459X.2011.00344.x

Ram, A. K. (2011). *Production of spray-dried honey powder and its application in bread*. [Master's thesis, Louisiana State University]. LSU Scholarly Repository. https://digitalcommons.lsu.edu/gradschool_theses/1743/

Ramli, A. S., Basrawi, F., Idris, D. M. N. D., Yusof, M. H., Ibrahim, T. K., Mustafa, Z., & Sulaiman, S. A. (2017). A new dewatering technique for stingless bees honey. In *MATEC Web of Conferences* (Vol. 131, p. 03014). EDP Sciences. https://doi.org/10.1051/matecconf/201713103014

Ramos, S., Martín, M. A., & Goya, L. (2017). Effects of cocoa antioxidants in type 2 diabetes mellitus. *Antioxidants*, *6*(4), 84. https://doi.org/10.3390/antiox6040084

Robert, S. D., & Al-Safi, I. A. (2009). Two varieties of honey that are available in Malaysia gave intermediate glycemic index values when tested among healthy individuals. *Biomedical Papers*, *153*(2), 145–148. https://doi.org/10.5507/bp.2009.024

Sathivel, S., Ram, A. K., Espinoza, L., King, J., Cueto, R., & Solval, K. M. (2013). Application of honey powder in bread and its effect on bread characteristics. *Journal of Food Processing and Technology*, *4*(11). 1000279. https://doi.org/10.4172/2157-7110.1000279

Shafi, F., Reshi, M., & Bashir, I. (2018). Chocolate processing. *International Journal of Advances Biological Research*, *8*(3), 408–419.

Tadera, K., Minami, Y., Takamatsu, K., & Matsuoka, T. (2006). Inhibition of α-glucosidase and α-amylase by flavonoids. *Journal of Nutritional Science and Vitaminology*, *52*(2), 149-153. https://doi.org/10.3177/jnsv.52.149

Tiefenbacher, K. F. (2017). Technology of main ingredients - Water and flours. In *Wafer and waffle: Processing and manufacturing* (pp. 15-121). Academic Press. https://doi.org/10.1016/B978-0-12-809438-9.00002-8

Tran, N., Tran, M., Truong, H., & Le, L. (2020). Spray-drying microencapsulation of high concentration of bioactive compounds fragments from *Euphorbia hirta* L. extract and their effect on diabetes mellitus. *Foods*, *9*(7), 881. https://doi.org/10.3390/foods9070881

Todorovic, V., Radojcic, I., Todorovic, Z., Jankovic, G., Dodevska, M., & Sobajic, S. (2015). Polyphenols, methylxanthines and antioxidant capacity of chocolates produced in Serbia. *Journal of Food Composition and Analysis*, *41*, 137–143. https://doi.org/10.1016/j.jfca.2015.01.018

Tomczyk, M., Zaguła, G., Tarapatskyy, M., Kačániová, M., & Dzugan, M. (2020). The effect of honey variety on the quality of honey powder. *Journal of Microbiology, Biotechnology and Food Sciences*, *9*(5), 949–954. https://doi.org/10.15414/jmbfs.2020.9.5.949-954

Tong, Q., Zhang, X., Wu, F., Tong, J., Zhang, P., & Zhang, J. (2010). Effect of honey powder on dough rheology and bread quality. *Food Research International*, *43*(9), 2284–2288. https://doi.org/10.1016/j.foodres.2010.08.002

Tonon, R. V., Brabet, C., & Hubinger, M. D. (2010). Anthocyanin stability and antioxidant activity of spray-dried açai (*Euterpe oleracea* Mart.) juice produced with different carrier agents. *Food Research International*, *43*(3), 907–914. https://doi.org/10.1016/j.foodres.2009.12.013

Yaghoobi, N., Al-Waili, N., Ghayour-Mobarhan, M., Parizadeh, S. M. R., Abasalti, Z., Yaghoobi, Z., Yaghoobi, F., Esmaeili, H., Kazemi-Bajestani, S. M. R., Aghasizadeh, R., Saloom, K. Y., & Ferns, G. A. A. (2008). Natural honey and cardiovascular risk factors; Effects on blood glucose, cholesterol, triacylglycerole, CRP, and body weight compared with sucrose. *The Scientific World Journal*, *8*, 961837. https://doi.org/10.1100/tsw.2008.64

Yang, B., Kealey, K., Chen, J., & Solval, K. M. (2022). Developing microencapsulated powders containing polyphenols and pectin extracted from Georgia-grown pomegranate peels. *LWT*, *154*, 112644. https://doi.org/10.1016/j.lwt.2021.112644

Yusuf, M., Pirman, P., Attahmid, N. F. U., Amri, I., & Andi, I. J.(2021). Identifications of polyphenols and α-amylase inhibitory activity of multi herbal formulation: Cocoa beans (*Theobroma cocoa*), buni (*Antidesma bunius* L. Spreng) and cinnamons (*Cinnamomum cassia*). In *Journal of Physics: Conference Series* (Vol. 1783, No. 1, p. 012004). IOP Publishing. https://doi.org/10.1088/1742-6596/1783/1/012004

Pertanika J. Trop. Agric. Sci. 46 (4): 1221 - 1232 (2023)

PERTANIKA JOURNALS

TROPICAL AGRICULTURAL SCIENCE

Journal homepage: http://www.pertanika.upm.edu.my/

Nutrient Uptake in Different Maize Varieties (*Zea mays* L.) Planted in Tropical Peat Materials

Ameera Abdul Reeza[1]*, Muhamad Amirul Falieq Baharuddin[1], Osumanu Haruna Ahmed[2] and Mohd Aizuddin Masuri[1]

[1]*Faculty of Plantation and Agrotechnology, Universiti Teknologi MARA, Kampus Jasin, Cawangan Melaka, 77300, Merlimau, Melaka, Malaysia*

[2]*Ibnu Sina Laboratory Centre, Universiti Islam Sultan Sharif Ali, Kampus Sinaut, Tutong TB1741, Brunei Darussalam*

ABSTRACT

Oligotrophic tropical peat soils are usually deemed unsuitable for cropping common crops such as maize due to low pH and nutrient deficiency. This research aims to compare potassium, calcium, and magnesium uptake between different varieties of maize planted in two types of peat materials. This study investigated the growth of selected maize varieties by comparing the nutrient uptake between three different varieties of maize (V1-Asia Manis, V2-Super A, and V3-Pearl Waxy) planted on hemic and sapric, respectively, without any application of fertilisers. Significant interactions were found where different maize varieties responded differently in the nutrient uptake when planted in different peat materials. Super A (V2) significantly recorded the highest uptake for all nutrients (679.71 mg) when planted in hemic, followed by V1 (422.03 mg) and V3 (314.77 mg) when planted in sapric. Super A was found to be superior to the two varieties, where it was more efficient in absorbing nutrients from the peat materials, having significantly higher dry matter weight (26.37 g) than V1 (19.26 g) and V3 (13.67 g). Hemic and sapric could support the growth of all three maize varieties up till the tasselling stage without any fertiliser application.

Keywords: Calcium, growth performance, hemic, magnesium, potassium, sapric

ARTICLE INFO

Article history:
Received: 06 April 2023
Accepted: 06 June 2023
Published: 31 October 2023

DOI: https://doi.org/10.47836/pjtas.46.4.09

E-mail addresses:
ameera@uitm.edu.my (Ameera Abdul Reeza)
2020977455@student.uitm.edu.my (Muhamad Amirul Falieq Baharuddin)
ahmed.haruna@unissa.edu.bn (Osumanu Haruna Ahmed)
aizuddin@uitm.edu.my (Mohd Aizuddin Masuri)
* Corresponding author

INTRODUCTION

Maize is an important staple crop in the Industrial Revolution and is in great demand globally, considering its importance as food, animal feed, additives in industrial products, scientific research, and economy (Ayiti &

ISSN: 1511-3701
e-ISSN: 2231-8542

Babalola, 2022). The demand and supply for maize worldwide for food and non-food products are usually on the rise, with nearly 15 million metric tons (MMT) used for animal feed, 4.25 MMT for industrial use while 1.36 MMT is used as food (Yadav et al., 2016). Concerning its value for domestic, economic, and industrial use, investing in the increase in maize production is an opportunity for any country.

However, the agriculture sector worldwide faces growing concerns over global grain security (Kalugina, 2014). Such issue has risen due to cultivated land conversion into urban and industrial construction as well as climate change (Hu et al., 2016). During the past decade, the consumption of natural resources has also increased due to the global population rise, and thus, demand for food, fibre, and biofuel has a significant impact on land and fertiliser consumption at local and global scales (Setiyono et al., 2010). Continuous cropping subsequently leads to nutrient mining, a major cause of low crop yields and unsustainable agriculture, especially in parts of the developing world, particularly in Southeast Asian regions.

Due to the scarcity of fertile land, farmers are now turning to marginal land, such as peatland, which has become a target for agricultural development over recent years (Lubis et al., 2019). The latest report by Omar et al. (2022) revealed that Southeast Asia has the largest areas of tropical peatlands in the world, where most peatlands in Southeast Asia are found in Indonesia (20.7 million ha), followed by Malaysia (2.6 million ha). Peatlands as land for farming possess an array of challenges physically, chemically, and biologically. Peatland has low productivity due to the lack of macro and micronutrients available for plants, especially with a low pH of 3.0-5.0 (Lubis et al., 2019; Omar et al., 2022). Previous studies suggested that pineapple is the only crop recommended and grown successfully on this soil, while various other crops are grown, with invariably poor yield. However, recent studies revealed that more crops can be grown in peats. As such, potatoes, sugar beet, celery, onions, carrots, lettuce, and market garden crops are commonly grown in drained fen or light peat soils in temperate regions, yet cereals still produce low yields (Finch et al., 2014). Conversely, several reports have shown that maize can be cultivated in tropical peatlands subject to chemical amelioration, such as liming and fertilisation (Lubis et al., 2019; Suswati et al., 2014, 2015). On the other hand, reports regarding new hybrid maize varieties that are capable of withstanding inadequate soil and climatic conditions have gained much attention (Harou et al., 2017), yet the applicability of these new hybrids to be grown and commercialised in organic soils as in contrast with the more commonly utilised mineral soils are severely limited. Also, most of these studies focussed on primary macronutrients such as N, P, and K in maize planted in mineral soils (Jiang et al., 2017; Ning et al., 2012; Q. Ma et al. 2021; Z. Ma et al., 2022) while other nutrients such as potassium, calcium, and magnesium are lacking especially with regards to planting in peat soils.

Given such a situation, it is imperative to assess the potential of peats as a growing media according to the types of peat since different kinds of peat respond differently to the growth and development of crops (Reeza, 2019; Reeza et al., 2021) due to their varied nutrient contents and other abiotic condition. Such information may provide significant importance in understanding the nutrient dynamics of the peat material brought upon by anthropogenic activities. In addition, with the newly introduced hybrid maize variety, there is a possibility that maize can be grown in peat, as these varieties may be able to withstand the acidity of peat materials. It is hypothesised that different maize varieties respond differently when planted in distinct types of peat materials and display different levels of nutrient uptake when planted within the same type. Hence, this research aims to compare the nutrient uptake between different varieties of maize planted in hemic and sapric peat materials. The comparison of the different types of maize varieties can determine which varieties have higher nutrient efficiency and are suitable to be planted in peat. Also, the use of peat can help to expand the area of maize cultivation so that maize will be able to be grown on a larger scale.

MATERIALS AND METHODS

Sampling and Collection of Peat Materials

The experiment was carried out in a greenhouse in the Faculty of Plantation and Agrotechnology, Universiti Teknologi MARA, Jasin campus, Malacca, Malaysia (2°13'44.9"N 102°27'20.8"E) from December 2021 to March 2022. The area's climate is categorised as equatorial rainforest, fully humid (Kottek et al., 2006) without apparent dry and wet seasons since Malaysia receives rain all year round of 2,600 mm per year. The mean annual temperature is 27.6°C, where the average maximum temperature falls around 32.7°C while the average minimum temperature is 24.2°C (Malaysian Meteorological Department [MetMalaysia], 2019).

Hemic and sapric peat materials were used in this study, where they were collected from a 10-year-old oil palm plantation in the faculty itself (2°13'38.1"N 102°27'33.4"E), where the peat is classified as shallow peat having depth of organic material layer of less than 1.5 m (Lim, 1989). They are classified as Tropohemists since most of the organic materials have been decomposed enough that the botanical origin of as much as two-thirds of them cannot be readily determined, or the fibres can be largely destroyed by rubbing between the fingers and that they have hemic soil materials dominant in the subsurface tier if there is no continuous mineral layer 40 cm or more thick that has its upper boundary in that tier (Andriesse, 1988). Surface (0–15 cm) and subsurface (20–40 cm) soil layers were identified as sapric and hemic peat materials, respectively, based on the degree of decomposition (H1–H10) according to the von Post scale (von Post, 1922). The peat materials were collected using an Eijkelkamp peat sampler and

gathered in burlap sacks. Bulk density was also taken where undisturbed peat samples were collected using a core sampler of stainless-steel rings (diameter 5.2 cm, height 6.0 cm) and later were oven-dried to a constant weight at 105ºC (gravimetric method; American Society for Testing and Materials [ASTM], 1988). Upon returning to the greenhouse, the peat materials were air-dried for 3 days to remove the excess water to be used as a potting medium. After the peat materials had dried, they were transferred into polybags (2.5 cm × 2.5 cm), where each polybag was filled with 3.5 kg of hemic and sapric peat materials individually.

Experimental Design and Treatments

There were 3 different hybrid maize varieties utilised in this study, which were V1-Asia Manis (SS932) and V2-Super A (SS232); both are of sweetcorn seeds resistant to rust and stalk rot, while V3-Pearl Waxy (WX100) is categorised as white waxy corn resistant towards rust and southern corn leaf blight. All three varieties are classified as non-genetically modified organisms (non-GMO) F1 hybrid maize seeds (Hefei Hefeng Seeds Co. Ltd., China). Seeds were sown on seedling trays for uniform growth and selection for transplanting into polybags. After the seedlings had grown 4 true leaves around two weeks after sowing, they were transferred to polybags in a greenhouse and were grown for 8 weeks (56 days) until they reached the tasselling stage, where it is the maximum growth stage achieved prior to the productive stage from January 2022 till February 2022. The average temperature in the greenhouse was 33.6°C with a mean relative humidity of 53.6%. As much as 600 ml of daily manual watering was performed on each polybag, which was done twice: early morning and late afternoon.

The experiment followed a completely randomised design (CRD) comprising two different peat materials (hemic and sapric) and three different hybrid maize varieties (V1-Asia Manis, V2-Super A, and V3-Waxy Corn). There were 144 experimental units altogether (2 peat types × 3 maize varieties × 3 replicates × 8 weeks). Destructive sampling was conducted for this study, where soil and plant samples were collected each week for 8 weeks [56 days after sowing (DAS)].

Soil and Plant Analysis

Prior to planting, the peat materials were analysed for pH, which was measured potentiometrically in soil suspensions consisting of a 1:10 volumetric ratio of peat sample to water (Reeza et al., 2021). Exchangeable calcium, magnesium, and potassium were determined using ammonium acetate (NH_4OAc, buffered at pH 4, Bendosen, Noway) (Reeza et al., 2021) and organic matter via loss in ignition method after placing samples in a muffle furnace at 300–550°C for 6 hr (Sutherland, 1998). Daily manual watering of about 1 L of water per polybag was performed. It is important to note that no fertiliser was added as this experiment was exclusively done to study the nutrient-

supplying ability of the peat materials without any interference from external additives.

For every week of destructive sampling, the whole plant was harvested (shoot and root), weighed before oven-drying at 60°C to constant weight, and measured using an electronic sensitive balance. These dried plant samples were then milled to bypass via a 0.5 mm sieve. Soil sampling was also taken weekly to determine the availability of K^+, Ca^{2+}, and Mg^{2+} via NH_4OAc buffered at pH 4 (Bendosen, Noway) (Reeza et al., 2021), while dry ashing method was used to determine nutrient content in the plant samples (Sahrawat et al., 2002). Nutrient uptake (potassium, calcium, and magnesium) was then calculated by multiplying plant dry weight by nutrient concentration obtained from the dry ashing method (mg/kg) according to the following formula (Nigussie et al., 2021):

$$Total\ nutrient\ uptake\left(\frac{mg}{polybag}\right) = Nutrient\ concentration\ in\ tissue\left(\frac{mg}{kg}\right) \times Plant\ dry\ weight\left(\frac{kg}{polybag}\right)$$

Statistical Analysis

Two-way analysis of variance (ANOVA) was performed to test for differences among the factors (peat types and maize varieties) using SPSS (version 21.0), while means of the treatments were compared based on Tukey's b test at the 5% probability level.

RESULTS AND DISCUSSION

Initial Soil Analysis

Initial soil physicochemical properties for hemic and sapric peat materials are presented in Table 1. It is important to note that the pH of the peat materials is relatively high (pH 5.0–5.7) compared to many other reports (pH 3.2–4.5) of similar region and climate (Afip & Jusoff, 2019; Hikmatullah & Sukarman, 2014). The pH, organic matter (OM), organic carbon (OC), and moisture content were lower in sapric compared to hemic due to the

Table 1
Initial physicochemical properties for hemic and sapric

Properties	Hemic	Sapric
pH	5.7 ± 0.4	5.04 ± 0.16
OM (%)	73.6 ± 2.94	62.9 ± 2.77
OC (%)	43.0 ± 1.34	36.6 ± 1.71
Moisture content (%)	73.63 ± 3.78	64.21 ± 2.98
Bulk density (g/cm^3)	0.15 ± 0.02	0.21 ± 0.03
von Post	H5	H8
Available K (mg/kg)	66.65 ± 2.60	35.84 ± 3.71
Available Ca (mg/kg)	225.64 ± 4.80	172.05 ± 3.06
Available Mg (mg/kg)	46.86 ± 3.04	35.68 ± 2.14

Note. OM = Organic matter; OC = Organic carbon

higher degree of decomposition, as shown in von Post (H8) compared to hemic (H5). Also, available K^+, Ca^{2+}, and Mg^{2+} were lower in sapric than hemic. Such findings were consistent with reports by Reeza et al. (2021) as well as Hikmatullah and Sukarman (2014), where sapric materials commonly display a reduction in OM, OC, and available nutrients due to the advanced degree of decomposition that leads to loss of organic materials and other physicochemical properties. In contrast, bulk density is slightly higher in sapric compared to hemic, justifying the higher maturity of peat soils that will be followed by increasing bulk density value (Hikamtullah & Sukarman, 2014) attributed to a decrease in porosity and fibre content as well as the increase in the mineral matter as a result of the further decomposition process.

However, the available nutrient contents were found to be lower than reports elsewhere (Arabia et al., 2020; Hikmatullah & Sukarman, 2014; Sahfitra et al., 2020), and this is possibly due to the origin of the peatland area, where oil palms have been planted for 10 years that may cause these nutrients to be depleted.

Dry Matter Weight and Nutrient Uptake for Different Maize Varieties Planted in Two Types of Peat Materials

The dry matter (DM) weight for V1, V2, and V3 planted in hemic and sapric peat upon harvest at 56 DAS is presented in Table 2. There were significant differences in DM between varieties, where V2 recorded significantly the highest DM, followed by V1 and V3. However, no significant differences were found when planted in the two types of peat materials except for V3. It can be inferred that although different types of peat materials had no influence on the DM for these hybrid maize varieties, significant discrepancies in their DM weight are evident, where V2 (Super A) yield the highest compared to other varieties.

Alternatively, there are significant interactions between peat types and maize varieties for nutrient uptake. Different maize varieties responded differently in nutrient uptake when planted in different peat materials (Table 3). Nevertheless, potassium is the most nutrient absorbed by all three varieties, followed by calcium and magnesium. The values obtained from the nutrient uptake in this study are consistent with the reports by Kassim et al. (2011), where the amount of nutrient uptake is in the following order: K > Ca > Mg. Also, V2 significantly recorded the highest uptake for all three nutrients, followed by V1 and V3 regardless of peat materials, justifying the highest DM obtained by V2 (Table 2).

Table 2
Dry matter weight between treatments at 56 days after sowing

Maize varieties	Dry matter weight (g)	
	Hemic	Sapric
V1	18.157^{Ab}	19.26^{Ab}
V2	25.35^{Aa}	26.37^{Aa}
V3	7.12^{Ac}	13.67^{Bc}

Note. Capital letters indicate mean separation between peat types while lowercase letters refer to mean separation among varieties using Tukey at $p = 0.05$

The K uptake was significantly higher when planted in sapric for V1 (339.55 mg) and V3 (248.453 mg); however, V2 was the only variety that performed better in hemic with the highest amount of K uptake (571.03 mg) compared to other varieties.

A similar observation was found in calcium uptake, where V1 and V3 showed significantly higher calcium absorption in sapric with 58.57 and 44.04 mg/plant, respectively, while V2 performed better in hemic with 73.79 mg/plant. However, no significant differences were obtained in magnesium uptake planted in the two types of peat materials, while significant differences were only detected in the uptake between varieties, where V2 recorded significantly higher magnesium uptake than the other two varieties.

The distinct response in nutrient uptake between varieties was also reported by Fosu-Mensah and Mensah (2016) as well as Singh and Gildhyal (1980), where different types of maize varieties showed significantly different nutrient uptake, particularly macronutrients. Furthermore, according to González-Fontes et al. (2017), genetic variation within and among crops in nutrient uptake efficiency (NUE) is well recognised where genotypic variability affects NUE and nutrient uptake influences some processes and plant mechanisms, including differences in uptake, movement in the root, shoot demand, and biomass production (DM weight).

At this point, no single fertiliser was added to these peat materials, and all the nutrients absorbed by these maize varieties were solely from the peat itself. Based on this study, it can be clearly understood that regardless of the types of peat materials, V2 might be a superior variety due to higher nutrient uptake efficiency as this variety was able to absorb and utilise higher amounts of nutrients (K, Ca, and Mg) resulting in significantly higher DM compared to the other two varieties when planted on the same type of peat materials.

Table 3
Nutrient uptake (K, Ca, and Mg) for different varieties and peat types at 56 days after sowing

Nutrient uptake (mg/plant)	Variety	Peat types	
		Hemic	Sapric
Potassium (K)	V1	273.03^{Bb}	339.55^{Ab}
	V2	571.03^{Aa}	360.22^{Ba}
	V3	158.54^{Bc}	248.45^{Ac}
Calcium (Ca)	V1	44.02^{Bb}	58.57^{Ab}
	V2	73.79^{Aa}	66.64^{Ba}
	V3	19.95^{Bc}	44.04^{Ac}
Magnesium (Mg)	V1	23.91^{Ab}	23.14^{Aa}
	V2	34.89^{Aa}	23.26^{Ba}
	V3	13.77^{Bc}	22.28^{Aa}

Note. Capital letters indicate significant differences between peat types, while small letters indicate significant differences between varieties for a particular nutrient uptake using Tukey at $p = 0.05$

Plant Height at 56 DAS

Plant height has a direct relationship with plant dry weight, which, as the height increases, so does the dry weight since it reflects the biomass of the plant itself. Hence, based on Table 4, the pattern of plant height increment is similar to that of dry weight, as described previously in Table 2. A significant interaction was only detected for V3, whose height was significantly higher in sapric than hemic. Super A significantly showed the maximum height, followed by Asia Manis and Pearl Waxy, regardless of peat materials. Therefore, it can be deduced that when the same type and amount of external sources such as medium of planting, water, sunlight, and nutrient supply are given to the three types of hybrid maize variety, Super A showed the highest and most rapid growth compared to Asia Manis and Pearl Waxy and it can be inferred that Super A is more efficient in using all the external sources to support its growth and development compared to the other two varieties above, hence justifying the name of the variety "Super" as being superior than the other varieties. Apart from that, tassels emerged rapidly at week 6, where the emergence was slightly faster when grown in sapric than hemic, although nutrient availability was significantly higher in the latter.

Table 4
Plant height between treatments at 56 days after sowing

Maize varieties	Plant height (cm)	
	Hemic	Sapric
V1	159.0^{Ab}	163.0^{Ab}
V2	186.0^{Aa}	180.0^{Aa}
V3	116.0^{Ac}	146.0^{Bc}

Note. Capital letters indicate mean separation between peat types while lowercase letters refer to mean separation among varieties using Tukey at $p = 0.05$

Analysis of Chemical Properties of Peat Materials at 56 DAS

The variation in the uptake of nutrients and DM of these hybrid maize varieties can be justified not only by their different genotypic variability but also by the distinct discrepancies in hemic and sapric's chemical properties during initial and after planting for 56 DAS as shown in Tables 1 and 5, respectively. Based on these tables, it is evident that generally, pH, OM, OC, and available nutrients (K^+, Ca^{2+}, Mg^{2+}) were higher in hemic compared to sapric, yet only V2 showed better growth and uptake of nutrients in hemic while V1 and V3 performed better in sapric.

The differences may be attributed to the different degrees of decomposition of these peat materials, which in turn influence the rate of nutrient release. It agrees with

Table 5
Selected chemical properties for hemic and sapric at 56 days after sowing

Properties	Hemic	Sapric
pH	6.24^{a}	5.8^{b}
OM (%)	69.39^{a}	66.41^{b}
OC (%)	40.25^{a}	38.52^{a}
Available K (mg/kg)	27.42^{a}	24.57^{b}
Available Ca (mg/kg)	326.44^{a}	176.75^{b}
Available Mg (mg/kg)	66.54^{a}	30.32^{b}

Note. OM = Organic matter; OC = Organic carbon; Small letters within rows indicate significant differences between peat types using Tukey at p=0.05

the findings by Veloo et al. (2015), where the stage of decomposition has the most significant effect on crop yield for peat soil. They reported that soils with sapric materials gave significantly better yields than soils with hemic materials, possibly because crop roots are mainly in contact with the highly decomposed sapric material, which is a good rooting and growth medium compared to the hemic material. Another probability is that hemic peat with a higher porosity level may not have good nutrient retention properties compared to sapric with lower porosity characteristics (Veloo et al., 2015).

The pH was found to be increased at 56 DAS irrespective of peat materials, and it was attributed to the rise in available Ca at 8 weeks of planting (Table 5), while there was a profound decrease in available K when compared to the initial condition of the peat materials (Table 1). The decrease in available K can be supported by the substantial uptake of this nutrient ranging between 158–578 mg/plant regardless of maize varieties compared to calcium and magnesium uptake varying between 14–74 mg/plant. Since the uptake of calcium and magnesium was much lower than potassium, the accumulation of these former nutrients was high in these peat materials, increasing pH. It is worth mentioning that all the maize varieties were able to grow well without showing any deficiency symptom of these nutrients up to the tasselling and silking stage, which may suggest that the nutrient content in hemic and sapric peat materials might be sufficient to support the growth these maize varieties since no fertilisers were added.

CONCLUSION

Different maize varieties have different preferences for the types of peat materials being used as a planting medium, and the variety V2 (SS232-Super A) performed better than V1 (SS232-Asia Manis) and V3 (WX100-Waxy Corn) in terms of dry matter weight, potassium, calcium, and magnesium uptake when planted in tropical hemic and sapric peat materials in the following order V2 > V1 > V3. Nonetheless, different maize varieties take up significantly different amounts of nutrients, yet both hemic and sapric could support the growth of maize without any application of fertiliser up till the tasselling stage. Further research can be implemented by extending the duration of the study till the harvesting stage to observe the yield differences between these varieties and elucidate the mechanism of the cause of why different varieties favour different types of soil.

ACKNOWLEDGEMENTS

The authors are very grateful for the financial and technical support from Universiti Teknologi MARA and the Ministry of Higher Education, Malaysia.

REFERENCES

Afip, I. A., & Jusoff, K. (2019). Properties of a tropical sapric peat poil in Sarawak. *Malaysian Journal of Soil Science*, *23*, 1-12.

American Society for Testing and Materials. (1988). *Annual book of ASTM standard: Construction, concrete and aggregates*. ASTM.

Andriesse, J. P. (1988). *Nature and management of tropical peat soils*. Food and Agriculture Organization of the United Nations.

Arabia, T., Basri, H., Manfarizah., Zainabun., & Mukhtaruddin. (2020). Physical and chemical characteristics in peat lands of Aceh Jaya District, Indonesia. In *IOP Conference Series: Earth and Environmental Science* (Vol. 499, No. 1, p. 012004). IOP Publishing. https://doi.org/10.1088/1755-1315/499/1/012004

Ayiti, O. E., & Babalola, O. O. (2022). Sustainable intensification of maize in the industrial revolution: Potential of nitrifying bacteria and archaea. *Frontiers in Sustainable Food Systems*, *6*, 827477. https://doi.org/10.3389/fsufs.2022.827477

Finch, H. J. S., Samuel, A. M., & Lane, G. P. F. (2014). *Lockhart and Wiseman's crop husbandry including grassland* (9th ed.). Woodhead Publishing.

Fosu-Mensah, B. Y., & Mensah, M. (2016). The effect of phosphorus and nitrogen fertilizers on grain yield, nutrient uptake and use efficiency of two maize (*Zea mays* L.) varieties under rain fed condition on Haplic Lixisol in the forest-savannah transition zone of Ghana. *Environmental Systems Research*, *5*, 22. https://doi.org/10.1186/s40068-016-0073-2

González-Fontes, A., Navarro-Gochicoa, M. T., Ceacero, C. J., Herrera-Rodríguez, M. B., Camacho-Cristóbal, J. J., & Rexach, J. (2017). Understanding calcium transport and signaling, and its use efficiency in vascular plants. In M. A. Hossain, T. Kamiya, D. J. Burritt, L. S. P. Tran, & T. Fujiwara (Eds.), *Plant macronutrient use efficiency* (pp. 165-180). Academic Press. https://doi.org/10.1016/B978-0-12-811308-0.00009-0

Harou, A. P., Liu Y., Barrett, C. B., & You, L. (2017). Variable returns to fertiliser use and the geography of poverty: Experimental and simulation evidence from Malawi. *Journal of African Economies*, *26*(3), 342–371. https://doi.org/10.1093/jae/ejx002

Hikmatullah., & Sukarman. (2014). Physical and chemical properties of cultivated peat soils in four trial sites of ICCTF in Kalimantan and Sumatra, Indonesia. *Journal of Tropical Soils*, *19*(3), 131-141. https://doi.org/10.5400/jts.2014.v19i3.131-141

Hu, F., Gan, Y., Chai, Q., Feng, F., Zhao, C., Yu, A., Mu, Y., & Zhang, Y. (2016). Boosting system productivity through the improved coordination of interspecific competition in maize/pea strip intercropping. *Field Crop Research*, *198*, 50–60. https://doi.org/10.1016/j.fcr.2016.08.022

Jiang, W., Liu, X., Qi, W., Xu, X., & Zhu, Y. (2017). Using QUEFTS model for estimating nutrient requirements of maize in the Northeast China. *Plant Soil and Environment*, *63*(11), 498–504. https://doi.org/10.17221/417/2017-PSE

Kalugina, Z. I. (2014). Agricultural policy in Russia: Global challenges and the viability of rural communities. *The International Journal of Sociology of Agriculture and Food*, *21*(1), 115–131. https://doi.org/10.48416/ijsaf.v21i1.158

Kassim, S., Ahmed, O. H., & Majid, N. M. A. (2011). Effectiveness of liquid organic-nitrogen fertilizer in enhancing nutrients uptake and use efficiency in corn (*Zea mays*). *African Journal of Biotechnology*, *10*(12), 2274-2281.

Kottek, M., Grieser, J., Beck, C., Rudolf, B., & Rubel, F. (2006). World map of the Köppen-Geiger climate classification updated. *Meteorologische Zeitschrift*, *15*(3), 259–263. https://doi.org/10.1127/0941-2948/2006/0130

Lim, J. S. (1989). Major soil mapping units in peninsular Malaysia. In *Proceedings of Workshop on Recent Development in Soil Genesis and Classification* (pp. 113–133). Malaysian Society of Soil Science.

Lubis, K., Siddik, S. S., & Setiado, H. (2019). Performance of some populations of maize (*Zea mays* L.) on peat soil applied sludge and ash of oil palm. In *IOP Conference Series: Earth and Environmental Science* (Vol. 260, No. 1, p. 012167). IOP Publishing. https://doi.org/10.1088/1755-1315/260/1/012167

Ma, Q., Jiang, C., Li, S., & Yu, W. (2021). Maize yield and nitrogen-use characteristics were promoted as consistently improved soil fertility: 6-year straw incorporation in Northeast China. *Plant Soil and Environment*, *67*(7), 383–389. https://doi.org/10.17221/434/2020-PSE

Ma, Z., Ren, B., Zhao, B., Liu, P., & Zhang, J. (2022). Optimising the root traits of summer maize to improve nutrient uptake and utilisation through rational application of urea ammonium nitrate solution. *Plant, Soil and Environment*, *68*(2), 98–107. https://doi.org/10.17221/335/2021-PSE

Malaysian Meteorological Department. (2019). *Annual report 2019*. MetMalaysia. https://www.flipsnack.com/7B5CF55569B/laporantahunan2019/full-view.html

Nigussie, A., Haile, W., Agegnehu, G., & Kiflu, A. (2021). Growth, nitrogen uptake of maize (*Zea mays* L.) and soil chemical properties, and responses to compost and nitrogen rates and their mixture on different textured soils: Pot experiment. *Applied and Environmental Soil Science*, *2021*, 9931763. https://doi.org/10.1155/2021/9931763

Ning, T. Y., Shao, G. Q., Li, Z. J., Han, H. F., Hu, H. G., Wang, Y., Tian, S. Z., & Chi, S.Y. (2012). Effects of urea types and irrigation on crop uptake, soil residual, and loss of nitrogen in maize field on the North China Plain. *Plant, Soil and Environment*, *58*(1), 1-8. https://doi.org/10.17221/156/2011-PSE

Omar, M. S., Ifandi, E., Sukri, R. S., Kalaitzidis, S., Christanis, K., Lai, D. T. C., Bashir, S., & Tsikouras, B. (2022). Peatlands in Southeast Asia: A comprehensive geological review. *Earth-Science Reviews*, *232*, 104149. https://doi.org/10.1016/j.earscirev.2022.104149

Reeza, A. A. (2019). Effect of liming and fertilizer application on mineralization of nitrogen in hemic and sapric of tropical peat material. *Pertanika Journal of Tropical Agricultural Science*, *42*(2), 779 – 790.

Reeza, A. A., Hussin, A., & Ahmed, O. H. (2021). Comparison of the effectiveness of three extractants in extracting potassium, calcium and magnesium from tropical peat soils. *Mires and Peat*, *27*(6), 1-10. https://doi.org/10.19189/MaP.2019.OMB.StA.1833

Sahfitra, A. A., Hanudin, E., Wulandari, C., & Utami, S. N. H. (2020). NPK uptake and growth of maize on ombrogenous peat as affected by the application of mycorrhizal fungal multi-spores and compound fertilizers. *Ilmu Pertanian (Agricultural Science)*, *5*(2), 76-85. https://doi.org/10.22146/ipas.47535

Sahrawat, K. L., Ravi Kumar, G., & Rao, J. K. (2002). Evaluation of triacid and dry ashing procedures for determining potassium, calcium, magnesium, iron, zinc, manganese, and copper in plant materials. *Communications in Soil Science and Plant Analysis*, *33*(1–2), 95–102. https://doi.org/10.1081/CSS-120002380

Setiyono, T. D., Waltersa, D. T., Cassmana, K. G., Wittb, C., & Dobermann, A. (2010). Estimating maize nutrient uptake requirements. *Field Crops Research*, *118*(2), 158–168. https://doi.org/10.1016/j.fcr.2010.05.006

Singh, R., & Ghildyal, B. P. (1980). Soil submergence effects on nutrient uptake, growth, and yield of five corn cultivars. *Agronomy Journal*, *72*(5), 737-741. https://doi.org/10.2134/agronj1980.00021962007200050011x

Suswati, D., Sunarminto, B. H., Shiddieq, D., & Indradewa, D. (2014). Use of ameliorants to increase growth and yield of maize (*Zea mays*

L.) in peat soils of West Kalimantan. *Journal of Tropical Soils*, *19*(1), 35-41. https://doi.org/10.5400/jts.2014.v19i1.35-41

Suswati, D., Sunarminto, B. H., Shiddieq, D., & Indradewa, D. (2015). Effect of ameliorants on nutrient uptake and maize productivity in peatlands. *Malaysian Journal of Soil Science*, *19*, 115-129.

Sutherland, R. A. (1998). Loss-on-ignition estimates of organic matter and relationships to organic carbon in fluvial bed sediments. *Hydrobiologia*, *389*, 153–167. https://doi.org/10.1023/A:1003570219018

Veloo, R., van Ranst, E., & Selliah, P. (2015). Peat characteristics and its impact on oil palm yield. *NJAS-Wageningen Journal of Life Sciences*, *72-73*(1), 33-40. https://doi.org/10.1016/j.njas.2014.11.001

von Post, L. (1922). Sveriges geologiska undersöknings torvinventering och några av dess hitills vunna resultat [The Swedish Geological Survey's peat inventory and some of the results so far]. *Svenska Mosskulturföreningens Tidskrift*, *36*, 1–27.

Yadav, O., Prasanna, B., Yadava, P., Jat, S., Kumar, D., & Dhillon, B., (2016). Doubling maize (*Zea mays*) production of India by 2025-challenges and opportunities. *Indian Journal Agricultural Science*, *86*(4), 427–434. https://doi.org/10.56093/ijas.v86i4.57427

Pertanika J. Trop. Agric. Sci. 46 (4): 1233 - 1244 (2023)

PERTANIKA JOURNALS

TROPICAL AGRICULTURAL SCIENCE

Journal homepage: http://www.pertanika.upm.edu.my/

Short Communication

Determination of Pneumococcal Serotypes by Sequetyping and Sequential Conventional Multiplex PCR in the Vaccine Era

Nurul Asyikin Abdul Rahman[1,2], Mohd Nasir Mohd Desa[1]*, Siti Norbaya Masri[3], Niazlin Mohd Taib[3], Nurshahira Sulaiman[1], Nurul Diana Dzaraly[1] and Hazmin Hazman[1]

[1]Department of Biomedical Science, Faculty of Medicine and Health Sciences, Universiti Putra Malaysia, 43400 Serdang, Selangor, Malaysia

[2]School of Biology, Faculty of Applied Sciences, Universiti Teknologi MARA Negeri Sembilan, Kuala Pilah Branch, 72000 Kuala Pilah, Negeri Sembilan, Malaysia

[3]Department of Medical Microbiology, Faculty of Medicine and Health Sciences, Universiti Putra Malaysia, 43400 Serdang, Selangor, Malaysia

ABSTRACT

Pneumococcal serotyping is required for epidemiological surveillance to guide vaccination strategy. DNA-based approaches are more affordable, but the combination of sequetyping and sequential conventional multiplex polymerase chain reaction (cmPCR) may complement one another. A total of 101 isolates were subjected to sequetyping and sequential cmPCR following previously published protocols, and the outputs were compared. The sequetyping method determined up to the serotype level for 99 isolates (98%). On the other hand, the sequential cmPCR technique identified 91 isolates (90.1%), with 63 of them (62.4%) up to the serotype level. Sequetyping generated discrete serotypes for 6A/B, 11A/D, 15A/F, and 15B/C as 6A (n = 11), 6B (n = 10), 11A (n = 5), 15C (n = 1), and 15A (n = 1). In conclusion, the *cpsB* gene sequetyping method produced a comparable output with sequential cmPCR, further discriminating some sub-serogroups among the isolate collection.

ARTICLE INFO

Article history:
Received: 01 March 2023
Accepted: 24 May 2023
Published: 31 October 2023

DOI: https://doi.org/10.47836/pjtas.46.4.10

E-mail addresses:
asyikin1945@uitm.edu.my (Nurul Asyikin Abdul Rahman)
mnasir@upm.edu.my (Mohd Nasir Mohd Desa)
sitinorbaya@upm.edu.my (Siti Norbaya Masri)
niazlin@upm.edu.my (Niazlin Mohd Taib)
nurshahira@upm.edu.my (Nurshahira Sulaiman)
dianadzaraly@gmail.com (Nurul Diana Dzaraly)
hazminhazman@gmail.com (Hazmin Hazman)
* Corresponding author

Keywords: Sequential conventional multiplex PCR, sequetyping, serotyping, *Streptococcus pneumoniae*

INTRODUCTION

Streptococcus pneumoniae (pneumococci) is a normal microflora of the upper respiratory tract. It is also an opportunistic pathogen that may cause non-invasive and invasive pneumococcal disease in

ISSN: 1511-3701
e-ISSN: 2231-8542

children worldwide. Pneumococcal disease is a global health problem that causes an estimated one million mortalities annually, mainly in children younger than five (Wahl et al., 2018).

Polysaccharide capsules (CPSs) are the main factors that enable pneumococci to evade the host's immune system. The capsular structural variation and antigen differentiate *S. pneumoniae* into 101 serotypes (Ganaie et al., 2021). Some *S. pneumoniae* serotypes are more commonly associated with clinical or carrier isolates, or both, which differ in invasiveness (Ganaie et al., 2020). Data from Southeast Asia showed that the most prevalent pathogenic serotypes were 19F, 23F, 14, 6B, 1, 19A, and 3, while the prevalence of *S. pneumoniae* in healthy children under the age of five was 6A/B, 23F, and 19F (Daningrat, 2022; Jauneikaite, 2012).

The most frequent serotypes in Malaysia across all pneumococcal diseases are 14, 6A/B, 23F, 19A, and 19F (Dzaraly et al., 2021). With regards to vaccines, the pneumococcal conjugate vaccine (PCV) Synflorix (PCV10, GlaxoSmithKline) covers four of the most widely disseminated serotypes in Malaysia, but Prevnar (PCV13, Pfizer) offers a better serotype-coverage than PCV10. The serotypes covered by the PCVs are referred to as vaccine types (VT). Malaysia recently implemented a pneumococcal vaccination policy incorporating PCV into the National Immunisation Programme in December 2020. The Synflorix pneumococcal vaccine has been included for the first two years of implementation and protects against ten serotypes: 1, 4, 5, 6B, 7F, 9V, 14, 18C, 19F, and 23F. Thus, accurate determination of *S. pneumoniae* serotypes in clinical and community settings is critical, as vaccine development relies on serotype prevalence data.

The conventional agglutination based-serotyping method, the Quellung reaction test, has been used for several decades to conduct epidemiological research on pneumococcal diseases. Despite being the "gold standard," it requires significant cost and expertise; hence, its use has been limited in specialised reference laboratories. Then, the commercial latex agglutination test is appropriate for laboratories with a rapid turnaround and fewer resources. This technique has the primary benefit of not needing sophisticated equipment for testing (Swarthout et al., 2021). Moreover, latex agglutination is suggested as a substitute for the Quellung approach for pneumococcal serotyping. Latex agglutination is among the simplest laboratory techniques for serotype identification; nevertheless, it has several disadvantages, such as weak outcomes leading to challenging interpretations and self-agglutinations that make typing infeasible (Batt et al., 2005). Inconsistencies arise due to laboratory errors and the high cost of antisera panels for Quellung and latex agglutination, suggesting that the DNA-based approach using PCR is a more affordable serotyping approach (Batt et al., 2005; Leung et al., 2012; Park et al., 2019).

PCR-specific serotyping approaches such as sequetyping and sequential

conventional multiplex PCR (cmPCR) were devised as the alternatives for Quellung and latex agglutination by amplifying capsular type-based DNA elements; this offers an economical, sensitive, and relatively straightforward serotyping approach compared to the conventional methods (Leung et al., 2012). Hence, the Centers for Disease Control and Prevention (CDC) develops protocols through a series of multiplex PCR, which uses primer combinations targeting various serotypes or serogroups. Several sets of serotype-specific primers are needed to facilitate detailed serotype evaluation, and currently, 41 primer sets have been available covering 22 single serotypes and 18 single serogroups through eight sequential multiplex PCR as updated by the CDC *Streptococcus* Laboratory at https://www.cdc.gov/streplab/pneumococcus/resources.html. However, sequential cmPCR has some limitations, including the need to run sequential reactions until the serotyping for the sample is obtained, which is time-consuming. In addition, sequential cmPCR detection can be affected by mutations in the target sequences, which can lead to false-positive or false-negative results.

Sequetyping is another method that uses a single primer set that can be used for *S. pneumoniae* serotyping. Sequetyping is previously claimed as a cost-effective, efficacious, and relatively straightforward serotyping approach offering appreciable coverage, including the serotypes not covered by PCVs, referred to as non-vaccine serotypes (NVT) (Leung et al., 2012). This technique uses only one amplification reaction followed by DNA sequencing to determine the pneumococcal serotypes (Leung et al., 2012). Therefore, it can be applied in laboratories that offer PCR and sequencing for determining a wider coverage of pneumococcal serotypes. The sequetyping method may provide a certain level of expediency over other previously reported serotyping methods. Thus, in this study, the performance between sequetyping and sequential multiplex PCR was evaluated in terms of serotype identification in our archived collection of local *S. pneumoniae* isolates.

MATERIALS AND METHODS

Ethical Clearance

This study was approved by the Ethics Committee for Research involving Human Subjects of Universiti Putra Malaysia (Reference: JKEUPM-2021-647). This study utilised old isolates collected from previous studies only for the objective of this study without any relation to the patient's background associated with the isolates (patients' data are restricted and not traceable).

Bacterial Isolates

A total of 101 hospital isolates from various isolation sites (sputum, pus, blood, tracheal aspirates, eye, and nasopharynx) collected in 2017–2019 were available in our archived culture collection at the Applied Microbiology Laboratory, Faculty of Medicine and Health Sciences, Universiti

Putra Malaysia. Isolates were re-identified for viability and purity following standard methods.

Identification of *S. pneumoniae* Using the Standard Bacteriological Method

A standard bacteriological method was used to identify all isolates as *S. pneumoniae*, including colonial morphology on Columbia agar with 5% sheep blood (Isolab Sdn Bhd, Malaysia), Gram-positive (Gram-positive diplococci in the chain), and a catalase test (negative reaction) (Sigma Aldrich, Switzerland). Furthermore, isolates were subjected to a standard confirmatory test such as a bile solubility (Hardy Diagnostics, USA) and susceptibility test with ethylhydrocupreine (Liofilchem, Italy) or optochin (Liofilchem, Italy).

DNA Extraction

Bacterial DNA was extracted from single colonies grown on an agar plate using the GeneAll ExgeneCell SV Mini genomic extraction kit (GeneAll, South Korea) according to the manufacturer's instructions.

Molecular Identification of *S. pneumoniae* Virulence Genes Using the *ply* and *lytA* Genes

The *S. pneumoniae* virulence genes *ply* and *lytA* were amplified using conventional PCR assays as a spp. verification following protocols by Seki et al. (2005) and Sheppard et al. (2004). The tube of PCR reactions mixed with a DNA template of *S. pneumoniae* ATCC 49619 served as a positive control, and the reaction mixture without the DNA template served as a negative control. All suspensions of the PCR tube reaction mixture of 25 µl were thoroughly mixed and run in the BioRad MyCycler™ thermal cycler (BioRad, USA).

Sequetyping Using *cpsB* Single Gene Primer

Sequetyping was performed using primers designed by Leung et al. (2012). The reaction mixtures contained 12.5 µl of MyTaq TM Red Mix Bioline (Meridien Biosciences, USA), 0.8 µl forward primer (*cps1*), 0.8 µl reverse primer (*cps2*), and 3 µl of genomic DNA that made up the final volume of 25 µl with nuclease-free sterile distilled water. The reaction cycle consisted of an initial denaturation step at 95°C for 5 min, followed by 30 amplification cycles of denaturation at 95°C for 30 s, annealing at 65°C for 30 s, extension at 72°C for 1 min, and the final extension at 72°C for 5 min. Amplified DNAs were sequenced at Apical Scientific Sdn. Bhd., (Malaysia) and searched for homology in the GenBank. All sequences were submitted to GenBank with accession numbers OP 081815, OP136953, OP235918, OP235920-OP235037, OP270727-OP270740, and OP270742-OP270793.

Sequential Conventional Multiplex PCR (cmPCR)

The serotypes of the pneumococcal isolates were determined by sequential cmPCR using the primer sequences recommended by the CDC (2021). The primers targeted the *glycosyltranferase* genes (*wzg*, *wzx*, *wzy*,

wciP, *wciN Beta*, *wciL*, *wcwL*, and *wcwV*). This study's combination of the CDC's recommended primers was based on the multiplex target sets formulated by Shakrin et al. (2013, 2014). The sequential reactions were based on six sets labelled as A, B, C, D, E, and F in the sequence of the serotype prevalence in Asia and Malaysia: the most prevalent serotypes/serogroups were targeted first, followed by the less prevalent serotypes/serogroups. Each set of primer pairs contained four serotypes/serogroups and an internal positive control pair of primers that targeted a conserved region of the pneumococcal capsular polysaccharide synthesis gene (*cpsA*). The reaction mixtures contained 12.5 µl of MyTaq™ Red Mix Bioline (Meridien Biosciences, USA), 2.0 µl of serotype-specific forward primer pairs, 2.0 µl of serotype-specific reverse primer pairs, 0.5 µl of *cpsA* forward and reverse primers, and 3 µl of genomic DNA, which made up the final volume of 25 µl with nuclease-free sterile distilled water. The reaction cycle consisted of an initial denaturation step at 95°C for 1 min, followed by 30 amplification cycles of denaturation at 95°C for 15 s, annealing at 54°C for 15 s, extension at 72°C for 10 s, and the final extension at 72°C for 5 min.

RESULTS

Characteristics and Identification of *S. pneumoniae*

All 101 isolates exhibited typical *S. pneumoniae* characteristics, including purplish, elongated diplococci under the microscope, alpha (α) hemolysis, sensitivity to 5 µg optochin disk (Liofilchem, Italy), and a solubility test with 2% sodium deoxycholate (Hardy Diagnostics, USA). Furthermore, the presence of *lytA* and *ply* genes in the 101 isolates further confirmed the identity of *S. pneumoniae*.

Sequetyping Employing *cpsB* Single Gene Primer for Serotype Identification

Ninety-nine of 101 (98%) pneumococcal isolates produced a positive signal with a 1,061 bp band. Two isolates (2%) were not amplified for the *cpsB* gene and were classified as non-typeable (NT). Upon sequencing and homology search, 16 different serotypes were determined. The most frequent was serotype 19F (n = 22; 21.8%) followed by 19A (n = 13; 12.9%); 14 (n = 12; 11.9%); 23F (n = 12; 11.9%); 6A (n = 11; 10.9%); 6B (n = 10; 9.9%); 11A (n = 5; 5%); 3 (n = 3; 3%); 1 (n = 2; 2%); 4 (n = 2; 2%); 35B (n = 2;2%); 13 (n = 1; 1%); 15A (n = 1; 1%); 15C (n = 1; 1%); 23A (n = 1; 1%), and 34 (n = 1; 1%) (Table 1).

Sequential cmPCR for Pneumococcal Serotype and Serogroup Determination

All 101 samples were positive for amplifying the internal positive control *cpsA* gene. However, 10 isolates (9.9%) could not be identified for any molecular target by the sequential cmPCR and were designated as NT. These include two isolates that could not be detected by sequetyping. Eleven serotypes and six serogroups were found in 91 (90.1%) isolates. The most frequent was serotype 19F (n = 22; 21.8%) followed by 6A/B (n = 21; 20.8%); 19A (n = 13;

Table 1
Serotype distribution by sequetyping and sequential conventional multiplex PCR

Serotypes	Sequetyping	Sequential cmPCR
1	2	2
3	3	(a)
4	2	2
6A/B	(b)	21
6A	11	(c)
6B	10	(c)
11A/D	(b)	5
11A	5	(d)
11D	0	(d)
13	1	(a)
14	13	12
15A/F	(b)	1
15A	1	(e)
15F	0	(e)
15B/C	(b)	1
15B	0	(f)
15C	2	(f)
19A	13	13
19F	22	22
23A	1	(g)
23F	12	12
34	1	(a)
35B	2	(a)
NT	2	10
Total	101	101

Note.
(a) = Primer not included in our multiplex set
(b) = Sequetyping able to discriminate to the serotype level/single serotype
(c) = Determined as 6A/B
(d) = Determined as 11A/D
(e) = Determined as 15A/F
(f) = Determined as 15B/C
(g) = Determined as non-typeable (NT)

12.9%); 14 (n = 12; 11.9%); 23F (n = 12; 11.9%); 11A/D (n = 5; 5%); 1 (n = 2; 2%); 4 (n = 2; 2%); 15B/C (n = 1; 1%); 15A/F (n = 1; 1%) (Table 1). The initial sequential cmPCR reaction covered 67.3% of the total isolates in Set A (serotypes 6A/B, 19A, 19F, and 23F), the most prevalent serotypes. The second reaction covered 14.9% in Set B (serotypes 1, 14, and 15B/C), and the third reaction covered 5% in Set C (serotype 11A/D) of the total isolates, respectively.

Comparison of *cpsB* Sequetyping and Sequential cmPCR

Table 1 compares the serotype distribution by sequetyping and sequential cmPCR. The result of sequetyping is in concordance with sequential cmPCR in most of the isolates. Sequetyping determined 99 isolates (98%) up to serotype level, while sequential cmPCR identified 91 isolates (90.3%) with 63 (62.4%) up to serotype level (Figure 1). Sequetyping could not amplify two isolates (2%), which also failed to be determined by the sequential cmPCR. Sequential cmPCR failed to amplify 10 isolates (9.9%) labelled NT, although all gave a positive result for the internal control *cpsA* gene. The highest serotype distribution was 19F (n = 22; 21.8%) when detected by sequetyping and sequential cmPCR. Meanwhile, the second most prevalent serotype was 19A (n = 13; 12.9%) by sequetyping and 6A/B (n = 21; 20.8%) by cmPCR. Furthermore, sequetyping identified four NVTs: 13, 23A, 34, and 35B, respectively. Serotype 3 is present in PCV13 but was not included in Shakira et al. (2013, 2014) formulation of the sequential multiplex sets of primers. Using sequetyping, serotype 23A was successfully amplified, but sequential cmPCR listed it as NT even though the primer was listed in our reaction sets. The

sequential cmPCR method identified some isolates as only 6A/B, 11A/D, 15A/F, and 15B/C (serogroup level) due to limited primers, while the sequetyping method discriminated the isolates as 6A (n = 11; 10.9%); 6B (n = 10; 9.9%); 11A (n = 5; 5%), and 15C (n = 1; 1%) (Figure 1).

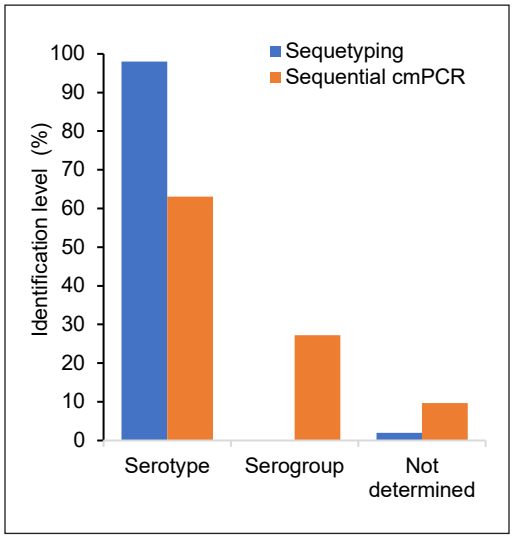

Figure 1. Comparison of serotyping outputs using sequetyping and sequential conventional multiplex PCR

Note. 'Not determined' refers to non-typeable (NT) isolates that cannot be detected using sequetyping and sequential cmPCR

DISCUSSION

Generally, DNA-based techniques allow the differentiation of a proportion of the pneumococcal serogroups and serotypes commonly associated with diseases. Although not all 101 serotypes can cause severe infections, accurately identifying *S. pneumoniae* serotypes is still necessary for prophylactic purposes. It is crucial to monitor the distribution of serotypes to manage strategy in disease control and prevention. Increasing numbers of pathogenic and carriage pneumococci are being investigated as part of post-PCV surveillance studies; therefore, rapid, accurate, and economical typing approaches are essential. Additionally, the proportion of IPD attributable to NVT gradually increases after PCVs are implemented (Løchen et al., 2020). Therefore, serotyping is important in screening for both VTs and NVTs.

In the sequential cmPCR in this study, six sets of CDC's recommended primer sequences (Set A–Set F) targeting 10 serogroups and 14 serotypes were employed to include the prevalent VTs in the Asian region and Malaysia (Shakrin et al., 2013, 2014). The sequential multiplex PCR (A to F) successfully identified 91 (90.1%) from a total of 101 isolates, with 63 (62.4%) of the isolates detected at the serotype level. Taking the overall reactions (Sets A to C), the sequential cmPCR based on Shakrin et al. (2013, 2014) formulation in this study showed a better coverage at 87.2% of the total isolates for the cumulative reactions 1, 2, and 3, as compared to the results of Park et al. (2019) at 79.4% in the same reactions. For the later study, Park et al. (2019) developed a modified sequential multiplex of conventional PCR using 30 primer sets to cover the predominant serotypes in Asian countries. It reflects the dynamic of conventional multiplex reactions that can always be subjected to improvement, but a technically and chemically workable PCR reaction in the presence of multiple targets usually requires sound optimisations and is not easily achieved.

Meanwhile, sequetyping is a more straightforward approach involving only a single gene amplification. Nevertheless, the amplified gene needs to be sequenced, which may look intricate, but the process is feasible due to the wide availability of service providers to continue with the downstream analysis. In this study, it was able to serotype 99 (98%) among the 101 isolates and discriminated serogroups 6A/B, 11A/D, 15A/F, and 15B/C as previously reported in the sequential cmPCR. Serotypes 6A and 6B, including 6C and 6D, could not be distinguished with sequential cmPCR alone due to the higher degree of genetic similarity that the current primers are not specific for the four sub-serotypes (Mauffrey et al., 2017; Pai et al., 2005). Jin et al. (2009) developed a serotype-specific primer targeting the *wciP* gene to differentiate serotypes 6A and 6B and another primer targeting the *wciN* gene to further differentiate serotypes 6A and 6C. Nevertheless, this adds extra steps; thus, more time and labour are needed to discriminate the serogroup. The *cpsB* gene sequetyping, on the other hand, can detect the specific sequence polymorphism at the nucleotide level to discriminate into 6A and 6B without the need to perform additional PCR reactions (Lawrence et al., 2000).

Several serotypes (9.9%) were undetectable by the sequential cmPCR in this study because of the limited primer coverage in the current multiplex sets. Whereas for serotype 23A, it was successfully determined by sequetyping but could not be amplified using the sequential cmPCR despite the primer being included in the current set of reactions. The misidentification might be due to the mutations in the *cps* locus that prevent amplification with the primers employed (Richter et al., 2013). There are 17 additional serotypes covered in the eight sequential sets as of the CDC's latest primer list, and the additional serotypes include the ones identified by the sequetyping in this study. It was observed that the sequetyping also failed to amplify the *cpsB* gene in two isolates (2%); this could be due to nucleotide variations or the absence of the targeted amplicons in the *cpsB* gene of these strains (Zhou et al., 2022). In the long run, sequetyping may benefit from the increasing availability of genomic information in public databases. Therefore, more studies are warranted to continuously update the database with the *cpsB* gene sequence of isolates from various geographical regions, particularly in view of the potential genetic diversity to establish the universality of the *cpsB* as the target for worldwide serotyping. This aspect has been a challenge regarding incomplete data, leading to incorrect serotype designations and assignments (Zhou et al., 2022).

Sequential cmPCR is an effective method as one reaction allows the simultaneous identification of one or more alleles or genes (Mauffrey et al., 2017). Nevertheless, due to the requirement of multiple PCR primers and reactions, the process may be time-consuming along the sequential steps, and unusual serotypes may remain undetected

even after a series of consecutive reactions (Leung et al., 2012; Zhou et al., 2022). Therefore, the sequetyping approach can be complementary as it is easy to perform and could detect a wide range of serotypes with a single amplification of the *cpsB* gene to fill up the gap left in the conventional multiplex approach (Leung et al., 2012). However, there are limitations to the *cpsB* gene amplifications in serotypes 25F, 37, 38, 39, and 43 as the *cpsB* gene is lacking, making these serotypes unidentifiable with this method (Leung et al., 2012; Mauffrey et al., 2017). To address this issue, additional measures, such as the Quellung and latex agglutination methods, need to be utilised to verify the likelihood of false-positive PCR outcomes since some serotypes cannot be entirely differentiated based solely on the *cps* sequence (Jin et al., 2016; Mauffrey et al., 2017).

Although sequetyping is easier and more convenient, it requires an additional step of sequencing, which incurs an additional cost but less PCR reaction compared to sequential cmPCR. Thus, in selective cases, a combination of *cpsB* sequetyping with sequential cmPCR can significantly increase the accuracy and effectiveness of serotyping and offer a financially viable alternative to the traditional agglutination-based serotyping for *S. pneumoniae* (Zhou et al., 2022). In addition, there has been a revolutionary advancement in whole genome sequencing (WGS) to generate comprehensive sequence data for a better-curated analysis of the possible serotype-related DNA sequences. With such data, the need for validation with the antisera test (Quellung) for certain serotypes that cannot be definitively differentiated from the *cps* sequences (Mauffrey et al., 2017) would probably not be necessary anymore. Nonetheless, WGS is still associated with high costs and requires bioinformatic expertise and digital platforms, which are only available in specialised and well-funded facilities.

CONCLUSION

This study showed that the *cpsB* gene sequetyping method might complement sequential cmPCR to discriminate further a range of serogroups such as 6A/B, 11A/D, 15A/F, and 15B/C. The combination of both would best suit the current need for surveillance until WGS becomes more affordable. As for the limitations pertaining to this study, we only investigated using *cpsB* sequetyping and sequential cmPCR, where the latter only targets 24 serotypes/serogroups of Asian prevalence due to limited resources. For a more meaningful validation, results should be verified by the gold standard: the Quellung technique or latex agglutination, especially for the NTs. The cmPCR requires more updated and extended serotype coverage with feasible primers-combinations that are doable in the sequential multiplex system. Meanwhile, this study and the associated discussion were based on culture steps prior to serotyping, where the strains have been propagated for purity with likely sufficient DNA for the downstream serotyping assay. In the case of direct DNA extraction from host samples,

cmPCR may not have sufficient sensitivity to amplify low DNA copy numbers, and the subsequent sequential multiplex PCR process will be a lot more challenging.

ACKNOWLEDGEMENTS

This work was supported by the Fundamental Research Grant Scheme (FRGS/1/2020/SKK0/UPM/02/10) of the Ministry of Higher Education Malaysia and the Research University Grant (GP-IPS/2022/9723900) of Universiti Putra Malaysia.

REFERENCES

Batt, S. L., Charalambous, B. M., McHugh, T. D., Martin, S., & Gillespie, S. H. (2005). Novel PCR-restriction fragment length polymorphism method for determining serotypes or serogroups of *Streptococcus pneumoniae* isolates. *Journal of Clinical Microbiology*, *43*(6), 2656–2661. https://doi.org/10.1128/JCM.43.6.2656-2661.2005

Centers for Disease Control and Prevention. (2021). *PCR-based methods for identification of* S. pneumoniae *serotypes/serogroups*. CDC. https://www.cdc.gov/streplab/pneumococcus/resources.html

Daningrat, W. O. D., Amalia, H., Ayu, I. M., Satzke, C., & Safari, D. (2022). Carriage of *Streptococcus pneumoniae* in children under five years of age prior to pneumococcal vaccine introduction in Southeast Asia: A systematic review and meta-analysis (2001–2019). *Journal of Microbiology, Immunology and Infection*, *55*(1), 6–17. https://doi.org/10.1016/j.jmii.2021.08.002

Dzaraly, N. D., Mohd Desa, M. N., Muthanna, A. R., Masri, S. N., Taib, N. M., Suhaili, Z., Sulaiman, N., Baharin, N. H. Z., Shuan, C. Y., Ariffin, Z., Rahman, N. I. A., Mohd Rani, F., Palanisamy, N. K., Soh, T. S. T., & Abdullah, F. H. (2021). Antimicrobial susceptibility, serotype distribution, virulence profile and molecular typing of piliated clinical isolates of pneumococci from east coast, Peninsular Malaysia. *Scientific Reports*, *11*, 8220. https://doi.org/10.1038/s41598-021-87428-z

Ganaie, F., Maruhn, K., Li, C., Porambo, R. J., Elverdal, P. L., Abeygunwardana, C., van der Linden, M., Duus, J. Ø., Sheppard, C. L., & Nahm, M. H. (2021). Structural, genetic, and serological elucidation of *Streptococcus pneumoniae* serogroup 24 serotypes: Discovery of a new serotype, 24C, with a variable capsule structure. *Journal of Clinical Microbiology*, *59*(7), e00540-21. https://doi.org/10.1128/JCM.00540-21

Ganaie, F., Saad, J. S., McGee, L., van Tonder, A. J., Bentley, S. D., Lo, S. W., Gladstone, R. A., Turner, P., Keenan, J. D., Breiman, R. F., & Nahm, M. H. (2020). A new pneumococcal capsule type, 10D, is the 100th serotype and has a large *cps* fragment from an oral streptococcus. *mBio*, *11*(3), e00937-20. https://doi.org/10.1128/mBio.00937-20

Jauneikaite, E., Jefferies, J. M., Hibberd, M. L., & Clarke, S. C. (2012). Prevalence of *Streptococcus pneumoniae* serotypes causing invasive and non-invasive disease in South East Asia: A review. *Vaccine*, *30*(24), 3503–3514. https://doi.org/10.1016/j.vaccine.2012.03.066

Jin, P., Wu, L., Oftadeh, S., Kudinha, T., Kong, F., & Zeng, Q. (2016). Using a practical molecular capsular serotype prediction strategy to investigate *Streptococcus pneumoniae* serotype distribution and antimicrobial resistance in Chinese local hospitalized children. *BMC Pediatrics*, *16*, 53. https://doi.org/10.1186/s12887-016-0589-7

Jin, P., Xiao, M., Kong, F., Oftadeh, S., Zhou, F., Liu, C., & Gilbert, G. L. (2009). Simple, accurate, serotype-specific PCR assay to differentiate *Streptococcus pneumoniae* serotypes 6A, 6B, and 6C. *Journal of Clinical Microbiology*,

47(8), 2470–2474. https://doi.org/10.1128/JCM.00484-09

Lawrence, E. R., Arias, C. A., Duke, B., Beste, D., Broughton, K., Efstratiou, A., George, R. C., & Hall, L. M. C. (2000). Evaluation of serotype prediction by *cpsA-cpsB* gene polymorphism in *Streptococcus pneumoniae*. *Journal of Clinical Microbiology*, *38*(4), 1319–1323. https://doi.org/10.1128/jcm.38.4.1319-1323.2000

Leung, M. H., Bryson, K., Freystatter, K., Pichon, B., Edwards, G., Charalambous, B. M., & Gillespie, S. H. (2012). Sequetyping: Serotyping *Streptococcus pneumoniae* by a single PCR sequencing strategy. *Journal of Clinical Microbiology*, *50*(7), 2419–2427. https://doi.org/10.1128/JCM.06384-11

Løchen, A., Croucher, N. J., & Anderson, R. M. (2020). Divergent serotype replacement trends and increasing diversity in pneumococcal disease in high income settings reduce the benefit of expanding vaccine valency. *Scientific Reports*, *10*, 18977. https://doi.org/10.1038/s41598-020-75691-5

Mauffrey, F., Fournier, É., Demczuk, W., Martin, I., Mulvey, M., Martineau, C., Lévesque, S., Bekal, S., Domingo, M.-C. C., Doualla-Bell, F., Longtin, J., & Lefebvre, B. (2017). Comparison of sequential multiplex PCR, sequetyping and whole genome sequencing for serotyping of *Streptococcus pneumoniae*. *PLOS One*, *12*(12), e0189163. https://doi.org/10.1371/journal.pone.0189163

Pai, R., Limor, J., & Beall, B. (2005). Use of pyrosequencing to differentiate *Streptococcus pneumoniae* serotypes 6A and 6B. *Journal of Clinical Microbiology*, *43*(9), 4820–4822. https://doi.org/10.1128/JCM.43.9.4820-4822.2005

Park, D., Kim, S. H., Bae, I. K., Kim, N. Y., Kook, J.-K., Park, Y.-H., & Shin, J. H. (2019). Evaluation of modified sequential multiplex PCR for *Streptococcus pneumoniae* serotyping. *Japanese Journal of Infectious Diseases*, *72*(4), 224–227. https://doi.org/10.7883/yoken.JJID.2018.422

Richter, S. S., Heilmann, K. P., Dohrn, C. L., Riahi, F., Diekema, D. J., & Doern, G. V. (2013). Evaluation of pneumococcal serotyping by multiplex PCR and quellung reactions. *Journal of Clinical Microbiology*, *51*(12), 4193–4195. https://doi.org/10.1128/JCM.01876-13

Seki, M., Yamashita, Y., Torigoe, H., Tsuda, H., Sato, S., & Maeno, M. (2005). Loop-mediated isothermal amplification method targeting the *lytA* gene for detection of *Streptococcus pneumoniae*. *Journal of Clinical Microbiology*, *43*(4), 1581-1586. https://doi.org/10.1128/jcm.43.4.1581-1586.2005

Shakrin, N. N. S. M., Balasubramaniam, S. D., Yusof, H. A., Mastuki, M. F., Masri, S. N., Taib, N. M., Nordin, S. A., Jamal, F., Clarke, S. C., & Desa, M. N. M. (2013). Evaluation of PCR-based approach for serotype determination of *Streptococcus pneumoniae*. *Tropical Biomedicine*, *30*(2), 338–344.

Shakrin, N. N. S. M., Masri, S. N., Taib, N. M., Nordin, S. A., Jamal, F., & Desa, M. N. M. (2014). Genotypic characterization of Malaysian human isolates of *Streptococcus pneumoniae* from carriage and clinical sources. *Comparative Immunology, Microbiology and Infectious Diseases*, 37(5–6), 347–354. https://doi.org/10.1016/j.cimid.2014.10.005

Sheppard, C. L., Harrison, T. G., Morris, R., Hogan, A., & George, R. C. (2004). Autolysin-targeted LightCycler assay including internal process control for detection of *Streptococcus pneumoniae* DNA in clinical samples. *Journal of Medical Microbiology*, *53*(3), 189–195. https://doi.org/10.1099/jmm.0.05460-0

Swarthout, T. D., Gori, A., Bar-Zeev, N., Kamng'ona, A. W., Mwalukomo, T. S., Bonomali, F., Nyirenda, R., Brown, C., Msefula, J., Everett, D., Mwansambo, C., Gould, K., Hinds, J.,

Heyderman, R. S., & French, N. (2021). Evaluation of pneumococcal serotyping of nasopharyngeal-carriage isolates by latex agglutination, whole-genome sequencing (PneumoCaT), and DNA microarray in a high-pneumococcal-carriage-prevalence population in Malawi. *Journal of Clinical Microbiology*, *59*(1), e02103-20. https://doi.org/10.1128/JCM.02103-20

Wahl, B., O'Brien, K. L., Greenbaum, A., Majumder, A., Liu, L., Chu, Y., Lukšić, I., Nair, H., McAllister, D. A., Campbell, H., Rudan, I., Black, R., & Knoll, M. D. (2018). Burden of *Streptococcus pneumoniae* and *Haemophilus influenzae* type b disease in children in the era of conjugate vaccines: Global, regional, and national estimates for 2000–15. *The Lancet Global Health*, *6*(7), e744–e757. https://doi.org/10.1016/S2214-109X(18)30247-X

Zhou, M.-L., Wang, Z.-R., Li, Y.-B., Kudinha, T., Wang, J., Wang, Y., Xiao, M., Xu, Y.-C., Liu, Z.-Y., & Hsueh, P.-R. (2022). Rapid identification of *Streptococcus pneumoniae* serotypes by *cpsB* gene-based sequetyping combined with multiplex PCR. *Journal of Microbiology, Immunology and Infection*, *55*(5), 870–879. https://doi.org/10.1016/j.jmii.2021.11.004

Pertanika J. Trop. Agric. Sci. 46 (4): 1245 - 1257 (2023)

PERTANIKA JOURNALS

TROPICAL AGRICULTURAL SCIENCE

Journal homepage: http://www.pertanika.upm.edu.my/

Genetic Variability and Antimicrobial Susceptibility Profile of *Mycoplasma gallisepticum* and Antimicrobial Susceptibility Profile of *Mycoplasma synoviae* Isolated from Various Bird Species in Peninsular Malaysia

Hossein Taiyari[1], Jalila Abu[1]*, Nik Mohd Faiz[1,3] and Zunita Zakaria[2,3]

[1]Department of Veterinary Clinical Studies, Faculty of Veterinary Medicine, Universiti Putra Malaysia, 43400 Serdang, Selangor, Malaysia
[2]Department of Veterinary Pathology and Microbiology, Faculty of Veterinary Medicine, Universiti Putra Malaysia, 43400 Serdang, Selangor, Malaysia
[3]Institute of Bioscience, Universiti Putra Malaysia, 43400 Serdang, Selangor, Malaysia

ABSTRACT

Mycoplasma gallisepticum (MG) and *M. synoviae* (MS) can infect many bird species. Susceptible species of birds are responsible for spillover infections from poultry to wild birds. In Malaysia, previous studies reported the detection of MG in free-flying birds, but there is a lack of information on the characterization and antimicrobial susceptibility profile of these isolates. Therefore, this study aims to molecular characterize and assess the minimum inhibitory concentration (MIC) of MG and MS isolated from different bird species, including aviary, free-flying, and pet birds. Altogether 54 choanal slit swab samples were collected. All the swab samples were subjected to isolation and polymerase chain reaction (PCR) detection. Positive samples were subjected to molecular characterization and MIC assay. Molecular characterization was done using targeted gene sequencing, and microdilution MIC assay was employed to determine the antimicrobial susceptibility profile of the isolates. Using both culture and PCR techniques, 5.6% (3/54) of the samples were positive for MG, while MS was detected in 29.6% (16/54) and 40.7% (22/54) of samples using culture and PCR, respectively. The partial sequence of the *mgc2* gene showed a distinct pattern of this gene in one of the MG isolates. Phylogenetic analysis of this isolate indicated that this isolate is a progeny of a Thailand poultry strain. Microdilution MIC assay indicated

ARTICLE INFO

Article history:
Received: 06 April 2023
Accepted: 19 June 2023
Published: 31 October 2023

DOI: https://doi.org/10.47836/pjtas.46.4.11

E-mail addresses:
hosseintaiyari@gmail.com (Hossein Taiyari)
jalila@upm.edu.my (Jalila Abu)
nikmdfaiz@upm.edu.my (Nik Mohd Faiz)
zunita@upm.edu.my (Zunita Zakaria)
* Corresponding author

ISSN: 1511-3701
e-ISSN: 2231-8542

100% resistance to erythromycin and chlortetracycline. The findings of this study indicate the possibility of avian interspecies transmission of MG and MS in Malaysia and the need for antimicrobial treatment dosage optimization.

Keywords: Bird species, microdilution, *Mycoplasma gallisepticum*, *Mycoplasma synoviae*, targeted gene sequencing

INTRODUCTION

Mycoplasma gallisepticum (MG) and *M. synoviae* (MS) are among the most significant mycoplasmal infections of birds (Friend, 1999; Luttrell & Fischer, 2007). Historically, MG and MS were thought to be host-specific and pathogenic bacteria primarily for poultry species (Raviv & Ley, 2013). However, the identification of MG as the causative agent of conjunctivitis outbreak in house finch (*Haemorhous mexicanus*) gave a new perspective on the pathogenicity of MG (Taiyari & Abu, 2020). The MG infection in house finch spread rapidly, and throughout its expansion, host jump events were reported among other passerine species (Dhondt et al., 2014). *Mycoplasma gallisepticum* was also reported to cause an outbreak in the wild turkey population (Davidson et al., 1982). Apart from wild turkey and house finch, MG and MS have been isolated from several species of free-ranging birds including pheasants, chukar partridge, grey partridge, peafowl, Bobwhite quail, Japanese quail, ducks, geese, yellow-naped Amazon parrot, greater flamingos, American goldfinches, pine grosbeaks, evening grosbeaks, purple finch, blue jay, pigeon, and red-legged partridge (Ferguson-Noel & Noormohammadi, 2013; Raviv & Ley, 2013). Identifying new natural hosts plays a crucial role in comprehending transmission routes and carriers of these important pathogens. From the past to the present, MG and MS infections have occurred in high numbers among poultry farms in Malaysia (Yasmin et al., 2014). A previous study in Malaysia detected MG in crows by polymerase chain reaction (PCR) (Ganapathy et al., 2007). It indicates the possible role of free-flying birds in the circulation and transmission of MG in Malaysia.

MG and MS infections are detected via culture, serological, and molecular techniques. The culture technique includes the isolation and subsequent identification step using immunofluorescence staining. Although the culture technique is laborious and time-consuming, its capability to identify all mycoplasma species with high specificity is still paramount (Levisohn & Kleven, 2000). PCR offers a rapid and convenient diagnosis of pathogenic mycoplasmas. However, few studies reported the false diagnosis of MG by PCR (Ganapathy & Bradbury, 1999; Kempf et al., 1997). The products of PCR can be used for genotyping and phylogenetic analysis of the isolates. Gene-targeted sequencing (GTS) is a reproducible typing method with satisfactory discriminatory power to separate the isolates (Ferguson et al., 2005). The *mgc2* gene of MG is responsible for encoding major surface proteins with pathogenic, antigenic, and immune evasion properties (Markham et al., 1993). Since different strains of MG have varied sizes of

the *mgc2* gene and only a single copy of this gene can be found in the MG genome, this gene was selected for genotyping of isolates in this study (Bencina, 2002).

Good biosecurity and consistent monitoring programs allow the poultry industry to control and prevent mycoplasmosis. Although these preventive programs have been successful in some aspects, the complete control of avian mycoplasmosis seems difficult due to large poultry populations, multi-age flocks, and unidentified reservoirs (Kleven, 2008). In addition, studies have shown that MG can survive in the environment longer than was previously assumed (Shah-Majid, 1988). This finding adds to the difficulties of controlling mycoplasmosis. Antibiotic treatment may be very beneficial and effective in reducing clinical signs and disease transmission, but the long-term use of antimicrobial agents may develop resistance (Reinhardt et al., 2005). Therefore, although antibiotic medications could prevent economic losses related to avian mycoplasmosis, these prevention programs should be considered for short periods (Kleven, 2008). Macrolides tend to be effective against avian mycoplasmosis (Kleven, 2008). Macrolides such as tylosin and erythromycin are Malaysia's first antibiotic therapy choice against mycoplasmosis. However, there is a lack of information on the antimicrobial minimum inhibitory concentration (MIC) of Malaysian MG and MS isolates. The guideline to conduct MIC tests for pathogenic avian mycoplasmas was described by Hannan (2000).

Therefore, this study aims to investigate the sustainability of MG and MS infections in non-poultry birds by characterizing the field isolates using molecular techniques and determining antimicrobial susceptibility profiles.

METHODS

Samples Descriptives

A total of 54 choanal slit swab samples were collected from various species of birds without clinical signs of avian mycoplasmosis. Some of these birds were kept as aviary birds on an ornamental farm. Aviary birds were inclusive of jungle fowl, guinea fowl, and peacock. The other group of birds was free-flying, including raptors and non-raptor species. Non-raptor species were caught using a mist net at an ornamental bird farm in Selangor, Malaysia. Pigeons and spotted doves were the non-raptor species. The public donated raptors to the University Veterinary Hospital (UVH) for rehabilitation. Barn owls, Asian brown wood owls, crested serpent eagles, and buffy fish owls were the raptor species. The rest of the birds were pet birds that were admitted to UVH. Budgerigar and mynah were the pet species. Descriptive of different bird categories are presented in Table 1. This study was approved by the Institutional Animal Care and Use Committee (IACUC) (UPM/IACUC/AUP-R069/2019).

Capture of Free-flying Birds

Free-flying birds were captured at the ornamental farm's site. Briefly, a mist net was set up and placed between the trees for six hours, which was done in the morning. Every twenty minutes, the trap was checked

Table 1
Descriptive of different bird categories

Category	Species of bird	No.
Aviary birds	Jungle fowl (*Gallus gallus*)	30
	Peafowl (*Pavo cristatus*)	3
	Guineafowl (*Numida meleagris*)	6
Free flying birds	Pigeon (*Columba livia domestica*)	5
	Spotted dove (*Spilopelia chinensis*)	2
	Barn owl (*Tyto alba*)	1
	Asian brown wood owl (*Strix leptogrammica*)	1
	Crested serpent eagle (*Spilornis cheela*)	1
	Buffy fish owl (*Ketupa ketupu*)	1
Pet birds	Budgerigar (*Melopsittacus undulatus*)	2
	Common myna (*Acridotheres tristis*)	2

for the presence of any bird. The trapped birds were restrained properly (Bailey, 2016) and subjected to sample collection.

Isolation Technique

Frey medium with 15% swine serum (FMS) (Merck, Germany) was prepared according to the literature (Ferguson-Noel & Kleven, 2016). A cotton swab with a plastic shaft was pre-wet with FMS prior to sample collection. Once the sample was collected for each bird, the swabs were kept inside individual FMS bottles and transported to the laboratory inside a cool box within 24 hr. Upon arrival at the laboratory, the bottles were incubated at 36°C. After 24 hr of incubation, broth cultures were subjected to FMS agar inoculation and PCR. Agar plates were incubated at 36°C under carbon dioxide (CO_2) conditions by putting them inside candle jars. Frey medium with 15% FMS agar inoculation was repeated for each sample when the broth cultures showed a color change from red to orange/yellow. Plates were monitored every three days under a stereo microscope for any sign of mycoplasma colonies.

According to the literature, the mycoplasma colonies were identified using immunofluorescence assay (IFA) (Ferguson-Noel & Kleven, 2016). A block of agar (0.5 cm × 0.5 cm) containing mycoplasma colonies was cut from each sample and subjected to IFA. For identification of MG colonies, a high-tittered MG-specific rabbit polyclonal antibody (IgG) conjugated with Alexa fluor 488 (Bioss Antibodies, USA [diluted with phosphate-buffered saline (PBS) 1:200]) was used in direct IFA. An indirect immunofluorescence technique was used to identify MS colonies (Ferguson-Noel & Kleven, 2016). This technique requires a specific primary antibody with the ability to detect MS. In addition, there should be a secondary antibody conjugated with fluorescein and capable of attaching to the primary antibody. This study used a diluted MS-specific chicken

polyclonal antibody (IgY) as the primary antibody (Abcam, United Kingdom). For the secondary antibody, goat anti-chicken IgY conjugated with phycoerythrin (PE) (Abcam, United Kingdom) was used. Stained agar blocks were observed under a fluorescent microscope.

DNA Extraction

For molecular detection, twenty-four hours after incubation of the samples, 1 ml of the initial broth cultures was pipetted into a 1.5 ml tube and subjected to the DNA extraction process using QIAamp DNA Mini Kit (Qiagen, USA) according to the manufacturer's recommendations. Briefly, 20 µl of proteinase K and 200 µl of AL buffer were added to the plaque, and then the mixture was vortexed for about 20 s to detach the plaque from the bottom of the tube. After that, the tube was incubated at 56°C for 1 hr. The tube was vortexed several times during the incubation period. After the incubation, 200 µl of 99% alcohol (Labchem, Malaysia) was added to the tube and vortexed for about 20 s. The entire tube contents were transferred to a spin column and then centrifuged at 6,000 × *g* for 1 min. The collection tube was discarded, and the spin column was placed on a new collection tube. About 500 µl of buffer AW1 was added to the spin column and centrifuged at 6,000 × *g* for 1 min. The collection tube was discarded, and the spin column was placed on a new collection tube. Approximately 500 µl of buffer AW2 was added to the spin column and centrifuged at 20,000 × *g* for 5 min. After discarding the collection tube, the spin column was placed on a 1.5 ml tube. Finally, 100 µl of buffer AE was added to the spin column, incubated at room temperature for 3 min, and centrifuged at 6,000 × *g* for 1 min to elute the DNA.

Polymerase Chain Reaction (PCR)

Universal 16S rRNA primers were used to detect MG and MS in multiplex PCR assay (Ferguson-Noel & Kleven, 2016; Moscoso et al., 2004; Nicholas & Baker, 1998). Two sets of primers targeting 16S rRNA gene of MG (MG-16S rRNA F:5′-GAC CTA ATC TGT AAA GTT GGT C-3′; MG-16S rRNA R:5′-GCT TCC TTG CGG TTA GCA AC-3′) and MS (MS-16S rRNA F:5' -GAG AAG CAA AAT AGT GAT ATC A-3'; MS-16S rRNA R:5' -CAG TCG TCT CCG AAG TTA ACA A- 3') were used. The reaction solution was prepared at 25 µl. Initial denaturation was at 94°C for 5 min, followed by 35 cycles of 94°C for 30 s, 55°C for 30 s, and 72°C for 30 s. A final extension was performed at 72°C for 5 min. Notably, ATCC 19610 and ATCC 25204 were positive controls in gel electrophoresis to detect MG and MS isolates, respectively.

Phylogenetic Analysis

Molecular characterization was done by targeting the partial sequence of the MG *mgc2* gene (Moscoso et al., 2004). Positive MG colonies were subjected to DNA extraction using QIAamp DNA Mini Kit (Qiagen, USA). The DNA extracts were then subjected to PCR assay for the MG *mgc2* gene. Initial denaturation was at 94°C for 5 min, followed by 35 cycles of

94°C for 30 s, 58°C for 30 s, and 72°C for 60 s, and final extension was performed at 72°C for 5 min. The PCR products were observed by gel electrophoresis. Samples that showed distinguished *mgc2* band size compared to the MG positive control were selected for targeted sequencing. Using CLUSTALW, the sequences of the isolates and positive controls were aligned. Percentage differences among sequences were calculated, and then a phylogenetic tree was constructed using MEGA7.

Antimicrobial Susceptibility Profile

The antimicrobial susceptibility profile of the isolates was determined according to Hannan (2000) as well as Tanner and Wu (1992). The antibiotics used in this study were inclusive of tilmicosin, tiamulin, enrofloxacin, doxycycline, erythromycin, lincomycin, chlortetracycline, tylvalosin, and tylosin. After preparing pure cultures, viable counting was performed to achieve the 10^4 color-changing units inoculum size of MG and MS isolates. Briefly, 10-fold serial dilutions of the stock cultures were made. From each serial dilution, 100 µl was pipetted in 100 µl of FMS in a 96-well plate (viable counting plate). The viable counting plate was incubated at 37ºC with the positive control tube containing one ml of stock culture and 9 ml of sterile FMS. The viable counting plate was monitored for color change three times per day. Once the 10^{-3} well of viable counting plate changed color from red to orange, the positive control tube of the same stock culture was subjected to MIC plate inoculation. After inoculating 100 µl of positive control into each MIC plate well, the MIC plate was incubated at 37ºC. A schematic view of the MIC plate is shown in Figure 1. The MIC plates were monitored

SENSITITRE
CMP1VEAH
Veterinary Reference Card

	1	2	3	4	5	6	7	8	9	10	11	12
A	TIL 0.06	TIL 0.12	TIL 0.25	TIL 0.5	TIL 1	TIL 2	TIL 4	TIL 8	TIL 16	TIL 32	TIL 64	TIL 128
B	TIA 0.015	TIA 0.03	TIA 0.06	TIA 0.12	TIA 0.25	TIA 0.5	TIA 1	TIA 2	TIA 4	TIA 8	TIA 16	TIA 32
C	ENRO 0.03	ENRO 0.06	ENRO 0.12	ENRO 0.25	ENRO 0.5	ENRO 1	ENRO 2	ENRO 4	ENRO 8	ENRO 16	ENRO 32	DOX 0.06
D	DOX 0.12	DOX 0.25	DOX 0.5	DOX 1	DOX 2	DOX 4	DOX 8	DOX 16	ERY 0.12	ERY 0.25	ERY 0.5	ERY 1
E	ERY 2	ERY 4	ERY 8	ERY 16	ERY 32	ERY 64	LIN 0.12	LIN 0.25	LIN 0.5	LIN 1	LIN 2	LIN 4
F	LIN 8	LIN 16	LIN 32	CTET 0.25	CTET 0.5	CTET 1	CTET 2	CTET 4	CTET 8	CTET 16	TVN 0.015	TVN 0.03
G	TVN 0.06	TVN 0.12	TVN 0.25	TVN 0.5	TVN 1	TVN 2	TVN 4	TVN 8	TVN 16	TVN 32	TVN 64	TVN 128
H	TYLT 0.06	TYLT 0.12	TYLT 0.25	TYLT 0.5	TYLT 1	TYLT 2	TYLT 4	TYLT 8	TYLT 16	TYLT 32	TYLT 64	POS

Figure 1. Schematic view of the customized sensititre plate used in this study (numbers inside each well indicate the antibiotic concentration in µg per ml)
Note. TIL = Tilmicosin; TIA = Tiamulin; ENRO = Enrofloxacin; DOX = Doxycycline; ERY = Erythromycin; LIN = Lincomycin; CTET = Chlortetracycline; TVN = Tylvalosin; TYLT = Tylosin; POS = Positive control

three times per day. Once the positive well of the MIC plate changed color from red/orange to yellow, the MIC plates were taken out from the incubator, and the initial MIC was recorded.

RESULTS

Detection of *M. gallisepticum* and *M. synoviae*

In the samples collected from aviary birds, MG was detected in 7% (3/41) of samples using both culture and PCR techniques. In aviary birds, 44% (18/41) and 32% (13/41) of samples had MS using PCR and culture, respectively.

In free-flying birds, 27% (3/11) and 36% (4/11) of the samples were positive for MS by culture and PCR, respectively. No MG was detected in the samples of free-flying birds. No MG and MS were detected in pet bird samples. Figure 2 demonstrates the multiplex PCR agarose gel result indicating the detection of MG and MS in some PCR products.

Phylogenetic Analysis of Isolates

After amplifying the *mgc2* gene using the strain-specific primers, the PCR product was sent for purification and gene-targeted sequencing. Figure 3 shows the gel electrophoresis result of the MG isolate PCR product using *mgc2* strain-specific primers. A total of 3 MG isolates were made in this study, but only one of them, which was isolated from a jungle fowl (accession number: ON645899), showed different *mgc2* band sizes in comparison to the positive control. The sequencing coverage of this gene was 269 bp. This sequencing coverage was used to construct a phylogenetic tree.

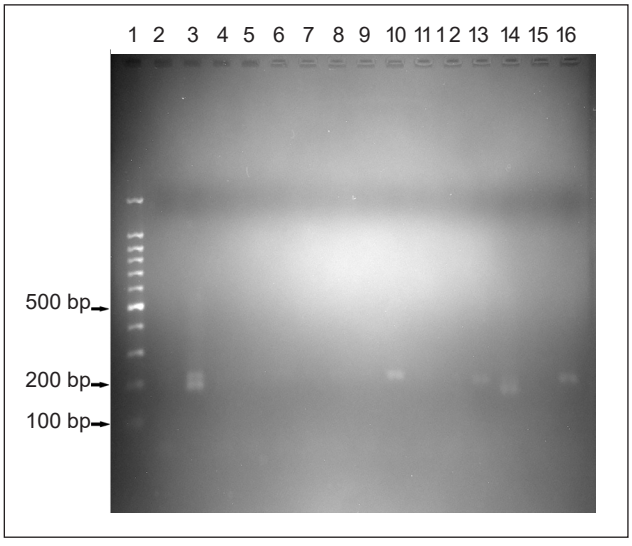

Figure 2. Multiplex polymerase chain reaction (PCR) agarose gel results indicating the detection of *Mycoplasma gallisepticum* and *M. synoviae* in some PCR products
Note. Lane 1 = 100 bp ladder; Lane 2 = Negative control; Lane 3 = Positive control; Lane 4-16 = Field samples

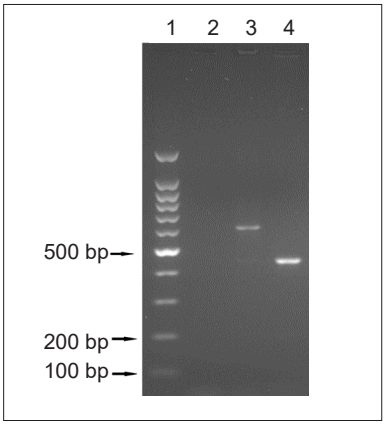

Figure 3. Gel electrophoresis result of the *Mycoplasma gallisepticum* isolates polymerase chain reaction product using *mgc2* strain-specific primers
Note. Lane 1 = 100 bp ladder; Lane 2 = Negative control; Lane 3 = Positive control; Lane 4 = Field isolate. The estimated product size for *the mgc2* gene of the field sample was 450 bp

Phylogenetic analysis of the partial sequence of this gene was done by constructing the neighbor-joining tree (Figure 4). According to this tree, the MG field isolate was found to be a progeny of a Thailand poultry strain (accession number: KX268616.1), although its *mgc2* pattern was not identical to other reference and international field isolates. Table 2 shows a list of isolates used to construct the phylogenetic analysis.

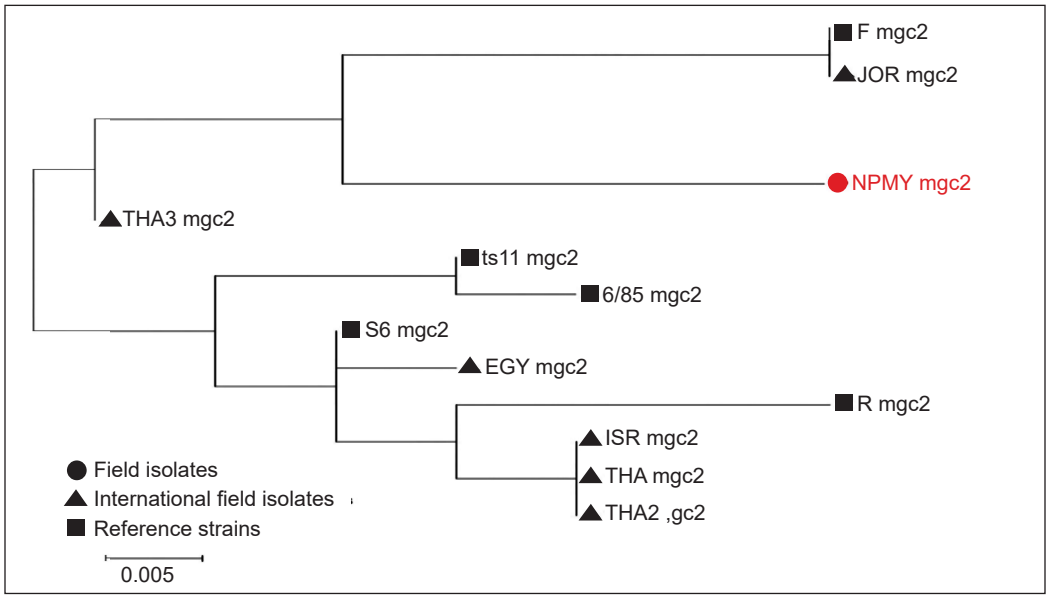

Figure 4. Phylogenetic tree of the *Mycoplasma gallisepticum* local strain (NPMY), international field isolates, and reference strains constructed based on *mgc2* partial gene sequence using the neighbor-joining algorithm. The country of origin of the international field isolates are shown as Egypt (EGY), Israel (ISR), Jordan (JOR), and Thailand (THA), respectively

Table 2
The isolates used in the phylogenetic analysis

Isolate name	Source	Country	Accession number
MG F	Reference strain		AY556230.1
MG JOR	Chicken	Jordan	HQ143379.1
MG NPMY	Jungle fowl	Malaysia	ON645899
MG THA	Chicken	Thailand	KX268618.1
MG THA2	Chicken	Thailand	KX268630.1
MG THA3	Chicken	Thailand	KX268617.1
MG ts-11	Reference strain		AY556232.1
MG 6/85	Reference strain		JQ770178.1
MG S6	Chicken	Thailand	KX268634
MG EGY	Chicken	Egypt	MW679029.1
MG R	Reference strain		AY556228.1
MG ISR	Chicken	Israel	HQ143377.1

Antimicrobial Minimum Inhibitory Concentration (MIC)

The antimicrobial MIC values of the MG PG31 reference strain were determined and compared to previous studies to optimize and validate the microdilution MIC protocol. Due to the failure to purify other isolate cultures, only three field isolates, including one MG isolate and two MS isolates, were successfully subjected to microdilution MIC. Results showed that all three isolates were resistant to erythromycin and chlortetracycline. The MIC values and the susceptibility profile of the isolates are shown in Table 3. The MG field isolates and one of the MS field isolates showed a multidrug-resistant (MDR) antimicrobial susceptibility profile.

DISCUSSION

This study aims to screen for the occurrence of MG and MS among various species of birds in Malaysia. Although the presence of MG among free-flying birds was detected by PCR in previous studies (Ganapathy et al., 2007), this study reported the isolation of MG and MS along with molecular characterization and determination of the antimicrobial susceptibility profile of the isolates. Most of the MG and MS isolates were collected from jungle fowl samples, indicating these microorganisms' affinity to fowl species. No MG was isolated from free-flying birds, although many free-flying culture samples showed mycoplasma colonies. It might be due to the overgrowth of commensal mycoplasmas inhibiting the growth of slow-growing MG (Bradbury, 2002; Ley, 2003). Isolation of MS from the free-flying birds' samples can indicate the significant role of free-flying birds in the circulation of avian mycoplasmosis. This finding is consistent with previous studies in which MS was detected in samples collected from pigeons (Benčina et al., 1987; Reece et al., 1986). Therefore, further studies investigating the phylogenetic analysis of MS isolated from free-flying birds are strongly suggested.

Molecular characterization of the field isolates indicated the presence of an MG field strain with a distinguished pattern of

Table 3
Antimicrobial minimum inhibitory concentration (MIC) values of Mycoplasma gallisepticum *(MG) and* M. synoviae (*MS) field isolates and reference strain*

Strain	MIC (μg/ml)								
	TIL	TIA	ENRO	DOX	ERY	LIN	CTET	TVN	TYLT
MG PG31	≤0.06	≤0.015	≤0.03	0.12	≤0.12	8	2	0.03	≤0.06
MG NPMY	≤0.06	0.06	2	0.5	64	0.5	8	0.03	0.12
MS NPMY1	≤0.06	0.25	0.25	0.25	64	2	8	0.12	0.25
MS NPMY2	32	1	32	0.5	64	4	8	0.25	4

Note. MG PG31 = Reference strain; MG NPMY = Local strain (isolated from aviary birds); MS NPMY1 = Local strain (isolated from free-flying birds); MS NPMY2 = Local strain (isolated from aviary birds); TIL = Tilmicosin; TIA = Tiamulin; ENRO = Enrofloxacin; DOX = Doxycycline; ERY = Erythromycin; LIN = Lincomycin; CTET = Chlortetracycline; TVN = Tylvalosin; TYLT = Tylosin

the *mgc2* gene. Phylogenetic analysis of this field strain showed that it is a progeny of a chicken MG field strain isolated in Thailand. This finding indicated the possible role of various bird species in the sustainability of avian mycoplasmosis by the occurrence of spillover infections between chicken and jungle fowl. It is consistent with a previous study indicating the strong possibility of spillover infection when the two species of birds belong to the same family (Dhondt et al., 2008; Farmer et al., 2005).

The antimicrobial susceptibility profile of the isolates was determined using microdilution MIC. The MIC values of the MG PG31 reference strain were compared to previous studies to validate the MIC assay. A consistent result was observed in the MIC value of the PG31 reference strain (Elbehiry et al., 2016; Gerchman et al., 2011, 2008; Khatoon et al., 2018; Li et al., 2010). Three field isolates, including one MG and two MS field isolates, were successfully subjected to the microdilution MIC assay. Failure to purify the isolates was the limit to success in determining the antimicrobial susceptibility profile of other isolates.

Considering the free-living nature of the study population and the MDR antimicrobial susceptibility profile of the isolates, these field strains may be transmitted from poultry, especially the MG isolated from jungle fowl. All the isolates showed resistance to erythromycin. This finding is consistent with previous studies that reported the resistance of MG field isolates to erythromycin (Bradbury et al., 1994; Taiyari et al., 2021; Tanner & Wu, 1992). The results of the microdilution MIC assay indicated resistance to enrofloxacin, lincomycin, chlortetracycline, and tylosin. These results agree with the increasing resistance of avian mycoplasmas against tetracyclines (Hannan et al., 1997), macrolides (Bradbury et al., 1994), and quinolones (Gerchman et al., 2011). However, tylosin, enrofloxacin, and tetracyclines are the most used and highly effective antimicrobial agents to control mycoplasmosis in poultry (Kleven, 2008). Enrofloxacin was less effective in treating MS infections in poultry (Stanley et al., 2001). In this study, one of the MS isolates was susceptible to enrofloxacin. It may be indicative of isolates that have not been transmitted from poultry.

CONCLUSION

This study investigated the role of non-poultry birds in the circulation of MG and MS in Malaysia. The culture and PCR results showed that MG and MS infections occur in the aviary and free-flying birds. Targeted gene sequencing of the isolates showed no identical pattern between the MG isolate and reference poultry strains used in this study. However, the phylogenetic analysis of the MG isolate showed that this isolate is a progeny of a poultry strain. The exposure of non-poultry birds to MDR, MG, and MS isolates might be another indication of the possible role of these birds in the circulation of disease. Unfortunately, this study could only evaluate 54 samples collected from different bird species in the Selangor state

of Malaysia. This caveat makes it difficult to draw a firm conclusion on this topic. However, results point out the possibility of MG and MS spillover infections. Therefore, constant surveillance is needed to identify MG and MS types isolated from non-poultry birds.

ACKNOWLEDGEMENTS

The study was supported by the Institute of Biosciences, Higher Institution Centre of Excellence (JBS HICoE) Grant No. 6369101 from the Ministry of Higher Education (MOHE), Government of Malaysia.

REFERENCES

Bailey, T. A. (2016). Capture and handling. In J. Samour (Ed.), *Avian medicine* (3rd ed., pp. 36–48). Mosby Ltd. https://doi.org/10.1016/B978-0-7234-3832-8.00004-3

Bencina, D. (2002). Haemagglutinins of pathogenic avian mycoplasmas. *Avian Pathology*, *31*(6), 535–547. https://doi.org/10.1080/0307945021000024526

Benčina, D., Dorrer, D., & Tadina, T. (1987). *Mycoplasma* species isolated from six avian species. *Avian Pathology*, *16*(4), 653-664. https://doi.org/10.1080/03079458708436413

Bradbury, J. M. (2002). Avian mycoplasmas. In F. T. W. Jordan, M. Alexander D. Pattison, & T. Faragher (Eds.), *Poultry diseases* (pp.178-193). Saunders.

Bradbury, J. M., Yavari, C. A., & Giles, C. J. (1994). *In vitro* evaluation of various antimicrobials against *Mycoplasma gallisepticum* and *Mycoplasma synoviae* by the micro-broth method, and comparison with a commercially-prepared test system. *Avian Pathology*, *23*(1), 105-115. https://doi.org/10.1080/03079459408418978

Davidson, W. R., Nettles, V. F., Couvillion, C. E., & Yoder Jr., H. W. (1982). Infectious sinusitis in wild turkeys. *Avian Diseases*, *26*(2), 402-405. https://doi.org/10.2307/1590112

Dhondt, A. A., DeCoste, J. C., Ley, D. H., & Hochachka, W. M. (2014). Diverse wild bird host range of *Mycoplasma gallisepticum* in Eastern North America. *PLOS One*, *9*(7), e103553. https://doi.org/10.1371/journal.pone.0103553

Dhondt, A. A., Dhondt, K. V., & McCleery, B. V. (2008). Comparative infectiousness of three passerine bird species after experimental inoculation with *Mycoplasma gallisepticum*. *Avian Pathology*, *37*(6), 635-640. https://doi.org/10.1080/03079450802499100

Elbehiry, A., Al-Dubaib, M., & Marzouk, E. (2016). Serological, rapid molecular characterization and antibiotic resistance for field isolates of *Mycoplasma gallisepticum* in chicken in Saudi Arabia. *Alexandria Journal for Veterinary Sciences*, *49*(2), 70-79. https://doi.org/10.5455/ajvs.224786

Farmer, K. L., Hill, G. E., & Roberts, S. R. (2005). Susceptibility of wild songbirds to the house finch strain of *Mycoplasma gallisepticum*. *Journal of Wildlife Diseases*, *41*(2), 317-325. https://doi.org/10.7589/0090-3558-41.2.317

Ferguson, N. M., Hepp, D., Sun, S., Ikuta, N., Levisohn, S., Kleven, S. H., & García, M. (2005). Use of molecular diversity of *Mycoplasma gallisepticum* by gene-targeted sequencing (GTS) and random amplified polymorphic DNA (RAPD) analysis for epidemiological studies. *Microbiology*, *151*(6), 1883-1893. https://doi.org/10.1099/mic.0.27642-0

Ferguson-Noel, N., & Kleven, S. H. (2016). *Mycoplasma* species. In S. M. Williams, L. Dufour-Zavala, M. W. Jackwood, M. D. Lee, B. Lupiani, W. M. Reed, E. Spackman, & P. R. Woolcock (Eds.), *A laboratory manual for the isolation, identification, and characterization*

of avian pathogens (pp. 63-70). American Association of Avian Pathologists.

Ferguson-Noel, N., & Noormohammadi, A. H. (2013). *Mycoplasma synoviae* infection. In D. E. Swayne, J. R. Glisson, L. R. McDougald, L. K. Nolan, D. L. Suarez, & V. L. Nair (Eds.), *Diseases of poultry* (pp. 875–943). Iowa State University Press.

Friend, M. (1999). Mycoplasmosis. In M. Friend & J. C. Franson (Eds.), *Field manual of wildlife diseases: General field procedures and diseases of birds* (pp.115–119). United States Geological Survey Publication.

Ganapathy, K., & Bradbury, J. M. (1999). Pathogenicity of *Mycoplasma imitans* in mixed infection with infectious bronchitis virus in chickens. *Avian Pathology*, *28*(3), 229-237. https://doi.org/10.1080/03079459994713

Ganapathy, K., Saleha, A. A., Jaganathan, M., Tan, C. G., Chong, C. T., Tang, S. C., Ideris, A., Dare, C. M., & Bradbury, J. M. (2007). Survey of *Campylobacter*, *Salmonella* and mycoplasmas in house crows (*Corvus splendens*) in Malaysia. *Veterinary Record*, *160*(18), 622-624. https://doi.org/10.1136/vr.160.18.622

Gerchman, I., Levisohn, S., Mikula, I., Manso-Silván, L., & Lysnyansky, I. (2011). Characterization of *in vivo*-acquired resistance to macrolides of *Mycoplasma gallisepticum* strains isolated from poultry. *Veterinary Research*, *42*(1), 90. https://doi.org/10.1186/1297-9716-42-90

Gerchman, I., Lysnyansky, I., Perk, S., & Levisohn, S. (2008). *In vitro* susceptibilities to fluoroquinolones in current and archived *Mycoplasma gallisepticum* and *Mycoplasma synoviae* isolates from meat-type turkeys. *Veterinary Microbiology*, *131*(3-4), 266-276. https://doi.org/10.1016/j.vetmic.2008.04.006

Hannan, P. C. T. (2000). Guidelines and recommendations for antimicrobial minimum inhibitory concentration (MIC) testing against veterinary mycoplasma species. *Veterinary Research*, *31*(4), 373-395. https://doi.org/10.1051/vetres:2000100

Hannan, P. C., Windsor, G. D., de Jong, A., Schmeer, N., & Stegemann, M. (1997). Comparative susceptibilities of various animal-pathogenic mycoplasmas to fluoroquinolones. *Antimicrobial Agents and Chemotherapy*, *41*(9), 2037-2040. https://doi.org/10.1128/AAC.41.9.2037

Kempf, I., Gesbert, F., & Guittet, M. (1997). Experimental infection of chickens with an atypical *Mycoplasma gallisepticum* strain: Comparison of diagnostic methods. *Research in Veterinary Science*, *63*(3), 211-213. https://doi.org/10.1016/S0034-5288(97)90022-9

Khatoon, H., Afzal, F., Tahir, M. F., Hussain, M., & Khan, S. U. (2018). Prevalence of mycoplasmosis and antibiotic susceptibility of *Mycoplasma gallisepticum* in commercial chicken flocks of Rawalpindi division, Pakistan. *Pakistan Veterinary Journal*, *38*(4), 446-448. https://doi.org/10.29261/pakvetj/2018.081

Kleven, S. H. (2008). Control of avian *Mycoplasma* infections in commercial poultry. *Avian Diseases*, *52*(3), 367-374. https://doi.org/10.1637/8323-041808-Review.1

Levisohn, S., & Kleven, S. H. (2000). Avian mycoplasmosis (*Mycoplasma gallisepticum*). *Revue Scientifique et Technique*, *19*(2), 425-442. https://doi.org/10.20506/rst.19.2.1232

Ley, D. H. (2003). *Mycoplasma gallisepticum* infection. In Y. M. Saif, H. J. Barnes, J. R. Glisson, A. M. Fadly, L. R. McDougald, & D. E. Swayne (Eds.), *Diseases of poultry* (pp. 722-744). Iowa State University Press.

Li, B.-B., Shen, J.-Z., Cao, X.-Y., Wang, Y., Dai, L., Huang, S.-Y., & Wu, C.-M. (2010). Mutations in 23S rRNA gene associated with decreased susceptibility to tiamulin and valnemulin in *Mycoplasma gallisepticum*. *FEMS Microbiology*

Letters, *308*(2), 144-149. https://doi.org/10.1111/j.1574-6968.2010.02003.x

Luttrell, P., & Fischer, J. R. (2007). Mycoplasmosis. In N. J. Thomas, D. B. Hunter, & C. T. Atkinson (Eds.), *Infectious diseases of wild birds* (pp. 317-331). Blackwell Publishing. https://doi.org/10.1002/9780470344668.ch16

Markham, P. F., Glew, M. D., Whithear, K. G., & Walker, I. D. (1993). Molecular cloning of a member of the gene family that encodes pMGA, a hemagglutinin of *Mycoplasma gallisepticum*. *Infection and Immunity*, *61*(3), 903-909. https://doi.org/10.1128/iai.61.3.903-909.1993

Moscoso, H., Thayer, S. G., Hofacre, C. L., & Kleven, S. H. (2004). Inactivation, storage, and PCR detection of mycoplasma on FTA® filter paper. *Avian Diseases*, *48*(4), 841-850. https://doi.org/10.1637/7215-060104

Nicholas, R., & Baker, S. (1998). Recovery of mycoplasma from birds. In R. Miles & R. Nicholas (Eds.), Mycoplasma *protocols: Methods in molecular biology*™ (Vol. 104, pp. 37-43). Humana Press. https://doi.org/10.1385/0-89603-525-5:37

Raviv, Z., & Ley, D. H. (2013). *Mycoplasma gallisepticum* infection. In D. E. Swayne, J. R. Glisson, L. R. McDougald, L. K. Nolan, D. L. Suarez, & V. L. Nair (Eds.), *Diseases of poultry* (pp. 877– 893). Wiley-Blackwell.

Reece, R. L., Ireland, L., & Scott, P. C. (1986). Mycoplasmosis in racing pigeons. *Australian Veterinary Journal*, *63*(5), 166–167. https://doi.org/10.1111/j.1751-0813.1986.tb02962.x

Reinhardt, A. K., Gautier-Bouchardon A. V., Gicquel-Bruneau M, Kobisch M, & Kempf I. (2005). Persistence of *Mycoplasma gallisepticum* in chickens after treatment with enrofloxacin without development of resistance. *Veterinary Microbiology*, *106*(1-2), 129-137. https://doi.org/10.1016/j.vetmic.2004.11.016

Shah-Majid, M. (1988). Survival and isolation of avian mycoplasmas from drinking water of infected chickens. *Pertanika*, *11*(3), 483-485.

Stanley, W. A., Hofacre, C. L., Speksnijder, G., Kleven, S. H., & Aggrey, S. E. (2001). Monitoring *Mycoplasma gallisepticum* and *Mycoplasma synoviae* infection in breeder chickens after treatment with enrofloxacin. *Avian Diseases*, *45*(2), 534-539. https://doi.org/10.2307/1593001

Taiyari, H., & Abu, J. (2020). House finch-associated *Mycoplasma gallisepticum* responsible for epizootic conjunctivitis in passerines. *Pertanika Journal of Tropical Agricultural Science*, *43*(1), 19-34.

Taiyari, H., Faiz, N. M., Abu, J., & Zakaria, Z. (2021). Antimicrobial minimum inhibitory concentration of *Mycoplasma gallisepticum*: A systematic review. *Journal of Applied Poultry Research*, *30*(2), 100160. https://doi.org/10.1016/j.japr.2021.100160

Tanner, A. C., & Wu, C.-C. (1992). Adaptation of the Sensititre® broth microdilution technique to antimicrobial susceptibility testing of *Mycoplasma gallisepticum*. *Avian Diseases*, *36*(3), 714-717. https://doi.org/10.2307/1591770

Yasmin, F., Ideris, A., Omar, A. R., Hair-Bejo, M., Tan, S. W., Tan, C. G., & Ahmad, K. (2014). Molecular detection of *Mycoplasma gallisepticum* by real time PCR. *Jurnal Veterinar Malaysia*, *26*(1), 1-7.

Pertanika J. Trop. Agric. Sci. 46 (4): 1259 - 1274 (2023)

PERTANIKA JOURNALS

TROPICAL AGRICULTURAL SCIENCE

Journal homepage: http://www.pertanika.upm.edu.my/

Effects of Nutritional and Culture Medium-based Approaches for Aquaponics System with Bio-floc Technology on Pak Choi and Catfish Growth Rates

Rory Anthony Hutagalung[1], Arka Dwinanda Soewono[2]*, Marten Darmawan[2] and Aldo Cornelius[1]

[1]Department of Biology, Faculty of Biotechnology, Atma Jaya Catholic University of Indonesia, Jenderal Sudirman No. 51, 12930, Jakarta, Indonesia
[2]Department of Mechanical Engineering, Faculty of Engineering, Atma Jaya Catholic University of Indonesia, Cisauk Raya BSD City, 15345, Banten, Indonesia

ABSTRACT

Aquaponics with bio-floc can potentially offer sustainable food production with zero waste as it allows farming plants and fish simultaneously, whereby the former use fish waste as their nutrient sources, while the latter receives cleaner water from the plants in a closed-loop system. In the aquaponics system, additional nutrients are usually added to support optimal plant growth, but it is suggested that the amount of such chemical nutrients should be controlled to prevent any harm to the fish. Furthermore, the plant and fish growth rates are influenced by the nutrients and the culture media used. This study aims to examine the effect of nutrition (full-nutrient and half-nutrient treatments) and different types of culture mediums (rockwool, rockwool-perlite, and rockwool-husk) on the growth rates of pak choi (*Brassica rapa*) and catfish (*Clarias gariepinus*) using split-plot design. Findings show that the half-nutrient treatment yielded a 17.12% higher plant growth rate and 23.87% heavier catfish weight than the full-nutrient treatment, but these treatments did not affect the fish survival rate. It was also observed that using different culture mediums did not result in any significant difference.

ARTICLE INFO

Article history:
Received: 25 April 2023
Accepted: 07 July 2023
Published: 31 October 2023

DOI: https://doi.org/10.47836/pjtas.46.4.12

E-mail addresses:
rory.hutagalung@atmajaya.ac.id (Rory Anthony Hutagalung)
arka.soewono@atmajaya.ac.id (Arka Dwinanda Soewono)
marten.darmawan@atmajaya.ac.id (Marten Darmawan)
ALDO.2015080078@student.atmajaya.ac.id (Aldo Cornelius)
* Corresponding author

Keywords: Aquaponics, *Brassica rapa*, *Clarias gariepinus*, culture medium, nutrition treatment

INTRODUCTION

As the growing population has spurred more demands for food supply and yet the land use for agriculture has become increasingly limited, food production efficiency is

ISSN: 1511-3701
e-ISSN: 2231-8542

essential to meeting the food demand. At the same time, the food consumption trend has changed toward fresh and healthy commodities, increasing fish and vegetable consumption worldwide (Kearney, 2010). Catering for such demands, aquaponics can be considered one of the potential solutions as it can produce fresh fish and plants in an integrated system. Compared to regular farming or aquaculture systems, aquaponics has the advantage of being able to control and manage the wastewater produced to reduce the environmental impact. Aquaponics can also be operated without vast agricultural land (da Rocha et al., 2017) and easily adopted by home-scale producers and local fish farmers in urban settings.

Aquaponics is a cultivation system that combines aquaculture with hydroponic techniques, wherein the water from the fish rearing tank is flowed to the plants and is returned to the fish farming system in a closed-loop system. The recirculation of water in aquaponics is a filter for any fish waste and decomposed food residue (Harmon, 2005). The water from the fish culture tank will be a source of nutrition for the plants, while the plants will act as a biofilter that can clean the water flowing back to the tank (Zhang et al., 2020). As the main benefit, the aquaponics system does not require commercial fertilizer to grow plants (Prayogo et al., 2021), making it more environmentally friendly. The aquaponics can further be augmented with a bio-floc system to support the nutrient circulation process, where a consortium of microorganisms processes the organic waste into bio-floc, which can be used as additional feed for fish with the rest channeled to plants. The bio-floc technology in the aquaponics system is also economical since it helps improve water quality under a zero water exchange system (Ahmad et al., 2017; Pinho et al., 2022).

Given its popularity, studies on aquaponics have been abundant, but the research focusing on the balanced needs of plants and fish, which are generally contradictory, has not been explored much because the types of commodities cultured—in this case, fish and plants usually have to be compatible to be farmed together. For aquaculture commodities, catfish (*Clarias gariepinus*) is a suitable fish species owing to their additional breathing apparatus called arborescent (Abd-Elmaksoud et al., 2008; Belão et al., 2015) and their tolerance to total dissolved solids (TDS) of up to 1,000 ppm in the water (Popoola et al., 2021), whereas for hydroponic farming, pak choi (*Brassica rapa*) is a commonly cultivated plant because of its relatively short cultivation period, simple farming and high dietary value (Echer et al., 2015; Ewert, 2004). Normally, pak choi can grow well at a nutrition concentration of 1,000–1,400 ppm, with optimum growth at 1,200 ppm and an ideal pH of 5.0-8.0 (Akasiska et al., 2014).

Nevertheless, aquaponics has an issue: the conflicting needs between plant growth and fish growth. Even though some nutrients are already available from the residual aquaculture waste, which contains organic nitrogen (N), phosphorus (P), and carbon (C) (Saba & Steinberg, 2012), the plants still

need additional nutrients that are not found in fish pellets. However, adding nutrients creates a dilemma between high nutritional requirements for plants and clean water quality (low nutrition) for fish. Adding more nutrients, however, may create a dilemma between high nutritional requirements for plants and clean water quality (low nutrition) for fish. While plants usually require high nutrient content and can benefit from the high TDS value in the circulating water in the aquaponics systems (Afolabi, 2020; Nozzi et al., 2018), large amounts of TDS are directly harmful to fish and indirectly decrease pH and oxygen solubility in the water. Therefore, the nutrients to be added should be restricted to the elements that plants need that exist in lower-than-desirable quantities in fish feed or waste, namely calcium (Ca), potassium (K), and iron (Fe) (Bittsanszky et al., 2016; Kasozi et al., 2019; Sastro, 2015).

The culture medium is another factor that may affect plant growth in aquaponics systems (Oladimeji et al., 2020). With its primary function to hold and provide plant roots with adequate moisture and oxygen and to support their weight, the culture medium is expected to be highly water absorbent, have good aeration, and be free of toxins. One of the most common mediums used in hydroponics is rockwool, which originates from heated basalt spun into a wool-like block. Rockwool is popular for its high water-holding capacity, good aeration, and sturdiness (Ingram et al., 2003). However, its solidity and sturdiness may hinder root movement, limiting the aeration inside the medium (Resh, 2015). The rockwool can be mixed with another medium, like perlite volcanic glass (alumina-silicate) that has been heated until it expands to increase the aeration. Perlite is light and resistant to bacteria degradation, and although it has a lower water-holding capacity than rockwool, perlite is usually used with another medium to provide better aeration in the medium (Ingram et al., 2003). Another medium commonly used is burnt rice husk. Not only is this medium able to hold water and aerate the medium well, but it can also absorb and neutralize toxic minerals in the water. Moreover, burnt rice husk is not easily decomposed by bacteria and can replace other growing media (Kaudal et al., 2016).

In conventional aquaculture systems, non-consumed fish feed and other waste are regularly discarded through water replacement or filtration because they are noxious to fish. However, in an aquaponics system combined with bio-floc technology, the waste is useful as additional fish feed after being processed by bacteria and other microorganisms. Floc-forming bacteria manipulate the carbon-nitrogen (C/N) ratio to convert the toxic nitrogenous waste into beneficial bacteria, forming microbial protein that can be used as an additional source of food for fish (Pattilo, 2017). Previous studies have shown that bio-floc technology can reduce fish feed by up to 20% (Ogello et al., 2014), potentially increasing the financial feasibility of aquaponics production. In addition, the floc-forming bacteria can help improve fish health and water quality, which is critical in the circulation system (Ahmad

et al., 2017; Gallardo-Collí et al., 2019). Given these advantages, bio-floc allows aquaponics to be a sustainable zero-waste food production system.

The present research aims to examine the growth rates of pak choi and catfish cultured through nutritional and culture medium-based approaches in the aquaponics system integrated with bio-floc technology. However, as the bio-floc implementation was still in the preliminary stage, the water quality parameters in the bio-floc application, such as the ammonia, nitrite, and nitrate levels, were beyond the scope of this study. This research will likely be the first to examine the potential use of a commercial nutrient solution in an aquaponics system with bio-floc to improve plant production while mitigating its adverse effect on fish health. The findings can eventually help enhance the productivity and profitability of aquaponics systems by indicating the optimal amount of nutrients (Ca, K, and Fe) that can be added to support plant growth without harming the fish.

MATERIALS AND METHODS

This research was conducted for eight months in the Aquaculture Laboratory, Atma Jaya Catholic University of Indonesia campus in Tangerang, West Java (6°19'S, 106°39'E, and altitude 44 m). The research began with an initial study on the design of the aquaponics system, which included water circulation from and to the hydroponic plots, a sunlight intensity system, and a feeding system. The primary process consisted of aquaponics installation, nutrient, and sample preparation, weekly monitoring and measurement, and final measurement and statistical analysis.

Aquaponics Installation and Experimental Design

A split-plot design was developed using six aquaponics sets, each containing a 1 m^3-square tank and ten hydroponic pipes with 90 holes, resulting in 540 holes available for growing plants. The tank was filled with fresh water, and bio-floc was grown by adding probiotic bacteria (EM4, Songgolangit Persada, Indonesia) for two weeks. When bio-floc was formed, 850 catfishes (*Clarias gariepinus*) of 1-month-old (9–11 cm) with an average weight between 4 to 5 g were put in each tank. The growing bio-floc was characterized by a change in the water color to greenish and the formation of small blackish-green clumps suspended in the water. The main plot was divided based on nutrient concentration (full-nutrient and half-nutrient), while the subplot was based on the culture medium (rockwool, rockwool-perlite, and rockwool-husk). Three aquaponics sets were used for the full-nutrient experiment and the rest for the half-nutrient one. Figure 1 shows the installation of the aquaponics system used in this study and the layout of each aquaponics set. Each set was equipped with a submersible impeller pump to circulate the water at a rate of 500 ± 5 L/hr. Intensive turbulent mixing generated by the air pump installed inside the tank and the returning waterfall from the hydroponic pipes would provide aeration for the aquaculture system.

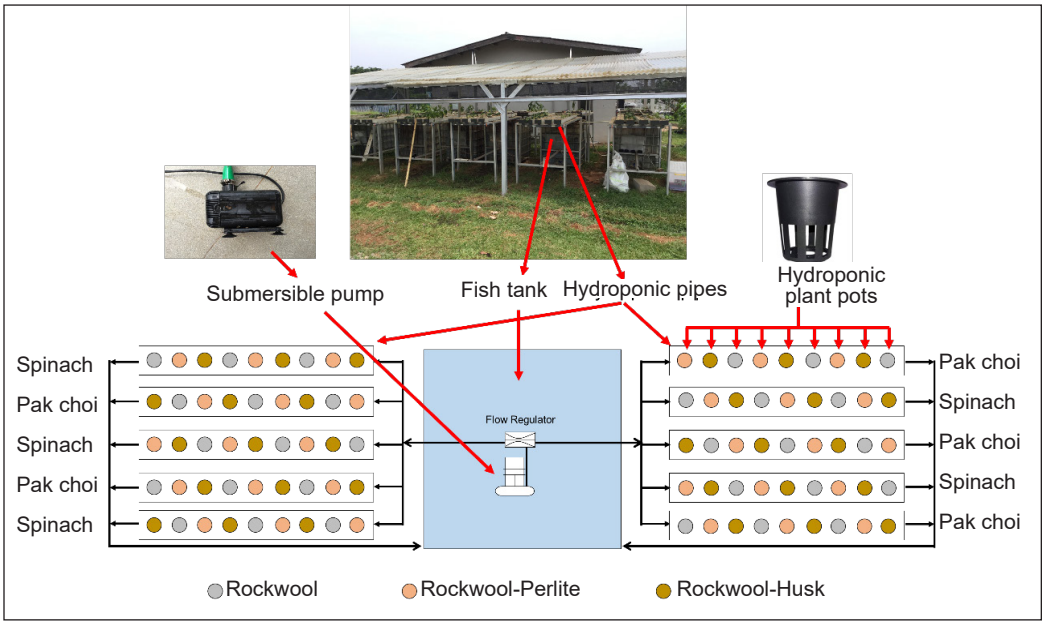

Figure 1. Aquaponics installation and layout

Lastly, nets were used to reduce excessive light intensity and protect the aquaponics from external conditions such as wind and rainfall. Initially, two types of plants were cultivated in the aquaponics systems: pak choi (*Brassica rapa*) and spinach (*Spinacia oleracea*). However, most spinach seeds failed to germinate; hence, the study would focus more on the pak choi.

Nutrient and Sample Preparation

The additional nutrition used for the plant was AB Mix nutrient (Agrifarm, Indonesia), which is well known in hydroponics farming. AB represents the two types of nutrients packaged separately, intended to prevent clumping when put together in the same package. The clumping usually occurs due to a chemical reaction between mineral salts or the crystallization of the nutrients. In detail, nutrient stock A represents macronutrients containing elements such as nitrogen (N) and phosphorus (P), while nutrient stock B represents micronutrients such as iron (Fe), copper (Cu), and chlorine (Cl). The composition of nutrients A and B for 1,000 L of water is shown in Table 1. The full-nutrient treatment was controlled using AB Mix at a final concentration of 1,200 ppm, while the

Table 1
The composition of AB Mix

Composition	Value (g)
Nutrient A	
Ammonium nitrate	616
Potassium nitrate	1176
Fe-EDTA	38
Nutrient B	
Manganese sulphate	8
Magnesium sulphate	790
Zinc sulphate	1.5
Copper sulphate	0.4
Potassium dihydrophosphate	335
Ammonium heptamolybdate	0.1
Boric acid	4

half-nutrient treatment was controlled at a final concentration of 600 ppm. For the half-nutrient treatment, 3.54 g of iron (II) sulfate ($FeSO_4$), 471.25 g of calcium carbonate ($CaCO_3$), and 462.55 g of potassium hydroxide (KOH) were also added.

Pak choi seeds were soaked and planted in rockwool measuring 3 × 3 × 3 cm^3, which were then sprayed with water using a sprayer. After ten days, the plants with four leaves were ready to be transferred to three different aquaponics pots, which contained only rockwool, rockwool-perlite, and rockwool-husk (according to medium treatments), respectively. Each was placed on an aquaponics plot with a nutrient flow technique (NFT) system.

Monitoring and Weekly Measurement

An Arduino-based control system was designed to monitor and maintain the water temperature, pH level, and dissolved oxygen (DO) in the aquaculture tanks, ensuring that the aquaponics ran optimally. The pH level in the tank was maintained at around 7.5, which is highly recommended for the optimal growth and development of catfish. At the same time, the dissolved oxygen was always preserved at a level above 3,000 ppm. As shown in Figure 2, the temperature, pH, and DO measurement data obtained from the Arduino sensor was hosted on the open-source analytical platform ThingSpeak Internet-of-Things.

Maintenance was also conducted daily to control the amount of TDS, as illustrated in Table 2. In the full-nutrient treatment, an AB Mix concentration of 600 ppm was initially added in week 1 and gradually increased to its final concentration of 1,200 ppm in week 4. Meanwhile, the AB Mix concentration in the half-nutrient treatment started at 300 ppm and rose to 600 ppm in the third and fourth week. Removal of any excess accumulated floc deposits in the fish tanks was conducted

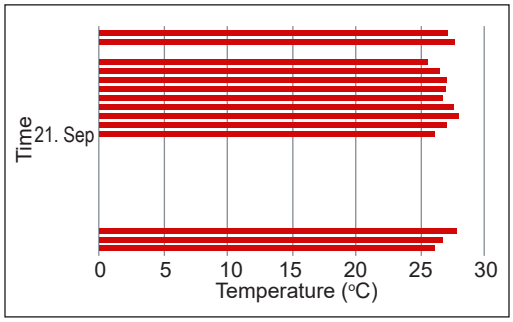

(a)

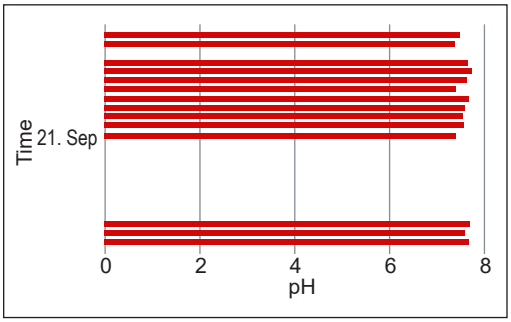

(b)

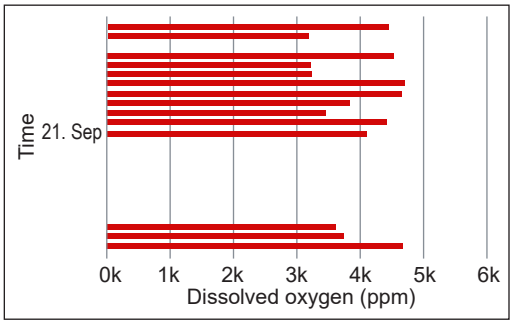

(c)

Figure 2. (a) Temperature; (b) pH; and (c) and dissolved oxygen measurement data

Table 2
The total dissolved solids maintenance provisions

Nutrition treatment	Initial	1st week	2nd week	3rd week	4th week
Full (ppm)	600	800	1,000	1,200	1,200
Half (ppm)	300	400	500	600	600

weekly to prevent clogging in the hydroponic pipes. In addition, visual inspections of the hydroponics sections were carried out twice weekly to ensure no solids were built on the plant's roots.

Final Measurement and Statistical Analysis

Final measurements were conducted during the fourth week. Two plants were taken from each culture medium treatment for final measurements for each nutrient treatment. The final measurement examined the stem weight, height, chlorophyll *a*, and chlorophyll *b*. The stem height was measured from the medium's surface to the plants' apical shoots. In contrast, the chlorophyll content was measured by following Harborne's (1998) method. A total of 0.1 g of leaves were crushed using a mortar until they became fine powder, after which 10 ml of 80% acetone (Sigma-Aldrich, Germany) was added. They were then centrifuged for 15 min at 1,593 × *g* and filtered using Whatman filter paper type 41. The chlorophyll content was measured using a spectrophotometer at 646 nm and 663 nm, with its levels determined using the following Equations:

$$\text{Chlorophyll } a = (12.21\ \lambda_{663} - 2.81\ \lambda_{646})\ \text{mg/L} \quad [1]$$

$$\text{Chlorophyll } b = (20.13\ \lambda_{646} - 5.03\ \lambda_{663})\ \text{mg/L} \quad [2]$$

The growth rates of pak choi and catfish were measured for 4 and 9 weeks, respectively, following their harvest cycle. The survival rate of the catfish was also measured at the end of the production cycle (week 9). Statistical Product and Service Solutions (SPSS) was used to determine the effect of different culture mediums and nutritional treatments on the growth rate of pak choi. The analysis used the analysis of variance test, where in case the analysis of the variance test yielded a significant difference (p <0.05), further analysis was conducted using the post-hoc Tukey's test. The number of leaves was analyzed using a non-parametric test (Kruskal-Wallis' test).

RESULTS

In the initial research stage, three main problems were encountered and solved: bio-floc accumulation in the hydroponic system that blocked the circulation, excessive sunlight that caused the plant to dry out, and nutrient deficiency. First, the water circulation in the hydroponic tank was easily clogged up by the bio-floc, blocking the circulation and causing the water to overflow. To address this issue, an additional water channel was created to return the

overflow to the tank. Secondly, the excessive sunlight intensity was reduced by installing the net (60% shade) on the roof and around the wall. The third problem, where the plants showed symptoms of malnutrition in the aquaponics system, as shown in Figure 3, was solved through the nutrient treatment conducted during the main experiment.

The experimental results showed that the half-nutrient treatment produced significantly higher plant height, number of leaves, weight growth, stem weight, stem height, chlorophyll *a*, and chlorophyll *b*, compared to the full nutrient (p<0.05), especially during the last week as summarized in Table 3. The chlorophyll *a* and b concentrations were obtained from Equations 1 and 2.

Figure 3. Malnutrition pak choi

The pak choi growth rates, as typified by the number of leaves, height, and weight, initially showed no difference in both treatments during the first week. In the second week, the full-nutrient treatment showed better results than the half-nutrient treatment regarding the number of leaves and height. However, as of the third week, the pak choi growth rate under the half-nutrient treatment was better on every measured variable (number of leaves, height, and weight growth) than the full-nutrient treatment (Figure 4). The error bars represent the standard errors from 36 random samples.

Regarding the culture mediums, no significant difference in the growth rates of pak choi cultivated in rockwool, rockwool-perlite, and rockwool-husk medium was observed on all measured variables (plant height, number of leaves, weight growth, stem weight, stem height, chlorophyll *a*, and chlorophyll *b*), as shown in Table 4.

The number of leaves and height from week 0 to week four did not significantly

Table 3
Pak choi growth rate in different nutrient treatment

	Treatment	
	Half-nutrient	Full-nutrient
Height (cm)	14.375 ± 0.221^{a}	13.177 ± 0.458^{b}
Total number of leaves	11.917 ± 0.2754^{a}	11.086 ± 0.483^{b}
Wet weight (g)	63.167 ± 0.829^{a}	56.444 ± 2.171^{b}
Stem weight (g)	22.667 ± 1.278^{a}	15.444 ± 0.978^{b}
Stem height (cm)	1.811 ± 0.116^{a}	1.383 ± 0.108^{b}
Chlorophyll *a* (µg/ml)	14.281 ± 1.223^{a}	11.842 ± 1.012^{b}
Chlorophyll *b* (µg/ml)	4.455 ± 0.386^{a}	3.524 ± 0.303^{b}

Note. Different subscripts mean that there is a statistically significant difference

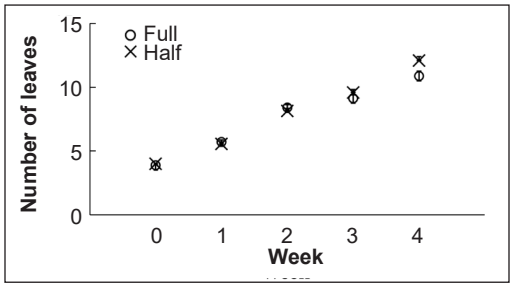

(a)

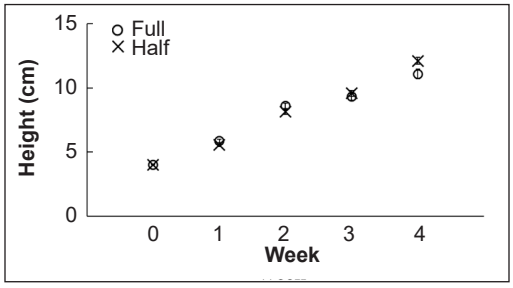

(b)

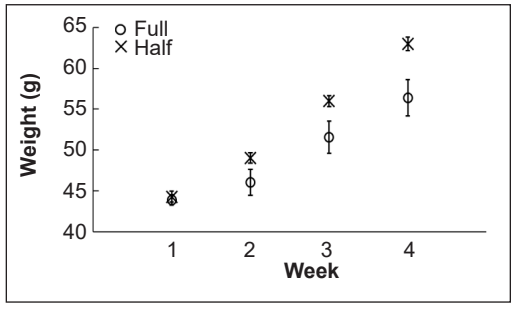

(c)

Figure 4. Comparisons of: (a) number of leaves; (b) height; and (c) weight of pak choi for full and half-nutrient treatments

differ in all treatments (Figures 5a and 5b). However, the weight growth of pak choi on rockwool was slightly better compared to that on other culture mediums (Figure 5c), especially during the last week, though the difference was not significant (p>0.05).

Regarding the catfish growth rate, the average weight under the full-nutrient treatment was lower, though not significantly (p>0.05), than that under the half-nutrient treatment starting from the first week of the experiment, as shown in Figure 6. The data points represent the average weight of sixty randomly selected catfishes from three different tanks for each treatment, and the error bars represent the standard error. Concerning the total production, 245 kg of marketable catfish (10–15 g per fish) were produced and sold at the end of this study, but approximately 20 kg of fish could not be sold as their size is too big (more than 1 kg per fish).

The growing bio-floc in the aquaculture tank was also observed in this study. The concentrations of settleable solids from bio-floc in the water tanks were measured weekly using a 500 ml Imhoff cone after 25

Table 4
Pak choi growth rate in the different medium treatment

	Treatment		
	Rockwool	Rockwool + Perlite	Rockwool + Husk
Height (cm)	13.714 ± 0.68[a]	13.565 ± 0.343[a]	13.788 ± 0.282[a]
Total number of leaves	11.596 ± 0.665[a]	11.542 ± 0.429[a]	11.667 ± 0.369[a]
Wet weight (g)	65.333 ± 2.952[a]	60.5 ± 1.887[a]	61.917 ± 1.209[a]
Stem weight (g)	20.667 ± 1.892[a]	17.667 ± 1.57[a]	18.883 ± 1.757[a]
Stem height (cm)	1.758 ± 0.125[a]	1.25 ± 0.145[a]	1.783 ± 0.132[a]
Chlorophyll a (µg/ml)	13.246 ± 0.602[a]	12.955 ± 0.522[a]	12.982 ± 0.59[a]
Chlorophyll b (µg/ml)	4.061 ± 0.209[a]	3.934 ± 0.184[a]	3.974 ± 0.202[a]

Note. Different subscripts mean that there is a statistically significant difference

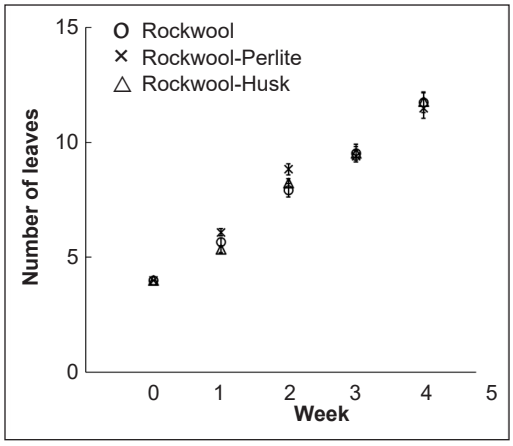

(a)

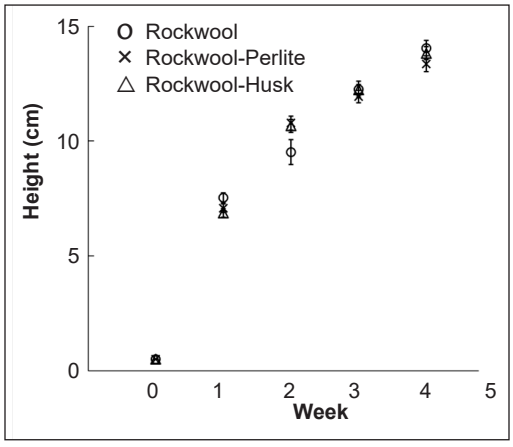

(b)

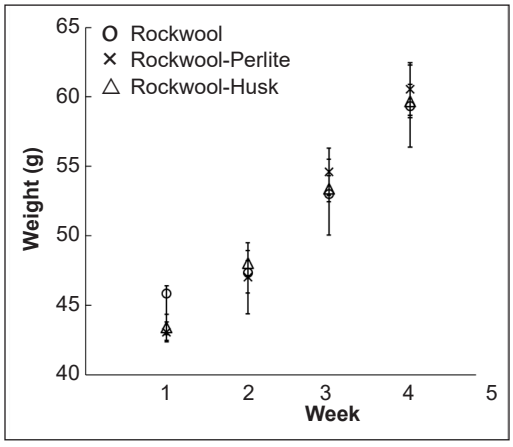

(c)

Figure 5. Comparisons of: (a) number of leaves; (b) height; and (c) wet weight of pak choi for different culture mediums

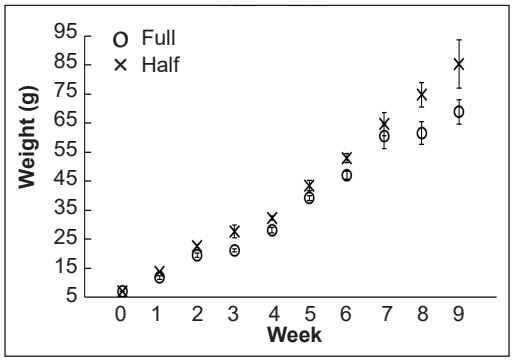

Figure 6. Catfish weight growth

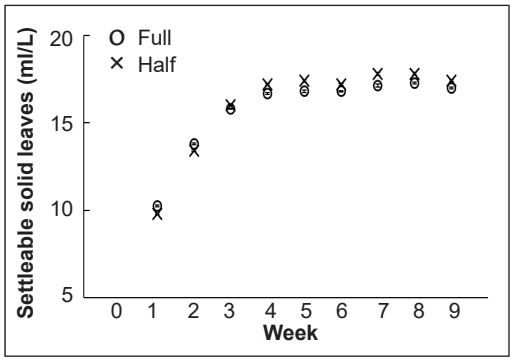

Figure 7. Settleable solids concentration in aquaculture tank

min of sedimentation. It was observed that the settleable solids increased for the first two weeks and started to stabilize around the third week, regardless of the nutrient treatment (Figure 7). It should be noted that further study is required to properly manage the use of bio-floc technology and its impact on aquaponics production.

DISCUSSION

The findings show no interaction between nutrition and culture medium treatments, each independent and not affecting the other. It was also observed that the half-nutrient treatment showed better products of pak choi

than the full-nutrient treatment, indicating that the addition of missing elements, namely Fe, Ca, and K, to the half-nutrient treatment made pak choi grow as effectively as it would do in a typical hydroponic system without harming the fish growth. Regarding the function of the missing elements, Fe is vital for plant respiration and chlorophyll formation, Ca stimulates root hair formation, stem hardening, and seed formation, and K helps the formation of protein and carbohydrates (Grusak, 2001). Other nutrients were available in fish feeds, continuously accumulating in the water. This study showed that the half-nutrient treatment was sufficient to promote plant growth, which suggests that aquaponics farmers can increase plant and fish production using a lower dose of a commercial nutrient solution, resulting in a lower operational cost.

As for the fish growth, the half-nutrient treatment yielded better results; the catfish became larger compared to the catfish size in the full-nutrient treatment, confirming the previous study's findings (Sarmento et al., 2020). In the half-nutrient treatment, the catfish were also able to adapt better compared to those in the full-nutrient treatment. Nevertheless, even though the catfish were tolerant to extreme conditions with low DO and high TDS because of their preference towards low-hardness water (Setiadi et al., 2019), it should be noted that the difference in growth rates between the two treatments was statistically not significant. This insignificance might be attributed to the limited number of replications (three times) for the fish growth experiment, necessitating further research with more replications to confirm the difference between the two treatments.

The culture medium treatment did not significantly affect the pak choi's growth, which is likely related to its long roots, which helped the plant obtain water more easily, regardless of the culture medium (Sundar & Chen, 2020). However, during the fourth week, the weight growth rate of the plants in the rockwool medium seemed higher than that in perlite and husk, which was possibly due to rockwool's better ability to store water than that of perlite and husk (Campbell et al., 2021; Ingram et al., 2003).

Similar to the previous research (Priadi et al., 2019), this study has found that the growth rate of pak choi was better in the half-treatment scenario, with the half-nutrient treatment yielding pak choi with better average height (14.38 cm), number of leaves (11.92), and wet weight (63.17 g) compared to the full-nutrient treatment. This slight difference indicates that the additional nutrient in the half-nutrient treatment can sufficiently compensate for the deficiency of Fe, Ca, and K nutrients in conventional aquaponics cultivation. In relation to the previous study by Nozzi et al. (2018) that demonstrates how adding supplements may accelerate plant growth but reduce the plant's nutritional quality, this study has presented the half-nutrient addition as a suitable concession to support the plant growth while maintaining most of its nutritional quality. Not only that, but the proper amount of the nutrient dose also

prevented any harm to the fish. Furthermore, this study attests to pak choi's suitability for aquaponic farming because it typically requires minimal supplement addition, tolerates low-medium ppm levels, and does not take too much space, resulting in efficient management and cost. Lastly, the findings confirm the suitability and positive effect of employing a bio-floc system on pak choi cultivation in aquaponics (Fimbres-Acedo et al., 2020).

This study also demonstrates what fish are suitable to farm in aquaponic systems. The water conditions in the aquaponic system are often turbid, resulting in low DO levels. Such an issue is even exacerbated with the addition of bio-floc technology (da Rocha et al., 2017). Therefore, the ideal types of fish to farm in aquaponic systems are those with an extra respiratory system and the ability to tolerate unfavorable environments. Furthermore, aquaponics is generally optimized for food production with high fish stocking density in the tank, meaning that the best fish to raise in aquaponics must be able to live in groups since the space between fish is limited (Setiadi et al., 2019). With all these considered, catfish are ideally suited for aquaponics due to their air-breathing capabilities and hardiness.

Nonetheless, the existing aquaponics system does still have some challenges. Firstly, the aquaponics system operated in this study is laboratory-scale, which may not properly replicate semi-commercial and large-scale commercial aquaponic operations. As commercial aquaponics normally seek a maximum production output (Palm et al., 2018), the aquaponics system in this research might not be financially sustainable since its intended design is not for economic production. Secondly, the application of bio-floc in this study is still in the preliminary stage, where critical water quality parameters in bio-floc technology, such as ammonia, nitrite, and nitrate, were not carefully maintained. Further research is needed to evaluate and optimize the water parameters and operating conditions to help maximize the bio-floc's effectiveness in increasing fish production in aquaponics. In addition, this study discovered that the current aquaponics system with bio-floc was less efficient because large floc deposits were still left at the end of the production cycle, which would likely require some cleansing. In light of the large number of floc deposits, it is therefore recommended that the number of fish and plants be balanced to reduce the excessive floc. Correspondingly, it is also suggested that the culture medium with larger pores be used to avoid clogging caused by the floc deposits since clogging can disrupt the plant's respiration due to the lack of aeration (Goddek et al., 2015). In future research, the leftover flocs should ideally be utilized as bio pellets to feed the fish to help minimize costs since fish food is one of the most significant cost factors during this study. Using bio pellets can then significantly improve the profitability of the aquaponics system.

Despite the current shortcomings, this study has demonstrated the potential

of aquaponics as a sustainable food cultivation system that allows the urban population to produce fresh food in their backyards or rooftops without the need for spacious farmland. The aquaponics integrated with bio-floc is also more environmentally friendly owing to its lower water consumption as a result of its zero or minimal water exchange during the operation. Legislators and policymakers can help to promote aquaponics as part of sustainable urban food production that can solve global food security issues.

CONCLUSION

The half-nutrient treatment showed better products of pak choi than the full-nutrient treatment on all measured variables (plant height, number of leaves, weight growth, stem weight, and stem height). The average growth rate of pak choi in the half-nutrient treatment was around 17.12% better than that in the full-nutrient treatment. This result indicates that the additional Fe, Ca, and K nutrients can compensate for the missing elements in the aquaponics system. However, as to the culture-medium treatment, there was no significant difference in the effects of rockwool, rockwool-perlite, and rockwool-husk mediums on pak choi's growth rate on every measured variable. Finally, the fish growth under the half-nutrient treatment was higher than that under the full-nutrient treatment, although the difference was not statistically significant. Further experiments with more replications should be conducted to confirm the difference.

ACKNOWLEDGEMENTS

This study was supported by the Institute for Research and Community Services of Atma Jaya Catholic University of Indonesia under Research Grant "Hibah Kompetitif 2019" No. 2019-RIA.

REFERENCES

Abd-Elmaksoud, A., Kassab, M. A., Sayed, A. A., & Fayed, M. H. (2008). Anatomical, light and scanning electron microscopic studies on the air breathing dendretic organ of the sharp tooth catfish (*Clarias gariepinus*). *Journal of Veterinary Anatomy*, *1*(1), 29–37. https://doi.org/10.21608/jva.2008.45452

Afolabi, K. A. (2020). *Productivity of kale (*Brassica oleracea *var.* acephala*) and Nile tilapia (*Oreochromis niloticus*) culture in aquaponic systems* [Master's thesis, The American University in Cairo]. AUC Knowledge Fountain. https://fount.aucegypt.edu/etds/1449/

Ahmad, I., Babitha Rani, A. M., Verma, A. K., & Maqsood, M. (2017). Biofloc technology: An emerging avenue in aquatic animal healthcare and nutrition. *Aquaculture International*, *25*, 1215–1226. https://doi.org/10.1007/s10499-016-0108-8

Akasiska, R., Samekto, R., & Siswadi. (2014). Pengaruh konsentrasi nutrisi dan media tanam terhadap pertumbuhan dan hasil sawi pakcoy (*Brassica parachinensis*) sistem hidroponik vertikultur [The effect of nutrient concentration and growing media on the growth and yield of mustard pak choi (*Brassica parachinensis*) in verticulture hydroponic system]. *Jurnal Inovasi Pertanian*, *13*(2), 46–61.

Belão, T. C., Zeraik, V. M., Florindo, L. H., Kalinin, A. L., Leite, C. A. C., & Rantin, F. T. (2015). Control of cardiorespiratory function in response to hypoxia in an air-breathing fish, the African sharptooth catfish, *Clarias gariepinus*. *Comparative Biochemistry and Physiology*

Part A: Molecular and Integrative Physiology, *187*, 130–140. https://doi.org/10.1016/j.cbpa.2015.05.010

Bittsanszky, A., Uzinger, N., Gyulai, G., Mathis, A., Junge, R., Villarroel, M., Kotzen, B., & Komives, T. (2016). Nutrient supply of plants in aquaponic systems. *Ecocycles*, *2*(2), 17–20. https://doi.org/10.19040/ecocycles.v2i2.57

Campbell, S. M., Anderson, S. L., Brym, Z. T., & Pearson, B. J. (2021). Evaluation of substrate composition and exogenous hormone application on vegetative propagule rooting success of essential oil hemp (*Cannabis sativa* L.). *PLOS One*, *16*(7), e0249160. https://doi.org/10.1371/journal.pone.0249160

da Rocha, A. F., Filho, M. L. B., Stech, M. R., & da Silva, R. P. (2017). Lettuce production in aquaponic and biofloc systems with silver catfish. *Rhamdia quelen*. *Boletim do Instituto de Pesca*, *44*, 64-73. https://doi.org/10.20950/1678-2305.2017.64.73

Echer, M. M., Dalastra, G. M., Hachmann, T. Lo, Klosowskı, E. S., & Guimarães, V. F. (2015). Agronomic performances of pak choi grown with different soil cover. *Horticultura Brasileira*, *33*(2), 261–266. https://doi.org/10.1590/S0102-053620150000200020

Ewert, F. (2004). Modelling plant responses to elevated CO_2: How important is leaf area index? *Annals of Botany*, *93*(6), 619–627. https://doi.org/10.1093/aob/mch101

Fimbres-Acedo, Y. E., Servín-Villegas, R., Garza-Torres, R., Endo, M., Fitzsimmons, K. M., Emerenciano, M. G. C., Magallón-Servín, P., López-Vela, M., & Magallón-Barajas, F. J. (2020). Hydroponic horticulture using residual waters from *Oreochromis niloticus* aquaculture with biofloc technology in photoautotrophic conditions with *Chlorella* microalgae. *Aquaculture Research*, *51*(10), 4340–4360. https://doi.org/10.1111/are.14779

Gallardo-Collí, A., Pérez-Rostro, C. I., & Hernández-Vergara, M. P. (2019). Reuse of water from biofloc technology for intensive culture of Nile tilapia (*Oreochromis niloticus*): Effects on productive performance, organosomatic indices and body composition. *International Aquatic Research*, *11*, 43–55. https://doi.org/10.1007/s40071-019-0218-9

Goddek, S., Delaide, B., Mankasingh, U., Ragnarsdottir, K. V, Jijakli, H., & Thorarinsdottir, R. (2015). Challenges of sustainable and commercial aquaponics. *Sustainability*, *7*(4), 4199–4224. https://doi.org/10.3390/su7044199

Grusak, M. A. (2001). Plant macro- and micronutrient minerals. In *eLS*. https://doi.org/https://doi.org/10.1038/npg.els.0001306

Harborne, J. B. (1998). *Phytochemical methods: A guide to modern techniques of plant analysis* (3rd ed.). Springer.

Harmon, T. S. (2005). The role of "aquaponics" in recirculating aquaculture systems. *International Journal of Recirculating Aquaculture*, *6*(1), 13–22. https://doi.org/10.21061/ijra.v6i1.1398

Ingram, D. L., Henley, R. W., & Yeager, T. H. (2003). *Growth media for container grown ornamental plants*. https://ufdc.ufl.edu/IR00004607/00001/pdf

Kasozi, N., Tandlich, R., Fick, M., Kaiser, H., & Wilhelmi, B. (2019). Iron supplementation and management in aquaponic systems: A review. *Aquaculture Reports*, *15*, 100221. https://doi.org/10.1016/j.aqrep.2019.100221

Kaudal, B. B., Chen, D., Madhavan, D. B., Downie, A., & Weatherley, A. (2016). An examination of physical and chemical properties of urban biochar for use as growing media substrate. *Biomass and Bioenergy*, *84*, 49–58. https://doi.org/10.1016/j.biombioe.2015.11.012

Kearney, J. (2010). Food consumption trends and drivers. *Philosophical Transactions of the Royal*

Society B: Biological Sciences, *365*, 2793–2807. https://doi.org/10.1098/rstb.2010.0149

Nozzi, V., Graber, A., Schmautz, Z., Mathis, A., & Junge, R. (2018). Nutrient management in aquaponics: Comparison of three approaches for cultivating lettuce, mint and mushroom herb. *Agronomy*, *8*(3), 27. https://doi.org/10.3390/agronomy8030027

Ogello, E. O., Musa, S. M., Mulanda Aura, C., Abwao, J. O., & Mbonge Munguti, J. (2014). An appraisal of the feasibility of tilapia production in ponds using biofloc technology: A review. *International Journal of Aquatic Science*, *5*(1), 21–39.

Oladimeji, A. S., Olufeagba, S. O., Ayuba, V. O., Sololmon, S. G., & Okomoda, V. T. (2020). Effects of different growth media on water quality and plant yield in a catfish-pumpkin aquaponics system. *Journal of King Saud University - Science*, *32*(1), 60–66. https://doi.org/10.1016/j.jksus.2018.02.001

Palm, H. W., Knaus, U., Appelbaum, S., Goddek, S., Strauch, S. M., Vermeulen, T., Haïssam Jijakli, M., & Kotzen, B. (2018). Towards commercial aquaponics: A review of systems, designs, scales and nomenclature. *Aquaculture International*, *26*, 813–842. https://doi.org/10.1007/s10499-018-0249-z

Pattilo, D. A. (2017). *An overview of aquaponic system: Hydroponic component*. https://www.ncrac.org/files/publication/hyroponic_components.pdf

Pinho, S. M., de Lima, J. P., David, L. H., Emerenciano, M. G. C., Goddek, S., Verdegem, M. C. J., Keesman, K. J., & Portella, M. C. (2022). FLOCponics: The integration of biofloc technology with plant production. *Reviews in Aquaculture*, *14*(2), 647–675. https://doi.org/10.1111/raq.12617

Popoola, O. M., Oguntade, S. T., & Adebayo, O. T. (2021). Growth performance and immunological response of African catfish (*Clarias gariepinus*) juveniles reared in biofloc system. *Journal of Agriculture and Rural Development in the Tropics and Subtropics*, *122*(1), 137–145. https://doi.org/10.17170/kobra-202105253967

Prayogo., Agustono., Rahardja, B. S., & Amin, M. (2021). Growth performance and nutrient composition of mustard green (*Brassica juncea*) cultured in aquaponics systems and hydroponic system. *Journal of Aquaculture and Fish Health*, *10*(3), 373–379. https://doi.org/10.20473/jafh.v10i3.26593

Priadi, D., Wibowo, H., & Mulyaningsih, E. S. (2019). The growth optimization of pak choy (*Brassica rapa* L. var. *chinensis*) in household-scale aquaponics system. *Jurnal Biodjati*, *4*(2), 175–183. https://doi.org/10.15575/biodjati.v4i2.4630

Resh, H. M. (2015). *Hydroponics for the home grower* (1st ed.). CRC Press. https://doi.org/10.1201/b18069

Saba, G. K., & Steinberg, D. K. (2012). Abundance, composition, and sinking rates of fish fecal pellets in the Santa Barbara Channel. *Scientific Reports*, *2*, 716. https://doi.org/10.1038/srep00716

Sarmento, R. L. T., Hakim, R. R., & Hermawan, D. (2020). The effect of AB Mix nutrition on growth performance of catfish (*Clarias gariepinus*) and lettuce (*Lactuca sativa*) cultivated in aquaponic systems. *Indonesian Journal of Tropical Aquatic*, *3*(2), 87–94.

Sastro, Y. (2015). Akuaponik: Budidaya tanaman terintegrasi dengan ikan, permasalahan keharaan dan strategi mengatasinya [Aquaponics: Integrated plant farming with fish, nutritional problems and strategies to overcome them]. *Buletin Pertanian Perkotaan*, *5*(1), 33–42.

Setiadi, E., Taufik, I., Widyastuti, Y. R., Ardi, I., & Puspaningsih, D. (2019). Improving productivity and water quality of catfish, *Clarias* sp. cultured in an aquaponic ebb-tide system using different filtration. In *IOP Conference*

Series: Earth and Environmental Science (Vol. 236, No. 1, p. 12026). IOP Publishing. https://doi.org/10.1088/1755-1315/236/1/012026

Sundar, L. S., & Chen, G. S. (2020). Study on the growth performance of lettuce (*Lactuca sativa*) and pak choi (*Brassica chinensis*) in different aquaponic growing systems. *Horticulturae*, *6*(4), 69. https://doi.org/10.3390/horticulturae6040069

Zhang, H., Gao, Y., Shi, H., Lee, C. T., Hashim, H., Zhang, Z., Wu, W.-M., & Li, C. (2020). Recovery of nutrients from fish sludge in an aquaponic system using biological aerated filters with ceramsite plus lignocellulosic material media. *Journal of Cleaner Production*, *258*, 120886. https://doi.org/10.1016/j.jclepro.2020.120886

Pertanika J. Trop. Agric. Sci. 46 (4): 1275 - 1292 (2023)

PERTANIKA JOURNALS

TROPICAL AGRICULTURAL SCIENCE

Journal homepage: http://www.pertanika.upm.edu.my/

Kinetics of Color Changes During Pretreatment Blanching of Pineapple (*Ananas Comosus*) Fruit Variety 'MD2'

Rosnah Shamsudin[1]*, Hasfalina Che Man[2,3], Siti Hajar Ariffin[1], Nazatul Shima Azmi[1] and Siti Nor Afiekah Mohd Ghani[1]

[1]Department of Process and Food Engineering, Faculty of Engineering, Universiti Putra Malaysia, 43400 Serdang, Selangor, Malaysia
[2]Department of Biological and Agricultural, Faculty of Engineering, Universiti Putra Malaysia, 43400 Serdang, Selangor, Malaysia
[3]SMART Farming Technology Research Center (SFRTC), Level 6, Tower Block, Faculty of Engineering, Universiti Putra Malaysia, 43400 Serdang, Selangor, Malaysia

ABSTRACT

Drying is an intensive unit operation used to preserve the pineapple fruit. In this study, the kinetics of color degradation in pineapple slices during blanching as pretreatment with combined microwave and convection drying at different temperatures (110, 120, 130, and 140°C) and drying times (5, 10, 20, 25, and 30 min) were determined. L*, b*, chroma, and total color difference (TCD) increased as the drying temperature and time increased. As for the a* parameter, it is not dependent on the drying temperature. In addition, blanching pretreatment prior to drying can affect and change the color of pineapple slices by increasing L*, a*, chroma, and TCD compared to no blanching. Nevertheless, it maintains the yellowness (b*) in pineapple slices. As for kinetic models, zero-order best described the changes of L*, a*, b*, chroma, and TCD, while first-order best pronounced the parameters L*, b*, chroma, and TCD. These findings would be useful in designing thermal processes and related calculations for the pineapple fruit.

Keywords: Blanching, color changes, kinetic models, MD2 variety, pineapple

ARTICLE INFO

Article history:
Received: 16 March 2023
Accepted: 23 May 2023
Published: 31 October 2023

DOI: https://doi.org/10.47836/pjtas.46.4.13

E-mail addresses:
rosnahs@upm.edu.my (Rosnah Shamsudin)
hasfalina@upm.edu.my (Hasfalina Che Man)
hajararriffin@upm.edu.my (Siti Hajar Ariffin)
nazatul_shima89@yahoo.com (Nazatul Shima Azmi)
fiekahfika@gmail.com (Siti Not Afiekah Mohd Ghani)
* Corresponding author

INTRODUCTION

Fresh pineapple fruit is extremely perishable and will go bad quickly if not handled properly due to the high water content (around 80%) of the fruit (Orsat et al., 2006). When extreme situations such as the

ISSN: 1511-3701
e-ISSN: 2231-8542

COVID-19 pandemic broke out in 2020, instability in the food supply chain affected the availability of food in the market through prolonged lockdowns and restrictions on immigration (Shahidi, 2020). Therefore, preservation techniques such as drying have become necessary for extending the shelf life.

Drying is the common method to preserve the high moisture content like pineapple. Drying is one of the oldest processing methods. It refers to removing moisture from solid material upon applying heat (Agarry et al., 2013). While drying fruit is a process where water is removed to retard the growth of microorganisms, as well as stop the occurrence of enzymatic or nonenzymatic browning reactions in the material matrix (Fan et al., 2006). In addition, fruits and vegetables are dried to extend shelf-life, enhance storage stability, minimize packaging requirements, and reduce transport weight (Karam et al., 2016). Kingsly et al. (2007) stated that drying also greatly affected the sensory and nutritional characteristics of the end product. Numerous drying techniques have been used for fruits and vegetables (Ahmed, 2011), such as solar drying (Lahsasni et al., 2004), microwave (Izli et al., 2018), and freeze-drying (Ceballos et al., 2012). Microwave drying was chosen as the drying method because it does not show a significant change in physicochemical properties. According to Abd Rahman (2020), microwave drying only shows minimal changes in the physicochemical properties, such as vitamin C and carotenoid compounds in mandarin citrus peels. It contrasts with hot air drying, which showed significant changes during elevated temperatures.

Application of physical pre-drying treatments such as blanching of solid food materials had been used commonly (Dandamrongrak et al., 2003). Blanching is a thermal treatment used prior to the food process (Xiao et al., 2017) to enhance the taste or texture of fruits and vegetables (Abdul Halim, 2021). The blanched products will cool rapidly or continue with the next processes, such as drying, freezing, frying, and canning (Abdul Halim, 2022; Xiao et al., 2017). Generally, vegetables and fruit are blanched to a predetermined temperature, and the time between 1 min and less than 10 min depends on the time required for the inactivation of peroxidase and polyphenol oxidase enzymes (Xiao et al., 2017). While drying, the pineapple fruit plant's tissues can experience several physical and chemical changes that substantially impact the quality. It includes shrinkage, color changes, ascorbic acid breakdown, and loss of rehydration capacity (Radojčin et al., 2021; Ramallo & Mascheroni, 2012). However, the temperature and duration of the blanching procedure for pineapple fruits are not defined. Hence, it is important to study the effect of blanching and drying on the kinetic color changes of pineapple fruits to determine the most suitable blanching and drying conditions to produce a good quality dried pineapple. Hidayat and Setyadjit (2019) reported the effect of blanching pretreatment on the physicochemical characteristics of potato powder samples.

They reported that the pretreatment affected the yield, color, water, and protein content and did not significantly affect ash, fat, or carbohydrate content. Alam et al. (2013) reported that carrot pomace became darker, corresponding to a decrease in the 'L' values and loss in redness ('a*' value decreased) and yellowness ('b*' value decreased) irrespective of blanching. Akter et al. (2010) investigated the effects of blanching with hot water and hot-air drying temperatures on the physicochemical properties, dietary fiber compositions, antioxidant activity, and hydration properties of ripe and soft persimmon peels. They found that blanched peels dried at 50°C had the highest dietary fiber compositions, swelling capacity, and antioxidant activity compared with those at high drying temperatures (60 and 70°C).

Agarry et al. (2013) conducted a study regarding the effect of blanching temperature-time combinations treatment conditions on the drying behavior of pineapple slices. The results show that the blanching temperature-time combinations affected drying rates and drying times. Blanching at 60 to 80°C for a short period (3 to 5 min) prior to drying showed increased mass transfer activity during the oven-drying process of pineapple slices. While blanching at 70 and 80°C for 10 min showed increased drying time compared with the unblanched pineapple samples (control). It could result from carbohydrate gelatinization and high water uptake (Agarry et al., 2013). Garba et al. (2015) observed that the effects of the blanching that resulted in higher drying rates were significant at a high temperature (80°C) and only marginal at a lower temperature (50°C).

The quality changes of the dried and blanched pineapple fruits were examined, and the influencing elements will be researched. The study used a model that can be used to predict how the color of pineapple fruits will vary over time in response to various blanching and drying settings. The first-order model and zero-order model were the kinetic models suggested based on the research found.

MATERIAL AND METHODS

Plant Materials

The pineapple fruit variety MD2 was supplied from the local farm at Sg. Merab, Kajang, Selangor, Malaysia. The pineapple fruits were harvested and delivered to Universiti Putra Malaysia on the same day. The fruits were from indices 4 (riped and matured), free from damage and pests. The fruits were then stored in room conditions at 25°C until further used.

Blanching

Pineapple slices were sliced into 60 cubes (Figure 1) for three different blanching temperatures, which were 0, 50, and 60°C (Agarry et al., 2013), respectively. The pineapple slices were immersed in a beaker filled with distilled water and heated using a water bath (Laft Technologies, Australia). For all temperatures, samples were blanched for up to 3 min, with 1 min cooled in the ice water to stop the heating process and analyzed for color properties.

Figure 1. Slices of pineapple fruit

Combined Microwave and Convection Drying

The pre-blanched samples were then further dried using a microwave oven with 1,220 W power (NN-J993, Panasonic, Japan) (Figure 2) at four different temperatures: 110, 120, 130, and 140°C. The temperatures were set up accordingly using the microwave oven control panel. First, press the convection button on the control panel (Figure 2a). Then, turn the left knob clockwise to set the temperature (Figure 2a). The drying time was varied at 5, 10, 15, 20, 25, and 30 min for each temperature, respectively, by turning clockwise the right knob on the control panel (Figure 2b) (Izli et al., 2018; Maskan, 2001). For every 5 min, the dried pineapple sample color was taken using a portable colorimeter (WR-18, FRU, China).

Color Analysis

The effect of blanching and combined microwave and convection drying were observed through color analysis. A colorimeter (WR-18, FRU, China) determined the samples' color after blanching and drying. The quantitative attribute of colorfulness, also known as

(a)

(b)

Figure 2. The microwave oven (a) left and (b) right control panel (NN-J993, Panasonic, Japan)

chroma (C) and total color difference (TCD), was calculated using Equations 1 and 2 (Izli et al., 2018):

$$C = \sqrt{a*^2 + b*^2} \quad (1)$$

$$TCD = \sqrt{(L* - L_o*)^2 + (a* - a_o*)^2 + (b* - b_o*)^2} \quad (2)$$

where, a* = Redness or greenness of the sample; a_0* = Redness or greenness of the standard tile; b* = Yellowness or blueness of the sample; b_0* = Yellowness or blueness of the standard tile; L* = Whiteness or brightness of the sample; and L_0* = Whiteness or brightness of the standard tile.

Mathematical Models and Kinetic Analysis for Color of Blenched and Dried Pineapple Fruit

The parameter of L*, a*, b*, C*, and TCD is used to estimate the color changes of pineapple slices. The two models were chosen to study the effect of color changes due to blanching and drying: zero order and first order. Equation 3 below shows the zero-order model equation (Maskan, 2001):

$$P = P_0 - kt \quad (3)$$

where, P is the parameter to be estimated, the subscript 0 indicates the parameter's initial value, t is the drying time, and k is the rate constant at temperature. The equation was then rearranged into Equation 4, as Gonçalves et al. (2010) proposed to plot the zero-order equation graph.

$$1 - \frac{P}{P_o} = kt \quad (4)$$

where, the y-axis is $\left(1 - \frac{P}{P_0}\right)$, the x-axis is the duration of drying in minutes (t), and the slope of the graph is determined as the kinetic reaction rate. Equation 5 shows the first-order equation model proposed by Gonçalves et al. (2010) and Maskan (2001):

$$\frac{P}{P_0} = e^{-kt} \quad (5)$$

Equation 5 is then converted into Equation 6 to plot the first-order graph:

$$\ln\left(\frac{P}{P_0}\right) = -kt \quad (6)$$

where, y-axis: $\ln\left(\frac{P}{P_0}\right)$; x-axis = duration of drying (t, min); and slope of the graph = kinetic reaction rate (-k).

Statistical Analysis

Using statistical tools SigmaPlot (version 18.0), data analysis and mass modeling prediction were carried out. The standard error of the estimate (SEE) and coefficient of determination (R^2) were chosen as the parameters to assess the applicability of the regression models. The models with higher R^2 and smaller SEE numbers were chosen as appropriate. The R^2 value near 1.00 for regression equations generally shows a good fit with the model (Shahbazi & Rahmati, 2012).

RESULT AND DISCUSSION

Color Characteristics of Pineapple Fruit

Pineapple fruits' flesh variety MD2 before blanching and drying was yellowish, translated in the color parameters shown

in Table 1. Before blanching and drying, the pineapple fruits' flesh has a value of 39.2 for the L* parameter indication on the brightness. Furthermore, the positive value of a* parameter is 2.4, which indicates a shift towards redness. The redness of the pineapple was based on the sugar content of the fruit (Ding & Syazwani, 2016). On the other hand, the positive value of the b* parameter, which is 37.3, suggests a shift towards yellowness. This finding was similar to the study by Romli et al. (2019), which detected the b* value was 33.20±0.83 for MD2 pineapple with index 4 maturity. The combination of the a* parameter (2.4) and b* parameter (37.3) shows that the color of the flesh of pineapple fruit is light yellow based on the CIELAB color chart.

Table 1
Initial characteristics of pineapple fruit variety MD2

Parameter	Initial value
L*	39.2
a*	2.4
b*	37.3
Chroma (C)	37.3
Total color difference (TCD)	0.0

Effect of Microwave Drying on the Color of Pineapple Fruits without Blanching as Pretreatment

Based on Figure 3, the value of L* had a slight increase (P<0.05) as the duration time increased (5 to 30 min) for all the temperatures. After drying, the value of L* at 110°C (5 min) is 39.3 and increased to 47 (25 min). However, at a duration of 30 min, the value of L* had decreased to 44.8. The same trends are also shown at temperature 120°C, where the L*value increases from minute 5 (51.7) to minute 25 (52.6) but decreases to 52.2 in minute 30. As for temperatures 130 and 140°C, the L* values increased from minute 5 to minute 25. According to Ramallo and Mascheroni (2012), the variations of L* values were not significant during pineapple drying. This parameter was not affected by process temperature. Similar observations about L* values were reported by Krokida and Maroulis (1999) during apple, banana, carrot, and potato drying.

Figure 4 shows the a* value for the flesh of pineapple fruits. It can be observed that the a* value at the temperature 140°C was the lowest compared to the other drying temperature. Drying at a temperature of 110°C showed the most significant increase from 13.5 (5 min) to 40.9 (30 min) (P<0.05). While for temperature 120°C, the a* value increased from 9.2 (5 min) to 26.0 (10 min) before decreasing to 6.5 at minute 20. Then

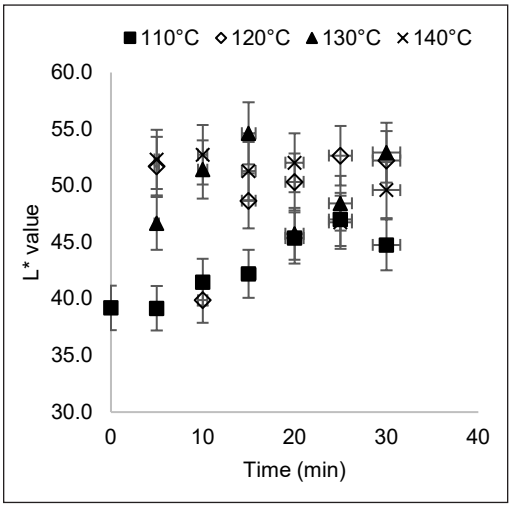

Figure 3. The effect of microwave drying (110, 120, 130, and 140°C) without blanching on the color parameters of pineapple fruits: Lightness (L*)

it increases again to 22.2 at minute 30. As for temperature 130℃, it was observed that a* value increased from 5.9 (5 min) to 14. 2 (30 min). The same increasing trend also shows at temperature 140℃. The increase in a* values as the drying temperatures increased, and the drying method lowered green pigmentation without increasing the yellow color (Ramallo & Mascheroni, 2012). Ramallo and Mascheroni (2012) reported that the increase of a* and b* parameters of pineapple fruit was independent of the drying temperature, where they found the relative visual yellow color (b* value) was slightly increased during drying at 45 and 60℃, and practically remained without changes during the drying at 75℃. The authors found that values of parameter b* remained constant during thermal processing at 70℃. Overall, the a* value is not dependent on the drying temperature as it does not show an increasing or decreasing trend, as Ramallo and Mascheroni (2012) stated.

Figure 5 shows that the value of b* after drying at 110℃ at 5 min is 51.5 and increased to 86.0 at 30 min. A similar trend can also be seen in temperatures 120 and 130℃. The result shows that the b* value increased significantly as temperature and duration time increased. Overall, it can be concluded that as the temperature and time of drying increases, the b* parameter also increases, resulting in the yellowness of fruit after drying.

Based on Figure 6, the value of chroma after drying at 110℃ at 5 min is 53.5 and increased to 95.2 at 30 min. For 120℃, the value of chroma at 5 min, that is 54.8, increases to 79.5 at 30 min. The same increasing trend also showed for temperature 130℃. While for temperature 140℃, the chroma's value decreases slightly from 37.3 (5 min) to 36.9 (30 min). This result is similar to the findings by Guine et al. (2012), where they stated that the chroma of dried pumpkin decreased significantly with freeze

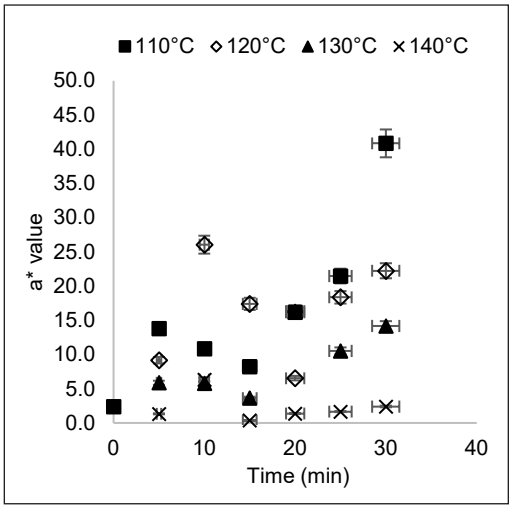

Figure 4. The effect of microwave drying (110, 120, 130, and 140℃) without blanching on the color parameters of pineapple fruits: Redness (a*)

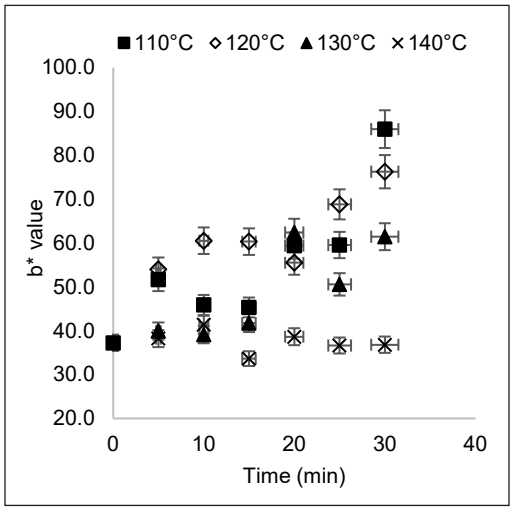

Figure 5. The effect of microwave drying (110, 120, 130, and 140℃) without blanching on the color parameters of pineapple fruits: Yellowness (b*)

drying. Since the chroma value was observed to increase for temperatures 110, 120, and 130°C and only decrease at temperature 140°C, it can be concluded that the effect of drying on the chroma color of the pineapple fruit is as the temperature and time of drying increases, the chroma value increases. The proportion of the grey component that defines a color is connected to the chroma parameter (Shamsudin et al., 2022). The intensity of the hue increased as the chroma rose.

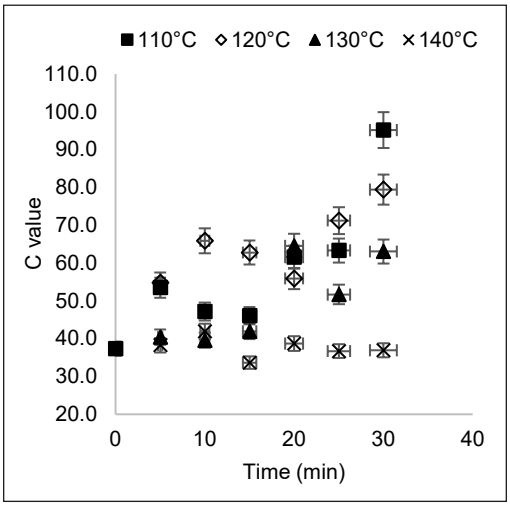

Figure 6. The effect of microwave drying (110, 120, 130, and 140°C) without blanching on the color parameters of pineapple fruits: Chroma value (C)

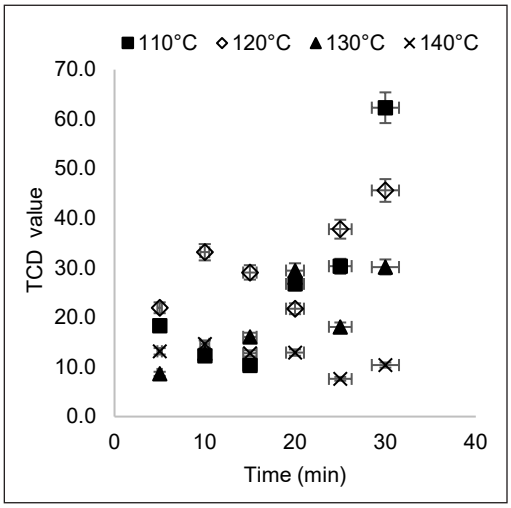

Figure 7. The effect of microwave drying (110, 120, 130, and 140°C) without blanching on the color parameters of pineapple fruits: Total color difference (TCD)

Based on Figure 7, the TCD value after drying increases as the time duration increases. At a temperature of 110°C, TCD increased from 18.4 at 5 min to 62.3 at 30 min. The same trend was observed at temperatures 110, 120, 130, and 140°C. A study by Mohammadi et al. (2008) also showed the same trend for TCD, stating that TCD increased as the air temperature increased.

Effect of Blanching Pretreatment and Drying on the Color of Pineapple Fruits

Figure 8 shows the effect of blanching on the color parameter L* of dried pineapple fruits. Based on the figure, the L* parameter for no blanched, blanched at 50°C, and blanched at 60°C shows the increasing trend as the time increased. Comparing no blanched

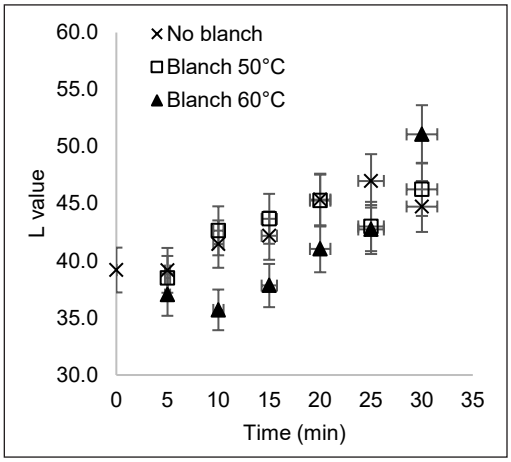

Figure 8. The effect of blanching (50 and 60°C) and microwave drying (110°C) on the color parameters of pineapple fruits: Lightness (L*)

and blanched at 50 and 60°C, the L* value at 60°C is lower than no blanch and blanch at 50°C at minute 5 to minute 25. While the L* value, when subjected to no blanched and blanched at 50°C, is nearly the same and does not show much difference. It may occur due to the lower temperature of blanching that does not affect the color of the pineapple slices. To conclude, blanching can affect the L* value by lowering it when the subject blanches at 60°C. The lower value of L* indicates the samples turn darker. A similar result was also observed by Deylami et al. (2016), where they discovered a significant (P<0.05) decrease in hunter L∗ value as the temperature of thermal treatment increased from temperature 60 to 100°C indicating that the mangosteen pericarp extracts became darker at higher temperatures.

Figure 9 shows the effect of blanching on color parameter a* of dried pineapple fruits. Based on Figure 9, the a* parameter, when blanched at a temperature of 60°C, has the highest a* value at minute 5 (20.3) until minute 20 (28.8) compared when no blanch and when blanched at 50°C. After minute 20, a* parameter for pineapple slices that blanch at 60°C decreases to 13.5 and then increases again to 16 at minute 30. While for conditions with no blanch and blanch at 50°C, their a* value does not show a significant difference (P>0.05) and is nearly the same. It may be due to the lower temperature of blanching that does not affect the color changes in pineapple slices. It has been proven by Verlinden et al. (2000) that a lower blanching temperature of 55°C reduces the physical breakdown of the fruit. The graph shows that the temperature of blanching pretreatment at 60°C increases the a* parameter, indicating the color of pineapples to shift to the redness.

Figure 10 shows the effect of blanching on color parameter b* of dried pineapple fruits. The different conditions of pretreatment, either no blanched, blanched 50°C, and

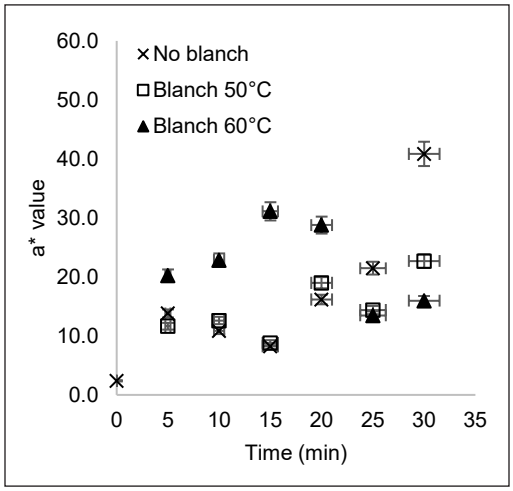

Figure 9. The effect of blanching (50 and 60°C) and microwave drying (110°C) on the color parameters of pineapple fruits: Redness (a*)

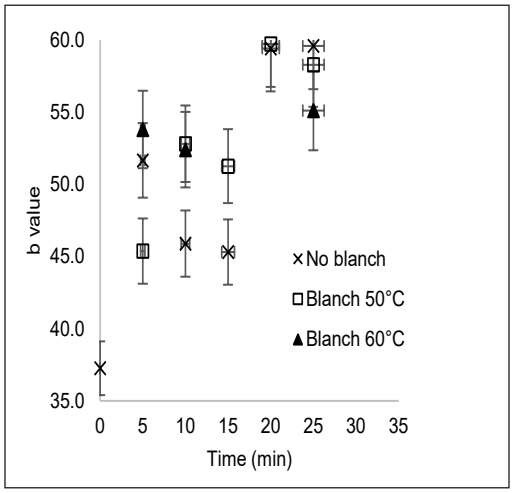

Figure 10. The effect of blanching (50 and 60°C) and microwave drying (110°C) on the color parameters of pineapple fruits: Yellowness (b*)

blanched 60°C independent of different pretreatment conditions. Figure 9 shows that the b* value for all three conditions is inconsistent with the presence of blanching or without blanching, making it independent of all three different pretreatment conditions.

Figure 11 shows the effect of blanching on the color parameter chroma of dried pineapple fruits. The chroma value for all conditions shows an increasing trend as time increases. Pineapple slices subjected to blanching at 60°C show the highest chroma value from minute 5 until minute 20. Then, the chroma value decreases to 56.8 (minute 25) and increases to 72.5 at minute 30. Pineapple slices subjected to no blanch and blanch at 50°C also show an increasing trend in chroma value, indicating an increase in intensity or saturation of the color. The vividness or saturation of color does change as the temperature and time of blanching increase (Demirhan & Özbek, 2015; Manjunatha et al., 2019; Onwude et al., 2016; Shamsudin et al., 2022).

Figure 12 shows the effect of blanching on the TCD parameter of dried pineapple fruits. Based on the figure, the TCD value for all conditions shows an increasing trend as the time increases from minute 5 to minute 30. Pineapple slices subjected to blanching at 60°C showed the highest TCD value compared to the other pretreatment conditions from minute 5 until minute 20. Then, the chroma value decreases to 21.3 (minute 25) and increases to 37.9 (minute 30). As for no blanch pineapple slices, it showed the lowest TCD value at minute 25. To conclude, the blanching pretreatment can affect the TCD value. As the temperature of blanching increases, the TCD value also increases. Overall, blanching pretreatment prior to drying can change the color of pineapple slices, turning the lightness of the pineapple darker and turning the color to redness when compared to no blanching. Nevertheless, it maintains the yellowness in the pineapple slice. Thus, in terms of color parameters, blanching pretreatment

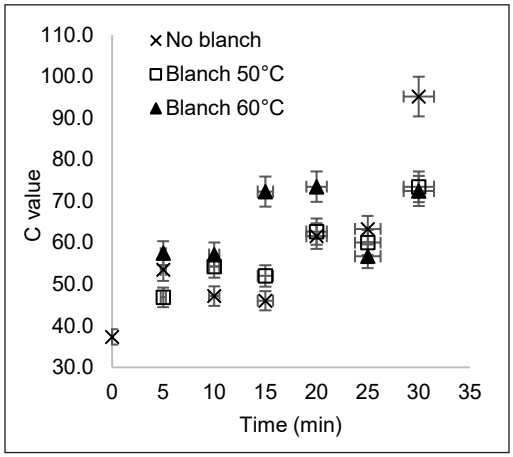

Figure 11. The effect of blanching (50 and 60°C) and microwave drying (110°C) on the color parameters of pineapple fruits: Chroma value (C)

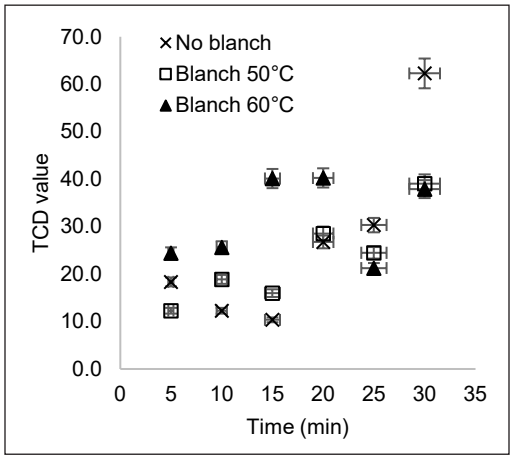

Figure 12. The effect of blanching (50 and 60°C) and microwave drying (110°C) on the color parameters of pineapple fruits: Total color difference (TCD)

is not suggested prior to drying since it can cause color degradation in pineapple slices compared to no blanching.

Modeling of Color Changes

Figure 13 shows L* values data fitted mn in the zero-order kinetic model. Based on Table 2, the k values for the L* parameter at 110, 120, 130, and 140°C for the zero-order model are -0.0066, -0.0097, -0.0117, and -0.0116, respectively. These values show the increasing trend, which also can be observed in the graph as in Figure 13 from temperature 110 to 130°C but decreased at temperature 140°C. As the slope of the graph becomes steeper with time, the k value also increases, which indicates the changes in the L* parameter. A similar trend was also observed for the first-order kinetic model. Based on Table 2, the k values for the L* parameter at 110, 120, 130, and 140°C for the first-order model are 0.0061, 0.0082, 0.0097, and 0.0061, respectively. Based on the tabulated data in Figure 14, it shows L*

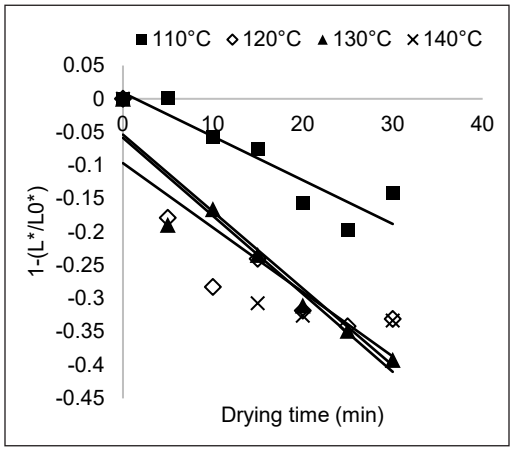

Figure 13. Zero-order kinetic model of the effect of microwave drying (110, 120, 130, and 140°C) on the color parameters of pineapple fruits: Lightness (L)

Table 2
The reaction rate (k) and coefficient of determination (R^2) for the first- and zero-order kinetic model of color parameter variations (L, a*, b*, C, and TCD) in dried pineapple fruit*

Parameter	Kinetic model	Temperature (°C)	k	R^2
L	Zero-order	110	-0.0066	0.8327
		120	-0.0097	0.7454
		130	-0.0117	0.9110
		140	-0.0116	0.8017
	First-order	110	0.0061	0.8408
		120	0.0082	0.7203
		130	0.0097	0.8857
		140	0.0061	0.8408
a	Zero-order	110	-0.4046	0.7152
		120	-0.2497	0.9107
		130	-0.1643	0.7429
		140	-0.0647	0.8586
	First-order	110	-0.0699	0.7293
		120	0.0621	0.7543
		130	0.0486	0.7391
		140	0.0483	0.5454
b	Zero-order	110	-0.0336	0.7320
		120	-0.0272	0.7888
		130	-0.0225	0.7091
		140	-0.0111	0.9147
	First-order	110	0.0218	0.7722
		120	0.0182	0.7469
		130	0.0174	0.7469
		140	0.0105	0.9203
C	Zero-order	110	-0.0406	0.7221
		120	-0.0292	0.7098
		130	-0.0252	0.7364
		140	-0.0109	0.8950
	First-order	110	0.0247	0.7699
		120	0.0208	0.8002
		130	0.0190	0.7726
		140	0.0103	0.9004
TDC	Zero-order	110	-0.0804	0.7114
		120	-0.0373	0.8445
		130	-0.0546	0.8256
		140	-0.0456	0.9839
	First-order	110	0.0472	0.8098
		120	0.0282	0.7041
		130	0.0356	0.8600
		140	0.0376	0.9693

data fitted in the first-order kinetic model. The zero-order and first-order kinetic models adequately described the degradation of L* values of pineapple slices over the entire temperature range. The coefficient of determination values (R^2) ranged between 0.7454 and 0.9110 for zero-order and 0.7203 and 0.8857 for the first-order kinetic model. This finding is supported by Chutintrasri and Noomhorm (2007), who discovered that the L* parameter followed the first-order kinetic reaction. In addition, Ansari et al. (2015) also found the same result where both models can be used adequately.

Based on Table 2, the value of k for a* parameter for zero order at temperatures 110, 120, 130, and 140°C were -0.4046, -0.2497, -0.1643, and -0.0647, respectively. These k value increase as the drying temperature increase from 110 to 140°C, which indicates the changes in a* parameter as the temperature change. Figure 15 shows that the slope (k) is steeper as temperature increases. The value of k for a* parameter for first order at temperatures 110, 120, 130, and 140°C were -0.0699, 0.0621, 0.0486, and 0.0483, respectively. These k value shows decreasing trends as the drying temperature increases, indicating the changes in a* parameter as the temperature increases. The data a* parameter was observed to be the best fit with zero order with the highest R^2 value (between 0.7152 to 0.9107) compared with the first order with a range between 0.5454 to 0.7543. The first-order kinetic model is presented in Figure 16. This result is agreed with Mohammadi et al. (2008), where they found that a* parameter followed the first-order model for color changes of kiwi fruit due to hot air drying.

Based on Table 2, the value of k for the b* parameter for zero order at temperatures 110, 120, 130, and 140°C were -0.0336, -0.0272, -0.0225, and -0.0111, respectively. Figure 17 shows that the slope indicating the k value decreases as temperature increases, which translates to lower k as temperature increases. A similar decreasing trend was also observed in the first-order kinetic model

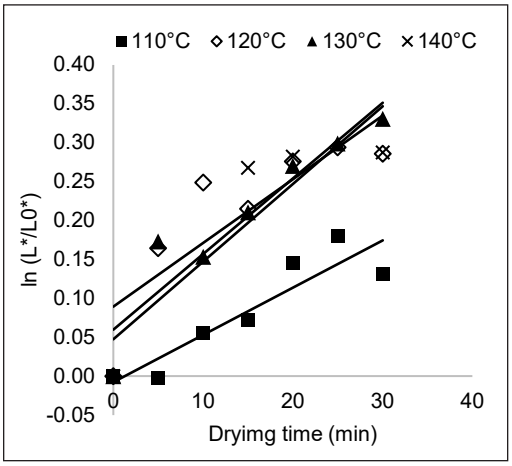

Figure 14. First-order kinetic model of the effect of microwave drying (110, 120, 130, and 140°C) on the color parameters of pineapple fruits: Lightness (L*)

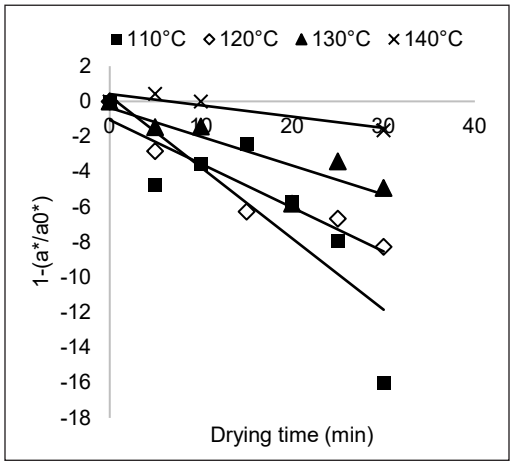

Figure 15. Zero order kinetic model of the effect of microwave drying (110, 120, 130, and 140°C) on the color parameters of pineapple fruits: Redness (a*)

where the k values were 0.0218 (110°C), 0.0182 (120°C), 0.0174 (130°C), and 0.0105 (140°C). Figure 18 shows the first-order graph for the b* parameter. The value R^2 for zero and first order is 0.7091-0.9147 and 0.7468-0.9147, respectively. High coefficient determination (R^2) for these models proves that the b* parameter changes best fit both models. Mohammadi et al. (2008) also observed the same result where first-order kinetic fits best. In addition, Ansari et al. (2015) also found the same result, where both models can be used adequately.

The values of k for the chroma parameter for zero order at temperatures 110, 120, 130, and 140°C were -0.0406, -0.0292, -0.0252, and -0.0109, respectively, as demonstrated in Table 2. The value of k is increasing as temperature increases. Figure 19 shows chroma values fitted with the zero-order kinetic model where the slope increases as the drying temperature increases, indicating the increase in the k value. A decreasing trend was observed in the first-order kinetic model where the k values were decreased from 0.0247 (110°C), 0.0208 (120°C), 0.0190 (130°C), and 0.0103 (140°C). Figure 20 shows the experimental data of chroma that fitted with the first model. Table 2 shows that the zero and first-order kinetic model best fits the chroma parameter with R^2 value

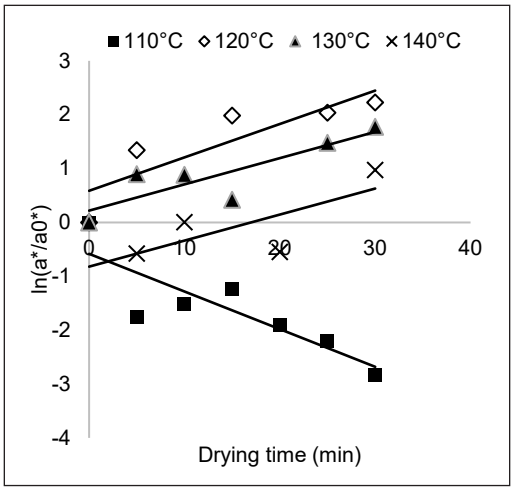

Figure 16. First-order kinetic model of the effect of microwave drying (110, 120, 130, and 140°C) on the color parameters of pineapple fruits: Redness (a*)

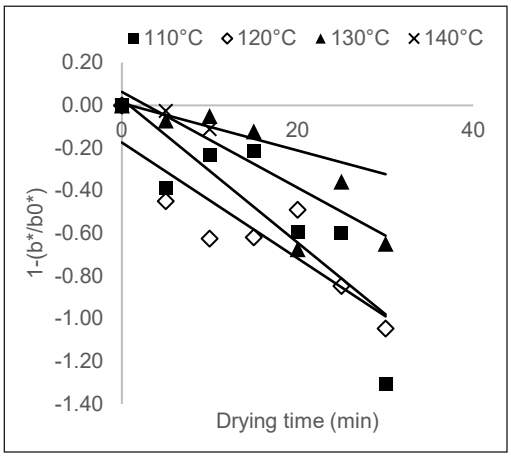

Figure 17. Zero order kinetic model of the effect of microwave drying (110, 120, 130, and 140°C) on the color parameters of pineapple fruits: Yellowness (b*)

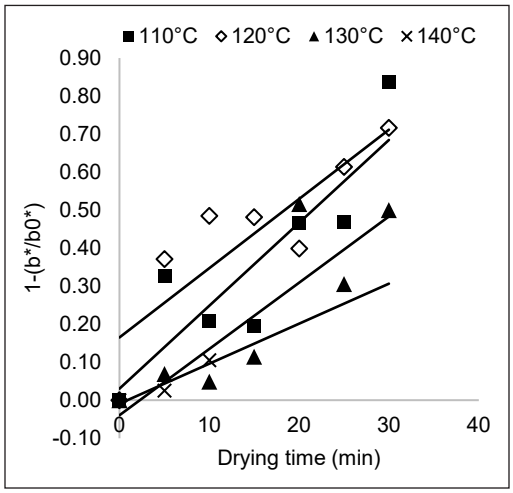

Figure 18. First-order kinetic model of the effect of microwave drying (110, 120, 130, and 140°C) on the color parameters of pineapple fruits: Yellowness (b*)

of 0.7098 to 0.8950 and 0.7699 to 0.9004, respectively. This finding agreed with the result of Demirhan and Özbek (2015), who found that the chroma best fits the first order for microwave drying the tea leaves.

Based on Table 2, the values of k for TCD for zero order at temperatures 110, 120, 130, and 140℃ were -0.0804, -0.0373, -0.0546, and -0.0456, respectively. These k values show inconsistent trends as the drying temperature increases, making it independent of drying time. Figure 21 shows the TCD values fitted in the zero-order kinetic model. A similar result was also observed for first-order kinetic, where the k value for TCD at temperatures 110, 120, 130, and 140℃ were 0.0472, 0.0282, 0.0356, and 0.0376. Figure 22 shows the

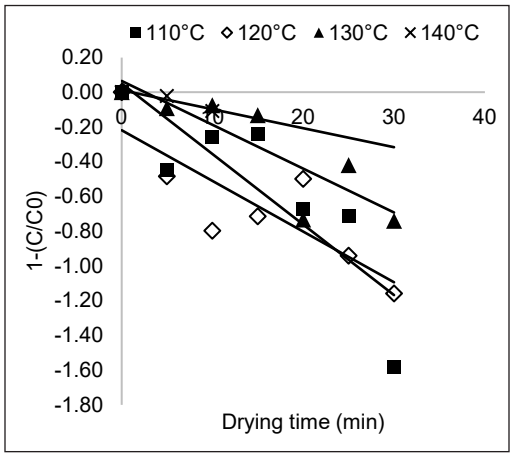

Figure 19. Zero-order kinetic model of the effect of microwave drying (110, 120, 130, and 140℃) on the color parameters of pineapple fruits: Chroma value (C)

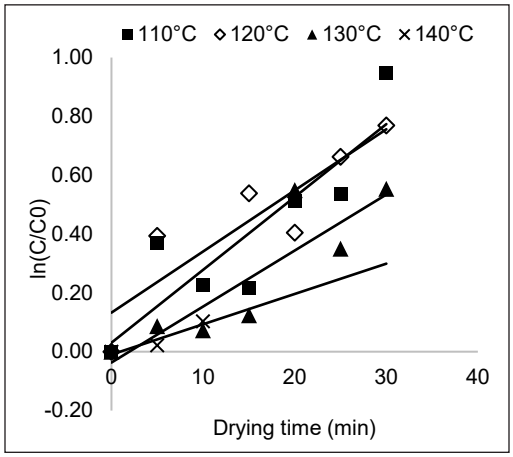

Figure 20. First-order kinetic model of the effect of microwave drying (110, 120, 130, and 140℃) on the color parameters of pineapple fruits: Chroma value (C)

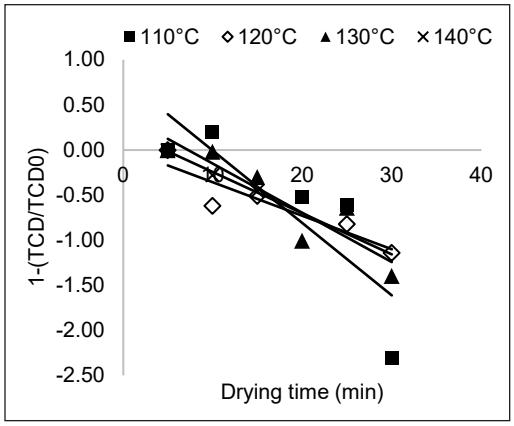

Figure 21. Zero-order kinetic model of the effect of microwave drying (110, 120, 130, and 140℃) on the color parameters of pineapple fruits: Total color difference (TCD)

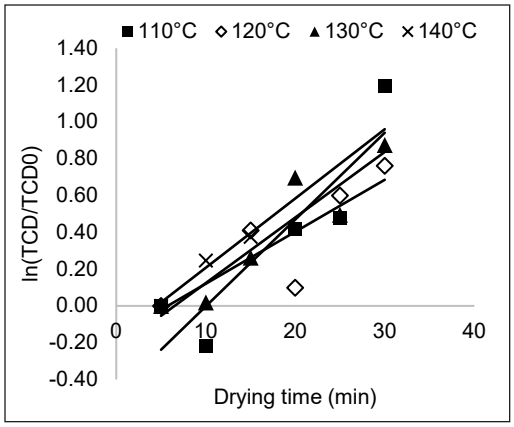

Figure 22. First-order kinetic model of the effect of microwave drying (110, 120, 130, and 140℃) on the color parameters of pineapple fruits: Total color difference (TC)

TCD data that fitted with the first model. Table 2 shows that the zero and first-order kinetic model best fits the TCD parameter with the R^2 value of 0.7114 to 0.9839 and 0.7041 to 0.9693, respectively. Chutintrasri and Noomhorm (2007) also found that the zero-order kinetic model fitted well to TCD.

CONCLUSION

Pre-blanching prior to drying affects the color of the pineapple as the L* value moves toward darker, reduces the a* value, and maintains the b* value by comparing it with the unblanched pineapple. Hence, pre-blanching is not suggested as it causes color degradation. During drying using the microwave technique, the L* values increased as the temperature as well as time increased. Meanwhile, the a* value showed no effect on the different temperatures or times of drying. Furthermore, the drying pineapple tended to gain yellowness and became saturated as the drying time and temperature increased. The kinetic modeling of color changes gives the result of L* b*, C, and TCD were all fitted with zero (R^2: 0.7091–0.9839) and first order (R^2: 0.7041–0.9693). As for the a* parameter, the kinetic modeling only fitted with zero order (R^2: 0.7152–0.9107). In conclusion, different drying time and temperature does give significant changes.

ACKNOWLEDGEMENTS

The authors express their gratitude to the Universiti Putra Malaysia for providing financial and technical support under grant GP-IPB/9687803 to conduct this research work.

REFERENCES

Abd Rahman, N. F. (2020). *Physicochemical and antioxidant properties of pamelo residues using different drying methods and kinetic models of naringin degradation* [Doctoral's thesis, Maejo University]. Maejo University Publications. http://ir.mju.ac.th/dspace/bitstream/123456789/454/1/6003507002.pdf

Abdul Halim, A. A. (2021). *Physical characteristics and effects of blanching treatment on the color and textural properties of dabai fruit (*Canarium odontophyllum *miq.)* variety "ngemah" [Unpublished Bachelor's dissertation]. Universiti Putra Malaysia.

Abdul Halim, A. A., Shamsudin, R., Ariffin, S. H., Zainol @ Abdullah, W. N. Z., & Azmi, N. S. (2022). Kinetic models on quality changes during heat blanching of some fruit and vegetables. *Advances in Agricultural and Food Research Journal*, *3*(1), a0000265. https://doi.org/10.36877/aafrj.a0000265

Agarry, S. E., Ajani, A. O., & Aremu, M. O. (2013). Thin layer drying kinetics of pineapple: Effect of blanching temperature – Time combination. *Nigerian Journal of Basic and Applied Sciences*, *21*(1), 1-10. https://doi.org/10.4314/njbas.v21i1.1

Ahmed, J. (2011). Drying of vegetables: Principles and dryer design. In N. K. Sinha (Ed.), *Handbook of vegetables and vegetable processing* (pp. 279–298). Blackwell Publishing Ltd. https://doi.org/10.1002/9780470958346.ch13

Akter, M. S., Ahmed, M., & Eun, J.-B. (2010). Effect of blanching and drying temperatures on the physicochemical characteristics, dietary fiber composition and antioxidant-related parameters of dried persimmons peel powder. *International Journal of Food Sciences*

and Nutrition, *61*(7), 702–712. https://doi.org/10.3109/09637481003757852

Alam, M. S., Gupta, K., Khaira, H., & Javed, M. (2013). Quality of dried carrot pomace powder as affected by pretreatments and methods of drying. *Agricultural Engineering International: CIGR Journal*, *15*(4), 236–243.

Ansari, S., Maftoonazad, N., Hossein, S. E., Farahnaky, A., & Asadi, G. H. (2015). Kinetic of color and texture changes in rehydrated figs. *Tarım Bilimleri Dergisi*, *21*(1), 108–122. https://doi.org/10.15832/tbd.47774

Ceballos, A. M., Giraldo, G. I., & Orrego, C. E. (2012). Effect of freezing rate on quality parameters of freeze dried soursop fruit pulp. *Journal of Food Engineering*, *111*(2), 360–365. https://doi.org/10.1016/j.jfoodeng.2012.02.010

Chutintrasri, B., & Noomhorm, A. (2007). Color degradation kinetics of pineapple puree during thermal processing. *LWT - Food Science and Technology*, *40*(2), 300–306. https://doi.org/10.1016/j.lwt.2005.11.003

Dandamrongrak, R., Mason, R., & Young, G. (2003). The effect of pretreatments on the drying rate and quality of dried bananas. *International Journal of Food Science and Technology*, *38*(8), 877–882. https://doi.org/10.1046/j.0950-5423.2003.00753.x

Demirhan, E., & Özbek, B. (2015). Color change kinetics of tea leaves during microwave drying. *International Journal of Food Engineering*, *11*(2), 255–263. https://doi.org/10.1515/ijfe-2014-0276

Deylami, M. Z., Rahman, R. A., Tan, C. P., Bakar, J., & Olusegun, L. (2016). Effect of blanching on enzyme activity, color changes, anthocyanin stability and extractability of mangosteen pericarp: A kinetic study. *Journal of Food Engineering*, *178*, 12–19. https://doi.org/10.1016/j.jfoodeng.2016.01.001

Ding, P., & Syazwani, S. (2016). Physicochemical quality, antioxidant compounds and activity of MD-2 pineapple fruit at five ripening stages. *International Food Research Journal*, *23*(2), 549-555.

Fan, L., Zhang, M., & Mujumdar, A. S. (2006). Effect of various pretreatments on the quality of vacuum-fried carrot chips. *Drying Technology*, *24*(11), 1481–1486. https://doi.org/10.1080/07373930600952826

Garba, U., Kaur, S., Gurumayum, S., & Rasane, P. (2015). Effect of hot water blanching time and drying temperature on the thin layer drying kinetics and anthocyanin degradation of black carrot (*Daucus carota* L.) shreds. *Food Technology and Biotechnology*, *53*(3), 324-330. https://doi.org/10.17113/ftb.53.03.15.3830

Gonçalves, E. M., Pinheiro, J., Abreu, M., Brandão, T. R. S., & Silva, C. L. M. (2010). Carrot (*Daucus carota* L.) peroxidase inactivation, phenolic content and physical changes kinetics due to blanching. *Journal of Food Engineering*, *97*(4), 574–581. https://doi.org/10.1016/j.jfoodeng.2009.12.005

Hidayat, T., & Setyadjit. (2019). Effect of pre-treatment on the physicochemical characteristics of potato powder dried by drum dryer. In *IOP Conference Series: Earth and Environmental Science* (Vol. 309, No. 1, p. 012056). IOP Publishing. https://doi.org/10.1088/1755-1315/309/1/012056

Izli, N., Izli, G., & Taskin, O. (2018). Impact of different drying methods on the drying kinetics, color, total phenolic content and antioxidant capacity of pineapple. *CyTA - Journal of Food*, *16*(1), 213–221. https://doi.org/10.1080/19476337.2017.1381174

Karam, M. C., Petit, J., Zimmer, D., Djantou, E. B., & Scher, J. (2016). Effects of drying and grinding in production of fruit and vegetable powders: A review. *Journal of*

Food Engineering, *188*, 32–49. https://doi.org/10.1016/j.jfoodeng.2016.05.001

Kingsly, R. P., Goyal, R. K., Manikantan, M. R., & Ilyas, S. M. (2007). Effects of pretreatments and drying air temperature on drying behaviour of peach slice. *International Journal of Food Science and Technology*, *42*(1), 65–69. https://doi.org/10.1111/j.1365-2621.2006.01210.x

Krokida, M. K., & Maroulis, Z. B. (1999). Effect of microwave drying on some quality properties of dehydrated products. *Drying Technology*, *17*(3), 449–466. https://doi.org/10.1080/07373939908917545

Lahsasni, S., Kouhila, M., Mahrouz, M., Mohamed, L. A., & Agorram, B. (2004). Characteristic drying curve and mathematical modeling of thin-layer solar drying of prickly pear cladode (*Opuntia ficus-indica*). *Journal of Food Process Engineering*, *27*(2), 103–117. https://doi.org/10.1111/j.1745-4530.2004.tb00625.x

Manjunatha, S. S., Mathews, A. T., & Patki, P. E. (2019). Modelling the kinetics of mass transfer and change in colour during deep fat frying of green peas (*Pisum sativum* L.) at different frying temperatures. *Heat Mass Transfer*, *55*, 3087–3102. https://doi.org/10.1007/s00231-019-02637-7

Maskan, M. (2001). Kinetics of colour change of kiwifruits during hot air and microwave drying. *Journal of Food Engineering*, *48*(2), 169–175. https://doi.org/10.1016/s0260-8774(00)00154-0

Mohammadi, A., Rafiee, S., Emam-Djomeh, Z., & Keyhani, A. (2008). Kinetic models for colour changes in kiwifruit slices during hot air drying. *World Journal of Agricultural Sciences*, *4*(3), 376–383.

Onwude, D. I., Hashim, N., Janius, R., Nawi, N. M., & Abdan, K. (2016). Color change kinetics and total carotenoid content of pumpkin as affected by drying temperature. *Italian Food Science*, *29*(1), 1-18.

Orsat, V., Changrue, V., & Vijaya Raghavan, G. S. (2006). Microwave drying of fruits and vegetables. *Stewart Postharvest Review*, *2*(6), 1–7. https://doi.org/10.2212/spr.2006.6.4

Radojčin, M., Pavkov, I., Bursać Kovačević, D., Putnik, P., Wiktor, A., Stamenković, Z., Kešelj, K., & Gere, A. (2021). Effect of selected drying methods and emerging drying intensification technologies on the quality of dried fruit: A review. *Processes*, *9*(1), 132. https://doi.org/10.3390/pr9010132

Ramallo, L. A., & Mascheroni, R. H. (2012). Quality evaluation of pineapple fruit during drying process. *Food and Bioproducts Processing*, *90*(2), 275–283. https://doi.org/10.1016/j.fbp.2011.06.001

Romli, R., Murad, M., Wan Nur Hafzan, W. M., & Haris, H. (2019). Physicochemical properties and sensory acceptability of pineapples of different varities and stages of maturity. *Food Research*, *3*(5), 491-500. https://doi.org/10.26656/fr.2017.3(5).060

Shahbazi, F., & Rahmati, S. (2012). Mass modeling of fig (*Ficus carica* L.) fruit with some physical characteristics. *Food Science and Nutrition*, *1*(2), 125–129. https://doi.org/10.1002/fsn3.20

Shahidi, F. (2020). Does COVID-19 affect food safety and security? *Journal of Food Bioactives*, *9*, 1-3. https://doi.org/10.31665/jfb.2020.9212

Shamsudin, R., Ariffin, S. H., Zainol @ Abdullah, W. N. Z., Azmi, N. S., & Abdul Halim, A. A. (2022). Quality evaluation of color and texture of the dabai fruit (*Canarium odontophyllum* Miq.) at different temperatures and times of blanching. *Pertanika Journal of Science and Technology*, *30*(4), 2427-2438. https://doi.org/10.47836/pjst.30.4.07

Verlinden, B. E., yuksel, D., Baheri, M., Baerdemaeker, J. D., & Dijk, C. V. (2000). Low temperature blanching effect on the changes in mechanical properties during subsequent cooking of three

potato cultivars. *International Journal of Food Science and Technology*, *35*(3), 331-340. https://doi.org/10.1046/j.1365-2621.2000.00391.x

Xiao, H.-W., Pan, Z., Deng, L.-Z., El-Mashad, H. M., Yang, X.-H., Mujumdar, A. S., Gao, Z.-J., & Zhang, Q. (2017). Recent developments and trends in thermal blanching – A comprehensive review. *Information Processing in Agriculture*, *4*(2), 101–127. https://doi.org/10.1016/j.inpa.2017.02.001

Pertanika J. Trop. Agri. Sci. 46 (4): 1293 - 1308 (2023)

PERTANIKA JOURNALS

TROPICAL AGRICULTURAL SCIENCE

Journal homepage: http://www.pertanika.upm.edu.my/

Watermoss Mulching Stimulates the Productivity and Physiochemical Properties of Strawberry in the Tropical Ecosystem of Southern Bangladesh

Joydeb Gomasta[1]*, Md. Rashedul Islam[2], Md. Alimur Rahman[2], Monirul Islam[3], Pronita Mondal[4], Jahidul Hassan[1] and Emrul Kayesh[1]

[1]Department of Horticulture, Bangabandhu Sheikh Mujibur Rahman Agricultural University, Gazipur-1706, Bangladesh

[2]Regional Agricultural Research Station, Bangladesh Agricultural Research Institute, Barishal-8211, Bangladesh

[3]Pomology Division, Horticulture Research Centre, Bangladesh Agricultural Research Institute, Gazipur-1701, Bangladesh

[4]Agroctechnology Discipline, Khulna University, Khulna-9208, Bangladesh

ABSTRACT

Strawberry is one of the most lucrative antioxidants and phytochemicals enriched temperate fruits. Nevertheless, good-quality fruit production requires special soil management practices like mulching and other strategies in tropical and sub-tropical regimes with short and dry winters. In the present research, strawberry var. BARI Strawberry-3 was cultivated using Asian watermoss (AW), water hyacinth (WH), paddy straw (PS), black polythene (BP), and silver polythene (SP) mulching along with control at the tropical weather-inclined southern part of Bangladesh from October 2018 to April 2019. The aim was to evaluate the comparative influences of those organic and synthetic mulches on root and shoot growth phenology along with subsequent reproductive behaviors, fruit yield, and fruit biochemical properties of strawberries under such an ecosystem. The experiment was conducted in a randomized complete block design with four replications. Mulching exhibited statistical superiority over control for strawberry growth, yield, and fruit quality indicators, where organic mulches performed better than others. Among the mulches, AW mulching produced the healthiest plant, having maximum plant height (20.40 cm), leaf number (23.33 per plant), canopy diameter (34.30 cm), single leaf area (100.06 cm^2), and root length (19.05 cm) resulting in

ARTICLE INFO

Article history:
Received: 02 June 2023
Accepted: 06 July 2023
Published: 02 November 2023

DOI: https://doi.org/10.47836/pjtas.46.4.14

E-mail addresses:
joydeb@bsmrau.edu.bd (Joydeb Gomasta)
rashedhrc@gmail.com (Md. Rashedul Islam)
alimurbd@yahoo.com (Md. Alimur Rahman)
monirbdku@gmail.com (Monirul Islam)
pronita.ku@gmail.com (Pronita Mondal)
jhassan@bsmrau.edu.bd (Jahidul Hassan)
ekayeshhrt@bsmrau.edu.bd (Emrul Kayesh)
*Corresponding author

ISSN: 1511-3701
e-ISSN: 2231-8542

the highest root and shoot biomass. Though the plants received AW mulch required maximum duration from transplanting to flowering (47.88 days) and flowering to harvest (29.60 days), those plants produced the highest number of flowers (21.20 per plant) as well as fruits (19.63 per plant), and ultimately the utmost fruit yield (370.02 g/plant and 15.42 kg/ha) being significantly dissonant from all other treatments. Thus, a 57.57% yield increase over control was recorded from AW mulching. Furthermore, statistically, the maximum total soluble solids (TSS) (9.93%), TSS/acidity ratio (17.37), and vitamin C (58.30 mg/100 g), but the minimum titratable acidity (0.57%) content of strawberry was noticed in AW treatment. WH and BP mulches had statistical consistency with the best treatment for a few attributes. Therefore, crop residues, aquatic plants, or their by-products can be used as mulch for quality strawberry production in dry winter, especially in tropical and subtropical regions.

Keywords: Fruit crop, organic and inorganic mulching, plant growth, tropical environment, yield and quality

INTRODUCTION

Sustainable fruit production requires balanced nutrients, cultural practices, and a favorable environment for optimal quality and high biological value. Strawberries (*Fragaria x ananassa* Duch.), being one of the most fascinating and important temperate fruits, are well adapted in diverse geographical areas and, therefore, can be grown in the tropics and sub-tropics (Bakshi et al., 2014) provided that effective management practices are ensured. Besides its pleasant taste and other organoleptic attributes, strawberry can be regarded as a functional fruit since the fruit contains significant levels of bioactive compounds such as phenols, flavonoids, vitamin C, and anthocyanins that have antioxidant activity to support human health and immunity (D'Urso et al., 2015; Fernandes et al., 2012).

Despite its diverse climatic adaptability, the crop is very sensitive to moisture and nutrient fluctuations due to its surface-feeding nature. Therefore, moisture and temperature conditions in the topsoil layer largely influence the crop's growth and development. In Bangladesh, it grows well in the winter, especially October-November, the best planting time to complete its life cycle before the temperature rises in March (Paul et al., 2017). Being a winter or dry season crop, it has to face a lot of natural adversities like poor soil moisture and temperature fluctuation, especially during flowering and fruiting in tropical and sub-tropical areas like Bangladesh. Again, as its fruits lay in soil, soil-dwelling pathogens can easily invade and destroy it. Hence, the application of mulching to the crop field is an appropriate intercultural operation that can facilitate several advantages of conserving soil moisture, suppressing weed growth, checking soil erosion, and preventing berries from direct contact (Barche et al., 2015; Sharma & Goel, 2017).

Moreover, mulches suppress extreme fluctuations in soil temperature (daily and seasonal), reducing soil moisture loss through evaporation and assisting in maintaining soil fertility (Iqbal et al., 2016; Slathia & Paul, 2012). However, mulching practices can be executed with locally available organic or commercially inorganic materials. Besides Bangladesh being a Gangetic Delta, stagnant water bodies as well as water logging for more than eight months a year has been common scenario particularly in the mid to southern part (Awal & Islam, 2020; M. H. R. Khan et al., 2015), where water hyacinth (*Eichhornia crassipes* L.) and Asian watermoss (*Salvinia cucullata* Roxb.) are the two very commonly observed noxious aquatic weeds (Islam & Atkins, 2007).

In addition, *Salvinia cucullata* is one of the base materials for floating bed agriculture in the wetlands and water-stagnant southern region of the country (Irfanullah et al., 2011; Mondal et al., 2022; Sunder, 2020). At the same time, water hyacinth and paddy straw are two of the easily obtainable and well-known mulch materials for crop production (L. Kaur et al., 2021; Parsottambhai & Rawat, 2020; Sarangi et al., 2021). Therefore, the present research using naturally occurring plant products and readily feasible colored polythene mulch materials was conducted to evaluate the vegetative and reproductive growth influencing the yield and physiochemical properties of strawberries in tropical conditions of southern Bangladesh.

MATERIALS AND METHODS

Experimental Site, Design, and Layout

The present research was conducted in the research field (22.7881°N and 90.2926°E) and laboratory of the Regional Agricultural Research Station (RARS), Bangladesh Agricultural Research Institute (BARI), Barishal, Bangladesh from October 2018 to April 2019. The soil characteristics of the experiment site were silty clay in texture with neutral to slightly alkaline in the top- and sub-soil under the Barisal series of Gangetic Alluvium Soil Tract (Agroecological Zone 13: Ganges Tidal Floodplain) and about 10 m above the sea level (Z. H. Khan et al., 1998). The site's climate is tropical, with a hot and dry summer, long and humid monsoon, and short and dry winter (Table 1).

The experiment was set in a randomized complete block design (RCBD) with four replications. Plants were spaced 60 cm × 40 cm on 1.6 m × 1.2 m beds, each bed representing a replication, and beds were raised 24 cm above the main field with 60 cm space between beds. Each bed had 8 plants in two adjacent rows 60 cm apart. Twenty-five-day-old strawberry saplings were transplanted in the well-prepared beds on November 14, 2018, followed by providing intercultural operations and fertilization as required. Well-acclimatized tissue-cultured saplings of the variety BARI Strawberry-3 were brought from the Biotechnology Division, BARI, Bangladesh, and kept in nursery condition for three days prior to planting. Five different types of naturally available and synthetic materials

viz., paddy straw (*Oryza sativa* L.), water hyacinth (*Eichhornia crassipes* L.), Asian watermoss (*Salvinia cucullata* Roxb.), silver shine polyethylene (Toughsheet, United Kingdom), and black polythene (Toughsheet, United Kingdom) in addition to control (no mulch) were used as mulch components. All types of mulches were applied two days prior to transplanting the saplings.

Table 1
Monthly mean temperature (maximum and minimum), relative humidity, wind speed, rainfall, and solar radiation from October 2018 to April 2019

Month	Air temperature (ºC)			Rainfall (mm)	Relative humidity (%)		Sunshine (hrs/day)	Solar Radiation (g-cal/cm^2/day)
	Max.	Min.	Mean		7 a.m.	1.30 p.m.		
October 2018	30.56	23.19	26.87	2.79	94.32	66.81	5.33	302.01
November 2018	29.91	14.42	21.31	0.60	94.40	40.93	6.62	296.20
December 2018	24.43	13.77	19.10	0.14	89.74	55.23	5.27	241.80
January 2019	25.93	12.06	18.99	0.00	88.35	35.97	6.87	292.06
February 2019	28.47	15.20	21.84	2.35	89.79	48.57	7.15	345.56
March 2019	31.61	20.54	26.07	1.23	88.23	51.23	7.94	417.06
April 2019	33.05	22.95	28.00	2.61	91.93	55.47	8.36	447.72

Note. Max. = Maximum; Min. = Minimum

Nutrient Analysis of Mulch Materials

Organic mulch samples as applied to crop were taken to the laboratory for their physical and nutritional analyses where paddy straw, water hyacinth, and Asian watermoss were analyzed for organic carbon (C), nitrogen (N), phosphorous (P), potassium (K), calcium (Ca), magnesium (Mg), sulfur (S), and boron (B) following the standard guidelines as described in Official Methods of Analysis (Baur & Endminger, 2012). Organic C content in mulch samples was determined according to the wet oxidation method and expressed in percent. N content in the mulches was determined in the Kjeldhal procedure, and P was estimated by the modified Olsen method. While K, Ca, and Mg content was determined using the ammonium acetate (NH_4OAc) (Merck, Germany) method. On the other hand, S and B content in the mulch materials were estimated by calcium dihydrogen phosphate (Merck, Germany) extraction procedure and calcium chloride (Wako, Japan) extraction method, respectively. No analysis was done for polythene mulches. The analysis report is presented in Table 2.

Table 2
Analysis report of paddy straw, water hyacinth, and Asian watermoss

Sample	Organic C (%)	N (%)	P (%)	K (%)	Ca (%)	Mg (%)	S (%)	B (ppm)
Paddy straw	0.32	0.44	0.12	1.42	0.35	0.24	0.075	10
Water hyacinth	1.79	1.16	0.19	0.61	2.78	1.43	0.097	215
Asian watermoss	2.41	1.86	0.42	1.18	5.30	2.72	0.206	173

Measurement of Growth and Yield of Strawberry

Vegetative growth of the strawberry plant as affected by mulching was assessed by measuring plant height (cm), number of leaves per plant, petiole length (cm), canopy diameter (cm), individual leaf area (cm^2), and leaf relative greenness as Soil Plant Analysis Development (SPAD) value were recorded at full blossom stage preferably at 75 days after transplanting. On the other hand, individual leaf area (cm^2) and SPAD value were measured by an electric leaf area meter (Model: LI 3000, LI-COR, USA) and portable chlorophyll meter (Model: SPAD-502Plus; Konica Minolta, Japan), respectively, at full blossom. Runners developed by the transplants were removed as and when noticed on any plant. Flowering started on December 29, 2018, and various reproductive data, namely the number of days required from transplanting to the first flowering and first harvest, flowering to harvest duration, number of flowers, and fruits per plant, were noted against each replication under treatment.

Fruit was harvested when the color of the fruit changed from pink to red. Harvesting was initiated on January 25, 2019. Immediately after harvest, fruits were weighed (g), followed by measuring the fruit length (cm) and diameter (cm); sepals were removed and stored at -20ºC for biochemical analyses from fruit flesh. Fresh fruit samples were also dried in an electric oven at 72 ± 3ºC for three days to assess the dry matter content. Plants were carefully taken out of the ground with rhizosphere soil after the fruit harvest, the root systems and shoots were separated, they were washed under running water, and fresh weight (g) was recorded. Root length (cm) was also estimated, and dry weight (g) of the shoot and root was measured by drying the samples at 60ºC in the oven for a week.

Assessment of Biochemical Attributes

The stored as well as harvested fresh fruits were utilized for biochemical analyses. TSS, titratable acidity, TSS/acidity ratio, and vitamin C were estimated using standard procedures (Baur & Endminger, 2012). At room temperature, TSS was determined using a digital refractometer (Model: PAL-α, ATAGO, Japan). Results were expressed as percentages. Titratable acidity (TA) was measured using 5 g of fruit pulp, homogenized with 20 ml of purified water, and filtered to obtain a pure extract. Each extract (5 ml) was titrated against sodium hydroxide solution (0.1 N NaOH) (Sigma-Aldrich, Germany) using a

phenolphthalein indicator. Results obtained were expressed in the percentage of citric acid. The ratio of TSS to titratable acidity was also assessed. Vitamin C was measured using 2,6-dichlorophenol indophenol dye (Sigma-Aldrich, Germany) and expressed in mg/100 g of fresh fruit.

Statistical Analysis

All the collected data were gathered, analyzed, and presented as treatment means ± standard errors (SE) of four replicates (8 plants at each replication) after performing a one-way analysis of variance (ANOVA) where treatment means were separated using Fisher's protected least significance difference (LSD) test at $p \leq 0.05$. Statistix 10.0 analytical software was used for data analysis.

RESULTS

Shoot and Root Growth

Plant height, number of leaves per plant, petiole length, canopy diameter, single leaf area, leaf relative greenness (SPAD value), as well as root length of strawberry plants at full blossom varied significantly ($p \leq 0.05$) among the treatments (Table 3; Figure 1). Significantly, the tallest strawberry plant was noticed in the T_3 treatment (20.40 cm), being statistically unique with that of T_2 (19.70 cm), followed by both T_4 and T_5 treatments, respectively. Control treatment (T_0) exhibited the shortest plants (15.48 cm) at full blossom (Figure 1a). The number of leaves at full blossom was counted significantly maximum in T_3 (23.33 per plant), statistically different from all other treatments, followed by T_2 treatment (21.55 leaves/plant). Leaf petiole length was measured statistically similarly in all the mulch treatments but different from T_0 plants with shorter petiole. Again, plants under T_3 mulching exhibited a significant maximum canopy diameter (34.30 cm) at full blossom, which had statistical harmony with the T_2 treatment (32.68 cm).

Furthermore, single leaf area (100.06 cm^2), as well as leaf SPAD value (49.35), was also noticed to be significantly maximum in T_3 treatment; plants under T_2 treatment had statistical harmony in terms of single leaf area (99.95 cm^2) and leaf SPAD value (48.43), and the two-polythene mulch treatment (T_4 and T_5) followed the best treatment (Figures 1c and 1d). Control plants exhibited statistical inferiority in terms of number of leaves (15.95 per plant), petiole length (11.15 cm), canopy diameter (26.13 cm), single leaf area (84.46 cm^2), and leaf relative greenness (SPAD value 46.10) at full blossom having statistical consonance with that of T_1 treatment (Table 3). Root growth (length) of the plants was estimated significantly the best in T_3 (22.78 cm) and the worst in control plants (16.10 cm) (Figure 1b).

Shoot and Root Biomass

Different organic and inorganic mulch treatments had significant ($p \leq 0.05$) and positive influences on fresh and dry weight of shoot and root of strawberries recorded after complete fruit harvest (Table 4). Among the treatments, plants cultured with T_3

Table 3
Effect of organic and inorganic mulches on the number of leaves per plant, petiole length, and canopy diameter of strawberry at full blossom

Treatment	Number of leaves per plant	Petiole length (cm)	Canopy diameter (cm)
T_0	15.95 ± 0.72 d	11.15 ± 0.31 b	26.13 ± 0.75 c
T_1	16.08 ± 0.64 d	12.85 ± 0.52 a	28.13 ± 0.76 c
T_2	21.55 ± 0.43 b	13.50 ± 0.39 a	32.68 ± 0.72 ab
T_3	23.33 ± 0.37 a	13.60 ± 0.49 a	34.30 ± 0.42 a
T_4	18.63 ± 0.87 c	13.45 ± 0.53 a	31.83 ± 0.68 b
T_5	19.48 ± 0.69 c	13.28 ± 0.40 a	32.05 ± 0.41 b
$LSD_{0.05}$	1.76	1.43	2.10
CV (%)	6.11	7.29	4.51
Level of significance	**	*	**

Note. Vertical bars on the top of the columns represent the standard errors of means of four replicates (n = 20). Different letters indicate the statistical differences among the treatments at $p \leq 0.05$. T_0 = Control; T_1 = Paddy straw; T_2 = Water hyacinth; T_3 = Asian watermoss; T_4 = Silver polythene; and T_5 = Black polythene

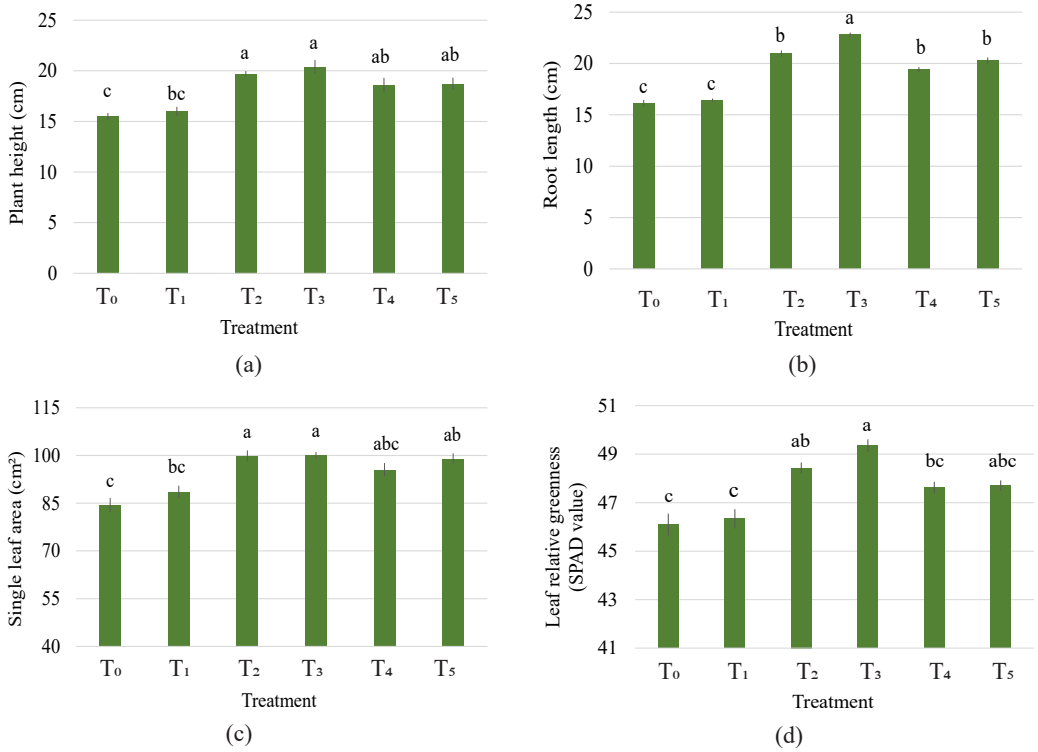

Figure 1. (a) Average plant height (cm), (b) root length (cm), (c) single leaf area (cm^2), and (d) leaf relative greenness (SPAD value) of strawberry var. BARI Strawberry-3 at full blossom as influenced by mulch treatments
Note. Vertical bars on the top of the columns represent the standard errors of means of four replicates (n = 20). Different letters indicate the statistical differences among the treatments at $p \leq 0.05$. T_0 = Control; T_1 = Paddy straw; T_2 = Water hyacinth; T_3 = Asian watermoss; T_4 = Silver polythene; and T_5 = Black polythene

treatment possessed statistically maximum shoot weight on fresh and dry basis (166.97 and 40.98 g, respectively), having statistical unity with T_2 and T_5 mulches for shoot fresh weight and dissonance from all the treatments for shoot dry weight. Similarly, root fresh and dry weight was recorded as the highest (19.05 and 13.78 g, respectively) in T_3, statistically consonant with that of T_2 mulch. The earlier trend control plants had the lightest root (12.10 and 8.98 g in fresh and dry weight basis, respectively).

Table 4
Effect of organic and inorganic mulches on fresh and dry biomass of shoot and root of strawberry

Treatment	Shoot fresh weight (g)	Shoot dry weight (g)	Root fresh weight (g)	Root dry weight (g)
T_0	113.15 ± 4.82 d	27.08 ± 1.04 e	12.10 ± 0.53 e	8.98 ± 0.38 e
T_1	126.45 ± 4.46 c	30.48 ± 1.04 d	13.43 ± 0.44 d	10.03 ± 0.36 d
T_2	160.28 ± 4.92 a	38.38 ± 1.09 b	17.95 ± 0.29 ab	13.05 ± 0.27 ab
T_3	166.97 ± 3.34 a	40.98 ± 0.69 a	19.05 ± 0.31 a	13.78 ± 0.24 a
T_4	145.08 ± 3.64 b	34.55 ± 0.98 c	15.95 ± 0.67 c	11.63 ± 0.38 c
T_5	158.80 ± 3.91 a	38.43 ± 0.73 b	17.15 ± 0.40 bc	12.58 ± 0.31 b
$LSD_{0.05}$	9.47	2.04	1.30	0.75
CV (%)	4.33	3.88	5.42	4.26
Level of significance	**	**	**	**

Note. Values are means ± standard errors of four independent replications (n = 20). Different letters within the column indicate statistically significant differences among the treatments according to LSD at $p \leq 0.05$. T_0 = Control; T_1 = Paddy straw; T_2 = Water hyacinth; T_3 = Asian watermoss; T_4 = Silver polythene; and T_5 = Black polythene

Reproductive Traits

Significant variations ($p \leq 0.05$) among the treatments were registered for the reproductive parameters of strawberries except for several days required for transplanting to the first-time fruit harvest (Table 5). Control plants-initiated flowering within the shortest possible time from transplanting (46.93 days) followed by T_2 (47.80 days) and T_3 (47.88 days) mulches. Plants under T_1 treatment took a longer time (52.55 days) to emerge the first flower. Again, the duration from flowering to harvesting ranged from 23.48 to 29.60 days, where fruits of control plants ripened early from flowering (23.48 days) being statistically identical with that of T_1 treatment (24.33 days) while significant maximum duration between flowering and harvesting (29.60 days) was recorded in T_3 treatment. Besides, the number of flowers and fruits was statistically different in different treatments, where T_3 mulch-treated plants produced maximum flowers

(21.20 per plant), as well as fruits (19.63 per plant) with a fruit set percentage of 92.66. Significantly, the minimum number of flowers (14.90 per plant) and fruits (12.98 per plant) was counted in control plants; T_1 plants had statistical parity with control treatment.

Table 5
Effect of organic and inorganic mulches on reproductive traits of strawberry

Treatment	Number of days required			Number of flowers per plant	Number of fruits per plant	Fruit set (%)
	Transplanting to the 1st flowering	Transplanting to the 1st harvest	Flowering to harvest			
T_0	46.93 ± 1.64 c	75.93 ± 2.80	23.48 ± 0.62 c	14.90 ± 1.00 c	12.98 ± 0.48 e	87.63 ± 2.76 bc
T_1	52.55 ± 1.18 a	82.30 ± 1.76	24.33 ± 0.69 c	15.50 ± 0.49 c	13.58 ± 0.44 de	87.73 ± 2.97 bc
T_2	47.80 ± 1.01 bc	80.05 ± 1.91	27.28 ± 0.57 b	18.73 ± 0.54 b	17.38 ± 0.36b	92.87 ± 1.28 a
T_3	47.88 ± 1.35 bc	80.63 ± 2.00	29.60 ± 0.28 a	21.20 ± 0.67 a	19.63 ± 0.44 a	92.66 ±0.99 a
T_4	51.38 ± 1.00 ab	79.63 ± 0.77	24.90 ± 0.50 c	18.00 ± 0.62 b	15.45 ± 0.85 cd	85.70 ± 2.32 c
T_5	48.58 ± 1.21 abc	80.33 ± 2.22	27.80 ± 0.58 b	18.75 ± 0.49b	17.20 ± 0.80 bc	91.60 ± 2.02 ab
$LSD_{0.05}$	4.00	6.09	1.58	2.12	1.89	4.93
CV (%)	5.40	5.06	4.01	7.90	7.84	3.64
Level of significance	*	NS	**	**	**	*

Note. Values are means ± standard errors of four independent replications (n = 20). Different letters within the column indicate statistically significant differences among the treatments according to LSD at $p \leq 0.05$. T_0 = Control; T_1 = Paddy straw; T_2 = Water hyacinth; T_3 = Asian watermoss; T_4 = Silver polythene; and T_5 = Black polythene

Yield Attributes

Except for individual fruit weight, strawberry yield characteristics such as fruit size (length and breadth) and fruit yield (g/plant and kg/ha) significantly ($p \leq 0.05$) differed in the different types of mulch treatments (Figure 2). Individual fruit weight of BARI Strawberry-3 under study ranged between 17.88 to 18.88 g (Figure 2a). Though fruit length was noted as a minimum in T_4 mulch (3.97 cm), fruit breadth was recorded as a minimum in control (T_0) plants (3.02 cm), whereas T_2 fruits had a maximum length (4.98 cm) and T_3 fruits got maximum breadth (3.57 cm) (Figure 2b). In addition, T_3 exhibited statistical superiority over other treatments in terms of fruit yield (370.02 g/plant and 15.42 kg/ha) followed by T_2 and T_5 mulches; contrarily, the minimum yield was obtained from untreated plots (234.83 g/plant and 9.78 kg/ha) (Figure 2c). Therefore, an increase in fruit yield over control was noted due to mulching, where a maximum 57.57% yield enhancement was noticed in the T_3 treatment and a minimum of 6.99% in the T_1 treatment; T_2 and T_5 mulching had a yield increment of 37.51 and 34.54%, respectively (Figure 2d).

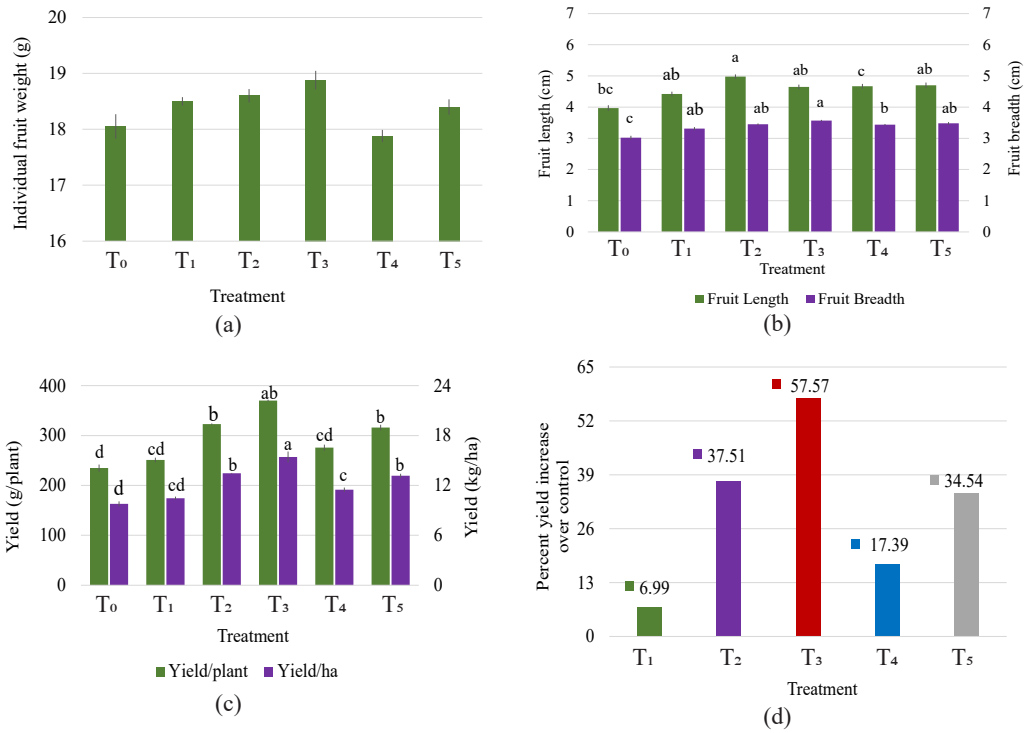

Figure 2. (a) Average individual fruit weight (g), (b) fruit length (cm) and breadth (cm), (c) fruit yield (g/plant and kg/ha), and (d) percent yield increase over control of strawberry var. Different organic and inorganic mulches influence BARI Strawberry-3

Note. Vertical bars on the top of the columns represent the standard errors of means of four replicates (n = 20). Different letters indicate the statistical differences among the treatments at $p \leq 0.05$. T_0 = Control; T_1 = Paddy straw; T_2 = Water hyacinth; T_3 = Asian watermoss; T_4 = Silver polythene; and T_5 = Black polythene

Physiochemical Properties of Fruit

Significant ($p \leq 0.05$) variations in fruit physical and biochemical attributes were noted due to organic and inorganic mulching in strawberries (Table 6). Fruits of all the treatments, except T_1, had statistically similar dry matter content numerically high in T_3 treatment (9.68%). Likely, fruits obtained from the T_3 treatment exhibited the highest TSS content (9.95%), while T_1 fruits showed minimum TSS (7.75%). TA was estimated maximum in the T_1 treatment (0.66%) and the same minimum TA (0.58%) in both T_3 and T_5 treatments. Consequently, the TSS/acidity ratio was significantly the highest (17.08:1) in the fruits of the T_3 treatment, being statistically different from all other treatments. Fruits under T_1 had statistically minimum TSS/acidity ratio (11.74:1). Furthermore, T_3-treated strawberry transplants produced fruits with significantly maximum vitamin C content (58.16 mg/100 g), which was statistically identical to that of T_2, T_4, and T_5 mulch treatments. Control treatments had fruits with statistically minimum vitamin C content (47.23 mg/100 g).

Table 6
Effect of different mulches on the content of fruit dry matter, total soluble solids, titratable acidity, TSS/acidity ratio, and vitamin C of strawberry

Treatment	Dry matter (%)	Total soluble solids (%)	Titratable acidity (%)	TSS/acidity ratio	Vitamin C (mg/100 g)
T_0	8.86 ± 0.32 ab	8.05 ± 0.21 cd	0.59 ± 0.01 b	13.59 ± 0.16 c	47.23 ± 1.74 c
T_1	8.22 ± 0.26 b	7.75 ± 0.24 d	0.66 ± 0.02 a	11.74 ± 0.07 d	51.94 ± 1.69 bc
T_2	9.42 ± 0.27 a	9.50 ± 0.39 ab	0.62 ± 0.02 ab	15.43 ± 0.17 b	56.62 ± 1.50 ab
T_3	9.68 ± 0.19 a	9.95 ± 0.17 a	0.58 ± 0.01 b	17.08 ± 0.05 a	58.16 ± 1.68 a
T_4	9.27 ± 0.34 a	8.95 ± 0.37 bc	0.58 ± 0.01 b	15.49 ± 0.93 b	57.24 ± 1.65 a
T_5	9.41 ± 0.21 a	9.35 ± 0.27 ab	0.61 ± 0.01 ab	15.26 ± 0.14 b	55.23 ± 1.13 ab
$LSD_{0.05}$	0.89	0.95	0.05	1.24	5.13
CV (%)	6.45	7.03	5.4	5.57	6.25
Level of significance	*	**	*	**	**

Note. Values are means ± standard errors of four independent replications (n = 20). Different letters within the column indicate statistically significant differences among the treatments according to LSD at $p \leq 0.05$. T_0 = Control; T_1 = Paddy straw; T_2 = Water hyacinth; T_3 = Asian watermoss; T_4 = Silver polythene; and T_5 = Black polythene

DISCUSSION

Mulching, an age-old cultural practice of curing the soil surface, is laying various covering materials on the soil/ground surface surrounding the plant base for the best possible outcome of making soil environment for plant growth, development, and efficient crop production. Besides many other soil management strategies, mulching measures can efficiently regulate soil temperature by reducing soil temperature in hot weather, maintaining soil temperature during the cold season, and improving the physical properties of the soil (Iqbal et al., 2016). In the present experimental site, the cultivable winter (rabi season) had almost no rain, atmospheric humidity below par, extreme day temperature, and solar radiation not up to the mark (Table 1). Studies also opined that winter occurs for no longer than three months, with hotter winter days in the southern region of Bangladesh, a phenomenon in recent years (M. H. R. Khan et al., 2019).

In such adversities, enhanced plant growth, development, yield, and fruit biochemical properties were noticed in organic and inorganic mulch-treated plants compared to the control. Appropriate mulching can accelerate plant root and shoot growth by generating congenial soil physical, chemical, and biological conditions that potentially increase the soil water holding capacity, microbial community, soil texture and aeration, and nutrient availability, making the soil more productive and fertile. All these conditions favor enhanced crop growth and yield even under adverse climate situations.

Qu et al. (2019) and Zhang et al. (2009) demonstrated that mulching promotes soil microbial activity by improving agro-physical properties, which augments soil nutrient uptake and improves vegetative growth. Mulching also improves crop-water use efficiency and reduces fertilizer leaching during excess irrigation and rains (Almeida et al., 2015; Barche et al., 2015; Iqbal et al., 2016). All these auspicious events might occur here to increase the shoot and root growth of strawberries that consequently influenced the accumulation and translocation of photosynthates to the sink, resulting in the significant quantity of fruits having eminent post-harvest qualities.

Similar instances of accelerated growth and development in strawberries due to mulching over control were noted in several studies (Abdalla et al., 2019; Bakshi et al., 2014; Deb et al., 2014; P. Kaur & Kaur, 2017; Patil et al., 2013; Sharma & Goel, 2017). Not only strawberry, mulching improves vegetative growth remarkably and yield in other similar crops like potato (Bhatta et al., 2020; Li et al., 2018), tomato (Biswas et al., 2016; Mendonça et al., 2021), and eggplant (R. R. Kumar et al., 2019).

Again, among the natural and synthetic mulches, Asian watermoss exhibited superiority over the other treatments in inducing strawberry yield and quality. Water hyacinth mulch had some resemblances in some cases. The results meant that organic mulch materials had a better impact than inorganic mulching in the present environmental and soil conditions. Again, the average air temperature at the early growth and reproductive stage went beyond 30°C, which was not congenial for strawberry growth. The rise in air temperature corresponds to the increment in soil temperature. Here, organic mulching with Asian water might prevent the soil temperature from rising excessively while not allowing the soil temperature to be too low by facilitating the slow release of ground temperature during the whole growth phase of the strawberry.

Regulation of temperature made proper ground for the soil microbes along with many more advantages for better crop growth and yield. D. Kumar and Sharma (2018), as well as Lal (2013), noticed that organic mulch had much soil cooling capacity than colored synthetic mulch. Soil temperature rise in extremely cool periods might be beneficial, but it may be pernicious in places where moderate to relatively higher air temperature prevails in winter. Organic mulches provide harbor and food for numerous soil microorganisms essential for promoting soil granulation and preserving soil health (Barche et al., 2015; Kader et al., 2017).

Besides, organic mulch has the maximum capacity to retain soil water and extends all sorts of basic soil properties by adding organic carbon to the soil during decomposition (Qu et al., 2019). As an organic mulch material, the use of water hyacinth mulch and the resultant improvement in crop growth, yield, and fruit nutrient contents have been reported (Adnan et al., 2017; Indulekha & Thomas, 2018; Sil et al., 2020). Though evidence of applying

Asian watermoss as mulching is scant (Arzoo et al., 2021), it has been widely used as the structural material for bed preparation in floating agriculture (Irfanullah et al., 2011; Mondal et al., 2022; Sunder, 2020), where it undergoes gradual decomposition, and the cultivated seedlings and vegetable crops receive necessary nutrients from it.

Again, as partial decomposition of organic mulches occurs in the field, Asian watermoss added more mineral matter due to its higher mineral compositions than water hyacinth and paddy straw mulch. Besides, the nutrient analysis also revealed that Asian watermoss had a C:N ratio with higher levels of organic C and mineralizable N. The moss *Salvinia* is also reported as highly potent organic manure (Hussain et al., 2018; Sangla et al., 2006). Thereby, there was every chance for the improvement of soil health most efficiently upon Asian watermoss mulching, which contributed to the best growth, yield, and biochemical properties of strawberries in the tropical southern region of Bangladesh.

CONCLUSION

Strawberry being a sensitive surface feeding winter fruit, the topsoil must have appropriate biological, chemical, and physical properties. It was noted that superior vegetative growth with maximum root and shoot biomass of strawberries was obtained from Asian watermoss mulching, and water hyacinth mulch had similar contributions. Reproductive growth, mainly the number of flowers and fruits, as well as fruit yield, was distinctly eminent in Asian water moss-applied plots. Once again, fruit quality characteristics followed similar trends. Overall, mulching had a statistically profound impact on strawberry production, and organic mulch performed better than inorganic mulch in the tropical ecosystem of southern Bangladesh.

ACKNOWLEDGEMENTS

The authors express profound respect and heartiest gratitude to the Bangladesh Agricultural Research Institute for providing logistic and physical support in accomplishing this research. Besides, the publication was supported by the "Research, extension and popularization of vegetables and spices cultivation on floating bed" Project with the funding code MoA-224117501.

REFERENCES

Abdalla, R. M., Attalah, S. Y., Badawy, I. F. M., & Aboalmajd, S. A. (2019). Effect of plastic mulching on strawberry fruit yield and quality. *Assiut Journal of Agricultural Sciences*, *5*(4), 126-141. https://doi.org/10.21608/ajas.2019.69810

Adnan, M. M., Rahim, M. A., Haque, T., & Hossain, M. M. (2017). Growth and yield performance of strawberry (*Fragaria* × *ananassa* Duch.) as influenced by variety and mulch materials. *Fundamental and Applied Agriculture*, *2*(1), 202-206.

Almeida, W. F. D., Lima, L. A., & Pereira, G. M. (2015). Drip pulses and soil mulching effect on american crisphead lettuce yield. *Engenharia Agrícola*, *35*(6), 1009-1018. http://doi.org/10.1590/1809-4430-Eng.Agric.v35n6p1009-1018/2015

Arzoo, A., Behera, B., & Hota, S. (2021). Impacts of waste biomass of *Salvinia cucullata* L. on growth, physiological and biochemical parameters of *Vigna unguiculata* L. *International Journal of Botany Studies*, *6*(3), 132-134.

Awal, M. A., & Islam, A. F. M. T. (2020). Water logging in south-western coastal region of Bangladesh: Causes and consequences and people's response. *Asian Journal of Geographical Research*, *3*(2), 9-28. https://doi.org/10.9734/ajgr/2020/v3i230102

Bakshi, P., Bhat, D. J., Wali, V. K., Sharma, A., & Iqbal, M. (2014). Growth, yield and quality of strawberry (*Fragaria* x *ananassa* Duch.) cv. Chandler as influenced by various mulching materials. *African Journal of Agricultural Research*, *9*(7), 701-706. https://doi.org/10.5897/AJAR2013.7983

Barche, S., Nair, R., & Jain, P. K. (2015). A review of mulching on vegetable crops production. *Ecology, Environment and Conservation*, *21*(2), 859-866. https://doi.org/10.13140/RG.2.2.14223.33440

Baur, F. J., & Endminger, L. G. (2012). *Official methods of analysis*. Association of Official Analytical Chemist.

Bhatta, M., Shrestha, B., Devkota, A. R., Joshi, K. R., Bhattarai, S., & Dhakal, U. (2020). Effect of plastic mulches on growth and yield of potato (*Solanum tuberosum* L.) in Dadeldhura, Nepal. *Journal of Agriculture and Natural Resources*, *3*(2), 228-240. https://doi.org/10.3126/janr.v3i2.32509

Biswas, S. K., Akanda, A. R., Rahman, M. S., & Hossain, M. A. (2016). Effect of drip irrigation and mulching on yield, water-use efficiency and economics of tomato. *Plant, Soil and Environment*, *61*(3), 97-102. https://doi.org/10.17221/804/2014-PSE

Deb, P., Sangma, D. K., Prasad, B. V. G., Bhowmick, N., & Dey, K. (2014). Effect of different mulches on vegetative growth of strawberry (cv. Tioga) under red and lateritic zone of west Bengal. *International Journal of Basic and Applied Biology*, *2*(2), 77-80.

D'Urso, G., d'Aquino, L., Pizza, C., & Montoro, P. (2015). Integrated mass spectrometric and multivariate data analysis approaches for the discrimination of organic and conventional strawberry (*Fragaria ananassa* Duch.) crops. *Food Research International*, *77*(Part 2), 264-272. https://doi.org/10.1016/j.foodres.2015.04.028

Fernandes, V. C., Domingues, V. F., de Freitas, V., Delerue-Matos, C., & Mateus, N. (2012). Strawberries from integrated pest management and organic farming: Phenolic composition and antioxidant properties. *Food Chemistry*, *134*(4), 1926-1931. https://doi.org/10.1016/j.foodchem.2012.03.130

Hussain, N., Abbasi, T., & Abbasi, S. A. (2018). Generation of highly potent organic fertilizer from pernicious aquatic weed *Salvinia molesta*. *Environmental Science and Pollution Research*, *25*, 4989-5002. https://doi.org/10.1007/s11356-017-0826-0

Indulekha, V. P., & Thomas, C. G. (2018). Utilization of water hyacinth as mulch in turmeric. *Journal of Tropical Agriculture*, *56*(1), 27-33.

Iqbal, M., Bakshi, P., Wali, V. K., Kumar, R., Bhat, D., & Jasrotia, A. (2016). Efficacy of organic and inorganic mulching materials on weed count, growth, and yield of aonla (*Emblica officinalis*) cv. NA 7. *Indian Journal of Agricultural Sciences*, *86*(4), 545-549. https://doi.org/10.56093/ijas.v86i4.57572

Irfanullah, H. M., Azad, M. A. K., Kamruzzaman, M., & Wahed, M. A. (2011). Floating gardening in Bangladesh: A means to rebuild lives after devastating flood. *Indian Journal of Traditional Knowledge*, *10*(1), 31-38.

Islam, T., & Atkins, P. (2007). Indigenous floating cultivation: A sustainable agricultural practice in the wetlands of Bangladesh. *Development in Practice*, *17*(1), 130-136. https://doi.org/10.1080/09614520601092733

Kader, M. A., Senge, M., Mojid, M. A., & Ito, K. (2017). Recent advances in mulching materials and methods for modifying soil environment. *Soil and Tillage Research*, *168*, 155-166. https://doi.org/10.1016/j.still.2017.01.001

Kaur, L., Kaur, A., & Brar, A. S. (2021). Water use efficiency of green gram (*Vigna radiata* L.) impacted by paddy straw mulch and irrigation regimes in north-western India. *Agricultural Water Management*, *258*, 107184. https://doi.org/10.1016/j.agwat.2021.107184

Kaur, P., & Kaur, A. (2017). Effect of various mulches on the growth and yield of strawberry cv. Chandler under tropical conditions on Punjab. *International Journal of Recent Trends in Science and Technology*, *25*(1), 21-25. https://doi.org/10.26611/202515

Khan, M. H. R., Rahman, A., Luo, C., Kumar, S., Islam, G. A., & Hossain, M. A. (2019). Detection of changes and trends in climatic variables in Bangladesh during 1988-2017. *Heliyon*, *5*(3), e01268. https://doi.org/10.1016/j.heliyon.2019.e01268

Khan, M. M. H., Bryceson, I., Kolivras, K. N., Faruque, F., Rahman, M. M., & Haque, U. (2015). Natural disasters and land-use/land-cover change in the southwest coastal areas of Bangladesh. *Regional Environmental Change*, *15*, 241-250. https://doi.org/10.1007/s10113-014-0642-8

Khan, Z. H., Mazumder, A. R., Mohiuddin, A. S. M., Hussain, M. S., & Saheed, S. M. (1998). Physical properties of some benchmark soils from the flood-plains of Bangladesh. *Journal of the Indian Society of Soil Science*, *46*(3), 442-446.

Kumar, D., & Sharma, R. (2018). Effect of mulching on growth, yield and quality in different varieties of summer squash (*Cucurbita pepo* L.). *International Journal of Current Microbiology and Applied Sciences*, *7*(6), 2113-2119. https://doi.org/10.20546/ijcmas.2018.706.251

Kumar, R. R., Singh, R., Sohane, R. K., & Singh, A. K. (2019). Effect of different type mulch on growth, yield attributes and yield of brinjal (*Solanum melogena*). *Current Journal of Applied Science and Technology*, *37*(6), 1-6. https://doi.org/10.9734/cjast/2019/v37i630333

Lal, B. R. (2013). Effect of mulching on crop production under rainfed condition - A review. *Agricultural Reviews*, *34*(3), 188-197. https://doi.org/10.5958/j.0976-0741.34.3.003

Li, Q., Li, H., Zhang, L., Zhang, S., & Chen, Y. (2018). Mulching improves yield and water-use efficiency of potato cropping in China: A meta-analysis. *Field Crops Research*, *221*, 50-60. https://doi.org/10.1016/j.fcr.2018.02.017

Mendonça, S. R., Ávila, M. C. R., Vital, R. G., Evangelista, Z. R., de Carvalho Pontes, N., & dos Reis Nascimento, A. (2021). The effect of different mulching on tomato development and yield. *Scientia Horticulturae*, *275*, 109657. https://doi.org/10.1016/j.scienta.2020.109657

Mondal, A. B., Azad, A. K., Ahmed, M. B., Mannan, A., Hossain, M., & Eaton, T. E. (2022). Influence of organic and inorganic fertilizers on floating bed cultivation of okra and cucumber during summer season in southern part of Bangladesh. *American Journal of Plant Sciences*, *13*(5), 600-612. https://doi.org/10.4236/ajps.2022.135040

Parsottambhai, S. M. K., & Rawat, M. (2020). Effect of mulching on growth, yield and quality of onion (*Allium cepa* L.): A review. *Journal of Pharmacognosy and Phytochemistry*, *9*(6), 1861-1863.

Patil, N. N., Rao, V. K., & Dimri, D. C. (2013). Effect of mulching on soil properties, growth and yield of strawberry cv. Chandler under mid hill conditions of Uttarakhand. *Journal of Hill Agriculture*, *48*(1), 42-47. https://doi.org/10.5958/2249-5258.2016.00008.7

Paul, C., Gomasta, J., & Hossain, M. M. (2017). Effects of planting dates and variety on growth and yield of strawberry. *International Journal of Horticulture, Agriculture and Food Science*, *1*(4), 1-12. https://doi.org/10.22161/ijhaf.1.4.1

Qu, B., Liu, Y., Sun, X., Li, S., Wang, X., Xiong, K., Yun, B., & Zhang, H. (2019). Effect of various mulches on soil physic-chemical properties and tree growth (*Sophora japonica*) in urban tree pits. *PLOS One*, *14*(2), e0210777. https://doi.org/10.1371/journal.pone.0210777

Sangla, L., Suppadit, T., & Pintasean, S. (2006). Fundamental utilization of floating mass

(*Salvinia cucullata* Roxb.) in agricultural aspect. *Journal of Social Development*, *8*(1), 313-323.

Sarangi, S. K., Maji, B., Sharma, P. C., Digar, S., Mahanta, K. K., Burman, D., Mandal, U. K., Mandal, S., & Mainuddin, M. (2021). Potato (*Solanum tuberosum* L.) cultivation by zero tillage and paddy straw mulching in the saline soils of the Ganges Delta. *Potato Research*, *64*, 277-305. https://doi.org/10.1007/s11540-020-09478-6

Sharma, V. K., & Goel, A. K. (2017). Effect of mulching and nitrogen on growth and yield of strawberry. *International Journal of Science, Environment and Technology*, *6*(3), 2074-2079.

Sil, M. C., Haque, M. Z., Shila, A., Howlader, M. H. K., & Ahmed, R. (2020). Effect of different mulches on growth and yield of Cauliflower in southern Bangladesh. *Journal of Environmental Science and Natural Resources*, *13*(1-2), 110-117.

Slathia, P. S., & Paul, N. (2012). Traditional practices for sustainable livelihood in Kandi belt of Jammu. *Indian Journal of Traditional Knowledge*, *11*(3), 548-552.

Sunder, K. (2020, September 11). The remarkable floating gardens of Bangladesh. *BBC*. https://www.bbc.com/future/article/20200910-the-remarkable-floating-gardens-of-bangladesh

Zhang, S., Lövdahl, L., Grip, H., Tong, Y., Yang, X., & Wang, Q. (2009). Effects of mulching and catch cropping on soil temperature, soil moisture and wheat yield on the Loess Plateau of China. *Soil and Tillage Research*, *102*(1), 78-86. https://doi.org/10.1016/j.still.2008.07.019

Pertanika J. Trop. Agri. Sci. 46 (4): 1309 - 1326 (2023)

PERTANIKA JOURNALS

TROPICAL AGRICULTURAL SCIENCE

Journal homepage: http://www.pertanika.upm.edu.my/

Effect of Deficiency-adjusted Macronutrients to Cure Brown Bast Syndrome in Rubber Tree (*Hevea brasiliensis*)

Nurul Atiqah Ahmad[1], Zulkefly Sulaiman[1,2]*, Mohd Yusoff Abdul Samad[1,3], Sarker Mohammad Rezaul Karim[2] and Monsuru Adekunle Salisu[4]

[1]*Institute of Plantation Studies, Universiti Putra Malaysia, 43400 Serdang, Selangor, Malaysia*
[2]*Department of Crop Science, Faculty of Agriculture, Universiti Putra Malaysia, 43400 Serdang, Selangor, Malaysia*
[3]*Department of Land Management, Faculty of Agriculture, Universiti Putra Malaysia, 43400 Serdang, Selangor, Malaysia*
[4]*Department of Agricultural Sciences, Faculty of Technical and Vocational, Universiti Pendidikan Sultan Idris, 53900 Tanjung Malim, Perak, Malaysia*

ABSTRACT

The brown bast (BB) syndrome causes a 15-20% loss of annual rubber (*Hevea brasiliensis*) production in Malaysia, and no sustainable remedy has been developed yet. Initial investigation showed a macronutrients deficiency in the bark of affected plants compared to non-affected plants. Therefore, this study was undertaken to know the effect of spraying the deficient macronutrients in curing BB syndrome and increasing latex productivity. The treatments were selected by adjusting deficient nutrients, especially in N, K, and S, compared to healthy plants. The treatments consisted of 13 combinations of nutrient concentrations and a control (no application on healthy rubber trees). One liter of individual treatment per tree was applied on the trunk of BB-affected trees once a week for one month. Data on latex production was collected one week after the last application and continued for up to three months. The results showed that the treatment T_9 (0.5% N, 0.8 mg/L K, and 0.2% S), in addition to other prescribed nutrients, made a 100% cure of BB syndrome after three weeks of application, and the nutrient contents of the bark of the affected plants appeared to be similar to the healthy plants. Applying these additional nutrients enhanced the latex production at the rate of 51.85 g/tapping/tree after two months of treatment application under the agro-ecosystem of FELCRA, Simpang Renggam, Johor, Malaysia. It is

ARTICLE INFO

Article history:
Received: 05 May 2023
Accepted: 27 June 2023
Published: 02 November 2023

DOI: https://doi.org/10.47836/pjtas.46.4.15

E-mail addresses:
atiqahahmad_94@yahoo.com (Nurul Atiqah Ahmad)
zulkefly@upm.edu.my (Zulkefly Sulaiman)
myusoffas@upm.edu.my (Mohd Yusoff Abdul Samad)
sarker.mohammad@upm.edu.my
(Sarker Mohammad Rezaul Karim)
salisuadekunle@gmail.com (Monsuru Adekunle Salisu)
*Corresponding author

ISSN: 1511-3701
e-ISSN: 2231-8542

a new finding to 100% cure BB syndrome and to increase the latex productivity in sustaining the rubber industry in Malaysia.

Keywords: Brown bast syndrome, *Hevea brasiliensis*, latex productivity, macronutrient, tapping frequency d3, tapping panel dryness, tapping system S/2

INTRODUCTION

Rubber (*Hevea brasiliensis*) is one of the significant economic plantations besides oil palm in Malaysia. The country plays an essential role in producing and exporting rubber worldwide. As per the first Economic Transformation Programs (ETPs) of Malaysia, the average national rubber productivity needs to be increased to 2,000 kg/ha by 2020 (Said & Ghani, 2012) since rubber is an important commodity under the National Key Economic Area (NKEA) of the country. However, since 2019, latex productivity has been reduced, with an average of 1,440 and 1,420 kg/ha in 2017 and 2018, respectively, due mainly to brown bast (BB) syndrome and other agronomic management problems. Rubber production has declined from 799.1 thousand tonnes in 2019 to 719 thousand tonnes in 2020. Meanwhile, rubber consumption in Malaysia increased from 1,075.7 thousand tonnes in 2019 to 1,170.1 thousand tonnes in 2020 (Malaysian Rubber Council [MRC], n.d.). Due to this decline in rubber production and increased demand, the country has relied on other countries to meet its rubber needs. According to MRC (n.d.), rubber imports in Malaysia increased from 1,677.4 thousand tonnes in 2019 to 1,702.1 thousand tonnes in 2020. Therefore, an increase in rubber productivity in Malaysia is of prime importance.

Brown bast or tapping panel dryness (TPD) is a syndrome related to partial or entire dryness of a rubber tapping panel. The syndrome is regarded as a physiological disorder that causes severe damage to the rubber trees if not treated immediately. TPD is characterized by the drying up the latex-producing tissues beneath the tree's bark, resulting in reduced or halted latex flow. This condition is a major concern for rubber plantations, significantly impacting latex production and overall yield. This disorder causes an imbalance between the latex regeneration and tapping process. The bark becomes brown, thick, and finally cracks in severe cases. Brown bast has been reported to cause a loss of 15-20% in rubber production in Malaysia (Nandris et al., 2004). Qi et al. (2014) reported that around 14.75% of rubber trees are damaged by tapping panel dryness. Another report says that about 12–50% of productive trees are affected by TPD in almost every rubber-growing region (Venkatachalam et al., 2007). TPD can persist for extended periods and cause significant economic losses for rubber plantations.

The exact cause of BB or TPD is not yet fully understood, and it is believed to result from a combination of physiological, anatomical, and environmental factors. Some possible contributing factors include hormonal imbalances, nutrient deficiencies, excessive or improper tapping practices, genetic factors, and environmental stressors

such as drought, extreme temperatures, or waterlogging (Venkatachalam et al., 2007). The researchers have been trying to develop methods to treat BB syndrome for a long time. As part of the efforts, the syndrome portion was isolated from healthy high bark to avoid infection in healthy parts of rubber trees (Keralafarmer, 2019), but that was unsuccessful. The injection of chemical stimulants such as ethephon to increase latex productivity tended to cause a high incidence of this physiological syndrome (Nazri, 2020). The introduction of a newly formulated ethephon and water-based stimulant (RRIM HYDROBEST™) by the Malaysian Rubber Board (MRB) (2009) indicated that this stimulant could improve land productivity and lower the incidence of TPD (Budiasih et al., 2020; Nazri, 2020; Sainoi & Sdoodee, 2012).

However, treatment with the stimulants depends on the cell biochemistry of the plants (Nik Hashyati et al., 2022) and, for longer use, affects the latex physiology (Lacote et al., 2010). Nik Hashyati et al. (2022) found that the bark dryness of rubber trees could be cured by treating them with a specific fertilizer formulation of macro and micronutrients in liquid form and spraying on the tree. In light of the findings mentioned above, it was speculated that there might be differences in nutrient contents in the bark, leaf, and soil ecosystems of healthy and BB-syndromed rubber plants, which must be solved. Therefore, this study was undertaken firstly to know if there is any difference in macronutrients in the ecosystems of BB-affected and non-affected rubber trees; secondly, if the difference exists whether adjustment of deficient nutrients can cure BB-syndrome, and thirdly, to know if the application of adjusted macronutrients can increase the yield of latex.

MATERIALS AND METHODS

Sampling Location and Climatic Conditions

The study was conducted at FELCRA, Simpang Renggam, Johor (1°44'55.1"N, 103°20'02.6°E) with the clone RRIM 2002 from November 2019 to February 2020. The area's three hundred and ninety trees, representing 56.52%, were infected by BB syndrome. Of these, 39 trees (10%) were randomly selected and used as study samples, and healthy plants were selected from the same area. The average temperature during the experiment was similar and varied from 33°C (November 2019) to 33.2°C (February 2020). The rainfall was high at the beginning and then reduced gradually. The flow was below: November 2019 = 67 mm, December 2019 = 84 mm, January 2020 = 47 mm, and February 2020 = 25 mm, respectively.

Pretreatment Nutrient Assessment and Treatment Determination

First, some affected and healthy plants' soil, leaf, and bark nutrient contents were analyzed. Significant differences were identified in N, K, and S contents, especially in the barks between the two groups of plants. Therefore, in the new formulation, the nutrient deficiency in the affected plants was adjusted based on healthy plants

(Table 1). The N, K, and S nutrient rates used in the formulation were based on the difference observed between affected and unaffected rubber trees. For example, BB-affected plants' N contents differ by 0.2 to 0.8%. Putting the lowest and highest values in the Box-Behnken design, the predicted formulation rates were estimated for use as treatments (Kumari et al., 2021). The different nutrient concentrations used in the study are shown in Table 1. Treatment T_1 represents the healthy rubber tree as the control, i.e., without treatment application. Treatments T_2 to T_{14} are estimated treatments, respectively. As per treatment specification, the nutrients of N, K, and S, which were obtained using ammonium nitrate, triple super phosphate, and ammonium sulfate that were purchased from RM Phosphate & Chemicals Pvt. Ltd. (Malaysia), were mixed, stirred, and diluted in 1.0 L of distilled water.

The treatments were applied directly to the tree base to 6 feet upright of the trunk using a hand sprayer once a week for one month. Thirty-nine soil, bark, and leaf samples were collected from affected and non-affected rubber trees. The leaves and the barks were dried in the oven at 50°C for three days. The soil samples were collected at a depth of 30 cm from the area 2 m away from the base of affected and non-affected rubber trees using an auger. The soil samples were then separated into two different depths: 0-15 and 15-30 cm, respectively. The samples were air-dried, ground, and sieved through a 2 mm sieve before analysis for their macronutrients, such as calcium (Ca), nitrogen (N), phosphorus (P), potassium (K), magnesium (Mg), and

Table 1
Concentration of additional nutrients used in the treatment formulation

Symbol	Rate		
	N (%)	K (mg/L)	S (%)
T_1 (control)	0	0	0
T_2	0.2	0.2	0.5
T_3	0.2	0.5	0.2
T_4	0.2	0.5	0.8
T_5	0.2	0.8	0.5
T_6	0.5	0.2	0.2
T_7	0.5	0.2	0.8
T_8	0.5	0.5	0.5
T_9	0.5	0.8	0.2
T_{10}	0.5	0.8	0.8
T_{11}	0.8	0.2	0.5
T_{12}	0.8	0.5	0.2
T_{13}	0.8	0.5	0.8
T_{14}	0.8	0.8	0.5

sulfur (S). The samples were also analyzed using appropriate methodologies to know their pH and electrical conductivity (EC). Leaf and bark analyses for the elements N and S were done using LECO CNS TruMac Analyzer (Netherlands) (Kowalenko et al., 2001). The macronutrients P and K were determined by the dry ashing method (Varley, 1966) using an auto-analyzer (LACHAT Instrument, QuikChem FIA+ 8000 series, Malaysia), while Ca and Mg were analyzed using atomic absorption spectroscopy (PerkinElmer PinAAcle 900T, USA). Soil pH was determined using a calibrated pH meter (Forster, 1995; Paul et al., 2017). EC analysis was carried out with a ratio of 1:5 of soil to water (Foster, 2015) using a conductivity meter.

Data Collection and Statistical Analysis

Data on latex yield were collected one week after the last treatment and continued for 3 months with the tapping system S/2 (half-spiral cut downward) and tapping frequency d3 (once every 3 days) to prevent stress on the rubber trees. The cup lump was weighed and recorded before and after the tapping collection.

The percentage of brown bast cure was measured by using a measuring tape and calculated by the formula below:

$$\% \text{ Brown bast cure} = \frac{\text{Total length of tapping cut} - \text{Length of cured tapping cut}}{\text{Total length of tapping cut}} \times 100\%$$

(Rhoades, 1993)

The experiment was conducted in a randomized complete block design (RCBD) with 3 replications. In the first stage of statistical analysis, a comparison between healthy rubber trees and BB-affected rubber trees was done using a *t*-test. In the second stage of the study, the variance (ANOVA) analysis was done to identify the significant effectiveness of applying the new formulation using the concerned elements shown in the first stage. All the data were analyzed using the statistical software SAS (version 9.4). The significant differences were determined using Tukey's honest significant difference (HSD) test at a 5% level of probability ($p \leq 0.05$).

RESULTS AND DISCUSSION

Soil pH, Soil EC, and Nutrient Contents in Soil, Leaf, and Barks

The results of nutrient analyses indicated no significant difference in soil nutrients between affected and unaffected rubber trees, as shown in Table 2. Soil pH ranged between 4.5 and 5.5 (Table 2), which is considered optimum acidic for rubber plantation (Daud, 2013; Priyadarshan, 2003), and the soil EC of both the affected and unaffected rubber trees was 1–2 dS/m (Table 2), which was in a non-saline state ("Wintering season," 2021).

Soil nutrient contents similarly influenced the nutrient contents of the leaf, as shown in Table 3. The insignificant difference in nutrient content in both soil and leaves was assumed to be the plant's adequate nutrient supply. However, the nutrient contents of the bark of BB-affected

rubber trees were significantly varied, especially in N and S contents, while the other nutrients, such as P, K, Ca, and Mg, were similar (Table 4). Bark and leaves usually correlate positively with their nutrient contents (Jones et al., 2019), but the authors found a difference between leaves and bark. Based on this difference, when a new formulation with additional fertilizers was made, it caused positive responses to the healthiness of the bark of the BB-affected rubber trees. After treatment with a new formulation of fertilizers, the nutrient contents of the bark tissues of BB-affected trees were increased, and they became like non-affected healthy trees (Table 5). The bark of plants can absorb nutrients when the fertilizers are applied directly to the trees.

Table 2
Differences in pH, EC, and macronutrients in soils of healthy and BB-affected rubber trees before treatment application at two soil depths

Rubber plant	Depth (cm)	pH	EC (dS/m)	N (%)	Available P (mg/kg)	K (mg/kg)	Ca (mg/kg)	Mg (mg/kg)	S (%)
Affected tree	0-15	5.232	2.090	0.073	12.677	42.030	210.200	22.633	0.065
Healthy tree		5.140	1.540	0.055	15.365	27.982	88.798	16.483	0.068
p-value		0.460^{ns}	0.187^{ns}	0.053^{ns}	0.607^{ns}	0.114^{ns}	0.063^{ns}	0.130^{ns}	0.203^{ns}
Affected tree	15-30	5.103	1.566	0.067	10.462	33.915	129.100	15.350	0.065
Healthy tree		4.947	1.687	0.070	10.208	30.032	68.513	13.033	0.066
p-value		0.381^{ns}	0.562^{ns}	0.827^{ns}	0.906^{ns}	0.563^{ns}	0.154^{ns}	0.423^{ns}	0.684^{ns}

Note. EC = Electrical conductivity; BB = Brown bast; ns = Not significant at $p>0.05$

Effect of New Formulation on Brown Bast Cure

The new formulation of fertilizers, especially of N, K, and S, caused a positive response to cure BB syndrome in rubber trees, leading to increased latex production. Figure 1 shows that before treatment application, the latex flow in T_1 (healthy tree) was good (100% latex flow), but the BB-affected plants represented by T_2 to T_{14} had no latex flow on the tapping cut. Figures 2, 3, 4, and 5 show the effect of treatments with new formulations on the percent cure of brown bast, respectively. For instance, Figure 2 indicates that, on average, 11.33% BB cure occurred after the first week of treatment application. Although the percent BB cure increased a bit, it was still significantly lower than the healthy plant (T_1), and no significant differences were observed between treatments, T_2 to T_{14}. However, significant increases (33%) were found in

the treated trees (T_2 to T_{14}) after two weeks of treatment application (Figure 3), and it caused a similar cure of healthy plants except for a few treatments (T_2, T_5, T_{12}, and T_{14}). More prominent results (69% increase) were observed after three weeks of treatment application (Figure 4).

The results indicated no significant difference between healthy trees and the treated trees (T_2 to T_{14}) regarding the percent cure of BB syndrome. Noticeably, T_9 produced a 100% brown bast cure after three weeks of treatment application, as shown in Figures 4 and 5, and was not significantly different from T_1. The effects of other treatments produced differential BB cures, but there was no significant difference between all other treatments. This result was in line with a previous similar study using both macro and micronutrients, which was conducted by Nik Hashyati et al. (2022), who observed that brown bast syndrome could be cured by the application of macro- and micronutrients in liquid form and applied on the affected trees.

Table 3
Differences in macronutrients between leaf tissue of healthy and BB-affected trees before treatment application

Rubber plant	N (%)	P (mg/kg)	K (mg/kg)	Ca (mg/kg)	Mg (mg/kg)	S (%)
Affected tree	2.779	302.7	3660.2	1,8621.7	812.7	0.244
Healthy tree	2.724	341.7	3,715.7	1,8282.2	985.8	0.24
p-value	0.765^{ns}	0.737^{ns}	0.686^{ns}	0.908^{ns}	0.449^{ns}	0.775^{ns}

Note. BB = Brown bast; ns = Not significant at $p>0.05$

Table 4
Differences in macronutrients between bark tissue of healthy and BB-affected trees before treatment application

Rubber plant	N (%)	P (mg/kg)	K (mg/kg)	Ca (mg/kg)	Mg (mg/kg)	S (%)
Affected tree	0.463	894.8	4,063.7	9,741.3	1,546	0.092
Healthy tree	0.559	958.3	4,206.8	9,263.8	1,496.8	0.105
p-value	0.023*	0.617^{ns}	0.282^{ns}	0.789^{ns}	0.785^{ns}	0.007*

Note. BB = Brown bast; ns = Not significant at $p>0.05$; * = Significant at $p\leq0.05$

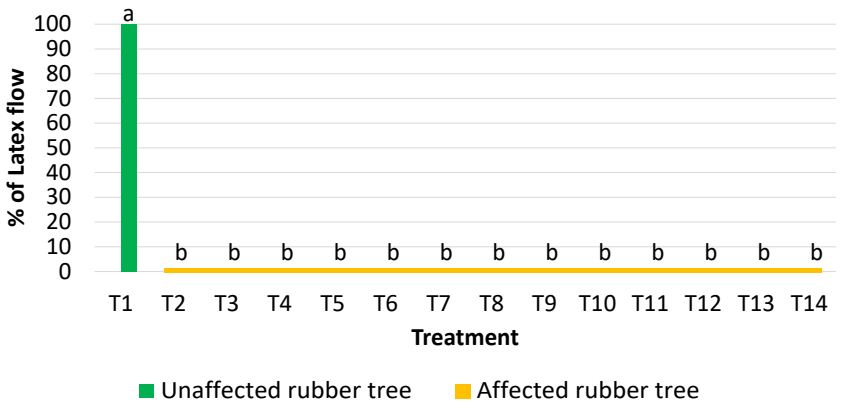

Figure 1. Initial percentage of latex yield of healthy trees and brown bast-affected trees

Note. Bars with the different letters are significantly different at $p \leq 0.05$ according to Tukey's honest significant difference test [T_1 = Control; T_2 = 0.2% N, 0.2 mg/L K, and 0.5% S; T_3 = 0.2% N, 0.5 mg/L K, and 0.2% S; T_4 = 0.2% N, 0.5 mg/L K, and 0.8% S; T_5 = 0.2% N, 0.8 mg/L K, and 0.5% S; T_6 =0.5% N, 0.2 mg/L K, and 0.2% S; T_7 = 0.5% N, 0.2 mg/L, and 0.8% S; T_8 = 0.5% N, 0.5 mg/L K, and 0.5% S; T_9 = 0.5% N, 0.8 mg/L, and 0.2% S; T_{10} = 0.5% N, 0.8 mg/L K, and 0.8% S; T_{11} = 0.8% N, 0.2 mg/L K, and 0.5% S; T_{12} = 0.8% N, 0.5 mg/L K, and 0.2% S; T_{13} = 0.8% N, 0.5 mg/L K, and 0.8% S; T_{14} = 0.8% N, 0.8 mg/L K, and 0.5% S]

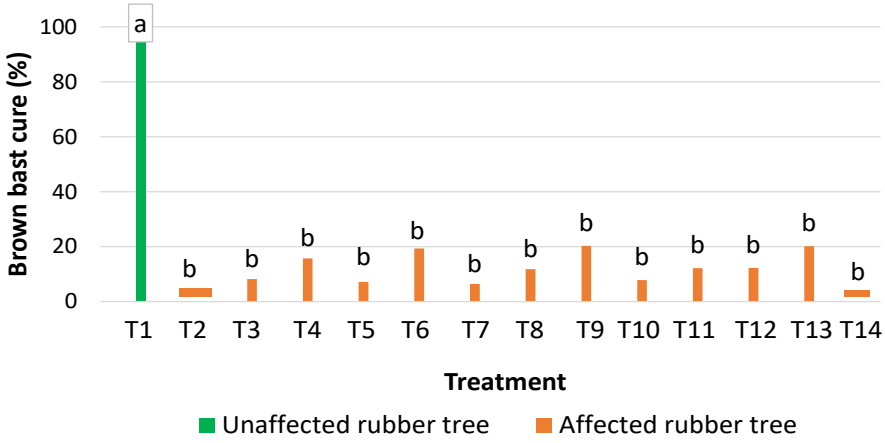

Figure 2. Percentage of brown bast cure after 1 week of treatment application

Note. Bars with the different letters are significantly different at $p \leq 0.05$ according to Tukey's honest significant difference test [T_1 = Control; T_2 = 0.2% N, 0.2 mg/L K, and 0.5% S; T_3 = 0.2% N, 0.5 mg/L K, and 0.2% S; T_4 = 0.2% N, 0.5 mg/L K, and 0.8% S; T_5 = 0.2% N, 0.8 mg/L K, and 0.5% S; T_6 =0.5% N, 0.2 mg/L K, and 0.2% S; T_7 = 0.5% N, 0.2 mg/L, and 0.8% S; T_8 = 0.5% N, 0.5 mg/L K, and 0.5% S; T_9 = 0.5% N, 0.8 mg/L, and 0.2% S; T_{10} = 0.5% N, 0.8 mg/L K, and 0.8% S; T_{11} = 0.8% N, 0.2 mg/L K, and 0.5% S; T_{12} = 0.8% N, 0.5 mg/L K, and 0.2% S; T_{13} = 0.8% N, 0.5 mg/L K, and 0.8% S; T_{14} = 0.8% N, 0.8 mg/L K, and 0.5% S]

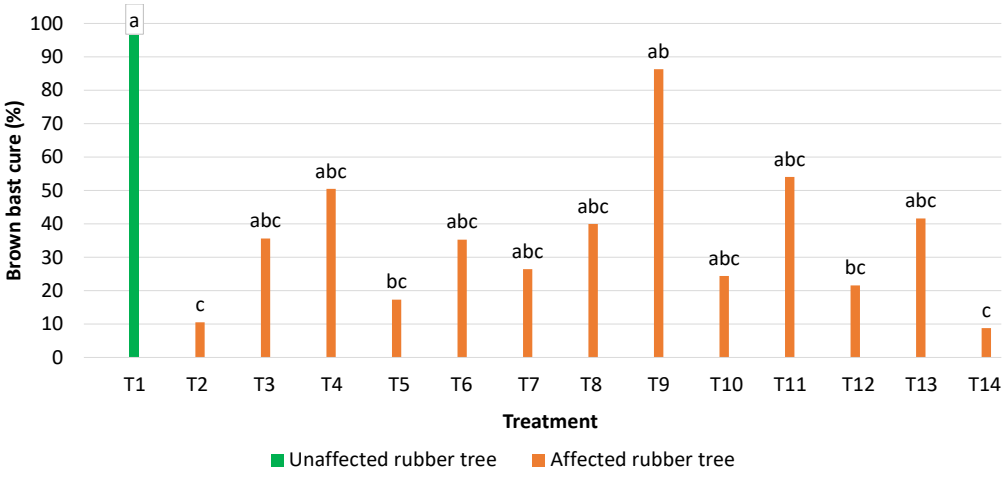

Figure 3. Percentage of brown bast cure after 2 weeks of treatment application

Note. Bars with the different letters are significantly different at $p \leq 0.05$ according to Tukey's honest significant difference test [T_1 = Control; T_2 = 0.2% N, 0.2 mg/L K, and 0.5% S; T_3 = 0.2% N, 0.5 mg/L K, and 0.2% S; T_4 = 0.2% N, 0.5 mg/L K, and 0.8% S; T_5 = 0.2% N, 0.8 mg/L K, and 0.5% S; T_6 =0.5% N, 0.2 mg/L K, and 0.2% S; T_7 = 0.5% N, 0.2 mg/L, and 0.8% S; T_8 = 0.5% N, 0.5 mg/L K, and 0.5% S; T_9 = 0.5% N, 0.8 mg/L, and 0.2% S; T_{10} = 0.5% N, 0.8 mg/L K, and 0.8% S; T_{11} = 0.8% N, 0.2 mg/L K, and 0.5% S; T_{12} = 0.8% N, 0.5 mg/L K, and 0.2% S; T_{13} = 0.8% N, 0.5 mg/L K, and 0.8% S; T_{14} = 0.8% N, 0.8 mg/L K, and 0.5% S]

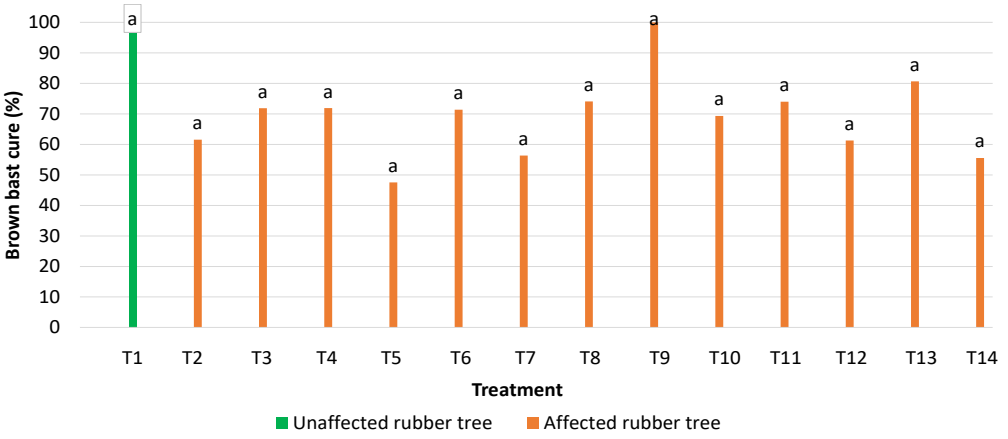

Figure 4. Percentage of brown bast cure after 3 weeks of treatment application

Note. Bars with the different letters are significantly different at $p \leq 0.05$ according to Tukey's honest significant difference test [T_1 = Control; T_2 = 0.2% N, 0.2 mg/L K, and 0.5% S; T_3 = 0.2% N, 0.5 mg/L K, and 0.2% S; T_4 = 0.2% N, 0.5 mg/L K, and 0.8% S; T_5 = 0.2% N, 0.8 mg/L K, and 0.5% S; T_6 =0.5% N, 0.2 mg/L K, and 0.2% S; T_7 = 0.5% N, 0.2 mg/L, and 0.8% S; T_8 = 0.5% N, 0.5 mg/L K, and 0.5% S; T_9 = 0.5% N, 0.8 mg/L, and 0.2% S; T_{10} = 0.5% N, 0.8 mg/L K, and 0.8% S; T_{11} = 0.8% N, 0.2 mg/L K, and 0.5% S; T_{12} = 0.8% N, 0.5 mg/L K, and 0.2% S; T_{13} = 0.8% N, 0.5 mg/L K, and 0.8% S; T_{14} = 0.8% N, 0.8 mg/L K, and 0.5% S]

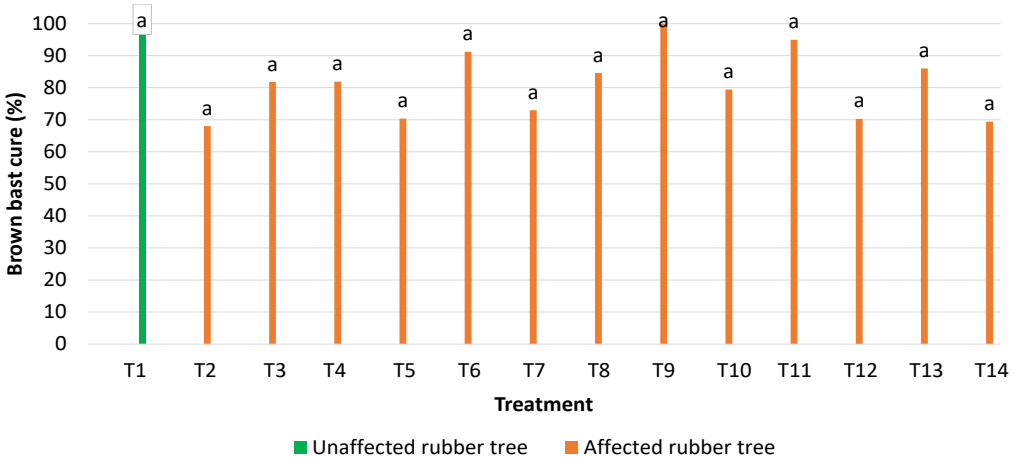

Figure 5. Percentage of brown bast cure after 4 weeks of treatment application

Note. Bars with the different letters are significantly different at $p \leq 0.05$ according to Tukey's honest significant difference test [T_1 = Control; T_2 = 0.2% N, 0.2 mg/L K, and 0.5% S; T_3 = 0.2% N, 0.5 mg/L K, and 0.2% S; T_4 = 0.2% N, 0.5 mg/L K, and 0.8% S; T_5 = 0.2% N, 0.8 mg/L K, and 0.5% S; T_6 =0.5% N, 0.2 mg/L K, and 0.2% S; T_7 = 0.5% N, 0.2 mg/L, and 0.8% S; T_8 = 0.5% N, 0.5 mg/L K, and 0.5% S; T_9 = 0.5% N, 0.8 mg/L, and 0.2% S; T_{10} = 0.5% N, 0.8 mg/L K, and 0.8% S; T_{11} = 0.8% N, 0.2 mg/L K, and 0.5% S; T_{12} = 0.8% N, 0.5 mg/L K, and 0.2% S; T_{13} = 0.8% N, 0.5 mg/L K, and 0.8% S; T_{14} = 0.8% N, 0.8 mg/L K, and 0.5% S]

Table 5
Effect of treatment application on the nutrient content of bark tissue

Factor	N	S	K	P	Mg	Ca
ANOVA analysis						
Treatment	0.847^{ns}	0.126^{ns}	0.777^{ns}	0.484^{ns}	0.090^{ns}	0.490^{ns}
Time	$<0.0001^{*}$	0.0002^{*}	0.280^{ns}	0.071^{ns}	0.676^{ns}	0.062^{ns}
Mean comparison of treatments	(%)	(%)	(%)	(%)	(%)	(%)
Time						
Before	0.409^{b}	0.088^{b}	0.430^{a}	0.101^{a}	0.076^{a}	1.232^{a}
After	0.619^{a}	0.113^{a}	0.457^{a}	0.162^{a}	0.079^{a}	1.311^{a}
Least significant difference (LSD)	0.052	0.012	0.050	0.066	0.012	0.083
Treatment						
T_1	0.522^{a}	0.142^{a}	0.403^{a}	0.112^{a}	0.043^{a}	1.413^{a}
T_2	0.595^{a}	0.097^{a}	0.507^{a}	0.118^{a}	0.085^{a}	1.316^{a}

Table 5 *(continue)*

Factor	N	S	K	P	Mg	Ca
T_3	0.480[a]	0.092[a]	0.415[a]	0.114[a]	0.064[a]	1.349[a]
T_4	0.534[a]	0.095[a]	0.501[a]	0.117[a]	0.077[a]	1.231[a]
T_5	0.513[a]	0.097[a]	0.421[a]	0.115[a]	0.092[a]	1.119[a]
T_6	0.460[a]	0.092[a]	0.423[a]	0.117[a]	0.086[a]	1.274[a]
T_7	0.555[a]	0.094[a]	0.415[a]	0.116[a]	0.098[a]	1.315[a]
T_8	0.533[a]	0.116[a]	0.512[a]	0.342[a]	0.077[a]	1.165[a]
T_9	0.473[a]	0.099[a]	0.427[a]	0.115[a]	0.084[a]	1.270[a]
T_{10}	0.515[a]	0.092[a]	0.444[a]	0.120[a]	0.056[a]	1.227[a]
T_{11}	0.477[a]	0.093[a]	0.423[a]	0.114[a]	0.080[a]	1.242[a]
T_{12}	0.481[a]	0.109[a]	0.472[a]	0.113[a]	0.082[a]	1.268[a]
T_{13}	0.515[a]	0.095[a]	0.411[a]	0.110[a]	0.071[a]	1.260[a]
T_{14}	0.546[a]	0.093[a]	0.445[a]	0.120[a]	0.092[a]	1.352[a]
LSD	0.241	0.055	0.229	0.305	0.057	0.384

Note. ns = Not significant at $p>0.05$; * = Significant at $p\leq0.05$; Means followed by the same letters in a column are not significantly different at $p>0.05$ using Tukey's honest significant difference test [T_1 = Control; T_2 = 0.2% N, 0.2 mg/L K, and 0.5% S; T_3 = 0.2% N, 0.5 mg/L K, and 0.2% S; T_4 = 0.2% N, 0.5 mg/L K, and 0.8% S; T_5 = 0.2% N, 0.8 mg/L K, and 0.5% S; T_6 =0.5% N, 0.2 mg/L K, and 0.2% S; T_7 = 0.5% N, 0.2 mg/L, and 0.8% S; T_8 = 0.5% N, 0.5 mg/L K, and 0.5% S; T_9 = 0.5% N, 0.8 mg/L, and 0.2% S; T_{10} = 0.5% N, 0.8 mg/L K, and 0.8% S; T_{11} = 0.8% N, 0.2 mg/L K, and 0.5% S; T_{12} = 0.8% N, 0.5 mg/L K, and 0.2% S; T_{13} = 0.8% N, 0.5 mg/L K, and 0.8% S; T_{14} = 0.8% N, 0.8 mg/L K, and 0.5% S]

The results indicate that the applications of deficient macronutrients could cure the brown bast problem in rubber trees and restore latex generation similar to healthy rubber trees, as shown in Figure 6. Adequate fertilizer application does not only positively impact economic growth but could equally minimize nutrient loss. Moreover, adequate nutrients could maintain rubber trees' healthy growth and yield (Njukeng et al., 2013). Keralafarmer (2010) stated that nutrient deficiency is one of the factors that cause brown bast in rubber trees. In Malaysia, no more study has been done on curing brown bast syndrome with the addition of deficient macronutrients. Therefore, this finding sheds new light on managing BB syndrome in rubber plantations.

It can be noted that there was a significant difference ($p<0.047$) between S and Mg contents in the bark of *H. brasiliensis* after treatment application, with a negative correlation (r=-0.539) between these elements (Table 6). The increased level of Mg in the rubber bark would decrease the level of S in the bark. Magnesium is generally essential for photosynthesis and latex production. However, the excessive use of fertilizer containing Mg would cause latex instability (Karunanayake &

(a) (b)

Figure 6. Experimental rubber trees: (a) before treatment application (no latex flow) and (b) after treatment application (with latex low)

Priyanthi Perera, 2006), resulting in pre-coagulation and increased brown bast problems. Phosphorus is another essential macronutrient that is necessary for the growth and development of rubber trees. It plays a significant role in the plant's photosynthesis, respiration, and energy transfer. Adequate phosphorus supply increases latex production and improves the quality of latex.

Sulfur is generally essential in protein synthesis, enzyme activation, and photosynthesis. According to Kashyap (2009), the sulfur requirement of plants is more significant than P. Meanwhile, Mg ranks as the least abundant macronutrient in plants compared to Ca, P, and S. Therefore, S was required in higher quantities than Mg.

Therefore, when the deficient macronutrients were supplied to the plant, especially applied directly to the trunk, the bark absorbed the nutrients, and the deficiency was recovered, which led the rubber trees to make regular latex flow.

Table 6
Correlation between nutrient content and brown bast cure of Hevea brasiliensis

	N	P	K	Ca	Mg	S
N	1.000	0.165 0.573	0.438 0.117	0.120 0.684	0.105 0.720	0.083 0.777
P	0.165 0.573	1.000	0.525 0.054	-0.404 0.152	0.001 0.997	0.321 0.263
K	0.438 0.117	0.525 0.054	1.000	-0.330 0.249	0.198 0.497	0.061 0.835

Table 6 *(continue)*

	N	P	K	Ca	Mg	S
Ca	0.120	-0.404	-0.330	1.000	-0.318	0.299
	0.684	0.152	0.249		0.268	0.299
Mg	0.105	0.001	0.198	-0.318	1.000	-0.539
	0.720	0.997	0.497	0.268		0.047
S	0.083	0.321	0.061	0.299	-0.539	1.000
	0.777	0.263	0.835	0.299	0.047*	

Note. * = Significant at $p \leq 0.05$

Effect of New Formulation on Moisture Content in Bark Tissue

The moisture content in the bark indicated a significant difference ($p<0.001$) between before and after treatment (Table 7). The moisture content before treatment application was higher (42.8%) than after treatment application (39.6%). Several factors can contribute to the development of this BB syndrome. Moisture content in the bark has been identified as a key factor of this syndrome (Cheng et al., 2019; Zhang et al., 2021).

High moisture levels in the bark create conditions that favor the growth of microorganisms, including fungi and bacteria, and can cause damage to the bark and cambium tissue. It can also lead to brown bast syndrome in rubber trees (Cheng et al., 2019). On the other hand, maintaining appropriate moisture levels in the bark can help prevent the development of brown bast syndrome.

The low moisture content in the bark after treatment initiates a greater ability of barks to absorb water. That also helped the plants to absorb nutrients and improved latex production. It also increases the viscosity of latex. According to Lin and Lai (2009), the rheological behavior of plant hydrocolloids can be improved by using water, and the viscosity results from the polymer charge in water.

Table 7
Effect of treatment application on the moisture contents of bark tissue

Factor	Moisture content
ANOVA analysis	
Treatment	0.115^{ns}
Time	$<0.001^{*}$
Mean comparison of treatment	(%)
Time	
Before	42.786^{a}
Factor	Moisture content
After	39.593^{b}
Least significant difference (LSD)	1.881

Table 7 *(continue)*

Factor	Moisture content
Treatment	
T_1	42.175[a]
T_2	43.820[a]
T_3	42.563[a]
T_4	40.973[a]
T_5	42.652[a]
T_6	37.562[a]
T_7	41.797[a]
T_8	43.222[a]
T_9	41.473[a]
T_{10}	37.792[a]
T_{11}	44.292[a]
T_{12}	41.067[a]
T_{13}	38.783[a]
T_{14}	38.477[a]
LSD	8.715

Note. ns = Not significant at $p>0.05$; * = Significant at $p\leq0.05$; Means followed by the same letters in a column are not significantly different at $p>0.05$ using Tukey's honest significant difference test [T_1 = Control; T_2 = 0.2% N, 0.2 mg/L K, and 0.5% S; T_3 = 0.2% N, 0.5 mg/L K, and 0.2% S; T_4 = 0.2% N, 0.5 mg/L K, and 0.8% S; T_5 = 0.2% N, 0.8 mg/L K, and 0.5% S; T_6 =0.5% N, 0.2 mg/L K, and 0.2% S; T_7 = 0.5% N, 0.2 mg/L, and 0.8% S; T_8 = 0.5% N, 0.5 mg/L K, and 0.5% S; T_9 = 0.5% N, 0.8 mg/L, and 0.2% S; T_{10} = 0.5% N, 0.8 mg/L K, and 0.8% S; T_{11} = 0.8% N, 0.2 mg/L K, and 0.5% S; T_{12} = 0.8% N, 0.5 mg/L K, and 0.2% S; T_{13} = 0.8% N, 0.5 mg/L K, and 0.8% S; T_{14} = 0.8% N, 0.8 mg/L K, and 0.5% S]

Effect of New Formulation on Latex Production

The effect of treatment application indicated a significant ($p<0.05$) increment in latex yield (Table 8). For instance, in December 2019, the healthy plants (T_1) had a higher latex yield (79.69 g/tapping/tree) than other treatments (T_2 to T_{14}), except for T_3 (62.09 g/tapping/tree). In January 2020, significant differences were noticed between T_1 with, T4 and T_{12}. However, there was no significant difference between T_1 with T_3, T_9, T_2, T_5, T_7, T_8, and T_{13}. The treatment T_3 produced the highest yield (57.73 g/tapping/tree) after two months of treatment application, similar to T_9 (51.73 g/tapping/tree). Macronutrients are essential nutrients required in large quantities by rubber trees to grow and produce high-quality latex (Chowdhury et al., 2019; Zhou et al., 2018). For example, an adequate nitrogen supply increases the number of latex vessels and the latex yield.

However, excessive nitrogen supply can lead to the production of low-quality latex. Potassium is an essential macronutrient that regulates the plant's water balance and enhances its stress resistance. It also increases the number of latex vessels, the latex yield, and the quality of latex. Calcium is important for the structural development of rubber trees and is related to the thickness and elasticity of the latex vessels, increases the latex yield, and improves the quality of latex. Magnesium is necessary for the synthesis of chlorophyll, which is essential for photosynthesis. Adequate magnesium supply also increases the latex yield and improves the quality of latex. In summary, macronutrients are crucial in rubber trees' growth and development and significantly affect latex production and quality. A balanced supply of these nutrients is essential for high latex yield and quality.

Salisu and Daud (2016) reported that the optimum fertilizer level was achieved at 150% of the standard dose (780 kg/ha of a

Table 8
Latex yield (g/tapping/tree) of rubber trees after treatment application

Factor	Latex yield			
	November 2019	December 2019	January 2020	February 2020
ANOVA analysis				
Treatment	<0.0001*	0.002*	0.046ns	0.002*
Mean comparison of treatment		(g)		
Treatment				
T_1	73.86[a]	79.69[a]	74.53[a]	62.20[a]
T_2	0[b]	14.67[c]	29.66[abc]	24.39[bcd]
T_3	0[b]	62.09[ab]	57.73[ab]	40.44[b]
T_4	0[b]	9.42[c]	10.40[c]	11.39[d]
T_5	0[b]	20.87[c]	52.11[abc]	37.81[bc]
T_6	0[b]	20.41[c]	20.14[bc]	20.30[bcd]
T_7	0[b]	32.33[bc]	38.56[abc]	30.57[bcd]
T_8	0[b]	10.71[c]	32.50[abc]	26.94[bcd]
T_9	0[b]	22.34[c]	51.85[abc]	26.57[bcd]
T_{10}	0[b]	15.68[c]	18.98[bc]	14.93[cd]
T_{11}	0[b]	40.41[bc]	22.48[bc]	20.77[bcd]
T_{12}	0[b]	6.51[c]	9.60[c]	7.93[d]
T_{13}	0[b]	36.36[bc]	43.17[abc]	30.44[bcd]
T_{14}	0[b]	16.33[c]	12.68[bc]	12.19[d]
Least significant difference	0.1055	56.259	70.499	38.734

Note. ns = Not significant at $p>0.05$; * = Significant at $p\leq0.05$; Means followed by the same letters in a column are not significantly different at $p>0.05$ using Tukey's honest significant difference test [T_1 = Control; T_2 = 0.2% N, 0.2 mg/L K, and 0.5% S; T_3 = 0.2% N, 0.5 mg/L K, and 0.2% S; T_4 = 0.2% N, 0.5 mg/L K, and 0.8% S; T_5 = 0.2% N, 0.8 mg/L K, and 0.5% S; T_6 =0.5% N, 0.2 mg/L K, and 0.2% S; T_7 = 0.5% N, 0.2 mg/L, and 0.8% S; T_8 = 0.5% N, 0.5 mg/L K, and 0.5% S; T_9 = 0.5% N, 0.8 mg/L, and 0.2% S; T_{10} = 0.5% N, 0.8 mg/L K, and 0.8% S; T_{11} = 0.8% N, 0.2 mg/L K, and 0.5% S; T_{12} = 0.8% N, 0.5 mg/L K, and 0.2% S; T_{13} = 0.8% N, 0.5 mg/L K, and 0.8% S; T_{14} = 0.8% N, 0.8 mg/L K, and 0.5% S]

blend of 10–16–9-2). A study by Chowdhury et al. (2019) reported a significant increase in latex yield by 18.3% with NPK fertilizers. Mokhatar et al. (2012) reported that the currently recommended fertilizer doses are insufficient, and for optimum growth, a precise fertilizer application should be considered to optimize fertilizer use efficiency. However, in February 2020, the latex yield was lowered in the treated rubber trees (T_2 to T_{14}) along with healthy plants compared to January yields, which might be due to annual wintering (February to May) and leaf senescence in Malaysia (Qi

et al., 2014). The wintering caused leaves to fall and disturbed photosynthetic activity, directly affecting latex production.

CONCLUSION

Since significant differences in macronutrient contents, especially in the bark of brown bast-affected rubber trees, are found, the nutrient-adjusted formulation of fertilizers is the best option to cure the brown bast disease and to improve the latex yield. Treatment T_9 comprised 0.5% N, 0.8 mg/L K, and 0.2% S is the best treatment (BB cure = 100%, yield = 51.85 g/tapping/tree) to cure the brown bast of rubber trees for the study area. The treatment T_3 (0.2% N, 0.5 mg/L K, and 0.2% S) can also be used, as it caused an 80% cure of BB syndrome after four weeks of treatment application and produced the highest latex yield (57.73 g/tapping/tree) after two months of treatment application. The curing of brown bast by applying this nutrient-adjusted formulation caused stability of latex flow, increment in nutrient content, and improved the latex yield. Therefore, it is recommended that first, the difference in macronutrients in the barks of BB-affected and healthy plants of any concerned area should be studied, and the deficiency, if any, should be adjusted in the liquid fertilizer formulation for treating the brown bast syndrome and to increase latex yield of rubber trees. It is the first report on the cure of brown bast syndrome in rubber trees by the trunk application of deficient-adjusted macronutrients.

ACKNOWLEDGEMENTS

The authors would like to thank Universiti Putra Malaysia (UPM) for the financial support (grant number 9645300) under the Graduate Research Fellowship (GRF) program of UPM to complete this research successfully. We would also like to thank the staff of FELCRA, Simpang Renggam, Johor, Malaysia for assisting in data collection and field selection. We gratefully acknowledge all the lab assistants of UPM Serdang, Selangor, who graciously contributed to the success of this work.

REFERENCES

Budiasih, R., Salim, M. A., Apriani, I., Hasani, S., & Subandi, M. (2020). Effect of stimulant (ethephon) application and tapping frequency on latex production of rubber tree (*Hevea brasiliensis* Muell. Arg.). *Bulgarian Journal of Agricultural Science*, *26*(4), 793–799.

Cheng, L., Li, H., Li, Z., Huang, Z., Lin, Y., Cai, L., & Yang, H. (2019). Effects of bark moisture content on brown bast disease incidence in rubber tree plantations. *Forests*, *10*(5), 386.

Chowdhury, S. A., Hossain, M. M., Uddin, M. K., & Rahman, M. M. (2019). Effects of different doses of NPK fertilizers on growth, yield and quality of latex in rubber (*Hevea brasiliensis*) trees. *Scientific Reports*, *9*(1), 1-8.

Daud, N. W. (2013). *Rubber plantation: Soil management and nutritional requirements*. UPM Press.

Forster, J. C. (1995). Soil sampling, handling, storage and analysis. In K. Alef & P. Nannipieri (Eds.), *Methods in applied soil microbiology and biochemistry* (pp. 49-121). Academic Press. https://doi.org/10.1016/B978-012513840-6/50018-5

Foster, H. L. (1971). Rapid routine soil and plant analysis without automatic equipment. *East African Agricultural and Forestry Journal*, *37*(2), 160-170. https://doi.org/10.1080/00128325.1971.11662519

Jones, J. M., Heineman, K. D., & Dalling, J. W. (2019). Soil and species effects on bark nutrient storage in a premontane tropical forest. *Plant and Soil*, *438*, 347-360. https://doi.org/10.1007/s11104-019-04026-9

Karunanayake, L., & Priyanthi Perera, G. M. (2006). Effect of magnesium and phosphate ions on the stability of concentrated natural rubber latex and the properties of natural rubber latex-dipped product. *Journal of Applied Polymer Science*, *99*(6), 3120-3124. https://doi.org/10.1002/app.22944

Kashyap, R. K. (2009). *Soil fertility, fertilizer, and integrated nutrient management*. Oxford Book Company.

Keralafarmer. (2010, 14 January). *Complete remedy for brown bast on rubber trees*. http://agropedia.iitk.ac.in/content/complete-remedy-brown-bast-rubber-trees

Keralafarmer. (2019, 30 December). *Brown bast in rubber trees can be cured*. http://agropedia.iitk.ac.in/content/remedy-bown-bast

Kowalenko, C. G. (2001). Assessment of Leco CNS-2000 analyser for simultaneously measuring total carbon, nitrogen, and sulphur in soil. *Communications in Soil Science and Plant Analysis*, *32*(13-14), 2065-2078. https://doi.org/10.1081/CSS-120000269

Kumari, P. V. K., Yarraguntla, S. R., Sharmila, M., & Gulibindala, E. (2021). Application of Box-Behnken design for formulation parameters of eslicarbazepine tablets. *Indian Journal of Pharmaceutical Sciences*, *83*(3), 575-583. https://doi.org/10.36468/pharmaceutical-sciences.808

Lacote, R., Gabla, O., Obouayeba, S., Eschbach, J. M., Rivano, F., Dian, K., & Gohet, E. (2010). Long-term effect of ethylene stimulation on the yield of rubber trees is linked to latex cell biochemistry. *Field Crops Research*, *115*(1), 94–98. https://doi.org/10.1016/j.fcr.2009.10.007

Lin, H.-Y., & Lai, L.-S. (2009). Isolation and viscometric characterization of hydrocolloids from mulberry (*Morus alba* L.) leave. *Food Hydrocolloids*, *23*(3), 840-848. https://doi.org/10.1016/j.foodhyd.2008.03.018

Malaysian Rubber Board. (2009). Fertilizer application and field maintenance. In *Rubber plantation and processing technologies* (pp. 23-25). Malaysia Rubber Board Kuala Press.

Malaysian Rubber Council. (n.d.). *Malaysian rubber production, consumption, and trade*. MRC. https://www.myrubbercouncil.com/industry/malaysia_production.php

Mokhatar, S. J., Daud, N. W., & Ishak, C. F. (2012). Response of *Hevea brasiliensis* (RRIM 2001) planted on an oxisol to different rates of fertilizer application. *Malaysian Journal of Soil Science*, *16*(1), 57-69.

Nandris, D., Moreau, R., Pellegrin, F., Chrestin, H., Abina, J., & Angui, P. (2004). Rubber tree (*Hevea brasiliensis*) bark necrosis syndrome II: First comprehensive report on causal stresses. *Plant Disease*, *88*(9), 1047. https://doi.org/10.1094/PDIS.2004.88.9.1047A

Nazri, A. Z. (2020). Transcriptome analyses of tapping panel dryness (TPD) in *Hevea brasiliensis* treated with latex stimulant RRIM HYDROBEST™. *Journal of Tropical Plant Physiology*, *12*(1), 13-26. https://doi.org/10.56999/jtpp.2020.12.1.2

Nik Hashyati, N. H., Sulaiman, Z., Salisu, M. A., Samad, M. Y. A., Mohamed, M. T. M., Mokhtar, M. S. J., Ghani, Z. A. B., & Adinan, A. (2022). Application of different rates and frequencies of rejuvenator for the treatments of brown bast syndrome on *Hevea brasiliensis*. *Indian Journal of Agricultural Research*, *56*(4), 469-473. https://doi.org/10.18805/ijare.af-678

Njukeng, J. N., Ehabe, E. E., Nkeng, G. E., Schicks, J., Kratz, S., & Schnug, E. (2013). Investigations on the nutritional status of *Hevea brasiliensis* plantations in the humid forest zone of Cameroon

Part 2: Establishment of macronutrient norms. *Journal for Kulturpflanzen*, *65*(10), 376-384. https://doi.org/10.5073/JFK.2013.10.02

Paul, V., Ramesh, K. V., & Pandey, R. (2017). Analysis of mineral nutrients: Sampling techniques and methods of digestion for plant samples. In *Manual of ICAR sponsored training programme for technical staff of ICAR institutes on "Physiological Techniques to Analyze the Impact of Climate Change on Crop Plants"* (pp. 77-81). Indian Agricultural Research Institute. https://doi.org/10.13140/RG.2.2.23335.44967

Priyadarshan, P. M. (2003). Contributions of weather variables for specific adaptation of rubber tree (*Hevea brasiliensis* Muell. Arg) clones. *Genetics and Molecular Biology*, *26*(4), 435–440. https://doi.org/10.1590/S1415-47572003000400006

Qi, D., Zhou, J., Xie, G., & Wu, Z. (2014). Studies on rubber (*Hevea brasiliensis*) trees exist plant type after planting and available tapping tree of rubber plantation in China. *American Journal of Plant Sciences*, *5*(20), 3017-3021. https://doi.org/10.4236/ajps.2014.520318

Rhoades, J. D. (1993). Electrical conductivity methods for measuring and mapping soil salinity. In D. L. Sparks (Ed.), *Advances in Agronomy* (Vol. 49, pp. 201- 251). Elsevier. https://doi.org/10.1016/S0065-2113(08)60795-6

Said, M. A. M., & Ghani, E. A. (2012, June 25-26). *R&D transformation programme for the natural rubber industry* [Paper presentation]. Proceeding of the 7th International Planters' Conference, Kuala Lumpur, Malaysia. https://rios.lgm.gov.my/cms/fedDigiContentDetail.jsp?searchText=&selTab=digiCon&id=vital1:80668&type=Article

Sainoi, T., & Sdoodee, S. (2012). The impact of ethylene gas application on young tapping rubber trees. *Journal of Agricultural Technology*, *8*(4), 1497-1507.

Salisu, M. A., & Daud, N. W. (2016). Effect of fertilizer rates and soil series on root morphological traits and root: shoot ratio of immature natural rubber (*Hevea brasiliensis*). *International Journal of Scientific and Engineering Research*, *7*(9), 1373–1378.

Varley, J. A. (1966). Automatic methods for the determination of nitrogen, phosphorous and potassium in plant material. *Analyst*, *91*, 119-126. https://doi.org/10.1039/AN9669100119

Venkatachalam, P., Thulaseedharan, A., & Raghothama, K. (2007). Identification of expression profiles of tapping panel dryness (TPD) associated genes from the latex of rubber tree (*Hevea brasiliensis* Muell. Arg.). *Planta*, *226*, 499–515. https://doi.org/10.1007/s00425-007-0500-8

Wintering season forces villagers to do odd jobs for extra income. (2021, February 23). *TheSun Daily*. https://www.thesundaily.my/home/wintering-season-forces-villagers-to-do-odd-jobs-for-extra-income-GF6869967

Zhang, Z., Li, X., He, J., & Zhang, L. (2021). Effects of bark moisture content and temperature on the occurrence of brown bast disease in *Hevea brasiliensis*. *Journal of Central South University of Forestry and Technology*, *41*(4), 22-28.

Zhou, L., Ye, X., Luo, Z., Peng, Y., & Chen, R. (2018). Effects of macro-nutrient fertilizer on latex yield and quality of *Hevea brasiliensis* Muell. Arg. *Journal of Plant Nutrition*, *41*(3), 328-339.

Pertanika J. Trop. Agri. Sci. 46 (4): 1327 - 1345 (2023)

PERTANIKA JOURNALS

TROPICAL AGRICULTURAL SCIENCE

Journal homepage: http://www.pertanika.upm.edu.my/

Cryopreservation of Bovine Oocyte Using Vitrification Solution and Cryotop Techniques

Nabila Jasmine Afifi Mohd Nawi[1], Habsah Bidin[2] and Mamat Hamidi Kamalludin[1,3]*

[1]Department of Animal Science, Faculty of Agriculture, Universiti Putra Malaysia, 43400 Serdang, Selangor, Malaysia
[2]Livestock Science Research Centre, MARDI Headquarters, 43400 Serdang, Selangor, Malaysia
[3]Institute of Tropical Agriculture and Food Security, Universiti Putra Malaysia, 43400 Serdang, Selangor, Malaysia

ABSTRACT

Cryopreservation is used to preserve biological samples over an extended period at ultra-low temperatures. This process evolved into vitrification, a more advanced and superior technology in which fluids or water molecules form a glass-like structure without forming ice crystals. Unlike fresh cells, cryopreservation is reported to reduce oocyte viability and developmental competency. This study employed two vitrification techniques, vitrification solution (VS) and Cryotop, to investigate the meiotic resumption in bovine. Oocytes were extracted from cow ovaries collected from slaughterhouses in Banting and Shah Alam, Selangor, Malaysia. The oocytes were grouped (A, B, and B') based on cumulus morphology and matured *in vitro* in a culture dish (humidified 5% carbon dioxide incubator at 38.5°C) for 20 to 24 hr. Oocytes were vitrified after maturation using straws or aids of Cryotop sheets, then submerged in liquid nitrogen and stored for five days before defrosting for cryoprotectant elimination. By using Giemsa staining, the maturation state of fresh and vitrified bovine oocytes was evaluated through five parameters: zygotene, pachytene, diakinesis, metaphase I, and metaphase II. The maturation rate demonstrated only slight differences in the three groups of oocytes treated with VS (A: 44.79%; B: 30.97%; B': 20.70%) and Cryotop (A: 39.42%; B: 37.27%; B': 28.97%), which were significantly lower than fresh oocytes (A: 55.83%; B: 44.82%; B': 56.17%). Both VS and Cryotop methods were viable options for cryopreserving oocytes, but the Cryotop technique was more effective in increasing the meiotic competence of poor-quality oocytes.

Keywords: Bovine, cryopreservation, Cryotop, oocyte, vitrification

ARTICLE INFO

Article history:
Received: 23 February 2023
Accepted: 24 May 2023
Published: 02 November 2023

DOI: https://doi.org/10.47836/pjtas.46.4.16

E-mail addresses:
gs56122@student.upm.edu.my (Nabila Jasmine Afifi Mohd Nawi)
habsahb@mardi.gov.my (Habsah Bidin)
mamath@upm.edu.my (Mamat Hamidi Kamalludin)
*Corresponding author

ISSN: 1511-3701
e-ISSN: 2231-8542

INTRODUCTION

Oocyte cryopreservation has been actively investigated due to its powerful applications in livestock and human reproduction for more than three decades (Dhali et al., 2018). The ability to preserve the viability of reproductive cells and tissues on long-term freezing facilitates its application in animal and human reproduction (Vladimirov et al., 2019). Nevertheless, oocyte cryopreservation results in lower pregnancy and survival rates compared to freshly derived gametes, namely sperm, oocytes, and embryos (Basirat et al., 2016; Tharasanit & Thuwanut, 2021; Vining et al., 2021).

Despite the progress achieved in using various procedures such as *in vitro* maturation (IVM), *in vitro* fertilisation (IVF), and *in vitro* culture (IVC), there is still a need to improve the cryopreservation technique of oocytes in buffalo and bovine embryos produced under *in vitro* conditions (Sanches et al., 2019). Although modest reproductive technologies such as artificial insemination (AI), embryo transfer (ET), and IVF have been successfully applied in bovine and resulting in the birth of live offspring, *in vitro* produced (IVP), embryos are still not fully optimised in bovine and other domestic species (Aguila et al., 2020; Saunders & Parks, 1999). The success rate of oocyte cryopreservation is typically low compared to non-cryopreserved oocytes (Tharasanit & Thuwanut, 2021), although they survived both the freezing and thawing processes (Tao & Del Valle, 2008). Cryopreserved oocytes were reported to be more difficult than embryos (Dhali et al., 2018), as oocytes depicted high susceptibility to intracellular ice formation and low surface area to volume ratio (Tharasanit & Thuwanut, 2021). Several factors are responsible for the lower efficiency of *in vitro* production of embryos compared to *in vivo*, which could impact the development of bovine oocytes and their ability to develop into blastocysts (Abd El-Aziz et al., 2016). The impact of oocyte metabolic changes on lipid composition and cryo-tolerance are among the factors that occur in *in vitro* culture conditions compared to *in vivo* (Idrissi et al., 2021).

Cryopreservation procedures must, therefore, be improved to enhance the quality and yield of transferable bovine embryos. Cryopreservation often uses a vitrification solution technique to preserve living cells such as oocytes, zygotes, and blastocysts (Nagy et al., 2020). Such procedures ensure a consistent supply of oocytes and embryos for subsequent assisted reproduction applications such as *in vitro* embryo production (IVEP), embryo transfer (ET), stem cell production, and gene editing (Dhali et al., 2018). The vitrification technique can be defined as a cryopreservation process of biological samples in which a glass-like solution solidifies without forming ice crystals (Aljaser, 2022). A critical stage in a successful cryopreservation procedure is selecting and optimising freezing and thawing rates. This technique requires rapid cooling rates and concentrated cryoprotectant solutions to properly vitrify

the oocytes (Fathi et al., 2018; Kader et al., 2009; Reyes & Jaramillo, 2016).

Cryoprotectants, known as cryoprotective additive (CPA) solutions, are vital in freezing and thawing processes to prevent damage to samples. Samples may be damaged due to intracellular ice crystal formation with uncontrolled dehydration during freezing and 'osmotic shock' or swelling injury due to multiple flows between CPA solutions during solution warming (Sydykov et al., 2018). Warming the solution to 37°C and thawing in descending order of concentrated CPA to obtain gradual rehydration will reduce the osmotic shock in cryopreserved samples post-thawing (Kader et al., 2009; Whaley et al., 2021). The solution needs to be warmed to maintain the viability of oocytes and facilitate a faster recovery rate after sample preservation (Whaley et al., 2021). However, some CPAs, such as dimethyl sulfoxide (DMSO), are toxic to cells, especially at temperatures above 4°C (Tonev et al., 2020). Exposure to high levels of CPA during vitrification is hazardous to oocytes, resulting in parthenogenetic activation and zona hardening, compromising the subsequent development of vitrified/thawed oocytes (Fathi et al., 2018). Rapid freezing and thawing in a culture medium are important to reduce CPA toxicity (Jain & Paulson, 2006; Whaley et al., 2021). The toxicity of CPA can also be reduced by utilising two permeable CPAs instead of one to reduce or mitigate the toxic effect of a single CPA (Angel-Velez et al., 2021; Mahmoud et al., 2016; Nagy et al., 2009).

The common choices of CPAs in a vitrification procedure are sucrose and trehalose, which are non-permeable and can lessen the osmotic stress that develops throughout the process. In contrast, permeable CPAs such as glycerol, ethylene glycol (EG), DMSO, and methanol can penetrate the cells and replace intracellular water to generate osmotic stress (Angel-Velez et al., 2021; Do et al., 2016). New vitrification devices have also been developed to diminish the volume of the vitrification solution to accelerate the cooling process according to sample size (Bottrel et al., 2019; Fathi et al., 2018). In the latest development, a cryo referred to as the Cryotop technique is utilised in the cryopreservation process, which uses a minimum amount of vitrification solution (Bottrel et al., 2019; Cobo et al., 2008; Kuwayama, 2007). This method was initially employed in the cryopreservation of human oocytes, resulting in a 91% oocyte survival rate, followed by a blastocyst development rate of 50% (Kuwayama et al., 2005). Recent findings also demonstrated improved results when employing the Cryotop method in humans, with cleaved embryo survival rates and embryo live birth rates of 91.63 and 25.64%, respectively (Keshavarzi et al., 2022). These findings indicated that a combination of cryo-device and concentrated cryoprotectant led to higher survival rates of oocyte and pregnancy in humans, which can be applied to other developmental stages such as zygotes, cleavages, and blastocysts in bovine.

The Cryotop technique consists of thin polypropylene strips in which oocytes are loaded in an extremely small amount of the vitrification solution, a plastic handle, and a straw cover (Liu & Li, 2020). Cryotop accelerates the cooling rate through an open method, whereby samples are directly exposed to sterilised liquid nitrogen to avoid cryoinjury during chilling (Hochi, 2022; Liu & Li, 2020). The Cryotop device serves as a vitrification container for embryos and oocytes (Liu & Li, 2020), resulting in a high post-thawing survival rate (Kuwayama et al., 2005). The cryo-device has been reported to be more effective as the method entails a different strategy during the cooling process in which various carrier devices are used (Sripunya et al., 2010).

Presently, the government's restriction on slaughtering female animals, unless they are no longer productive, infertile, or diseased has contributed to the poor availability of cow ovaries in the local slaughterhouses. When there is abundant availability, the cryopreservation of bovine oocytes would be a suitable preservation measure to address the limited supply (Aljaser, 2022). Comparisons between two cryopreservation techniques, namely conventional and advanced cryo-device approaches, could offer improved guidelines for implementing these methods in bovine reproductive biotechnologies. Thus, this study aims to compare the Cryotop technique with the conventional cryopreservation method using a vitrification solution (VS). The meiotic resumption of the cryopreserved bovine oocytes was evaluated to determine the efficiency of the two techniques.

MATERIALS AND METHODS

Experimental Design

Oocytes with three different groups of cumulus cell layer (A, B, and B') were randomly assigned to the control group or unvitrified oocyte (Treatment 1), and two different freezing procedures: vitrification solution (Treatment 2) and Cryotop technique (Kitazato Supply Co., Japan) (Treatment 3). The meiotic status of the control group was determined immediately after IVM, whereas the two vitrification treatments were performed after IVM and freezing. After IVM, all oocytes were fixed, stained, and evaluated for their meiotic stages: zygotene, pachytene, diakinesis, metaphase I, and metaphase II.

Bovine Ovaries Collection

A total of 42 slaughtered native breed cattle from the slaughterhouse were sampled to collect ovaries. The cattle were slaughtered primarily owing to old age, illness, and sterility. Cattle ovaries were collected twice weekly from the local slaughterhouse in Banting and Shah Alam, Selangor, Malaysia and transported within two hours to the Gamete Laboratory, Livestock Science Research Centre, Malaysian Agricultural and Research Development Institute (MARDI) in Serdang. The ovaries were kept in phosphate-buffered saline (PBS, Sigma, USA) at 30 to 37°C during transportation from the slaughterhouse to the laboratory. Oocytes were obtained from the ovaries by slicing through the vesicular follicles using a sterile scalpel blade (Davachi et al., 2014), as shown in Figure 1 and were rinsed

with PBS supplemented with 10% foetal bovine serum (FBS, Hexcel-Berlin GmbH, Germany) before being subjected to IVM.

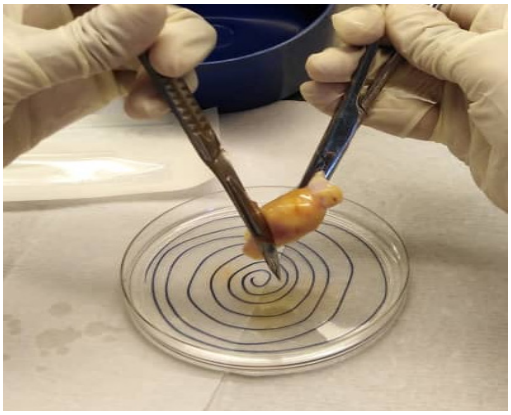

Figure 1. Oocytes were extracted from a bovine ovary using the slicing procedure

In vitro Maturation (IVM)

Cumulus-oocytes-complexes (COCs) were washed twice in tissue culture medium (TCM199, Sigma, USA) before being transferred and incubated in maturation droplets. The maturation droplet was prepared using TCM199 added with 0.1 M 17β-oestradiol (Sigma, USA) and 50 µm cysteamine solution (v/v) (Sigma, USA) and covered with mineral oil (Sigma, Canada). The COCs were loaded into the droplets according to the groups: Group A: packed and dense cumulus cell layer, Group B: less packed and less dense cumulus cell layer, and Group B': partial cumulus cell layer or almost naked (Bidin, 2005; Bidin et al., 2012) as in Figure 2. The oocytes were matured at 38.5°C in a humidified, 5% CO_2 incubator for 20 to 24 hr.

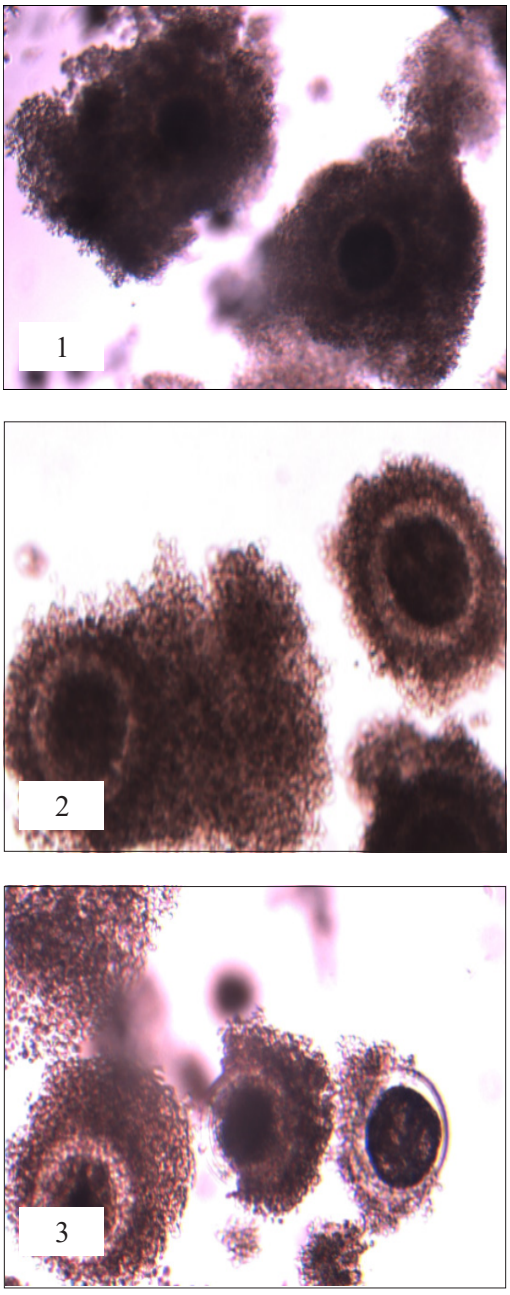

Figure 2. Oocytes used were differentiated based on the layer of cumulus cells around the oocytes (100× magnification)

Cryopreservation Technique

All media involved in the vitrification and thawing processes were kept at room temperature, except for the warming solution, which was kept at 37°C. Initially, matured oocytes were denuded and washed twice in TCM199 and added with 10% FBS for a few minutes. Two vitrification techniques, VS (Experiment 1) and Cryotop vitrification technique (Experiment 2), were used for this experiment. The VS solution for the conventional vitrification procedure was prepared according to Valdez et al. (1992), whereas the Cryotop device, together with the freezing and thawing media, was purchased from Kitazato Supply Co. (Japan).

Experiment 1: Conventional Vitrification Technique-freezing Technique. The vitrification process started by transferring the denuded matured oocytes into a 4-well plate containing 10% glycerol (Sigma, USA), VS1, VS2, and 1 M sucrose (Sigma, USA). Vitrification media was synthesised by preparing modified Dulbecco's Phosphate-Buffered Saline (m DPBS, Sigma, USA) upon mixing DPBS (Sigma, USA) with 15% FBS (Hexcel-Berlin GmbH, Germany). A 10% (v/v) glycerol (Sigma, USA) was prepared in m DPBS, whereas VS1 and VS2 were prepared using glycerol (Sigma, USA) and EG (Sigma, Germany) in m-DPBS in a ratio of 1:2:7 and 1:1:2, respectively. Denuded oocytes were incubated in 10% glycerol (Sigma, USA) for 5 min and later in the vitrification media twice for 6 min, 5 min in VS1 and immediately transferred to VS2 for another 1 min. In less than 1 min, m DPBS cleansed straw was loaded with 3 to 5 oocytes in VS2 with 1 M sucrose (Sigma, USA) at both ends of the straw, as shown in Figure 3. All straws were then submerged in a liquid nitrogen tank for storage.

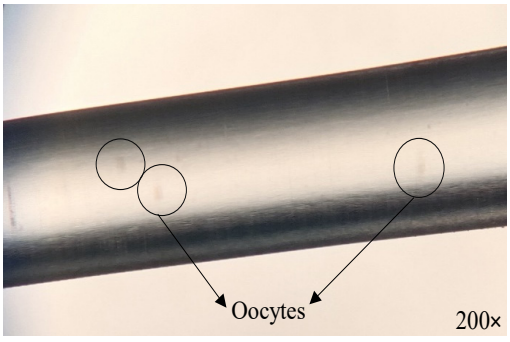

Figure 3. Matured oocytes were loaded into the conventional straw in VS2 solution for storage

Thawing Process. Thawing is required to remove the excess CPAs from the previous freezing technique. The EG (Sigma, Germany) and glycerol (Sigma, USA), which were used as CPAs in this study, were eliminated through a five-step procedure using thawing solutions from higher to lower concentrations of sucrose, starting from 1, 0.75, 0.50, 0.25, and 0.125 M in descending order. The sucrose concentration was prepared using m DPBS (Sigma, USA) mixed with sucrose (Sigma, USA). In the thawing process, oocytes were transferred into m DPBS containing sucrose with concentrations of 1, 0.75, 0.50, 0.25, and 0.125 M in sequence for 5 min each (Figure 4) before being transferred into m-DPBS. Oocytes were washed thrice in m-DPBS and transferred into TCM 199

(Sigma, USA) media supplemented with 17β-oestradiol (Sigma, USA). Finally, the oocytes were cultured in a humid, 5% CO_2 incubator at 38.5°C for 30 min before the fixing procedure.

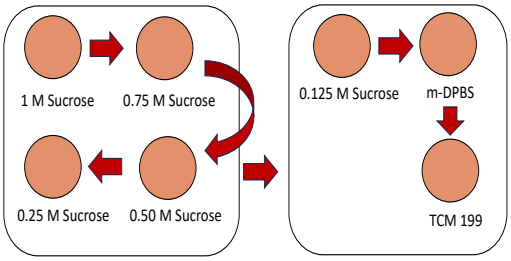

Figure 4. Vitrified oocytes were defrosted for 5 min each in descending concentrations of sucrose in the conventional straw thawing technique

Experiment 2: Cryotop Vitrification Technique-freezing Technique. Oocytes were vitrified using the Cryotop vitrification technique, consisting of a Cryotop device and commercial Cryotop media based on the manufacturer's instructions (Kitazato Supply Co., Japan). The latter comprises basic medium (BS), equilibration solution (ES), and vitrification solutions 1 (VS1) and 2 (VS2). A repro plate was prepared by adding 20 µl BS and 300 µl each of VS1 and VS2. The oocytes were transferred and left at the bottom of the 20 µl BS for several seconds. Oocytes were then equilibrated thrice by 1) adding a layer of 20 µl ES gently on the top of the BS and gently pushing the oocyte down the well and left for 3 min, followed by 2) 20 µl ES for 3 min before being supplemented with 3) 240 µl ES on top of the layer of the mixture from steps 1 and 2 for another 6 to 9 min. Oocytes were then exposed to the vitrification solution starting with VS1 for 30 s by sucking and releasing oocytes at various points using Pasteur pipettes and transferred into VS2 with a similar step to VS1 for another 30 s. A stereomicroscope was used to retrieve 3 to 5 oocytes and subsequently loaded into the Cryotop sheet (Figure 5) within less than 1 min of the oocyte's immersion in VS2. Almost all traces of BS, ES, and VS1 solutions from previous exposure covering the oocytes were eliminated, leaving only a small volume of less than 1 µl of VS2. Cryotop were plunged into liquid nitrogen after 1 min in a styrofoam container for storage before thawing.

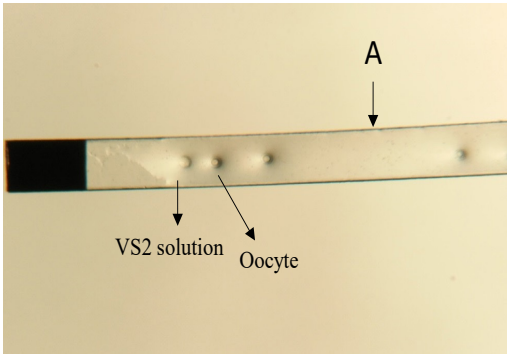

Figure 5. Oocytes were loaded onto Cryotop sheet (A) with a minimum amount of VS2 solution

Thawing of Vitrified Oocytes. The Cryotop sheet was removed from its protective cover, and the end of the polypropylene strip was immediately placed in the thawing solution (TS) for 1 min. Later, oocytes were carefully removed from the cryo-devices through gentle shaking and sucking in the oocytes using a 1 µl micropipette. After 1 min, the oocytes came off naturally from the Cryotop

sheet and transferred into the dilution solution (DS) using a 1 µl micropipette for 3 min. Oocytes were then incubated and washed twice in the first washing solution (WS1) for 5 min, followed by another minute in the second washing solution (WS2). The oocytes were then washed in a culture medium, placed in a culture dish containing the appropriate culture medium to prevent contamination, and further incubated to equilibrate for 1 hr (oocytes stabilise), as shown in Figure 6.

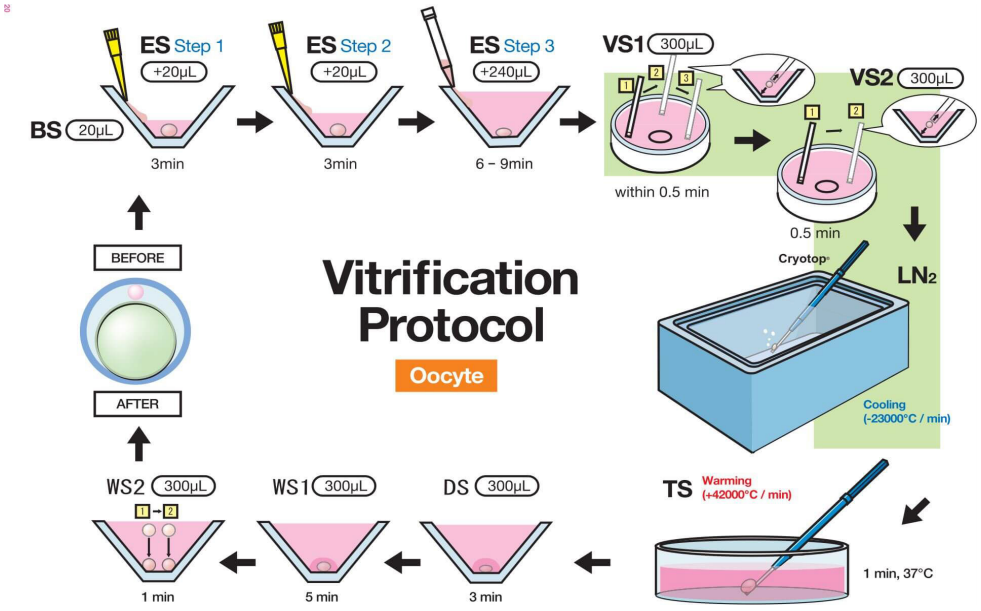

Figure 6. The procedure of freezing and thawing of bovine oocytes as per the manufacturer's instructions (Source: EXTOLSEED Oocyte and Sperm Bank, 2018)

Note. BS = Basic solution; ES = Equilibration solution; VS1 = Vitrification solution 1; VS2 = Vitrification solution 2; TS = Thawing solution; DS = Dilution solution; WS1 = Washing solution 1; WS2 = Washing solution 2

Fixing and Giemsa's Staining

Fixing and Giemsa's staining were performed as described by Bidin (2005). Both fresh and vitrified oocytes were retrieved using a stereomicroscope and treated with 1% hypotonic trisodium citrate solution (Sigma, Germany) individually for 3 min. Oocytes were immediately placed onto microscopic slides, and excess hypotonic trisodium citrate solution was removed before fixing with 1:1 (v/v) methanol (R&M Chemicals, United Kingdom) and acetic acid solution (Merck, Germany). The oocytes were then blow-dried. The microscopic slides were immersed in a Coplin jar containing the fixative solution of methanol and acetic acid (3:1) and kept overnight at 2°C. The slides were air-dried the next day and stained with 4% Giemsa solution (Sigma, Germany) for 3 min. After that, the slides were cleaned in xylene solution (Merck, Germany) for another 3 min and mounted with dibutyl

phthalate polystyrene xylene (DPX, Merck, Germany) before observation.

Evaluation of Meiotic Progression

The stages of nuclear maturation of stained oocytes were observed under a phase contrast microscope (Zeiss, Germany) at 100×, 200×, 400×, and 1,000× magnifications. The meiotic stages were categorised as zygotene, pachytene, diakinesis, first metaphase (MI), and second metaphase (MII). Oocytes arrested at MII were considered to have accomplished maturation *in vitro* (Figure 7), while germinal vesicle and MI were considered immature *in vitro*. An unidentified chromosome (OUC) is in a state where the chromosome is condensed or structurally abnormal and cannot be identified.

Data Analysis

The data on bovine oocytes' meiotic progression were analysed using Statistical Product and Service Solutions (SPSS, version 24). A one-way analysis of variance (ANOVA) with Duncan's multiple range comparison test was performed to assess the differences between the treatment means. The mean values were considered statistically significant at $p<0.05$.

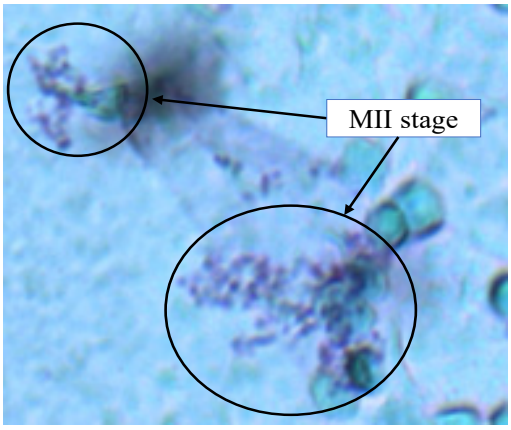

Figure 7. Stained metaphase II (MII) oocytes were observed under 400× magnification

RESULTS AND DISCUSSION

This study focused on the maturation rate of bovine oocytes as an indicator of meiotic competence and capability to resume meiosis at various stages, namely, zygotene, pachytene, diakinesis, metaphase I (MI), metaphase II (MII), and unidentified chromosomes under *in vitro* conditions. The meiotic resumption of vitrified bovine oocytes compared to the fresh oocytes as control is shown in Table 1. Significant differences ($p<0.05$) were observed in the zygotene, MI, MII, and unidentified chromosomes in the three treatments but not in the pachytene and diakinesis stages.

In terms of maturation rate, the mean percentage for MII recorded was significantly different ($p<0.05$) compared to the oocytes exposed to either vitrification or Cryotop treatments. The mean percentage of oocytes arrested at MII in the control group, Cryotop, and VS treatments were 52.27, 35.22, and 32.15%, respectively. Significant differences ($p<0.05$) were observed in the mean percentage of MI stage in control oocytes (1.54%) compared to the VS (9.57%) and Cryotop treatments (10.90%). Thus, in the present study, the maturation stage reflected that the meiotic competence of cryopreserved oocytes was lower than that of fresh oocytes. This result suggests that the cryopreserved oocytes

are probably susceptible to physical and chemical stress to resume their meiosis (Iussig et al., 2019); thus, the oocytes are less capable of surviving the cooling and warming procedures compared to normal fresh oocytes.

Table 1
The effects of conventional vitrification solution and Cryotop techniques on the mean percentage of meiotic stages in bovine oocytes

Treatment	Meiotic stages ± SEM						
	n	Zygotene	Pachytene	Diakinesis	MI	MII	OUC
Control	99	5.62 ± 2.87$^{a, x}$	8.18 ± 2.99$^{a, x}$	0.40 ± 0.40$^{a, x}$	1.54 ± 0.97$^{a, x}$	52.27 ± 6.52$^{b, y}$	8.18 ± 2.75$^{a, xy}$
Vitrification solution	115	5.29 ± 1.88$^{a, x}$	7.52 ± 2.72$^{ab, x}$	3.43 ± 1.98$^{a, x}$	9.57 ± 2.79$^{ab, y}$	32.15 ± 5.08$^{c, x}$	16.12 ± 3.98$^{b, y}$
Cryotop	95	16.67 ± 4.23$^{b, y}$	8.10 ± 2.50$^{ab, x}$	3.08 ± 1.49$^{a, x}$	10.90 ± 2.55$^{ab, y}$	35.22 ± 5.20$^{c, x}$	5.51 ± 2.09$^{a, x}$

Note.
$^{a, b, c}$ = Means within a row with different superscripts were significantly different at $p<0.05$;
$^{x, y}$ = Means within columns with different superscripts were significantly different at $p<0.05$;
n = Number of oocytes; Zy = Zygotene; Pa = Pachytene; Dia = Diakinesis; MI = Metaphase I;
MII = Metaphase II; OUC = Oocytes with unidentified chromosome
SEM = Standard error of the mean

In the zygotene stage, there were significant differences ($p<0.05$) in the mean percentage of control (5.62%) and VS (5.29%) treatments compared to Cryotop (16.67%), as shown in Table 1. Immature oocytes (GV stage) were more resistant using the Cryotop technique. A recent study reported that the DNA of the GV stage oocytes is more resistant to cryopreservation since it is relatively compact in the meiotic state and protected by the nuclear membrane (Peinado et al., 2022). Compared to the control at 8.18%, a significantly higher percentage of oocytes with unidentified chromosomes was observed in the VS-cryopreserved group compared to Cryotop-cryopreserved oocytes at 16.12 and 5.51%, respectively. This condition may result from the structural or molecular changes during the vitrification process using carriers or cryo-devices, thereby causing the microtubule's spindle to depolymerise and disorganise. These events would limit the viability and developmental potential of the oocytes (Mogas, 2018).

In addition, the conditions of oocyte donors in the present study in terms of breed, age, body scores, and parity numbers were unknown as the oocytes were harvested from slaughterhouse ovaries. It is a pertinent point as donor conditions affect the survival rate of oocytes (Tharasanit & Thuwanut, 2021). During the vitrification treatments, oocytes were exposed to various conditions, including chemical toxicity, osmotic shifts, and mechanical and thermal stresses, which may further reduce the oocytes' competence *in vitro*. As a result, the mean percentage

of vitrified oocytes with unidentified chromosomes increased compared to controls (Tharasanit & Thuwanut, 2021). Another reason might be technical errors while using the carriers to preserve the oocytes. Technical competence of personnel is very important in the vitrification techniques, especially during the handling and loading of oocytes, which must be accomplished within a short time. Moreover, it is difficult to visualise the oocytes in the highly concentrated solution, which could delay the vitrification process.

The mean percentage of various meiotic stages of A, B, and B' of bovine oocytes are shown in Table 2. In the control treatment, significant differences ($p<0.05$) were observed in oocytes reaching the MII stage compared to other stages in each group of oocytes. A higher mean percentage was observed in the MII stage compared to other meiotic stages, specifically in group B' followed by groups A and B at 56.17, 55.83, and 44.82%, respectively. However, no oocytes in groups B and B' were observed to reach the diakinesis stage in the control treatment.

Table 2
The effects of conventional vitrification solution and Cryotop techniques on the mean percentage of meiotic stages in three groups of bovine oocytes

Treatment	Group	Meiotic stages of oocytes ± SEM						
		n	Zygotene	Pachytene	Diakinesis	MI	MII	OUC
Control	A	34	9.17 ± 4.86$^{a, x}$	9.17 ± 4.36$^{a, x}$	1.19 ± 1.19$^{a, x}$	0.60 ± 0.60$^{a, x}$	55.83 ± 11.84$^{b, x}$	2.62 ± 1.79$^{a, x}$
	B	29	7.69 ± 7.12$^{a, x}$	10.62 ± 7.33$^{a, x}$	0.00 ± 0.00$^{a, x}$	1.65 ± 1.65$^{a, x}$	44.82 ± 11.99$^{b, x}$	6.65 ± 3.93$^{a, x}$
	B'	36	0.00 ± 0.00$^{a, x}$	4.76 ± 3.23$^{a, x}$	0.00 ± 0.00$^{a, x}$	2.38 ± 2.38$^{a, x}$	56.17 ± 10.59$^{b, x}$	15.26 ± 6.83$^{a, x}$
Vitrification solution	A	46	5.34 ± 3.04$^{a, x}$	9.26 ± 6.49$^{a, x}$	9.17 ± 5.69$^{a, x}$	9.31 ± 4.10$^{a, x}$	44.79 ± 9.49$^{b, x}$	11.02 ± 5.82$^{a, x}$
	B	34	6.94 ± 3.94$^{a, x}$	7.13 ± 3.49$^{a, x}$	1.11 ± 1.11$^{a, x}$	5.28 ± 3.14$^{a, x}$	30.97± 8.47$^{b, x}$	9.68 ± 3.71$^{a, x}$
	B'	35	3.57 ± 2.84$^{ab, x}$	6.17 ± 3.81$^{ab, x}$	0.00 ± 0.00$^{a, x}$	14.11 ± 6.61$^{abc, x}$	20.70 ± 7.93$^{bc, x}$	27.67 ± 9.42$^{c, x}$
Cryotop	A	35	13.78 ± 5.20$^{a, x}$	6.09 ± 3.96$^{a, x}$	0.00 ± 0.00$^{a, x}$	6.09 ± 2.78$^{a, x}$	39.42 ± 9.58$^{b, x}$	3.85 ± 2.60a$^{, x}$
	B	32	11.36 ± 5.45$^{a, x}$	12.18 ± 5.55$^{a, x}$	6.68 ± 3.55$^{a, x}$	15.20 ± 5.41$^{a, x}$	37.27 ± 7.65$^{b, x}$	1.92 ± 1.92$^{a, x}$
	B'	28	24.87 ± 10.24$^{bc, x}$	6.03 ± 3.27$^{ab, x}$	2.56± 2.56a$^{, x}$	11.41 ± 4.63$^{abc, x}$	28.97 ± 10.07$^{c, x}$	10.77 ± 5.25$^{abc, x}$

Note.
$^{a, b, c}$ = Means within a row with different superscripts were significantly different at $p<0.05$; ^{x}= Means within the column within a group with similar superscripts were not significantly different at $p>0.05$; n = Number of oocytes; MI = Metaphase I; MII = Metaphase II; OUC = Oocytes with unidentified chromosome
SEM = Standard error of the mean

In the VS treatment, groups A and B oocytes depicted significant differences (p<0.05) in MII compared to other meiotic stages. In group B' oocytes, a significant difference (p<0.05) was observed in unidentified chromosomes compared to other meiotic stages. Meanwhile, no significant difference at all meiotic stages was observed across the groups in the VS treatment. Although not significant, a higher mean percentage of oocytes in MII was observed in group A (44.79%), followed by groups B (30.97%) and B' (20.70%) oocytes. In the VS technique, the mean percentage of oocytes with unidentified chromosomes in groups A, B, and B' was 11.02, 9.68, and 27.67%, respectively. In contrast, no group B' oocytes reached the diakinesis stage.

Group B' oocytes had the highest mean percentage of unidentified chromosomes in comparison to groups A and B in the VS technique. It could be due to the warming and cooling steps in the vitrification process of the oocytes that were detrimental, thereby leading to cryodamage and affecting the oocytes' viability (Thrasanit & Thuwanut, 2021). In addition, the sensitivity of oocytes to cryopreservation varied depending on their meiotic stage (Rienzi et al., 2010). In this study, the oocytes' ability to enter the meiotic phase could be explained by maturation media containing serum and cysteamine to encourage oocyte growth (Bidin, 2005). The Cryotop had a similar trend as the control and VS techniques in which no significant difference was observed across the three groups of oocytes in all meiotic stages. However, a significantly (p<0.05) higher percentage of oocytes were observed in groups A and B oocytes reaching MII compared to other meiotic stages. The mean percentage recorded was 39.42, 37.27, and 28.97% for groups A, B, and B', respectively. For group B' oocytes, a significant difference (p<0.05) was observed in the diakinesis (2.56%) and MII (28.97%) stages compared to other stages. Oocytes in group B' were less likely to meiotically arrest in diakinesis, which might be attributed to poor cell-to-cell communication that lowers the cyclic adenosine monophosphate (cAMP) levels (Bidin, 2005).

The disconnection of the junctional competence in group B' oocytes could result from its characterisation, which is either a partial or almost complete lack of cumulus cells (Bidin, 2005). Although not significantly different, group B' oocytes had higher percentages of oocytes reaching zygotene (24.87%) and incidences of oocytes with unidentified chromosomes (10.77%). These might be due to insufficient cysteamine supplementation in the maturation media or the failure of the inferior quality of group B' oocytes to support full meiotic progression. The result might also stem from the cumulus cell dispersion component within the collection in group B', which results in meiotic arrest in this phase (Bidin, 2005). Cumulus cells are crucial in oocyte meiotic maturation and meiosis, which are necessary for ovulation, fertilisation, and subsequent early embryo development (Turathum et al., 2021). Therefore, understanding the involvement of oocyte grouping can be crucial in predicting

oocyte quality and subsequent embryonic development competence.

The percentage of meiotic resumption of fresh bovine oocytes (control), compared to conventional VS- and Cryotop-vitrified oocytes of three groups of oocytes, are presented in Table 3. A similar trend was observed, where A, B, and B' groups of oocytes of all treatments recorded the highest mean percentage of oocytes reaching MII. In group A oocytes, no significant difference was observed for all meiotic stages between the three treatments, although the mean percentage of oocytes reaching the MII stage was relatively higher in control (55.83%), VS (44.79%), and Cryotop (39.42%) groups. However, a significant difference ($p<0.05$) was observed in MII upon comparing the other meiotic stages within treatments in group A oocytes. In group B oocytes, significant differences ($p<0.05$) were observed in the diakinesis and MI stages of Cryotop treatment compared to other oocyte groups and treatments. Nevertheless, the diakinesis stage of group B oocyte was not detected in the control treatment.

Table 3
The mean percentage of meiotic stages in three groups of oocytes using conventional vitrification solution and Cryotop techniques

Group	Treatment	Stages						
		n	Zygotene	Pachytene	Diakinesis	MI	MII	OUC
A	Control	34	9.17 ± 4.86$^{a, x}$	9.17 ± 4.36$^{a, x}$	1.19 ± 1.19$^{a, x}$	0.60 ± 0.60$^{a, x}$	55.83 ± 11.84$^{b, x}$	2.62 ± 1.79$^{a, x}$
	Vitrification solution	46	5.34 ± 3.04$^{a, x}$	9.26 ± 6.49$^{a, x}$	9.17 ± 5.69$^{a, x}$	9.31 ± 4.10$^{a, x}$	44.79 ± 9.49$^{b, x}$	11.02 ± 5.82$^{a, x}$
	Cryotop	35	13.78 ± 5.20$^{a, x}$	6.09 ± 3.96$^{a, x}$	0.00± 0.00$^{a, x}$	6.09 ± 2.78$^{a, x}$	39.42 ± 9.58$^{b, x}$	3.85 ± 2.60$^{a, x}$
B	Control	29	7.69 ± 7.12$^{a, x}$	10.62 ± 7.33$^{a, x}$	0.00 ± 0.00$^{a, x}$	1.65 ± 1.65$^{a, x}$	44.82 ± 11.99$^{b, x}$	6.65 ± 3.93$^{a, x}$
	Vitrification solution	34	6.94 ± 3.94$^{a, x}$	7.13 ± 3.49$^{a, x}$	1.11 ± 1.11$^{a, x}$	5.28 ± 3.14$^{a, xy}$	30.97 ± 8.47$^{b, x}$	9.68 ± 3.71$^{a, x}$
	Cryotop	32	11.36 ± 5.45$^{a, x}$	12.18 ± 5.55$^{a, x}$	6.68 ± 3.55$^{a, y}$	15.20 ± 5.41$^{a, y}$	37.27 ± 7.65$^{b, x}$	1.92 ± 1.92$^{a, x}$
B'	Control	36	0.00 ± 0.00$^{a, x}$	4.76 ± 3.23$^{a, x}$	0.00 ± 0.00$^{a, x}$	2.38 ± 2.38$^{a, x}$	56.17 ± 10.59$^{b, y}$	15.26 ± 6.83$^{a, x}$
	Vitrification solution	35	3.57 ± 2.84$^{ab, x}$	6.17 ± 3.81$^{ab, x}$	0.00± 0.00$^{a, x}$	14.11 ± 6.61$^{abc, x}$	20.70 ± 7.93$^{bc, x}$	27.67 ± 9.42$^{c, x}$
	Cryotop	28	24.87 ± 10.24$^{bc, y}$	6.03 ± 3.27$^{ab, x}$	2.56 ± 2.56$^{a, x}$	11.41 ± 4.63$^{abc, x}$	28.97 ± 10.07$^{c, x}$	10.77 ± 5.25$^{abc, x}$

Note.
$^{a, b, c}$ = Means within a row with different superscripts were significantly different at $p<0.05$; $^{x, y}$ = Means within columns within a group with different superscripts were significantly different at $p<0.05$; n = Number of oocytes; MI = Metaphase I; MII = Metaphase II; OUC = Oocytes with unidentified chromosome

The phenotype of increased aneuploidy and lower developmental competence may be related to alterations in mitochondrial distribution at the level of cytoplasmic maturation (Rybska et al., 2018). In all treatments, a significant difference (p<0.05) was recorded in MII compared to other stages in group B oocytes. The highest MII that was achieved in group B oocytes was recorded in the control (44.82%), followed by Cryotop (37.27%) and VS (30.97%), respectively. These results indicated that the cryo-device, which only requires a minimum volume of solution for cryopreservation, could be less detrimental and thus sustain the structural integrity of oocytes (Cobo et al., 2008; Kuwayama, 2007). Group B' oocytes depicted statistically significant differences (p<0.05) between the three zygotene and MII stages treatments. In the MII stage, significant differences (p<0.05) were observed in control (56.17%) compared to Cryotop (28.97%) and VS (20.70%), the lowest being group B'.

It was not surprising that the survivability of fresh oocytes was higher compared to the vitrified oocytes. The sub-lethal damage caused the impaired meiotic progression of vitrified oocytes due to the cooling or warming procedures (Sripunya et al., 2010). The fresh oocytes had a higher percentage of meiosis rate since the detrimental effects of osmosis less impacted them through several equilibration and dilution and morphological injuries compared to vitrified oocytes (Sripunya et al., 2010). The structural and morphological damages were reported in vitrified-warmed oocytes, as stated by Amidi et al. (2018). Oocyte survivability following vitrification is impacted given that the plasma membrane of oocytes is permeable to the mutual flow of both impermeable and permeable CPAs when compared to zygote and embryo (Díez et al., 2012; Hajarian et al. 2011). The highest mean percentage of 24.87% of the zygotene stage in the Cryotop treatment was significantly different (p<0.05) when compared to other oocyte groups in other treatments. However, the zygotene stage was not observed in group B' oocytes of the control group. It could result from mitochondrial dysfunction, which interferes with the assembly of the meiotic spindle and reduces ATP synthesis. The meiotic spindle is responsible for chromosomal segregation (Sasaki et al., 2019). In addition, the cellular function of bovine oocytes can be affected by several factors, such as cortical granules, cytoskeleton, and lipid droplets, which are sensitive to freezing and warming processes in cryopreservation (Prentice & Anzar, 2010).

Across the three groups of oocytes, group B' oocytes revealed the most promising outcomes in terms of the number of oocytes reaching MII. In this study, supplementation of 50 µm cysteamine/β-mercaptoethanol (antioxidants) in the IVM maturation medium for a period of 20 to 24 hr for all groups of oocytes, was expected to enhance the developmental competence of lower quality group B' oocytes, as stated by Bidin (2005). It was supported by a recent finding, which suggested the positive effect of cysteamine as an antioxidative agent in

the culture medium of IVM (Magata et al., 2021). The low-molecular-weight thiols, including cysteamine/β-mercaptoethanol, promote the formation of intracellular glutathione (GSH) in IVM media (Budani & Tiboni, 2020). *In vitro* matured oocytes have lower levels of GSH; therefore, the addition of antioxidants facilitated increased GSH levels in the cytoplasm of oocytes. GSH is important in the *in vitro* process for the maturation of oocyte cytoplasm (Nikseresht et al., 2017).

In addition, the highest mean percentage of unidentified chromosomes was recorded in group B' oocyte (27.67%) in the VS treatment compared to the control (15.26%) and Cryotop (10.77%) treatments. Despite having no oocytes in the diakinesis stage, group B' oocytes had a significantly higher ($p<0.05$) percentage of oocytes with unidentified chromosomes. Oocytes with unidentified chromosomes were higher in the VS procedure using straw compared to the Cryotop technique across all treatments. It could be due to the utilisation of a larger volume of highly concentrated solution in VS, which may have deleterious effects on the oocytes when exposed to liquid nitrogen. Besides, the technique used for inserting the samples inside the straw in the vitrification method may be detrimental to the oocytes (Rao et al., 2012). The detrimental effects during the cryopreservation procedure might elicit altered gene expression, apoptosis, and the release of oocyte-derived substances, thereby leading to cryodamage (Rao et al., 2012). Significant differences ($p<0.05$) were observed in diakinesis and MII stages compared to other meiotic stages for Cryotop treatment. Specifically, group B' oocytes recorded the lowest MII stage compared to control and VS treatments and the only treatment observed for oocytes arrested in diakinesis.

CONCLUSION

In general, fresh oocytes (control) had the highest percentage of maturation compared to the vitrification techniques. Both vitrification techniques, namely conventional VS and Cryotop, successfully maintained the maturation rate and survivability of vitrified bovine oocytes in all three groups of oocytes (A, B, and B'). In group A oocytes, a higher mean percentage was observed in the VS technique than in Cryotop. On the contrary, a higher mean percentage of MII stage in groups B and B' oocytes was observed in Cryotop compared to the conventional VS technique. These findings indicated that both vitrification techniques could be used in terms of the survival rate of bovine oocytes. Nevertheless, further studies on evaluating the effects of both vitrification techniques through IVF technique are necessary to determine the developmental competence of cryopreserved bovine oocytes.

ACKNOWLEDGEMENTS

This study was supported by the 'IVEP and twin birth in cattle' Project under the Ruminant Industry Development Grant (Grant no.: K-RLC97-1001-KSR999), New Source of Wealth (SKB) under Malaysian Agriculture Research and Development Institute (MARDI). The authors would like

to thank all the staff of the Animal Breeding Programme, MARDI for their technical assistance and the Banting and Shah Alam abattoirs staff for their cooperation in collecting the ovaries.

REFERENCES

Abd El-Aziz, A. H., Mahrous, U. E., Kamel, S. Z., & Sabek, A. A. (2016). Factors influencing *in vitro* production of bovine embryos: A review. *Asian Journal of Animal and Veterinary Advances*, *11*(12), 737–756. https://doi.org/10.3923/ajava.2016.737.756

Aguila, L., Treulen, F., Therrien, J., Felmer, R., Valdivia, M., & Smith, L. C. (2020). Oocyte selection for *in vitro* embryo production in bovine species: Noninvasive approaches for new challenges of oocyte competence. *Animals*, *10*(12), 2196. https://doi.org/10.3390/ani10122196

Aljaser, F. S. (2022). Cryopreservation methods and frontiers in the art of freezing life in animal models. In Y. Bozkurt & M. N. Bucak (Eds.), *Animal reproduction*. IntechOpen. https://doi.org/10.5772/intechopen.101750

Amidi, F., Khodabandeh, Z., & Mogahi, M. H. N. (2018). Comparison of the effects of vitrification on gene expression of mature mouse oocytes using cryotop and open-pulled straw. *International Journal of Fertility and Sterility*, *12*(1), 61–67. https://doi.org/10.22074/ijfs.2018.5112

Angel-Velez, D., De Coster, T., Azari-Dolatabad, N., Fernandez-Montoro, A., Benedetti, C., Pascottini, O. B., Woelders, H., Soom, A. V., & Smits, K. (2021). New alternative mixtures of cryoprotectants for equine immature oocyte vitrification. *Animals*, *11*(11), 3077. https://doi.org/10.3390/ani11113077

Basirat, Z., Rad, H. A., Esmailzadeh, S., Jorsaraei, S. G. A., Hajian-Tilaki, K., Pasha, H., & Ghofrani, F. (2016). Comparison of pregnancy rate between fresh embryo transfers and frozen-thawed embryo transfers following ICSI treatment. *International Journal of Reproductive Biomedicine*, *14*(1), 39–46.

Bidin, H. (2005). *IVF performance of different qualities of oocyte using co-culture and chemically-defined medium in Malaysian cattle* [Unpublished Doctoral dissertation]. Universiti Malaya.

Bidin, H., Osman, N. A., & Kamaruddin, M. (2012). Effects of oestradiol-17β on the development of cattle oocytes. In *Proceedings of the 5th International Conference on Animal Nutrition 2012 Malacca, Malaysia* (pp. 314-316). Malaysian Agricultural Research and Development Institute.

Bottrel, M., Ortiz, I., Pereira, B., Díaz-Jiménez, M., Hidalgo, M., Consuegra, C., Morató, R., Mogas, T., & Dorado, J. (2019). Cryopreservation of donkey embryos by the cryotop method: Effect of developmental stage, embryo quality, diameter and age of embryos. *Theriogenology*, *125*, 242–248. https://doi.org/10.1016/j.theriogenology.2018.11.011

Budani, M. C., & Tiboni, G. M. (2020). Effects of supplementation with natural antioxidants on oocytes and preimplantation embryos. *Antioxidants*, *9*(7), 612. https://doi.org/10.3390/antiox9070612

Cobo, A., Bellver, J., Domingo, J., Pérez, S., Crespo, J., Pellicer, A., & Remohí, J. (2008). New options in assisted reproduction technology: The Cryotop method of oocyte vitrification. *Reproductive Biomedicine Online*, *17*(1), 68–72. https://doi.org/10.1016/s1472-6483(10)60295-7

Davachi, N. D., Shahneh, A. Z., Kohram, H., Zhandi, M., Dashti, S., Shamsi, H., & Moghadam, R. (2014). *In vitro* ovine embryo production: The study of seasonal and oocyte recovery method effects. *Iranian Red Crescent Medical Journal*, *16*(9), e20749. https://doi.org/10.5812/ircmj.20749

Dhali, A., Kolte, A. P., Mishra, A., Roy, S. C., & Bhatta, R. (2018). Cryopreservation of oocytes and embryos: Current status and

opportunities. In D. S. Sheriff (Ed.), *Infertility, assisted reproductive technologies and hormone assays*. IntechOpen. https://doi.org/10.5772/intechopen.81653

Díez, C., Muñoz, M., Caamaño, J. N., & Gómez, E. (2012). Cryopreservation of the bovine oocyte: Current status and perspectives. *Reproduction in Domestic Animals*, 47(s3), 76–83. https://doi.org/10.1111/j.1439-0531.2012.02029.x

Do, V. H., Walton, S., Catt, S., & Taylor-Robinson, A. W. (2016). Requirements for cryopreservation of *in vitro*-produced bovine embryos by a standard method of vitrification. *Journal of Veterinary Science and Animal Husbandry*, *4*(1), 102. https://doi.org/10.15744/2348-9790.4.102

EXTOLSEED Oocyte and Sperm Bank (2018). *Thawing (Kitazato)*. https://extolseed.com/vitrification-and-warming-kitazato/thawing-kitazato/

Fathi, M., Moawad, A. R., & Badr, M. R. (2018). Production of blastocysts following *in vitro* maturation and fertilization of dromedary camel oocytes vitrified at the germinal vesicle stage. *PLOS One*, *13*(3), e0194602. https://doi.org/10.1371/journal.pone.0194602

Hajarian, H., Wahid, H., Rosnina, Y., Daliri, M., Dashtizad, M., Karamishabankareh, H., & Abas Mazni, O. (2011). Cryotop and development of vitrified immature bovine oocytes. *Brazilian Journal of Veterinary and Animal Sciences*, *63*(1), 67–73. https://doi.org/10.1590/s0102-09352011000100011

Hochi, S. (2022). Cryodevices developed for minimum volume cooling vitrification of bovine oocytes. *Animal Science Journal*, *93*(1), e13683. https://doi.org/10.1111/asj.13683

Idrissi, S. J., Le Bourhis, D., Lefevre, A., Emond, P., Le Berre, L., Desnoës, O., Joly, T., Buff, S., Maillard, V., Schibler, L., Salvetti, P., & Elis, S. (2021). Lipid profile of bovine grade - 1 blastocysts produced either *in vivo* or *in vitro* before and after slow freezing process. *Scientific Reports*, *11*, 11618. https://doi.org/10.1038/s41598-021-90870-8

Iussig, B., Maggiulli, R., Fabozzi, G., Bertelle, S., Vaiarelli, A., Cimadomo, D., Ubaldi, F. M., & Rienzi, L. (2019). A brief history of oocyte cryopreservation: Arguments and facts. *Acta Obstetricia et Gynecologica Scandinavica*, *98*(5), 550-558. https://doi.org/10.1111/aogs.13569

Jain, J. K., & Paulson, R. J. (2006). Oocyte cryopreservation. *Fertility and Sterility*, *86*(4), 1037–1046. https://doi.org/10.1016/j.fertnstert.2006.07.1478

Kader, A. A., Choi, A., Orief, Y., & Agarwal, A. (2009). Factors affecting the outcome of human blastocyst vitrification. *Reproductive Biology and Endocrinology*, *7*, 99. https://doi.org/10.1186/1477-7827-7-99

Keshavarzi, S., Eftekhari, A. D., Vahabzadeh, H., Mehrafza, M., Taheripanah, R., Asgharnia, M., Esfandyari, S., Ghazifard, A., Hosseinirad, H., & Paktinat, S. (2022). A comparative study of post-warming survival rates and clinical outcomes of human blastocysts vitrified/warmed by CryoTouch and Cryotop methods. *JBRA assisted Reproduction*, *26*(4), 568–573. https://doi.org/10.5935/1518-0557.20210116

Kuwayama, M. (2007). Highly efficient vitrification for cryopreservation of human oocytes and embryos: The Cryotop method. *Theriogenology*, *67*(1), 73–80. https://doi.org/10.1016/j.theriogenology.2006.09.014

Kuwayama, M., Vajta, G., Kato, O., & Leibo, S. P. (2005). Highly efficient vitrification method for cryopreservation of human oocytes. *Reproductive BioMedicine Online*, *11*(3), 300–308. https://doi.org/10.1016/s1472-6483(10)60837-1

Liu, S., & Li, F. (2020). Cryopreservation of single-sperm: Where are we today? *Reproductive Biology and Endocrinology*, *18*, 41. https://doi.org/10.1186/s12958-020-00607-x

Magata, F., Ideta, A., Matsuda, F., Urakawa, M., & Oono, Y. (2021). Glutathione ethyl ester improved the age-induced decline in the developmental competence of bovine oocytes. *Theriogenology*, *167*, 37–43. https://doi.org/10.1016/j.theriogenology.2021.03.004

Mahmoud, K. G. M., El-Sokary, M. M. M., Kandiel, M. M. M., El-Roos, M. E. A. A., & Sosa, G. M. S. (2016). Effects of cysteamine during *in vitro* maturation on viability and meiotic competence of vitrified buffalo oocytes. *Iranian Journal of Veterinary Research*, *17*(3), 165–170.

Mogas, T. (2018). Update on the vitrification of bovine oocytes and *in vitro*-produced embryos. *Reproduction, Fertility, and Development*, *31*(1), 105–117. https://doi.org/10.1071/rd18345

Nagy, Z. P., Chang, C.-C., Shapiro, D., Bernal, D. P., Kort, H. I., & Vajta, G. (2009). The efficacy and safety of human oocyte vitrification. *Seminars in Reproductive Medicine*, *27*(6), 450–455. https://doi.org/10.1055/s-0029-1241054

Nagy, Z. P., Shapiro, D., & Chang, C.-C., (2020). Vitrification of the human embryo: A more efficient and safer in vitro fertilization treatment. *Fertility and Sterility*, *113*(2), 241-247. https://doi.org/10.1016/j.fertnstert.2019.12.009

Nikseresht, M., Toori, M. A., Rahimi, H. R., Fallahzadeh, A. R., Kahshani, I. R., Hashemi, S. F., Bahrami, S., & Mahmoudi, R. (2017). Effect of antioxidants (β-mercaptoethanol and cysteamine) on assisted reproductive technology *in vitro*. *Journal of Clinical and Diagnostic Research: JCDR*, *11*(2), BC10–BC14. https://doi.org/10.7860/JCDR/2017/21778.9298

Peinado, I., Moya, I., García-Valverde, L., Francés, R., Ribes, R., Polo, P., Gómez-Torres, M. J., & Monzó, A. (2022). Potential development of vitrified immature human oocytes: influence of the culture medium and the timing of vitrification. *International Journal of Molecular Sciences*, *24*(1), 417. https://doi.org/10.3390/ijms24010417

Prentice, J. R., & Anzar, M. (2010). Cryopreservation of mammalian oocyte for conservation of animal genetics. *Veterinary Medicine International*, *2011*, 146405. https://doi.org/10.4061/2011/146405

Rao, B. S., Mahesh, Y. U., Charan, K. V., Suman, K., Sekhar, N., & Shivaji, S. (2012). Effect of vitrification on meiotic maturation and expression of genes in immature goat cumulus oocyte complexes. *Cryobiology*, *64*(3), 176–184. https://doi.org/10.1016/j.cryobiol.2012.01.005

Reyes, J. N. V., & Jaramillo, L. C. (2016). Cryopreservation method and composition of the vitrification solution affect viability of *in vitro* bovine embryos. *Revista Colombiana de Ciencias Pecuarias*, *29*, 130–137. https://doi.org/10.17533/udea.rccp.v29n2a06

Rienzi, L., Romano, S., Albricci, L., Maggiulli, R., Capalbo, A., Baroni, E., Colamaria, S., Sapienza, F., & Ubaldi, F. (2010). Embryo development of fresh 'versus' vitrified metaphase II oocytes after ICSI: A prospective randomized sibling-oocyte study. *Human Reproduction*, *25*(1), 66–73. https://doi.org/10.1093/humrep/dep346

Rybska, M., Knap, S., Jankowski, M., Jeseta, M., Bukowska, D., Antosik, P., Nowicki, M., Zabel, M., Kempisty, B., & Jaśkowski, J. M. (2018). Cytoplasmic and nuclear maturation of oocytes in mammals – Living in the shadow of cells developmental capability. *Medical Journal of Cell Biology*, *6*(1), 13–17. https://doi.org/10.2478/acb-2018-0003

Sanches, B. V., Zangirolamo, A. F., & Seneda, M. M. (2019). Intensive use of IVF by large-scale dairy programs. *Animal Reproduction*, *16*(3), 394–401. https://doi.org/10.21451/1984-3143-AR2019-0058

Sasaki, H., Hamatani, T., Kamijo, S., Iwai, M., Kobanawa, M., Ogawa, S., Miyado, K., & Tanaka, M. (2019). Impact of oxidative stress on age-associated decline in oocyte developmental competence. *Frontiers in Endocrinology*, *10*, 811. https://doi.org/10.3389/fendo.2019.00811

Saunders, K. M., & Parks, J. E. (1999). Effects of cryopreservation procedures on the cytology and fertilization rate of *in vitro*-matured bovine oocytes. *Biology of Reproduction*, *6*(1), 178–187. https://doi.org/10.1095/biolreprod61.1.178

Sripunya, N., Somfai, T., Inaba, Y., Nagai, T., Imai, K., & Parnpai, R. (2010). A comparison of cryotop and solid surface vitrification methods for the cryopreservation of *in vitro* matured bovine oocytes. *Journal of Reproduction and*

Development, *56*(1), 176–181. https://doi.org/10.1262/jrd.09-108h

Sydykov, B., Oldenhof, H., Sieme, H., & Wolkers, W. F. (2018). Storage stability of liposomes stored at elevated subzero temperatures in DMSO/sucrose mixtures. *PLOS One*, *13*(7), e0199867. https://doi.org/10.1371/journal.pone.0199867

Tao, T., & Del Valle, A. (2008). Human oocyte and ovarian tissue cryopreservation and its application. *Journal of Assisted Reproduction and Genetics*, *25*, 287–296. https://doi.org/10.1007/s10815-008-9236-z

Tharasanit, T., & Thuwanut, P. (2021). Oocyte cryopreservation in domestic animals and humans: Principles, techniques and updated outcomes. *Animals*, *11*(10), 2949. https://doi.org/10.3390/ani11102949

Tonev, I. D., Hristova, S. H., Zhivkov, A. M., & Mincheff, M. S. (2020). Cytotoxic effect of dimethyl sulfoxide (DMSO) on hematopoietic stem cells: Influence of the temperature and the incubation time. *Bulgarian Chemical Communications*, *52*(Special Issue B), 40–43. https://doi.org/10.34049/bcc.52.B.0011

Turathum, B., Gao, E.-M., & Chian, R.-C. (2021). The function of cumulus cells in oocyte growth and maturation and in subsequent ovulation and fertilization. *Cells*, *10*(9), 2292. https://doi.org/10.3390/cells10092292

Valdez, C. A., Abas Mazni, O., Takahashi, Y., Fujikawa, S., & Kanagawa, H. (1992). Successful cryopreservation of mouse blastocysts using a new vitrification solution. *Journal of Reproduction and Fertility*, *96*(2), 793–802. https://doi.org/10.1530/jrf.0.0960793

Vining, L. M., Zak, L. J., Harvey, S. C., & Harvey, K. E. (2021). The role of apoptosis in cryopreserved animal oocytes and embryos. *Theriogenology*, *173*, 93–101. https://doi.org/10.1016/j.theriogenology.2021.07.017

Vladimirov, I. K., Tacheva, D., & Dobrinov, V. (2019). The present and future of embryo cryopreservation. In B. Wu & H. L. Feng (Eds.), *Embryology: Theory and practice*. IntechOpen. https://doi.org/10.5772/intechopen.80587

Whaley, D., Damyar, K., Witek, R. P., Mendoza, A., Alexander, M., & Lakey, J. R. T. (2021). Cryopreservation: An overview of principles and cell-specific considerations. *Cell Transplantation*, *30*, 1-12. https://doi.org/10.1177/0963689721999617

Pertanika J. Trop. Agri. Sci. 46 (4): 1347 - 1357 (2023)

PERTANIKA JOURNALS

TROPICAL AGRICULTURAL SCIENCE

Journal homepage: http://www.pertanika.upm.edu.my/

Species Identification of Sea Bamboo (*Isis hippuris*) Using *COI*-based DNA Barcoding

La Ode Alirman Afu[1,2], Anis Chamidah[3], Uun Yanuhar[4] and Maftuch[5]*

[1]Doctoral Program, Faculty of Fisheries and Marine Sciences, Brawijaya University, Malang 65145, East Java, Indonesia

[2]Department of Marine Science, Faculty of Fisheries and Marine Sciences, Halu Oleo University, Kendari 93232, Southeast Sulawesi, Indonesia

[3]Department of Fisheries Product Technology, Faculty of Fisheries and Marine Sciences, Brawijaya University, Malang 65145, East Java, Indonesia

[4]Department of Aquatic Resources Management, Faculty of Fisheries and Marine Sciences, Brawijaya University, Malang 65145, East Java, Indonesia

[5]Department of Aquaculture, Faculty of Fisheries and Marine Sciences, Brawijaya University, Malang 65145, East Java, Indonesia

ABSTRACT

Conservation and effective management of marine ecosystems and biodiversity requires accurate species identification. This study classifies sea bamboo (*Isis hippuris*) specimens using DNA barcoding, a technique widely recognized for its speed, accuracy, and objectivity. This study examines the *cytochrome c oxidase subunit I* (*COI*) gene analysis for species identification. *Isis hippuris* was collected from two stations (coral and seagrass areas) of Tanjung Tiram Waters, South Konawe, Southeast Sulawesi. Genomic DNA was extracted from the base, main, and lateral stem of *I. hippuris*. Polymerase chain reaction (PCR) was used to amplify the mtDNA of *I. hippuris* with HCO2198 and LCO1490 primers. The highest quality PCR product based on the *COI* gene was chosen for sequencing analysis. The study revealed that *COI* gene analysis could only be performed on the base and main stem of the *I. hippuris*. Samples from coral and seagrass-coral areas on lateral stems were not further analyzed due to low concentration and purity values, which could potentially fail DNA sequencing. Each part of *I. hippuris* may have unique genetic differences. This study highlights the advantages of DNA sequencing in providing a unique genetic fingerprint for each species, enabling accurate species identification. This research provides insight into using DNA barcoding for sea bamboo species identification.

Keywords: *COI* gene analysis, conservation, DNA barcoding, management strategies, sea bamboo (*Isis hippuris*)

ARTICLE INFO

Article history:
Received: 10 May 2023
Accepted: 07 July 2023
Published: 17 November 2023

DOI: https://doi.org/10.47836/pjtas.46.4.17

E-mail addresses:
laode.alirmanafu@gmail.com (La Ode Alirman Afu)
achamidah@ub.ac.id (Anis Chamidah)
doktoruun@ub.ac.id (Uun Yanuhar)
maftuch@ub.ac.id (Maftuch)
*Corresponding author

ISSN: 1511-3701
e-ISSN: 2231-8542

INTRODUCTION

Conservation of marine biodiversity is essential for maintaining the equilibrium of the environment. Biodiversity is the variety of genes, species, and ecosystems that make life on Earth (Laxmi et al., 2015; Watson et al., 2012). Due to changing complex interactions, the environment, ecosystem degradation, and anthropogenic pressures have decreased marine species' populations, including the sea bamboo (*Isis hippuris*) (Díaz et al., 2019). It is essential to strengthen conservation management to protect sea bamboo (*Isis* spp.) as a fish species and prevent overexploitation. This effort is in line with the Convention on International Trade in Endangered Species (CITES) recommendations (Edrus & Suman, 2013), especially considering its important function in the commerce of jewelry (Cooper et al., 2011). The pace of reduction in biodiversity is equivalent to the extinction rates during the previous five big extinction events on Earth, and it is happening now (Hoegh-Guldberg & Bruno, 2010; Pimm et al., 2014).

The success of biodiversity conservation measures is inconsistent, and their implementation is not widely spread (Lunt et al., 2013). There has been a growing awareness of the significance of biodiversity and the need for conservation and efficient management of marine ecosystems in recent years. Appropriate species identification is critical in understanding marine species' diversity and distribution and formulating efficient conservation strategies. The agreement permits local and regional governments to manage environmental activities and strive for regional conservation standards. However, conventional species identification methods, such as morphological analysis of the product's identifiable portion using morphology, can be subjective and time-consuming (Posthouwer et al., 2018). DNA barcoding, a molecular method, has become increasingly popular for species identification because of its rapid, accurate, and objective approach.

Mitochondrial DNA sequencing is a highly reliable and commonly used molecular method that is a specific molecular marker for investigating parental analysis, population genetics, and species identification. It also supports long-term ecosystem sustainability, as highlighted in various studies (Ceruso et al., 2019; Ravago-Gotanco & Kim, 2019; Saad, 2019). The precision, speed, and cost-effectiveness of DNA barcoding have been highlighted in prior studies, making it a useful policy tool for species identification (Clark, 2015). Researchers in taxonomy, genetics, and evolutionary biology from all over the world are interested in this method since it is well known for its effectiveness in identifying species (Hellberg et al., 2016).

DNA sequences can be used as a reliable species identifier through DNA barcoding. While some studies have used multiple genes for species identification, a single gene is recommended for a universal animal identification system. The *COI* mitochondrial gene can be used for DNA barcoding techniques to meet global demand for animal identification.

Researchers rely on the National Center for Biotechnology Information (NCBI), Barcode of Life Data System (BOLD), and International Nucleotide Sequence Database Collaboration (INSDC) databases for short nucleotide sequences. The mitochondrial *COI* gene is the most used gene for DNA barcoding in animal groups. These findings are supported (Hebert et al., 2003; Wallace et al., 2012).

Recent research stated that DNA barcoding is a highly effective technique for identifying various species, especially those with similar morphological features. One example of such a species is *I. hippuris*, where DNA barcoding has been used to distinguish between different species and identify specimens of the same species (Bineesh et al., 2017). The method can detect subtle genetic differences between closely related species, assess intraspecific genetic diversity (Verma, 2017), and identify cryptic species that are morphologically indistinguishable but genetically distinct (A. Kumar & Verma, 2017). The significance of this lies in its potential to aid conservation initiatives by safeguarding endangered species before their extinction while also enabling the detection of genetic diversity within species and identifying populations that are in danger of disappearing (Verma, 2018).

Isis hippuris can have several practical applications, including identifying areas for sampling, focusing research efforts, and developing conservation strategies. This information can be used to establish protected areas, restore habitats, and regulate the exploitation of this species. The ecological and conservation information can also be used to design long-term sustainability management strategies for *I. hippuris*.

MATERIALS AND METHODS

Sampling Site

The sample of *I. hippuris* was obtained from Tanjung Tiram Waters, South Konawe, Southeast Sulawesi, Indonesia. The sampling location was classified into two stations, including the coral area (ST 1: 122°40'8.808" E; 4°1'19.414" S) and the coral-seagrass area (ST 2: 122°40'24.070" E; 4°2'3.032" S) (Figure 1). A unique number was assigned and cataloged for each sample to ensure accurate identification. Samples were stored at recommended temperatures until DNA extraction was performed. This strict sampling protocol ensures the reliability of subsequent DNA barcoding analysis and provides valuable insights into the conservation and management of marine ecosystems. This study used three different parts of *I. hippuris*, including the base stem, main stem, and lateral stem (Figure 2), to assess the effectiveness of DNA barcoding in identifying species and their potential impacts on marine ecosystem conservation and management.

DNA Isolation and Extraction

PCR was used to investigate the genetic composition of *I. hippuris*. The genomic DNA of *I. hippuris* was extracted using gSYNC™ DNA Extraction Kit GS300

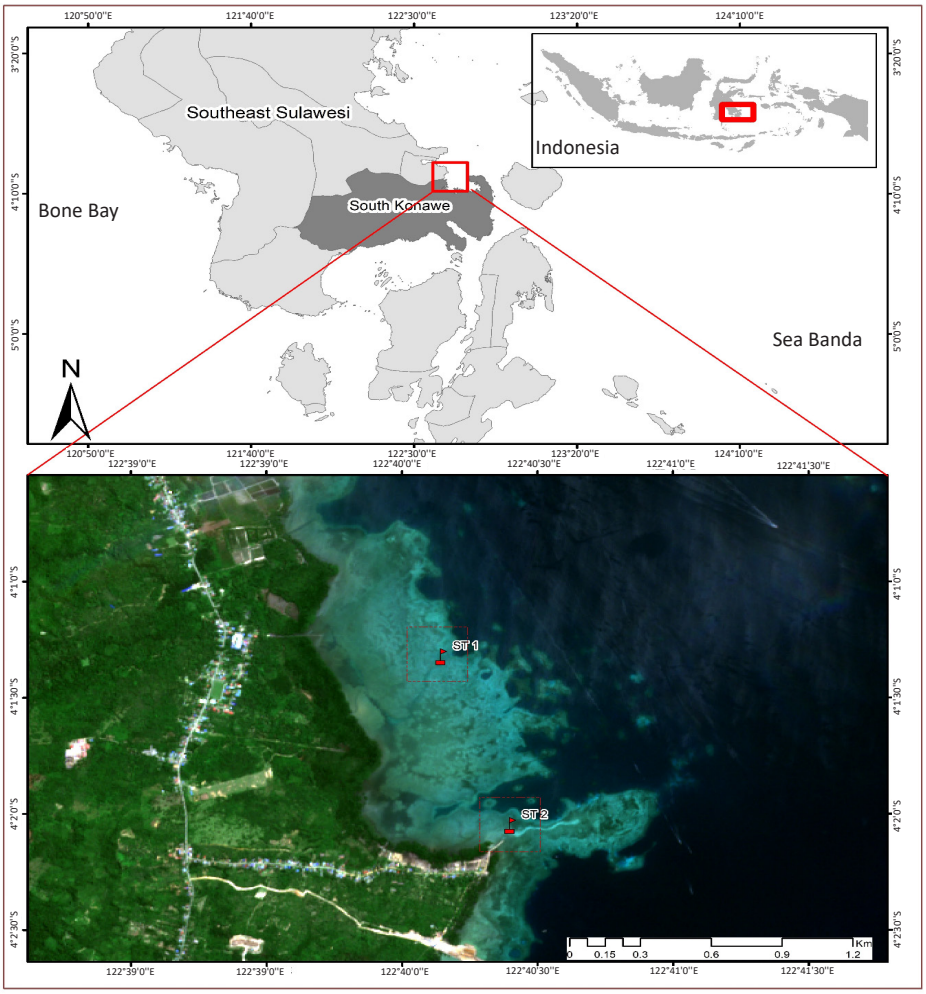

Figure 1. Sampling stations in the coral area (ST 1) and seagrass-coral area (ST 2)

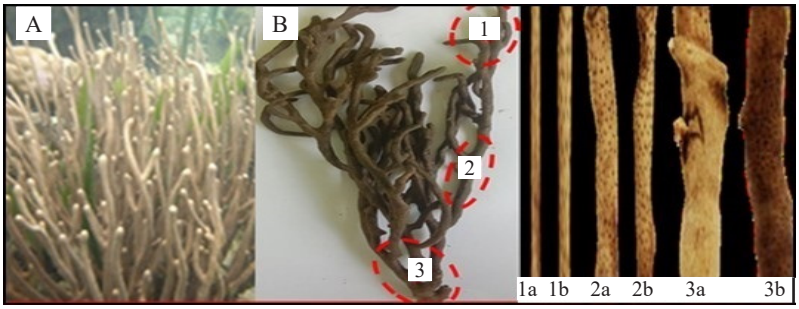

Figure 2. External morphology of soft coral specimens: (A) *Isis hippuris* colony; (B) Samples processed for DNA analysis (1. Lateral stem; 2. Main stem; 3. Stem base) to be extracted DNA
Note. 1a = Lateral stem (area seagrass – coral); 1b = Lateral stem (coral area); 2a = Main stem (area seagrass – coral); 2b = Main stem (coral area); 3a = Stem base (area seagrass – coral); 3b = Stem base (coral area)

(Geneaid Biotech Ltd., Taiwan) and then amplified using PCR with MyTaq HS Red Mix (Bioline Reagent Ltd., United Kingdom). The DNA of *I. hippuris*, preserved with absolute ethanol (EtOH, PT. SMART-LAB, Indonesia), was washed with TE buffer 2-3 times to remove the preservation. Incubation time for the lysis stage was 18 min with 205 µl GBT buffer and the DNA ligation stage using 205 µl EtOH (PT. SMART-LAB, Indonesia). The DNA purity was determined at A260/A280 nm. The obtained DNA of *I. hippuris* was categorized as high quality and quantity, as evidenced by the purity of the purified DNA was 1.8 to 2.0 and a concentration of 200 ng/L.

Amplification of Mitochondrial DNA

The PCR technique was done to amplify the mtDNA of *I. hippuris* using HCO2198 (Forward: 5'- TAA ACT TCA GGG TGA CCA AAA AAT CA 3') and LCO1490 (Reverse: 5' GGT CAA CAA ATC ATA AAG ATA TTG G 3') primers (Black et al., 1994). The following conditions were used for amplification: pre-denaturation for 3 min at 95°C, followed by 35 cycles consisting of 94°C for 45 s for denaturation, 60°C for 45 s for annealing, 1 min for extension, 6 min for post-extension, and 10 min of storage at 4°C. Then, the PCR results were visualized using a 1.5% agarose gel stained with ethidium bromide (EtBr) (Bio-Rad Laboratories, USA) and 1x TAE buffer solution (40 mM Trisacetate and 1 mM EDTA) (Invitrogen™, Thermo Fisher Scientific Inc., USA) in an electrophoretic machine under UV illumination (100 V).

DNA Sequencing

Selecting the highest quality PCR product derived from the *COI* gene is essential in the sequencing analysis. The PCR product was then used for sequencing (1st BASE DNA Sequencing Services, Singapore). The obtained sequences of *I. hippuris* have been published in the National Center for Biotechnology Information (NCBI) database (https://www.ncbi.nlm.nih.gov/nuccore/?term=OR165098%3AOR165101%5Baccn%5D) with accession number OR165098:OR165101[accn].

Data Analysis

Molecular Evolutionary Genetics Analysis (MEGA X) version 11.0 software was used to analyze the nucleotide sequences, including reading and editing the individual sequence results, conducting bioinformatics analysis, and examining homology (S. Kumar et al., 2018). Nucleotide sequence alignment was performed using the CLUSTALX application (Thompson, 1997), and nucleotide sequence homology analysis was carried out via the Basic Local Alignment Search Tool-Nucleotide (BLAST-N) program on the NCBI website (www.ncbi.nlm.nih.gov). This analysis provided valuable information on the genetic variations and similarities between the samples, which the evolutionary relationships and genetic diversity of the species can conclude.

RESULTS AND DISCUSSION

The *COI* gene of three different parts of *I. hippuris* (stem base, main stem, and

lateral stem) was amplified using the PCR. The electrophoresis findings of the PCR product with LCO1490/HCO2198 primers are shown in Figure 3. The results significantly influenced the quality of the DNA samples and the efficacy of the PCR procedure. The use of diverse sections and distinct regions enabled a comprehensive exploration of the genetic diversity of the studied species, which can provide vital insights into the ecological and evolutionary processes of the species. These findings have important implications for understanding the species' population structure, geographic distribution, and potential for adaptation to changing environments.

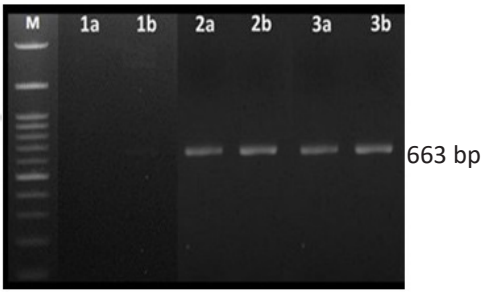

Figure 3. Electrophoresis of *COI* gene mtDNA PCR products primer LCO1490/HCO2198 *Isis hippuris*

Note. M = Marker size 1 kb; 1a = Lateral stem (area seagrass – coral); 1b = Lateral stem (coral area); 2a = Main stem (area seagrass – coral); 2b = Main stem (coral area); 3a = Stem base (area seagrass – coral); 3b = Stem base (coral area)

The genetic diversity of the *COI* genes in multiple samples from various locations and populations has been examined. The DNA sequence data acquired from these samples has provided valuable insights into the variation in *COI* gene sequences and genetic distinctions among populations. This investigation authenticated the species identity of the samples, which was accomplished through BLAST analysis. By contrasting the DNA sequences of the samples with those of reference sequences in the NCBI database, the most closely matching species and their level of similarity were determined (Table 1). The BLAST analysis entailed comparing the DNA sequences of samples with those of numerous species in the NCBI database to confirm their species identity, which is crucial for comprehending their biological characteristics and behaviors.

Table 1
BLAST analysis result based on NCBI for species identification

No.	Sample ID	Query cover (%)	Identification (%)	Species identified
1	1a	-	-	-
2	1b	-	-	-
3	2a	97	99.55	*Isis hippuris*
4	2b	99	99.26	*Isis hippuris*
5	3a	97	99.40	*Isis hippuris*
6	3b	96	99.70	*Isis hippuris*

Note. 1a = Lateral stem (area seagrass – coral); 1b = Lateral stem (coral area); 2a = Main stem (area seagrass – coral); 2b = Main stem (coral area); 3a = Stem base (area seagrass – coral); 3b = Stem base (coral area)

Analysis of population structure and genetic diversity are critical components of effective conservation and management strategies of marine biodiversity. However, morphology-based identification of marine species is challenging due to the high degree of morphological similarity, which makes DNA barcoding and mitochondrial DNA sequencing very important tools for accurate species identification and phylogenetic analysis. The use of *COI* genes has been widely recognized as valuable genetic markers. Several studies have emphasized their importance for conservation management decisions, including fishing site design and regulation.

Bingpeng et al. (2018), Cooke et al. (2016), and Wang et al. (2017) have highlighted the need to analyze population structure and genetic diversity using *COI* genes to promote resource recovery, population zoning, sustainable harvesting and utilization, biodiversity conservation, and fisheries management (Han et al., 2008; Palumbi, 2003; Thai et al., 2006). However, it is critical to carefully select DNA extraction sites to ensure accurate specimen identification, as *COI* gene expression may vary depending on the sampling site (Ceruso et al., 2019; Meriam et al., 2015; Saad, 2019; Sari et al., 2015). This study underscores this point, suggesting that additional markers or sequencing methods may be needed to assess genetic diversity and fully characterize the species, especially in environmental factors affecting its distribution.

The isolation of DNA plays an important role in the successful extraction, purification, and quantification of DNA. DNA isolation involves cell lysis, extraction, and precipitation of lipids, proteins, polysaccharides, and inorganic and organic compounds. These contaminants can reduce DNA quality and interfere with subsequent analyses' success (Muhammad et al. 2016). Secondary structures in primers can inhibit the PCR process and decrease PCR product yield; thus, these secondary structures should be avoided (Ozturk & Can, 2017). Primer dimers can be caused by amplifying them, leading to non-specific PCR products (Dieffenbach et al., 1993). The species-specific primers for *I. hippuris* with a target base length of ~663 bp have been applied to all six samples. The absence of DNA bands in some samples may be due to suboptimal PCR conditions or primer design.

The identification of species in *I. hippuris* was performed on six samples, three from coral and three from seagrass-coral areas. Samples 1a and 1b (samples from coral and seagrass-coral areas on lateral stem) were not further analyzed due to low concentration and purity values, as shown in Figure 3, which could potentially fail DNA sequencing. Samples 2a, 2b, 3a, and 3b were amplified using the DNA LCO1490/HCO2198 primers. Each part of *I. hippuris* may have unique genetic differences. However, only two parts could be identified from the results, including the main and base stems. It can be used as a benchmark for time efficiency in conservation activities. The same gene

may be expressed with different intensities in different body parts, which can provide insight into gene regulation and phenotypic differences between sites. Furthermore, research on the genetics of *I. hippuris* has not been carried out.

The PCR products were sequenced and aligned to obtain nucleotide base sequences, and species identification was carried out based on the Gen Bank reference database. The species identification was performed on samples using the LCO1490/HCO2198 primers. Based on the BLAST sequence analysis, the detected species in the samples were identified as *I. hippuris*. Homology sequence analysis and comparison with Gen Bank using NCBI BLAST showed consistent percentage values. Drancourt et al. (2000) explained that homology values greater than or equal to 99% indicate the same species, while values greater than or equal to 97% indicate species within the same genus. Data on closely related species are important to analyze to determine the relationship between the sample sequence data and Gen Bank (Kuske et al., 2006).

The identification of *I. hippuris* could only be performed on certain parts, including the base of the stem and main stem, due to unique morphological characteristics or physical characteristics found on those parts. There was noisy data with weak signals in sequencing analysis results, resulting in short sequences because the DNA template in the PCR reaction was too much or too little, degradation of the DNA template, contaminated DNA, and no priming site. Therefore, accurate identification of specimens requires sampling from appropriate sections. In addition, this study highlights the importance of genetic diversity for the growth, development, and regeneration of species and the potential for genetic diversity to determine the ability of corals to adapt to changes in environment, climate, and disease (Perwati, 2009). The results of this study increase the understanding of genetic diversity within *I. hippuris* populations and emphasize the need to carefully select DNA extraction sites when investigating the genetic diversity of marine organisms.

In addition, environmental variables such as ocean currents, tides, and geological changes can affect marine life's genetic makeup, making understanding population structure and genetic diversity even more important. Lind et al. (2009) and Ovenden et al. (2013) have shown that environmental variables can alter a species's distribution, affecting its genetic makeup. DNA barcoding has immense potential in conserving and managing marine ecosystems by facilitating species identification, particularly in cases where morphological differences are challenging to discern. This advanced technology enables precise monitoring and management of marine species and their habitats and can also aid in identifying endangered or vulnerable species. However, the application of *COI* genetic analysis may be restricted to specific subgroups of *I. hippuris*, which can limit its usefulness in precise species identification. Various physical conditions can also affect the genetic makeup of marine species.

CONCLUSION

COI gene analysis could only be performed on the base and main stem of the *I. hippuris*. The lateral stem of *I. hippuris* from coral and seagrass-coral areas was not further analyzed due to low concentration and purity values, which could potentially fail DNA sequencing. Each part of *I. hippuris* may have unique genetic differences. This study highlights the advantages of DNA sequencing in providing a unique genetic fingerprint for each species, enabling accurate species identification. This research provides insight into using DNA barcoding for sea bamboo species identification.

ACKNOWLEDGEMENTS

The authors thank the Indonesian Ministry of Education, Culture, Research, and Technology for providing the BPPDN scholarship and funding this research (No: 554/UN10.F40/KM.01.00/2023).

REFERENCES

Bineesh, K. K., Gopalakrishnan, A., Akhilesh, K. V., Sajeela, K. A., Abdussamad, E. M., Pillai, N. G. K., Basheer, V. S., Jena, J. K., & Ward, R. D. (2017). DNA barcoding reveals species composition of sharks and rays in the Indian commercial fishery. *Mitochondrial DNA Part A: DNA Mapping, Sequencing, and Analysis*, *28*(4), 458–472. https://doi.org/10.3109/19401736.2015.1137900

Bingpeng, X., Heshan, L., Zhilan, Z., Chunguang, W., Yanguo, W., & Jianjun, W. (2018). DNA barcoding for identification of fish species in the Taiwan Strait. *PLOS One*, *13*(6), e0198109. https://doi.org/10.1371/journal.pone.0198109

Ceruso, M., Mascolo, C., Anastasio, A., Pepe, T., & Sordino, P. (2019). Frauds and fish species authentication: Study of the complete mitochondrial genome of some Sparidae to provide specific barcode markers. *Food Control*, *103*, 36-47. https://doi.org/10.1016/j.foodcont.2019.03.028

Clark, L. F. (2015). The current status of DNA barcoding technology for species identification in fish value chains. *Food Policy*, *54*, 85-94. https://doi.org/10.1016/j.foodpol.2015.05.005

Cooke, S. J., Martins, E. G., Struthers, D. P., Gutowsky, L. F., Power, M., Doka, S. E., Dettmers, J. M., Crook, D. A., Lucas, M. C., Holbrook, C. M., & Krueger, C. C. (2016). A moving target-incorporating knowledge of the spatial ecology of fish into the assessment and management of freshwater fish populations. *Environmental Monitoring and Assessment*, *188*(4), 239. https://doi.org/10.1007/s10661-016-5228-0

Cooper, E. W. T., Torntore, S. J., Leung, A. S. M., Shadbolt, T., & Dawe, C. (2011). *Guide to the identification of precious and semi-precious corals in commercial trade*. https://www.traffic.org/site/assets/files/5642/guide_to_the_identification_of_precious_and_semi-precious_corals_in_commercial_trade.pdf

Díaz, S., Settele, J., Brondízio, E. S., Ngo, H. T., Guèze, M., Agard, J., Arneth, A., Balvanera, P., Brauman, K., Butchart, S. H., Chan, K. M., Garibaldi, L. A., Ichii, K., Liu, J., Mazhenchery Subramanian, S., Midgley, G., Miloslavich, P., Molnár, Z., Obura, D., … Zayas, C. N. (Eds.). (2019). *Summary for policymakers of the global assessment report on biodiversity and ecosystem services*. Intergovernmental Science-Policy Platform on Biodiversity and Ecosystem Services. https://doi.org/10.5281/zenodo.3553579

Dieffenbach, C. W., Lowe, T. M., & Dveksler, G. S. (1993). General concepts for PCR primer design. *PCR Methods and Applications*, *3*(3), S30–S37. https://doi.org/10.1101/gr.3.3.s30

Drancourt, M., Bollet, C., Carlioz, A., Martelin, R., Gayral, J. P., & Raoult, D. (2000). 16S ribosomal DNA sequence analysis of a large collection

of environmental and clinical unidentifiable bacterial isolates. *Journal of Clinical Microbiology*, *38*(10), 3623–3630. https://doi.org/10.1128/JCM.38.10.3623-3630.2000

Edrus, I. N., & Suman, A. (2013). Kebijakan perlindungan dan konservasi hewan oktokoralian/bambu laut (*Isis hippuris* Linnaeus 1758) [Policy for the protection and conservation of octocoralians/sea bamboo (*Isis hippuris* Linnaeus 1758)]. *Jurnal Kebijakan Perikanan Indonesia*, *5*(2), 107-112. https://doi.org/10.15578/JKPI.5.2.2013.107-112

Han, Z. Q., Gao, T. X., Yanagimoto, T., & Sakurai, Y. (2008). Genetic population structure of *Nibea albiflora* in the Yellow Sea and East China Sea. *Fisheries Science*, *74*, 544-552. https://doi.org/10.1111/j.1444-2906.2008.01557.x

Hebert, P. D., Cywinska, A., Ball, S. L., & deWaard, J. R. (2003). Biological identifications through DNA barcodes. *Proceedings of the Royal Society of London Series B: Biological Sciences*, *270*(1512), 313-321. https://doi.org/10.1098/rspb.2002.2218

Hellberg, R. S., Pollack, S. J., & Hanner, R. H. (2016). Seafood species identification using DNA sequencing. In A. M. Naaum & R. H. Hanner (Eds.), *Food safety and quality systems in developing countries* (pp. 113-132). Academic Press. https://doi.org/10.1016/B978-0-12-801592-6.00006-1

Hoegh-Guldberg, O., & Bruno, J. F. (2010). The impact of climate change on the world's marine ecosystems. *Science*, *328*(5985), 1523-1528. https://doi.org/10.1126/science.1189930

Kumar, A., & Verma, A. K. (2017). Biodiversity loss and its ecological impact in India. *International Journal on Biological Sciences*, *8*(2), 156-160.

Kumar, S., Stecher, G., Li, M., Knyaz, C., & Tamura, K. (2018). MEGA X: Molecular Evolutionary Genetics Analysis across computing platforms. *Molecular Biology and Evolution*, *35*(6), 1547-1549. https://doi.org/10.1093/molbev/msy096

Kuske, C. R., Barns, S. M., Grow, C. C., Merrill, L., & Dunbar, J. (2006). Environmental survey for four pathogenic bacteria and closely related species using phylogenetic and functional genes. *Journal of Forensic Sciences*, *51*(3), 548–558. https://doi.org/10.1111/j.1556-4029.2006.00131.x

Laxmi, R., Arya, S., Sultana, A., & Das, S. K. (2015). Assessment and impact of industrial effluents on River Yamuna ecosystem. *International Journal of Current Research*, *7*(9), 19956-19963.

Lind, C. U., Evans, B. S., Knauer, J., Taylor, J. J. U., & Jerry, D. R. (2009). Decreased genetic diversity and a reduced effective population size in cultured silver-lipped pearl oysters (*Pinctada maxima*). *Aquaculture*, *286*(1-2), 12-19. https://doi.org/10.1016/j.aquaculture.2008.09.009

Lunt, I. D., Byrne, M., Hellmann, J. J., Mitchell, N. J., Garnett, S. T., Hayward, M. W., Martin, T. G., Mcdonald-maddden, E., Williams, S. E., & Zander, K. K. (2013). Using assisted colonisation to conserve biodiversity and restore ecosystem function under climate change. *Biological Conservation*, *157*, 172–177. https://doi.org/10.1016/j.biocon.2012.08.034

Meriam, T., Wafa, T., Khawla, T., Tarek, H., Abdeljelil, G., & Mhamed, E. (2015). Genetic diversity and population structure of *Sepia officinalis* from the Tunisian cost revealed by mitochondrial COI sequences. *Molecular Biology Reports*, *42*, 77-86. https://doi.org/10.1007/s11033-014-3743-z

Muhammad, H., Iqbal, Z., Iqbal, M. U., Younas, T., & Bashir, Q. (2016). An efficient method for DNA isolation from fish fin. *Pakistan Journal of Agricultural Science*, *53*(4), 843-850. https://doi.org/10.21162/PAKJAS%2F16.3998

Ovenden, J. R., Berry, O., Welch, D. J., Buckworth, R. C., & Dichmont, C. M. (2013). Ocean's eleven: A critical evaluation of the role of population, evolutionary and molecular genetics in the management of wild fisheries. *Fish and Fisheries*, *16*(1), 125-159. https://doi.org/10.1111/faf.12052

Ozturk, A. R., & Can, T. (2017). A multiplex primer design algorithm for target amplification of continuous genomic regions. *BMC Bioinformatics*, *18*, 306. https://doi.org/10.1186/s12859-017-1716-7

Palumbi, S. R. (2003). Population genetics, demographic connectivity, and the design of marine reserves. *Ecological Applications*, *13*(sp1), 146-158. https://doi.org/10.1890/1051-0761(2003)013[0146:PGDCAT]2.0.CO;2

Perwati, L. K. (2009). Analisis derajat ploidi dan pengaruhnya terhadap variasi ukuran stomata dan spora pada *Adiantum raddianum* [Analysis of ploidy degree and its effect on variations in stomata and spore size in *Adiantum raddianum*]. *Bioma: Berkala Ilmiah Biologi*, *11*(2), 39-44. https://doi.org/10.14710/bioma.11.2.39-44

Pimm, S. L., Jenkins, C. N., Abell, R., Brooks, T. M., Gittleman, J. L., Joppa, L. N., Raven, P. H., Roberts, C. M., & Sexton, J. O. (2014). The biodiversity of species and their rates of extinction, distribution, and protection. *Science*, *344*(6187), 1246752. https://doi.org/10.1126/science.1246752

Posthouwer, C., Veldman, S., Abihudi, S., Otieno, J. N., van Andel, T. R., & de Boer, H. J. (2018). Quantitative market survey of non-woody plants sold at Kariakoo Market in Dar es Salaam, Tanzania. *Journal of Ethnopharmacology*, *222*, 280-287. https://doi.org/10.1016/j.jep.2018.04.039

Ravago-Gotanco, R., & Kim, K. M. (2019). Regional genetic structure of sandfish *Holothuria* (*Metriatyla*) *scabra* populations across the Philippine archipelago. *Fisheries Research*, *209*, 143-155. https://doi.org/10.1016/J.FISHRES.2018.09.021

Saad, Y. (2019). Analysis of 16s mitochondrial ribosomal DNA sequence variations and phylogenetic relations among some Serranidae fishes. *South African Journal of Animal Science*, *49*(1), 80-89. https://doi.org/10.4314/sajas.v49i1.10

Sari, A., Duran, M., Sen, A., & Bardakci, F. (2015). Investigation of Chironomidae (Diptera) relationships using mitochondrial *COI* gene. *Biochemical Systematics and Ecology*, *59*, 229-238. https://doi.org/10.1016/j.bse.2015.01.005

Thai, B. T., Pham, T. A., & Austin, G. M. (2006). Genetic diversity of common carp in Vietnam using direct sequencing and SSCP analysis of the mitochondrial DNA control region. *Aquaculture*, *258*(1-4), 228-240. https://doi.org/10.1016/j.aquaculture.2006.03.025

Thompson, J. D., Gibson, T. J., Plewniak, F., Jeanmougin, F., & Higgins, D. G. (1997). The CLUSTAL_X windows interface: Flexible strategies for multiple sequence alignment aided by quality analysis tools. *Nucleic Acids Research*, *25*(24), 4876-4882. https://doi.org/10.1093/nar/25.24.4876

Verma, A. K. (2017). Genetic diversity as buffer in biodiversity. *Indian Journal of Biology*, *4*(1), 61-63. https://doi.org/10.21088/ijb.2394.1391.4117.9

Verma, A. K. (2018). Ecological balance: An indispensable need for human. *Journal of Experimental Zoology India*, *21*(1), 407-409.

Wallace, L. J., Boilard, S. M. A. L., Eagle, S. H. C., Spall, J. L., Shokralla, S., & Hajibabaei, M. (2012). DNA barcodes for everyday life: Routine authentication of Natural Health Products. *Food Research International*, *49*(1), 446-452. https://doi.org/10.1016/j.foodres.2012.07.048

Wang, B., Xie, F., Li, J. N., Wang, G., Li, C., & Jiang, J. P. (2017). Phylogeographic investigation and ecological niche modelling of the endemic frog species *Nanorana pleskei* revealed multiple refugia in the eastern Tibetan Plateau. *PeerJ*, *5*, e3770. https://doi.org/10.7717/peerj.3770

Watson, J. E. M., Rao, M., Ai-Li, K., & Yan, X. (2012). Climate change adaptation planning for biodiversity conservation: A review. *Advances in Climate Change Research*, *3*(1), 1-11. https://doi.org/10.3724/SP.J.1248.2012.00001

Pertanika J. Trop. Agri. Sci. 46 (4): 1359 - 1374 (2023)

PERTANIKA JOURNALS

TROPICAL AGRICULTURAL SCIENCE

Journal homepage: http://www.pertanika.upm.edu.my/

Microscale Dynamics of Larval Fish Assemblages in the Straits of Malacca Nearshore Coincided with Lunar Phases

Ali Md. Yeakub[1], Fatimah Md. Yusoff[1,2], Natrah Fatin Mohd Ikhsan[1,2] and Zafri Hassan[1,2]*

[1]International Institute of Aquaculture and Aquatic Sciences, Universiti Putra Malaysia, 70150 Port Dickson, Negeri Sembilan, Malaysia
[2]Department of Aquaculture, Faculty of Agriculture, Universiti Putra Malaysia, 43400 Serdang, Selangor, Malaysia

ABSTRACT

Marine fish larvae are an integral part of the marine environment because their abundance can become an ecological indicator. The abundance is dependent on the environmental variations that include but are not limited to lunar phases and diel changes, both of which predictably influence them to drift between inshore and outshore of the nearshore system. This study determined the effects of those environmental variations at the spatio-temporal level on the larval fish abundance along the Negeri Sembilan coastline of the Straits of Malacca, Malaysia. Samples were collected using a Bongo net of 300 μm in mesh size during the inter-monsoon season of March through April 2021 ($n = 32$). Larval fish density for the 32 samples ranged between 1 and 31 larvae/m^3. There were 18 larval fish families identified from the study, with the most sampled larvae of Engraulidae, contributing to 24.20% of 892 total fish larvae identified. Other families with notable abundance were Gobiidae (16.30%), Blennidae (13.15%), Ambassidae (10.40%), Apogonidae (9.95%), and Leiognathidae (3.73%). The larval fish abundance was significantly higher during the new lunar phase than the full lunar phase ($P < 0.01$). Although there were marginal differences between the night and day as well as between outshore and inshore in some of the samples, there was no significant difference within both diel changes and shore distances. The study indicated that the dynamics in the larval fish assemblages in the study area were markedly attributed to lunar phases.

Keywords: Diel change, lunar phase, marine fish larvae, nearshore marine, the Straits of Malacca

ARTICLE INFO

Article history:
Received: 28 February 2023
Accepted: 29 May 2023
Published: 17 November 2023

DOI: https://doi.org/10.47836/pjtas.46.4.18

E-mail addresses:
yeakubali106@gmail.com (Ali Md. Yeakub)
fatimahyus@gmail.com (Fatimah Md. Yusoff)
natrah@upm.edu.my (Natrah Fatin Mohd Ikhsan)
mzafri@upm.edu.my (Zafri Hassan)
*Corresponding author

ISSN: 1511-3701
e-ISSN: 2231-8542

INTRODUCTION

Larval fish life history is distinguished by specific eco-morphological characteristics that the larvae are adapted to during the early fish life stages (Catalán et al., 2020). Biotic and abiotic factors influence the adaptations. The biotic factors include but are not limited to prey and predator availability (Ferreira et al., 2020), digestive tract development, visual acuity, and swimming performance of larvae (Makrakis et al., 2005). At the same time, the abiotic factors can include habitats (Ara et al., 2020), daylight cycle (Picapedra et al., 2018), and water quality (Colombano et al., 2021; McGeady et al., 2021). The adaptations during the initial stage of the life cycle are critical because the survival rate is relatively as low as 10% and reduces to around 2–3% as the larvae start their first feeding (Ferreira et al., 2020).

In the marine ecosystem, fish larvae drift in the nearshore littoral zone during the ontogenetic developmental stage (Polte et al., 2017), where varying challenges affect their survival rate (Ridho et al., 2020). Natural circadian rhythms also influence larval fish assemblages in the coastal marine water. The nearshore coastal region fits the larval retention hypothesis in that it is an important nursery ground due to high bioavailability, low predation risk, and suitable physio-chemical characteristics (Díaz-Astudillo et al., 2017; Pattrick & Strydom, 2014a).

Activities around the area are also affected by diel patterns. During this stage, fish larvae depend on the light given the less developed eyes in their early development. Nearshore depths between 0 and 100 m harbor the highest larvae concentrations, where zooplankton density increases during the night, attributed to the lunar cycle (Olivar et al., 2018).

The lunar illumination cycle is the key driving element in the dispersion of fish larvae in the water column. It is the factor that affects vertical migration of the fish larvae in the marine ecosystem resulting in diel variation in the larval assemblages (Wang et al., 2022). The migration is mainly due to feeding, where they move to the epipelagic zone at night before returning to the mesopelagic zone to digest the food and excrete waste (Dove et al., 2021; Irigoien et al., 2014).

The lunar phases also cause cyclical variations in nighttime illumination (moonlight intensity), geomagnetic fields, gravitational pull, tidal amplitude, hormonal secretion, and gene expression for the cryptochrome gene (Ikegami, Takeuchi, Hur, et al., 2014). Melatonin hormone secretion can induce larval fish activity at night during the lunar phase. Hormone secretion occurs greatly at night during the new moon phase compared to the full moon phase (Ikegami, Takeuchi, & Takemura, 2014).

The variability in the biotic and abiotic in relation to larval assemblages indicates spawning occurrence in the nearshore environment. The information is important for fisheries management, especially when targeted fisheries and fishing ground limits are concerned. While acquiring gravid fishes as an indicator of the occurrence of spawning events at a specific time or locality can be challenging, deduction from larval fish assemblages should be able to provide

such information. Therefore, the objective of this study was to determine the effects of lunar phases, diel variations, and shoreline distance on larval fish assemblages in the Malacca Strait's nearshore marine ecosystem.

MATERIALS AND METHODS

Study Area

The study was carried out on the Negeri Sembilan coastline, which accounts for about 5% of Peninsular Malaysia's total coastline length of 48 km on the strait. The whole of Peninsular Malaysia is of tropical climate, where the coastal environment is largely affected by monsoon winds throughout the year, southwest and northeast monsoons. Fieldwork for this study was carried out during inter-monsoon of the transition monsoon between northeast and southwest, i.e., March until April 2022.

Selection of Sampling Stations

Sampling stations were primarily selected based on the following limits: (1) in Zone A fishing area, which is designated by the Department of Fisheries Malaysia (DOF), essentially within less than 2.5 km offshore, (2) spatially equal distance of 2 km from each station across the coastal limits of Zone A fishing area and Negeri Sembilan state maritime borders with Lukut and Tanjung Tuan as the extreme-most points, (3) four replicate stations that are associated with coastal towns and landmarks, and (4) two distances seaward from the nearest coastal towns or landmarks i.e., 0.5 km (hereafter inshore) and 2.5 km (hereafter outshore).

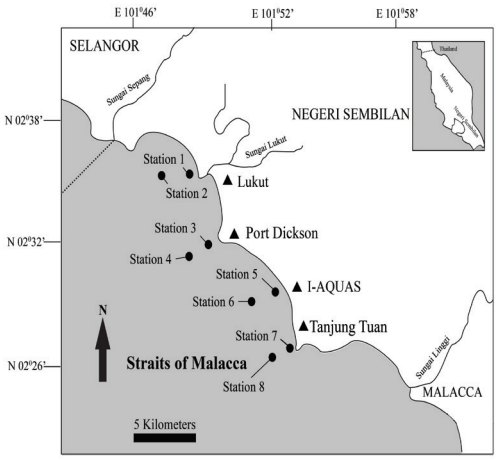

Figure 1. Sampling stations in the nearshore zone of the Straits of Malacca along the Negeri Sembilan shoreline.

Altogether, eight sampling stations were selected for the study based on the criteria (Figure 1). Sampling stations 1–4 are associated with the coastal towns of Lukut and Port Dickson, and sampling stations 5-8 are associated with landmarks of the International Institute of Aquaculture and Aquatic Sciences (IAQUAS) and Tanjung Tuan.

Broken lines perpendicular to Sungai Sepang and Sungai Linggi are arbitrary state maritime borders between Negeri Sembilan and other states

Fieldwork

Thirty-two (32) samples were collected during the inter-monsoon season of March through April 2021. All samples from the fieldwork were collected during spring tide to control for the effect of tides on larval fish assemblages. Altogether, the 32 samples consisted of samples from 2 lunar phases

× 2 distances from the shore × 2 diel × 4 replicate stations. The sampling scheme essentially culminated in eight spatio-temporal treatments, i.e.: (a) New Lunar + Inshore + Day, (b) New Lunar + Inshore + Night, (c) New Lunar + Outshore + Day, (d) New Lunar + Outshore + Night, (e) Full Lunar + Inshore + Day, (f) Full Lunar + Inshore + Night, (g) Full Lunar + Outshore + Day, and (h) Full Lunar + Outshore + Night.

Sample Collection and Preservation

Larval fish were collected by using a set of Bongo nets of 300 µm mesh size (mouth diameter 0.60 and 3 m long). The net was towed horizontally at the water sub-surface from a moving boat at a constant speed of 2.5 knots for 10 min. Larval fish samples collected from the tows were preserved in 5% formalin (Sigma-Aldrich, USA). The 5% formalin solution was buffered with sodium tetraborate de-carbohydrate, i.e., borax (Sigma-Aldrich, USA), to neutralize the pH (Joshi & Sreekumar, 2015). All collected samples were transported to the laboratory for taxonomic identification.

Water Quality and Diversity Indices

The following *in situ* environmental variables were measured using YSI™ 556 multi-parameter probes (USA) at every sampling station: seawater dissolved oxygen (mg/L), and water sub-surface temperature (°C), salinity (ppt), pH, and turbidity (mg/L).

Identified larvae for each sample were tallied to measure diversity indices based on the following formula:

a. Relative abundance and its complement (complementary Simpson, 1-D), Simpson (1949), $1-D=1-\sum_{i=1}^{R}\left(\frac{n_i(n_i-1)}{N(N-1)}\right)$ where R = total number of family in the sample, n_i = number of individuals in family i, and N = total number of species in the sample.

b. The proportion of larvae for each family of Shannon-Weiner H', Shannon (1948), $H'=\sum_{i=1}^{R} ln(p_i)$, where R = the number of individuals in the family i, and p_i = proportions of individuals that belong to species i.

c. Evenness of the larvae over the number of families, Pielou (1966) $J'=\frac{H'}{H'_{max}}$, where H' = derived from Shannon-Wiener diversity index, and H'_{max} = the maximum possible value of H'.

Larval Fish Density and Abundance Estimation

Larval fish abundance was determined by quantifying the number of individuals per unit volume of water (larvae/m^3). Dilution depends on the turbidity of the collected samples, where more turbid water requires a higher dilution factor as compared to the less turbid water samples. Then, taxonomic identification began with grouping a few preliminary water samples containing larval fish into generic groups based on their morphological characteristics: pre-flexion, flexion, and post-flexion. Larval fish were then identified to the lowest possible taxa by using identification keys provided by preceding researchers (Jeyaseelan & Ramamathan, 1998; Kawaguchi, 2003; Konishi et al., 2012; Lies & Carson-Ewart, 2004; Okiyama,1989).

Data Analysis

The probability of occurrence of each identified family during the fieldwork was calculated based on tabulated presence and absence data from the 32 samples. Essentially, the probability of occurrence for each family is $p(\text{occurrence}) = \left(\frac{n_p}{N}\right)$,where n_p = number of samples, where at least one individual was present, and N = total number of samples analyzed in the study.

Overall differences in density and diversity indices were compared among the eight sampling stations to ascertain that the variation was due to chance. Three-way analyses of variance (ANOVA) were performed to evaluate the effect of lunar phases simultaneously, distance from the shore and diel variations, and their interactions on the larval fish density and diversity indices. The normality of response variables was tested prior to running the ANOVA tests by using the Shapiro-Wilk's lambda test. The homogeneity of variance of the tested groups was checked using Levene's test. Data that failed to meet the normality assumption were log-transformed in the analyses. Additionally, a one-way ANOVA was performed on eight spatio-temporal treatments of the combined factors to test whether there were differences in larval fish density among treatments. Significant ANOVA tests were subject to Tukey's honestly significant difference (HSD) post-hoc test to determine group differences.

Water quality parameters significantly different among the lunar phases were used as predictors in linear regression models to determine their effects on larval fish density. All ANOVA tests were performed with $\alpha = 0.05$ or essentially at 95% confidence intervals in RStudio 2022.07.1 with relevant R packages (Team, 2020).

RESULTS

Fish Larvae Assemblage

There were 892 fish larvae recovered from the study, with 18 families identified from 32 samples. More than half of the 18 families, i.e., 10, were present at every level of each factor (Table 1). Three of the 18 families, i.e., Ophidiidae, Pomacentridae, and Sciaenidae, were absent from the inshore samples, while Eleotrida, Kyphosidae, Tetraodontidae, and Uranoscopidae were absent from the outshore samples. Pomacentridae was the only family that was absent during the new lunar phase.

During the full lunar phase, more families were absent from the renumeration, and they were Eleotridae, Kyphosidae, Ophidiidae, Sciaenidae, Tetraodontidae, and Uranoscopidae (Figure 2). As expected, more families were recovered from night samples as opposed to day samples, with Uranoscopidae being the only absent from the former samples. Engraulidae had the highest probability of occurrence, $p(\text{occurrence}) = 0.91$, while the lowest was Tetraodontidae, $p(\text{occurrence}) = 0.03$ (Figure 2). Apart from Engraulidae, Ambassidae ($p = 0.84$), Blennidae ($p = 0.78$), Apogonidae ($p = 0.59$), and Gobiidae ($p = 0.5$) are families with 50% occurrence from the 32 samples.

Table 1
Checklist of fish larvae family identified from the samples by the three environmental factors tested in the study

Locality	Station / Shore distance	Lunar phase	Diel	Family																		Total Family
				Ambassidae	Apogonidae	Belonidae	Blenniidae	Carangidae	Clupeidae	Eleotridae	Engraulidae	Gobiidae	Kyphosidae	Leiognathidae	Nemipteridae	Ophidiidae	Pomacentridae	Sciaenidae	Scombridae	Tetraodontidae	Uranoscopidae	
Lukut	Station 1 (Inshore)	Full	Night	✓	×	×	✓	×	✓	×	✓	✓	×	×	×	×	×	×	×	×	×	5
			Day	×	×	✓	×	✓	×	×	×	✓	×	×	✓	×	×	×	✓	×	×	5
		New	Night	✓	×	×	✓	×	×	×	✓	✓	×	×	×	×	×	×	✓	×	×	5
			Day	✓	×	×	✓	×	×	×	✓	✓	×	×	×	×	×	×	✓	×	×	5
	Station 2 (Outshore)	Full	Night	✓	✓	✓	✓	✓	×	×	✓	✓	×	✓	✓	×	✓	×	×	×	×	10
			Day	×	✓	×	✓	×	×	×	✓	×	×	×	×	×	×	×	×	×	×	3
		New	Night	✓	✓	×	✓	×	×	×	✓	✓	×	✓	✓	×	×	×	✓	×	×	9
			Day	×	✓	×	×	×	×	×	×	✓	×	✓	×	×	×	×	✓	×	×	1
Port Dickson	Station 3 (Inshore)	Full	Night	✓	✓	×	✓	✓	×	×	✓	✓	×	✓	✓	×	×	×	×	×	×	8
			Day	✓	×	✓	✓	✓	×	×	✓	×	×	×	×	×	×	×	×	×	×	4
		New	Night	✓	✓	×	×	×	×	×	✓	✓	×	×	×	×	×	×	✓	×	×	5
			Day	✓	✓	×	✓	×	×	×	✓	×	×	×	×	×	×	×	×	×	×	4
	Station 4 (Outshore)	Full	Night	✓	×	✓	✓	✓	✓	×	✓	✓	×	✓	✓	×	×	×	×	×	×	6
			Day	✓	✓	×	✓	×	✓	×	✓	×	×	×	×	×	×	×	×	×	×	5
		New	Night	✓	✓	✓	✓	✓	✓	×	✓	✓	×	✓	✓	×	×	✓	×	×	×	12
			Day	✓	✓	×	✓	×	✓	×	✓	×	×	✓	✓	×	×	✓	×	×	×	6

Table 1 *(continue)*

Locality	Station / Shore distance	Lunar phase	Diel	Family																				
				Ambassidae	Apogonidae	Belonidae	Blenniidae	Carangidae	Clupeidae	Eleotridae	Engraulidae	Gobiidae	Kyphosidae	Leiognathidae	Nemipteridae	Ophidiidae	Pomacentridae	Sciaenidae	Scombridae	Tetraodontidae	Uranoscopidae	Total Family
I-AQUAS	Station 5 (Inshore)	Full	Night	✓	×	×	×	×	×	×	✓	×	×	×	×	×	×	×	×	×	×	2
			Day	✓	✓	×	×	×	×	×	×	×	×	×	×	×	×	×	×	×	×	2
		New	Night	✓	✓	×	✓	×	×	✓	✓	✓	✓	✓	✓	×	×	✓	✓	✓	×	11
			Day	✓	✓	×	✓	×	×	×	✓	×	×	×	✓	×	×	✓	✓	×	×	6
	Station 6 (Outshore)	Full	Night	✓	×	×	✓	×	✓	×	✓	×	×	✓	×	×	×	×	×	×	×	5
			Day	×	×	×	×	×	×	×	×	×	×	×	×	×	×	×	×	×	×	1
		New	Night	✓	×	×	✓	×	×	×	✓	×	×	✓	×	×	×	×	✓	×	×	5
			Day	✓	×	×	✓	✓	×	×	✓	×	×	×	×	×	×	×	×	×	×	5
Tanjung Tuan	Station 7 (Inshore)	Full	Night	✓	✓	×	✓	✓	✓	×	✓	✓	×	✓	×	×	×	×	×	×	×	7
			Day	✓	✓	×	×	×	×	×	✓	×	×	×	×	×	×	×	×	×	×	4
		New	Night	✓	✓	×	✓	×	✓	✓	✓	✓	✓	✓	✓	×	×	×	✓	×	×	10
			Day	✓	✓	×	✓	✓	×	×	✓	✓	×	✓	×	×	×	×	✓	×	✓	8
	Station 8 (Outshore)	Full	Night	✓	×	×	✓	✓	✓	×	✓	✓	×	✓	×	×	×	×	✓	×	×	9
			Day	×	✓	×	✓	×	✓	×	✓	×	×	✓	×	×	×	×	×	×	×	4
		New	Night	✓	×	×	✓	×	×	×	✓	✓	×	✓	×	×	×	×	×	×	×	7
			Day	✓	✓	×	✓	×	×	×	✓	×	×	✓	×	×	×	×	✓	×	×	7

Note. ✓ = Presence; × = Absence

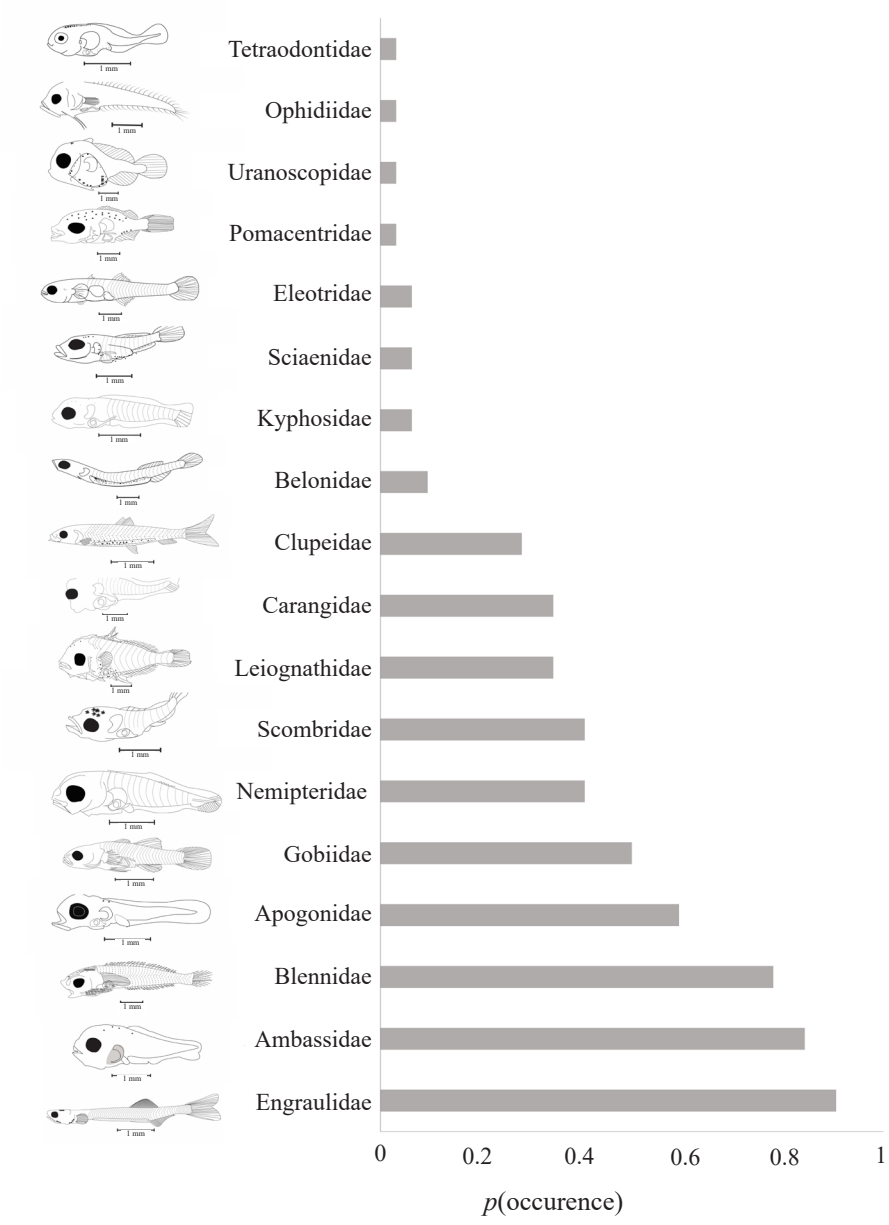

Figure 2. Probability of occurrence for identified larval fish family from all samples (n = 32)

Larval fish density for the 32 samples ranged between 1 and 31 larvae/m^3. Comparison among stations revealed that the diversity indices corroborated the larval fish density despite no significant differences (Figure 3). The F statistic and p-value for larval fish density was $F_{7,24} = 0.64$, p-value = 0.72, whereas diversity indices comparison of Shannon was $F_{7,24} = 0.81$, p-value = 0.59, Simpson $F_{7,24} = 0.96$, p-value = 0.48, and Evenness $F_{7,24} = 1.24$, p-value = 0.32. The outcomes indicated that larval

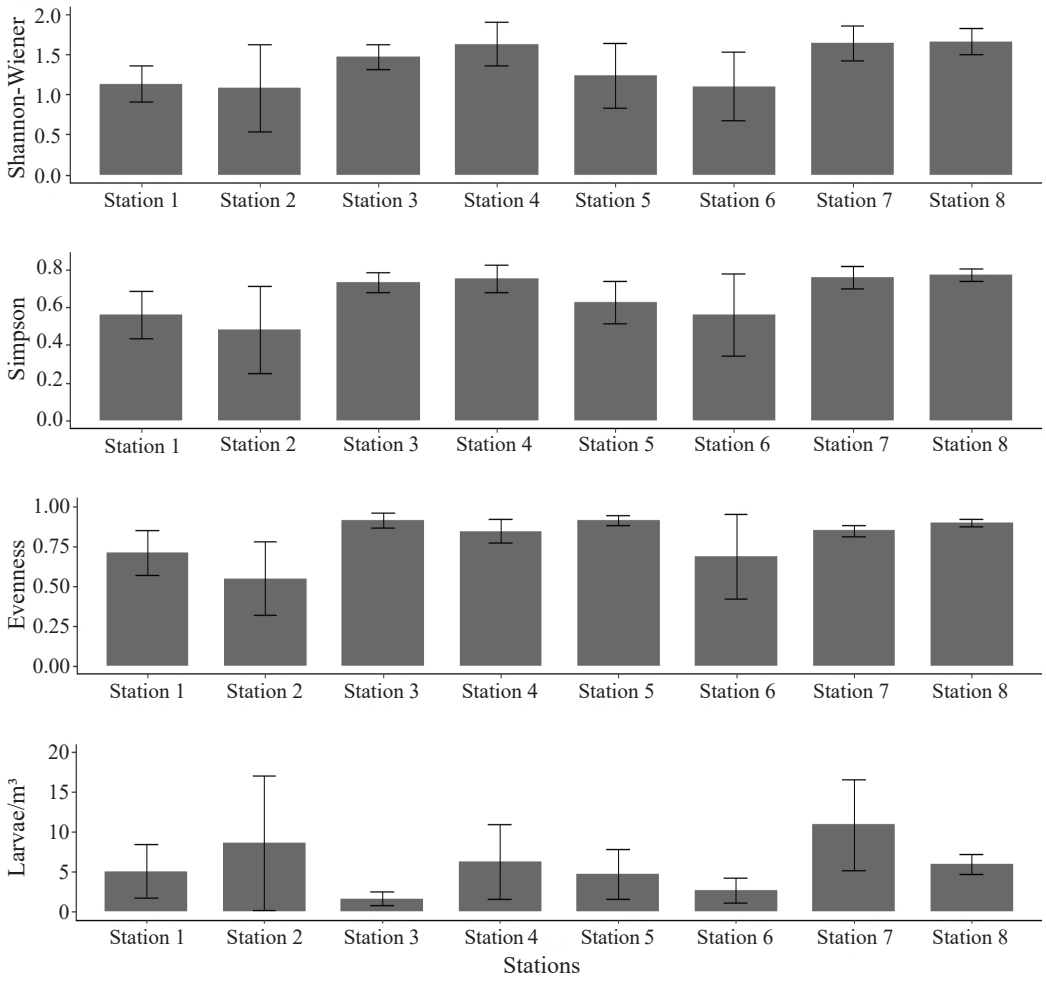

Figure 3. Mean ± SE for diversity indices, (a) Shannon-Wiener, (b) Simpson, (c) Pielou's Evenness, and (d) larval fish density

fish density in the study area was random and not inherent in their locality within the geo-limit of the study.

Effects of Lunar Phase, Shore Distance, and Diel Change on Larval Fish Density and Diversity

Three-way ANOVA analyses using original and log-transformed data (equal variance, Levene's $s_{7,24} = 0.478$, p-value = 0.841) revealed the same outcomes (Table 2). The lunar phase was the only factor that showed a significant difference ($p < 0.001$). Mean ± standard error density for samples collected during the new lunar phase (10 ± 1 larvae/m^3) was nine times higher than during the full lunar phase (2 ± 3 larvae/m^3). There were no significant two-way or three-way interactions among the main effects ($p > 0.05$). The outcome essentially revealed the significant role of lunar phases over other spatial factors in determining larval fish density.

Table 2
Three-way analysis of variance outputs for main effects of shore distance, lunar phase, diel factors, and their interactions. Similar outputs were obtained for log-transformed data (numbers in brackets)

Effect	F-statistic $_{df1=1,\ df2=24}$	p-value
Distance	0.015 (0.026)	0.902 (0.874)
Lunar phase	14.565 (21.373)	0.000837* (0.000108*)
Diel	2.341 (0.44)	0.139 (0.514)
Distance × Lunar phase	0.012 (0.093)	0.914 (0.762)
Distance × Diel	0.724 (0.044)	0.403 (836)
Lunar phase x Diel	2.195 (1.106)	0.151 (0.303)
Distance × Lunar phase × Diel	1.515 (1.359)	0.23 (0.255)

Note. * = Significant result at 95% confidence intervals

A follow-up analysis of one-way ANOVA on the spatio-temporal treatments using original and log-transformed data resulted in the same significant outcome, $F_{7,24} = 3.052$, p-value = 0.019 vs. 0.010, respectively. The post-hoc analysis further revealed that the combined factor of new lunar phase, inshore, and night treatment significantly marked the highest density, while the combined factor of full lunar phase, inshore, and day treatment significantly resulted in the lowest density (Figure 4). Overall, samples from new lunar phase fieldwork recorded higher larval fish mean density than those of the full lunar phase.

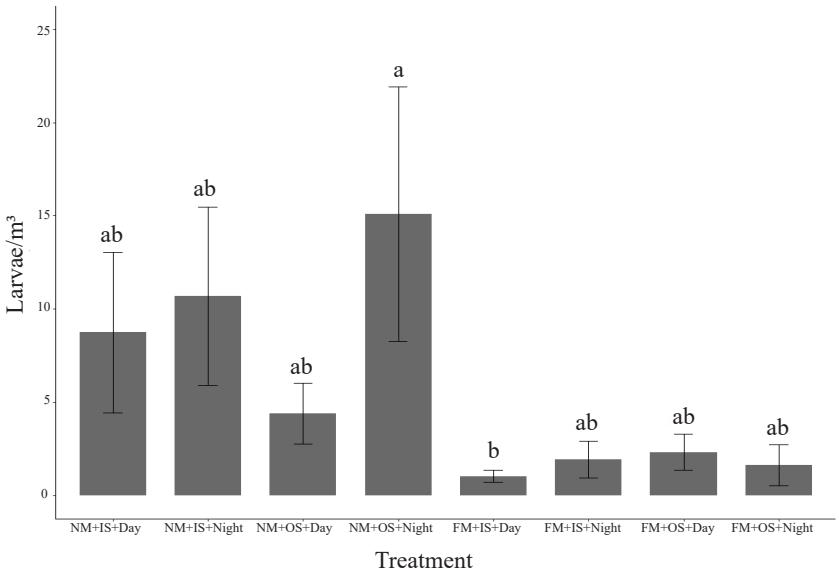

Figure 4. Mean ± SE larval fish density for eight spatio-temporal treatments of three factors with two levels each. The same scripts on top of the upper error bars indicate Tukey's honestly significant difference in post-hoc results.

Note. NM = New lunar; FM = Full lunar phase; IS = Inshore; OS = Outshore

Variation in Water Quality Parameters

Except for water temperature and total dissolved solids (TDS), all other water quality parameters measured during the study (pH, salinity, and dissolved oxygen) were not significantly different between the two levels of each factor (lunar phases, diel changes, and shore distance) tested in this study. Lunar phase ($F_{1,30}$ = 5.55; p-value = 0.03) and shore distance ($F_{1,30}$ = 7.66; p-value = 0.01) were significant factors that affected water temperature and TDS, respectively. The mean ± SE water temperature during the full lunar phase (29.4 ± 0.07°C) was significantly higher than that of the new lunar phase (29.2 ± 0.09°C). Additionally, the TDS of outshore water was significantly higher than inshore water (30.1 ± 0.01 mg/L vs. 29.7 ± 0.13 mg/L).

However, multiple linear regression, water temperature, and TDS were not significant factors in predicting larval fish density during the study period (Table 3). The coefficient of determination of the linear model of both water quality parameters was low in that those predictors insignificantly explained only 2.3% of the variance in the larval fish density ($F_{2, 29}$ = 0.343, p-value = 0.713, R^2 = 0.023).

Table 3
Parameter estimates of multiple linear regression on larval fish density

Effect	Estimates	Standard error	*t*-value	*p*-value
Intercept	112.47	138.00	0.82	0.42
Temperature (°C)	-2.96	3.97	-0.75	0.46
Total dissolved solids (mg/L)	-0.67	3.44	-0.19	0.85

DISCUSSION

Numerous marine fishes use the nearshore coastal habitats, including the inshore regions of the continental shelf, as an important habitat for at least part of their life cycles. A wide variety of fish species inhabit the oceanic regions, from large pelagic fish such as tuna that migrate to reproduce close to the littoral zone to those that spend their entire lives in the open ocean (Olivar et al., 2018). For example, Carangidae were abundant in spring and summer in seas less than 60 m deep (Chen & Li, 2003), whereas the majority of Nemipteridae larvae occupied sediment bottoms between 60 and 80 m deep (Guobao et al., 2002). Diverse fish need varying depths for spawning, where the depth influences the geographical distribution of spawning grounds and larval occurrence (Feng et al., 2021; Lelièvre et al., 2014). Due to the absence of a swimbladder and incomplete fin development, larval fish involuntarily change their habitat through drifting or along with water currents, ocean waves, and diel vertical migration. The drifting behavior explains why larval fish density decreases with depth or distance from the shoreline.

Engraulidae were the greatest family composition found in all stations in

the study area, followed by Gobiidae, Blennidae, Ambassidae, Apogonidae, and Leiognathidae. A previous study stated that Engraulidae fish larvae were found mostly in waters less than 20 m deep in the Yangtze River Estuary (Li et al., 2018). The abundance of larval fish was greater inshore than in the deepest offshore area (Tiedemann & Brehmer, 2017). However, the current study has not found any evidence to indicate that inshore larval fish distribution, abundance, and density are significantly higher than offshore. Another study found that inshore catches were Gobiidae, and offshore catches were Engraulidae mainly (Pattrick et al., 2021). In this study, Gobiidae occurred only in the Mangrove Lukut estuarine habitat as it is an estuarine resident species (Chu et al., 2019; Vorsatz et al., 2021). However, in the current study, larval fish density in nearshore and outshore has no significant difference due to micro spatial sampling as it is still in fishing Zone A. Larval fish movement is regulated by the day and night variation.

Diel vertical migration of larval fish is an exogenous process. The highest abundance and richness are higher during the night (Arévalo-Frías & Mendoza-Carranza, 2015). The highest catches of larvae and early juveniles have been made during the night and ebb tide. Engraulidae dominates larvae at night during the dry or summer season and mostly in pre-flexion larvae (Pattrick & Strydom, 2014b). Larval fish abundance and density are higher during the nighttime than during the daylight hours (Islam et al., 2007; Olivar & Beckley, 2022; Wang et al., 2022). The current study corroborated the past findings. Another study supported that diel variation did not show any significant trends in a study carried beach surf zone in southwest Spain (Gutiérrez-Martínez et al., 2021).

The fish larvae were abundant at night because when daylight decreases in intensity during nightfall, the condition stimulates larval migration toward surface layers. After all, the fish larvae respond to increased illumination from the full moon, as opposed to during daylight, when they move deeper waters (Picapedra et al., 2015). During this crepuscular period of low light levels, the risk of predation is reduced but, at the same time, enables vision of food in the surface layers. This activity is viewed as a multi-adaptive approach that confers advantages in terms of predator avoidance, bioenergetic efficiency, and zooplankton foraging (Mehner, 2014).

The phases of the moon cause cyclical variations in nighttime illumination (moonlight intensity), geomagnetic fields, gravitational pull, tidal amplitude, hormonal secretion, and gene expression for the cryptochrome gene (Ikegami, Takeuchi, & Takemura, 2014). Melatonin hormone secretion can induce larval fish activity at night during the lunar phase, where the inducement is greater during the new than the full lunar phase (Ikegami, Takeuchi, Hur, et al., 2014). There are mixed findings with regard to the role of lunar phases on larval fish assemblages. However, there was evidence to indicate that the increased abundance was not significant during the

new lunar phase (Mwaluma, 2014); at least two studies corroborated with our findings that larval fish abundance is significantly highest during the lunar phase (Jaxion-Harm & Speight, 2016; Pattrick et al., 2022). However, the assemblages may vary among families as Engraulidae were seen the highest during the third quarter and full lunar phases (Díaz-Astudillo et al., 2017), while Ambassidae, Apogonidae, Gobiidae, and Leiognathidae were present during new and full lunar nights (Krumme et al., 2015). The selective presence of these families during certain lunar phases indicates that their spawning may be associated with the atmospheric cycle as well.

CONCLUSION

The new lunar phase appeared to augment larval fish assemblages in the Straits of Malacca along the Negeri Sembilan shoreline in Malaysia. It was possibly because of spawning events during the previous full lunar phase. Diel variation and coastal area within the Department of Fisheries Malaysia's Zone A fishing ground had a trivial influence on the aggregation of early development of marine fishes in the study area. Despite numerous research on fish larvae in the straits, ours was the first to demonstrate lunar phases as a possibly non-random element influencing larval fish assemblages in the nearshore zone.

ACKNOWLEDGEMENTS

Funding for this research comes from the Ministry of Higher Education (MoHE) of Malaysia and is supported by the Science and Technology Research Partnership for Sustainable Development (SATREPS), an auspice of the Japan Science and Technology Agency (JST) and the Japan International Cooperation Agency (JICA). We duly thank Universiti Teknologi Malaysia (UTM) for engaging Universiti Putra Malaysia for the water quality assessment under their MoHE Long-Term Research Grant Scheme (LRGS) project (JPT.S(BPKI)2000/011/06/01 Jld.9(80)) entitled "Development of Advanced Hybrid Ocean Thermal Energy Conversion (OTEC) Technology for Low Carbon Society & Sustainable Energy System".

REFERENCES

Ara, R., Amin, S. M. N., Yusoff, F. M., Arshad, A., & Romano, N. (2020). Larval fish assemblage, diversity and habitat ecology in the Matang Mangrove Ecosystem, Perak, Malaysia. *Journal of Environmental Biology*, *41*, 1316–1325. https://doi.org/10.22438/jeb/41/5(SI)/MS_25

Arévalo-Frías, W., & Mendoza-Carranza, M. (2015). Influence of temporal and spatial factors on abundance and richness of fish early stages in shallow tropical estuaries. *Environmental Biology of Fishes*, *98*, 891–904. https://doi.org/10.1007/s10641-014-0324-x

Catalán, I. A., Reglero, P., & Álvarez, I. (2020). Research on early life stages of fish: A lively field. *Marine Ecology Progress Series*, *650*, 1–5. https://doi.org/10.3354/meps13491

Chen, G., & Li, Y. (2003). Distribution of the Carangidae fishes in the continental shelf waters of northern South China Sea. *Journal of Shanghai Ocean University*, *12*(2), 146–151.

Chu, C., Loh, K. H., Ng, C. C., Ooi, A. L., Konishi, Y., Huang, S. P., & Chong, V. C. (2019). Using DNA barcodes to aid the identification of larval fishes in tropical estuarine waters (Malacca Straits,

Malaysia). *Zoological Studies*, *58*, 30. https://doi.org/10.6620/ZS.2019.58-30

Colombano, D. D., Litvin, S. Y., Ziegler, S. L., Alford, S. B., Baker, R., Barbeau, M. A., Cebrián, J., Connolly, R. M., Currin, C. A., Deegan, L. A., Lesser, J. S., Martin, C. W., McDonald, A. E., McLuckie, C., Morrison, B. H., Pahl, J. W., Risse, L. M., Smith, J. A. M., Staver, L. W., ... Waltham, N. J. (2021). Climate change implications for tidal marshes and food web linkages to estuarine and coastal nekton. *Estuaries and Coasts*, *44*, 1637-1648. https://doi.org/10.1007/s12237-020-00891-1

Díaz-Astudillo, M., Castillo, M. I., Cáceres, M. A., Plaza, G., & Landaeta, M. F. (2017). Oceanographic and lunar forcing affects nearshore larval fish assemblages from temperate rocky reefs. *Marine Biology Research*, *13*(10), 1015–1026. https://doi.org/10.1080/17451000.2017.1335872

Dove, S., Tiedemann, M., & Fock, H. O. (2021). Latitudinal transition of mesopelagic larval fish assemblages in the eastern central Atlantic. *Deep-Sea Research Part I: Oceanographic Research Papers*, *168*, 103446. https://doi.org/10.1016/j.dsr.2020.103446

Feng, Y., Yao, L., Zhao, H., Yu, J., & Lin, Z. (2021). Environmental effects on the spatiotemporal variability of fish larvae in the western Guangdong waters, China. *Journal of Marine Science and Engineering*, *9*(3), 316. https://doi.org/10.3390/jmse9030316

Ferreira, A. S. A., Stige, L. C., Neuheimer, A. B., Bogstad, B., Yaragina, N., Prokopchuk, I., & Durant, J. M. (2020). Match–mismatch dynamics in the Norwegian–Barents Sea system. *Marine Ecology Progress Series*, *650*, 81–94. https://doi.org/10.3354/MEPS13276

Guobao, C., Yongzhen, L., & Pimao, C. (2002). Spawning ground of *Nemipterus bathybius* in northern continental shelf waters of South China Sea. *Journal of Zhanjiang Ocean University*, *22*(6), 20–25.

Gutiérrez-Martínez, M., Muñoz-Lechuga, R., Rodríguez-García, C., Sanz-Fernández, V., & Cabrera-Castro, R. (2021). Spatial-temporal patterns of fish and macroinvertebrate communities in sandy beach surf zones: Short and medium-term variations. *Journal of Sea Research*, *168*, 101993. https://doi.org/10.1016/j.seares.2020.101993

Ikegami, T., Takeuchi, Y., & Takemura, A. (2014). Lunar clock in fish reproduction. In H. Numata & B. Helm (Eds.), *Annual, lunar, and tidal clocks: Patterns and mechanisms of nature's enigmatic rhythms* (pp. 163–178). Springer. https://doi.org/10.1007/978-4-431-55261-1_9

Ikegami, T., Takeuchi, Y., Hur, S. P., & Takemura, A. (2014). Impacts of moonlight on fish reproduction. *Marine Genomics*, *14*, 59–66. https://doi.org/10.1016/j.margen.2013.11.007

Irigoien, X., Klevjer, T. A., Røstad, S., Martinez, U., Boyra, G., Acuña, J. L., Bode, A., Echevarria, F., Gonzalez-Gordillo, J. I., Hernandez-Leon, S., Agusti, S., Aksnes, D. L., Duarte, C. M., & Kaartvedt, S. (2014). Large mesopelagic fish's biomass and trophic efficiency in the open ocean. *Nature Communications*, *5*, 3271. https://doi.org/10.1038/ncomms4271

Islam, M. S., Hibino, M., & Tanaka, M. (2007). Tidal and diurnal variations in larval fish abundance in an estuarine inlet in Ariake Bay, Japan: Implication for selective tidal stream transport. *Ecological Research*, *22*(1), 165–171. https://doi.org/10.1007/s11284-006-0001-4

Jaxion-Harm, J., & Speight, M. R. (2016). Distribution of fish larvae within a weakly tidal mangrove lagoon. *Marine and Freshwater Research*, *68*(2), 396–400. https://doi.org/10.1071/MF15292

Jeyaseelan, M. J. P., & Ramamathan, N. (1998). *Manual of fish eggs and larvae from Asian mangrove waters*. Unesco Publishing.

Joshi, K. K., & Sreekumar, K. M. (2015). Basics of sample collection, preservation and species identification of finfish. In K. K. Joshi, M. S. Varsha, V. L. Sruthy, V. Susan, & P. V. Prathyusha (Eds.), *Summer school on recent*

advances in marine biodiversity conservation and management (pp. 134-137). Central Marine Fisheries Research Institute.

Kawaguchi, K. (2003). *Guide for sampling and identification of fish larvae in the straits of Malacca*. Unri Press.

Konishi, Y., Chayakul, R., Chamchang, C., & Duangdee, T. (2012). *Early stages of marine fishes in Southeast Asian Region*. http://repository.seafdec.or.th/handle/20.500.12067/566

Krumme, U., Grinvalds, K., Zagars, M., Elferts, D., Ikejima, K., & Tongnunui, P. (2015). Tidal, diel, and lunar patterns in intertidal and subtidal mangrove creek fish assemblages from southwest Thailand. *Environmental Biology of Fishes*, *98*, 1671-1693. https://doi.org/10.1007/s10641-015-0393-5

Lelièvre, S., Vaz, S., Martin, C. S., & Loots, C. (2014). Delineating recurrent fish spawning habitats in the North Sea. *Journal of Sea Research*, *91*, 1–14. https://doi.org/10.1016/j.seares.2014.03.008

Li, J. S., Lin, N., & Ling, J. Z. (2018). Temporal variation in the composition and abundance of fish larvae and juveniles off the Yangtze River Estuary in spring and summer. *Journal of Fisheries Science China*, *25*(3), 586-594. https://doi.org/10.3724/SP.J.1118.2018.17265

Lies, J. M., & Carson-Ewart, B. M. (Eds.). (2004). *The larvae of Indo-Pacific coastal fishes: An identification guide to marine fish larvae*. Brill.

Makrakis, M. C., Nakatani, K., Bialetzki, A., Sanches, P. V., Baumgartner, G., & Gomes, L. C. (2005). Ontogenetic shifts in digestive tract morphology and diet of fish larvae of the Itaipu Reservoir, Brazil. *Environmental Biology of Fishes*, *72*, 99–107. https://doi.org/10.1007/s10641-004-6596-9

McGeady, R., Lordan, C., & Power, A. M. (2021). Shift in the larval phenology of a marine ectotherm due to ocean warming with consequences for larval transport. *Limnology and Oceanography*, *66*(2),543–557. https://doi.org/10.1002/lno.11622

Mehner, T. (2014). Partial diel vertical migration of sympatric vendace (*Coregonus albula*) and fontane cisco (*Coregonus fontanae*) is driven by density dependence. *Canadian Journal of Fisheries and Aquatic Sciences*, *72*(1), 116–124. https://doi.org/10.1139/cjfas-2014-0009

Mwaluma, J. M., Kaunda-Arara, B., & Rasowo, J. (2014). Diel and lunar variations in larval supply to Malindi Marine Park, Kenya. *Western Indian Ocean Journal of Marine Science*, *13*(1), 57–67.

Okiyama, M. (1989). *An atlas of the early-stage fishes in Japan*. Tokai University Press.

Olivar, M. P., & Beckley, L. E. (2022). Latitudinal variation in diversity and abundance of mesopelagic fishes associated with change in oceanographic variables along 110°E, south-east Indian Ocean. *Deep-Sea Research Part II: Topical Studies in Oceanography*, *198*, 105053. https://doi.org/10.1016/j.dsr2.2022.105053

Olivar, M. P., Contreras, T., Hulley, P. A., Emelianov, M., López-Pérez, C., Tuset, V., & Castellón, A. (2018). Variation in the diel vertical distributions of larvae and transforming stages of oceanic fishes across the tropical and equatorial Atlantic. *Progress in Oceanography*, *160*, 83–100. https://doi.org/10.1016/j.pocean.2017.12.005

Pattrick, P., & Strydom, N. (2014a). Recruitment of fish larvae and juveniles into two estuarine nursery areas with evidence of ebb tide use. *Estuarine, Coastal and Shelf Science*, *149*, 120–132. https://doi.org/10.1016/j.ecss.2014.08.003

Pattrick, P., & Strydom, N. A. (2014b). Larval fish variability in response to oceanographic features in a nearshore nursery area. *Journal of Fish Biology*, *85*(3), 857–881. https://doi.org/10.1111/jfb.12477

Pattrick, P., Minguzzi, M., Weidberg, N., & Porri, F. (2022). Ecological value of the earliest human manipulated coastal habitats: Preliminary insights into the nursery function of a pre-colonial stonewalled fish trap in South Africa. *Regional Studies in Marine Science*, *52*, 102266. https://doi.org/10.1016/j.rsma.2022.102266

Pattrick, P., Weidberg, N., Goschen, W. S., Jackson, J. M., McQuaid, C. D., & Porri, F. (2021). Larval fish assemblage structure at coastal fronts and the influence of environmental variability. *Frontiers in Ecology and Evolution*, *9*, 684502. https://doi.org/10.3389/fevo.2021.684502

Picapedra, P. H. S., Lansac-Tôha, F. A., & Bialetzki, A. (2015). Diel vertical migration and spatial overlap between fish larvae and zooplankton in two tropical lakes, Brazil. *Brazilian Journal of Biology*, *75*(2), 352–361. https://doi.org/10.1590/1519-6984.13213

Picapedra, P. H. S., Sanches, P. V., & Lansac-Tôha, F. A. (2018). Effects of light-dark cycle on the spatial distribution and feeding activity of fish larvae of two co-occurring species (Pisces: Hypophthalmidae and Sciaenidae) in a Neotropical floodplain lake. *Brazilian Journal of Biology*, *78*(4), 763–772. https://doi.org/10.1590/1519-6984.179070

Pielou, E.C. (1966). The *measurement* of diversity in different types of biological collections. *Journal of Theoretical Biology*, *13*, 131-144.

Polte, P., Kotterba, P., Moll, D., & von Nordheim, L. (2017). Ontogenetic loops in habitat use highlight the importance of littoral habitats for early life-stages of oceanic fishes in temperate waters. *Scientific Reports*, *7*, 42709. https://doi.org/10.1038/srep42709

Ridho, M. R., Patriono, E., Sarno, S., & Wirda, S. (2020). Diversity of fish larvae around the estuary of the Banyuasin river, South Sumatera province. *BIOVALENTIA: Biological Research Journal*, *6*(2), 45-51. https://doi.org/10.24233/biov.6.2.2020.181

Shannon, C. E. (1948). A mathematical theory of communication. *The Bell System Technical Journal*, *27*, 379–423. https://doi.org/10.1145/584091.584093

Simpson, E. H. (1949). Measurement of diversity. *Nature*, *163*, 688. https://doi.org/10.1038/163688a0

Team, R. (2020). *RStudio: Integrated development for R*. http://www.rstudio.com/

Tiedemann, M., & Brehmer, P. (2017). Larval fish assemblages across an upwelling front: Indication for active and passive retention. *Estuarine, Coastal and Shelf Science*, *187*, 118–133. https://doi.org/10.1016/j.ecss.2016.12.015

Vorsatz, L. D., Pattrick, P., & Porri, F. (2021). Ecological scaling in mangroves: The role of microhabitats for the distribution of larval assemblages. *Estuarine, Coastal and Shelf Science*, *253*, 107318. https://doi.org/10.1016/j.ecss.2021.107318

Wang, Y.-C., Tsai, S.-C., & Chen, W.-Y. (2022). Diel vertical distribution patterns of pelagic fish larvae in Yilan Bay, Taiwan. *Journal of Marine Science and Technology*, *29*(6), 6. https://doi.org/10.51400/2709-6998.2557

Pertanika J. Trop. Agri. Sci. 46 (4): 1375 - 1390 (2023)

PERTANIKA JOURNALS

TROPICAL AGRICULTURAL SCIENCE

Journal homepage: http://www.pertanika.upm.edu.my/

Performance of Climbing Perch (*Anabas testudineus*) and Bok Choy (*Brassica chinensis*) in Aquaponics Systems Using Nutrient Film Technique in Indonesian Small-scale Livestock

Achmad Arif Syarifudin[1], Prayogo[1], Suciyono[1]*, Hapsari Kenconojati[1], Muhammad Browijoyo Santanumurti[2,3], Arafik Lamadi[4] and Ciptaning Weargo Jati[5]

[1]*Aquaculture Study Program, School of Health and Life Science, Universitas Airlangga, 68422 Banyuwangi, East Java, Indonesia*

[2]*Department of Aquaculture, Faculty of Fisheries and Marine, Universitas Airlangga, 60115 Surabaya, East Java, Indonesia*

[3]*Department of Marine Biology, Faculty of Marine Sciences King Abdulaziz University, 21589 Jeddah, Mekkah, Kingdom of Saudi Arabia*

[4]*Aquaculture Study Program, Faculty of Fisheries and Marine, Gorontalo University, 96128 Gorontalo, Indonesia*

[5]*Aquaculture Study Program, Faculty of Agriculture, Universitas Lampung, 35141, Lampung, Indonesia*

ABSTRACT

The Nutrient Film Technique (NFT) in aquaponics is a closed aquaculture system favored by Indonesian aquaculturists due to its environmental friendliness and can be applied on a small scale. Climbing perch (*Anabas testudineus*) has the potential to be cultured in this system as small-scale livestock. This research aims to determine the performance of the NFT aquaponics system of *Anabas testudineus* and *Brassica chinensis* with different stock densities. A completely randomized design within four stock density treatments and five replications was applied to this study. The results showed that the specific growth rate, survival rate, and feed conversion rate (FCR) of *A. testudineus* differed significantly across treatments ($p < 0.05$). The best performance of specific growth rate (1.96 ± 0.15%), FCR (1.31 ± 0.13), and survival rate (88 ± 4.69%) were shown in the second treatment (50 fish/tank). On the other hand, the fourth treatment (100 fish/tank) yielded the tallest *B. chinensis* at 20.7 ± 0.90 cm and a leaf number of 10.68 ± 0.28. Higher fish stocking density resulted in a slower fish

ARTICLE INFO

Article history:
Received: 29 March 2023
Accepted: 26 May 2023
Published: 27 November 2023

DOI: https://doi.org/10.47836/pjtas.46.4.19

E-mail addresses:
achmad.syarifudin@japfa.com (Achmad Arif Syarifudin)
prayogo@fpk.unair.ac.id (Prayogo)
suciyono@fpk.unair.ac.id (Suciyono)
hapsari@fpk.unair.ac.id (Hapsari Kenconojati)
m.browijoyo.s@fpk.unair.ac.id (Muhammad Browijoyo Santanumurti)
arafik_lamadi@ung.ac.id (Arafik Lamadi)
ciptaning.jati@fp.unila.ac.id (Ciptaning Weargo Jati)
*Corresponding author

ISSN: 1511-3701
e-ISSN: 2231-8542

growth rate but a faster plant growth rate. It can be concluded that the aquaponics system of NFT with a density of 50 fish/tank could be applied to small-scale livestock. The amount of organic matter that plant roots can use as nutrients is the factor that determines the growth rate of *B. chinensis*.

Keywords: Aquaponics, climbing perch, Nutrient Film Technique, stocking density

INTRODUCTION

Anabas testudineus is an economically important fish with high nutritional value in South and Southeast Asia, including Indonesia (Agustinus & Minggawati, 2020; Ahmadi et al., 2021; Khatun et al., 2019). In Indonesia, this fish is the main ingredient for processing local typical food on Borneo island, where the total demand in 2017 was more than six thousand tons (Lemae & Lasmi, 2019). The increasing demand causes the availability of this fish at consumption size to decrease (Hidayat et al., 2016). The climbing perch can be cultured in closed system cultivation, although Indonesian farmers still rarely cultivate this species. In conventional aquaculture, *A. testudineus* has slow growth (Ahmed et al., 2015; Kohinoor et al., 2009) due to several factors, including sex, genetics, age, water quality, stocking density, and feeding type (Ahmed et al., 2015; Susila, 2016). Technically, a closed system culture is more environmentally friendly, especially due to the minimized use of water, land, and total organic matter wasted on the environment (Hu et al., 2015; Nuryadi et al., 2009).

Aquaponics is combined aquaculture and hydroponics in a single system (Anantharaja et al., 2017; Resh, 2022), it can maintain water balance by the plants (Ebeling & Timmons, 2012; Hu et al., 2015), continuously reduce the waste produced by fish through low-level organisms. However, low dissolved oxygen (DO) hindered closed systems such as aquaponics. Hence, only certain species could survive (Uddin et al., 2016). This system allows for cultivating *A. testudineus* fish with low or medium stocking densities (Kohinoor et al., 2007; Uddin et al., 2016). *Anabas testudineus* has an extra organ (labyrinth) that allows them to live in low DO levels of 0.12–3.80 mg/L (Akbar et al., 2016; Maidie et al., 2015).

However, water quality, including DO, affects fish's survival and growth (Putra et al., 2016). Increased stocking density is a profitable method of intensifying cultivation. However, information about the cultivation of this fish in aquaponics systems with high stocking densities is still lacking. This research cultured *A. testudineus* in a closed system with different stocking densities to determine the best growth rate, survival rate, and feed efficiency due to a lack of information on the subject. Research related to *A. testudineus* in aquaponics systems has been reported by combining it with other plants such as malabar spinach (*Basella alba*) or cum spinach (*Spinacia oleracea*) (Anantharaja et al., 2017; Subhasmita et al., 2021).

However, the aquaponic combination between *A. testudineus* and bok choy (*Brassica chinensis*) has not been reported.

Bok choy, or Chinese cabbage, is a plant with high demand for consumption and good nutritional content (Wu et al., 2019). The use of *B. chinensis* in aquaponics has been widely practiced, such as tilapia or bonylip barb fish, because these plants do not need large spaces for cultivation (Albani et al., 2023; Hadiroseyani et al., 2023). This research is expected to be able to determine the performance of climbing perch (*A. testudineus*) and bok choy (*B. chinensis*) in aquaponics systems using NFT in Indonesian small-scale livestock. NFT is an aquaponic system that continuously flows water over the plant's root from the fish tank (Setiawan, 2018). NFT is used in this study for its benefits, such as being widely used, uniform nutrient concentration, faster plant growth, and adequate water supply (Wibisono & Kristyawan, 2021). Furthermore, correlations between fish production parameters and water quality, as well as plant growth, were investigated.

MATERIALS AND METHODS

Time and Place

This research was carried out in a small-scale closed system rearing tank at Airlangga University, Banyuwangi Campus, East Java, from February to April 2021 and was conducted in accordance with Law No. 18 of 2002 on the National System for Research, Development, and Application of Science and Technology of the Republic of Indonesia. The research was conducted with the approval of the School of Health and Life Sciences, Universitas Airlangga (Letter of Assignment from the Academic Vice Director of the School of Health and Life Sciences, Universitas Airlangga, 193/UN3.1.16/KP/2021).

Fish Origin and Husbandry

Approximately 1,250 *A. testudineus* seeds with an average weight of 3.13 ± 0.09 g from fish farmers in Demak, Central Java, Indonesia, were used in this study. The biomass was maintained for sixty days in plastic buckets (water volume 70 L). The temperature of the water and DO was maintained between 24.7–28.9°C and 4.12–5.25 mg/L. At the same time, the pH parameters ranged from 7.2 to 7.4. Commercial fish feed (PF 1000™, Prima Feed, Indonesia) was used during rearing (Table 1).

Table 1
The commercial fish feed content in this study

Content	Percentage (%)
Protein	39
Fat	5
Fiber	6
Ash	12
Water	10

Note. Size = 1.3-1.7 mm

Research Design

A completely randomized design (CRD) was used to treat differences in stocking density. Four treatments and five replications were performed, where the first treatment (T1) was filled with 25 seeds stocking density, the second treatment (T2) had 50 seeds, the third (T3), and the fourth treatment (T4) had

75 and 100 seeds, respectively. A bucket with 50 L of water volume was used as the cultivation medium.

Preparation of Nutrient Film Technique

A total of 20 buckets were perforated on the sides to keep the water level constant, and then 10 net pots with a hanging model were assembled in a plastic bucket using a wire in a circle, and the net pot was filled with activated charcoal and rockwool. Following washing and drying, each container was filled with 50 L of water, and *Nitrobacter*, as a probiotic (Nitro-Bac, Indonesia), with a density of 2 x 10^{14} as much as 0.01 ppm was added (Beauty et al., 2012). Furthermore, up to 50% of the net pot is filled with charcoal and rockwool. Activated charcoal is added to absorb dissolved gases, heavy metals, and odors in the water. The aquaponic system used in this study was the NFT system since the water continuously flowed over the roots of *B. chinensis* (Figure 1). NFT is an aquaponic system that continuously flows water over the plant's root from the fish tank (Setiawan, 2018).

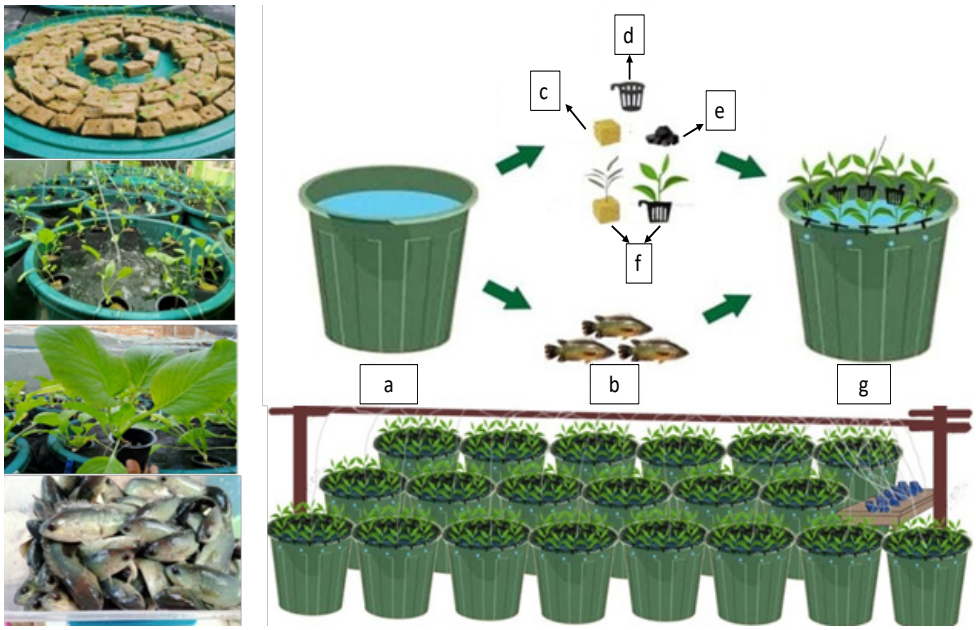

Figure 1. Site of close system aquaponics: a = floating aquaponics design; b = fish of *Anabas testudineus*; c = rockwool media; d = net pot as rockwool media; e = charcoal; f = combination of the rockwool and charcoal in the net pot for *Brassica chinensis* installation; g = establishment of the aquaponic system

Animal and Plant Preparation

Before being stocked in each tank, the fish were acclimatized for physiological adjustments to the new environment. Meanwhile, the *B. chinensis* seeds (Garuda Seed, Indonesia) were grown on wet

rockwool media perforated with water and kept in a closed container until germinated. After germinating, the seed was sowed in direct sunlight for 1–2 weeks to allow roots to develop before being transferred to a net pot when it has four leaves.

Fish Observation Parameters

The fish observation parameters were survival rate, feed conversion rate (FCR), and specific growth rate determined using the formula according to Uddin et al. (2016). The fish's weight is determined using a scale (CAS MWP 300). The formulas were followed:

$$\text{Survival rate (\%)} = \frac{\text{Initial number of fish} - \text{Final number of fish}}{\text{Initial number of fish}} \times 100\%$$

$$\text{Feed conversion rate (FCR)} = \frac{\text{Feed fed (g)}}{\text{Fish weight gain}}$$

$$\text{Specific growth rate (\%)} = \frac{\text{Final weight} - \text{Initial weight}}{\text{Day(s) of culture}} \times 100\%$$

Plant Observation and Water Quality

Water quality parameters such as pH (AMTAST EC910, USA) and temperature (AMTAST EC910, USA) were checked daily in this study, while ammonia (NH_3), nitrite (NO_2^-), and nitrate (NO_3^-) (Hitachi, Japan), as well as DO (AMTAST EC910, USA) were checked once per week. Furthermore, the *B. chinensis*'s growth was calculated based on the number of leaves that grew, and the growth rate of stem height was measured with a vernier caliper (Kenmaster, Indonesia) with an accuracy of 0.05 mm.

Data Analysis

Duncan's multiple range test (DMRT) and analysis of variance (ANOVA) were used to determine the significant differences between each treatment in production parameters, such as survival rate and growth rate, as well as feed consumption rate. A level of significance of 0.05 was used to compare the differences between treatments. Principal component analysis (PCA) was used to correlate a water quality parameter and a specific growth rate of fish and plants. In addition, the results of the water quality and production parameters were used to determine the similarity of each treatment using clustering analysis.

RESULTS AND DISCUSSION

Specific Growth Rate

The result of the specific growth rate showed *A. testudineus* with different values (Table 2). The weekly growth rate is in Figure 2, with a boxplot of the initial and final length of *A. testudineus*. The first treatment (T1) differed significantly ($p < 0.05$) from the second (T2) and the third (T3). However, T1 was not significantly different ($p > 0.05$) from the fourth treatment (T4). The specific growth rate is the percentage of regular body weight in individuals (Hossain et al., 2012). The parameter was affected by the rate at which organisms consume and convert food into energy. Furthermore, space competition and DO were the limiting factors inhibiting growth (Anantharaja et al., 2017; Hossain et al., 2012; Khatune-Jannat et al., 2012). In this study, the specific growth rate of

A. testudineus was found to be inversely proportional to solid density. T1 had the lowest specific growth rates with 1.35% or 0.06 g/ind/day. These results are the same as the growth rate carried out by Hanafie (2020), 1.14 g/ind/day in a bioflock system with a stocking density of 1 fish/L.

However, in this study, the best specific growth rate is greater than that of Agustinus and Minggawati (2020), as well as Hidayat et al. (2016), with respective values of 1.13, 1.8, and 1.72%. T2 had the highest (1.96%, or 0.12 g/ind/day). The specific growth rate of *A. testudineus* is quite low since it has a negative allometric growth pattern, where length increases faster than body weight (Kumar et al., 2013). Nonetheless, the best results of this study were lower than the best treatment in Uddin's (2016) study of 2.52%. Furthermore, the high stocking density impacts the amount of feed provided (Lemae & Lasmi, 2019), resulting in high metabolic waste and organic content (Hossain et al., 2012). Fishes could absorb only about 25% of the feed, with the remaining 75% wasted in the water (Akbar et al., 2016). Feed waste mineralized by bacteria into NH_3 is toxic to the environment's waters (Gichana et al., 2018; Nuryadi et al., 2009). In high concentrations, NH_3 can damage gill tissue and reduce appetite (Liew et al., 2013). As a result, most energy is spent on adaptation rather than growth.

Table 2
The growth (mean±standard deviation), feed conversion rate (FCR), and survival rate of Anabas testudineus *over eight weeks in a Nutrient Film Technique aquaponics system using* Brassica chinensis

Parameters	Unit	Treatment 1	Treatment 2	Treatment 3	Treatment 4
Initial weight	g/ind	3.04 ± 0.05	3.27 ± 0.09	3.19 ± 0.04	3.13 ± 0.07
Final weight	g/ind	5.30 ± 0.07	7.03 ± 0.12	6.31 ± 0.06	5.73 ± 0.05
Initial biomass	g	76.04 ± 1.17	163.30 ± 4.60	238.95 ± 2.68	313.20 ± 6.65
Final biomass	g	171.51 ± 8.91	528.04 ± 42.94	693.54 ± 35.69	744.14 ± 78.13
Specific growth rate	%	1.35 ± 0.105^{a}	1.96 ± 0.15^{b}	1.77 ± 0.09^{b}	1.44 ± 0.17^{a}
Survival rate	%	86.40 ± 4.56^{b}	88.00 ± 4.69^{b}	84.60 ± 4.38^{ab}	78.40 ± 5.85^{a}
FCR	-	1.77 ± 0.09^{a}	1.31 ± 0.13^{c}	1.63 ± 0.09^{ab}	1.54 ± 0.16^{b}
Final feed consumption	g	202.97 ± 18.37	513.56 ± 24.88	735.69 ± 19.62	850.95 ± 48.34

Note. Treatments 1-4 = 25, 50, 75, and 100 fish/50 L with a rearing period of 60 days, respectively. Different superscripts in the same column show that there are significant differences ($p < 0.05$)

Survival Rate

There is no significant difference ($p > 0.05$) between the first (T1) and second (T2) treatments (Table 2). Meanwhile, the third (T3) and fourth (T4) treatments differ significantly. T2 had the highest survival rate, followed by T3, T1, and T4. Decreasing water quality, stress, and disease are all factors that affect survival rates (Hu et al., 2015). The survival rate date indicated the

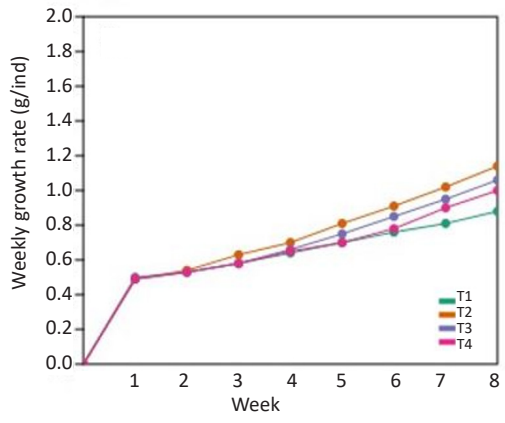

(a)

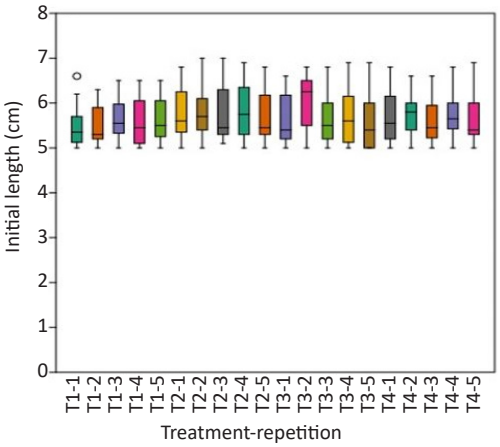

(b)

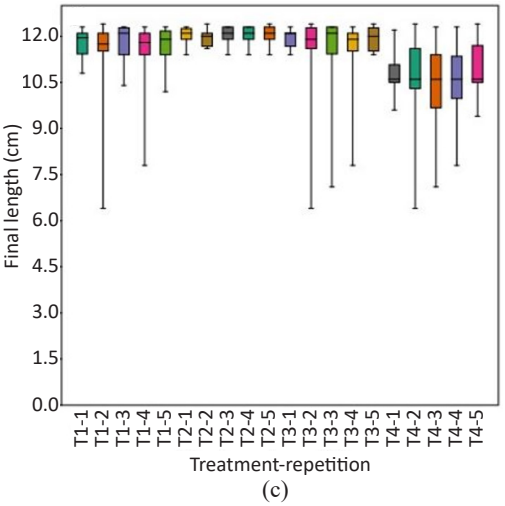

(c)

Figure 2. (a) The specific growth rate of *Anabas testudineus*, (b) box plot of the initial length of *A. testudineus*, and (c) box plot of the final length of *A. testudineus*

Note. Different colors in figures b and c are intended to make it easier to read the data. There were 5 biological replicates for 1 treatment. T1–T4 (Treatments 1-4) = 25, 50, 75, and 100 fish/50 L with a rearing period of 60 days, respectively

viability and tolerance of the fish. This study had the highest survival rate of 88%, higher than the research by Uddin (2016) with 83.33%. This result also showed that NFT aquaponics with *B. chinensis* for *A. testudineus* will increase the survival rate because the previous research was carried out in a cage of a lake while this research was carried out with NFT aquaponics.

NFT aquaponics has the advantage of maintaining water balance and continuously reducing the waste produced by fish through low levels (Ebeling & Timmons, 2012; Hu et al., 2015). Aquaponic also has the advantage of being done in a narrow room and is not easily affected by environmental conditions such as rivers (closed system) (Krastanova et al., 2022). As with all treatments, the highest mortality rate occurred in the second week. It was caused by the increased amount of feed given, as well as the fact that *B. chinensis*' nitrification and filtration processes were not optimal. These findings indicated that each organism has a certain level of tolerance for changes in water quality (Zhang et al., 2019). A concentration of NH_3 greater than 3 ppm is toxic and causes mass death (Akbar et al., 2016; Zhang et al., 2019). However, the subsequent week's improvement in water quality was consistent with forming an ecosystem in the aquaponics system because roots are a medium for developing

nitrifying bacteria, and increasing plant size and number of roots can maximize NO_3^- absorption in water (Gichana et al., 2018; Mantelin & Touraine, 2004).

Feed Conversion Rate (FCR)

Table 2 shows that stocking density was not the only factor that had the most influence on the FCR value, where the best value (T2) is 1.31, followed by T4 and T3. On the other hand, the lowest stocking density (T1) resulted in the lowest FCR, affected by the way *A. testudineus* scavenges for food in groups (Zworykin, 2018). However, the value of the FCR in this study was classified as good for the *Anabas* genus, where the value was still better than that of Akbar et al. (2016) and Kohinoor et al. (2013), with the best FCR of 1.81 and 3.2, respectively. Controlled water quality through plant absorption improves fish appetite. Thus, the aquaponics system also increases the fish growth rate, fresh weight, and feed conversion efficiency (Yang & Kim, 2020).

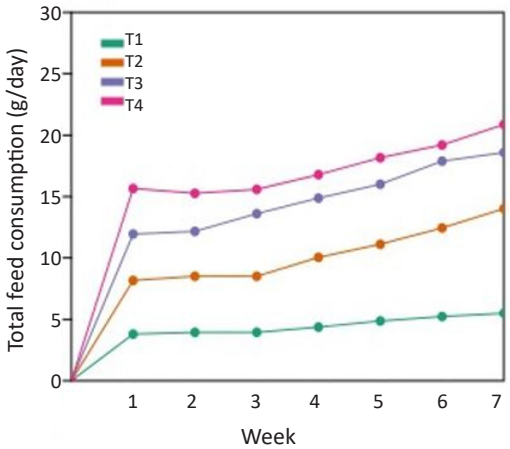

Figure 3. The daily feed consumption per week
Note. T1–T4 (Treatments 1–4) = 25, 50, 75, and 100 fish/50 L with a rearing period of 60 days, respectively

The daily feed consumption per week is shown in Figure 3.

Water Quality Parameters

Table 3 shows that the temperature, pH, DO, NH_3, NO_2^-, and NO_3 influence water quality parameters in cultivating *A. testudineus* and *B. chinensis* in the NFT aquaponic system. The average value of water quality parameters is still appropriate for the growth of *A. testudineus*. However, the parameters NH_3, NO_2^-, and NO_3^- had values that exceeded the quality standard at periods. The metabolism of fish and feed residues causes this condition. Water quality plays an important role in aquaculture because water is a living medium for fish (Gichana et al., 2018). The results of temperature measurements in this study ranged from 27.41 to 27.60°C. This temperature is classified as suitable for the life of *A. testudineus* since temperatures <25°C can reduce fish appetite (Rahmadi et al., 2021; Zworykin, 2018). On the contrary, if the temperature is too high, it will cause the water to become denser, which reduces DO. Furthermore, the oxygen solubility in this study ranged from 4.78 to 5.30 ppm. DO is important in overhauling organic matter (bacteria) and fish respiration (Riedel et al., 2013). The oxygen level is still within the tolerance limits of *A. testudineus* (Akbar et al., 2016). DO solubility < 4 ppm can cause a decrease in appetite and the development of anaerobic bacteria (Mahasri et al., 2018).

On the other hand, the pH measurement in this study was 7.28–7.31. This value is within the optimal limit for the growth of *A.*

Table 3
Results of measuring the water quality during sixty days of culture in a Nutrient Film Technique aquaponics system

Parameters	Unit	Treatment 1	Treatment 2	Treatment 3	Treatment 4
Temperature	°C	27.41 ± 0.14	27.60 ± 0.23	27.58 ± 0.18	27.50 ± 0.17
pH		7.28 ± 1.56	7.28 ± 1.56	7.28 ± 1.54	7.31 ± 1.88
Dissolved oxygen	mg/L	5.30 ± 0.52	4.90 ± 0.62	4.83 ± 0.51	4.78 ± 0.48
Ammonia	mg/L	0.06 ± 0.02	0.05 ± 0.02	0.08 ± 0.02	0.09 ± 0.03
Nitrite	mg/L	0.04 ± 0.01	0.04 ± 0.02	0.05 ± 0.01	0.06 ± 0.01
Nitrate	mg/L	6.07 ± 1.41	7.01 ± 1.29	5.63 ± 0.61	4.96 ± 0.76

Note. Treatments 1–4 = 25, 50, 75, and 100 fish/50 L with a rearing period of 60 days, respectively

testudineus (Akbar et al., 2016). Increasing the pH value affects the performance of nitrifying bacteria, causing high NH_3 and NO_2^- values, which are harmful to fish (Hu et al., 2015; Khatune-Jannat et al., 2012). The pH value affects the development and growth of aerobic nitrification bacteria (Anantharaja et al., 2017), whereas probiotic bacteria are agents of decomposing organic matter in water. The accumulation of feed that is not utilized must be able to be decomposed by nitrifying bacteria so that it does not become toxic compounds (NH_3). NH_3 in water is toxic because the ion is uncharged and soluble in fat, so it can easily enter biological membranes, and the threshold limit in aquaculture waters ranges from <0.1 ppm (Liew et al., 2013). Meanwhile, NH_3 concentration in this study ranged from 0.05 to 0.09 ppm, which is still within range. In some fish species, NH_3 concentration >0.07 ppm can damage fish tissue and cause death.

However, the limiting value for NH_3 toxicity depends on the species, size, metal, and active compound (Liew et al., 2013). The research found that the highest NH_3 concentration value was in the second week. It was suspected that the role of bok choy in absorbing NH_3 was not optimal (Wu et al., 2019). Furthermore, the measurement of NO_2^- concentration in the study was 0.04–0.06 ppm. NO_2^- is the result of the oxidation of NH_3 in the NO_2^- stage carried out by *Nitrosomonas* bacteria (Vadivelu et al., 2007). This value is still within the threshold for *A. testudineus* cultivation. NO_2^- concentration increased in the second week because of the low water temperature and the minimal development of NO_3^- microbial populations (Maidie et al., 2015). Furthermore, the concentration of NO_3^- in this study was 4.96–7.01 ppm. Based on the Indonesian Government Regulation No. 82/2001, this value is classified as safe for fish aquaculture activities (Tallar & Suen, 2016). NO_3 concentrations that exceed the threshold cause eutrophication and stimulate phytoplankton blooms.

Growth of *B. chinensis*

The growth rate of *B. chinensis* showed a significant difference ($p < 0.05$) between the T4 with T1, T2, and T3 (Table 4). On the other hand, there was no significant difference between the three treatments (T1, T2, and T3). The best *B. chinensis* plant height was found in the T4 with 20.7 ± 0.90 cm and the lowest in T1 with a value of 19.18 ± 0.25 cm. The leaf amount also showed a significant difference ($p < 0.05$). There was not a significant difference in T4 (10.68 ± 0.28) with T3 (10.26 ± 0.43), but significantly different with T1 (9.12 ± 0.15) and T2 (10.16 ± 0.32). The best number of *B. chinensis* plants was found in the T4; the lowest was T1. This result indicated that higher fish density would decrease the fish growth but increase the plant growth in aquaponics. It can be caused by a variety of factors, such as poor seedlings, the lack of light, nutrient availability, and pests (Harahap et al., 2020; Nuryadi et al., 2009; Wang et al., 2022). Nutrient availability is the key factor since higher fish density will increase the nutrients in the water from the feces, fish excreta, or uneaten feed (Bao et al., 2019). The effect of low stocking densities results in organic matter that is not optimal for *B. chinensis* as nutrients (Silva et al., 2017). *Brassica chinensis* is an oriental vegetable that grows well in tropical regions. Its local market price is higher, and it has a fibrous taproot that can reach 3–5 cm (Silva et al., 2017). *Brassica chinensis*' growth rate (Figure 4) is influenced by nutrient availability in water and absorption ability (Harahap et al., 2020; Wang et al., 2022).

Table 4
Measurement of the growth (mean standard deviation) of stem height and number of leaves from Brassica chinensis *during sixty days of culture in a Nutrient Film Technique aquaponics system*

Parameters	Unit	Treatment 1	Treatment 2	Treatment 3	Treatment 4
Initial stem height	cm	4.12 ± 0.11	4.38 ± 0.11	4.22 ± 0.19	4.22 ± 0.08
Final stem height	cm	19.18 ± 0.20^{a}	19.22 ± 0.05^{a}	19.40 ± 1.18^{a}	20.74 ± 0.90^{b}
Initial number	leaf	3.54 ± 0.09	3.86 ± 0.05	3.72 ± 0.10	3.7 ± 0.14
Final number	leaf	9.12 ± 0.15^{a}	10.16 ± 0.32^{b}	10.26 ± 0.43^{c}	10.68 ± 0.28^{c}

Note. Treatments 1-4 = 25, 50, 75, and 100 fish/50 L with a rearing period of 60 days, respectively. Different superscript letters denote statistically significant treatment differences ($p < 0.05$). Only the final results were examined by statistic

This study found a correlation between water quality parameters and a specific growth rate of fish and plants. PCA presents the relationship of water quality in Figure 5a. The data showed that DO, NH_3, and NO_2^- affect the performance of *A. testudineus* while temperature and NO_3^- affect the growth of *B. chinensis*. DO is an important element for growth because oxygen plays a role in respiration and metabolic processes in fish (Little et al., 2020). When the DO concentration decreased, respiration and

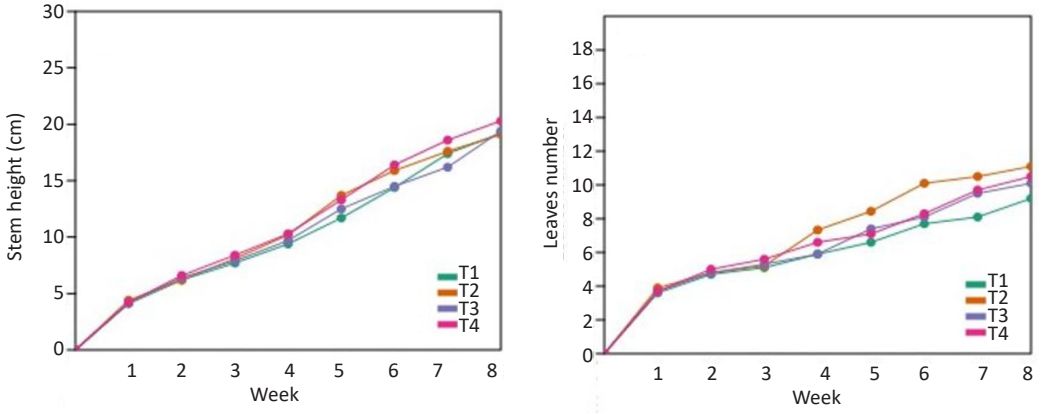

(a) (b)

Figure 4. (a) The growth of stem (cm) from weekly sampling during eight weeks, (b) The growth of leaf from weekly sampling during eight weeks

Note. T1–T4 (Treatments 1–4) = 25, 50, 75, and 100 fish/50 L with a rearing period of 60 days, respectively

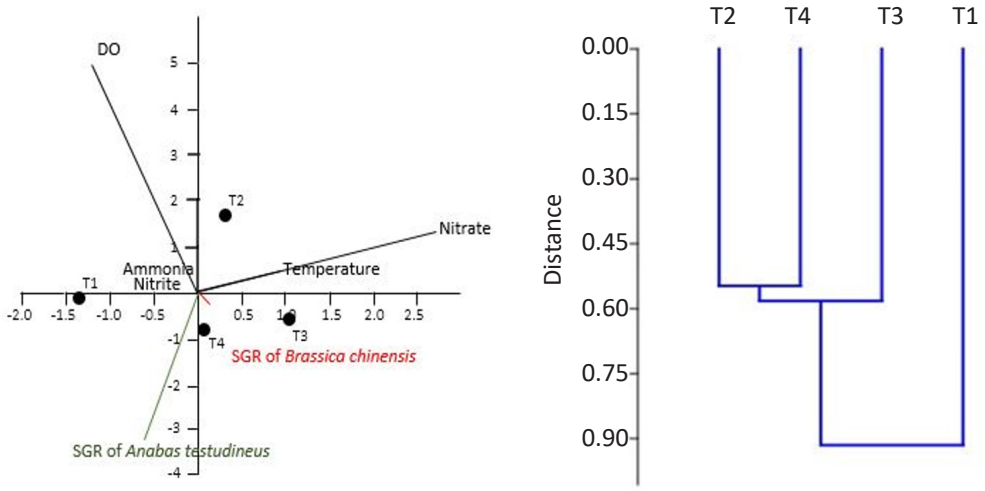

(a) (b)

Figure 5. (a) Scatter plot correlation between water quality by principal component analysis; (b) Clustering treatment

Note. SGR = Specific growth rate; T1–T4 (Treatments 1–4) = 25, 50, 75, and 100 fish/50 L with a rearing period of 60 days, respectively

feeding activity also decreased. It causes the growth rate to decrease, and the possibility of disease attacks increases. NH_3 can also affect fish growth because it can cause stress for fish in the waters. When stressed, fish will use the nutrients in their bodies to survive, so their growth is not optimal (Xu et al., 2021). NO_2^- can reduce growth by increasing methemoglobin formation, disrupting osmoregulation, and changing normal physiology (Ciji & Akhtar, 2020). Temperature can affect the plant since high temperatures cause heat stress and slow growth (Hinojosa et al., 2019). NO_3

has a role as a signal molecule for plant metabolism, physiology, growth, and development (Vega et al., 2019).

The results of the water quality and production parameters were used to determine the similarity of each treatment using clustering analysis (Figure 5b). The results showed that T2 and T4 were the best results. However, the growth of *B. chinensis* was not the highest for 50 fish/tank, while the growth of *A. testudineus* was not the highest for 100 fish/tank. Higher fish stocking density resulted in a slower fish growth rate but a faster plant growth rate. Nutrient availability is the key factor since higher fish density will increase the nutrients in the water from the feces, fish excreta, or uneaten feed (Bao et al., 2019). The effect of low stocking densities results in organic matter that is not optimal for *B. chinensis* as nutrients (Silva et al., 2017).

CONCLUSION

Stocking density influenced the growth rate, FCR, and survival rate of *A. testudineus* and *B. chinenses* cultured in closed aquaponics. The treatment with a stocking density of 50 and 100 fish/tank showed the best results. However, the growth of *B. chinensis* was not the highest for 50 fish/tank, while the growth of *A. testudineus* was not the highest for 100 fish/tank. Higher fish stocking density resulted in a slower fish growth rate but a faster plant growth rate. Higher fish stocking density indicated more organic matter. The amount of organic matter absorbed by plant roots is the factor of *B. chinensis's* growth speed.

ACKNOWLEDGEMENTS

The authors express their gratitude to the School of Health and Life Science (SIKIA), Universitas Airlangga, Indonesia as the funder of our research with the grand number of Keputusan Rektor No. 477/UN3/2021. The authors also express gratitude to King Abdulaziz University, Saudi Arabia; Gorontalo State University and Lampung University, Indonesia for the collaboration and access to finish this research.

REFERENCES

Agustinus, F., & Minggawati, I. (2020). Pertumbuhan ikan betok (*Anabas Testudineus*) yang dipelihara menggunakan hapa di kolam tanah [Growth of climbing perch (*Anabas testudineus*) reared using hapa in earthen ponds]. *Jurnal Ilmu Hewani Tropika*, *8*(2), 89-92.

Ahmadi, A., Lilimantik, E., & Mahreda, E. S. (2021). Marketing efficiency of the climbing perch (*Anabas testudineus*) cultured with bioflock system. *Egyptian Journal of Aquatic Biology and Fisheries*, *25*(2), 561-572. https://doi.org/10.21608/EJABF.2021.165912

Ahmed, G. U., Rahman, M. M., Alam, M. N., Alam, M. B., & Sarker, B. (2015). Impact of stocking density on growth and production performance of Vietnamese koi (*Anabas testudineus*) in semi-intensive culture system at Muktaghasa region of Mymensingh district. *Research in Agriculture Livestock and Fisheries*, *2*(2), 335-341. https://doi.org/10.3329/ralf.v2i2.25019

Akbar, J., Mangalik, A., & Fran, S. (2016). Application of fermented aquatic weeds in formulated diet of climbing perch (*Anabas testudineus*). *International Journal of Engineering Research and Science*, *2*(5), 240-243.

Albani, R. I., Budiardi, T., Hadiroseyani, Y., & Ekasari, J. (2023). The production performance

of Nile tilapia *Oreochromis niloticus* and mineral balance in aquaponic, biofloc, and aquabioponic culture systems. *Jurnal Akuakultur Indonesia*, *22*(1), 66-79. https://doi.org/10.19027/jai.22.1.66-79

Anantharaja, K., Mohapatra, B. C., Pillai, B. R., Kumar, R., Devaraj, C., & Majhi, D. (2017). Growth and survival of climbing perch, *Anabas testudineus* in Nutrient Film Technique (NFT) aquaponics system. *International Journal of Fisheries and Aquatic Studies*, *5*(4), 24-29.

Bao, W., Zhu, S., Jin, G., & Ye, Z. (2019). Generation, characterization, perniciousness, removal and reutilization of solids in aquaculture water: A review from the whole process perspective. *Reviews in Aquaculture*, *11*(4), 1342-1366. https://doi.org/10.1111/raq.12296

Beauty, G., Yustiati, A., & Grandiosa, R. (2012). Pengaruh dosis mikroorganisme probiotik pada media pemeliharaan terhadap kelangsungan hidup dan pertumbuhan benih mas koki (*Carassius auratus*) dengan padat penebaran berbeda [The effect of the dose of probiotic microorganisms on maintenance media on the survival and growth of goldfish (*Carassius auratus*) with different stocking densities]. *Jurnal Perikanan Kelautan*, *3*(3), 1-6.

Ciji, A., & Akhtar, M. S. (2020). Nitrite implications and its management strategies in aquaculture: A review. *Reviews in Aquaculture*, *12*(2), 878-908. https://doi.org/10.1111/raq.12354

Ebeling, J. M., & Timmons, M. B. (2012). Recirculating aquaculture systems. *Aquaculture production systems*, 245-277. In J. H. Tidwell (Ed.), *Aquacultrue production system* (pp. 245-277). Wiley-Blackwell. https://doi.org/10.1002/9781118250105.ch11

Gichana, Z. M., Liti D., Waidbacher, H., Zollitsch, W., Drexler, S., & Waikibia, J. (2018). Waste management in recirculating aquaculture system through bacteria dissimilation and plant assimilation. *Aquaculture International*, *26*, 1541-1572. https://doi.org/10.1007/s10499-018-0303-x

Hadiroseyani, Y., Diatin, I., Faozar, M. F., & Vinasyiam, A. (2023). Nursery of bonylip barb fish *Osteochilus hasselti* in an aquaponics system. *Jurnal Akuakultur Indonesia*, *22*(1), 55-65. https://doi.org/10.19027/jai.22.1.55-65

Hanafie, A. (2020). Laju pertumbuhan ikan papuyu (*Anabas testudineus* Bloch) sistem bioflok dengan sumber probiotik yang berbeda [Growth rate of papuyu fish (*Anabas testudineus* Bloch) biofloc system with different probiotic sources]. *Prosiding Seminar Nasional Lingkungan Lahan Basah*, *5*(2), 104-112.

Harahap, M. A., Harahap, F., & Gultom, T. (2020). The effect of Ab mix nutrient on growth and yield of pak choi (*Brassica chinensis* L.) plants under hydroponic wick system condition. In *Journal of Physics: Conference Series* (Vol. 1485, No. 1, p. 012028). IOP Publishing. https://doi.org/10.1088/1742-6596/1485/1/012028

Hidayat, R., Carman, O., & Alimuddin. (2016). Sexual dimorphism related to growth in climbing perch *Anabas testudineus*. *Jurnal Akuakultur Indonesia*, *15*(1), 8-14. https://doi.org/10.19027/jai.15.8-14

Hinojosa, L., Matanguihan, J. B., & Murphy, K. M. (2019). Effect of high temperature on pollen morphology, plant growth and seed yield in quinoa (*Chenopodium quinoa* Willd.). *Journal of Agronomy and Crop Science*, *205*(1), 33-45. https://doi.org/10.1111/jac.12302

Hossain, M. A., Sultana, Z., Kibria, A. S. M., & Azimuddin, K. M. (2012). Optimum dietary protein requirement of a Thai strain of climbing perch, *Anabas testudineus* (Bloch, 1792) fry. *Turkish Journal of Fisheries and Aquatic Sciences*, *12*(2), 217-224. https://doi.org/10.4194/1303-2712-v12_2_04

Hu, Z., Lee, J. W., Chandran, K., Kim, S., Brotto, A. C., & Khanal, S. K. (2015). Effect of plant species on nitrogen recovery in aquaponics. *Bioresource Technology*, *188*, 92-98. https://doi.org/10.1016/j.biortech.2015.01.013

Khatun, D., Hossain, M. Y., Rahman, M. A., Islam, M. A., Rahman, O., Abul, M., Azad, M. A. K., Sarmin, M. S., Parvin, M. F., Tausif, A., Haque, A. T. U., Mawa, Z., & Hossain, M. A. (2019). Life-history traits of the climbing perch *Anabas testudineus* (Bloch, 1792) in a wetland ecosystem. *Jordan Journal of Biological Sciences*, *12*(2), 175-182.

Khatune-Jannat, M., Rahman, M. M., Bashar, M. A., Hasan, M. N., Ahamed, F. & Hossain, M. Y. (2012). Effects of stocking density on survival, growth and production of Thai climbing perch (*Anabas testudineus*) under fed ponds. *Sains Malaysiana*, *41*(10), 1205-1210.

Kohinoor, A. H. M., Islam, A. K. M. S., Jahan, D. A., Zaher, M., & Hussain, M. G. (2007). Monoculture of climbing perch, Thai koi, *Anabas testudineus* (Bloch) under different stocking densities at on-farm. *Bangladesh Journal of Fisheries Research*, *11*(2), 173–180.

Kohinoor, A. H. M., Islam, M. S., Jahan, D. A., Khan, M. M., & Hussain, M. G. (2013). Growth and production performances of crossbred climbing perch koi, *Anabas testudineus* in Bangladesh. *International Journal of Agricultural Research, Innovation and Technology*, *2*(1),19-25. https://doi.org/10.3329/ijarit.v2i1.13990

Kohinoor, A. H. M., Jahan, D. A., Khan, M. M., Ahmed, S. U., & Hussain, M. G. (2009). Culture potentials of climbing perch, *Anabas testudineus* (Bloch) under different stocking densities at semi-intensive management. *Bangladesh Journal of Fisheries Research*, *13*(2), 115-120.

Krastanova, M., Sirakov, I., Ivanova-Kirilova, S., Yarkov, D., & Orozova, P. (2022). Aquaponic systems: Biological and technological parameters. *Biotechnology and Biotechnological Equipment*, *36*(1), 305-316. https://doi.org/10.1080/13102818.2022.2074892

Kumar, K., Lalrinsanga, P. L., Sahoo, M., Mohanty, U. L., Kumar, R., & Sahu, A. K. (2013). Length-weight relationship and condition factor of *Anabas testudineus* and *Channa* species under different culture systems. *World Journal of Fish and Marine Sciences*, *5*(1), 74-78. https://doi.org/10.5829/idosi.wjfms.2013.05.01.64201

Lemae., & Lasmi, L. (2019). Studi pengaruh kemunduran mutu terhadap kandungan gizi ikan Betok (*Anabas testudineus*) dari daerah Mandor [Study of the effect of quality deterioration on the nutritional content of climbing perch (*Anabas testudineus*) from the Mandor area]. *Jurnal Ilmu Perikanan*, *8*(1), 20-26. https://doi.org/10.26618/octopus.v8i1.2491

Liew, H. J., Sinha, A. K., Nawata, C. M., Blust, R., Wood, C. M., & De Boeck, G. (2013). Differential responses in ammonia excretion, sodium fluxes and gill permeability explain different sensitivities to acute high environmental ammonia in three freshwater teleosts. *Aquatic Toxicology*, *126*, 63-76. https://doi.org/10.1016/j.aquatox.2012.10.012

Little, A. G., Loughland, I., & Seebacher, F. (2020). What do warming waters mean for fish physiology and fisheries? *Journal of Fish Biology*, *97*(2), 328-340. https://doi.org/10.1111/jfb.14402

Mahasri, G., Saskia, A., Apandi, P. S., Dewi, N. N., & Usuman, N. M. (2018). Development of an aquaculture system using nanobubble technology for the optimation of dissolved oxygen in culture media for nile tilapia (*Oreochromis niloticus*). In *IOP Conference Series: Earth and Environmental Science* (Vol. 137, No. 1, p. 012046). IOP Publishing. https://doi.org/10.1088/1755-1315/137/1/012046

Maidie, A., Sumoharjo., Asra, S. W., Ramadhan, M., & Hidayanto, D. N. (2015). Pengembangan pembenihan ikan betok (*Anabas testudineus*) untuk skala rumah tangga [Development of climbing perch (*Anabas testudineus*) breeding for household scale]. *Media Akuakultur*, *10*(1), 31-37. https:/doi.org/10.15578/ma.10.1.2015.31-37

Mantelin, S., & Touraine, B. (2004). Plant growth-promoting bacteria and nitrate availability: Impacts on root development and nitrate uptake. *Journal of Experimental Botany*, *55*(394), 27-34. https://doi.org/10.1093/jxb/erh010

Nuryadi., Sutrisno., & Puspaningsih, D. (2009). Fitoremediasi kolam pemeliharaan ikan dengan memanfaatkan sayuran [Phytoremediation of fish rearing ponds using vegetables]. *Media Akuakultur*, *4*(1), 50-53. https://doi.org/10.15578/ma.4.1.2009.50-53

Putra, D. F., Fanni, M., Muchlisin, Z. A., & Abbas, M. A. (2016). Growth performance and survival rate of climbing perch (*Anabas testudineus*) fed *Daphnia* sp. enriched with manure, coconut dregs flour and soybean meal. *Aquaculture, Aquarium, Conservation and Legislation*, *9*(5), 944-948.

Rahmadi, R., Syahril, A., Nur, F. M., Maulida, S., & Muchlisin, Z. A. (2021). Embryogenesis of climbing perch fish *Anabas testudineus* (Bloch 1792) at incubation temperature of 28°C. In *IOP Conference Series: Earth and Environmental Science* (Vol. 869, No. 1, p. 012061. IOP Publishing. https://doi.org/10.1088/1755-1315/869/1/012061

Resh, H. M. (2022). *Hydroponic food production: A definitive guidebook for the advanced home gardener and the commercial hydroponic grower* (8th ed.). CRC Press. https://doi.org/10.1201/9781003133254

Riedel, T. E., Berelson, W. M., Nealson, K. H., & Finkel, S. E. (2013). Oxygen consumption rates of bacteria under nutrient-limited conditions. *Applied and Environmental Microbiology*, *79*(16), 4921-4931. https://doi.org/10.1128/AEM.00756-13

Setiawan, N. D. (2018). Otomasi pencampur nutrisi hidroponik sistem NTF (Nutrient Film Technique) berbasis Arduino Mega 2560 [Automation of hydroponic nutrient mixing NTF (Nutrient Film Technique) system based on Arduino Mega 2560]. *Jurnal Teknik Informatika UNIKA Santo Thomas*, *3*(2), 78-82. https://doi.org/10.17605/jti.v3i2.292

Silva, L., Escalante, E., Valdés-Lozano, D., Hernández, M., & Gasca-Leyva, E. (2017). Evaluation of a semi-intensive aquaponics system, with and without bacterial biofilter in a tropical location. *Sustainability*, *9*(4), 592. https://doi.org/10.3390/su9040592

Subhasmita, C., Tripathy, M. K., Nanda, S., Patra, S. K., Sahu, B., Pattanaik, S. S., & Rout, S. K. (2021). Optimization of stocking density and its effects on climbing perch (*Anabas testudineus*) cum spinach (*Spinacia oleracea*) based aquaponic system. *Journal of The Inland Fisheries Society in India*, *53*(3-4), 143-150.

Susila, N. (2016). Pengaruh padat penebaran terhadap kelangsungan hidup larva ikan Betok (*Anabas testudineus*) yang dipelihara dalam baskom [Effect of stocking density on the survival rate of climbing perch larvae (*Anabas testudineus*) reared in container]. *Journal of Tropical Animal Science*, *5*(2), 72-75.

Tallar, R. Y., & Suen, J.-P. (2016). Aquaculture Water Quality Index: A low-cost index to accelerate aquaculture development in Indonesia. *Aquaculture International*, *24*, 295-312. https://doi.org/10.1007/s10499-015-9926-3

Uddin, K. B., Moniruzzaman, M., Bashar, M. A., Basak, S., Islam, A. K. M. S., Mahmud, Y., Lee, S., & Bai, S. C. (2016). Culture potential of Thai climbing perch (*Anabas testudineus*) in experimental cages at different stocking densities in Kaptai Lake, Bangladesh. *Aquaculture, Aquarium, Conservation and Legislation*, *9*(3), 564-573.

Vadivelu, V. M., Keller, J., & Yuan, Z. (2007). Free ammonia and free nitrous acid inhibition on the anabolic and catabolic processes of *Nitrosomonas* and *Nitrobacter*. *Water Science and Technology*, *56*(7), 89-97. https://doi.org/10.2166/wst.2007.612

Vega, A., O'Brien, J. A., & Gutiérrez, R. A. (2019). Nitrate and hormonal signaling crosstalk for plant growth and development. *Current Opinion in Plant Biology*, *52*, 155-163. https://doi.org/10.1016/j.pbi.2019.10.001

Wang, C., Yue, L., Cheng, B., Chen, F., Zhao, X., Wang, Z., & Xing, B. (2022). Mechanisms of growth-promotion and Se-enrichment in *Brassica chinensis* L. by selenium nanomaterials: Beneficial rhizosphere microorganisms, nutrient availability, and photosynthesis. *Environmental*

Science: Nano, *9*, 302-312. https://doi.org/10.1039/D1EN00740H

Wibisono, V., & Kristyawan, Y. (2021). An efficient technique for automation of the NFT (Nutrient Film Technique) hydroponic system using Arduino. *International Journal of Artificial Intelligence and Robotics*, *3*(1), 44-49. https://doi.org/10.25139/ijair.v3i1.3209

Wu, W., Gao, H., Chen, H., Fang, X., Han, Q., & Zhong, Q. (2019). Combined effects of aqueous chlorine dioxide and ultrasonic treatments on shelf-life and nutritional quality of bok choy (*Brassica chinensis*). *LWT*, *101*, 757-763. https://doi.org/10.1016/j.lwt.2018.11.073

Xu, Z., Cao, J., Qin, X., Qiu, W., Mei, J., & Xie, J. (2021). Toxic effects on bioaccumulation, hematological parameters, oxidative stress, immune responses and tissue structure in fish exposed to ammonia nitrogen: A review. *Animals*, *11*(11), 3304. https://doi.org/10.3390/ani11113304

Yang, T., & Kim, H.-J. (2020). Effects of hydraulic loading rate on spatial and temporal water quality characteristics and crop growth and yield in aquaponic systems. *Horticulturae*, *6*(1), 9. https://doi.org/10.3390/horticulturae6010009

Zhang, W., Xie, H. Q., Li, Y., Jin, T., Li, J., Xu, L., Zhou, Z., Zhang, S., Ma, D., Hahn, M. E., & Zhao, B. (2019). Transcriptomic analysis of *Anabas testudineus* and its defensive mechanisms in response to persistent organic pollutants exposure. *Science of The Total Environment*, *669*, 621-630. https://doi.org/10.1016/j.scitotenv.2019.02.440

Zworykin, D. D. (2018). The behavior of climbing perch, *Anabas testudineus*, with novel food in individual and social conditions. *Journal of Ichthyology*, *58*, 260–264. https://doi.org/10.1134/S0032945218020169

Pertanika J. Trop. Agri. Sci. 46 (4): 1391 - 1405 (2023)

PERTANIKA JOURNALS

TROPICAL AGRICULTURAL SCIENCE

Journal homepage: http://www.pertanika.upm.edu.my/

Gibberellic Acid and Tween 20 Increases Napier Grass Tolerance to Synthetic Pyrethroid

Khanitta Somtrakoon[1], Wilailuck Khompun[2], Chonlada Dechakiatkrai Theerakarunwong[2] and Waraporn Chouychai[2]*

[1]Department of Biology, Faculty of Science, Mahasarakham University, Mahasarakham 44150, Thailand
[2]Department of Science, Faculty of Science and Technology, Nakhonsawan Rajabhat University, Nakhonsawan 60000, Thailand

ABSTRACT

The wide use of synthetic pyrethroids has increased their contamination in agricultural soil, so removing this pollutant from agricultural sites is necessary. Phytoremediation offers promise for agricultural soil decontamination as it is an environmentally friendly and green method. In this study, Napier grass cv. Pakchong 1 (*Pennisetum purpureum* x *Pennisetum Americanum*), cuttings with or without soaking in gibberellic acid (GA_3) with and without the surfactant Tween 20, were planted in synthetic pyrethroid contaminated soil for 20 days. The results showed that the synthetic pyrethroid reduced shoot and root growth, reduced the pigment content and increased the proline content in the leaves of Napier grass cv. Pakchong 1, and GA_3 soaking alone was the most appropriate method to alleviate synthetic pyrethroid phytotoxicity. However, planting with Napier grass cv. Pakchong 1 did not enhance soil biodegradation of cypermethrin, deltamethrin, permethrin, and fenvalerate. Napier grass did not accumulate synthetic pyrethroids within the shoot and root tissue, as the bioconcentration factor for each compound was below 1. Indigenous soil microorganisms caused a decrease in these synthetic pyrethroids. Napier grass could tolerate and grow well in pyrethroid-contaminated soil, and a method to enhance the plant's capacity to remove pyrethroid from the soil should be developed.

Keywords: Cypermethrin, deltamethrin, gibberellin, Napier grass, Tween 20

ARTICLE INFO

Article history:
Received: 02 February 2023
Accepted: 12 June 2023
Published: 27 November 2023

DOI: https://doi.org/10.47836/pjtas.46.4.20

E-mail addresses:
khanitta.s@msu.ac.th (Khanitta Somtrakoon)
wililuck.k@nsru.ac.th (Wilailuck Khompun)
chonlada.d@nsru.ac.th (Chonlada Dechakiatkrai Theerakarunwong)
waraporn.c@nsru.ac.th (Waraporn Chouychai)
*Corresponding author

ISSN: 1511-3701
e-ISSN: 2231-8542

INTRODUCTION

Agricultural and public health use of insecticides worldwide has increased environmental contamination. Synthetic pyrethroids are short-lived in the environment and have low acute toxicity to mammals when compared with organochlorine, organophosphorus, and

carbamate pesticides, but it is highly toxic to fish and bees (Thatheyus & Selvam, 2013). Synthetic pyrethroids were synthesised as analogues and derivatives of pyrethrin. This compound was an analogue of pyrethrum, a natural compound extracted from *Chrysanthemum cinerariaefolium* and *Chrysanthemum cineum*, which have been used as natural insecticides for a long time. However, synthetic pyrethroids were more toxic and environmentally recalcitrant than natural pyrethrum. There are many synthetic pyrethroids widely used in Thailand, including type I pyrethroids (without a cyano group), such as permethrin and type II pyrethroids (with a cyano group), such as cypermethrin, fenvalerate, and deltamethrin (Thatheyus & Selvam, 2013). However, the high use in agriculture of pyrethroid pesticides can cause environmental contamination in agricultural areas and should be a concern.

There have been many reports of synthetic pyrethroid contamination. Cypermethrin was reported to show a high frequency of contamination in agricultural soil in Jordan (Kailani et al., 2021). Deltamethrin was reported to contaminate agricultural soil in northern Portugal as 15.7–101.7 ng/g soil during the summer (Bragança et al., 2019). Permethrin and deltamethrin are pyrethroid pesticides reported contaminating tea plantation areas in the Citarum watershed, Indonesia. Permethrin was found at 0.18–0.28 µg/g soil in the wet season and 0.16–0.32 µg/g soil in the dry season, while deltamethrin was found only in the wet season at a concentration of 0.09-0.12 µg/g soil (Ariyani et al., 2020). The soil concentration of synthetic pyrethroid in Thailand has been rarely found, but cypermethrin has been reported as the main insecticide used in rice farms in Ang Thong and Pranakhon Si Ayutthaya Provinces, central Thailand (Maneepitak & Cochard, 2014). This contamination increases the chance of human exposure to this pesticide, and phytoremediation of pyrethroid-contaminated soil in agricultural areas will be an appropriate method for environmental remediation.

The phytoremediation of synthetic pyrethroid contamination in soil, such as cypermethrin and deltamethrin, is still limited (Aioub et al., 2019), while some aquatic plants (*Eichornia crassipes* and *Pistia strateotes*) and algae (*Chaetomorpha sutoria*, *Sirogonium sticticum*, and *Zygnema* sp.) could remove 58–76% of the pyrethroid contamination in water within seven days (Riaz et al., 2017). However, phytoremediation is safe and environmentally friendly for synthetic pyrethroid removal from agricultural soil. The low water solubility and high log K_{ow} of cypermethrin limit the plant uptake and accumulation in shoot biomass (Aioub et al., 2019; Zhu & Zhang, 2008). A possible mechanism for pyrethroid phytoremediation could be phytostimulation of rhizospheric bacteria activity via root exudate (Pilon-Smits, 2005). Several reports are showing that synthetic pyrethroid is biodegradable. Soil bacteria biodegraded cypermethrin to 3-phenoxybenzoic acid and a derivative of cyclopropanecarboxylic acid (Akbar et al., 2015). There was a report that *Plantago major*, a plant in the Plantaginaceae family,

in combination with surfactant addition, 1% 2-hydroxypropyl-beta-cyclodextrin (HPßCD), could stimulate 70–80% removal of cypermethrin in soil (10 µg/g starting concentration) within 14 days (Aioub et al., 2019).

Phytoremediation is the most interesting method for managing pyrethroid-contaminated soil in agricultural areas of Thailand and using plants that grow well in Thailand. Napier grass (*Pennisetum purpureum*) is a popular forage crop for economic ruminants cultivated widely in central and northeastern parts of Thailand (Thongruang et al., 2021). This plant species was selected for use in the phytoremediation of pyrethroid-contaminated soil because this grass species can grow in low-quality soil and under a wide range of soil pH values, produces large amounts of biomass, and tolerates many pollutant-contaminants in soil (Osman et al., 2020; Ramadhan et al., 2015). Napier grass has been reported for phytoremediation of both organic and inorganic pollutants. For example, planting Napier grass in oil-contaminated soil for 40 days could decrease the total hydrocarbons in the soil (Bobor & Omosefe, 2019) and decrease the chlorobenzene in the soil within 150 days (Alvarenga et al., 2017). Co-planting between Napier grass and corn stimulated petroleum hydrocarbon removal to 83% within two weeks (Ayotamuno et al., 2006). The application of a synthetic surfactant has been reported to increase pyrethroid removal (Aioub et al., 2019). Normally, a surfactant increases the bioavailability of the pollutant and then increases microbial biodegradation and plant root uptake (Somtrakoon & Chouychai, 2021). Tween 20 has been reported to increase the absorption of organochlorine by *Miscanthus sinensis* (Mamirova et al., 2021). Even though there were no previous reports about synthetic pyrethroid phytoremediation with Napier grass, it could be possible to use this grass species for synthetic pyrethroid phytoremediation.

The phytotoxicity of pollutants normally retard plant growth and results in limited success of phytoremediation. Synthetic pyrethroid has also been reported to limit the growth of many plant species, such as corn and onion (Aveek et al., 2009). Plant growth regulators have often been reported to alleviate the toxicity of pollutants to plants. Among these, GA_3 is a plant growth regulator that could protect plants from pollutant toxicity and enhance the organic pollutant removal from soil. Ridge guard from seeds immersed in 1.0 mg/L GA_3 or watered with 10.0 mg/L GA_3 could increase the pyrene biodegradation after being planted in pyrene-contaminated soil for 30 days (Somtrakoon & Chouychai, 2022). Corn seed pretreatment with 0.1 mg/L GA_3 decreased hexachlorocyclohexane (HCH) contamination in soil (97.4% of initial concentration) when compared with soil planted with non-pretreated corn (35.7% of initial concentration) (Chouychai et al., 2015). Seeds immersion in 10.0 mg/L GA_3 could alleviate endosulfan toxicity to *Brassica chinensis* growing in 40 mg/kg alpha-endosulfan contaminated soil (Chouychai, 2012). In this study, the efficacy of Napier grass, cv. Pakchong 1 (*Pennisetum purpureum* x *Pennisetum*

americanum) cuttings to enhance synthetic pyrethroid biodegradation and the effect of Tween 20, a synthetic surfactant, and GA_3 on synthetic pyrethroid phytotoxicity and biodegradation, were studied. It will be useful for improving phytoremediation efficacy for pesticide contamination in agricultural soil in Thailand.

MATERIALS AND METHODS

Plant and Soil Preparation

Napier grass cv. Pakchong 1 (*Pennisetum purpureum* x *Pennisetum americanum*) was obtained as commercial stem cuttings from Nong Bo Sub-district, Muang Ubon Ratchathani District, Ubon Ratchathani Province, Thailand. The stem cuttings were soaked in water for seven days after being received before being used. The soil used in this experiment was collected from Takhianluan Sub-district, Muang District, Nakhonsawan Province, Thailand. This soil was a sandy loam that was characterised previously (Chouychai et al., 2022). This soil was non-contaminated with 8 synthetic pyrethroids (bifenthrin, lambda-cyhalothrin, permethrin, cyfluthrin, cypermethrin, fenvalerate, and deltamethrin) confirmed by gas chromatography—micro-electron capture detector (GC-μECD) with a limit of detection as 0.01 mg/kg. This soil was spiked with the two commercial pyrethroid pesticides (Good Knock©, Thailand) that contained 10% (w/v) cypermethrin and 3% (w/v) deltamethrin (Delta©, Thailand) to a final concentration of cypermethrin, deltamethrin, permethrin, and fenvalerate in soil at 26.70, 116.20, 1.00 and 0.35 mg/kg, respectively. The details of the pyrethroid analysis will be explained below in the pyrethroid analysis.

Experimental Design

Gibberellic acid (GA_3, purity 90%, Sigma-Aldrich, China) was used in this study. There were two experimental designs, one for phytotoxicity and another for phytoremediation (Table 1). Each experimental design was completely randomise design (CRD) with one factor, six treatments per experiment and four replicates per treatment. A non-planted treatment with pyrethroid contamination and pyrethroid contamination + Tween 20 application was set as a control for pyrethroid biodegradation. After rooting, stem cuttings of Napier grass cv. Pakchong 1 in the GA_3 treatment were soaked in water or 0.01 mg/l GA_3 for 24 hours before being transferred to soil. This concentration of GA_3 has been reported to induce the growth of Napier grass cv. Pakchong 1 in non-contaminated soil (Phetsuwan et al., 2023). The pots used in this experiment were 7" in diameter, each containing 1 kg of dry soil. The cuttings were inoculated vertically into the soil. There were two stem cuttings per pot and four pots per treatment, and each pot was watered daily with 20 ml/pot. For the surfactant application treatments, Tween 20 (QRëC, New Zealand) with 1x of critical micelle concentration (CMC) were added to each pot at 20 ml/pot on the first day of the experiment. The surfactant used in this study was adapted from our previous work (Somtrakoon & Chouychai, 2021).

Table 1
Experimental design for pyrethroid phytotoxicity and pyrethroid phytoremediation

Treatment	Soil contamination	Planted with Napier grass	Gibberellic acid (GA_3) applied to plant cuttings	Surfactant application applied to soil
		For pyrethroid phytotoxicity		
1	Non-contamination	Planted	None	No
2	Non-contamination	Planted	GA_3	No
3	Pyrethroid	Planted	None	No
4	Pyrethroid	Planted	GA_3	No
5	Pyrethroid	Planted	None	Tween 20
6	Pyrethroid	Planted	GA_3	Tween 20
		For pyrethroid phytoremediation		
1	Pyrethroid	Non-planted	-	No
2	Pyrethroid	Non-planted	-	Tween 20
3	Pyrethroid	Planted	None	No
4	Pyrethroid	Planted	GA_3	No
5	Pyrethroid	Planted	None	Tween 20
6	Pyrethroid	Planted	GA_3	Tween 20

Plant Growth Analysis

Plants from each treatment were collected on day 20 after planting to determine the plant growth parameters, including the number of leaves and stems per plant, shoot length, root length, shoot fresh weight, shoot dry weight, root fresh weight, and root dry weight. The chlorophyll and carotenoid contents in the leaves were determined according to Lichtenthaler (1987). Briefly, 200 mg of fresh leaves were crushed with 100% acetone (Ajax Finechem, Australia), and the volume was adjusted to 15 ml. The absorbances were measured at 663.2, 646.8, and 470 nm, and the concentration of each pigment (µg/ml) was calculated as follows:

Chlorophyll *a* (Chl *a*) content = (12.5 *A663.2) - (2.79* A646.8)

Chlorophyll *b* (Chl *b*) content = (21.51*A646.8) - (5.1*A663.2)

Total chlorophyll content = Chl *a* + Chl *b*

Carotenoid content = (1000* A470) - (1.8* Chl *a*) - (85.02* Chl *b*)/198

In addition, the relative water content in the leaves was analysed by [(total fresh weight – bag weight) – dry weight)/(turgid weight – dry weight)]*100% as described in Sade et al. (2015). The leaf's proline content was analysed with spectrophotometry by measuring the absorbance of the leaf solution at 520 nm. The leaf solution was extracted by sulphosalicylic, following which it was reacted with the acid ninhydrin and extracted with toluene before being

measured (John et al., 2008). The specific root length was calculated by root length/root dry weight (Calvelo Pereira et al., 2010), and the root-to-shoot ratio was calculated by root dry weight/shoot dry weight (Xu et al., 2018).

Pyrethroid Analysis

One kg of soil per pot was collected and sent for analysis of the pyrethroid pesticide concentration in the soil at the Central Laboratory Thailand, Ltd., Khon Kaen branch, using an in-house method based on the QuEChERS method using GC-μECD with a limit of detection as 0.01 mg/kg and in addition, dried shoots and roots of Napier grass cv. Pakchong 1 were collected and sent for analysis of the pyrethroid pesticide accumulation in plant tissue at the Central Laboratory Thailand, Ltd., Khon Kaen branch using an in-house method based on the QuEChERS method using GC-μECD with a limit of detection of 0.01 mg/kg. Each synthetic pyrethroid's bioconcentration factors (BCF) were calculated for each synthetic pyrethroid concentration in the harvested plant/each synthetic pyrethroid concentration in planted soil. A BCF higher than one showed the potential of plants to phytoaccumulate (Hammami et al., 2016).

Statistical Analysis

One-way analysis of variance (ANOVA) and Duncan's tests were used for variance analysis and pairwise comparison.

RESULTS AND DISCUSSION

Effect of Gibberellic Acid and Tween 20 on Napier Grass cv. Pakchong 1 Growth in Pyrethroid Contaminated Soil

Synthetic pyrethroids were significantly toxic to the growth of Napier grass cv. Pakchong 1. Shoot length, shoot fresh weight, and shoot dry weight of Napier grass grown in pyrethroid-contaminated soil were significantly lower than those grown in non-contaminated soil (Table 2). The shoot length of Napier grass cv. Pakchong 1 grown in non-contaminated soil was 44.5 ± 0.61 cm, while the shoot length of those grown in pyrethroid-contaminated soil was 31.0 ± 0.91 cm. In addition, the root length, root fresh weight, root dry weight, and root-to-shoot ratio of Napier grass growing in pyrethroid-contaminated soil were decreased when compared with those growing in non-contaminated soil. The root thickness tended to decrease, as shown by increasing the specific root length from 3.18 ± 0.06 m/g in non-contaminated soil to 4.82 ± 0.35 m/g (Table 3 and Figure 1).

Soaking with GA_3 could significantly increase the shoot length, shoot fresh weight, and shoot dry weight of Napier grass grown in pyrethroid-contaminated soil compared with plants not stimulated with GA_3. This stimulating effect on shoot growth was not seen when comparing cuttings that were soaked and not soaked with GA_3 in non-contaminated soil. The shoot length of Napier cuttings soaked and not soaked with GA_3 in pyrethroid-contaminated soil were 44.4 ± 0.47 and 31.0 ± 0.91 cm, respectively,

while those in non-contaminated soil were 38.0 ± 0.41 and 44.5 ± 0.61 cm, respectively (Table 1). However, the positive effect of GA_3 on root growth was less than on shoot growth. Soaking with GA_3 significantly increases only the root dry weight of Napier grass grown in pyrethroid-contaminated soil. This effect of GA_3 is similar to our previous study with hexachlorocyclohexane (HCH) (Chouychai et al., 2015) and polycyclic aromatic hydrocarbons (PAHs) (Somtrakoon & Chouychai, 2022). GA_3 is a plant hormone that controls plants' normal shoot and root growth (Hedden & Sponsel, 2015), and the application of exogenous GA_3 in this study was adequate to induce shoot growth of Napier grass in pyrethroid-contaminated soil.

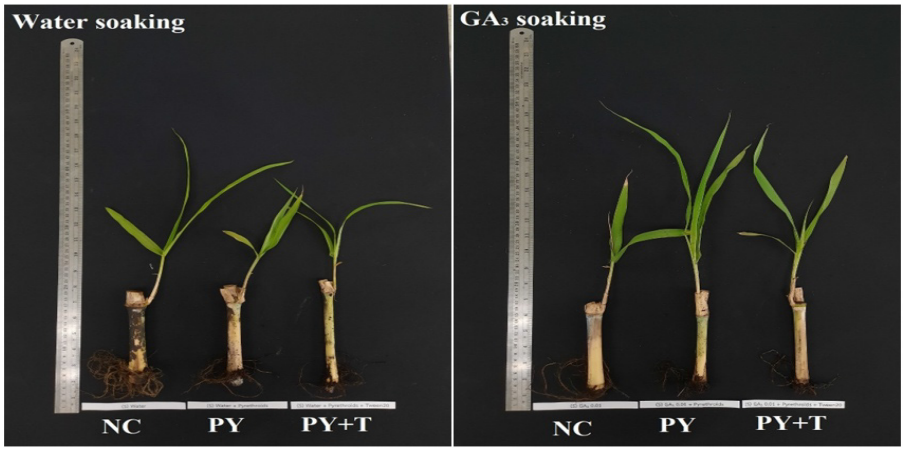

Figure 1. Shoot and root of Napier grass cv. Pakchong 1 soaking in water or 0.01 mg/L gibberellic acid (GA_3) and growing in different soil that was non-contaminated soil (NC), pyrethroid-contaminated soil with (PY + T) or without Tween 20 addition (PY) for 20 days

The positive effect of Tween 20 on Napier grass was less than GA_3. In addition, Tween 20 only increased the shoot length and shoot dry weight and did not enhance the root growth of Napier grass soaked with water and growing in pyrethroid-contaminated soil. It contrasts with Triton X-100 and Tween 80 in addition to *Impatiens balsamina* planted in 100 mg/kg anthracene and fluoranthene-contaminated soil, in which the shoot growth of the plants exposed to both surfactants was decreased (Somtrakoon & Chouychai, 2021). Tween 20, in addition to pyrethroid-contaminated soil and planted with GA_3-soaked cuttings, did not enhance the growth of Napier grass over that which received only GA_3. Depending on shoot and root growth, GA_3 soaking was appropriate to improve the Napier grass health in pyrethroid-contaminated soil.

Growth in pyrethroid did not affect the chlorophyll *b*, carotenoid, and relative water contents of Napier grass, and treatment with GA_3 or Tween 20 did not enhance these plant traits. For example, the carotenoid contents

Table 2
Shoot growth of Napier grass receiving gibberellic acid (GA_3) and Tween 20 and growing in non-contaminated soil or pyrethroid-contaminated soil for 20 days

Treatment	Shoot length (cm)	Shoot fresh weight (g)	Shoot dry weight (g)	Number of leave/cutting	Number of shoot/cutting
NC + Water-Np	44.5 ± 0.61 a	25.5 ± 0.52 a	14.7 ± 0.67 a	3.2 ± 0.25 a	1.0 ± 0.00
NC + GA_3-Np	38.0 ± 0.41 bc	26.7 ± 0.60 ab	15.2 ± 1.38 a	3.5 ± 0.29 a	1.0 ± 0.00
Pyrethroid + Water-Np	31.0 ± 0.91 d	19.3 ± 0.38 e	10.4 ± 0.36 b	2.8 ± 0.25 a	1.0 ± 0.00
Pyrethroid + Tween 20 + Water-Np	37.0 ± 0.41 c	21.4 ± 0.95 de	14.5 ± 0.56 a	3.0 ± 0.00 a	1.0 ± 0.00
Pyrethroid + GA_3-Np	44.4 ± 0.47 a	23.9 ± 0.90 bc	13.4 ± 0.66 a	3.2 ± 0.25 a	1.0 ± 0.00
Pyrethroid + Tween 20 + GA_3-Np	39.0 ± 0.71 b	22.5 ± 0.75 cd	14.3 ± 0.42 a	3.2 ± 0.25 a	1.0 ± 0.00

Note. Different lowercase letters showed significant difference ($P < 0.05$) between different treatment in same column; NC = Non-contaminated soil; Water-NP = Water soaking Napier grass cutting, GA_3-Np = GA_3 soaking Napier grass cutting

Table 3
Root growth of Napier grass receiving gibberellic acid (GA_3) and Tween 20 and growing in non-contaminated soil or pyrethroid-contaminated soil for 20 days

Treatment	Root length (cm)	Root fresh weight (g)	Root dry weight (g)	Root-to-shoot ratio	Specific root length (m/g)
NC + Water-Np	25.2 ± 0.63 a	0.76 ± 0.03 a	0.08 ± 0.003 a	0.005 ± 0.000 a	3.18 ± 0.06 b
NC + GA_3-Np	23.0 ± 0.41 b	0.68 ± 0.04 b	0.08 ± 0.003 a	0.005 ± 0.000 a	2.99 ± 0.16 b
Pyrethroid + Water-Np	16.1 ± 0.31 c	0.34 ± 0.03 c	0.03 ± 0.003 d	0.003 ± 0.000 c	4.82 ± 0.35 a
pyrethroid + Tween 20 + Water-Np	16.2 ± 0.25 c	0.33 ± 0.02 c	0.04 ± 0.003 cd	0.003 ± 0.000 c	4.23 ± 0.34 a
Pyrethroid + GA_3-Np	16.2 ± 0.25 c	0.39 ± 0.02 c	0.05 ± 0.004 bc	0.004 ± 0.000 b	3.27 ± 0.33 b
pyrethroid + Tween 20 + GA_3-Np	17.0 ± 0.41 c	0.40 ± 0.02 c	0.06 ± 0.006 b	0.004 ± 0.000 b	3.15 ± 0.39 b

Note. Different lowercase letters showed significant difference ($P < 0.05$) between different treatment in same column; NC = Non-contaminated soil; Water-NP = Water soaking Napier grass cutting, GA_3-Np = GA_3 soaking Napier grass cutting

in the leaves of Napier grass were between 0.12–0.15 mg/g FW for plants grown in non-contaminated soil and between 0.07–0.16 mg/g FW for plants growing in pyrethroid-contaminated soil (Table 4). However, pyrethroid contamination decreased the

chlorophyll *a* and total chlorophyll contents and increased the proline content in the leaves of Napier grass. Both GA_3 and Tween 20 applications increased the chlorophyll *a* and total chlorophyll contents in the leaves of Napier grass grown in pyrethroid-contaminated soil. However, only GA_3-treated Napier grass grown in pyrethroid-contaminated soil contained proline in the leaves (11.5 mg/g FW) at the same level as plants grown in non-contaminated soil (9.8 mg/g FW). Application of Tween 20 could decrease the proline content (14.9 mg/g FW) when compared with plants grown in pyrethroid-contaminated soil that did not receive Tween 20 (19.4 mg/g FW), but the proline content was still significantly higher than that growing in non-contaminated soil (9.8 mg/g FW) (Table 4).

Table 4
Chlorophyll, carotenoid, relative water, and proline content in leaves of Napier grass receiving gibberellic acid (GA_3) and Tween 20 and growing in non-contaminated soil or pyrethroid-contaminated soil for 20 days

Treatment	Chlorophyll *a* content (mg/g FW)	Chlorophyll *b* content (mg/g FW)	Total chlorophyll content (mg/g FW)	Carotenoid content (mg/g FW)	Relative water content (%)	Proline content (µg/g FW)
NC + Water-Np	0.67 ± 0.02 a	0.27 ± 0.03 a	0.94 ± 0.04 a	0.15 ± 0.02 a	55.4 ± 3.84 a	9.8 ± 0.74 c
NC + GA_3-Np	0.60 ± 0.07 a	0.35 ± 0.07 a	0.95 ± 0.03 a	0.12 ± 0.04 a	59.9 ± 4.18 a	10.1 ± 0.37 c
Pyrethroid + Water-Np	0.38 ± 0.05 b	0.17 ± 0.03 a	0.54 ± 0.03 b	0.07 ± 0.01 a	54.7 ± 10.44 a	19.4 ± 0.81 a
Pyrethroid +Tween 20 + Water-Np	0.60 ± 0.07 a	0.19 ± 0.02 a	0.79 ± 0.09 a	0.15 ± 0.02 a	67.9 ± 9.50 a	14.9 ± 0.98 b
Pyrethroid+ GA_3-Np	0.62 ± 0.06 a	0.24 ± 0.05 a	0.86 ± 0.07 a	0.14 ± 0.01 a	72.4 ± 12.48 a	11.5 ± 1.95 c
Pyrethroid + Tween 20 + GA_3-Np	0.68 ± 0.06 a	0.28 ± 0.08 a	0.96 ± 0.06 a	0.16 ± 0.03 a	61.8 ± 7.12 a	12.5 ± 0.68 bc

Note. Different lowercase letters showed significant difference ($P < 0.05$) between different treatment in same column; NC = Non-contaminated soil; Water-NP = Water soaking Napier grass cutting, GA_3-Np = GA_3 soaking Napier grass cutting

The toxicity of synthetic pyrethroid to Napier grass was the same as that reported for *Allium cepa*, *Lathyrus sativas*, and *Zea mays* exposed to 0.2-0.8 g/L cypermethrin 12 hr before germination. Cypermethrin significantly decreased the shoot and root length, mitotic index, chlorophyll content, and moisture content for all three plants (Aveek et al., 2009). GA_3 soaking could alleviate these toxicities to Napier grass, including decreasing the proline content in leaves. It indicates that GA_3 could decrease the pyrethroid stress to plants, which is advantageous for phytoremediation. The

proline content in plants often increases when exposed to stress, and it has been reported to function as a protein stabiliser, hydroxyl radical, singlet oxygen scavenger and inhibitor of lipid peroxidation (Siddiqui et al., 2011). Reports show that GA_3 could alleviate pollutant phytotoxicity and increase biodegradation of organic pollutants. GA_3 stimulated root growth, and then the healthy root could stimulate the growth and function of soil bacteria that could degrade the pollutant in the rhizosphere via the rhizodegradation process (Alagić et al., 2015) or plant-microbe interactions in the root zone (Chaudhry et al., 2005). Applying GA_3 alone or in combination with Tween 80 could increase the plant dry weight of *Tagetes patula* grown in benzo[a]pyrene and cadmium-contaminated soil (Sun et al., 2013).

Effect of Gibberellic Acid and Tween 20 on Pyrethroid Phytoremediation with Napier Grass cv. Pakchong 1

There were four pyrethroid pesticide groups found in contaminated soil, which were 26.7 mg/kg cypermethrin, 116.2 mg/kg deltamethrin, 1.00 mg/kg permethrin, and 0.35 mg/kg fenvalerate, at the beginning of the experiment (Table 5). After 20 days, the concentrations of cypermethrin, deltamethrin, and felvalorate decreased significantly in non-planted soil, while the concentration of permethrin in the soil did not decrease significantly. In addition, the accumulation of cypermethrin, deltamethrin, and permethrin in the shoots and roots of Napier grass cv. Pakchong 1 is limited as the bioconcentration factor was below 1, while fenvalerate was not found in any plant tissue (Table 6). Pyrethroid accumulation was not found in Napier grass growing in non-contaminated soil. These results contrast with aquatic plants that could remove synthetic pyrethroid from water by 58–76% within seven days (Riaz et al., 2017). It showed that the decrease in the synthetic pyrethroid in soil within 20 days did not occur by plant accumulation but depended on the activity of indigenous soil bacteria.

There has been a report that cypermethrin was degraded more rapidly in non-sterilised soil (with soil bacteria) than in sterilised soil (low soil bacteria by autoclaving at 120ºC for 20 min on two consecutive days). After 28 days, 2.89% of cypermethrin (starting concentration = 10 mg/kg) was removed in sterilised soil, while 8.41% of cypermethrin was removed in non-sterilised soil (Xie & Zhou, 2008). These bacteria could degrade cypermethrin, deltamethrin, and fenvalorate but could not degrade permethrin. Adding Tween 20 into non-planted soil or that planted with Napier grass did not enhance any pyrethroid removal in the soil. This effect was the same as with Tween 20 addition into phenanthrene-contaminated soil in which Tween 20 inhibited phenanthrene biodegradation (Zhou et al., 2008). The failure of the surfactant application has been reported. Tween 80 addition did not enhance PAH-phytoremediation by *Impatiens balsamina* but could enhance PAH biodegradation in non-planted soil when used with salicylic acid (Somtrakoon & Chouychai, 2021).

GA_3-stimulated Napier grass cutting did not exhibit any enhanced pyrethroid removal.

When comparing with cypermethrin biodegradation in soil planted with *Plantago major* (60% removal) for 14 days and a starting concentration of 10 mg/kg (Aioub et al., 2019), Napier grass cv. Pakchong 1 soaked in GA_3 was more effective with 66.3% cypermethrin removal (starting concentration was 26.7 mg/kg and planted for 20 days), while the effect of Napier grass cv. Pakchong 1 soaked in water was the same as *Plantago major* (59.6% removal). However, planting Napier grass cv. Pakchong 1 soaked with GA_3 or Tween 20 was less effective than *Plantago major* and liquid silicon dioxide addition (80% removal) (Aioub et al., 2019). The cultivation of Napier grass was stimulated with GA_3 and could tolerate synthetic pyrethroid-contaminated soil well, but the capacity to remove pyrethroid from the soil is limited and should be improved.

Table 5
Pyrethroid remaining in soil after planting with Napier grass for 20 days

Treatment	Cypermethrin (mg/kg)	Deltamethrin (mg/kg)	Permethrin (mg/kg)	Fenvalerate (mg/kg)
Starting concentration	26.7 ± 4.89 a	116.2 ± 26.4 a	1.00 ± 0.41 a	0.35 ± 0.06 a
No plant	14.0 ± 3.56 b	53.0 ± 20.3 b	0.7 ± 0.18 a	0.18 ± 0.04 b
No plant + Tween 20	17.8 ± 0.37 ab	97.9 ± 1.42 ab	1.0 ± 1.00 a	0.23 ± 0.02 b
Napier-water	10.8 ± 0.94 b	66.5 ± 7.20 b	0.8 ± 0.07 a	0.19 ± 0.02 b
Napier-water + Tween 20	12.0 ± 0.89 b	70.7 ± 5.02 b	0.9 ± 0.06 a	0.19 ± 0.01 b
Napier-GA_3	9.0 ± 0.49 b	56.2 ± 1.23 b	0.6 ± 0.02 a	0.16 ± 0.00 b
Napier-GA_3 + Tween 20	13.5 ± 2.37 b	91.1 ± 15.52 ab	0.9 ± 0.13 a	0.20 ± 0.04 b

Note. Different lowercase letters showed significant difference ($P < 0.05$) between different treatment in same column; GA_3 = Gibberellic acid

Table 6
Pyrethroid accumulation in plant tissue of Napier grass after planting for 20 days

Treatment	Cypermethrin	Deltamethrin	Permethrin
Shoot concentration (mg/kg)			
Napier-water	0.11	0.14	0.04
Napier-water + Tween 20	0.04	B.D.	0.04
Napier-GA_3	0.23	0.40	0.07
Napier-GA_3 + Tween 20	0.05	0.07	B.D.
Root concentration (mg/kg)			
Napier-water	0.11	0.20	0.05
Napier-water + Tween 20	0.03	0.05	0.01
Napier-GA_3	B.D.	0.01	B.D.

Table 6 *(Continue)*

Treatment	Cypermethrin	Deltamethrin	Permethrin
Napier-GA_3 + Tween 20	0.01	0.01	B.D.
Bioconcentration factor			
Napier-water	0.020	0.005	0.106
Napier-water + Tween 20	0.006	0.001	0.056
Napier-GA_3	0.025	0.007	0.111
Napier-GA_3 + Tween 20	0.004	0.001	-

Note. GA_3 = Gibberellic acid

CONCLUSION

Napier grass cv. Pakchong 1 could grow in synthetic pyrethroid-contaminated soil, but the shoot, root growth, and pigment content in leaves decreased. Soaking stem cuttings of Napier grass in 0.01 mg/L GA_3 before planting in synthetic pyrethroid-contaminated soil could stimulate growth and alleviate plant stress. Napier grass cv. Pakchong 1 enhanced the removal of cypermethrin, deltamethrin, and fenvalerate significantly within 20 days, and it did not accumulate all pyrethroid pesticides within plant tissue. In addition, Tween 20 addition to soil and GA_3-soaked cuttings did not stimulate synthetic pyrethroid removal from soil. The application of GA_3 is appropriate to induce the growth of Napier grass, but the method to enhance pyrethroid in Napier grass planting soil should be further developed.

ACKNOWLEDGEMENTS

The authors thank the Nakhon Sawan Rajabhat University and Thailand Science Research and Innovation (TSRI) Grant Year 2022 for the financial support under Grant No. FRB650025/0199 Project No. 2558225.

REFERENCES

Aioub, A. A. A., Li, Y., Qie, X., Zhang, X., & Hu, Z. (2019). Reduction of soil contamination by cypermethrin residues using phytoremediation with *Plantago major* and some surfactants. *Environmental Science Europe*, *31*, 26. https://doi.org/10.1186/s12302-019-0210-4

Akbar, S., Sultan, S., & Kertesz, M. (2015). Determination of cypermethrin degradation potential of soil bacteria along with plant growth-promoting characteristics. *Current Microbiology*, *70*, 75-84. https://doi.org/10.1007/s00284-014-0684-7

Alagić, S. Č., Maluckov, B. S., & Radojičić, V. B. (2015). How can plants manage polycyclic aromatic hydrocarbons? May these effects represent a useful tool for an effective soil remediation? A review. *Clean Technology and Environmental Policy*, *17*, 597–614. https://doi.org/10.1007/s10098-014-0840-6

Alvarenga, A. C., Sampaio, R. A., Pinho, G. P., Cardoso, P. H. S., de P. Sousa, I., & Barbosa, M. H. C. (2017). Phytoremediation of chlorobenzenes in sewage sludge cultivated with *Pennisetum purpureum* at different times. *Revista Brasileira de Engenharia Agrícola e Ambiental*, *21*(8), 573-578. https://doi.org/10.1590/1807-1929/agriambi.v21n8p573-578

Ariyani, M., Pitoi, M. M., Koesmawati, T. A., Maulana, H., Endah, E. S., & Yusiasih, R. (2020). Pyrethroid residues on tropical soil of an Indonesian tea plantation: Analytical method development, monitoring, and risk assessment. *Sustainable Environment Research*, *30*, 15. https://doi.org/10.1186/s42834-020-00055-7

Aveek, S., Jyoti, P. S., Jaydeb, J., & Somashree, M. (2009). Effect of cypermethrin on growth, cell division and photosynthetic pigment content in onion, maize and grass pea. *Research Journal of Chemistry and Environment*, *23*(8), 126-129.

Ayotamuno, J. M., Kogbara, R. B., & Egwuenum, P. N. (2006). Comparison of corn and elephant grass in the phytoremediation of a petroleum-hydrocarbon-contaminated agricultural soil in Port Harcourt, Nigeria. *Journal of Food, Agriculture and Environment*, *4*(3&4), 218-222.

Bobor, L. O., & Omosefe, B. E. (2019). Elephant grass (*Pennisetum purpureum*) mediated phytoremediation of crude oil-contaminated soil. *Nigerian Journal of Environmental Sciences and Technology*, *3*(1), 105-111.

Bragança, I., Lemos, P. C., Delerue-Matos, C., & Domingues, V. F. (2019). Assessment of pyrethroid pesticides in topsoils in northern Portugal. *Water, Air and Soil Pollution*, *230*, 166. https://doi.org/10.1007/s11270-019-4209-7

Calvelo Pereira, R., Monterroso, C., & Macías, F. (2010). Phytotoxicity of hexachlorocyclohexane: Effect on germination and early growth of different plant species. *Chemosphere*, *79*(3), 326-333. http://doi.org/10.1016/j.chemosphere.2010.01.035

Chaudhry, Q., Blom-Zandstra, M., Gupta, S. K., & Joner, E. J. (2005). Utilising the synergy between plants and rhizosphere microorganisms to enhance breakdown of organic pollutants in the environment. *Environmental Science and Pollution Research*, *12*, 34-48. https://doi.org/10.1065/espr2004.08.213

Chouychai, W. (2012). Effect of some plant growth regulators on lindane and alpha-endosulfan toxicity to *Brassica chinensis*. *Journal of Environmental Biology*, *33*(4), 811-816.

Chouychai, W., Kruatrachue, M., & Lee, H. (2015). Effect of plant growth regulators on phytoremediation of hexachlorocyclohexane-contaminated soil. *International Journal of Phytoremediation*, *17*(11), 1053-1059. https://doi.org/10.1080/15226514.2014.989309

Chouychai, W., Sangdee, A., & Somtrakoon, K. (2022). Effect of *Streptomyces* inoculation on *Ipomoea aquatica* and *Pachyrhizus erosus* grown under salinity and low water irrigation conditions. *Pertanika Journal of Tropical Agricultural Science*, *45*(2), 411-432. https://doi.org/10.47836/pjtas.45.2.05

Hammami, H., Parsa, M., Mohassel, M. H. R., Rahimi, S., & Mijani, S. (2016). Weeds ability to phytoremediate cadmium-contaminated soil. *International Journal of Phytoremediation*, *18*(1), 48-53. https://doi.org/10.1080/15226514.2015.1058336

Hedden, P., & Sponsel, V. (2015). A century of gibberellin research. *Journal of Plant Growth Regulation*, *34*, 740-760. https://doi.org/10.1007/s00344-015-9546-1

John, R., Ahmad, P., Gadgil, K., & Sharma, S. (2008). Effect of cadmium and lead on growth, biochemical parameters and uptake in *Lemna polyrrhiza* L. *Plant Soil and Environment*, *54*(6), 262–270. https://doi.org/10.17221/2787-PSE

Kailani, M. H., Al-Antary, T. M., & Alawi, M. A. (2021). Monitoring of pesticides residues in soil samples from the southern districts of Jordan in 2016/2017. *Toxin Reviews*, *40*(2), 198-214. https://doi.org/10.1080/15569543.2019.1580747

Lichtenthaler, H. K. (1987). Chlorophylls and carotenoids: Pigments of photosynthetic

biomembranes. In L. Packer & R. Douce (Eds.), *Methods in enzymology* (Vol. 148, pp. 350-382). Academic Press. https://doi.org/10.1016/0076-6879(87)48036-1

Mamirova, A., Pidlisnyuk, V., Amirbekov, A., Ševců, A., & Nurzhanova, A. (2021). Phytoremediation potential of *Miscanthus sinensis* And. in organochlorine pesticides contaminated soil amended by Tween 20 and activated carbon. *Evironmental Science and Pollution Research*, *28*, 16092-16106. https://doi.org/10.1007/s11356-020-11609-y

Maneepitak, S., & Cochard, R. (2014). Uses, toxicity levels, and environmental impacts of synthetic and natural pesticides in rice fields – A survey in Central Thailand. *International Journal of Biodiversity Science, Ecosystem Services and Management*, *10*(2), 144-156, https://doi.org/10.1080/21513732.2014.905493

Osman, N. A., Roslan, A. M., Ibrahim, M. F., & Hassan, M. A. (2020). Potential use of *Pennisetum purpureum* for phytoremediation and bioenergy production: A mini review. *Asia-Pacific Journal of Molecular Biology and Biotechnology*, *28*(1), 14-26. https://doi.org/10.35118/apjmbb.2020.028.1.02

Phetsuwan, A., Kunpratum, N., Pooam, M., Somtrakoon, K., & Chouychai, W. (2023). Application of salicylic acid and gibberellic acid increase stem cutting growth of *Pennisetum purpureum* cv. Mahasarakham and *Pennisetum purpureum* x *Pennisetum americanum*. *Pertanika Journal of Tropical Agricultural Science*, *46*(3), 735-754. https://doi.org/10.47836/pjtas.46.3.01

Pilon-Smits, E. (2005). Phytoremediation. *Annual Review of Plant Biotechnology*, *56*, 15-39. https://doi.org/10.1146/annurev.arplant.56.032604.144214

Ramadhan, A., Njunie, M. N., & Lewa, K. K. (2015). Effect of planting material and variety on productivity and survival of Napier grass (*Pennisetum purpureum* Schumach) in the coastal lowlands of Kenya. *East African Agricultural and Forestry Journal*, *81*(1), 40-45. https://doi.org/10.1080/00128325.2015.1040647

Riaz, G., Tabinda, B. A., Iqbal, S., Yasar, A., Abbas, M., Khan, A. M., Mahfooz, Y., & Baqar, M. (2017). Phytoremediation of organochlorine and pyrethroid pesticides by aquatic macrophytes and algae in freshwater systems. *International Journal of Phytoremediation*, *19*(10), 894-898. https://doi.org/10.1080/15226514.2017.1303808

Sade, N., Galkin, E., & Moshelion, M. (2015). Measuring *Arabidopsis*, tomato and barley leaf relative water content (RWC). *Bio-Protocol*, *5*(8), e1451. https://doi.org/10.21769/BIOPROTOC.1451

Siddiqui, M. H., Al-Whaibi, M. H., & Basalah, M. O. (2011). Interactive effect of calcium and gibberellin on nickel tolerance in relation to antioxidant systems in *Triticum aestivum* L. *Protoplasma*, *248*, 503–511. https://doi.org/10.1007/s00709-010-0197-6

Somtrakoon, K., & Chouychai, W. (2021). Potential of salicylic acid and synthetic surfactant on anthracene and fluoranthene remediation by *Impatiens balsamina*. *Walailak Journal of Science and Technology*, *18*(2), 7001. https://doi.org/10.48048/wjst.2021.7001

Somtrakoon, K., & Chouychai, W. (2022) Gibberellic acid treatment improved pyrene phytoremediation efficiency of ridge gourd (*Luffa acutangula* (L.) Roxb.) in soil. *Soil and Sediment Contamination: An International Journal*, *31*(2), 253-263. https://doi.org/10.1080/15320383.2021.1926419

Sun, Y., Xu, Y., Zhou, Q., Wang, L., Lin, D., & Liang, X. (2013). The potential of gibberellic acid (GA_3) and Tween-80 induced phytoremediation of co-contamination of Cd and Benzo[a] pyrene (B[a]P) using *Tagetes patula*. *Journal of Environmental Management*, *114*, 202-208. https://doi.org/10.1016/j.jenvman.2012.09.018

Thatheyus, A. J., & Selvam, A. D. G. (2013). Synthetic pyrethroids: Toxicity and biodegradation. *Applied Ecology and Environmental Sciences*, *1*(3), 33-36. https://doi.org/10.12691/aees-1-3-2

Thongruang, S., Kleawkleaur, K., Prombut, P., & Manatrinon, S. (2021). Comparisons in yields, forage characteristics, sweetness and nutritive values of sweet grass (*Pennisetum purpureum* cv. Mahasarakham) and Napier Pak Chong 1 grass (*Pennisetum purpureum* x *Pennisetum americanum*) at different cutting ages. *Khon Kaen Agriculture Journal*, *49*(5), 1092-1102. https://doi.org/10.14456/kaj.2021.97

Xie, W., & Zhou, J. (2008). Cypermethrin persistence and soil properties as affected by long-term fertilizer management. *Acta Agriculturae Scandinavica, Section B – Soil and Plant Science*, *58*(4), 314-321. https://doi.org/10.1080/09064710701743096

Xu, Z.-M., Mei, X.-Q., Tan, L., Li, Q.-S., Wang, L.-L., He, B.-Y., Guo, S.-H., Zhou, C., & Ye, H.-J. (2018). Low root/shoot (R/S) biomass ratio can be an indicator of low cadmium accumulation in the shoot of Chinese flowering cabbage (*Brassica campestris* L. ssp. *chinensis* var. *utilis* Tsen et Lee) cultivars. *Environmental Science and Pollution Research*, *25*, 36328-36340. https://doi.org/10.1007/s11356-018-3566-x

Zhou, Y., Zhang, J., Su, E., Wei, G., Ma, Y., & Wei, D. (2008). Phenanthrene biodegradation by an indigenous *Pseudomonas* sp. ZJFo8 with TX100 as surfactant. *Annals of Microbiology*, *58*, 439-442. https://doi.org/10.1007/BF03175540

Zhu, L., & Zhang, M. (2008). Effect of rhamnolipids on the uptake of PAHs by ryegrass. *Environmental Pollution*, *156*(1), 46-52. https://doi.org/10.1016/j.envpol.2008.01.004

Pertanika J. Trop. Agri. Sci. 46 (4): 1407 - 1421 (2023)

PERTANIKA JOURNALS

TROPICAL AGRICULTURAL SCIENCE

Journal homepage: http://www.pertanika.upm.edu.my/

Determination of Antioxidant Activity, Phenolic Compounds, and Toxicity of Methanolic and Ethanolic Extracts of Pink Pigmented Facultative Methylotrophs (PPFM) Bacteria Pigment

Nur Isti'anah Ramli[1], Faridah Abas[1,3], Intan Safinar Ismail[2,3], Yaya Rukayadi[1,3]* and Shahidah Md Nor[4]

[1]Department of Food Science, Faculty of Food Science and Technology, Universiti Putra Malaysia, 43400 Serdang, Selangor, Malaysia
[2]Department of Chemistry, Faculty of Science, Universiti Putra Malaysia, 43400 Serdang, Selangor, Malaysia
[3]Natural Medicines and Products Research Laboratory (NaturMeds), Institute of Bioscience (IBS), Universiti Putra Malaysia, 43400 Serdang, Selangor, Malaysia
[4]Department of Technology and Natural Resources, Universiti Tun Hussein Onn Malaysia, Hab Pendidikan Tinggi Pagoh, KM 1, Jalan Panchor, 84600 Panchor, Johor, Malaysia

ABSTRACT

Pink-pigmented facultative methylotrophs bacteria are a plant's surface inhabitant, especially at the leaf. They are known as *Methylobacterium* species. The antioxidant activity, phenolic compounds, and level of toxicity of this bacteria pigment have been studied. Recently, no previous research focused on the same bacterium found in *Melicope lunu-ankenda* (Gaertn.) T. G. Hartley, which is a component of the Malaysian *ulam* leaf. This study employed the 2,2-diphenyl-1-picrylhydrazyl (DPPH), ferric ion reducing antioxidant power (FRAP), and 2,2'-azino-bis (3-ethylbenzothiazoline-6-sulfonic acid) (ABTS) radical scavenging assays, along with total phenolic content determination to assess the antioxidant activities of the methanolic and ethanolic pigment extract. Additionally, the consumption safety level of the pigment extract used brine shrimp lethality assay. From these findings, ethanolic pigment extract has a higher antioxidant capacity than methanolic extract. The DPPH half-maximal inhibitory concentration (IC_{50}) value of methanolic pigment extract is higher than ethanolic extract (0.72 ± 0.04 mg/ml), but the IC_{50} value is *vice versa* for ABTS (4.59 ± 2.17 mg/ml). Furthermore, ethanolic extracts have a high FRAP assay value (1.09 ± 0.19 mg/mg of trolox equivalent at 0.78 mg/ml sample) and phenolic content (1.39 ± 0.07 mg/mg of gallic acid equivalent at 0.78 mg/ml sample) compared to methanolic pigment extracts. Fortunately, the methanolic and ethanolic pigment extract's lethal concentration values

ARTICLE INFO

Article history:
Received: 28 March 2023
Accepted: 29 May 2023
Published: 27 November 2023

DOI: https://doi.org/10.47836/pjtas.46.4.21

E-mail addresses:
nuribtr@gmail.com (Nur Isti'anah Ramli)
faridah_abas@upm.edu.my (Faridah Abas)
safinar@upm.edu.my (Intan Safinar Ismail)
yaya_rukayadi@upm.edu.my (Yaya Rukayadi)
shahidahmn@uthm.edu.my (Shahidah Md Nor)
*Corresponding author

ISSN: 1511-3701
e-ISSN: 2231-8542

(4.52 and 9.94 mg/ml) are considered safe for food application since their toxicity level is higher than 1 mg/ml.

Keywords: Antioxidant activity, bacteria pigment, *Methylobacterium* sp., phenolic compound, pink pigmented facultative methylotrophs, toxicity

INTRODUCTION

The bacteria known as pink-pigmented facultative methylotrophs (PPFM) live mostly on the surface of leaves, especially *ulam* leaves, in the phyllosphere. They can solely obtain their energy and carbon from single-carbon molecules or multi-carbon growth substrates (Green, 2014). Their cell body's appearance of reddish pink reflects the presence of carotenoid pigment (Madhaiyan, 2003). However, similar to bacteriochlorophylls, which serve as the light-harvesting pigment, carotenoids in PPFM pigment can also contribute to the process of light absorption (Boronat & Rodrguez-Concepción, 2015). Also, they can withstand more UV radiation than other types of bacteria since too much UV exposure can lead to the formation of oxidants in cells (Dreyer, 2016; Santos et al., 2013). Oxidants, which are unstable and chemically reactive entities, are generally referred to as free radicals, and they need to be managed to prevent unfavourable events in the biological system (Pawar et al., 2015). The greatest significant free radicals in the body are known as reactive oxygen species (ROS). These species interact with nearby macromolecules to stabilise themselves, producing an oxidative stress state that ultimately causes cell death (Cheeseman & Slater, 1993; Dekkers et al., 1996; Halliwell & Gutteridge, 2015).

Bacteria, especially pigmented ones, are constantly exposed to various harmful environmental conditions, including desiccation, freezing, UV radiation, and changes in heavy metal concentrations, which cause ROS to produce and build up in the body gradually (Dring, 2005). They thus turn on their antioxidant defence systems to neutralise ROS since excess ROS damages their cellular structures and function and causes them to die (Fridovich, 1986; Hajam et al., 2022). Hence, the antioxidant compounds found in their cells, including carotenoids, phenolic compounds, and flavonoids, are essential for their survival (Nagy et al., 2018; Photolo et al., 2020; Zeb, 2020). Some examples of antioxidant compounds found in *Methylobactrium* sp. are myxol (carotenoid) and phenol, 2,5-bis(1,1-dimethylethyl) (phenol) (Photolo et al., 2020; Stepnowski et al., 2004). The activity of antioxidant and phenolic compound content of ML8 pigment extract was evaluated through various assays, which are DPPH radical scavenging, ABTS radical scavenging, FRAP, and total phenolic content (TPC) due to the bacteria pigment benefits. Moreover, the toxicity of these pigment extracts was also determined to establish a safe dosage for consumption. In this study, the brine shrimp (*Artemia salina*) lethality bioassay was employed as a quick, easy, and effective method to evaluate the toxicity of a range of compounds such as natural plant extracts, poisonous chemicals, different hazardous

metal substances, and organic compounds, as highlighted in studies conducted by Lu and Yu (2019), Wu (2014), as well as Yu and Lu (2018).

Artemia salina, a class Crustacea and phylum Arthropoda member, can survive in hypersaline surroundings. *Artemia* sp. is a widely used biological model in low-cost toxicity bioassays conducted in laboratory settings, owing to its quick hatching, easy accessibility, and susceptibility to harmful compounds. This organism's small size, well-understood biological and ecological characteristics, and ability to adapt to various testing environments make it easy to operate in labs (Lu & Yu, 2019; Yu & Lu, 2018). Additionally, *Artemia* sp. has a unique ability to reproduce sexually and asexually in water with a 0.4–3.4 M salinity range and varying ionic environments. Its life cycle includes the cyst stage (the most resilient of all animal life history stages) and motile stages (that are among the best osmoregulators in the animal kingdom), making it a popular model for various studies, including toxicity tests (Norouzitallab, 2015; Ríos & Gajardo, 2004). In addition, research has indicated that this species has a similar toxicity mechanism to mammalian creatures. The *A. salina* test and the findings from toxicity studies conducted on a mouse fibroblast cell line, for instance, did not show any appreciable changes, according to Rajabi et al. (2015). However, according to Hamidi et al. (2014), the toxicity test results using mice and *A. salina* have a high correlation in determining the lethal concentration (LC_{50}).

MATERIALS AND METHODS

Materials

The methanol and ethanol pigment extracts of PPFM bacteria were prepared previously in several steps. The PPFM bacteria was initially isolated from *M. lunu-ankenda* leaf, cultured and purified on *Pseudomonas* agar media (BD Difco™, USA). The pure culture of the isolated PPFM bacteria (labelled as ML8) was grown in modified King's B broth media (contained peptone [BD Difco™, USA], magnesium sulphate heptahydrate [Systerms, Malaysia], potassium dihydrogen phosphate and glycerol (anhydrous) [R & M Chemicals, United Kingdom]) for cell enrichment for 5 days to obtain its pigment. Then, the cell was collected through centrifugation, and its pigment was extracted using selected solvents, followed by a drying process with several drying equipment, including a rotary evaporator. Those bacteria pigment extracts were tested on several related antioxidant capacity measurement activities, as well as a toxicity evaluation. They are DPPH, FRAP, ABTS radical scavenging assays, and TPC. Also, the brine shrimp method was used for toxicity level evaluation. In detail, the chemicals used are methanol, 2.0 N Folin-Ciocalteau's phenol reagent, ascorbic acid, potassium dichromate (R & M Chemicals, United Kingdom), sodium carbonate anhydrous (Systerm, Malaysia), trolox, and gallic acid monohydrate (Acros Organics, USA). Then, DPPH (free radical) powder (Alfa Aesar, Thermo Fisher Scientific, USA), ABTS diammonium salt, quercetin dehydrate, sodium acetate

anhydrous, potassium peroxodisulfate, and iron (III) chloride (Sigma-Aldrich, USA), glacial acetic acid, hydrochloric acid (HCl) 37% (EMSURE®, Merck, Germany), 2,4,6-tri(2-pyridyl)-1,3,5-triazine (TPTZ) (Merck, Germany), sodium chloride (QRëC, Thailand), and brine shrimp eggs were bought from supplier at Seri Kembangan (Malaysia). A microplate spectrophotometer (BioTek Model EL800, USA), with Gen5™ software (version 1.06.10) was used for absorbance reading in the DPPH assay while microplate spectrophotometer from Benchmark Plus Microplate model (BIO-RAD 170-6930, USA) equipped with Microplate Manager® software (version 5.2.1) was used to read absorbance for ABTS scavenging, FRAP, and TPC assays. All aqueous solutions were prepared using distilled water, and all purchased chemical reagents were of analytical grade. All antioxidant assays were done in minimal light to avoid technical errors during the experiment sessions.

Methods

DPPH Radical Scavenging Assay. In a 96-well microplate, samples were prepared at concentrations of 5–0.04 mg/ml (methanol extract), 2.5–0.02 mg/ml (ethanol extract), and 0.8–0.01 mg/ml for ascorbic acid. Then, 0.2 mM fresh DPPH solution was prepared using DPPH powder (Alfa Aesar, Thermo Fisher Scientific, USA) and methanol (R & M Chemicals, United Kingdom) referring to the modified method of Nor et al. (2023) and Prieto (2012). Next, the volume of the DPPH solution was mixed with the volume of the sample solution with a 1:1 ratio and incubated for 30 min at room temperature. The absorbance was then read at 515 nm. The result was shown by calculating the percentage of scavenging activity according to the equation below:

$$\%\ \text{DPPH scavenging} = \left(\frac{\text{A control} - [\text{A sample} - \text{A colour sample}]}{\text{A control}}\right) \times 100\%$$

where % DPPH scavenging = the percentage of radical scavenging activity, A control = absorbance of solvent with DPPH, A sample = absorbance of the sample with DPPH, and A colour sample = absorbance of the sample.

The results were plotted as the percentage (%) of scavenging activity versus the sample's concentration to obtain the IC_{50} inhibition concentration value. The IC_{50} value represents the sample amount that can reduce 50% of the DPPH radical, as defined by Ismail et al. (2013). The antioxidant capacity was stated in per cent inhibition (%I).

FRAP Assay. By slight modification of Pawar et al. (2015) and Sahib et al. (2012) FRAP method, the preparation of a working FRAP reagent was done by mixing 300 mM acetate buffer (pH 3.6, Sigma-Aldrich, USA), 10 mM TPTZ solution (Merck, Germany, which was diluted in 40 mM HCl [EMSURE®, Merck, Germany]), and 20 mM iron (III) chloride (Sigma-Aldrich, USA) in a ratio of 10:1:1. Then, the working FRAP reagent solution (150

µl) was mixed with a sample (20 µl) in each well of a 96-well microplate. The sample and standard (Trolox, Acros Organics, USA) were prepared as follows: 50–0.4 mg/ml (methanol extract), 5–0.04 mg/ml (ethanol extract), and 0.5–0.004 mg/ml (standard), respectively. After adding the sample to the FRAP reagent, it was placed in the dark at 37°C for incubation at 30 min, and the absorbance was read at 595 nm. The antioxidant activity of the extract was stated as trolox equivalents of 100 mg TE/g of crude sample extract.

ABTS Radical Scavenging Assay. This kind of scavenging assay was conducted based on the protocol described by Hussin et al. (2019), Pawar et al. (2015), and Verma et al. (2009) with slight amendments. The stock solutions of 7 mM ABTS (Sigma-Aldrich, USA) and 2.45 mM potassium peroxodisulfate (Sigma-Aldrich, USA) were prepared freshly before use. Then, those stock solutions were mixed with a 1:1 ratio and placed at room temperature for 16 hr under dark conditions to produce the ABTS radical cation. The working solution was then diluted to an absorbance reading of 0.70 ± 0.2 units at 734 nm, resulting in the $ABTS^{\cdot+}$ solution. A sample (50–0.4 mg/ml) and a standard (quercetin) solution (1.00–0.01 mg/ml) were prepared accordingly. A volume of 195 µl $ABTS^{\cdot+}$ solution was added to react with 5 µl samples for 60 s, and the absorbance was read at 734 nm. The collected data of antioxidant activity for the ABTS scavenging assay was calculated and presented similarly to the DPPH scavenging assay.

TPC Assay. Samples at concentrations of 50–0.4 mg/ml (methanol extract), 5–0.04 mg/ml (ethanol extract), and 0.5–0.004 mg/ml standard (gallic acid) were prepared to conduct the TPC assay adapted from Ismail et al. (2013). The assay was performed by adding a 10 µl sample with 75 µl of 0.2 N Folin-Ciocalteau's phenol reagent (R & M Chemicals, United Kingdom), and the reaction was let to occur at room temperature for 5 min, and subsequently, 75 µl of 6% sodium carbonate (Systerm, Malaysia) was added. The absorbance value at 725 nm was taken after 90 min of incubation at room temperature. A calibration curve was prepared using a series concentration of standard solutions. The TPC result was expressed as 100 mg gallic acid equivalents (GAE)/g of sample weight based on the equation below, as adapted from Singh et al. (2015):

$$C = \frac{V}{m} \times c$$

where C = total phenolic content mg GAE/g dry extract, c = concentration of gallic acid from the calibration curve (mg/ml), V = volume of sample (ml) and reagent mixture, and m = mass of sample (g).

Toxicity Study

The toxicity evaluation in this study was divided into two parts: the hatching of brine shrimp from eggs and the lethally evaluated nauplii. This species can survive on its egg yolk reserves for up to 5 days after hatching (Sanders, 2008), making any lethal effect on them solely due to any foreign compounds' exposure during toxicity studies.

Hatching of Brine Shrimp (*Artemia salina* sp.). The eggs of the species of brine shrimp, namely *A. salina* sp., were obtained from a supplier in Seri Kembangan, Selangor, Malaysia. A method based on Ramli (2018) was used to hatch the eggs with slight modifications. The eggs were hatched using artificial seawater by mixing 10 g of sodium chloride (QRëC, Thailand) with 400 ml of distilled water under good aeration and light conditions for a few days. After incubation for about 24–36 hr, the nauplii were separated from their eggshells by attracting them with light on one side, collected, and transferred into a Petri dish for further action (Figure 1).

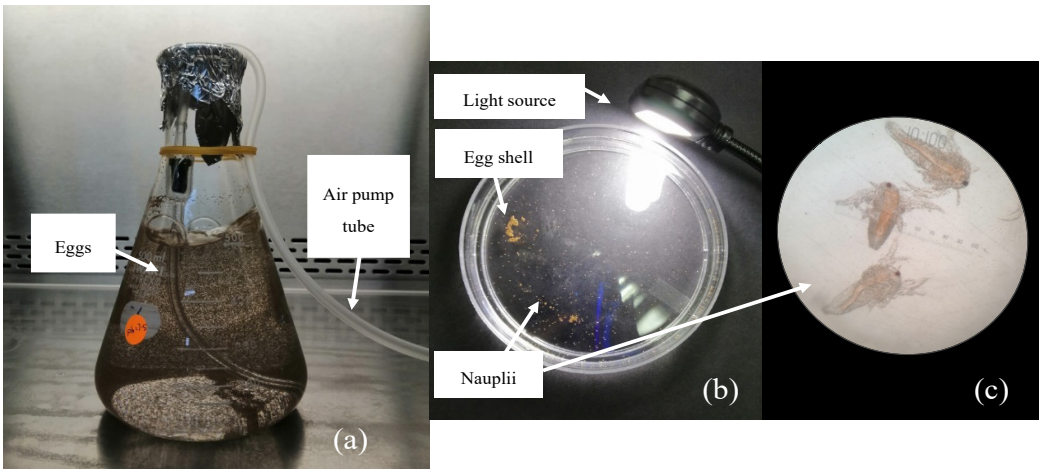

Figure 1. (a) Brine shrimp eggs hatching condition; (b) Nauplii of brine shrimp in a Petri dish; (c) Nauplii at 100× magnification

Brine Shrimp (*Artemia salina* sp.) Lethality Assay. A series of sample concentrations were prepared to range from 0.08–10 mg/ml and 0.01–1.25 mg/ml for potassium dichromate (R & M Chemicals, United Kingdom). Ten nauplii were incubated for 24 hr in each test tube containing 2 ml of solution (Figure 2). The percentage of mortality was calculated using the equation:

$$\% \text{ Mortality} = \left(\frac{\text{Number of dead nauplii}}{\text{Initial number of live nauplii}} \right) \times 100\%$$

The LC_{50} of the sample was calculated based on Probit analysis, and the regression line was achieved by plotting the logarithm of concentration versus the mortality per cent based on the Probit scale (Waghulde et al., 2019). The results were documented by examining the live nauplii for every hour. Potassium dichromate is a suitable reference toxicant for aquatic toxicity testing, as recommended by the U. S. Environmental Protection Agency (2002), with an LC_{50} value of 0.06 to 0.28–0.30 mg/ml (Ramli, 2018; Sahgal et al., 2010; Syahmi et al., 2010).

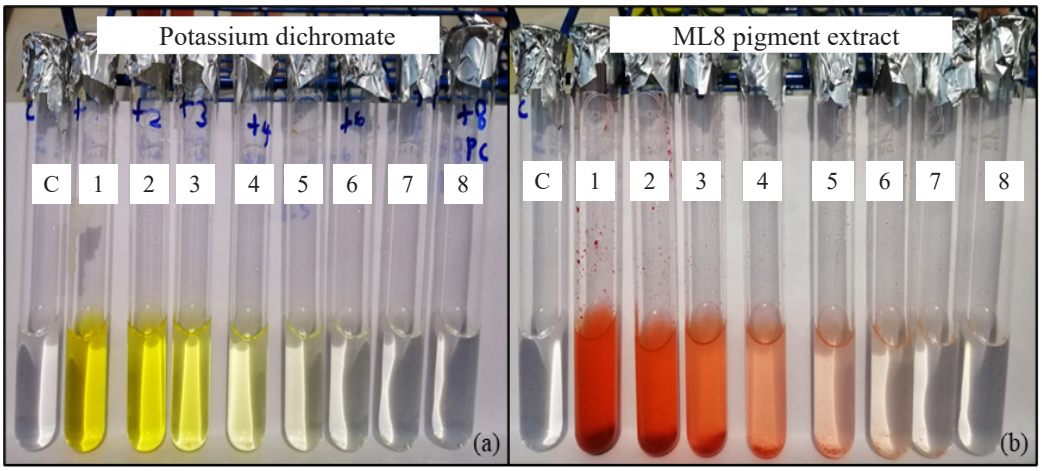

Figure 2. Serial dilution for toxicity analysis. (a) No. 1-8 = control, 1.25, 0.63, 0.31, 0.16, 0.08, 0.04, 0.02, 0.01 mg/ml; (b) No. 1–8 = control, 10.0, 5.00, 2.50, 1.25, 0.63, 0.31, 0.16, 0.08 mg/ml

RESULTS AND DISCUSSION

Using DPPH, FRAP, and ABTS tests, as well as TPC analysis and brine shrimp lethality assay, the antioxidant and toxicity properties of ML8 methanolic and ethanolic pigment extracts were assessed. All the data were examined and documented.

Antioxidant Activities and Phenolic Content of Pigment Extract

The free radical scavenging activities of ML8 pigment extracts were tested against commercial DPPH reagents, demonstrating a linear relationship with concentration. Increased concentration shows the rise of the DPPH scavenging activity. Ethanolic-extract ML8 pigment exhibits 21.34 ± 4.05% of scavenging activity for 0.08 mg/ml of pigment extract and rises to 77.00 ± 3.57% when the concentrations are increased to 0.63 mg/ml with an IC_{50} value of 0.36 ± 0.03 mg/ml. These activities are higher than those of methanol extract, which exhibits 15.50 ± 3.12% and 45.86 ± 1.95%, respectively, with an IC_{50} value of 0.72 ± 0.04 mg/ml (Figure 3). In contrast, methanolic extract ML8 pigment has a good ABTS scavenging activity (13.95 ± 1.57 to 53.81 ± 1.09% with an IC_{50} value of 4.59 ± 2.17 mg/ml) as compared to ethanolic extract (14.96 ± 6.01 to 52.22 ± 4.93 with an IC_{50} value of 6.30 ± 0.31mg/ml, respectively) at 0.78 to 6.25 mg/ml of sample concentration (Figure 4).

However, the analysis of FRAP showed that the ethanolic extract of the ML8 pigment had significant levels of trolox equivalent (TLX Eq.), followed by the methanolic extract of the same pigment. The ethanolic extract showed increasing orders of FRAP values, ranging from 1.09 ± 0.19 for 0.78 mg/ml to 8.77 ± 1.52 mg of TLX Eq./mg for 6.25 mg/ml of sample. In contrast, the methanolic extract exhibited low levels of TLX Eq., despite exhibiting better ABTS scavenging than the ethanolic extract (Figure 5). The TPC of all tested

samples ranged from 0.22 to 11.16 mg/mg of GAE. The ethanol extract of the ML8 pigment had the highest phenolic content (11.16 ± 0.55 mg GAE/mg), whereas the methanol extract had a low value of TPC (Figure 6).

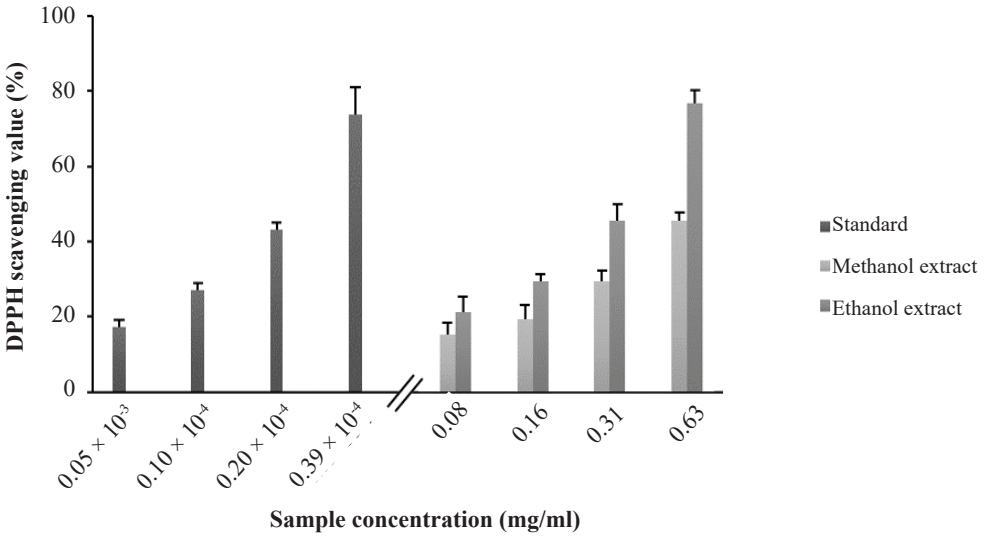

Figure 3. Antioxidant activities of ML8 pigment extract by 2,2-diphenyl-1-picrylhydrazyl (DPPH) radical scavenging assay

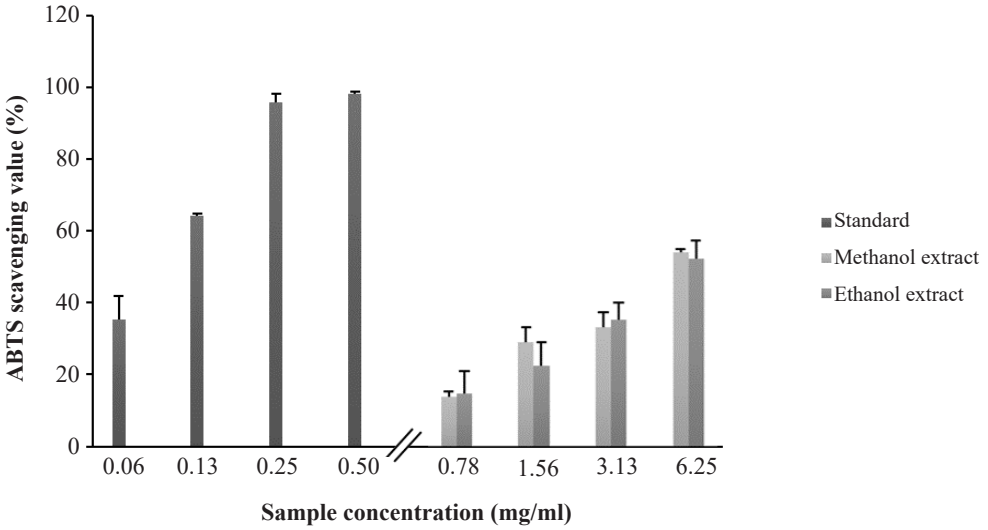

Figure 4. Antioxidant activities of ML8 pigment extract by 2,2'-azino-bis(3-ethylbenzothiazoline-6-sulfonic acid) (ABTS) radical scavenging assay

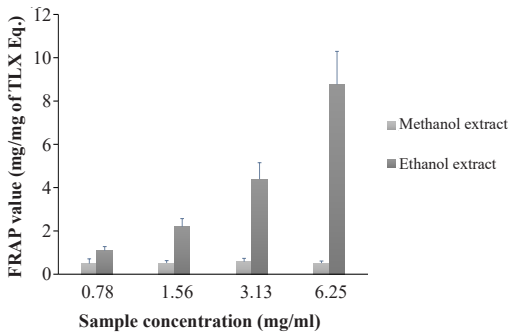

Figure 5. Antioxidant activity of ML8 pigment extract by ferric ion reducing antioxidant power (FRAP) assay

Note. TLX Eq. = Trolox equivalents

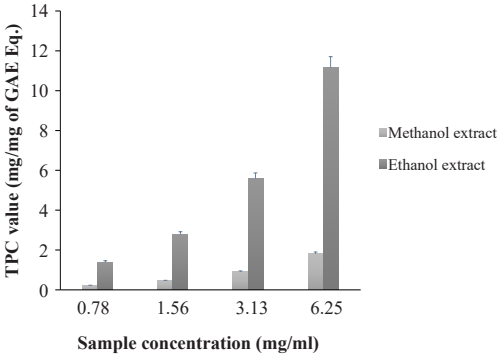

Figure 6. Antioxidant activity of ML8 pigment extract by total phenolic content (TPC) assay

Note. GAE Eq. = Gallic acid equivalents

In contrast, when compared to the IC_{50} values of the pigment extracts of several marine epiphyte species, including *Pseudomonas koreensis* (JX915782), *Serratia rubidaea* (JX915783), and *Pseudomonas argentinensis* (JX915781), high antioxidant activity was observed in both pigment extracts in all DPPH and ABTS scavenging assays (Pawar et al., 2015). Moreover, they displayed a low FRAP value and phenolic content. This finding suggests that various pigmented bacterial species may have various antioxidant properties in response to extract compounds in their pigments.

However, the antioxidant activity levels of the two pigment extracts vary. To be more specific, ethanolic extract ML8 pigment exhibits excellent activity in both DPPH and FRAP assays in addition to having a high phenolic content, whereas methanolic extract ML8 pigment exhibits good antioxidant activity in the ABTS assay but low phenolic content. The somewhat differing polarity index of the solvents (methanol and ethanol) used to extract the ML8 pigment may have an impact on both the type of compounds extracted and the yield value percentage. According to Abarca-Vargas et al. (2016), Torres et al. (2011), and Zullaikah et al. (2019), the polarity indices of methanol and ethanol are 5.1 and 5.2, respectively, making them both polar solvents. Though the polarity index value of ethanol is more polar than methanol, it is more likely to extract phenolic compounds, including polar carotenoids.

The extracted pigment from six microalgae strains from industrial wastewater using methanol and ethanol solvent extraction found that methanol extraction had a slightly lower phenolic content, but a greater carotenoid concentration compared to ethanol extraction (Safafar et al., 2015). Meanwhile, Do et al. (2014) found that the methanol extract of *Limnophilca aromatica* had a lower phenolic concentration than the ethanol extract. *Methylobacterium* sp. has been identified to contain alkaloids, flavonoids, steroids, and various types of

carotenoids, including astaxanthin, lutein, canthaxanthin, -carotene, spheroidene 1,1'- or 2,2'-dihydroxylycopene, and 2'-dehydroxymyxol, which most probably accountable to produce antioxidant activity, according to Photolo et al. (2020) and Stepnowski et al. (2004).

The interaction of chemical reagents with antioxidant molecules in the pigment extract during the antioxidant assay could contribute to the variation in antioxidant activity value. The Folin-Ciocalteu phenol's reagent, used to oxidise phenolic compounds, reacts with a mixture of tungstate and molybdate in a basic media, and any substance or molecule reacting with this solution increases the phenolic concentration. Such substances include organic acids, Fe^{2+}, sodium metabisulphite, sulphite, sugars, proteins, aromatic amines, ascorbic acid, and other enediols and reductones (Cerretani & Bendini, 2010).

The effect of a high phenolics ratio is further supported by Gil et al. (2002) when compared to the carotenoid content of numerous fruit species, including ripe nectarines, peaches, and plums, which generally have high antioxidant activity. Hence, based on the TPC, it is predicted that ethanolic ML8 pigment extracts with higher phenolic content will exhibit a better connection with antioxidant activity than methanolic pigment extracts. Furthermore, the FRAP mechanism that involves a compound's ability to convert Fe^{3+} to Fe^{2+} demonstrates the transfer of an electron rather than a hydrogen atom. In an acidic environment, this test allowed the reaction to decrease the ionisation potential that drives hydrogen atom transfer and increase the redox potential, which is the main reaction mechanism. When TPTZ is present during the reduction of Fe^{3+} to Fe^{2+}, a coloured complex with Fe^{2+} is formed due to the reaction, as described by Cerretani and Bendini (2010).

In phenolic compounds, the extent of conjugation and the degree of hydroxylation are connected to the reducing power. Similar molecules react in the FRAP assay because the reaction picks up substances with redox potentials value (lower than 700 mV) comparable to ABTS. Nevertheless, this assay is not sensitive enough to detect substances that work via hydrogen transfer (radical quenching), such as thiols (as glutathione) and proteins (Cerretani & Bendini, 2010). The lower FRAP score of the methanol extract of ML8 pigment, as compared to the ethanol extract, may be attributed to the possibility of higher concentrations of the mentioned chemicals in the former.

According to Cerretani and Bendini (2010), $ABTS^{\cdot+}$ and $DPPH^{\cdot}$ radicals can be neutralised via direct reduction through electron transfers or radical quenching via hydrogen atom transfers. In the ABTS assay, the decay of the radical cation $ABTS^{\cdot+}$ resulting from the oxidation of ABTS by other substances is spectrophotometrically observed. Although $ABTS^{\cdot}$ is relatively stable, it reacts energetically with molecules and can donate hydrogen atoms or electrons, leading to the disappearance of the blue/ green colour of the radical. A substance

having a lower redox potential than ABTS (680 mV) can reduce the $ABTS^{\cdot+}$. The DPPH radical is one of the few stable organic nitrogen radicals that produces deep purple solutions.

However, the reaction between $ABTS^{\cdot+}$ and $DPPH^{\cdot}$ can proceed slowly in the presence of many individual phenols or phenolic extracts. Additionally, the ABTS radical scavenging assay has some drawbacks, such as poor selectivity of $ABTS^{\cdot+}$ in the interaction with the hydrogen atom donors and ineffective aromatic OH-groups for antioxidation activity, as reported by Cerretani and Bendini (2010). Since these chemicals (aromatic OH-groups) may be abundantly available in methanolic extract based on compound analysis, this circumstance may explain the greater antioxidant activity value in the ABTS experiment compared to ethanol extraction of ML8 pigment.

In contrast, the selectivity of $DPPH^{\cdot}$ in the interaction with hydrogen donors is expected to be higher than $ABTS^{\cdot+}$ as it does not react with only one OH-group in aromatic acids. However, steric accessibility is one of the main limitations since smaller molecules have an easier entry to the radical position, resulting in increased apparent antioxidant action based on Cerretani and Bendini (2010). Due to this, the ethanol extract of the ML8 pigment may show more antioxidant activity compared to methanol in the DPPH experiment.

Nevertheless, research by Photolo et al. (2020) showed substantial DPPH radical scavenging by a pigment extract from a *Methylobacterium* species with an IC_{50} value greater than ascorbic acid. Most often, the EC_{50} (also known as IC_{50}) is the concentration that results in a 50% reduction in the initial DPPH concentration, where it is used to indicate a sample's hydrogen-donating potential measured in the DPPH test (Cerretani & Bendini, 2010). It demonstrates the excellent antioxidant activity of ethanol-extract ML8 pigments.

Toxicity Effect of Extracted Pigment on Brine Shrimp

This study found that the nauplii's mortality rate has a strong positive correlation with the concentration of ML8 pigment extract; the LC_{50} value was obtained through the best-fit line of the percentage of nauplii killed versus the concentration of ML8 pigment extract and potassium dichromate (Supplementary Figures A-C) and is presented in Table 1. Additionally, the brine shrimp lethality assay results revealed that extract ML8 pigments are not toxic to brine shrimp, with LC_{50} values of 4.52 mg/ml (methanol extract) and 9.94 mg/ml (ethanol extract).

Table 1
Toxicity value of ML8 pigment extract using brine shrimp lethality assay

No.	Sample	LC_{50} (mg/ml)
1.	Potassium dichromate	0.05
2.	ML8 pigment methanol extract	4.52
3.	ML8 pigment ethanol extract	9.94

Commonly, potassium dichromate is used as a positive control because of its well-known toxicity and was found to give brine shrimp toxication effect of exposure with an LC_{50} of 0.05 mg/ml. In contrast, brine shrimp in a test tube containing only artificial seawater showed no death and was a negative control. Syahmi et al. (2010) verified that crude extracts with LC_{50} values < 1 mg/ml are considered toxic, while those with values > 1 mg/ml are safe for human consumption. Therefore, the ML8 pigment extract is biologically safe for humans with LC_{50} values of 4.52 mg/ml and 9.94 mg/ml, while potassium dichromate is toxic.

CONCLUSION

The findings of all evaluated antioxidant activities, except for ABTS and phenolic substances, indicated that ethanolic ML8 pigment extract has a greater value than methanolic ML8 pigment extract. Furthermore, neither pigment extract was poisonous and could be used in the food sector for human consumption.

ACKNOWLEDGMENTS

The authors thank Universiti Putra Malaysia for providing all the necessary facilities and funds through the Putra Grant-Putra Graduate Initiative (GP-IPS/2017/9588200) and Graduate Research Fellowship.

REFERENCES

Abarca-Vargas, R., Pena Malacara, C. F., & Petricevich, V. L. (2016). Characterization of chemical compounds with antioxidant and cytotoxic activities in *Bougainvillea* × *buttiana* Holttum and Standl, (var. Rose) extracts. *Antioxidants*, *5*(4), 45. https://doi.org/10.3390/antiox5040045

Boronat, A., & Rodríguez-Concepción, M. (2015). Terpenoid biosynthesis in prokaryotes. In J. Schrader & J. Bohlmann (Eds.), *Biotechnology of isoprenoids: Advances in biochemical engineering/biotechnology* (Vol. 148, pp. 3–18). Springer. https://doi.org/10.1007/10_2014_285

Cerretani, L., & Bendini, A. (2010). Rapid assays to evaluate the antioxidant capacity of phenols in virgin olive oil. In V. R. Preedy & R. R. Watson (Eds.), *Olives and olive oil in health and disease prevention* (pp. 625–635). Academic Press. https://doi.org/10.1016/B978-0-12-374420-3.00067-X

Cheeseman, K. H., & Slater, T. F. (1993). An introduction to free radical biochemistry. *British Medical Bulletin*, *49*(3), 481–493. https://doi.org/10.1093/oxfordjournals.bmb.a072625

Dekkers, J. C., van Doornen, L. J., & Kemper, H. C. (1996). The role of antioxidant vitamins and enzymes in the prevention of exercise-induced muscle damage. *Sports Medicine*, *21*, 213–238. https://doi.org/10.2165/00007256-199621030-00005

Do, Q. D., Angkawijaya, A. E., Tran-Nguyen, P. L., Huynh, L. H., Soetaredjo, F. E., Ismadji, S., & Ju, Y.-H. (2014). Effect of extraction solvent on total phenol content, total flavonoid content, and antioxidant activity of *Limnophila aromatica*. *Journal of Food and Drug Analysis*, *22*(3), 296–302. https://doi.org/10.1016/j.jfda.2013.11.001

Dreyer, M. (2016). *Adaption of two* Methylobacterium *strains isolated from rainwater to simulated stress factors in the atmosphere* [Master's thesis, Aarhus University]. Studerende. https://studerende.au.dk/fileadmin/bioscience/Uddannelse/Specialerapporter_og_abstracts/2016-03-18_Morten_Dreyer_Speciale.pdf

Dring, M. J. (2005). Stress resistance and disease resistance in seaweeds: The role of reactive oxygen metabolism. *Advances in Botanical Research*, *43*, 175–207. https://doi.org/10.1016/S0065-2296(05)43004-9

Fridovich, I. (1986). Biological effects of the superoxide radical. *Archives of Biochemistry and Biophysics*, *247*(1), 1–11. https://doi.org/10.1016/0003-9861(86)90526-6

Gil, M. I., Tomás-Barberán, F. A., Hess-Pierce, B., & Kader, A. A. (2002). Antioxidant capacities, phenolic compounds, carotenoids, and vitamin C contents of nectarine, peach, and plum cultivars from California. *Journal of Agricultural and Food Chemistry*, *50*(17), 4976–4982. https://doi.org/10.1021/jf020136b

Green, P. N. (2014). Taxonomy of methylotrophic bacteria. In J. C. Murrell & H. Dalton (Eds.), *Methane and methanol utilizers: Biotechnology handbooks* (pp. 23–84). Springer. https://doi.org/10.1007/978-1-4899-2338-7_2

Hajam, Y. A., Rani, R., Ganie, S. Y., Sheikh, T. A., Javaid, D., Qadri, S. S., Pramodh, S., Alsulimani, A., Alkhanani, M. F., Harakeh, S., Hussain, A., Haque, S., & Reshi, M. S. (2022). Oxidative stress in human pathology and aging: Molecular mechanisms and perspectives. *Cells*, *11*(3), 552. https://doi.org/10.3390/cells11030552

Halliwell, B., & Gutteridge, J. M. C. (2015). *Free radicals in biology and medicine* (5th ed.). Oxford University Press. https://doi.org/10.1093/acprof:oso/9780198717478.001.0001

Hamidi, M. R., Jovanova, B., & Panovska, T. K. (2014). Toxicological evaluation of the plant products using brine shrimp (*Artemia salina* L.) model. *Macedonian Pharmaceutical Bulletin*, *60*(1), 9–18. https://doi.org/10.33320/MACED.PHARM.BULL.2014.60.01.002

Hussin, M., Hamid, A. A., Abas, F., Ramli, N. S., Jaafar, A. H., Roowi, S., Majid, N. A., & Dek, M. S. P. (2019). NMR-based metabolomics profiling for radical scavenging and anti-aging properties of selected herbs. *Molecules*, *24*(17), 3208. https://doi.org/10.3390/molecules24173208

Ismail, A., Azlan, A., Khoo, H.-E., Prasad, K.N., & Kong, K.-W. (2013). *Antioxidant assays: Principles, methods and analyses*. Universiti Putra Malaysia Press.

Lu, Y., & Yu, J. (2019). A well-established method for the rapid assessment of toxicity using *Artemia* spp. model. In H. E.-D. Saleh (Ed.), *Assessment and management of radioactive and electronic wastes*. IntechOpen. https://doi.org/10.5772/intechopen.85730

Madhaiyan, M. (2003). *Molecular aspects, diversity and plant interaction of facultative methylotrophs occurring in tropical plants* [Unpublished Doctoral dissertation]. Tamil Nadu Agricultural University.

Nagy, V., Agócs, A., Deli, J., Gulyás-Fekete, G., Illyés, T. Z., Kurtán, T., Turcsi, E., Béni, S., Dékány, M., Ballot, A., & Vasas, G. (2018). Carotenoid glycoside isolated and identified from cyanobacterium *Cylindrospermopsis raciborskii*. *Journal of Food Composition and Analysis*, *65*, 6–10. https://doi.org/10.1016/j.jfca.2017.06.003

Nor, S. M., Ding, P., & Chun, T. J. (2023). Locule position and thawing duration affect postharvest quality of freshly cryo-frozen musang king durian fruit. *Pertanika Journal of Tropical Agricultural Science*, *46*(2), 517-528. https://doi.org/10.47836/pjtas.46.2.09

Norouzitallab, P. (2015). *Use of* Artemia *as model organism to study epigenetic control of phenotypes relevant for aquaculture species* [Unpublished Doctoral dissertation]. Ghent University.

Pawar, R., Mohandass, C., Sivaperumal, E., Sabu, E., Rajasabapathy, R., & Jagtap, T. (2015). Epiphytic marine pigmented bacteria: A prospective source of natural antioxidants. *Brazilian Journal of Microbiology*, *46*(1), 29–39. https://doi.org/10.1590/S1517-838246120130353

Photolo, M. M., Mavumengwana, V., Sitole, L., & Tlou, M. G. (2020). Antimicrobial and antioxidant properties of a bacterial endophyte, *Methylobacterium radiotolerans* MAMP 4754, isolated from *Combretum erythrophyllum* seeds. *International Journal of Microbiology*, *2020*, 9483670. https://doi.org/10.1155/2020/9483670

Prieto, J. M. (2012). Procedure: preparation of DPPH radical, and antioxidant scavenging assay. *DPPH Microplate Protocol*, 1–3.

Rajabi, S., Ramazani, A., Hamidi, M., & Naji, T. (2015). *Artemia salina* as a model organism in toxicity assessment of nanoparticles. *DARU Journal of Pharmaceutical Sciences*, *23*, 20. https://doi.org/10.1186/s40199-015-0105-x

Ramli, S. (2018). *Antimicrobial activity, phytochemical and toxicity analyses of salam [*Syzygium polyanthum *(Wight) Walp.] leaf extract and its application in food* [Unpublished Doctoral dissertation]. Universiti Putra Malaysia.

Ríos, D. L. P., & Gajardo, G. (2004). The brine shrimp *Artemia* (Crustacea, Anostraca): A model organism to evaluate management policies in aquatic resources. *Revista Chilena de Historia Natural*, *77*(1), 3–4. https://doi.org/10.4067/S0716-078X2004000100001

Safafar, H., Van Wagenen, J., Møller, P., & Jacobsen, C. (2015). Carotenoids, phenolic compounds and tocopherols contribute to the antioxidative properties of some microalgae species grown on industrial wastewater. *Marine Drugs*, *13*(12), 7339–7356. https://doi.org/10.3390/md13127069

Sahgal, G., Ramanathan, S., Sasidharan, S., Mordi, M. N., Ismail, S., & Mansor, S. M. (2010). Brine shrimp lethality and acute oral toxicity studies on *Swietenia mahagoni* (Linn.) Jacq. seed methanolic extract. *Pharmacognosy Research*, *2*(4), 215-220. https://doi.org/10.4103/0974-8490.69107

Sahib, N. G., Hamid, A. A., Saari, N., Abas, F., Dek, M. S. P., & Rahim, M. (2012). Anti-pancreatic lipase and antioxidant activity of selected tropical herbs. *International Journal of Food Properties*, *15*(3), 569–578. https://doi.org/10.1080/10942912.2010.494754

Sanders, J. M. (2008). *Time post-hatch caloric value of* Artemia salina. https://digitalcommons.uri.edu/cgi/viewcontent.cgi?article=1085&context=srhonorsprog

Santos, A. L., Moreirinha, C., Lopes, D., Esteves, A. C., Henriques, I., Almeida, A., Domingues, M. R. M., Delgadillo, I., Correia, A., & Cunha, A. (2013). Effects of UV radiation on the lipids and proteins of bacteria studied by mid-infrared spectroscopy. *Environmental Science and Technology*, *47*(12), 6306-6315. https://doi.org/10.1021/es400660g

Singh, C. B., Devi, M. C., Thokchom, D. S., Sengupta, M., & Singh, A. K. (2015). Phytochemical screening, estimation of total phenols, total flavonoids and determination of antioxidant activity in the methanol extract of *Dendrobium denudans* D. Don stems. *Journal of Pharmacognosy and Phytochemistry*, *4*(4), 6-11.

Stepnowski, P., Blotevogel, K. H., & Jastorff, B. (2004). Extraction of carotenoid produced during methanol waste biodegradation. *International Biodeterioration and Biodegradation*, 53(2), 127–132. https://doi.org/10.1016/j.ibiod.2003.11.001

Syahmi, A. R. M., Vijayarathna, S., Sasidharan, S., Latha, L. Y., Kwan, Y. P., Lau, Y. L., Shin, L. N., & Chen, Y. (2010). Acute oral toxicity and brine shrimp lethality of *Elaeis guineensis* Jacq., (oil palm leaf) methanol extract. *Molecules*, *15*(11), 8111–8121. https://doi.org/10.3390/molecules15118111

Torres, L. G., Velasquez, A., & Brito-Arias, M. A. (2011). Ca-alginate spheres behavior in presence of some solvents and water-solvent mixtures. *Advances in Bioscience and Biotechnology*, *2*, 8–12. https://doi.org/10.4236/abb.2011.21002

U. S. Environmental Protection Agency. (2002). *Methods for measuring the acute toxicity of effluents and receiving waters to freshwater and marine organisms* (5th ed.). US EPA. https://www.epa.gov/sites/default/files/2015-08/documents/acute-freshwater-and-marine-wet-manual_2002.pdf

Verma, B., Hucl, P., & Chibbar, R. N. (2009). Phenolic acid composition and antioxidant capacity of acid and alkali hydrolysed wheat bran fractions. *Food Chemistry*, *116*(4), 947–954. https://doi.org/10.1016/j.foodchem.2009.03.060

Waghulde, S., Kale, M. K., & Patil, V. (2019). Brine shrimp lethality assay of the aqueous and ethanolic extracts of the selected species of

medicinal plants. *Proceedings*, *41*(1), 47. https://doi.org/10.3390/ecsoc-23-06703

Wu, C. (2014). An important player in brine shrimp lethality bioassay: The solvent. *Journal of Advanced Pharmaceutical Technology and Research*, *5*(1), 57-58.

Yu, J., & Lu, Y. (2018). *Artemia* spp. Model - A well-established method for rapidly assessing the toxicity on an environmental perspective. *Medical Research Archives*, *6*(2). https://doi.org/10.5772/intechopen.85730

Zeb, A. (2020). Concept, mechanism, and applications of phenolic antioxidants in foods. *Journal of Food Biochemistry*, *44*(9), e13394. https://doi.org/10.1111/jfbc.13394

Zullaikah, S., Jessinia, M. C. P., Yasmin, M., Rachimoellah, M., & Wu, D. W. (2019). Lipids extraction from wet and unbroken microalgae *Chlorella vulgaris* using subcritical water. *Materials Science Forum*, *964*, 103–108. https://doi.org/10.4028/www.scientific.net/MSF.964.103

SUPPLEMENTARY DATA

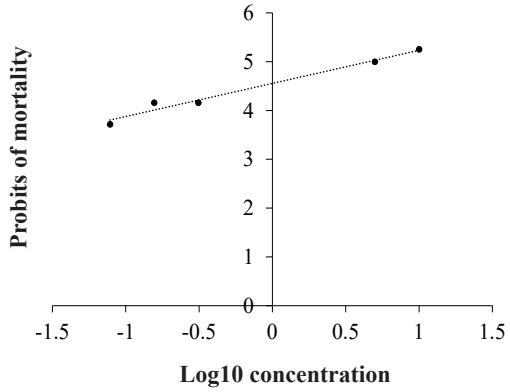

Figure A. Standard curve of brine shrimp lethality assay after being treated with ML8 pigment methanol extract

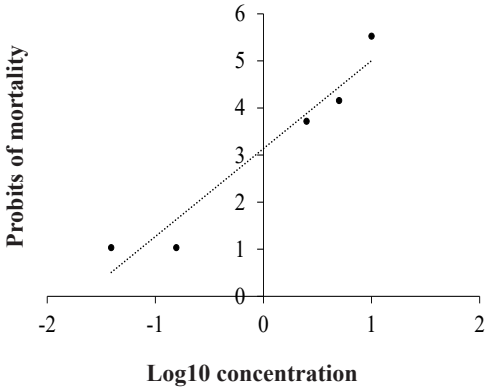

Figure B. Standard curve of brine shrimp lethality assay after being treated with ML8 pigment ethanol extract

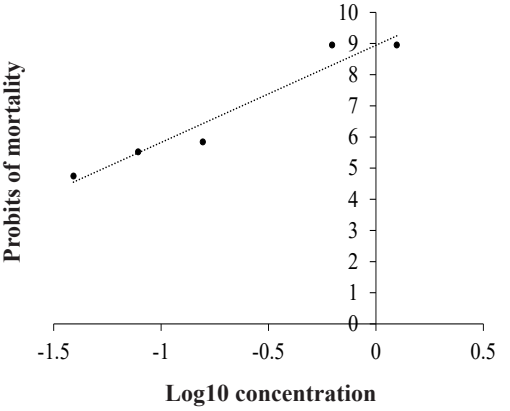

Figure C. Standard curve of brine shrimp lethality assay after being treated with potassium dichromate

REFEREES FOR THE PERTANIKA
JOURNAL OF TROPICAL AGRICULTURAL SCIENCE

Vol. 46 (4) Nov. 2023

The Editorial Board of the Pertanika Journal of Tropical Agricultural Science wishes to thank the following:

Abdul Rahman Omar
(UPM, Malaysia)

Ali Reza Radkhah
(UT, Iran)

Alimon Abd. Razak
(UGM, Indonesia)

Amin Ismail
(UPM, Malaysia)

Arief Budiman
(UGM, Indonesia)

Chew Bee Lynn
(USM, Malaysia)

Chonchanok Muangnapoh
(Chula, Thailand)

Didik Wahyudi
(UIN Malang, Indonesia)

Dzolkhifli Omar
(UPM, Malaysia)

Falah Hasan Baiee
(UoK, Iraq)

Felix Ogar Takim
(Unilorin, Nigereia)

Ika Roostika
(ICABIOGRAD, Indonesia)

Imad Abdelhamid El Haci
(CRAPC, Algeria)

Intan Faraha A Ghani
(UNISEL, Malaysia)

Isao Yumoto
(AIST, Japan)

Ismatul Nurul Asyikin Ismail
(USIM, Malaysia)

Jamal Ragheb Said Qasem
(UJ, Jordan)

Janna Ong Abdullah
(UPM, Malaysia)

Jesse Jay Villanueva
(MSU Main, Philippines)

Khanitta Somtrakoon
(MSU, Thailand)

Lesley Maurice Bilung
(UNIMAS, Malaysia)

Lingan Rajendran
(TNAU, India)

Loh Kar Hoe
(UM, Malaysia)

Loh Kar Hoe
(UM, Malaysia)

Mahmoud Nasr
(E-JUST, Egypt)

Mark Pyron
(BSU, USA)

Matthew Recsetar
(UA, USA)

Mohammad Amdadul Haque
(BARI, Bangladesh)

Mohammad Hassan Salehi
(SKU, Iran)

Mohd Effendy Abdul Wahid
(UMT, Malaysia)

Mok Wen Jye
(UMT, Malaysia)

Naeem Khan
(UFL, USA)

Naeem Sarwar
(BZU, Pakistan)

Najiah Musa
(UMT, Malaysia)

Narender Singh
(KUK, India)

Nazahatul Anis Amaludin
(UMK, Malaysia)

Neni Kartini Che Mohd Ramli
(UiTM, Malaysia)

Noor Akhmazillah Mohd Fauzi
(UTHM, Malaysia)

Nor Azlina Abd Aziz
(UM, Malaysia)

Nor Hazlina Mat Saat
(MARDI, Malaysia)

Noraini Mohd Jaafar
(UPM, Malaysia)

Norazian Mohd. Hassan
(IIUM, Malaysia)

Norhafizah Md Zain
(UMK, Malaysia)

Nur Fatihah Abdul Halid
(UMS, Malaysia)

Nur Sabrina Ahmad Azmi
(IIUM, Malaysia)

Piotr Salachna
(ZUT, Poland)

Piyada Theerakulpisut
(KKU, Thailand)

Piyaporn Waranusuntigul
(SDU, Thailand)

Raihana Zahirah Edros
(UMP, Malaysia)

Ramisah Shah Mohamed
(UMT, Malaysia)

Satyen Mondal
(BSMRAU, Bangladesh)

Shamsul Anuar
(UPM, Malaysia)

Sharina Omar
(UPM, Malaysia)

Sheikh Mohammad Masum
(SAU, Bangladesh)

Songchai Wiriyaumpaiwong
(MSU, Thailand)

Srinivasan Velusamy
(CDC, USA)

Tan Geok Hun
(UPM, Malaysia)

Tan Yee Shin
(UM, Malaysia)

Tengku Farizan Izzi Che Ku Jusoh
(UniSZA, Malaysia)

Wan Zaliha Wan Sembok
(UMT, Malaysia)

Zarul Hazrin Hashim
(USM, Malaysia)

AIST	*– National Institute of Advanced Industrial Science and Technology*
BARI	*– Bangladesh Agricultural Research Institute*
BSMRAU	*– Bangabandhu Sheikh Mujibur Rahman Agricultural University*
BSU	*– Ball State University*
BZU	*– Bahauddin Zakariya University*
CDC	*– Centers for Disease Control and Prevention*
Chula	*– Chulalongkorn University*
CRAPC	*– Centre de Recherche Scientifique et Technique en Analyses Physico-Chimiques*
E-JUST	*– Egypt-Japan University of Science and Technology*
ICABIOGRAD	*– Indonesian Center for Agricultural Biotechnology and Genetic Resource*
IIUM	*– International Islamic University Malaysia*
KKU	*– Khon Kaen University*
KUK	*– Kurukshetra University*
MARDI	*– Malaysian Agricultural Research and Development Institute*
MSU	*– Mahasarakham University*
MSU Main	*– Mindanao State University Research and Development*
SAU	*– Sher-e-Bangla Agricultural University*
SDU	*– Suan Dusit University*
SKU	*– Shahrekord University*
TNAU	*– Tamil Nadu Agricultural University*
UA	*– University of Arizona*
UFL	*– University of Florida*
UGM	*– Universitas Gadjah Mada*
UIN Malang	*– Universitas Islam Negeri Maulana Malik Ibrahim*
UiTM	*– Universiti Teknologi MARA*
UJ	*– University of Jordan*
UM	*– Universiti Malaya*
UMK	*– Universiti Malaysia Kelantan*
UMP	*– Universiti Malaysia Pahang*
UMS	*– Universiti Malaysia Sabah*
UMT	*– Universiti Malaysia Terengganu*
Unilorin	*– University of Ilorin*
UNIMAS	*– Universiti Malaysia Sarawak*
UNISEL	*– Universiti Selangor - Kampus Bestari Jaya*
UniSZA	*– Universiti Sultan Zainal Abidin*
UoK	*– University of Kufa*
UPM	*– Universiti Putra Malaysia*
USIM	*– Universiti Sains Islam Malaysia*
USM	*– Universiti Sains Malaysia*
UT	*– University of Tehran*
UTHM	*– Universiti Tun Hussein Onn Malaysia*
ZUT	*– Zachodniopomorski Uniwersytet Technologiczny w Szczecinie*

While every effort has been made to include a complete list of referees for the period stated above, however if any name(s) have been omitted unintentionally or spelt incorrectly, please notify the Chief Executive Editor, *Pertanika* Journals at executive_editor.pertanika@upm.edu.my

Any inclusion or exclusion of name(s) on this page does not commit the *Pertanika* Editorial Office, nor the UPM Press or the university to provide any liability for whatsoever reason.

Pertanika Journal of Tropical Agricultural Science
Vol. 46 (4) Nov. 2023

Content

Pertanika Editorial Office, Journal Division,
Putra Science Park,
1st Floor, IDEA Tower II,
UPM-MTDC Center,
Universiti Putra Malaysia,
43400 UPM Serdang,
Selangor Darul Ehsan
Malaysia

http://www.pertanika.upm.edu.my
Email: executive_editor.pertanika@upm.edu.my
Tel. No.: +603- 9769 1622

PENERBIT UPM UNIVERSITI PUTRA MALAYSIA PRESS

http://www.penerbit.upm.edu.my
Email: penerbit@upm.edu.my
Tel. No.: +603- 9769 8851

ISSN 1511-3701
11>
9 771511 370234